The Effects of Birth Weight and Accelerated Weight on Body Composition and Appetite Regulation

A thesis submitted for the degree of Doctor of Philosophy from Imperial College London

Gina Julieth Sanchez Canon

Imperial College London
Division of Investigative Science
and
Metabolic and Molecular Imaging Group
Faculty of Medicine

2014

Abstract

The link between early life and development of metabolic disorders and obesity in later life has been the focus of many studies over the past decades. Fetal life and early infancy are two of the most critical periods of physiological and metabolic development and plasticity, and thus, are periods whereby a stimulus can cause long term consequences on the health of an individual (developmental programming).

Accelerated weight gain during early life *per se* or in combination with extreme birth weights (low/high birth weight) have been postulated as factors that can affect the development of individuals with later consequences in health. However, there is not a clear understanding of the specific contribution at different ages to impaired health neither of the mechanisms involved in these alterations.

In this thesis, I used an isogenic murine model with natural birth weight variation within a normal range to investigate the effects of extreme birth weights on body composition and appetite regulation at different stages of life. I compared low and high birth weights phenotypes during lactation, at the time of weaning, and a young adulthood as well as early matured age. Mice were challenged to a moderate high fat diet for 12 weeks after weaning in order to assess the effects of both birth weight and a hypercaloric feed on body composition and hypothalamic neural activity.

At weaning, adiposity was positively related to birth weight and weight gain but negatively related to growth rate. Low birth weight male mice (**LBWm**) had a lower plasma glucose concentration but similar levels of insulin to High birth weight male mice (**HBWm**), indicating a degree of hyperinsulinemia. Low birth weight females (**LBWf**) were hyperinsulinemic and hyperglycemic compared to High birth weight females (**HBWf**). There was an upregulation in the expression of genes related to insulin signaling, adipogenesis/lipid metabolism and thermoregulation in Subcutaneous Adipose Tissue (SAT) of **LBWm** mice compared to **HBWm** mice but the contrary was seen in **LBWf** mice in respect to their counterpart.

LBWm mice caught up in weight with **HBWm** mice at younger age than the equivalent catch up in female mice. Birth weight and diet impacted body fat patterning and appetite regulation differently in both young males and females. However, at week 51 of age (early matured age), diet seemed to override the effects of birth weight on total body fat. **LBWm** mice tended to have smaller adipocytes than young and matured **HBWm** mice, especially when fed a **HF** diet, and this pattern was independent of fat mass.

In conclusion, the current study suggests that extreme birth weights in an isogenic mouse model (within natural birth weight variation), as well as postnatal nutrition influenced growth, glucose / lipid metabolism, body fat patterning and appetite regulation in an age-gender dependent manner.

Acknowledgements

I would like to thank my supervisor Prof. Jimmy Bell and Gary Frost for giving the opportunity to do this project and for their support over these years. I am very grateful with Prof. Jimmy Bell for giving me the freedom and encouragement to pursue this long journey.

I am also very greatful with each member of the Metabolic and Molecular Imaging Group especially Jelena, Louise, Meliz and Sarah. Thank you for your patient and for the time spent together. Thank you to Aine and Ana for your help too.

I would like to thank also Jordi and Marzena for their assistance in the BIC.

Finally, I would like to thank my parents and siblings for being there for me all the time. I could not thank enough to my parents for their inconditional support and love at all times. Thank you to my dear husband who has been patient and caring with me, especially when writing this thesis.

Este trabajo se lo dedico de corazón a mis padres quienes siempre me han apoyado incondicionalmente. A mi madre doy gracias por su amor, su dedicación y sacrificio durante todos esto años. A mi padre, por su buen ejemplo y por inculcarme rectitud y respeto hasta el último de sus días junto a nosotros. A mis hermanos, por ser mis mejores amigos. A mis pequeños grandes sobrinos por ser lo que son. A mi esposo, por ser ese complemento que siempre había esperado.

Gracias a todas las personas quienes bien o mal me dieron fuerza para seguir adelante.

A Dios doy gracias por darme todo cuanto he necesitado y he anhelado.

Declaration of Contributors

The work presented in this thesis was performed by the author. The contribution to this thesis from a third party is detailed below:

Segmentation analysis using Slice Omatic (Tomovision) software for the quantification of fat content and distribution was performed by a blind operator from Vardis group.

Abbreviations

2D = two dimensional

a-MSH= Alpha Melanocyte Stimulating Hormone

ACC = Acetyl-Coenzyme A Carboxylase

Actb/B-actin= Actin beta

Adrb3= Beta-3 adrenergic receptor

AEBSF = 4(2Aminoethyl) benzenesulfonyl fluoride hydrochloride

AGA= Appropriate for Gestational Age

AgRP= Agouti Related Peptide

ARC= Arcuate Nucleus

ATGL = Adipose Triglyceride Lipase

AUC= Area Under the Curve

BAT= Brown Adipose Tissue

BBB= Blood Brain Barrier

BMI= Body Mass Index

Bpm= Breaths per minute

CEBP= CCAAT Enhancer Binding Protein

cAMP = Cycling Adenosine Monophosphate

CART= Cocaine and Amphetamine Regulated Transcript

CAT= Computerised Axial Tomography

CCK= Cholecystokinin

cDNA= Complementary DNA

CI= Confidence Interval

CLAMS = Comprehensive Lab Animal Monitoring System

CNS= Central Nervous System

Ct = Threshold cycle

CVDs= Cardio Vascular Diseases

DEPC-treated water = Diethylpyrocarbonate treated water

DEXA = Dual Energy X-ray Absorptiometry

DMEM= Dulbecco's Modified Eagle Medium

DNA= Deoxyribonucleic acid

dNTPs = Deoxynucleotide Triphosphates

DPPIV= Dipeptidyl Peptidase four

dsDNA = double-stranded DNA

dT = deoxy –Thymine nucleotides

DTT= Dithriothreitol DTT

EDTA= Ethylenediaminetetraacetic acid

ER= Endoplasmic Reticulum

F-SEMS= Fast Spin Echo Multislice

FAS/FASN = Fatty Acid Synthase

FE= Feed Efficiency

FFM= Fat Free Mass

fMRI = Functional Magnetic Resonance Imaging

FOV= Field of View

GEE= Generalised Estimating Equation

GIP= Glucose-dependent Insulinotropic Peptide

GLM= General Linear Model

GLP-1= Glucagon Like Peptide 1

GLUT4/ Sic2a4= Glucose Transport 4/ Solute carrier family 2 (facilitated glucose transporter), member 4

^{1}H MRS = Proton Magnetic Resonance Spectroscopy

HBW= High Birth Weight

HBWf= High Birth Weight females

HBWm= High Birth Weight males

HF= High fat

Hprt = Hypoxanthine-guanine phosphoribosyltransferase

HSD= Tukey's high significance difference

HSL= Hormone Sensitive Lipase

i.p. = Intraperitoneal

i.v. = Intravenous

IAT= Internal Adipose Tissue

IHCL= Intrahepatocellular Lipid Content

IL-6= Interleukin 6

IPGTT= Intraperitoneal Glucose Tolerance Test

IR= Insulin Receptor

IRS= Insulin Receptor Substrate

LBW= Low Birth Weight

LBWf= Low Birth Weight females

LBWm= Low Birth Weight males

LGA= Large for Gestational Age

Ln= Naturally log transformed

LPL= Lipoprotein Lipase

LSD= Fisher's Least Significant Difference

MCP-1/CCL2= Monocyte Chemoattractant Protein-1

MEMRI= Manganase-Enhanced MRI

MGL= Monoglyceride Lipase

MGs= Monoglycerides

MMHMAG = Milliplex MAG Mouse Metabolic Hormone

Mn^{+2}= Manganese ions

$MnCl_2$= Manganese chloride

MRI= Magnetic Resonance Imaging

mRNA= messenger Ribonucleic Acid

MRS= Magnetic Resonance Spectroscopy

MSCs= Mesenchymal Stem Cells

NF= Normal fat

NPE= Normalised Percentage Enhancement

NPY = Neuropeptide Y

PAI-1= Plasminogen Activator Inhibitor-1

PAR= Predictive Adaptive Response

PKC- λ= Protein Kinase C-Lambda

PKC-Z= Protein Kinase C-Zeta

Pe= Periventricular nucleus

PET= Positron Emission Tomography

PGC1a= Peroxisome Proliferator Activated Receptor Gamma (PPARG) coactivator 1 alpha

PIK3= Phosphatidylinositol 3 Kinase

PIP-2= Phosphatidylinositol (4,5) bisphosphate

PIP3= Phosphatidylinositol (3,4,5) triphosphate

PKB/Akt = Protein kinase B

POMC = Proopiomelanocortin

PPARG = Peroxisome Proliferator Activated Receptor Gamma

PRESS= Point Resolved Spectroscopy

PVN = Paraventricular Nucleus

ROI= Regions of Interest

RT-PCR= Reverse Transcriptase Polymerase Chain Reaction

RT-qPCR= Real Time quantitative Polymerase Chain Reaction

RT= Room Temperature

SAT= Subcutaneus Adipose Tissue

SEM= Standard error of the mean

SEMS= Spin Echo Multislice

SI= Signal Intensities

SPULS= Single pulse sequence

SREBP1c/Serbf1= Steroid Regulatory Element Binding Protein 1c

ssDNA = Single-stranded DNA

Streptavidin-PE = Streptavidin-PhycoErythrin

SVF= Stromal Vascular Fraction

SW= Spectral Width

TE= Echo Time

TG= Triglyceride

TNF-alpha/a= Tumor Necrosis Factor alpha

TR = Repetition Time

TZDs= Thiazolidinediones

UCP-1= Uncoupling Protein 1

UCPs= Uncoupling Proteins

VMH = Ventromedial Hypothalamus

WAT= White Adipose Tissue

WC= Waist Circumference

WHO= World Health Organisation

Table of Contents

Table of Figures and Tables

1. Introduction

1.1 Early Life Programming

Clinical and experimental studies have demonstrated that there are associations between the early nutritional environment, patterns of postnatal growth and the development of obesity and altered fat distribution, cardiovascular diseases (CVDs), insulin resistance and type 2 diabetes in adult life (Fall, Osmond et al. 1995, Loos, Beunen et al. 2002, Cripps, Martin-Gronert et al. 2005).

Clinical and animal studies are widely supporting the concept of Developmental Programming whereby a stimulus, occurring during a critical period of developmental plasticity, has long-term consequences on the health of an individual (Gluckman and Hanson 2004, Desai, Beall et al. 2013). Fetal and early infancy are two of the most critical periods of physiological and metabolic development and thus, are periods that could be linked to the onset of the metabolic syndrome and related disorders, such as obesity, cardiovascular risk, hypertension and renal dysfunction (Hales and Barker 1992).

Low birth weight and infant and /or early childhood catch-up growth have been associated with a significant risk of adult obesity (Dietz 1994, Ong 2006). High birth weight associated with maternal obesity, with or without gestational diabetes, has also been related to an increased risk of obesity in children and adults. However, some studies have demonstrated a positive

relationship between high birth weight, insulin sensitivity and lean body mass (Seidman, Laor et al. 1991, Hales and Ozanne 2003, Singhal, Wells et al. 2003, Bouhours-Nouet, Dufresne et al. 2008). Overall, it has been shown that early life environment can permanently affect the metabolism of an individual.

Studies in young rodents (3 months of age) have demonstrated that low birth weight offspring had an improved glucose tolerance with reduced plasma insulin levels, which suggested improved insulin sensitivity at this age (Hales, Desai et al. 1996, Ozanne, Wang et al. 1998). This phenotype seems to be altered with age, such that by 15 months, the male offspring had impaired glucose tolerance and females developed glucose intolerance by 21 months (Fernandez-Twinn, Wayman et al. 2005).

Developmental programming seems to be the result of different complex interconnected mechanisms, but the underlying mechanisms are not well understood. Therefore, it is important to increase our understanding of the relationship between early life and altered metabolic processes.

Different hypotheses have been postulated throughout the years involving early life factors that could be associated with the susceptibility to become obese or metabolically unhealthy. Some of these hypotheses are described in the following sections.

1.1.1 Thrifty genotype hypothesis

James V. Neel proposed the “thrifty genotype” hypothesis for the first time in 1962 (Neel 1962) to explain the high incidence of obesity and type 2 diabetes mellitus among the Pima Indians in the United States. He proposed that genes that predispose to diabetes (thrifty genes) were historically advantageous for hunter gatherer populations especially childbearing women allowing them to store fat during times of plenty for later use in times of famine. However, these thrifty genes became detrimental in the modern world of constant abundance of food. (Scott, Mohlke et al. 2007, Sladek, Rocheleau et al. 2007). Neel tried to find more evidence of this hypothesis under the presumption that if a propensity to develop diabetes were an evolutionary adaptation, diabetes would have been an established condition in those populations currently experiencing a high frequency of diabetes. However, Neel did no find any evidence of diabetes among these populations earlier in the century (Spielman, Fajans et al. 1982).

Because it is no longer thought that hunter-gatherer faced the challenges of feast/famine, a modified “thrifty genotype” hypothesis argues that periods of famine and seasonal shortage of food that occurred only during the agricultural period, may have exerted enough pressure to select for thrifty genes (Prentice, Hennig et al. 2008).

Genetic predisposition to obesity has been observed in animal studies such as the *ob/ob* model and in clinical studies of its human homologue leptin deficiency (Zhang, Proenca et al. 1994). However, failure to find similar

mutations in the general obese population opened the door for a polygenic etiology of obesity (more than one gene) rather than a monogenic obesity (only one gene). Indeed 22 other gene associations with obesity have been suggested in some studies (see table 1.1.1.1), including members of the leptin-melanocortin pathway, proinflammatory cytokines and uncoupling proteins (Walley, Blakemore et al. 2006).

Gene symbol	Full name	Chromosomal location	Number of studies	*P*-value
ACE	Angiotensin I-converting enzyme (peptidyl-dipeptidase A) 1	17q24.1	6	0.05–0.0023
ADIPOQ	Adiponectin, C1Q and collagen domain containing	3q27	11	0.05–0.001
ADRB2	Adrenergic, beta-2-, receptor, surface	5q31–q32	20	0.05–0.0001
ADRB3	Adrenergic, beta-3-, receptor	8p12–p11.2	29	0.05–0.001
DRD2	Dopamine receptor D2	11q23.2	5	0.03–0.002
GNB3	Guanine nucleotide binding protein (G protein), beta polypeptide 3	12p13.31	14	0.05–0.001
HTR2C	5-hydroxytryptamine (serotonin) receptor 2C	Xq24	10	0.05–0.0001
IL6	Interleukin 6 (interferon, beta 2)	7p21	6	0.03–0.003
INS	Insulin	11p15.5	7	0.05–0.0002
LDLR	Low density lipoprotein receptor (familial hypercholesterolaemia)	19p13.2	5	0.04–0.001
LEP	Leptin (obesity homologue, mouse)	7q31.3	10	0.05–0.003
LEPR	Leptin receptor	1p31	16	0.04–0.0001
LIPE	Lipase, hormone-sensitive	19q13.2	5	0.05–0.002
MC4R	Melanocortin 4 receptor	18q22	8	0.04–0.002
NR3C1	Nuclear receptor sub-family 3, group C, member 1 (glucocorticoid receptor)	5q31	10	0.05–0.001
PLIN	Perilipin	15q26	5	0.05–0.0008
PPARG	Peroxisome proliferative activated receptor, gamma	3p25	30	0.05–0.001
RETN	Resistin	19p13.2	5	0.048–0.001
TNF	Tumor necrosis factor (TNF superfamily, member 2)	6p21.3	9	0.05–0.004
UCP1	Uncoupling protein 1 (mitochondrial, proton carrier)	4q28–q31	10	0.05–0.001
UCP2	Uncoupling protein 2 (mitochondrial, proton carrier)	11q13.3	11	0.05–0.001
UCP3	Uncoupling protein 3 (mitochondrial, proton carrier)	11q13	12	0.049–0.0005

Table 1.1.1.1 Genes with five or more positive associations of variants with obesity related phenotypes (Walley, Blakemore et al. 2006).

1.1.2 Thrifty phenotype hypothesis

Hales and Barker introduced the thrifty phenotype hypothesis, which proposes that poor early life nutrition produces permanent changes in glucose-insulin metabolism leading to the development of diseases in adulthood such as type 2 diabetes and cardiovascular alterations (Hales and Barker 2001). It is proposed that poor nutrition *in utero* causes an adaptive response in development of organs. To optimise the growth of certain essential organs, such as the brain, nutrients are diverted away from other tissues, such as the viscera, thereby improving perinatal survival. This altered growth permanently changes the structure and function of the body.

One of the most recognised causes of poor nutrition in early life is maternal undernutrition (Hales and Barker 2001, Cripps, Martin-Gronert et al. 2005, Martin-Gronert and Ozanne 2005). However, other influences, such as placental function, may also be involved. The combination of undernutrition during fetal life and infancy followed by overnutrition in childhood and adulthood implies the transition from chronic under nutrition to adequate nutrition triggers glucose intolerance (possibly due to decrease beta cell numbers) and other metabolic abnormalities including obesity (Fall, Stein et al. 1998).

1.1.3 Predictive adaptive response

The Predictive Adaptive Response (PAR) hypothesis, proposed by Gluckman and Hanson (Gluckman, Hanson et al. 2005), extends Barker hypothesis to nutritional imbalance both undernutrition and overnutrition during early life. This hypothesis suggests that prenatally programmed predisposition will confer survival benefits if a postnatal nutrition is maintained as predicted *in utero*. However, it will predispose the individual to an imbalanced metabolism if the postnatal diet mismatches the prenatal nutritional resource. The failure to develop metabolic alterations in adult life may indicate that the adult diet is within the predictive adaptive range.

1.2 Birth Weight and Accelerated Growth

1.2.1 Birth weight

A number of epidemiological studies have shown that birth weight as well as early accelerated growth and excess childhood weight gain are associated with an increased risk of adult cardiovascular diseases, hypertension, glucose intolerance, insulin resistance, type 2 diabetes and obesity (Hales and Barker 2001, Martin-Gronert and Ozanne 2005, Bieswal, Ahn et al. 2006, Mook-Kanamori, Durmus et al. 2011).

Low birth weight, as a measure of adverse intrauterine environment, has been used as an indicator of obesity and other complications later in life. A vast number of studies have shown an inverse association between birth weight and truncal fat in adulthood, which at the same time suggests a role for fetal development in determining adult fat distribution (Parsons, Power et

al. 1999, Te Velde, Twisk et al. 2003). The prevalence of impaired glucose tolerance or type 2 diabetes inversely associated with birth weight has been confirmed in different populations worldwide (China, UK, India, Pima Indians, black South African children, and others) (Hales, Barker et al. 1991, McCance, Pettitt et al. 1994, Barker 1998, Stanner and Yudkin 2001, Yajnik, Fall et al. 2003). Overall, fetal adaptation to intrauterine suboptimal conditions may alter fetal physiology, endocrine response, metabolism, and neural circuits resulting in the survival of the fetus but being detrimental later in life. Both environmental and genetic factors and their interactions may contribute to both fetal and postnatal growth and their link with long-term disease risks.

Recent investigations have focused on the impact of a high birth weight on later life, but contradictory effects have been reported. Some studies have reported that a high birth weight is associated with an increased risk of later life obesity, as measured by a positive relation with adult body mass index (BMI: ≥30 kg/m^2) (Seidman, Laor et al. 1991, Dietz 1994, Curhan, Willett et al. 1996, Parsons, Power et al. 1999). Other studies have suggesed that the association of high birth weight and disease is influenced by maternal diabetes, family history of diabetes, and specific ethnicities such as the Pima Indians in Arizona, USA (McCance, Pettitt et al. 1994, Wei, Sung et al. 2003).

Conversely, a retrospective study of an Icelandic population, who have one of the highest incidences of high birth weight in the world, found that they

had low incidence of both coronary diseases and high blood pressure in adults (Gunnarsdottir, Birgisdottir et al. 2004). This study also showed high birth weight was positively related to BMI in adulthood but these infants were not at increased risk of adult obesity (defined as BMI ≥30Kg/m^2). A protective effect of high birth weight against very high truncal fat was seen in both genders.

Similarly, studies from France have shown that high birth weight and early weight gain are positively related to insulin sensitivity and low central fat deposition. This has been referred to as a metabolic healthy obese phenotype (Bouhours-Nouet, Dufresne et al. 2008).

As BMI is associated with both total lean mass and fat mass, the positive association between birth weight and BMI later in life might be associated with lean mass rather than fat mass (Singhal, Wells et al. 2003). Shinghal proposes that this possible relationship could explain the paradoxical results obtained in different investigations. Indeed, it may be the case that birth weight may program body composition rather than simply predisposing to a big body size in adulthood.

1.2.2 Accelerated growth

Poor fetal growth alone (low birth weight) or in synergy with poor infant growth, and restricted fetal growth followed by accelerated infant growth or rapid growth in infancy by itself have been implicated in metabolic alterations in adulthood (Dulloo, Jacquet et al. 2006, Ong 2006).

Accelerated growth has been described as a phenomenon seen in young children as well as in other mammals after a period of growth restriction, when the restraints upon growth are removed (Gafni and Baron 2000). Growth acceleration shows a rate above the expected limits for chronological age and/or maturity for a period of time, followed by a progressive deceleration until normal growth is reached (Williams 1981). This catch up, at least after fetal growth retardation, seems to be related to a faster proportion of fat accretion rather than lean muscle (Dulloo 2006). The fat distribution in these infants tends to be located centrally rather than peripherally. Moreover, central adiposity seems to be positively related to metabolic disturbances at young and adult ages (Mook-Kanamori, Durmus et al. 2011).

Different studies have concluded that early catch up growth during infancy exacerbates central fat deposition, hypertension and insulin resistance (Ong 2006). Other studies have shown that neonatal catch up growth in weight normalised both neurobehavioral and cardiovascular phenotypes, but led to insulin resistance and high-fat diet-induced diabetes (Hermann, Miller et al. 2009). However, others have shown that restricted perinatal growth is an independent risk factor for the development of type 2 diabetes, hypertension and coronary heart disease from childhood and onwards (Eriksson, Forsen et al. 2007, Bouhours-Nouet, Dufresne et al. 2008). Overall, the evidence indicates that in general, early life is a highly sensitive period that can affect mammalian metabolism permanently but the specific alterations involving birth weight and or accelerated growth are still under investigation.

1.3 Obesity, Definition and Other Aspects

The World Health Organisation (WHO) defines obesity, as an abnormal or excessive fat accumulation that presents a risk to health whose main cause is an energy imbalance between calories consumed and calories expended (World Health Organisation 2013).

The Body Mass Index (BMI) is the most widely and easy obtainable index to classify overweight and obesity worldwide. It is defined as an individual's weight in kilograms divided by the square of their height in metres (kg/m^2). An adult with a BMI of 30 or more is generally considered obese and an individual with a BMI equal to or greater than 25 is considered overweight (World Health Organisation 2013). Pediatric overweight is defined as a BMI equal to or greater than 95^{th} percentile for age, sex, and ethnicity (Must, Dallal et al. 1991).

BMI like other anthropometric measurements may not correspond to the same degree of fatness in different populations due, in part, to different body fat distribution (Consultation 2004, Flegal, Shepherd et al. 2009). Waist circumference (WC) is widely used as a surrogate of central fat content, but is unable to distinguish between different fat compartments (intra abdominal adipose tissue and abdominal subcutaneous tissue). Moreover, total body/trunk fat, waist to hip ratio, and skin fold thickness measurements cannot predict differences in internal stores of adipose tissue (Thomas, Parkinson et al. 2012). Therefore, health risks associated with increasing BMI and/or other anthropometric measurements may differ for different

populations (He, Horlick et al. 2002, Yajnik, Fall et al. 2003).

Overweight and obesity are a major risk factor for non-communicable diseases such as cardiovascular diseases, diabetes, musculoskeletal disorders (i.e., osteoarthritis) and cancers (colon, endometrial and breast cancer), which were the leading cause of deaths in 2008 (World Health Organisation 2013). WHO estimates indicate that approximately 1.4 billion adults were classified as overweight and 500 million people classified as obese (World Health Organisation 2013). Statistical modeling has projected that there will be 65 million more obese adults in the USA and 11 million more obese adults in the UK by 2030 and thus, an increase in non-communicable diseases. The treatment of these chronic diseases are estimated to cost to the health service an exorbitant increment of £2 billion per year in the UK and average of $58 billion per year in the USA by 2030 (Wang, McPherson et al. 2011).

Epidemiological studies indicate that not only is adult obesity increasing alarmingly, but children are also critically affected. The international obesity task force has reported that 1 in 10 children (approximately 155 million) worldwide aged between 5 and 17 years were overweight in 2008. In 2011, the estimated number of overweight children under five was more than 40 million. Approximately 30 million of these children are living in developing countries, especially in urban settings, with the remaining 10 million in developed countries (World Health Organisation 2013).

Overweight and obese children are at a high risk of a continuous obesogenic phenotype through their lives and therefore will be more prone to subsequent metabolic alteration such as insulin resistance, diabetes and cardiovascular complications (Yu, Han et al. 2011, World Health Organisation 2013). Therefore, it is imperative to understand the mechanisms underlying the onset of obesity at an early age to be able to tackle the vicious cycle of obesity from a better approach such that the epidemic can be controlled.

1.3.1 Origins of obesity

Egger and Swinburg proposed the term “obesogenic environment” as the driving force for the increasing prevalence of obesity in our society (Egger and Swinburn 1997, Swinburn, Egger et al. 1999, Swinburn and Egger 2001). This obesogenic environment where inexpensive, easily available, and high calorie food, combined with societal pressure and a high physical inactivity and genetic susceptibility drive the increment of obesity and non communicable diseases such as diabetes, Cardio Vascular Diseases (CVD) and metabolic syndrome in our population (Egger and Swinburn 1997). They proposed three main causes affecting the balance of body fat: biological, behavioural and environmental. This equilibrium is mediated by energy intake and energy expenditure, but moderated by physiological adjustments during periods of energy imbalance (Figure 1.3.1.1).

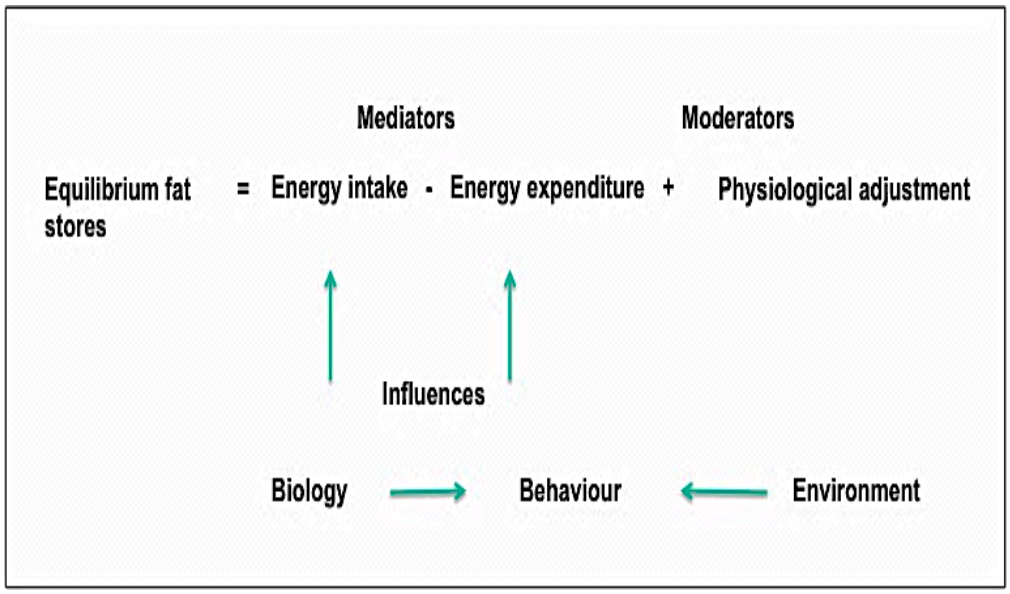

Figure 1.3.1.1 Ecological paradigm that include the factors that are related to obesity (Egger and Swinburn 1997).

It is now well known that there is a complex net of behavioural, societal, genetic and environmental factors that in combination or individually can contribute to the onset of obesity.

Important maternal and placental effects have been added to the list of factors that increase the risk of developing metabolic diseases in the progeny (Armitage, Khan et al. 2004, Poston 2010). Epidemiological studies and animal models have demonstrated that both maternal malnutrition (under/over nutrition) and body composition before and during pregnancy can adversely influence the progeny response to a later obesogenic environment or mismatched postnatal environment (Samuelsson, Matthews et al. 2008, Poston 2010). Moreover, the response to this new environment might be maladaptive when plasticity declines throughout life and therefore it generates detrimental conditions in the individual. Therefore, interventions in

older or middle-aged adults may not be as successful as interventions in early life.

1.4 Adipose Tissue

Adipose tissue is an endocrine organ capable of controlling the metabolism of several organs in humans and animals. It is formed mainly of adipocytes, but also contains blood vessels, connective tissue matrix (connective tissue and reticular fibres), nerve fibres, and the Stromal Vascular Fraction (SVF) of cells including preadipocytes (undifferentiated adipocytes), mesenchymal stem cells, endothelial progenitor cells, fibroblasts, and immune cells (Kershaw and Flier 2004, Vazquez-Vela, Torres et al. 2008) (Figure 1.4.1).

The composition of the stromal vascular fraction can differ between depots and physiological state. As an endocrine organ, adipose tissue also produces hormones such as leptin, estrogen and cytokines (adipokines) such as resistin, adiponectin, Monocyte Chemoattractant Protein-1 (MCP-1), Plasminogen Activator Inhibitor-1 (PAI-1), proteins of the renin-angiotensin system and Tumor Necrosis Factor alpha (TNF-alpha) (Vazquez-Vela, Torres et al. 2008). It has also been indentified as a major site of metabolism of sex steroids (Siiteri 1987).

Previously, adipose tissue was seen as an inactive tissue whose primary functions were storage of energy, structural support and protection of the internal organs (Zhang, Proenca et al. 1994). However, it is now known that it is a complex tissue that has an important secretory function of endocrine

and paracrine factors (adipokines). Within its endocrine functions are included regulation of metabolism, immune responses and neuroendocrine effects.

Adipose tissue also has the ability to receive efferent signals from the autonomic and central nervous system through the receptors they express. Therefore, adipose tissue composition and structure can impact its metabolic and endocrine function as well as the organs where it exerts its effects. An example of this is the adverse effect of an excessive accumulation adipose tissue causing obesity and relative metabolic disorders such as the metabolic syndrome. However, the development of the metabolic syndrome seems to be related to an abnormal distribution of fat with an increased internal deposition of fat (visceral adipose tissue) rather than a total subcutaneous fat or total body fat accretion (Ouchi, Parker et al. 2011).

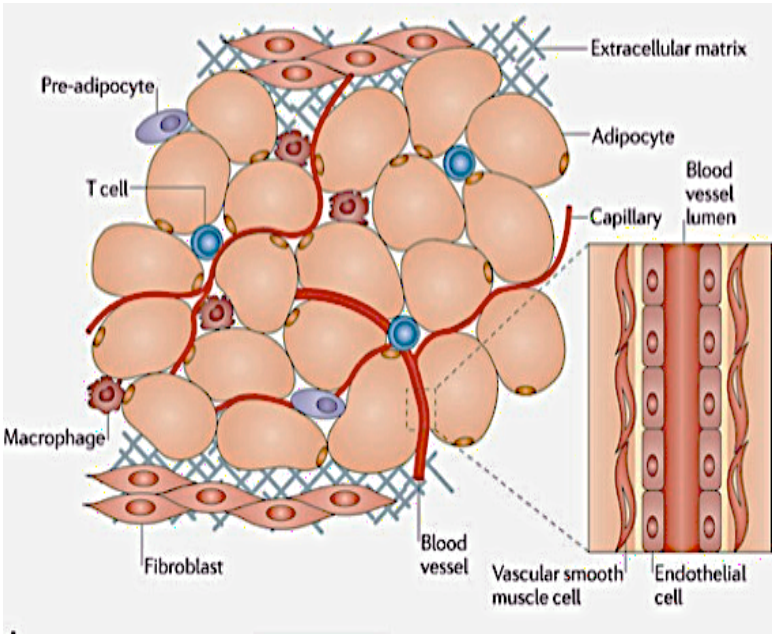

Figure 1.4.1 Illustration of adipose tissue structure, containing adipocytes, preadipocytes, T-cells, macrophages, fibroblasts, blood vessels, endothelial cells and Extracellular Matrix (ECM) (Ouchi, Parker et al. 2011).

1.4.1 Types of adipose tissue

There are two main types of adipose tissue: White Adipose Tissue (WAT) and Brown Adipose Tissue (BAT) containing mainly white adipocytes and brown adipocytes respectively. Recent studies have demonstrated the presence of a third type of adipocyte within the WAT. This adipocyte is known as “beige” or “brite” adipocyte (Wu, Bostrom et al. 2012, Lee, Swarbrick et al. 2013).

1.4.1.1 White Adipose Tissue (WAT)

Functions of WAT include energy storage in the form of triglycerides, insulation, cushioning of vital organs, and secretion of hormones (Torres-Leal, Fonseca-Alaniz et al. 2010).

White adipocyte cells are spherical, but they may appear polyhedral or oval when crowded within the adipose tissue. They store energy in unilocular lipid droplets in the form of triglycerides. This droplet flattens and displaces the nucleus to the periphery, occupying approximately 95% of the entire cell body. They also contain a small amount of mitochondria as well as fewer sympathetic nerve fibres and blood vessels than BAT (Cinti 2005, Gesta, Tseng et al. 2007).

White adipocytes are the main storage tissue of excess energy derived from food that is used when the energy demand exceeds intake. It is found throughout the body, but the distribution varies depending on genetics, gender, age, sensitivity to hormones and glucocorticoids. It has been reported that adipose tissue from different depots are distinct and that these differences may contribute to the type of obesity and metabolic status of an individual (Trujillo and Scherer 2006).

The distribution of WAT is typically classified as being subcutaneous WAT (beneath the skin throughout the body), and internal WAT that refers to the deeper inner body adipose tissue surrounding organs (Abate and Garg 1995).

Subcutaneous WAT in rodents can be divided into anterior subcutaneous WATs including the bilateral superficial subcutaneous adipose tissue between the skin and muscle fascia posterior to the lower segment of the upper limbs, and the inguinal subcutaneous WAT (attached dorsally along the pelvis to the thigh of the hindlimb). It can also be described as the flank or posterior subcutaneous WAT (divided into dorsolumbar, inguinal, and gluteal portion) (Frontini and Cinti 2010).

Internal WAT depots can be further categorised depending on the location. Intrathoratic adipose tissue that includes mediastinal, pericardial and retrosternal adipose tissue (very small compartments in rodents when compared to humans); intrabdominal or visceral WAT (inside the abdominal cavity) includes the gonadal WAT (surrounding the uterus and ovaries in females and the epididymis and testes in males), retroperitoneal WAT (located within the abdominal cavity along the dorsal wall of the abdomen, surrounding the kidneys and when massive extend into the pelvis), mesenteric WAT (lining the outer surface of the intestines), and omental WAT (surrounding the stomach; very small in rodents when compared to humans). In female mice, perirenal, periovarian, parametrial and perivesical fat form a single anatomical structure called the abdomino-pelvic depots (Frontini and Cinti 2010) (figure 1.4.1.1.1).

Adipose tissue is also found in the bone marrow fat (yellow bone marrow), mammary fat, around the lungs, in the adventitia of major blood vessels, and intramuscular adipose tissue (Ouchi, Parker et al. 2011, Sanchez-

Gurmaches and Guertin 2014) (figure 1.4.1.1.1).

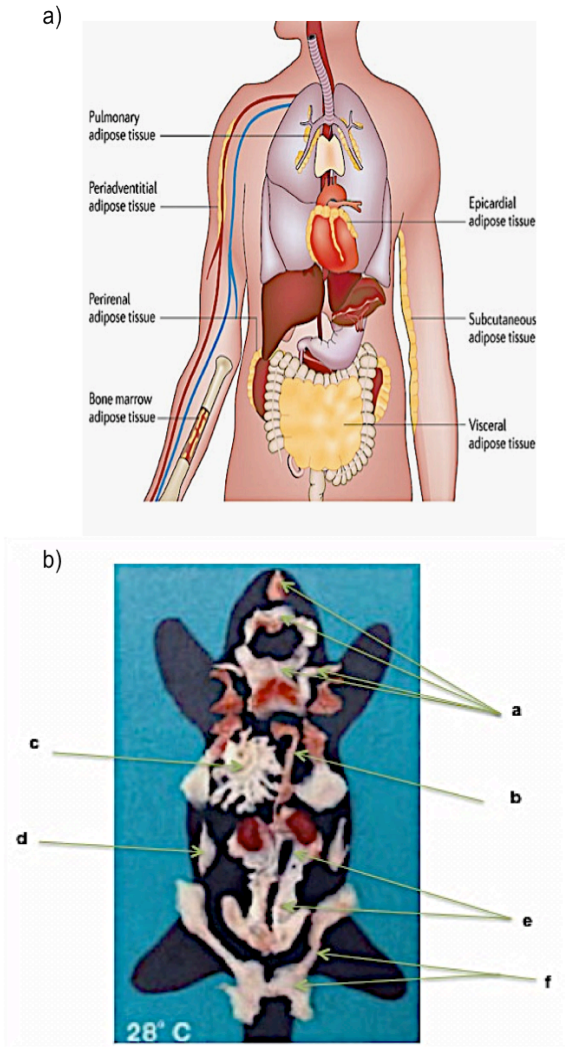

Figure 1.4.1.1.1 White adipose tissue distribution in humans and a female mouse. Distribution of WAT in humans a). Distribution of WAT in a female mouse acclimatised at 28˚C b): a) Anterior subcutaneous WAT (cervical, interscapular, subscapular, and axillothoracic), and f) posterior subcutaneous WAT (dorsolumbar, inguinal, and gluteal); b) mediastinal WAT, c) mesenteric; d) retroperitoneal; e) periovarian (gonadal) and perirenal WAT. Figure a) adapted from Ouchi et al, 2011(Ouchi, Parker et al. 2011) and figure b) adapted from the original (Frontini and Cinti 2010).

1.4.1.2 Brown Adipose Tissue (BAT)

Brown adipocytes store energy for thermogenesis as perilipin coated lipid droplets and glycogen granules. Brown adipocytes have a polygonal shape, central nucleus, and multilocular lipid droplets with more space in the cell for the high number of mitochondria needed for fatty acid oxidation (non-shivering thermogenesis) in the form of heat by uncoupling the respiratory chain of oxidative phosphorylation within mitochondria. BAT also has a rich supply of blood vessels and nerves (sympathetic nerve fibres mainly), and perivascular mesenchymal cells (niche of preadipocytes). This rich supply in addition to the high mitochondrial density give rise to the dark red-brown colour, compared to the pale white colour of the WAT (Klaus 1997, Lee, Swarbrick et al. 2013, Bartelt and Heeren 2014).

PPAR Gamma coactivator 1 alpha (PGC1alpha) is known as the master regulator of mithocondrial biogenesis and brown adipogenesis. PGC1a stimulates the synthesis of Uncoupling Protein 1 (UCP-1) by activating its promoter. It was first identified as a protein highly expressed in BAT and not in WAT. However, it has been shown that it also expressed in WAT and that cold exposure or beta-adrenergic agents can stimulate its expression. The expression of PGC1a and UCP-1 are closely associated to energy production (thermogenesis) (Enerback, Jacobsson et al. 1997, Puigserver, Wu et al. 1998, Lin, Wu et al. 2004, Leone, Lehman et al. 2005, Lee, Swarbrick et al. 2013).

Although WAT is found in both small mammals and humans, it was previously believed that BAT was only present in small rodents and infants but not in adults. Recently studies using Positron Emission Tomography (PET) have demonstrated the presence of fat with high metabolic activity in adults in the cervical, supraclavicular, axillary and paravertebral regions. Furthermore, brown adipocytes have been discovered in the visceral depots, mainly near the aorta. These fat depots were found to increase their activity following cold exposure or adrenergic stimulation. These findings have helped to confirm the active presence of BAT in adults. BAT generates heat via the mitochondrial Uncoupling Protein, protecting against hypothermia and excessive accumulation of white adipose fat (obesity) (figure 1.4.1.2.1) (Cypess, Lehman et al. 2009, Saito, Okamatsu-Ogura et al. 2009, Lee, Swarbrick et al. 2013).

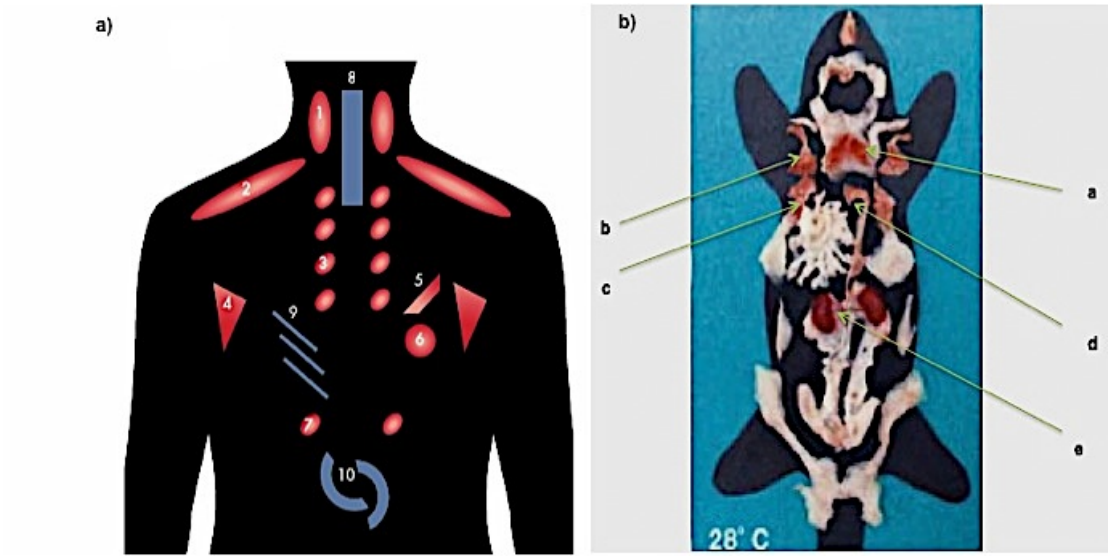

Figure 1.4.1.2.1 Brown adipose tissue distribution in humans a) and in a female mouse acclimatized at 28˚C b). In figure a): 1.Cervical BAT, 2.Supraclavicular BAT, 3.Paravertebral BAT, 4.Axillary BAT, 5.Mediastinal BAT, 6.Pericardial BAT, 7.Perirenal BAT, 8.Trachea-oesophageal BAT, 9.Intercostal BAT, 10.Mesenteric BAT. Red colour in figure a) reveals the distribution of BAT by PET scanning and histology and blue colour the BAT distribution by histology alone. In figure b): a) Interscapular BAT; b) Cervical BAT; c) Axillar BAT; d) Mediastinic BAT, and e) Perirenal BAT. Figures adapted from the originals (Frontini and Cinti 2010, Lee, Swarbrick et al. 2013).

1.4.1.3 Brown Like Adipocytes

Recent studies have demonstrated the existence of a different type of paucilocular (intermediate) brown adipocytes known as brown like-adipocytes or “beige”/“brite” adipocytes within the WAT (Petrovic, Walden et al. 2010, Seale, Conroe et al. 2011, Walden, Hansen et al. 2012, Wu, Bostrom et al. 2012). These beige cells have a dual function: when energy intake exceeds energy expenditure, the surplus energy can be stored in beige fat cells (basal condition) and these beige cells take on a more white morphology (figure 1.4.1.3.1). Moreover, certain stimuli including cold, sympathetic stimulation via catecholamines and beta-adrenergic receptors, hormones (irisin), and pharmaceutical stimulation such as Thiazolidinediones (TZDs) can activate beige fat cells resulting in increased energy dissipation in the form of heat activating the expression of genes /proteins such as PGC1a and its downstream target UCP-1 as in classical BAT.

Although both BAT and beige adipocytes are thermogenic, they seem to be regulated differently (Kozak 2000, Coulter, Bearden et al. 2003). Moreover, beige fat cell express different genes compared to white adipocytes. It has also been observed that the subcutaneous adipose tissue depots have a higher susceptibility toward expression of UCP-1 and other brown fat cell genes as compared to the visceral white adipose tissue (Cousin, Cinti et al. 1992, Cinti 2012).

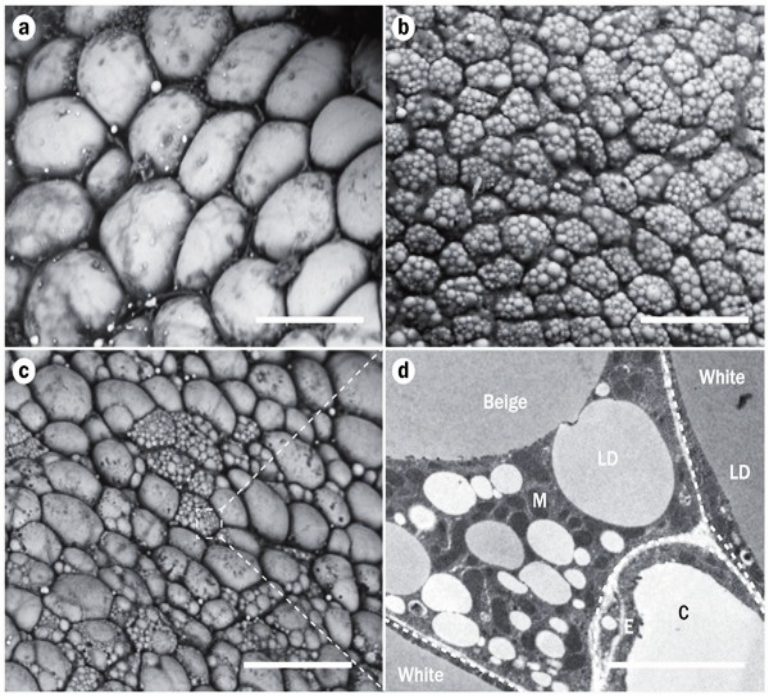

Figure 1.4.1.3.1 Morphology of mouse adipose tissue by electron microscopy. White adipocytes in inguinal WAT containing a single lipid droplet a). Brown adipocytes in interscapular brown adipose tissue containing multilocular lipid droplets b). Browning of WAT (induced by pharmacological activation of β3-adrenergic receptors) leads to formation of islets of multilocular beige adipocytes within inguinal WAT c). Beige adipocytes within WAT showing their high mitochondrial content d). Scale bars: a–c, 50 μm; d, 5 μm. Abbreviations: C, capillary; E, endothelial cell; LD, lipid droplet; M, mitochondria; WAT, white adipose tissue (Bartelt and Heeren 2014).

1.4.2 Transcriptional control of adipogenesis and lipid metabolism

BAT and WAT originate from Mesenchymal Stem Cells (MSCs), which can differentiate into adipocytes, osteoblasts, chondrocytes and myoblasts. These stem cells reside in the vascular stroma of adipose tissue as well as in the bone marrow (Covas, Panepucci et al. 2008).

1.4.2.1 Adipogenesis

Adipogenesis, or the formation of adipocytes, involves two stages of commitment and differentiation. With an appropriate stimulation, MSCs undergo a process of commitment in which they are recruited to an adipocyte lineage (preadipocytes). In the second phase, which is the terminal differentiation, the adipocyte takes on the characteristics of the mature adipocyte.

This process is controlled by the interaction of different transcription factors such as CCAAT Enhancer Binding protein alpha, beta and delta (CEBP-alpha, beta, delta); Peroxisome Proliferator Activated Receptor $Gamma_{1-2}$ ($PPARG_{1-2}$). Augmented expression of CEBP alpha and PPARGs are critical elements for the retention of the adipocyte phenotype (Rosen, Hsu et al. 2002, Wang, Shi et al. 2006, Huang and Tindall 2007). The action of PPARGs is mediated through two protein isoforms: $PPARG_1$ and $PPARG_2$. The expression of the latter is limited to adipose tissue whereas the former is constitutively expressed (Spiegelman, Puigserver et al. 2000).

Recruitment of new small adipocytes seems to decrease insulin resistance by increasing the capacity of lipid storage. This is due in part to PPARGs, which increase Glucose Transport 4 (GLUT4), uncoupling proteins and adiponectin (Vazquez-Vela, Torres et al. 2008).

1.4.2.2 Lipid metabolism: lipogenesis and lipolysis in adipocytes

Steroid Regulatory Element Binding Protein 1c (SREBP1c) has been identified as a proadipogenic factor that stimulates PPARGs expression and also as a mediator of glucose metabolism and lipogenesis via insulin regulation. Some of its downstream lipogenic gene targets are Fatty Acid Synthase (FAS), and Acetyl-Coenzyme A Carboxylase (ACC) (Gosmain, Dif et al. 2005). However other studies have suggested that SREBP1c is not associated with lipogenesis in adipocytes as it is in liver (Sekiya, Yahagi et al. 2007). mRNA expression has also been found to be upregulated in models of lipodystrophy (Shimomura, Hammer et al. 1998), but others studies have seen a downregulation in adipose tissue of diabetic obese humans suggesting in general than an alteration on its regulation may impaired insulin sensitivity of adipose tissue (Sewter, Berger et al. 2002) (figure 1.4.2.2.1).

Lipoprotein lipase (LPL) and fatty acid synthase (FAS) are two enzymes involved in adipose tissue lipid (triglyceride) accumulation. Whilst FAS is implicated in the *de novo lipogenesis (Vazquez-Vela, Torres et al. 2008),* LPL regulates the hydrolysis of circulating triglycerides. The local tissues reuptake the resulting fatty acids and monoacylglycerols helping in the

accumulation of lipids in adipose tissues, cardiac, skeletal muscle, islets and macrophages (Wang and Eckel 2009) (figure 1.4.2.2.1).

Triglycerides stored in lipid droplets are first hydrolysed by the enzyme Adipose Triglyceride Lipase (ATGL) to diacylglycerols. Subsequently, diacylglycerols are hydrolysed by the Hormone Sensitive Lipase (HSL) and finally by Monoglyceride Lipase (MGL), producing free fatty acids and glycerol. Perilipin A is a protein that surrounds the lipid droplet inhibiting hydrolysis. Beta-adrenergic stimulation and the Protein Kinase A-dependent phosphorylation of HSL and perilipin activate the translocation of HSL from the cytoplasm to the lipid droplet inducing intracellular lipolysis.

Insulin has antilipolytic effects and in fed states decreases the mobilization of lipids from adipose tissue inhibiting lipolytic enzymes such as HSL (Fredrikson, Tornqvist et al. 1986, Egan, Greenberg et al. 1992, Brasaemle, Rubin et al. 2000, Holm 2003, Villena, Roy et al. 2004, Vazquez-Vela, Torres et al. 2008) (figure 1.4.2.2.1).

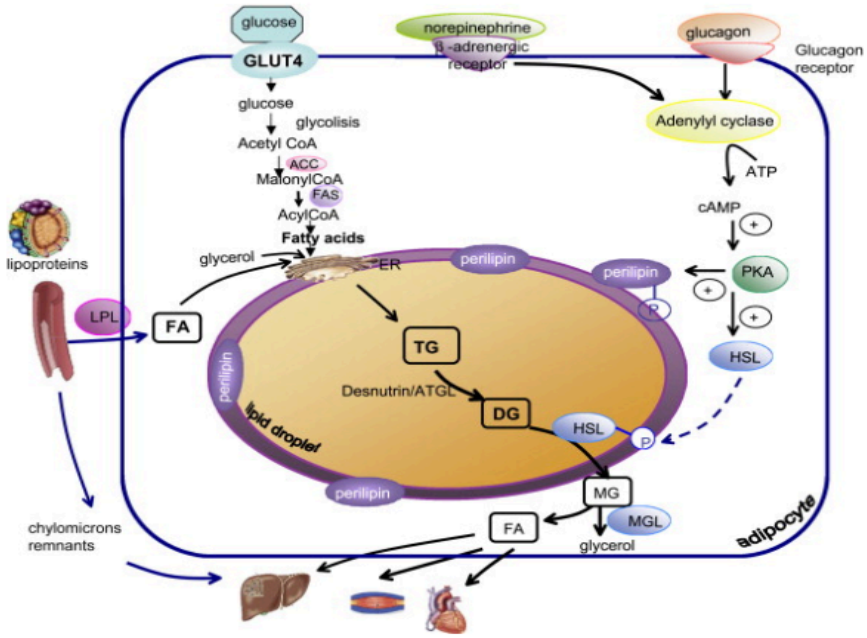

Figure 1.4.2.2.1 Lipid metabolism in adipocyte cells. Glucose excess is oxidized via glycolysis to acetyl-CoA in the adipocyte and then converted into acyl-CoA, which are then esterified in the Endoplasmic Reticulum (ER) to Triglycerides (TG). Subsequently they are then translocated into the lipid droplet. Fatty Acids (FA) obtained from lipoproteins are also esterified into TG and stored. Under fasting conditions, lipolysis is activated by G-protein-coupled receptors resulting in an increase in Cycling Adenosine Monophosphate (cAMP) that phosphorylates the protein perilipin located in the membrane of the lipid droplet. cAMP also phosphorylates the hormone-sensitive lipase (HSL) triggering its translocation from the cytoplasm to the lipid droplet and induces the hydrolysis of diglycerides produced by the ATGL to form monoglycerides (MGs). MGs are then released to non-adipose tissues, mainly for energy purposes. (Adapted from Vasquez -Vela et al) (Vazquez-Vela, Torres et al. 2008).

1.4.3 Adipose tissue and adipokines

Adipose tissue has the ability to produce and secrete hormones and cytokines and therefore is considered an endocrine organ. The adipose derived factors are known as adipokines and these participate in the regulation of energy balance. The expression of these factors is generally high in adipose tissue but their expression is not limited to adipocytes. As such, their action is not specifically related to adipocyte function. Some of these adipokines are described below.

1.4.3.1 Adiponectin

Adiponectin has both autocrine and paracrine effects. Its concentration in serum has been positively related to benefitial effects on insulin sensitivity, inflammation, lipid profiles and cardioprotection and angiogenesis. A strong correlation between adiponectin and LPL activity has been linked to improved lipid clearance and insulin sensitivity. Adiponectin receptors have been found in skeletal, cardiac and smooth muscle, adipose tissue, endothelial cells and liver and thus it is implicated in their functioning (von Eynatten, Schneider et al. 2004, Berg and Scherer 2005, Trujillo and Scherer 2005).

1.4.3.2 Leptin

Leptin in both human and rodents is produced mainly by adipocytes and smaller amounts can be synthetised in placenta, gastric parietal cells, ovary and liver (Campfield, Smith et al. 1995, Cripps, Martin-Gronert et al. 2005). It is thought to regulate energy homeostasis by reducing food intake, weight gain and increasing energy expenditure in adults. It is produced by adipose tissue in proportion to the body fat content rather than body mass.

Leptin also plays a role in signaling food deprivation with an extensive reduction on fasting, which is disproportionate to changes in fat mass (Trayhurn, Thomas et al. 1995). It has also been demonstrated that leptin regulates adipose tissue growth through its action on the central nervous system in the hypothalamic nuclei. Other studies have shown that leptin receptors are also present in others organs such as liver, skeletal muscle, heart, kidneys and pancreas, among others (Hoggard, Mercer et al. 1997, Lollmann, Gruninger et al. 1997). The leptin receptor is expressed in adipocytes suggesting an autocrine and paracrine role of the leptin hormone. It appears that leptin stimulates lipolysis of intracellular triglycerides and reduces the gene expression of SREBP1c and ACC; therefore inhibits lipogenesis and stimulate fatty acid oxidation reducing the possibility of ectopic fat deposition and thus lipotoxicity (Fruhbeck, Aguado et al. 1997, Unger and Orci 2002).

Others functions of leptin are stimulation of hematopoiesis, angiogenesis and accelerated wound healing. It also influences immune response and

sympathetic nervous system, and regulates bone mass (Kershaw and Flier 2004). Hyperleptinemia during obesity is associated with leptin resistance. This leptin resistance or reduction of sensitivity to leptin action could be due to malfunction at different levels such as altered leptin transport across the Blood Brain Barrier (BBB) or impairment in the leptin-signaling cascade (Kershaw and Flier 2004).

Experimental studies in neonatal rodents have demonstrated that leptin does not exert its biological effects on body weight regulation and feed intake during the neonatal period (Mistry, Swick et al. 1997, Proulx, Richard et al. 2002). Plasma leptin concentrations are high in neonates. Leptin actions seem to be developmentally regulated to optimise growth and survival of neonates enhancing their ability to increase thermoregulatory metabolic rates in order to maintain body temperature without suppressing food intake (Mistry, Swick et al. 1997). Furthermore, Bouret et al have found that leptin also modulates development of the neural circuitries in the hypothalamus (Bouret and Simerly 2004).

1.4.3.3 Resistin

The hormone resistin is expressed mainly in white adipocytes in rodents but in humans tends to be expressed in stromal vascular cells in adipose tissue. It is also found in BAT and the mammary gland (Steppan, Bailey et al. 2001). Its role and mechanism of action are not completely understood. It has been suggested that resistin antagonises insulin effects in glucose metabolism. In the liver for example, it has been shown that administration of resistin results

in severe hepatic but not peripheral insulin resistance and increased expression of gluconeogenic enzymes in liver. Transgenic overexpression of resistin results in increased fasting glucose and glucose intolerance suggesting an insulin resistant state (Rajala, Obici et al. 2003, Banerjee, Rangwala et al. 2004, Rangwala, Rich et al. 2004). It has also been shown that resistin alters lipid metabolism increasing the secretion of triglycerides from the liver. (Sato, Kobayashi et al. 2005).

1.4.3.4 Proinflammatory adipocytokines

Proinflammatory factors are predominantly produced by the cells within the stromal vascular fraction of the adipose tissue. Dyslipidemia, insulin resistance and obesity have been linked to chronic low-grade inflammation. Cytokines involved in the inflammatory response are not only produced by immune cells but also by adipose tissue. This suggests that obesity is an inflammatory state or that these cytokines are involved in the maintenance of fuel homeostasis (Yu and Ginsberg 2005). Inflammation is characterised by abnormal cytokine production and other regulators of inflammatory signaling.

1.4.3.4.1 Tumor Necrosis Factor alpha (TNF-a)

TNF-a expression seems to be increased in the adipose tissue of obese mammals and has been associated with whole body insulin resistance. TNF-a induces lipolysis in adipose tissue leading to elevation of fatty acid levels. Additionally, it reduces the expression of genes involved in adipogenesis and lipogenesis in adipocytes (Ruan, Hacohen et al. 2002). Conversely in liver TNF-a increases the expression of genes involved in *de*

novo lipogenesis and decreases the expression of those involved in fatty acid oxidation (Grunfeld and Feingold 1992). Although TNF-a levels are low in circulation and there is no clear correlation with obesity and insulin resistance, its tissue expression levels seem to be linked positively with both conditions (Yu and Ginsberg 2005). This means that TNF-a association with insulin resistance may be more related to local conditions rather than its general increased in periphery.

1.4.3.4.2 Interleukin 6 (IL-6)

IL-6 unlike TNF-a is secreted by the adipose tissue and enters the circulation where its concentration is relatively high. Plasma levels have been found to correlate positively with fat mass, insulin resistance and free fatty acids levels. *In vitro* studies have indicated that IL-6 increases leptin and lipolysis whereas suppressing LPL activity contributes to the metabolic changes related to obesity. However, it seems to have an opposite role in the central nervous system. Centrally, IL-6 is negatively related to fat mass in obesity. Its administration in rodents increases energy expenditure suggesting a protective role against obesity (Wallenius, Wallenius et al. 2002, Stenlof, Wernstedt et al. 2003, Kershaw and Flier 2004, Trujillo, Sullivan et al. 2004).

1.4.3.4.3 Monocyte Chemotactic Protein 1 (MCP-1/CCL_2)

MCP-1 is one of the key chemokines (attracts and activate immune cells) that regulate migration and infiltration of monocytes/macrophages into inflammation by inducing leukocyte-endothelial adhesion and promoting transendothelial migration. Recently, other functions have been attributed to

MCP-1 including angiogenesis. It is produced by a vast number of cells such as epithelial and endothelial cells, fibroblasts, keratinocytes, smooth muscle cells, mesothelial, mesangial cells, chondrocytes, osteoblasts, liver, astrocytes, microglia, mononuclear cells, eosinophils, mast cells and adipocytes (Van Coillie, Van Damme et al. 1999). Some reports have positively associated circulating MCP-1 levels with insulin resistance, hyperglycemia, type 2 diabetes and obesity (Panee 2012). Mice with MCP-1 receptors deletion gain as much weight as wild-type mice on a high-fat diet, but do not have adipose tissue inflammation and maintain their insulin sensitivity (Ouchi, Parker et al. 2011).

1.5 Insulin

Insulin is an anabolic hormone composed of two polypeptide chains (A-B) containing 51 amino acids secreted from the pancreatic beta cells in response to increased blood glucose following ingestion of a meal. Insulin exerts its actions through binding to specific receptors in cells, primarily on adipocytes, liver and muscle cells. The primary action of insulin is to regulate glucose concentration in blood by stimulating glucose uptake into muscle and adipose tissue and by suppressing glucose production in the liver promoting glycogenesis and concomitantly reducing glucagon secretion from pancreatic alpha cells to reduce production of glucose via glycogenolysis and gluconeogenesis. Other functions of insulin include stimulation of protein synthesis in the liver and muscle, free fatty acid uptake and synthesis in adipose tissue, inhibition of lipolysis and proliferation of cell growth such as adipose tissue growth and adipocyte differentiation via different adipokines

and transcription factors such as PPARG (Gerich, Schneider et al. 1974, Saltiel and Kahn 2001).

The secretion of insulin after a meal occurs into two phases. The first phase releases preformed insulin, rapidly followed by a second phase of insulin synthesis and slow sustained release. Long-term release of insulin occurs when high levels of glucose are maintained in blood (Gerich, Schneider et al. 1974). Other factors are known to stimulate the release of insulin apart from the potent glucose. These include increased concentration of some amino acids in circulation such as arginine, leucine and lysine; the incretins Glucagon Like Peptide 1 (GLP-1), and Glucose-dependent Insulinotropic Peptide (GIP) derived from the intestinal L and K cells respectively, Cholecystokinin (CCK), parasympathetic release of acetylcholine and via beta-2 adrenergic receptors. Insulin release is inhibited by noradrenaline, release of catecholamines (alpha-2 adrenergic receptors), and by the sympathetic nervous system (Nakaki, Nakadate et al. 1980, Holst 1994, Drucker 2001, Cawston and Miller 2010).

In energy balance regulation, insulin acts as both a short-term and long term signal. It is released in response to changes in energy levels such as meal ingestion, but it seems that its circulating levels are positively related to fat mass. In the hypothalamus region of the brain it acts on receptors in the Arcuate Nucleus (ARC) and Ventromedial Hypothalamus (VMH) and increases energy expenditure. Exogenous administration of insulin in the hypothalamus leads to a reduction in food intake. However in type 2

diabetes, patients placed on exogenous insulin treatment tend to gain weight as the anorexigenic effect is overcome by the antilipolytic effect of insulin (Henry, Gumbiner et al. 1993, Benoit, Clegg et al. 2004, Cripps, Martin-Gronert et al. 2005).

1.5.1 Insulin signaling

Insulin signaling is mediated by a series of molecular pathways. In the presence of insulin, the Insulin Receptor (IR) localised in caveola invaginations in the plasma membrane binds to insulin through its alpha subunits inducing trans-autophosporylation of the beta subunits, which become active (Gustavsson, Parpal et al. 1999, Karlsson, Thorn et al. 2004).

Following the phosphorylation of IR at tyrosine residues intracellular signaling proteins are recruited and can be phosphorylated by docking on the phosphorylated IR. Among these are members of the Insulin Receptor Substrate (IRS). Consequently after interaction with the IR tyrosines residues the IRS are phosphorylated. This creates docking sites for other intracellular proteins with SH2 domains. The insulin signal is transduced via a cascade of phosphorylations and dephosphorylations that constitute the insulin signaling inside the adipocyte. Downstream signaling occurs through two main kinase domains: the mitogenic and metabolic pathways. These pathways are a complex network of feedbacks and cross talks with other pathways in the cell (White 1998).

The IR-mediated tyrosine phosphorylation of IRS-1 activates a metabolic signaling pathway by binding to the regulatory subunit p85 of the Phosphatidylinositol 3 Kinase (PIK3). Then the catalytic subunit p110 is activated and this phosphorylates Phosphatidylinositol (4,5) bisphosphate (PIP2) conforming phosphatidylinositol (3,4,5) triphosphate (PIP3). Protein kinase B (PKB/Akt) is then recruited to the plasma membrane and Akt is phosphorylated at threonine 308 and serine 403 for maximal activation. Another target of PIK3 in adipocytes is the atypical Protein Kinase C-Zeta and Lambda (PKC-Z/ λ). Both PKB/Akt and PKC appear to be important for insulin stimulation of insulin-dependent Glucose Transporter 4 (GLUT4) translocation to the plasma membrane to induce and enhanced glucose uptake (Tanti, Grillo et al. 1997, Farese 2001, Saltiel and Kahn 2001, Hietakangas and Cohen 2009) (figure 1.5.1.1).

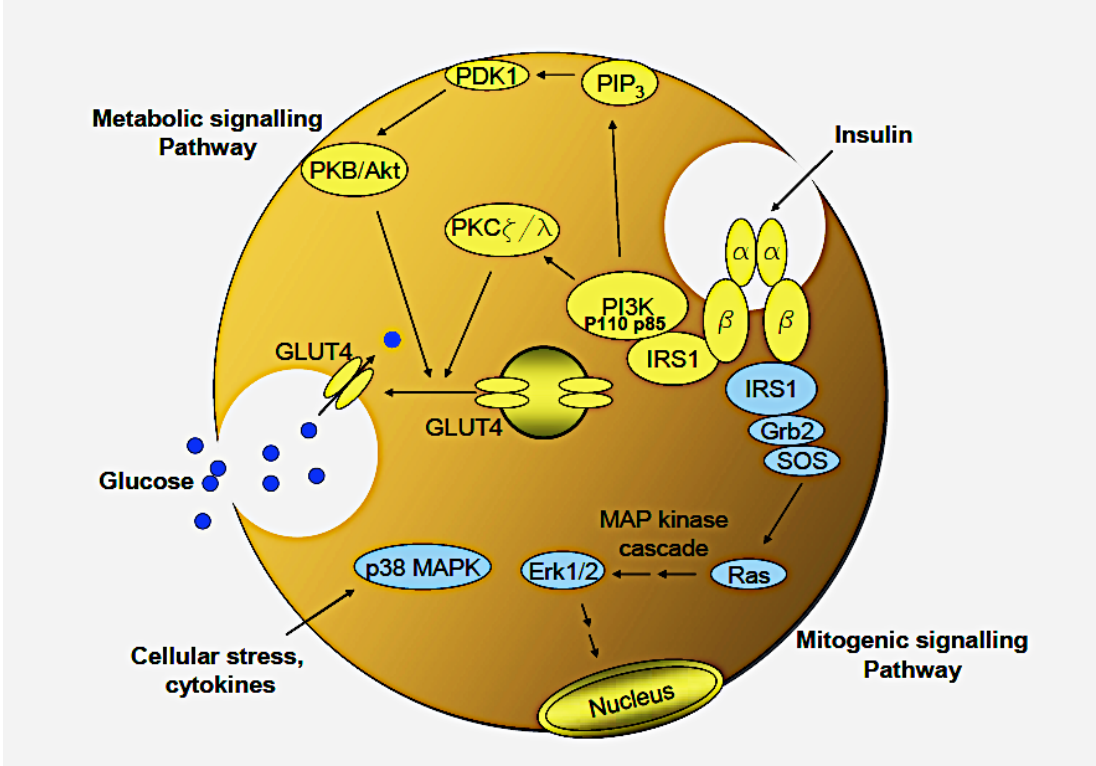

Figure 1.5.1.1 Insulin signaling pathways in an adipocyte. Both the metabolic and mitogenic pathways are illustrated (Adapted from Danielsson, 2007) (Danielsson 2007).

1.5.2 Insulin resistance

Insulin resistance is defined as the loss of the normal effect that insulin would have at its normal circulating concentration. In the presence of insulin resistance, insulin would not exert its function as in normal subjects. Defects in insulin function impair the suppression of glucose production in the liver and this will continue to produce glucose and release it into circulation. The most common cause of insulin resistance is the impaired signaling that can occur beyond the receptor (protein and gene expression). The lack of signal to reduce glucose in circulation will incur in the hyperresponsiveness of the pancreas to produce more insulin causing an increase in insulin concentration in periphery (hyperinsulemia), which initially will compensate for the effects of insulin resistance. Eventually, the system will fail in maintaining glucose levels at a normal level and hyperglycemia will develop, later progressing to type 2 diabetes (Dinneen, Gerich et al. 1992, Weyer, Bogardus et al. 1999, Kahn, Hull et al. 2006).

1.5.2.1 Insulin resistance and adipose tissue distribution

A vast number of studies have demonstrated that there is a link between adipose tissue mass and metabolic alterations such as insulin resistance and type 2 diabetes(Abate and Garg 1995, Ozanne, Lewis et al. 2004, Giorgino, Laviola et al. 2005). However, it is not only the total amount of fat mass that accounts for this relationship but in particular the sites where the fat is deposited in the body. Furthermore, it has been postulated that excess accumulation of visceral fat is associated with these metabolic changes

independently of overall body fat mass (Abate and Garg 1995, Giorgino, Laviola et al. 2005). One of the reasons postulated is that visceral fat secretes its hormones and lipids into the portal system, which has direct access to the liver. This increases the delivery of lipids to the liver, overloading its capacity in comparison to that it receives from to systemic subcutaneous fat (Unger, Clark et al. 2010). This overload will then increase the risk of lipotoxicity. Other possible reasons are metabolic and endocrine differences between different fat depots (Van Harmelen, Reynisdottir et al. 1998). Visceral fat for example seemed to recruit more proinflammatory macrophages than subcutaneous adipose tissue and activation of PPARG is lower in the former. This seems to be in accordance with the high lipolytic activity of visceral fat. As insulin inhibits lipolysis, the reduction of this effect can also be linked to the lower insulin sensitivity of these adipocytes (Sauma, Franck et al. 2007).

Adipose tissue expansion involves both increments in cell number (hyperplasia) and by increasing the size of existing mature adipocytes (hypertrophy) through the deposition of lipid. Overfeeding has been associated with a hypertrophic growth of adipocytes. These enlarged adipocytes become resistant to the antilipolytic effect of insulin, which leads to a greater release of free fatty acids into circulation (Iozzo 2009). These in turn are stored in ectopic sites such as muscle and liver increasing the risk of insulin resistance and further development of type 2 diabetes. In humans, visceral adipocytes have been found to be more enlarged than subcutaneous adipocytes (Boden 1997, Lundgren, Buren et al. 2004).

1.6 Hypothalamus and Appetite Regulation

The integration of different signals in the central nervous system is pivotal for the regulation of energy homeostasis in response to food intake and energy expenditure. Peripheral signals related to acute and long-term energy status (i.e, incretins, leptin and insulin) are integrated in the brain by neural networks primarily in the hypothalamus and brainstem generating an appropriate response balancing the expression of satiety (anorexigenic) and hunger (orexigenic) neurotransmitters (Elmquist, Coppari et al. 2005, Chaudhri, Parkinson et al. 2006).

The hypothalamus regulates food intake and energy balance, and other responses such as immune response and reproduction (Butte, Wong et al. 2004, Welt, Chan et al. 2004). It is subdivided in different nuclei carefully interconnected.

The Arcuate Nucleus (ARC) is located in the mediobasal hypothalamus adjacent to the third ventricle and it is directly above the median eminence, which is one of the circumventricular organs characterised by a partially permeable blood brain barrier (Ciofi 2011). This positioning of the ARC allows it to be an ideal integrator of peripheral signals such as circulating nutrients and hormonal signals of energy status including leptin, insulin, glucose, sex hormones and glucocorticoids (Tong, Zhao et al. 1990, Glaum, Hara et al. 1996, Sato, Kobayashi et al. 2005). The ARC nucleus has a number of inputs from other areas in the brain including other hypothalamic

nuclei, the hindbrain, limbic areas (amygdala) and cortical areas (somatosensory cortex) (DeFalco, Tomishima et al. 2001).

ARC neurons are known as first order neurons because of their partial contact with the circulation. It contains two main populations of neurons involved in the control of energy balance. The first population of neurons coexpresses Neuropeptide Y (NPY) and Agouti Related Peptide (AgRP). The second population expresses Proopiomelanocortin (POMC), which is cleaved to produce Cocaine and Amphetamine Regulated Transcript (CART) and alpha Melanocyte Stimulating Hormone (alpha-MSH). The first population of neurons increase food intake and decrease energy expenditure (orexigenic). They are inhibited by leptin and activated by ghrelin, a gut hormone that signals meal initiation (Cone, Cowley et al. 2001, Cowley, Smith et al. 2003, van den Top, Lee et al. 2004). The second population of hormones are activated by leptin (anorexigenic) (Cheung, Clifton et al. 1997). Both populations of hormones project to a second order of neurons in other hypothalamic nuclei including the Ventromedial Hypothalamus (VMH) and the Paraventricular Hypothalamus (PVN).

Along with the hypothalamus, centres in the brain stem also play an important role in appetite regulation interacting with hypothalamic centres such as PVN and lateral hypothalamus as well as receiving inputs from the vagus nerve, which links the gastrointestinal tract and brain (Ritter 2004). In addition to food intake and energy expenditure, other factors such as pleasure and preference of certain tastes and textures (hedonic responses)

involving brain reward centres intervene in the energy homeostasis (Saper, Chou et al. 2002) (figure 1.6.1).

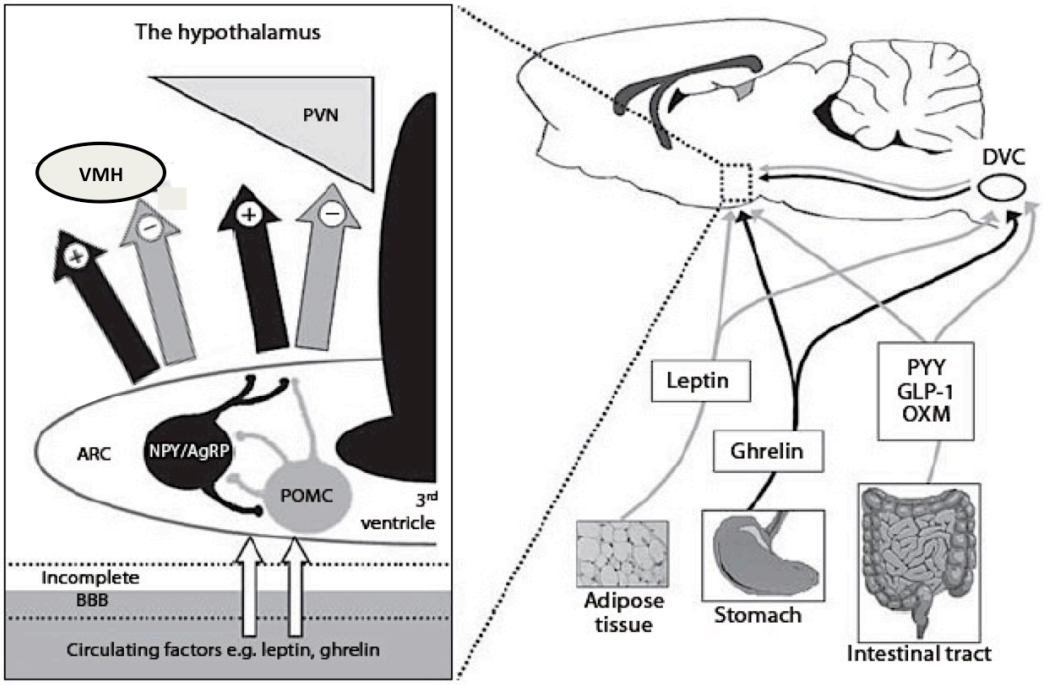

Figure 1.6.1 The appetite regulation circuits in hypothalamus and brain stem. Peripheral signals enter in the hypothalamus and brainstem through a partial permeable blood brain barrier. These signals alter the activity of anorexigenic and orexigenic neurotransmitters regulating appetite and energy homeostasis. Adapted from Parkinson et al 2009 (Parkinson, Chaudhri et al. 2009).

1.7 Hypothesis and Aims of Thesis

1.7.1 Hypothesis

Birth weight and accelerated weight gain modulate body fat patterning and hypothalamic function. Exposure to a high fat diet postnatally amplifies the impact of birth weight and that response is sex-age dependent.

1.7.2 Aims

- To elucidate the effects of birth weight and post weaning diet on fat content and its distribution as well as appetite regulation.
- To assess the association between weight gain and fat content and its distribution with appetite.
- To provide evidence of early metabolic alterations linked to deterioration of health later in life.
- To explore the potential underlying mechanism associated with early life programming of appetite and body composition.

1.7.2.1 Primary outcomes

- Measurements *in vivo* of body fat content and distribution using MRS and MRI techniques at weaning (3 weeks of age) and 15 weeks of age. In addition, MRS will be used to quantify hepatic lipid content.
- Manganase-Enhanced MRI (MEMRI) will be used to determine *in vivo* neural activity in the hypothalamic centres ARC, PVN, VMH and Pe, which are associated with appetite control.
- Biochemical analysis of plasma metabolites associated with metabolic

alterations such as insulin, leptin, resistin, GIP, ghrelin and some proinflammatory cytokines.

- Assessment of gene expression in adipose tissue. This will add information to underpin the early adaptations of the organisms that can program an adverse metabolic profile later in life.

2. Material and Methods

2.1. Study 1. Effects of Birth Weight and Accelerated Growth on Body Composition and Appetite Regulation at Lactation (From Birth Until 3 Weeks of Life)

2.1.1 Animals

All protocols were conducted in accordance with the UK Animals (Scientific Procedures) Act, 1986. C57BL/6J female mice (6-8 weeks old; Harlan U.K) and male mice (8-10 weeks old; Harlan U.K) were used as parental animals and were maintained on a standard rodent chow (RM3, Special Diet Services Ltd, UK) prior to the experiment. All mice were acclimatised during 7 days from arrival at the animal husbandry unit and housed in individually ventilated cages under controlled conditions (12h:12h dark-light cycle and 21-23°C) with *ad libitum* access to food and water.

2.1.2 Diet composition

The diet used for this study was a standard purified 20% protein diet (TD 91352, 20% kcal protein intake, Harlan Teklad). The macronutrient composition of this diet is shown in table 2.1.2.1.

Macronutrients	Protein diet
Protein (% by weight) **(% kcal)**	20.3 **21.5**
Carbohydrate (% by weight) **(% kcal)**	65.3 **71.4**
Fat (% by weight) **(% kcal)**	5.5 **13.1**
Kcal/g	3.8

Table 2.1.2.1 Nutritional composition of the diet used in study 1. The diet used in this study was a standard 20 % protein diet. Values in grey correspond to the percentage of each macronutrient in terms of weight. Values in bold correspond to the percentage kilocalories from each component of the diets. Last row correspond to the number of kilocalories per gram of food.

2.1.3 Study design

The diagram of the study design is shown in figure 2.1.4.1. After 7 days of acclimatisation, mice were mated, and copulation was confirmed by the presence of a vaginal plug. At conception (day0), pregnant female mice were separated from the male mice and housed individually, and were fed a normal 20% protein purified diet as mentioned above.

Litters were adjusted to 5-7 pups/litter/dam to obtain similar conditions as possible during lactation. Pups were kept within the same litter until weaning.

Mice were classified into two groups according to their birth weights but were kept within the same litter during the lactation period until the time of weaning at 3 weeks of life. These two groups were: 1) Low birth weight mice (**LBW**) and 2) High birth weight mice (**HBW**). **LBW** mice were defined as mice with a birth weight below the 10th percentile within the colony (≤1.18g) and **HBW** as mice with a birth weight higher than the 90th percentile within the colony (≥1.38g). Cut off values were calculated from a preliminary study taken into account birth weights from a colony of approximately 10-15 litters for both males (**m**) and females (**f**).

2.1.4 Methods

Birth weight was recorded 24 hours after delivery. Body weight was monitored weekly throughout lactation until week 3 of age (time of weaning). Whole body MRS and MRI, and localised liver MRS was performed at the end of lactation (3 weeks of life). Pups were dissected at the end of the study and biochemical analysis was performed on plasma samples. Tissues were harvested and adipose signaling was assessed (see figure 2.1.4.1). Details of these methods are described in section 2.4.

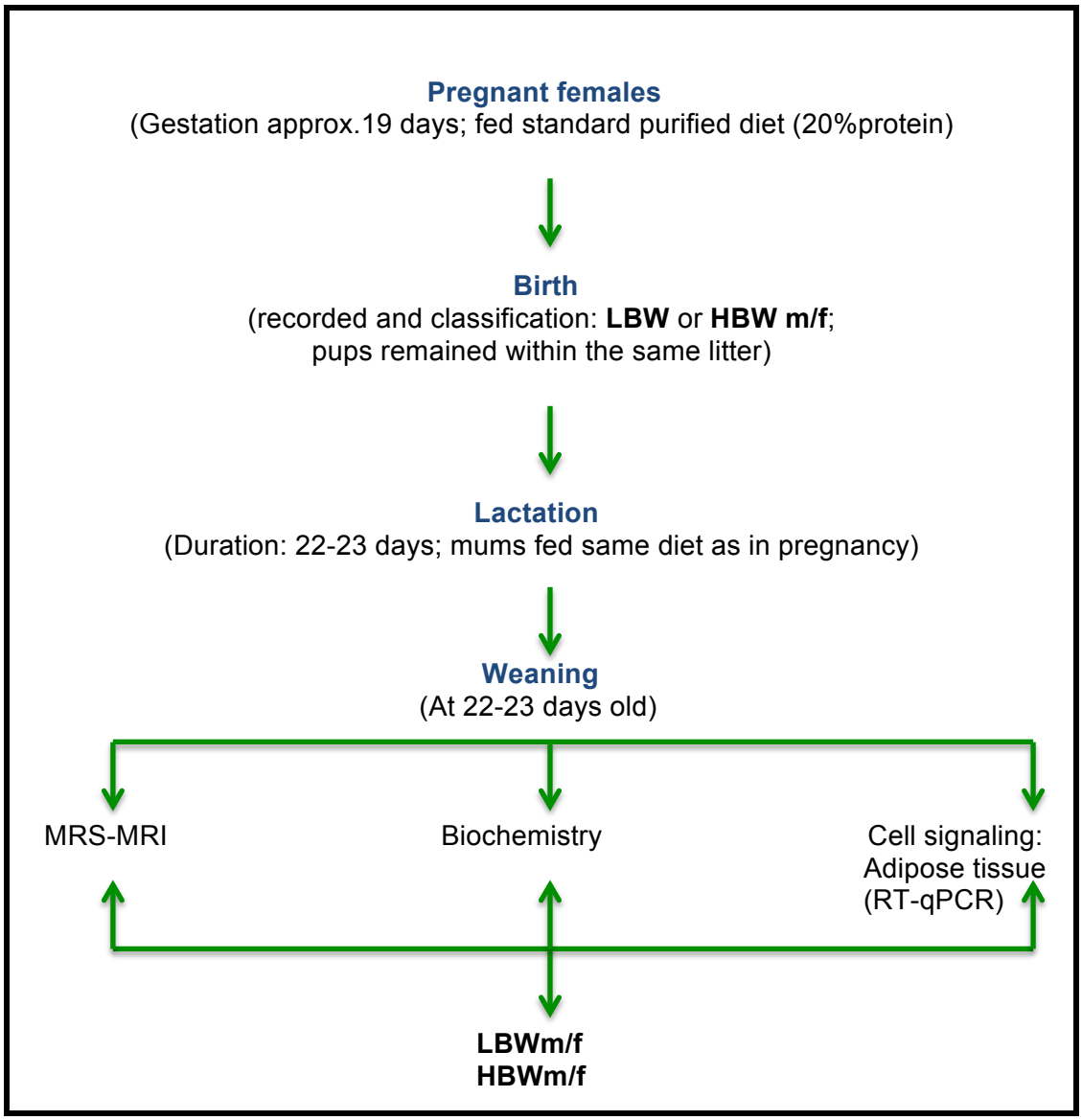

Figure 2.1.4.1 Protocol designed for study 1. Pregnant females were caged individually and kept on a standard purified diet from pregnancy until weaning (3 weeks old). Pups were classified into two groups according to their birth weights in either Low birth weight male/ female mice (**LBWm/f**) or High birth weight male/female mice (**HBWm/f**). Whole body MRS and MRI, and localised liver MRS was performed in pups at weaning (22-23 days of life). Tissue samples were collected at weaning (n=8-10). Adipose tissue signaling was assessed using RT-qPCR (n=6-8).

2.2 Study 2. Effects of Birth Weight and Diet on Body Composition and Appetite Regulation in Young Mice (From Week 3 of Life Until Week 15)

2.2.1 Animals

All protocols were conducted in accordance with the UK Animals (Scientific Procedures) Act, 1986. C57BL/6J offspring mice were housed in individually ventilated cages under controlled conditions (12h:12h dark-light cycle and 21-23°C) with *ad libitum* access to food and water.

2.2.2 Diet composition

The two diets used in this study were a purified normal fat control diet (TD 05072, 9% kcal fat intake) and purified moderated high fat diet (TD 05073, 27% kcal fat intake). Anhydrous milk fat was used as the source of saturated fat in both diets. The macronutrient composition of the diets is shown in table 2.2.2.1.

Macronutrients	Control diet	Moderate high fat
Protein (% by weight) **(% kcal)**	17.7 **19.6**	17.7 **17.3**
Carbohydrate (% by weight) **(% kcal)**	64.5 **71.4**	56.6 **55.4**
Fat (% by weight) **(% kcal)**	3.6 **9.0**	12.4 **27.3**
Kcal/g	3.6	4.1

Table 2.2.2.1 Nutritional composition of the two diet used in study 2. The two diet used in this study were a purified control fat diet (9%kcal fat intake) and a moderated high fat diet (27% kcal fat intake). Values in grey correspond to the percentage of each macronutrient in terms of weight. Values in bold correspond to the percentage kilocalories from each component of the diets. Last row correspond to the number of kilocalories per gram of food.

2.2.3 Study design

The diagram of the study design is shown in figure 2.2.3.1. Offspring were obtained and maintained until weaning as aforementioned in study 1 (section 2.1). At weaning (week 3 of life), mice were separated from their litters and divided by birth weight into two categories taking into account the parameters mentioned in study 1 (section 2.1.3). These two groups were: Low birth weight mice (**LBW**) and High birth weight mice (**HBW**). Offspring was further subdivided by diet using the diets described in section 2.2.2 and by gender: male (**m**) or female (**f**) mice. In total, four groups were formed per gender as

follow: 1). Low birth weight mice fed a Normal Fat diet (**LBW-NF**), 2). High birth weight mice fed a Normal Fat diet (**HBW-NF**), 3). Low birth weight mice fed a High Fat diet (**LBW-HF**) and 4). High birth weight mice fed a High Fat diet (**HBW-HF**).

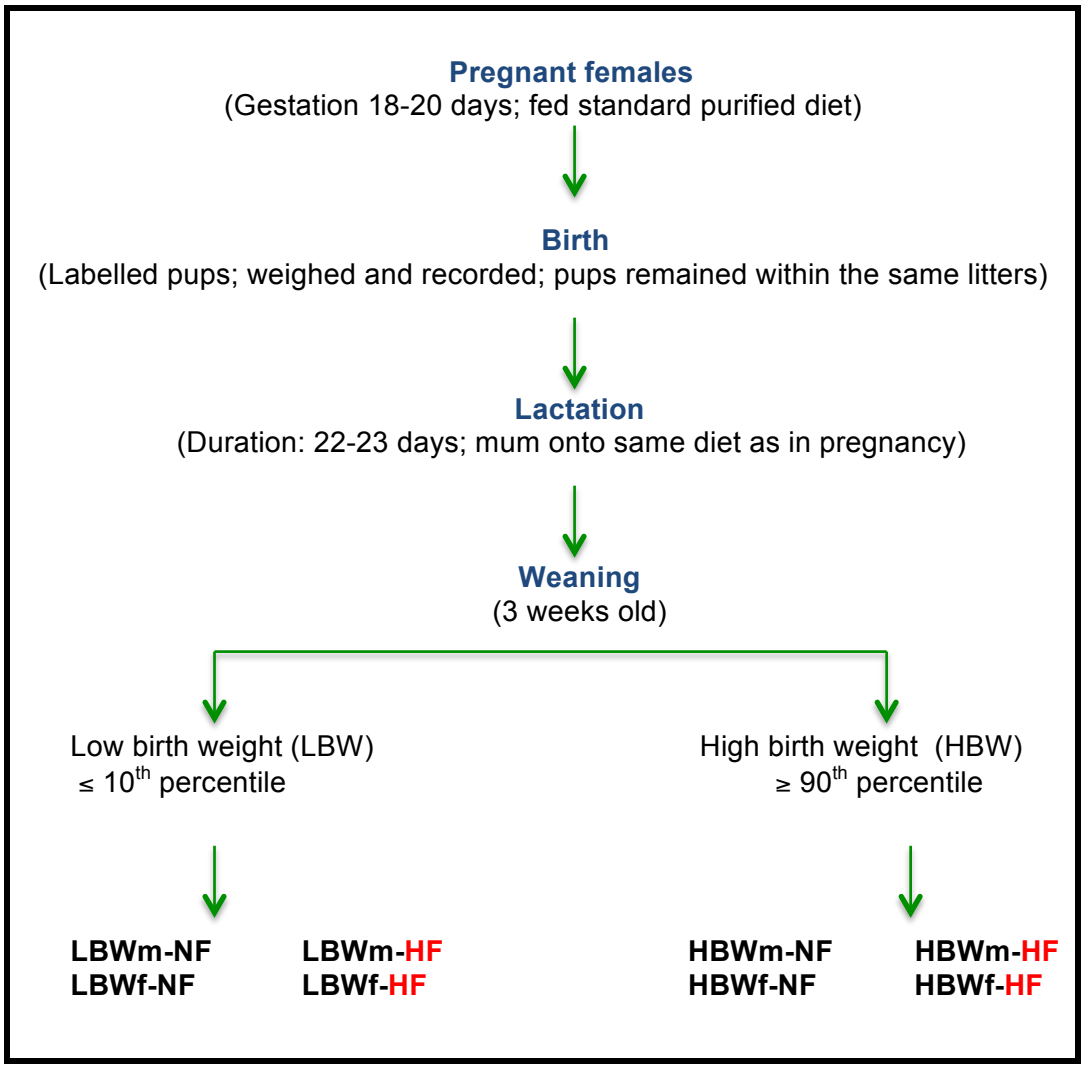

Figure 2.2.3.1 Diagram of the protocol designed for study 2. Offspring was obtained as mentioned in study 1 (section 2.1). At weaning, offspring was divided into eight groups depending on their birth weight and the diet given, and by gender: Low birth weight males fed a normal fat diet (**LBWm-NF**); Low birth weight males fed a high fat diet (**LBWm-HF**); High birth weight males fed a normal fat diet (**HBWm-NF**); High birth weight males fed a high fat diet (**HBWm-HF**); Low birth weight females fed a normal fat diet (**LBWf-NF**); Low birth weight females fed a high fat diet (**LBWf-HF**); High birth weight females fed a normal fat diet (**HBWf-NF**) and High birth weight females fed a high fat diet (**HBWf-HF**).

2.2.4 Methods

The diagram of this study is shown in figure 2.2.4.1. Body weight and kilocaloric intake were monitored weekly. Whole body MRS and MRI, and localised liver MRS were performed at age 14 weeks, and MEMRI was performed at age 15 weeks.

An Intraperitoneal Glucose Tolerance Test (IPGTT) was performed at week 14 of age to assess glucose tolerance. Tissues were harvested at 15 weeks old. Samples of gonadal and subcutaneous adipose tissue were taken for adipocyte extraction and analysis of adipocyte number and distribution. Different subsets of mice were used for each procedure when possible to minimise stress related metabolic changes in mice. Details of these methods are described in section 2.4.

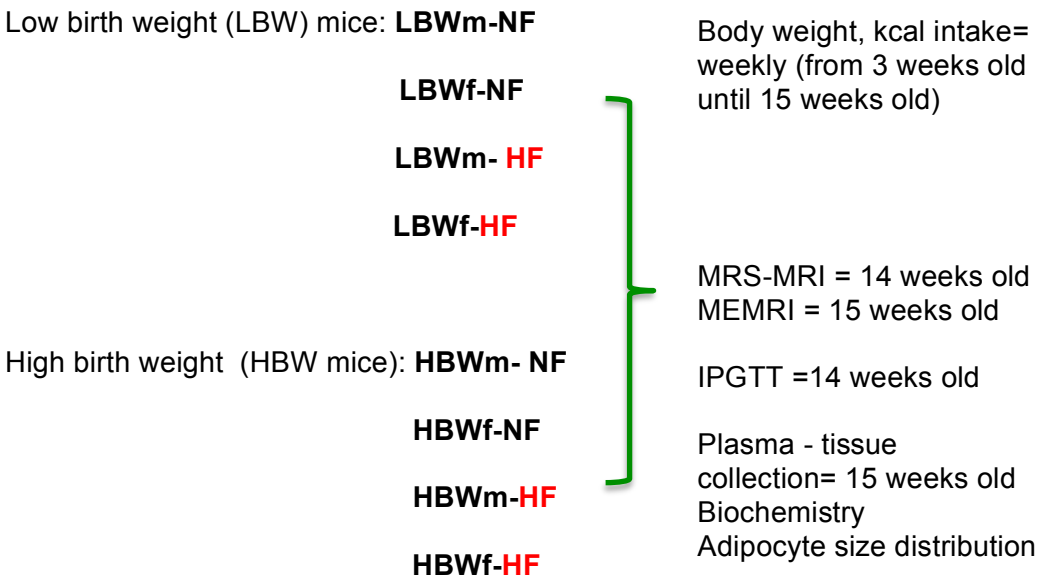

Figure 2.2.4.1 Diagram of the methods for study 2. Mice were weaned and groups were formed as mentioned above in study 2 (study design 2.2.3) Body weight and kilocaloric intake were recorded weekly. Whole body MRS and MRI, and localised liver MRS was performed in mice at 14 weeks old, to assess body composition and liver fat content. MEMRI was performed in mice at week 15 to assess neural activity in the hypothalamus. IPGTT was performed at week 14 in a different subset of animals. Tissue samples were collected at the end of the study (15 weeks old). Adipocyte size distribution was assessed in both gonadal and subcutaneous adipose tissue in males only.

2.3 Study 3. Effects of Birth Weight and Diet on Body Composition in Matured Mice (from 16 weeks old to 51 weeks old)

2.3.1 Animals

All protocols were conducted in accordance with the UK Animals (Scientific Procedures) Act, 1986. C57BL/6J offspring mice were housed in individually ventilated cages under controlled conditions (12h:12h dark-light cycle and 21-23°C) with *ad libitum* access to food and water.

2.3.2 Diet composition

The two diets used in this study were a purified normal fat control diet (TD 05072, 9% kcal fat intake) and purified moderated high fat diet (TD 05073, 27% kcal fat intake). Anhydrous milk fat was used as the source of saturated fat in both diets as in study 2. The macronutrient composition of the diets is shown in table 2 (section 2.2.2).

2.3.3 Study design

The study design for this study was followed as described in the study 2 (section 2.2.3). Mice were kept until the age of 51 weeks and maintained on the same diets as described in the study 2 throughout post weaning life.

2.3.4 Methods

The diagram of this study is shown in figure 2.3.4.1 Body weight and kilocaloric intake were monitored weekly. Adipose tissue index was calculated from the weight of gonadal, mesenteric, retroperitoneal and subcutaneous adipose tissues of mice at the end of the study (51 weeks old). Tissues were harvested and weighed at the end of the study and metabolic markers were assessed in plasma samples. Samples of gonadal and subcutaneous adipose tissue were taken for adipose cell extraction and analysis of adipose cell number and distribution. Details of these methods are described in section 2.4.

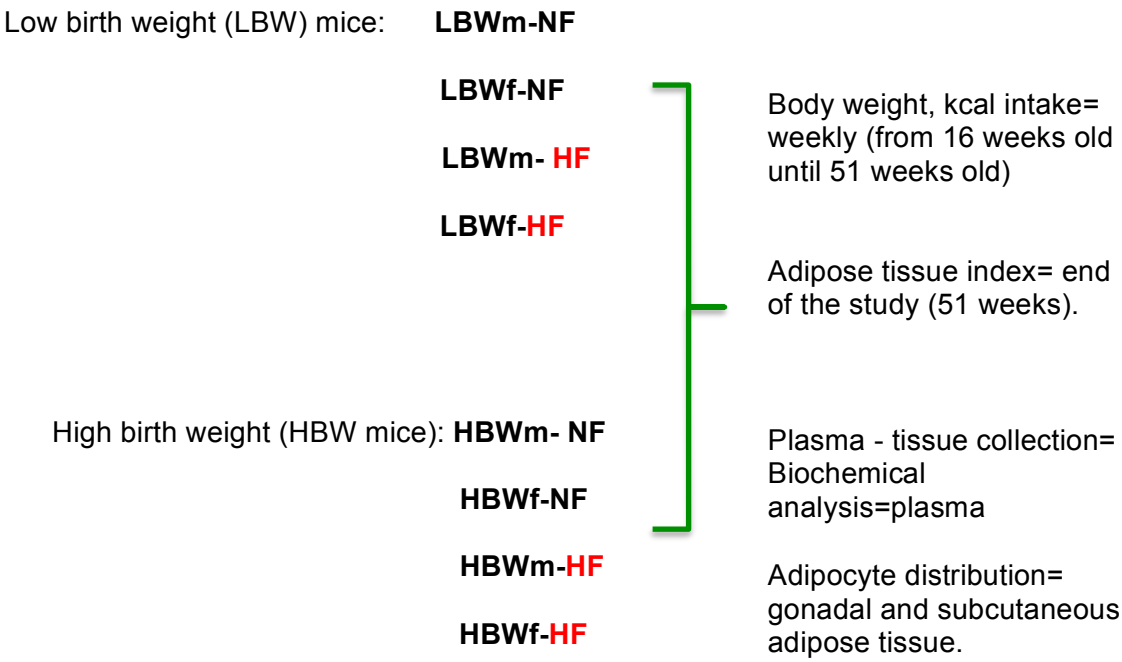

Figure 2.3.4.1 Diagram of the methods for study 3. Mice were weaned and groups were formed as described in study 2 (study design 2.2.3) Body weight and kilocaloric intake were recorded weekly. Adipose tissue index was calculated from the pad weight of gonadal, mesenteric, retroperitoneal and subcutaneous adipose tissues. Tissue samples were collected at the end of the study (51 weeks old).

2.4 Methods Used to Study the Effects of Birth Weight and Accelerated Weight on Body Composition and Appetite Regulation

2.4.1 Whole body ^{1}H MRS and MRI as a tool to study body composition and liver fat content; brief overview

In this project, body adiposity was assessed using whole body Magnetic Resonance Imaging (MRI) and Proton Magnetic Resonance Spectroscopy (^{1}H MRS) and hepatic fat content was quantified using localised ^{1}H MRS.

Magnetic Resonance Imaging (MRI) is a powerful non-invasive imaging technique used for functional, anatomical and molecular studies in humans and animal models. It has also the advantages of a high spatial resolution and better contrast resolution between soft tissues (such as brain, muscle, adipose tissue, etc.) compared to other invasive techniques such as Computerised Axial Tomography (CAT) or Dual Energy X-ray Absorptiometry (DEXA) (Makowski, Wiethoff et al. 2009). Moreover, it is ideal for longitudinal studies, as unlike CAT or DEXA it does not use radiation.

MRI is a technique that allows an accurate and reproducible measurement of compartmental adipose tissue stores that could not be predicted from indirect measurements such as Body Mass Index (BMI) and waist to hip ratio.

While MRI gives information about structural conditions of tissues (distribution, localisation and volume), MRS provides biochemical analysis of those tissues and fluids (chemical composition) (Ross, Leger et al. 1991).

Proton Magnetic Resonance Spectroscopy (^{1}H MRS) has been used to detect and quantify whole body fat and ectopic fat in organs such as liver, muscle, heart and pancreas (Thomas, Parkinson et al. 2012). Whole body ^{1}H MRS takes advantage of the differential behaviour of protons associated with lipids versus water when placed in a magnetic field and thus, yielding discrete peaks of proton resonance frequency that correspond to body lipid and body water (Ross, Leger et al. 1991, Mystkowski, Shankland et al. 2000). When ectopic fat is quantified, MRI is used to localise the organ of interest and it is combined with MRS to obtain total lipid content versus water content.

2.4.1.1 Preparation of animals for whole body MRS and MRI

Mice were fasted overnight for 16-18 hours. Before scanning, anesthesia was induced with a 4-3% oxygen-isofluorane mix via a facemask. This mix was maintained at 2% oxygen-2% isofluorane according to respiration and body temperature during the scan. Respiration and temperature were monitored using a standard monitoring equipment (SA Instruments, Inc). The temperature was kept at 37°C and the respiration rate maintained at 60-80 breaths per minute (bpm) approximately. Mice were positioned dorsally in a whole body birdcage coil and scanned in a 4.7T Unity Inova MR scanner (Agilent Technologies) as shown in figure 2.4.1.1.2.

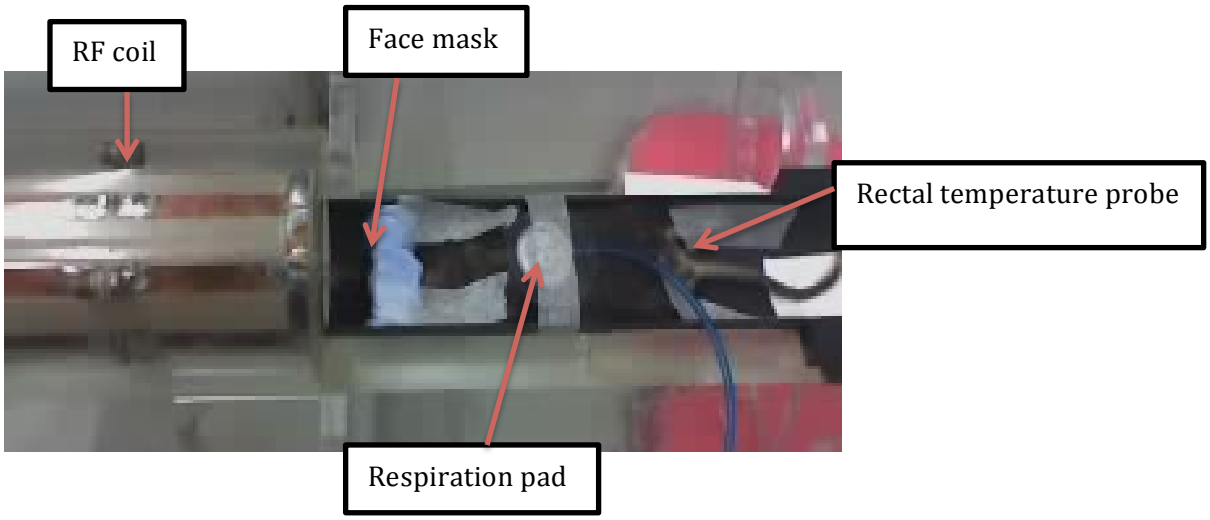

Figure 2.4.1.1.2 Positioning a mouse on a bed before placing it inside the radiofrequency coil (RF coil). The mouse was prepared for scanning in a dorsal position. A rectal temperature probe was placed to control the temperature at 37°C and a breathing pad was placed on the chest centrally to monitor the respiration.

2.4.1.3 Parameters used for whole body MRI

Following a preliminary image to determine the correct positioning of the mouse in the bore of the scanner (scout image figure 2.4.1.3.1.a), consecutive transverse MR images were collected using a T1-weighted Spin Echo Multislice (SEMS) sequence with the following parameters:

Orientation: transverse

Repetition time (TR): 2.2s

Echo time (TE): 20ms

Field of view (FOV): 45mm x 45mm,

Matrix size: 256 x 192

Averages: 2

Slice thickness: 2mm

Slices: interleaved

Number of slices: 45-50

The images collected were converted into stack images and saved into the appropriate format using ImageJ (Rasband). Image segmentation analysis was performed using a SliceOmatic^{TM} software (Tomovision®, Montreal, Canada) to provide volumes and mass of total, internal and subcutaneous adipose tissue depots. A trained analyst blinded to the study performed the analysis. The images obtained are T_1-weighted images and thus, adipose tissue appears brighter compared to other tissues. Pixels of this contrast were manually assigned as adipose tissue and tagged in a particular color for better quantification (figure 2.4.1.3.1b and c).

To calculate the volume of adipose tissue, the following equation was used:

Volume of adipose tissue (mm^3)= (FOV / matrix size) ^{2} x number of pixels x slice thickness (mm)

Imaging parameters described above for FOV, matrix size and slice thickness were used along for the calculation of volumes with the number of pixels highlighted for a specific adipose tissue depot.

The calculated volumes were then converted into adipose tissue mass in grams by using the density of adipose tissue (0.92 g/mm^3). The equation used for this conversion was:

Adipose tissue mass (g)= adipose tissue volume (mm^3) x 0.92 g/ mm^3

This adipose tissue mass was then expressed as percentage adipose tissue in respect to individual body weights:

% Adiposity= 100x adipose tissue (g) /body weight (g)

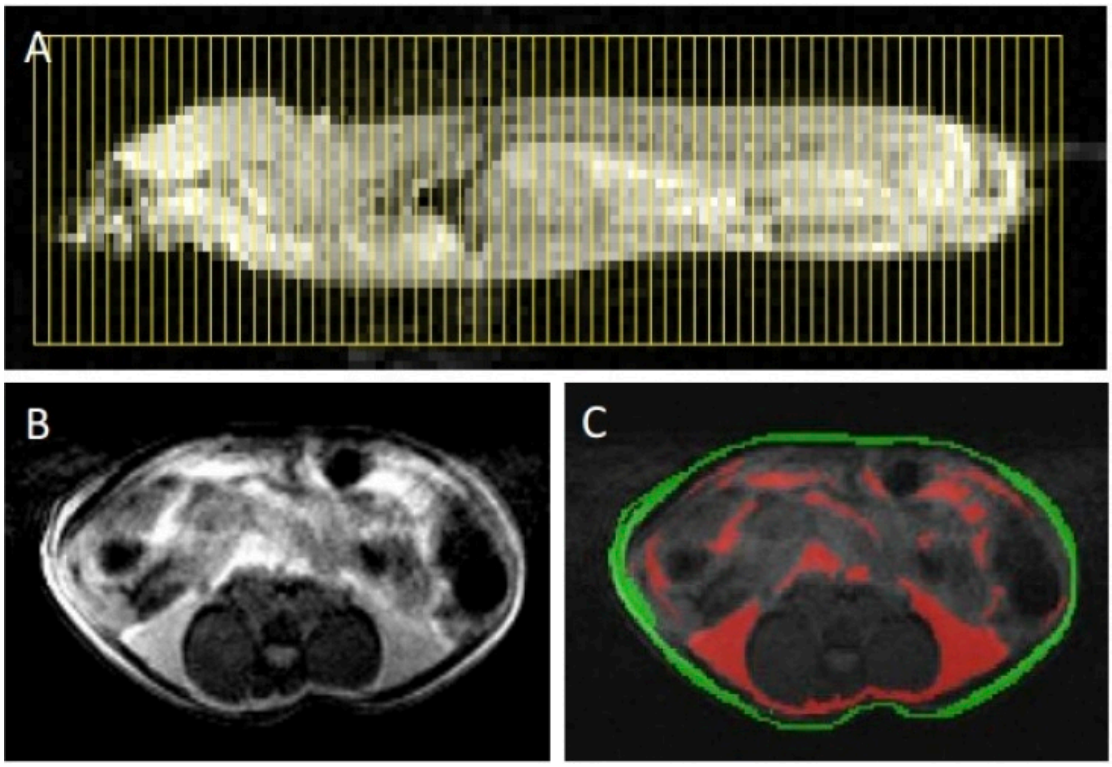

Figure 2.4.1.3.1 Images across the body using MRI. A) A sagittal scout image through the whole mouse body (head to tail, left to right) including 50 slices (in yellow) placed where they will be acquired. B) A representative image of a transverse slice acquired in the abdominal region and C) the same slice after fat segmentation (subcutaneous adipose tissue in green and internal adipose tissue in red). (Picture kindly provided by Dr. Jelena Anastasovska).

2.4.1.4 Parameters used for whole body ^{1}H MRS

Whole body ^{1}H MRS was performed using a single pulse sequence (SPULS) with the following parameters:

Repetition time (TR): 10 s

Pulse angle: 45°

Averages: 4

Spectral width (SW): 20.000 Hz

The spectra obtained (peaks) were analysed using MNOVA version 8.0 (Santiago de Compostela, Spain). After automated Fourier transformation, an exponential line broadening (apodisation) of 1.5 Hz was applied. After this, spectra were phasing and baseline corrected. Areas under the curve for individual spectra were obtained using line integrals. The water peak obtained was referenced at 4.7 ppm and the lipid peak referenced at 1.2-1.3 ppm. The lipid integral represents the lipid content as a percentage of the water integral (figure 2.4.1.4.1).

To calculate whole body adiposity, the individual lipid and water integrals from above were employed. Lean mass was predicted using the equation lean mass= 0.38*(integral water) as described by Mystkowski (Mystkowski, Shankland et al. 2000). The percentage of total body adiposity was therefore calculated using the following equation:

Total adiposity (%)= Lipid integral / (lipid integral + water integral + 0.38 x (water integral). Value of the water integral was assumed to be 1 for correspondent percentage assignation of lipid peaks.

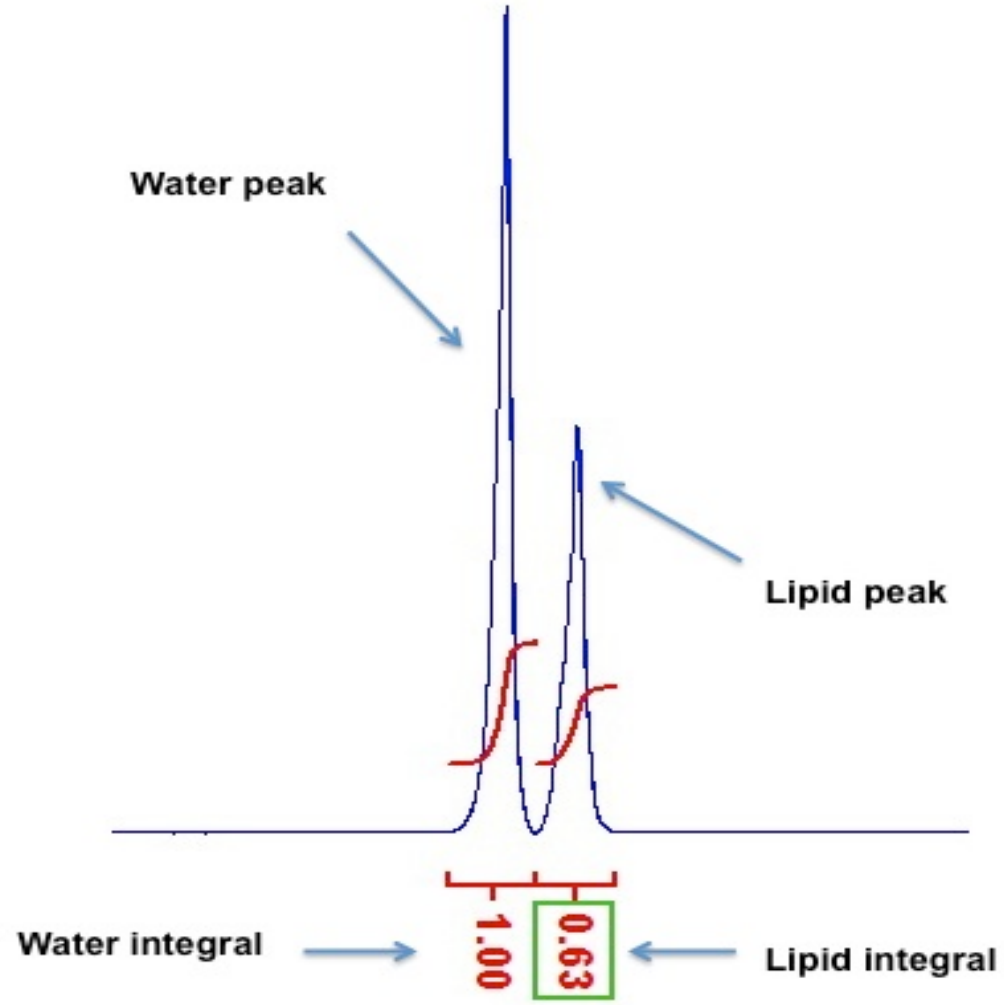

Figure 2.4.1.4.1 A representative whole body spectrum of a mouse obtained using MNOVA software. Integrals of water and lipid peaks are highlighted above. Lipid content in this spectrum is 63% relative to the water content of the mouse. The percentage of whole body adiposity was 31.34% obtained by substituting the fat integral (0.63) and water integral (1) into the equation mentioned above. Water integral was always 1 for all individuals.

2.4.1.5 Parameters used for localised ^{1}H hepatic MRS

To be able to visualise the liver for fat quantification, MRI was performed as described in section 2.4.1.3. When liver images were obtained, a Point Resolved Spectroscopy (PRESS) sequence was used, placing a single voxel on the top left of the liver (figure 2.4.1.5.1). The following parameters were applied:

Voxel size: 2x2x2 mm^3

TR: 10 s

TE: 9 ms

Averages: 64

Spectral width: 20.000 Hz

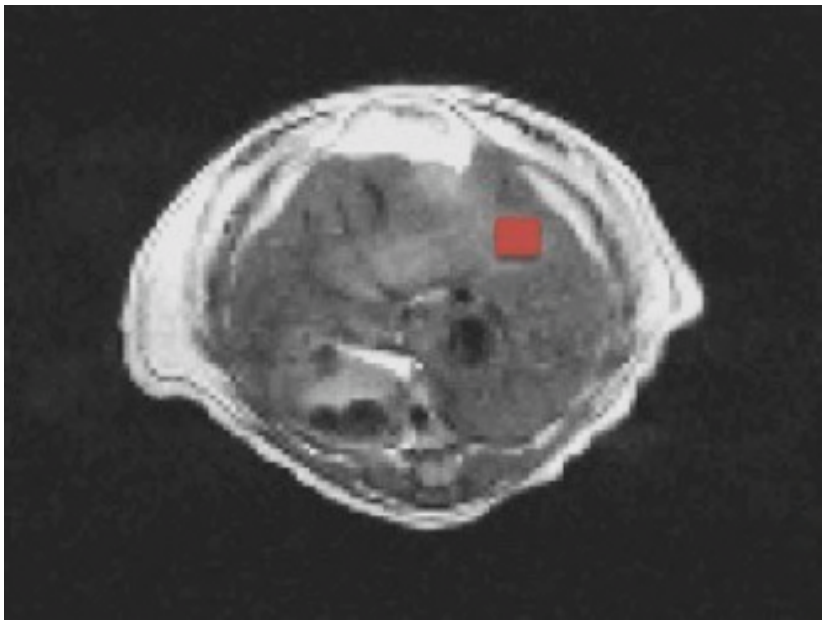

Figure 2.4.1.5.1 A transverse MR image slice through the liver, with a 2x2x2mm^3 voxel placed on the top left of the liver (in respect to the location of the mouse). Attention was paid to the placement of the voxel to ensure ^{1}H MR spectra are acquired from the same location in all individuals. A dead space was left between the voxel and possible interferences such as fat areas, presence of vessels or borders of the liver in order to keep a homogeneous area of quantification.

2.4.2 Manganese Enhanced Magnetic Resonance Imaging (MEMRI) as a tool to study hypothalamic activity

Manganese Enhanced MRI (MEMRI) is an emerging contrast agent based technique used for high resolution imaging of animal brain *in vivo* for anatomical, functional and neural connectivity studies (Pautler 2004).

MEMRI relies on the shortening effect of divalent manganese ions (Mn^{2+}) on the T_1 relaxation times of tissue water. As a consequence of this effect, T_1-weighted images become brighter in areas with sufficient manganese accumulation (Lin and Koretsky 1997). Mn^{2+} ions are also a calcium (Ca^{2+}) analog and therefore can be taken up by excitable cells, such as neurons and cardiac cells via voltage-gated Ca^{2+} channels. Influx of Ca^{2+} into neurons is necessary for release of neurotransmitters, which is the result of neural activation. This supports the notion that the uptake of Mn^{2+} by a neuron is directly coupled to its physiologic activity and function.

Others advantages of Mn^{2+} in MRI is that these ions accumulate in the activated neural tissue and have a slow clearance from the stimulated region of the brain. This allows the measurement of peak, or steady state activity during the two-hour period of the scan used in this project. Our laboratory has previously shown that Mn^{2+} can enter key appetite centres within the hypothalamus. *Kuo et al* and *Anastasovksa et al* have shown that this technique is able to detect significant changes in neural activity by Mn^{+2} uptake in experiments involving gut hormone administration and nutritional

interventions (Parkinson, Chaudhri et al. 2009, Anastasovska, Arora et al. 2012).

2.4.2.1 Preparation of animals for MEMRI

MEMRI was performed to visualise and quantify neural activity in specific regions of the hypothalamus in the brain associated with appetite. Before scanning, anesthesia was induced with a 4-3% oxygen-isofluorane mix via a facemask. This mix was maintained at 2% oxygen-(1.0-1.5)% isofluorane according to respiration and body temperature during the scan, using a standard monitoring equipment (SA Instruments, Inc). The temperature was kept at 37°C and the respiration maintained at around 90-100 bpm before manganese infusion and at 30-50 bpm after infusion. Mice were positioned ventrally in a bed and mice were cannulated in the tail vein using a 27G butterfly cannula connected via an infusion line to a syringe containing 100mM $MnCl_2$ solution that was placed in a syringe pump (Harvard Apparatus). The head of the mice were placed and fixed in a transmit-receive birdcage head coil and scanned in a 9.4T Unity Inova MR scanner (Agilent Technologies) as shown in figure 2.4.2.1.2.

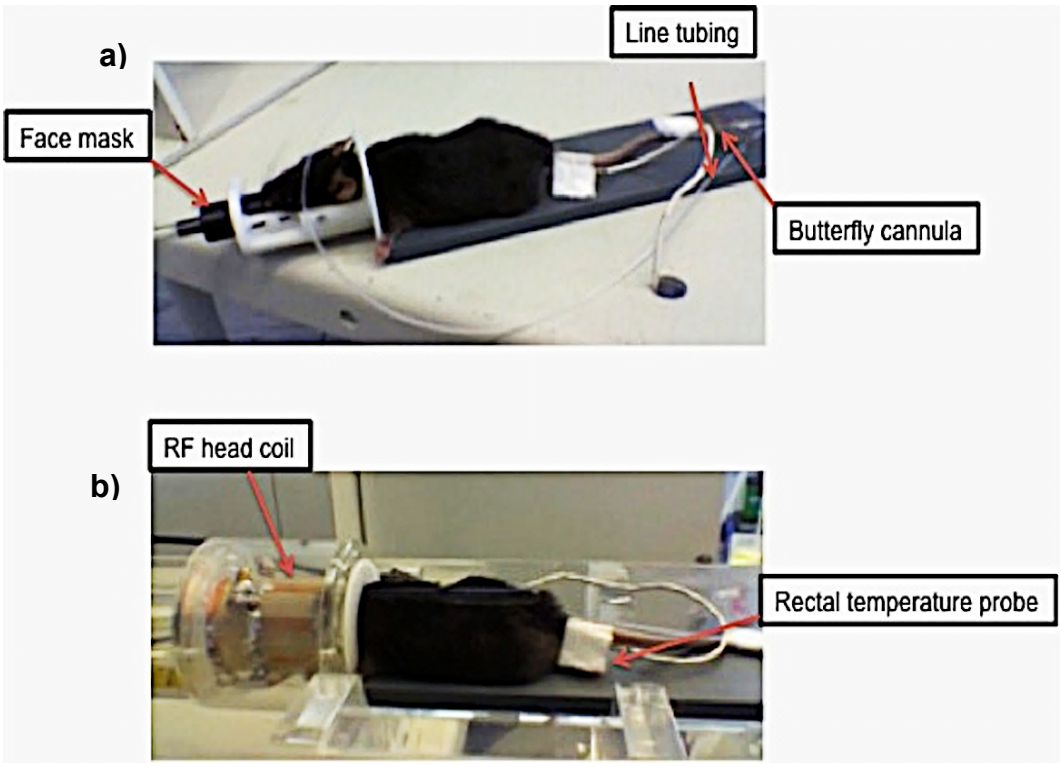

Figure 2.4.2.1.2 Set up of a mouse for MEMRI. a) Mouse set up in the bed with its head restrained in a head holder and with the i.v. cannula (butterfly) placed in the tail vein for infusion of $MnCl_2$ solution. b) Mouse head placed inside the RF coil, which was placed inside a cradle in a specific position, so that once placed inside the bore of the scanner it will remain isocentred. Anaesthesia is maintained through a face mask. Breathing rate and temperature are monitored via a breathing pad and the rectal temperature probe respectively connected to a standard monitoring system.

2.4.2.2 Parameters used for MEMRI

Following a preliminary image to determine the correct positioning of the mouse head in the bore of the scanner, transverse MR images were acquired repeatedly in an array, 66 times, using a two dimensional (2D) Fast Spin Echo Multislice (F-SEMS) sequence with the following parameters:

Orientation: transverse

TR: 1.8s

ETL: 6ms

Effective TE: 5.20 ms

FOV: 25mmx25mm

Matrix size: 192x192

Averages: 2

Slice thickness: 0.4mm

Slices: interleaved

Number of slices per array: 46

Array: 66 acquisitions of the 46 slices, each 1 min 55 seconds long, with 1-second time gap between acquisitions.

Slices were piloted so that the whole brain was covered (scout image figure 2.4.2.2.1). Correction for inhomogeneities in the magnetic field (shimming) was performed using a fast-map automated shimming on a 4x4x4 mm^3 voxel placed in the brain.

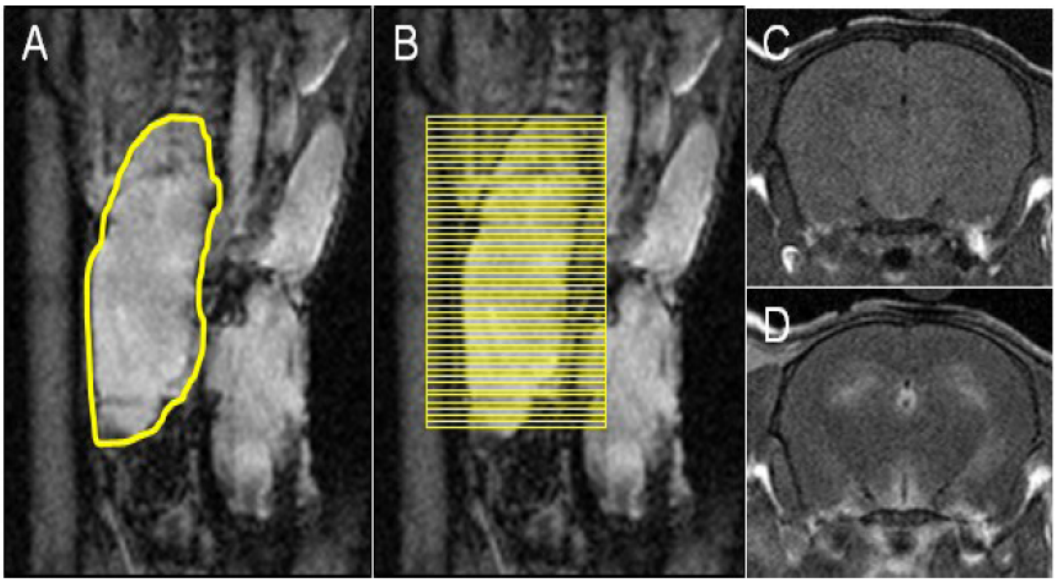

Figure 2.4.2.2.1 Piloting of the transverse MRI images across the brain. a) A sagittal pilot image (scout image) through the mouse head, with the brain delineated in yellow. b) A sagittal scout image of the brain with the 46 slices placed in the location where they will be acquired. c) A transverse slice acquired in the hypothalamus before and d) after $MnCl_2$ infusion. (Picture kindly provided by Dr. Jelena Anastasovska).

At the end of the third acquisition, $MnCl_2$ infusion was started using a syringe pump at a rate of 0.2ml/g of Fat Free Mass (FFM)/hour at a dose of 0.5mmol/g of FFM. Each mouse received a volume of 5ul of 100mM $MnCl_2$ per gram of fat free body mass. Fat free mass (FFM) was calculated using the integral of the lipid peak from the whole body MRS by using the equation described by *Mystkowski et al., 2000*) and converting percentages to grams as followed:

Fat Free Mass (FFM)= (100-% adiposity) x 0.01 x total body mass (body weight).

Motion correction was applied to acquire images and then registered to a brain atlas (*Dorr et al, 2008*) by using the tools from AFNI (Medical College of Wisconsin) and FSL (FMRIB, UK). Specific Regions of Interest (ROI) were identified and manually delineated using the brain atlas aforementioned as a model for further regional specific measurement of Signal Intensities (SI) throughout the 66 arrays per each slice (ARC, VMH, PVN, Pe nuclei; figure 2.4.2.2.1). Each SI measurement collected was normalised to that of the 4^{th} ventricle, which is outside the Blood Brain Barrier (BBB). As the 4^{th} ventricle lies outside the BBB, it was chosen as a suitable control for the correction for the differences in rates at which $MnCl_2$ is entering to the brain. This normalisation was assumed to correct any differences in the dose of $MnCl_2$ received to the brain of each mouse. The 4^{th} ventricle was also used as a reference for successful arrival of $MnCl_2$ to the brain and to evaluate differences in the circulation among animals. The Normalised Percentage Enhancement (NPE) in SIs was calculated for each mouse by calculating the percentage change of SI measurement from baseline SI (before $MnCl_2$ infusion).

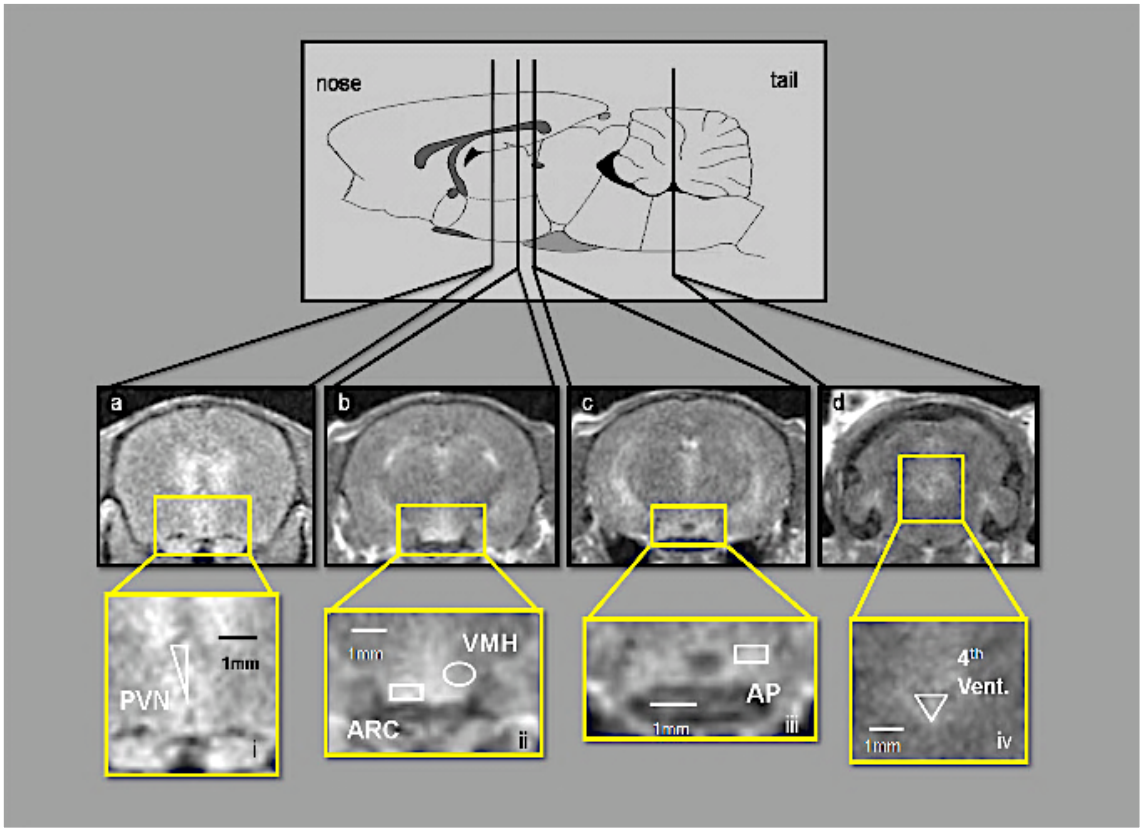

Figure 2.4.2.2.1 Regions of Interest (ROI) highlighting appetite centres analysed in hypothalamus by MEMRI. The diagram on the top shows the mouse brain with the location of the slices shown below it (a-c). These pictures are transverse images through the hypothalamus (shown within a highlighted yellow square, which has been enlarged in the images below (i-iv), after IV $MnCl_2$ infusion. The ROIs used for SIs measurements in the hypothalamus were drawn, highlighting the approximate location of the following regions: PVN: Paraventricular Nucleus (a,i), ARC: Arcuate Nucleus and VMH: Ventromedial Hypothalamic nucleus (b,ii), AP: Anterior Pituitary (c,iii) and 4^{th} ventricle (d,iv). (Picture kindly provided by Dr. Meliz Sahuri).

2.4.3 Intraperitoneal Glucose Tolerance Test (IPGTT)

Intraperitoneal glucose tolerance test measures the changes in blood glucose levels over a 2-hour interval following the administration of an intraperitoneally injected glucose load from the body. Altered changes in blood glucose levels (clearance of glucose) help to identify disturbances in glucose metabolism in conjunction with other parameters such as fasting glucose and insulin levels.

Mice were fasted overnight for 16-18 hours before glucose measurements. Baseline (fasting) glucose concentrations were determined before injecting the mice intraperitoneally with 2g/Kg body weight of 20% D-glucose. Blood glucose concentrations were detected after 15,30,60 and 120 minutes of the glucose load. Glucose levels were measured using a commercially available glucometer and glucose strips (Boots Stores, UK and Abbott Diabetes care UK respectively). Glucose tolerance was analysed at each time point and by calculating the area under the curve (AUC).

2.4.5 Tissue harvesting

Tissues were collected between 10:00 and 12:00 pm from fed mice. Anaesthesia was induced with a 4-3% oxygen-isoflurane mix and maintained at 3-2% with the same mix. Blood samples were taken by cardio puncture and collected in EDTA-coated vacutainers. Protein inhibitors were added to blood samples to avoid further protein degradation (100µl/ml plasma of AEBSF (Pefabloc Sc. Roche), 10µl protease inhibitor cocktail (Sigma, UK) and DPPIV inhibitor (Millipore, USA)). Blood was gently inverted to mix and

then centrifuged for 15 minutes at 4500 rpm at 4°C. Plasma was separated and aliquoted in 1.5 ml eppendorf tubes and stored at -80°C for further analysis.

Different organs were collected and frozen on dry ice and then stored at -80°C. White adipose tissue (subcutaneous, gonadal, retroperitoneal and mesenteric), brown adipose tissue, liver, pancreas, kidneys, heart and hind limb muscle were dissected and weighed in an analytical balance. Brains were weighed and immediately fast frozen with isopentane (2-methyl butane), which was cooled with dry ice first (placing the isopentane in a beaker throughout the process). Brains were immersed in isopentane for 25 seconds and then stored at -80°C as with the others harvested tissues for further analysis.

2.4.6 Adipocytes extraction for cell counting and distribution

Samples of adipose tissue (subcutaneous and gonadal adipose tissue) were used to extract adipocytes for cell quantification and to assess the relative distribution of these cells using a Beckman Coulter Multisizer 4 (MIAMI, FL, USA). The principle of this instrument is based on an electrical conductivity difference between particles and common diluent (Isoton II, Beckman Instruments). Particles act as insulators and diluents as good conductors.

The particles suspended in an electrolyte are made to pass through a small aperture in which an electrical current path has been established. As each particle displaces electrolyte in the aperture, a pulse essentially proportional

to the particle volume is produced. Particles in the range of 1 to 500μm can be counted and measured volumetrically.

Subcutaneous and gonadal adipose tissues were dissected and immediately weighed. A collagenase solution was prepared with a 4% albumin in a concentration of 1mg of collagenase (Type I; Sigma Aldrich (C0130) per milliliter of Dulbecco's Modified Eagle Medium (DMEM, Gibco®). Samples of 40-50 mg of tissue were minced and digested in a bijou tube containing 1ml of the collagenase solution described before per each 0.5mg of adipose tissue. Subsequently, minced tissues were incubated at 37°C in a shaking water bath (145 cycles/min) for 90 minutes. The cell suspension produced was then gently filtered in a 250μm diameter nylon mesh, washed three times with DMEM media enriched with 4% albumin and 1mg of trypsin inhibitor per 40ml of media.

Adipocytes layer (top layer) was transferred to a clean sterilin tube and resuspended in DMEM + 4 % albumin and kept in the shaking water bath (135 cycles/min) for 15-20 minutes at 37 °C. After this, cell suspensions were counted using the Coulter Counter Multisizer 4. Cell suspensions were swirled before counting to ensure even suspension. Blank readings using 100 ml of isoton buffer were performed before proceeding with the cell counting. 500μl of the cell suspensions was added to 100ml isoton buffer and counted using a 200μm diameter aperture under continuing stirring. The effective cell size range used was 20μm to 120μm. Cells size distribution was calculated as relative frequencies (%).

2.4.7 Biochemical analysis in plasma

A Milliplex MAG Mouse Metabolic Hormone (MMHMAG) panel was used to assess metabolic biomarkers in plasma samples (Millipore, USA). Milliplex MAG is an immunofluorescence technique that uses fluorescent coded magnetic beads (microspheres) as the substrate on which assays are performed. These microspheres are internally color-coded with two different fluorescent dyes. In the assay, the beads capture a specific analyte from the sample, and then a biotinylated detection antibody is introduced. The reaction is then incubated with Streptavidin-PhycoErythrin (Streptavidin-PE) conjugate to capture the biotinylated protein of interest. The Streptavidin binding protein is conjugated to the reporter molecule (chromophore) PE for the final detection. The microspheres in each well of the plate are then quantified by the Mag Pix system, which is a fluorescent-based detection system that uses imaging technology for precise quantification.

The microspheres pass through a laser, which excites the internal dyes marking the microsphere set. A second laser excites the chromophore PE whose fluorescence signal is quantified. Subsequently, high-speed digital signal processors identify each individual microsphere and quantify the concentration of each biomarker based on the fluorescent reporter signals. The software used to quantify the results was xPonent software for curve fitting analysis (Luminex Corp, US) incorporated in the Mag Pix system. This system uses a magnetic field to force the beads onto solid surface where they can be imaged and quantify.

The assay was performed according to the manufacturer's protocol using undiluted plasma (see figures 2.4.7.1 and 2.4.7.2 for a brief description). The volume of sample used in this assay was 10µl and 10 metabolic biomarkers were quantified per sample: insulin, leptin, glucagon, resistin, MCP-1, GIP, C-peptide, ghrelin, TNF-alpha and IL-6.

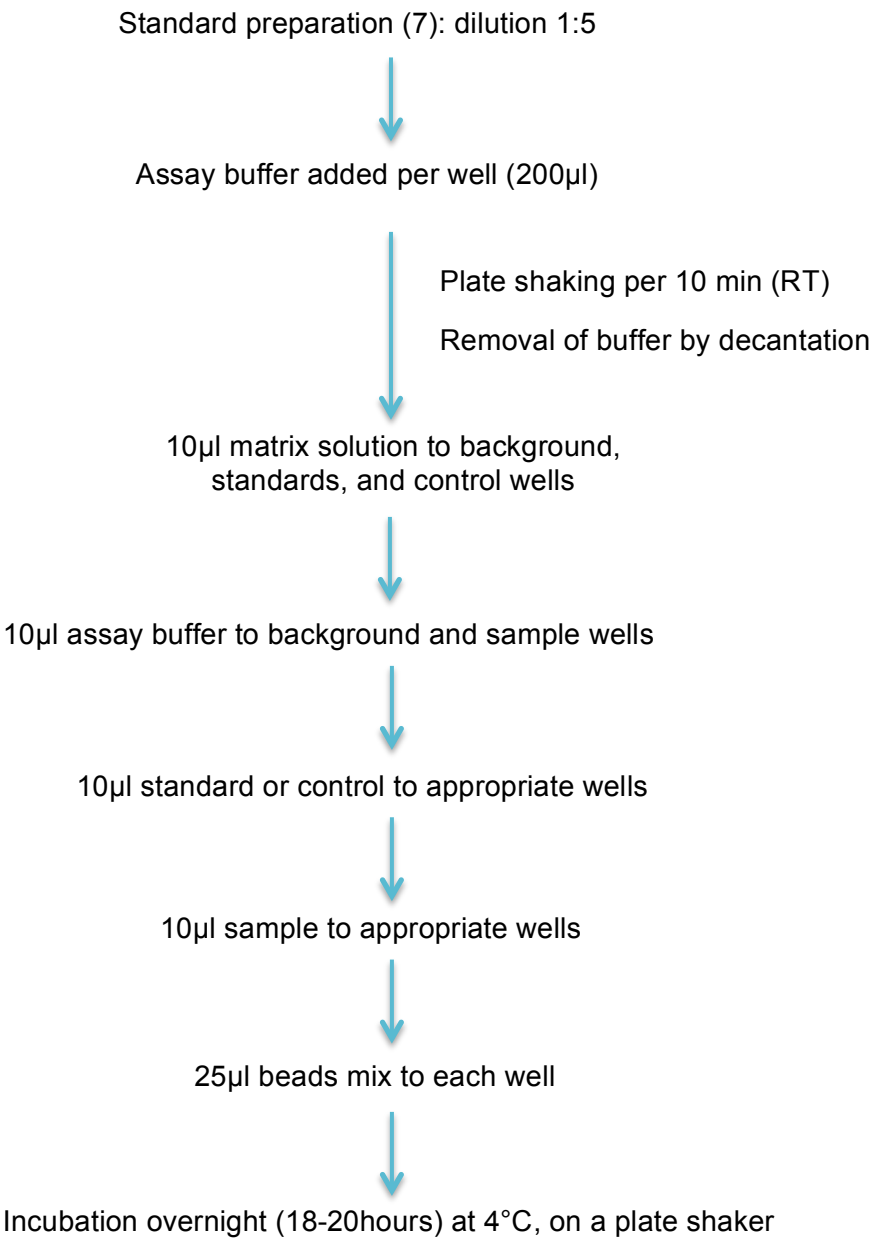

Figure 2.4.7.1 Schematic of the protocol used for the Milliplex MAG Mouse Metabolic Hormone (MMHMAG) panel on day 1. Protocol followed according to the manufacturer's guidance.

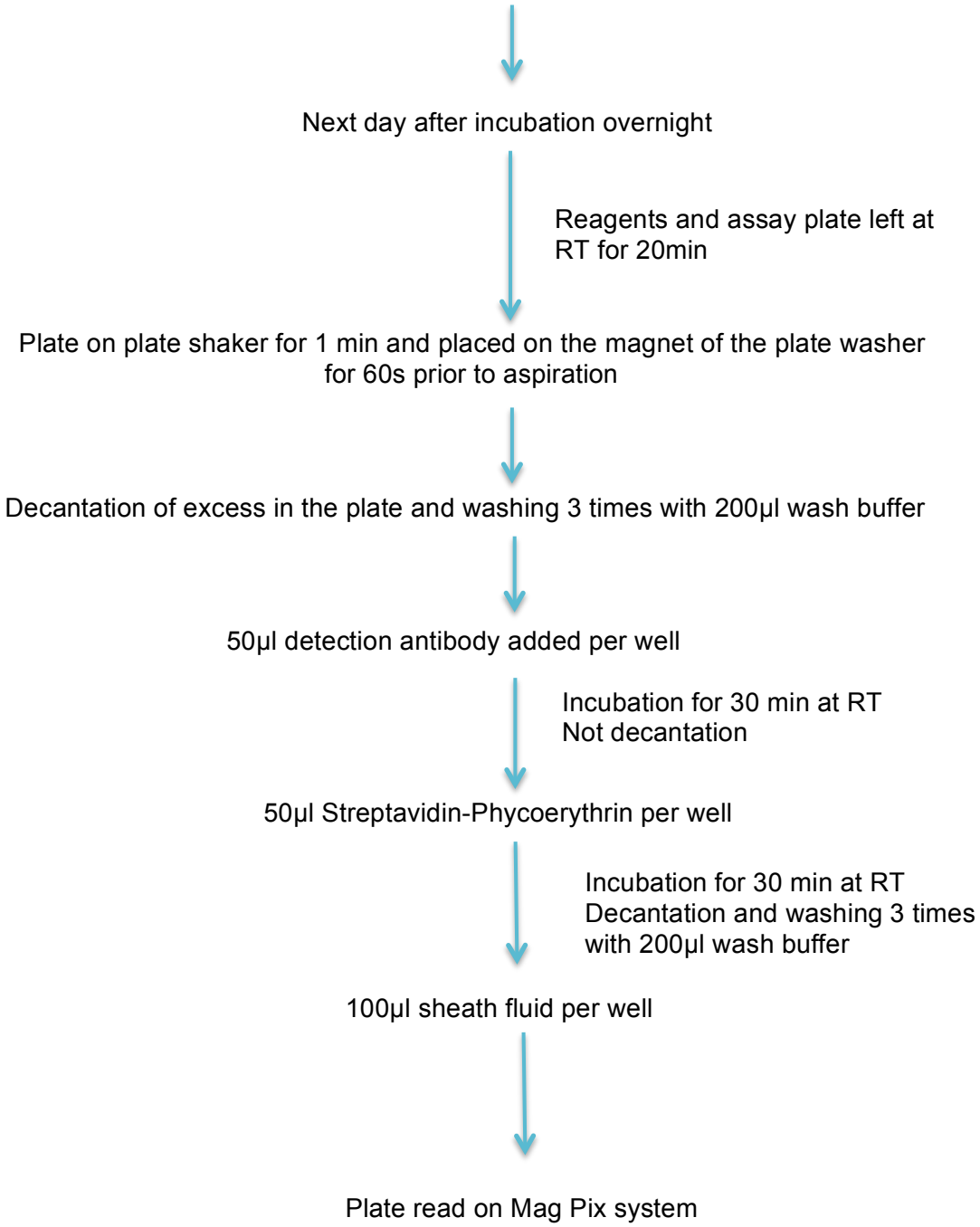

Figure 2.4.7.2 Schematic of the protocol used for the Milliplex MAG Mouse Metabolic Hormone (MMHMAG) panel in day 2. Sheath fluid or flow cell-liquid stream carries and aligns the cells so that they pass single file through the light beam for sensing. Protocol followed according to the manufacturer's guidance.

2.4.8 Gene expression analysis

2.4.8.1 RNA extraction

Adipose tissue (subcutaneous adipose tissue) RNA was extracted using a RNeasy Lipid Tissue Mini Kit, which integrates a phenol/guanidine-based sample lysis and silica-membrane purification of total RNA. QIAzol lysis reagent was used as homogeniser to facilitate lysis of adipose tissue and inhibition of RNases. General protocol can be seen in figure 2.4.8.1.2.

40-50mg of frozen adipose tissue was placed in 2ml microcentrifuge tubes, and kept on dry ice during this step. Care was taken when weighing and placing tissues in tubes in order to avoid thawing during handling. Subsequently, tubes were placed at room temperature and tissues were disrupted and homogenised by placing one steel bead (5mm mean diameter) to each microcentrifuge tube, adding 1ml QIAzol lysis reagent immediately after, and placing tubes in a TissueLyser Adapter set 2x24 for 2 minutes at 20Hz twice (rotating the rack of tubes before repeating the process for even homogenisation).

Lysates (homogenates) were pipetted into new 1.5 ml tubes and kept at room temperature for 5 minutes. 200µl chloroform were added and tubes were securely cap and vigorously shaken for 15 seconds by hand, before being left a further 2-3 minutes at room temperature. Samples were then centrifuged at 12000 x g for 15 minutes at 4°C. The aqueous phase (containing the RNA) was transferred to a new 1.5ml eppendorf tube and 1 volume (usually 600µl) of 70% ethanol was added to the aqueous phase and

mixed by vortexing to precipitate the RNA. Samples were transferred to the RNeasy spin column (which was placed in a 2ml eppendorf tube) and centrifuged for 15 seconds at ≥8000 x g at 23°C and flow through discarded. Membranes (columns) were washed with two different buffers (included in the kit) as specified in the manufacturer's protocol. Subsequently, columns were left to dry for 10 minutes at room temperature in a new 1.5ml eppendorf tube. Finally, RNA was eluted using 30µl RNase-free water and centrifuging for 1 minute at ≥8000 x g. RNA was stored at -80°C until further use.

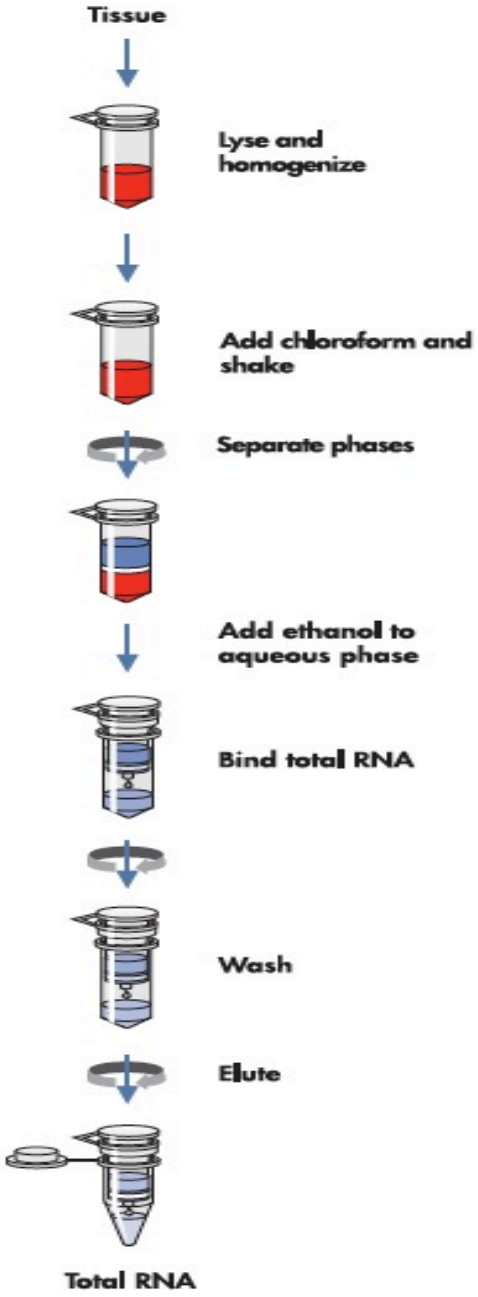

Figure 2.4.8.1.2 RNA Extraction procedure. Steps required for the extraction of RNA form adipose tissue, using RNeasy Lipid Tissue Mini Kit, Qiagen. Procedure was followed as described in the manufacturer's protocol. Figure reproduced from manufacture's handbook.

2.4.8.2 RNA quantification and cDNA synthesis

The amount of RNA extracted (as described above) was quantified using a NanoDrop 2000 spectrophotometer (Thermo Scientific, USA). The Nanodrop measures RNA quantity using only 1-2 µl of the sample. The sample is pipetted directly onto an optical measurement surface. A drop of the RNA (diluted in RNAase free water) is held in place by inherent surface tension during the analysis. The 260nm/280nm was automatically calculated. The ratio of absorbance at 260nm and 280nm was used to assess the purity of RNA. A ratio of approximately 2.0 was accepted as pure RNA as indicated in the manufacturer manual. Approximately 500-800ng/µl was obtained per adipose tissue sample.

2.4.8.3 cDNA synthesis

Complementary DNA (cDNA) synthesis is the first step of the two-step quantitative reverse transcriptase Polymerase Chain Reaction (RT-qPCR). cDNA is generated by the enzyme reverse transcriptase (RT), which has the ability to use the information in the RNA to generate the DNA that is complementary to the messenger RNAs (mRNAs) that encodes proteins of interest. mRNA is transcribed into complementary DNA (cDNA) by using the RT with access to the four Deoxynucleotide Triphosphates (dNTPs) and a short sequence of deoxy –Thymine nucleotides (oligo$(dT)_{20}$) primers to be able to initiate synthesis *de novo*. Subsequently, mRNA is removed by using an RNAase enzyme (RNAaseOUT^{TM}) leaving a single stranded cDNA ready for the secondreal time Polymerase chain Reaction (RT-PCR).

2µg of subcutaneous adipose tissue RNA was used to synthesise cDNA as described in the Thermoscript Reverse Transcriptase Polymerase Chain Reaction RT-PCR System protocol (Invitrogen, UK). This system is used for the detection and analysis of RNA molecules in a two-step RT-qPCR process. RNA was added to a mix of oligo $(dT)_{20}$ primer, 10mM deoxyribonucleotide triphosphate mix (dNTP), and Diethylpyrocarbonate (DEPC)-treated water or RNAase-free water. RNA was denatured by incubation in a thermal cycler preheated at 65°C for 5 minutes and immediately placed on ice. The samples were then incubated with 5x cDNA synthesis buffer, 0.1M Dithriothreitol (DTT; it stabilises and facilitates the enzymatic activity of the RT and RNAase inhibitor), DEPC-treated water, RNAaseOUT™ enzyme, and avian Thermoscript Reverse Transcriptase. cDNA synthesis was completed by incubating the samples at 50°C for 60 minutes and ending the reaction at 85°C for 5 minutes, after which the samples were stored at -20°C until real-time PCR was performed.

2.4.8.4 Real time quantitative PCR Polymerase Chain Reaction (RT-qPCR)

Gene expression in subcutaneous tissue was determined by Real Time Quantitative Polymerase Chain Reaction (RT-qPCR). Sequence specific primers bind to the cDNA previously obtained in the first step of the RT-qPCR (section 2.4.8.3). The amount of amplified product is measured at each PCR cycle by using fluorescent probes and reading the signal emitted from the dyes while performing the thermal cycling.

The real time PCR reaction consists of three important steps that make up each cycle. These steps are: 1) Denaturation at 95°C, where high temperature incubation “melts” the double-stranded DNA (dsDNA) into single-stranded DNA (ssDNA) and loosen secondary structures in single stranded DNA. 2) Annealing at 60°C, during which primers of the gene of interest hybridise to complementary ssDNA. 3) Extension at 60°C; once primers are hybridised they are elongated, making a copy of the gene of interest.

4µl of cDNA was mixed with 5µl of RNAase water, (10-20ng of cDNA) 10 µl of TaqMan Universal Master Mix II no UNG, 1 µl of TaqMan gene of interest, for a total volume of 20µl per reaction. Samples and mix were added in triplicate to a MicroAmp Fast 96-well reaction plate (Applied Biosystems, USA), including a 1:5 serial dilution of the cDNA templates used for each primer.

Actin beta (Actb) and Hypoxanthine-guanine phosphoribosyltransferase (Hprt) (TaqMan, Life Technologies, UK) were tested to find the best control for normalisation. No significant differences were found between groups. Therefore, Actb was chosen as control for normalisation of all genes of interest. Plates were sealed with a PCR-specific seal (Invitrogen, UK) then placed in a preheated Applied Biosystems 7500 Fast Real-Time PCR System at a cycling program of polymerase activation at 95°C for 10 minutes, 40 cycles of denaturation at 95°C for 15 seconds and annealing and extension at 60°C for 1 minute.

Baseline was set at the range of 3 to 15 cycles of amplification. The threshold was set at 0.1 for all readings. The threshold is the level of signal that reflects a statistically significant increase over the calculated baseline signal. It is set above the background and within the exponential growth phase of the amplification curve. The threshold cycle (Ct) is the cycle number at which the fluorescent signal of the reaction crosses the threshold. This value is proportionate to the initial amount of cDNA copy number. List of TaqMan genes of interest used for the gene expression assays are shown in table 2.4.8.4.1.

Gene expression level was analysed using a comparative quantification method delta delta Ct values. This method assesses the fold change compared to a calibrator sample (control or group of reference). Cts for genes of interest in both the calibrator and test samples are adjusted in relation to a reference (housekeeper) gene (B-actin) Ct from the same two samples (calibrator and test sample). The delta delta value is then used to determine the fold change or difference in expression of the gene of interest in respect to the control or reference group (Bookout & Mangelsdorf, 2003; Bookout et al., 2006). Equations used for the analysis are described below.

Delta Ct sample= Av Ct_s gene of interest - Av Ct_s B-actin

Delta Ct calibrator= Av Ct_c gene of interest - Av Ct_c B-actin

$$\text{St.dev. delta Ct} = \sqrt{(\text{st. dev. B-actin})^2 + (\text{st. dev. GOI})^2}$$

Delta delta Ct= delta Ct sample - delta Ct calibrator

St.dev. delta delta Ct= St. dev. delta Ct

Fold induction for each sample relative to calibrator = $2^{(-\text{delta delta Ct})}$

St.dev. fold change= (ln2) (st.dev. delta delta Ct)($2^{-\text{delta delta Ct}}$)

Gene Symbol	Gene Name	TaqMan Assay ID
C/EBP alpha	CCAAT/ enhancer binding protein (C/EBP) alpha	Mm00514283_s1
Glut4/Sic2a4	Solute carrier family 2 (facilitated glucose transporter), member 4	Mm01245502_m1
HSL	Hormone sensitive lipase	Mm00495359_m1
IRS	Insulin receptor substrate 1	Mm01278327_m1
PGC-1a	Peroxisome proliferative activated receptor, gamma, coactivator 1 alpha	Mm01208835_m1
PIK3cb/p110beta	Phosphatidylinositol 3-kinase, catalytic, beta polypeptide or p110beta	Mm00659576_m1
PrKCZ	Protein kinase C, zeta	Mm00776345_g1
PPARG2	Peroxisome proliferator activated receptor gamma	Mm01184322_m1
UCP-1	Uncoupling protein 1 (mitochondrial, proton carrier)	Mm01244861_m1
Serbf1/SREBP1c	Sterol regulatory element binding transcription factor-1	Mm00550338_m1

Table 2.4.8.4.1 Genes used for gene expression analysis using subcutaneous adipose tissue as tissue of interest.

2.4.5 Statistics

Normal distribution was assessed using a Kolmogorov-Smirnov test and homogeneity of variances was assessed using the Levene's test. Data that did not have a normal distribution was analysed using a Mann-Whitney test or other non-parametric analysis. Whether homogeneity of variances was significant, a test for unequal variances, or natural log transformation of the data followed by a parametric test was used for the analysis. Data was reported as means ±SEM if a parametric analysis was used or as medians with interquartile range (25%-75%) if a non-parametric test was used for the analysis. Natural log transformed data was presented as means with a 95% confidential interval. P values ≤ 0.05 were considered statistically significant. Analysis was performed and reported separately by sex.

A two factorial analysis General Linear Model (GLM, 2x2) was used to assess the effects of birth (LBW-HBW) and postnatal diets (NF-HF), and their interactions on body fat content, food intake and feed efficiency in study 2. When interactions were significant, simple main effects were analysed. A mixed general linear model followed by an appropriate post hoc analysis was used for body weight analysis or as specified. One-way ANOVA was used for between groups analysis for biochemical analysis, gene expression, and adipose cell distribution followed by a protected Fisher's least significant difference (LSD) post hoc analysis or Tukey's high significance difference (HSD) post hoc analysis if necessary. Area Under the Curve (AUC) was used for IPGTT analysis as well as a time point Mann-Whitney analysis.

The software used for the statistical analysis was SPSS (IBM Statistics) and GraphPad (San Diego, CA, USA; version 4) when required.

MEMRI analysis was conducted using Generalised Estimating Equation (GEE) for continuous data (STATA 9.1 software; Stata Corp, College Station, TX, USA) as described in previous publications (Kuo, Herlihy et al. 2006, Anastasovska, Arora et al. 2012).

3. Study 1. The Effects of Birth Weight and Accelerated Growth on Body Composition and Appetite Regulation During Lactation (Birth to 3 Weeks)

3.1 The Effects of Birth weight and Accelerated Growth on Body Weight During Lactation (Birth to 3 Weeks)

The protocol of this study is described in section 2.1. Pregnant females were caged individually and fed a standardised purified diet (20% protein kcal intake). After 24 hours of delivery, pups were weighed and labelled and kept within the same litter until the time of weaning, which was at the end of lactation (3 weeks old). As described in study 1 (section 2.1.3), mice were classified as either Low birth weight male/female mice (**LBWm/f**) or High birth weight male/female mice (**HBWm/f**). The average body weight at birth of all litters was 1.28 ±0.1g with no significant differences between genders: males (**m**)= 1.28 ±0.1g and females (**f**)=1.29±0.1g; p=0.81, *unpaired student t-test*. Figures 3.1.1 and 3.1.2 show the growth curve during lactation of both males and females respectively.

3.1.1 Body weight in Males

Males with a High birth weight (**HBWm**) were significantly heavier than those males with a Low birth weight (**LBWm**) throughout lactation (figure 3.1.1.1 and table 3.1.1.1).

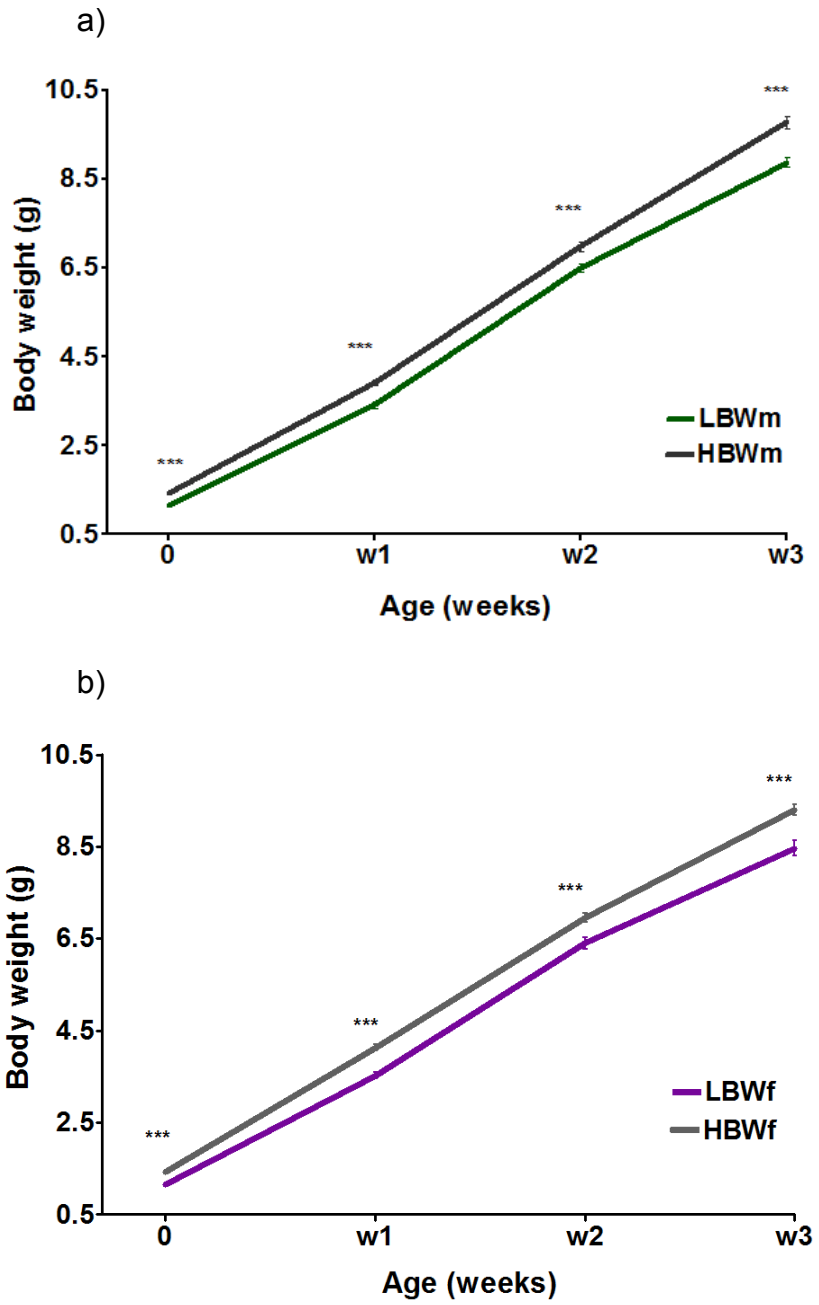

Figure 3.1.1.1 Body weight of High birth weight male and female mice (**HBWm/f)** and Low birth weight male and female mice **(LBWm/f**) throughout lactation (birth to 3 weeks). Data for male a) and female offspring b). Statistical analysis was performed using repeated measures ANOVA followed by a Tukey's high significance difference (HSD) post hoc test. Data presented as mean ±SEM. **LBWm** n=83, **HBWm** n=83; **LBWf** n=70; **HBWf** n=58. ***p≤0.001.

Males Age (Weeks)	LBWm Body weight (g) n=83	HBWm Body weight (g) n=83	P value
Birth (week0)	1.15 ± 0.01	1.43± 0.01***	**<0.001**
Week 1	3.44 ±0.06	4.06±0.06***	**<0.001**
Week 2	6.28±0.09	7.01±0.09***	**<0.001**
Week 3	8.57±0.12	9.91±0.12***	**<0.001**

Table 3.1.1.1 Body weight of male mice (**HBWm and LBWm**) from birth to week 3. Statistical analysis was performed using repeated measures ANOVA followed by a Tukey's high significance difference (HSD) post hoc test. Data presented as mean ±SEM. **LBWm** n=83, **HBWm** n=83.

3.1.2 Body weight in Females

Female offspring had a similar phenotype to that seen in males. High birth weight females (**HBWf**) were heavier at all time points during lactation than Low birth weight females (**LBWf**) as shown in figure 3.1.2.1 and table 3.1.2.1.

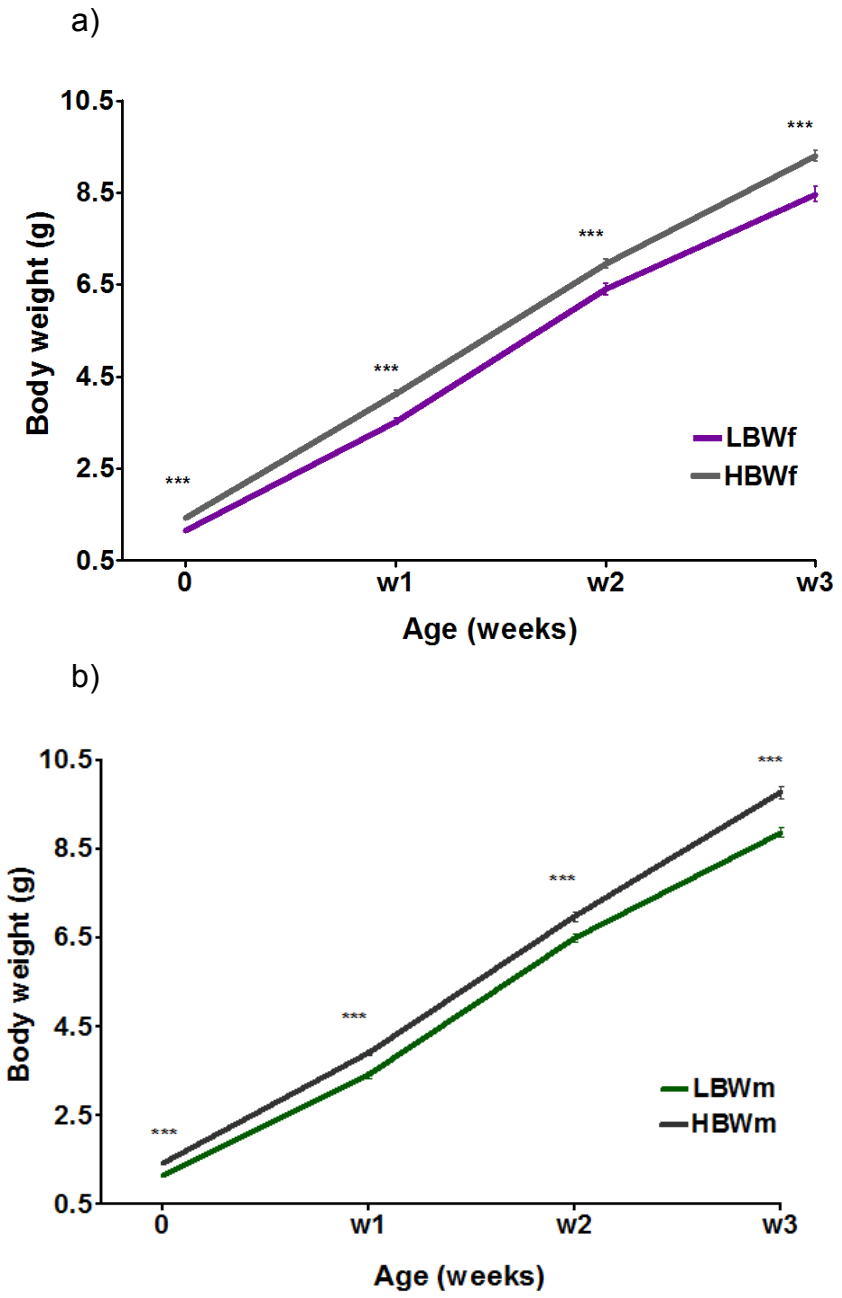

Figure 3.1.2.1 Body weight of High birth weight female and male mice (**HBWf/m)** and Low birth weight female and male mice **(LBWf/m**) throughout lactation (birth to 3 weeks). Data for female a) and male offspring b). Statistical analysis was performed using repeated measures ANOVA followed by a Tukey's high significance difference (HSD) post hoc test. Data presented as mean ±SEM. **LBWf** n=70; **HBWf** n=58; **LBWm** n=83, **HBWm** n=83. ***p≤0.001.

Females Age (Weeks)	LBWf Body weight (g) n=70	HBWf Body weight (g) n=58	P value
Birth (week0)	1.15 ± 0.01	1.42± 0.01***	**<0.001**
Week 1	3.56 ±0.06	4.1±0.06***	**<0.001**
Week 2	6.31±0.1	6.89±0.11***	**<0.001**
Week 3	8.41±0.12	9.31±0.13***	**<0.001**

Table 3.1.2.1 Body weight of female mice (**HBWf and LBWf**) from birth to week 3. Statistical analysis was performed using repeated measures ANOVA followed by a Tukey's high significance difference (HSD) post hoc test. Data presented as mean ±SEM. **LBWf** n=70, **HBWf** n=58.

At birth, similar body weights between **LBWf** and **LBWm** groups were observed as well as between **HBWf** and **HBWm** groups. Females were heavier than their respective male groups at week 1. However, by week 2, **LBWm** were heavier 0.03g compared to **LBWf**, and **HBWm** 0.11g heavier than **HBWf** mice. This phenotype was maintained at week 3 with a major difference of 0.61g between **HBWm** and **HBWf** followed by 0.16g between **LBWm** and **LBWf**.

3.1.3 Body weight gain in Males

HBWm gained more absolute weight than **LBWm** (**HBWm=** 8.434±0.139g, **LBWm=** 7.365±0.096g; **p<0.001**, two-tailed *unpaired student t-test*; figure 3.1.3.1a*)*. However, the change in growth over lactation (growth rate) showed that **LBWm** mice significantly accelerated their growth rate in respect to their counterparts (**HBWm=** 583.1 ±8.37%, **LBWm=** 648.3 ±9.11%; **p<0.001**, two-tailed *unpaired student t-test*; figure 3.1.3.1b; growth rate per day at lactation: **HBWm=** 0.28 ±0.004g/d, **LBWm=** 0.309 ±0.004g/d; **p<0.001**, two-tailed *unpaired student t-test*). Although **LBWm** mice accelerated their growth rate, it was not enough for them to catch up in weight at the time of weaning in respect to the **HBWm** mice (**LBWm =** 8.57±0.12, **HBWm=** 9.92±0.12; **p<0.001**).

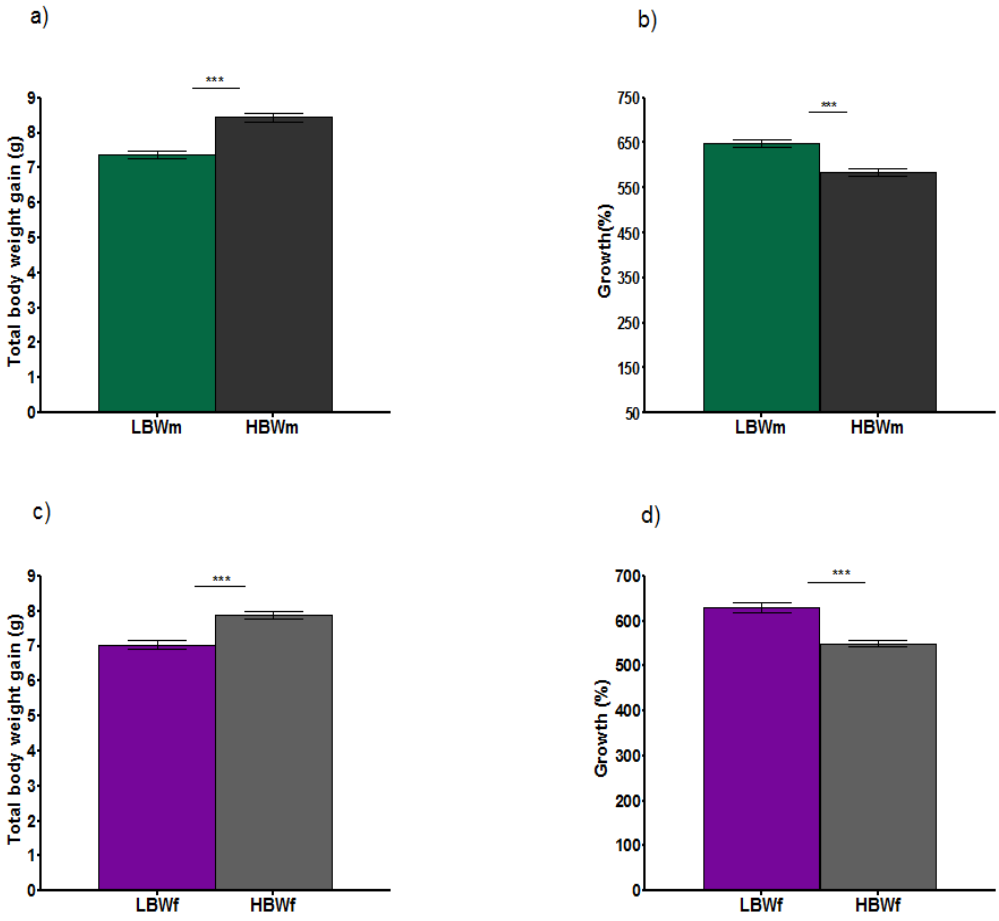

Figure 3.1.3.1 Total body weight gain and growth rate of male and female offspring at lactation (birth to 3 weeks). Total body weight gain (absolute weight gain in grams) a) and c) and total growth rate (as percentage body weight at week 3) b) and d). Figures on the top correspond to male mice and data below to female mice. Statistical analysis was performed using a two-tailed *unpaired student t-test*. Data presented as mean ±SEM. **LBWm** n=81, **HBWm** n=75; **LBWf** n=72; **HBWf** n=52. *** p≤0.001.

3.1.4 Body weight gain in Females

HBWf offspring, similarly to the respective male group, gained more absolute weight in grams than **LBWf** (**HBWf=** 7.88±0.102, **LBWf=** 7.03±0.127; **p<0.001**, two-tailed *unpaired student t-test;* figure 3.1.4.1a) but their growth velocity was slower than the **LBWf** as seen in the male group ((**HBWf=** 549.4±7.47, **LBWf=** 630.1±11.72; **p<0.001**, two-tailed *unpaired student t-test*; figure 3.1.4.1b; growth rate per day at lactation: **HBWf=** 0.262 ±0.003g/d, **LBWf=** 0.30±0.006g/d; **p<0.001**, two-tailed *unpaired student t-test* with Welch's correction). Despite having acceleration in growth, **LBWf** mice did not catch up on weight with the **HBWf** by the time of weaning at week 3 as **LBWm** mice (**LBWf=** 8.407±0.116, **HBWf=** 9.31±0.128; **p<0.001**).

Females did grow slower than their respective male groups. **LBWf** grew 2.81% less than **LBWm**, and **HBWf** 5.78% in relation to **HBWm** mice.

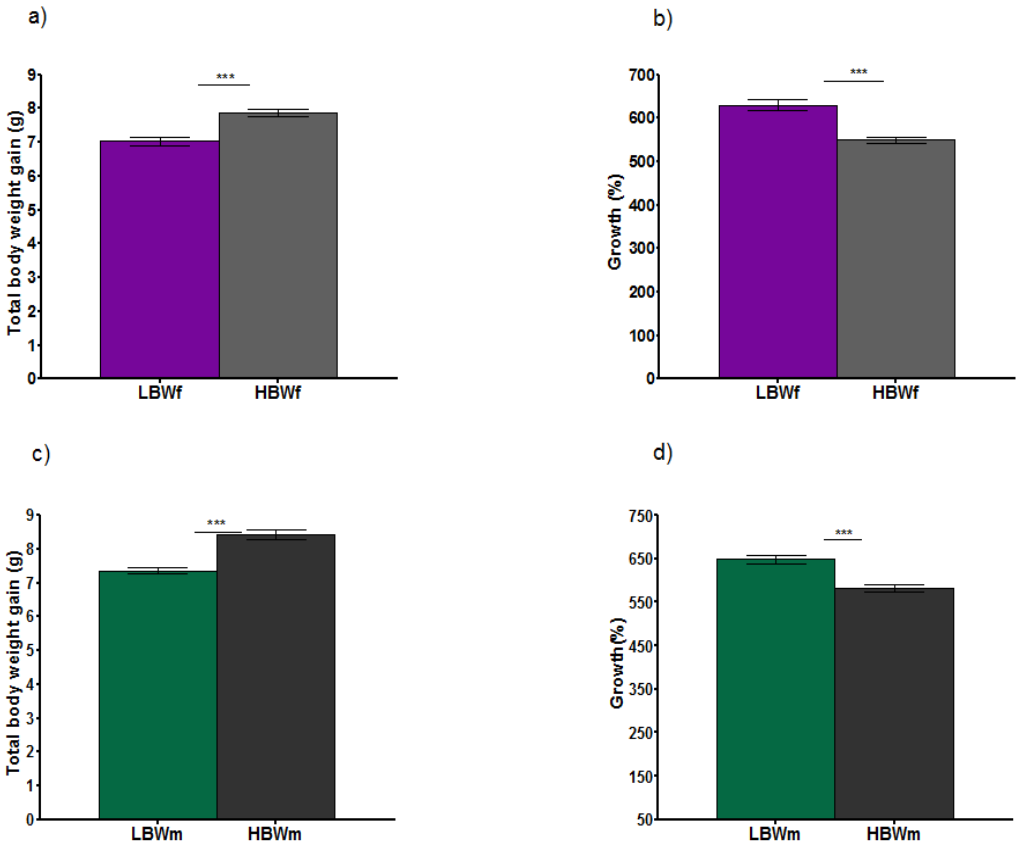

Figure 3.1.4.1 Total body weight gain and relative body weight gain of female and male offspring at lactation (birth to 3 weeks). Total body weight gain a) and c) and total growth rates (as percentage body weight at week 3) b) and d). Figures on the top correspond to female mice and data below to male mice. Statistical analysis was performed using a two-tailed *unpaired student t-test*. Data presented as mean ±SEM. **LBWf** n=72; **HBWf** n=52; **LBWm** n=81, **HBWm** n=75. *** p≤0.001.

3.2 The Effects of Birth Weight and Accelerated Growth on Total Body Adiposity and Intrahepatocellular Lipid Content at Weaning (3 Weeks)

3 weeks old pups were fasted for 3 hours before assessing non-invasively the whole body adiposity and intrahepatocellular lipid content using ^{1}H MRS and MRI techniques. Detailed information of the parameters of these methods is provided in section 2.4.1.

As mentioned before in section 3.1.1, **HBWm** had a higher body weight than **LBWm** by the time of weaning at week 3 (**HBWm=** 9.92±0.12, **LBWm =** 8.57±0.12; **p<0.001**).

3.2.1 Whole body adiposity and intrahepatocellular lipid content (IHCL) in Males

Whole body adiposity showed that **HBWm** had a higher adiposity compared to **LBWm** (**HBWm=** 6.255±0.563%, **LBWm=** 3.899±0.586%; **p=0.015**, figure 3.2.1.1).

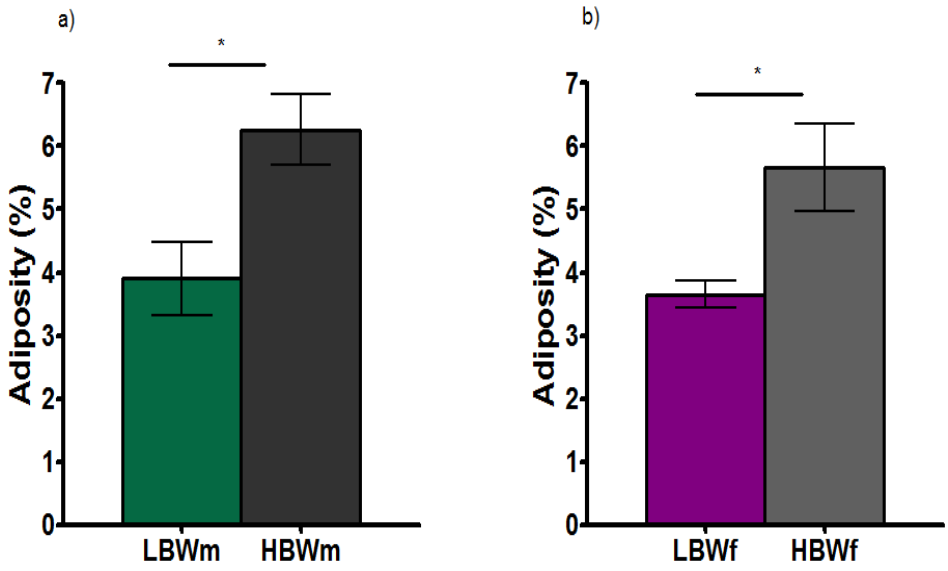

Figure 3.2.1.1 Percentage whole body adiposity of male and female offspring at weaning (3 weeks). Figure a) corresponds to male offspring and figure b) to female offspring. Whole body adiposity was assessed using ^{1}H MRS. Statistical analysis was performed using a two-tailed *unpaired student t-test*. Data presented as mean ±SEM. **LBWm** n=7; **HBWm** n=6; **LBWf** n=6; **HBWf** n=6. * p≤0.05.

Intrahepatocellular lipid content (IHCL) in **LBWm** mice was reduced significantly than **HBWm** mice (**LBWm**= 1.325±0.229, **HBWm**= 2.808±0.334; p=0.007; figure 3.2.1.2).

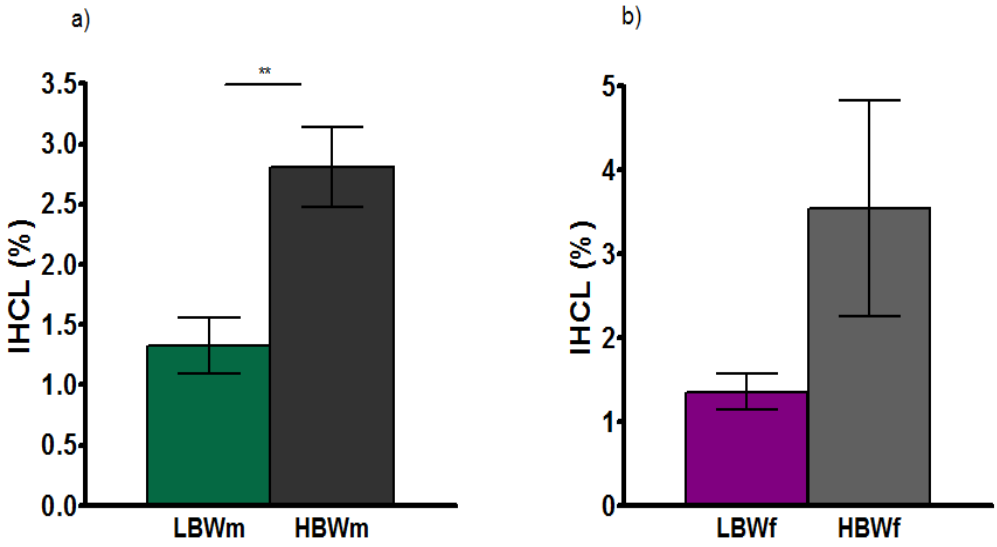

Figure 3.2.1.2 Intrahepotcellular lipid content (IHCL%) measured in male and female offspring at weaning. Figure a) corresponds to male offspring and figure b) to female offspring. IHCL as percentage was assessed using localised ^{1}H MRS. Statistical analysis was performed using a two-tailed *unpaired student t-test*. Data presented as mean ±SEM. **LBWm** n=5; **HBWm** n=5; ** p≤0.01.

3.2.2 Whole body adiposity and intrahepatocellular lipid content (IHCL) in Females

As in males, **LBWf** had less adiposity than **HBWf** (**LBWf=** 3.651±0.213%, **HBWf=** 5.661±0.686%; **p=0.038**; figure 3.2.2.1).

Male mice did have more fat than female mice but the difference between both **HBWf** and **HBWm** is more pronounced than in **LBWm/f** (difference between **HBWf** vs. **HBWm=** 0.604%, **LBWf** vs. **LBWm=** 0.248%).

IHCL content was not significantly reduced in females, but similar pattern was seen as in **LBWm** with a lower lipid percentage in **LBWf** compared to **HBWf** (**LBWf=**1.358±0.209, **HBWf=**2.496 ±0.929; p=0.156 figure 3.2.2.2).

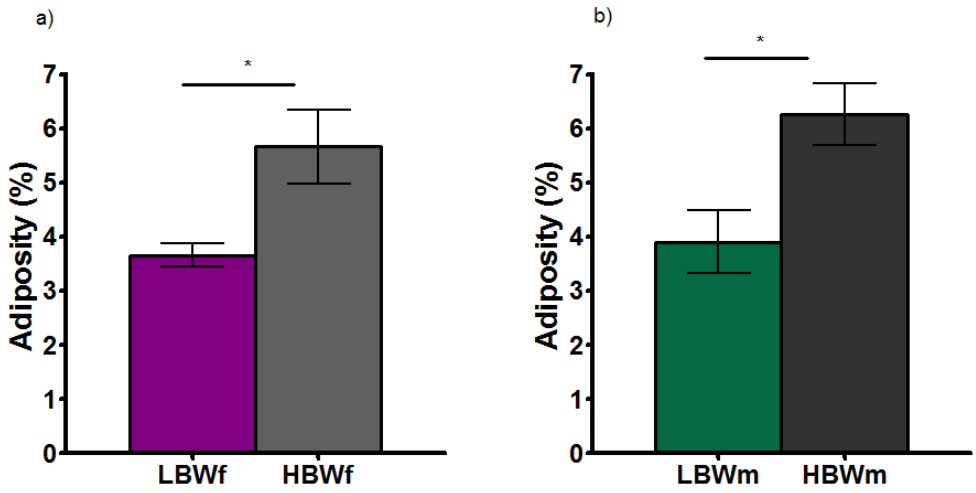

Figure 3.2.2.1 Percentage whole body adiposity of female and male offspring at weaning (3 weeks). Figure a) corresponds to female offspring and figure b) to male offspring. Whole body adiposity was assessed using ^{1}H MRS. Statistical analysis was performed using a two-tailed *unpaired student t-test* with *Welch's correction* test. Data presented as mean ±SEM. **LBWf** n=6; **HBWf** n=6; **LBWm** n=7; **HBWm** n=6. * p≤0.05.

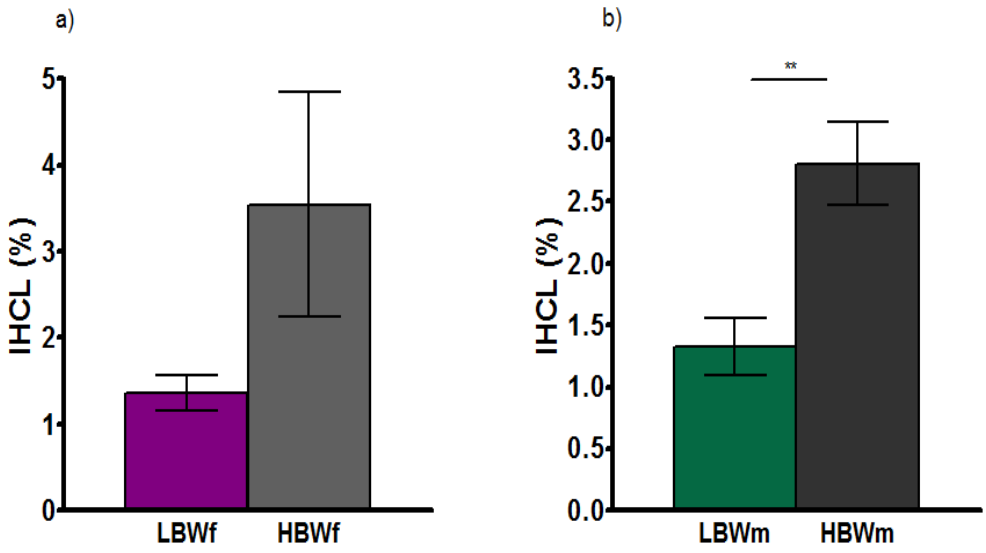

Figure 3.2.2.2 Intrahepatocellular lipid content (IHCL%) measured in female and male offspring at weaning. Figure a) corresponds to female offspring and figure b) to male offspring. IHCL as percentage was assessed using localised ^{1}H MRS. Statistical analysis was performed using a two-tailed *unpaired student t-test with Welch's correction*. Data presented as mean ±SEM. **LBWf** n=5; **HBWf** n=5;p=0.156; **LBWm** n=5; **HBWm** n=5; ** p≤0.01.

3.3 The Effects of Birth Weight and Accelerated Growth on Adipose Tissue Distribution at Weaning (3 Weeks)

3 weeks old pups were fasted for 3 hours before assessing non-invasively adipose tissue content and distribution by using MRI for localisation and subsequent quantification and distribution of adipose tissue by segmentation analysis, as described in section 2.4.1.

3.3.1 Adipose tissue distribution in Males

Total body fat in **LBWm** was significantly lower than in **HBWm** (**LBWm**=1.714±0.191g; **HBWm**=2.728±0.353g; **p=0.021**; figure 3.3.1.1a). This significant difference was not maintained when normalising to body weight but it followed the same pattern (**LBWm**=18.86±2.152%; **HBWm**=26.08±2.879%; p=0.071; figure 3.3.1.1b). This matches the pattern obtained using whole body ^{1}H MRS aforementioned (figure 3.2.1.1).

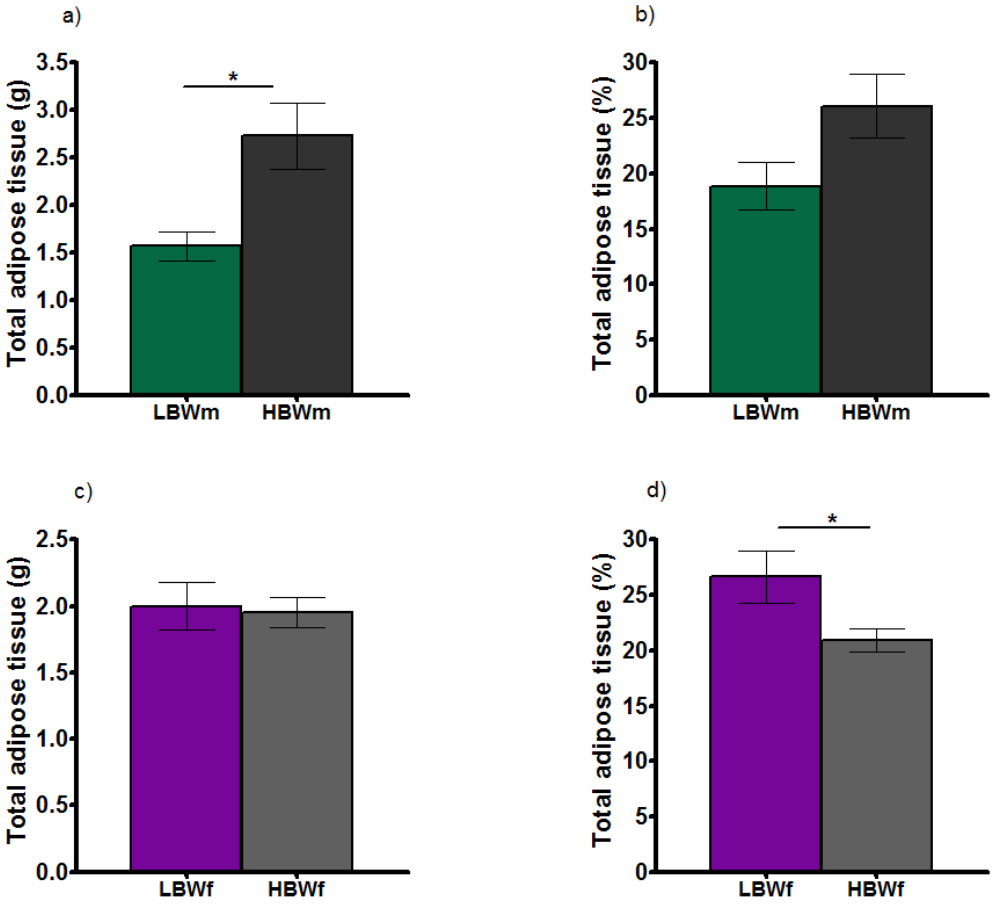

Figure 3.3.1.1 Total body fat content from male and female offspring at weaning. Total adipose tissue content in grams a) and c) and as a percentage of body weight b) and d). Figures on the top correspond to males and figures below to females. Total fat content was measured by using images generating by MRI and subsequent segmentation analysis. Statistical analysis was performed using a two-tailed *unpaired student t-test.* Data presented as mean ±SEM. **LBWm** n=7; **HBWm** n=6; **LBWf** n=5; **HBWf** n=6. * p≤0.05.

A comparison of subcutaneous adipose tissue showed **LBWm** had significantly less subcutaneous adipose tissue than **HBWm** mice, both in absolute values and relative to body weight (**LBWm**=1.103±0.06g; **HBWm**=1.632±0.117; **p=0.001**; figure 3.3.1.2a; **LBWm**=12.75±0.894%; **HBWm**=15.67±0.687; **p=0.034**; figure 3.3.1.2b).

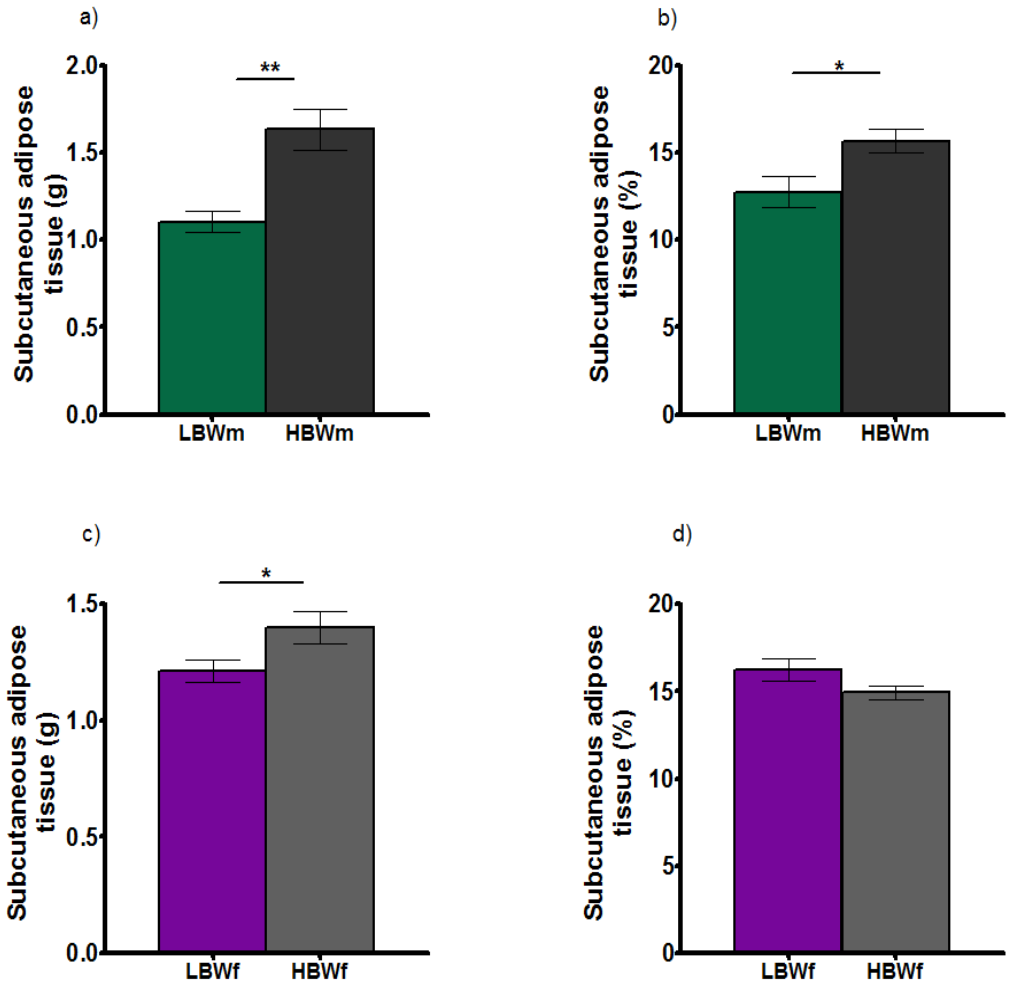

Figure 3.3.1.2 Subcutaneous adipose tissue content from male and female offspring at weaning. Subcutaneous adipose tissue content in grams a) and c) and as a percentage of body weight b) and d). Figures on the top correspond to males and figures below to females. Subcutaneous adipose tissue was quantified from MR images using segmentation analysis. Statistical analysis was performed using a two-tailed *unpaired student t-test.* Data presented as mean ±SEM. **LBWm** n=7; **HBWm** n=6; **LBWf** n=5; **HBWf** n=6. * p≤0.05, **p≤0.01.

Analysis of absolute internal adipose content (grams) showed **LBWm** had a significantly lower internal adipose tissue (**LBWm**=0.508±0.107g; **HBWm**=1.096±0.254; **p=0.048**; figure 3.3.1.3a. However, when analysing internal adipose tissue as a percentage of body weight, a similar pattern was observed, but the differences did not reach statistical significance (**LBWm**=6.111±1.394%; **HBWm**=10.41±2.305; p=0.131; figure 3.3.1.3b).

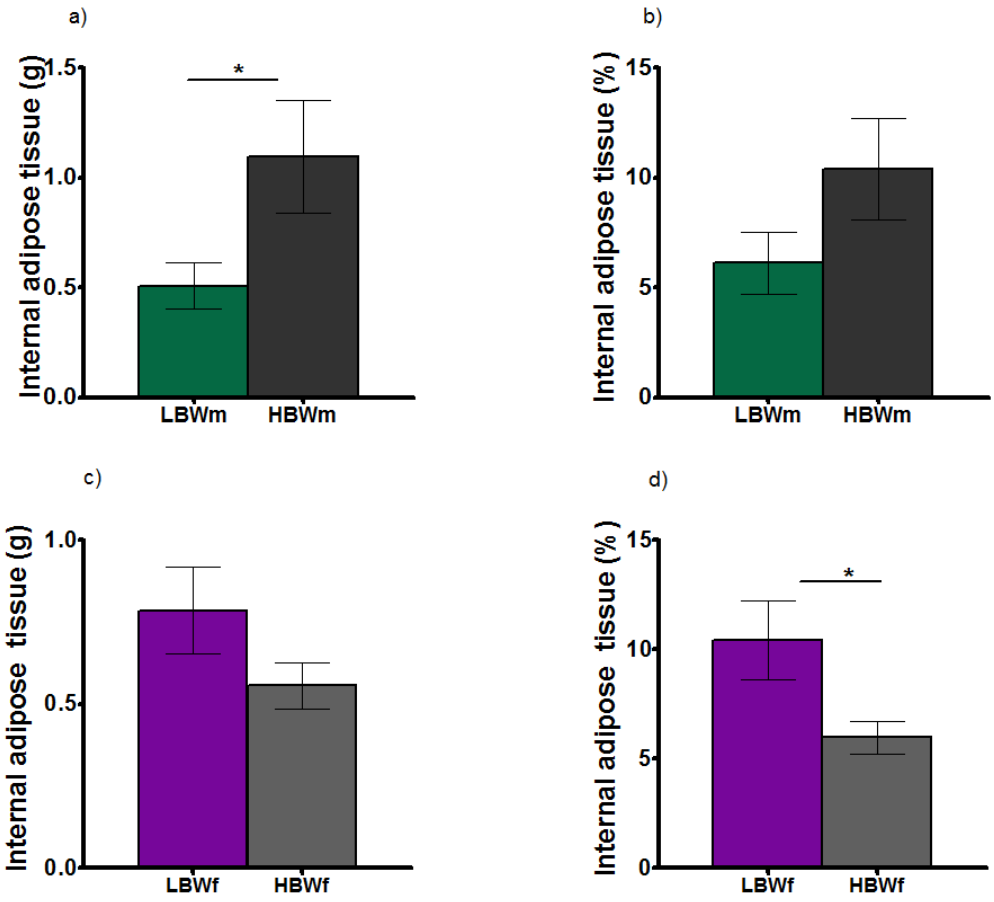

Figure 3.3.1.3 Internal adipose tissue content from male and female mice offspring at weaning. Internal adipose tissue content in grams a) and c) and as a percentage of body weight b) and d). Figures on the top correspond to males and figures below to females. Internal adipose tissue was quantified from MR images using segmentation analysis. Statistical analysis was performed using a two-tailed *unpaired student t-test.* Data presented as mean ±SEM. **LBWm** n=7; **HBWm** n=6. **LBWf** n=5; **HBWf** n=6. *p≤0.05.

Assessment of internal:subcutaneous adipose tissue ratio did not show significant differences between groups (**LBWm**=0.463±0.089; **HBWm**=0.648±0.13; p=0.257; figure 3.3.1.4).

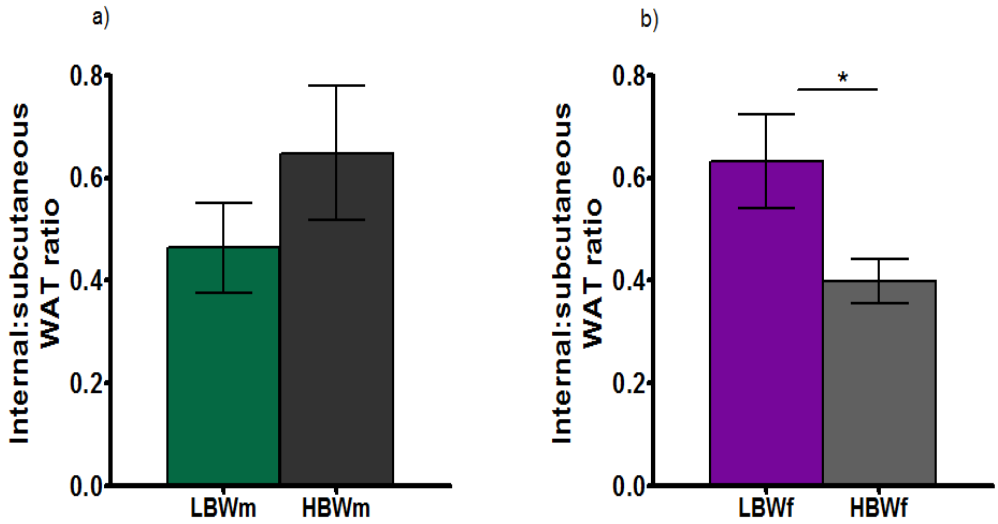

Figure 3.3.1.4 Internal to subcutaneous adipose tissue ratio from male and female offspring at weaning. Figure a) corresponds to males and figure b) to females. Statistical analysis was performed using a two-tailed *unpaired student t-test.* Data presented as mean ±SEM. **LBWm** n=7; **HBWm** n=6; **LBWf** n=5; **HBWf** n=6. *p≤0.05.

3.3.2 Adipose tissue distribution in Females

Assessment of total body fat content between female groups showed no apparent significant differences in absolute total adipose tissue content (**LBWf=**1.999±0.178g; **HBWf=**1.956±0.114g; p=0.838; figure 3.3.2.1a). However, when normalising to current body weight, a significant difference was seen between groups (**LBWf=**26.66±2.345%; **HBWf=**20.91±1.02%; **p=0.04**; figure 3.3.2.1b). This contrast with the results obtained using whole body adiposity by ^{1}H MRS, which shows significant reduced adiposity in **LBWf** (figure 3.2.2.1).

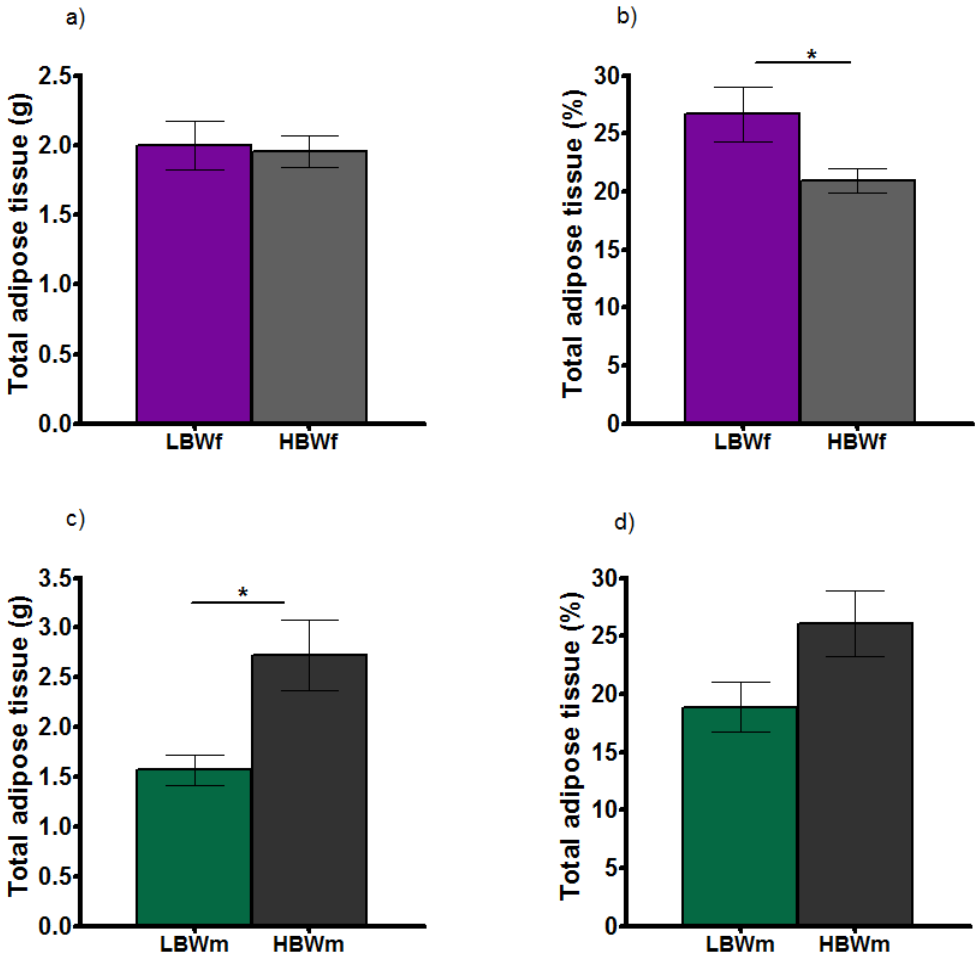

Figure 3.3.2.1 Total body fat content from female and male offspring at weaning. Total adipose tissue content in grams a) and c) and as a percentage of body weight b) and d). Figures on the top correspond to females and figures below to males. Total fat content was quantified from MR images using segmentation analysis. Statistical analysis was performed using a two-tailed *unpaired student t-test.* Data presented as mean ±SEM. **LBWf** n=5; **HBWf** n=6; **LBWm** n=7; **HBWm** n=6. *p≤0.05.

A comparison of subcutaneous adipose tissue between females showed **LBWf** had significantly less subcutaneous adipose tissue than **HBWf** but (**LBWf=**1.214±0.047g; **HBWf=**1.4±0.05g; **p=0.05**; figure 3.3.2.2a). When normalising subcutaneous adipose tissue to body weight differences were not statistically significant between groups (**LBWf=**16.23±0.633%; **HBWf=**14.93±0.407%; p=0.107; figure 3.3.2.2b).

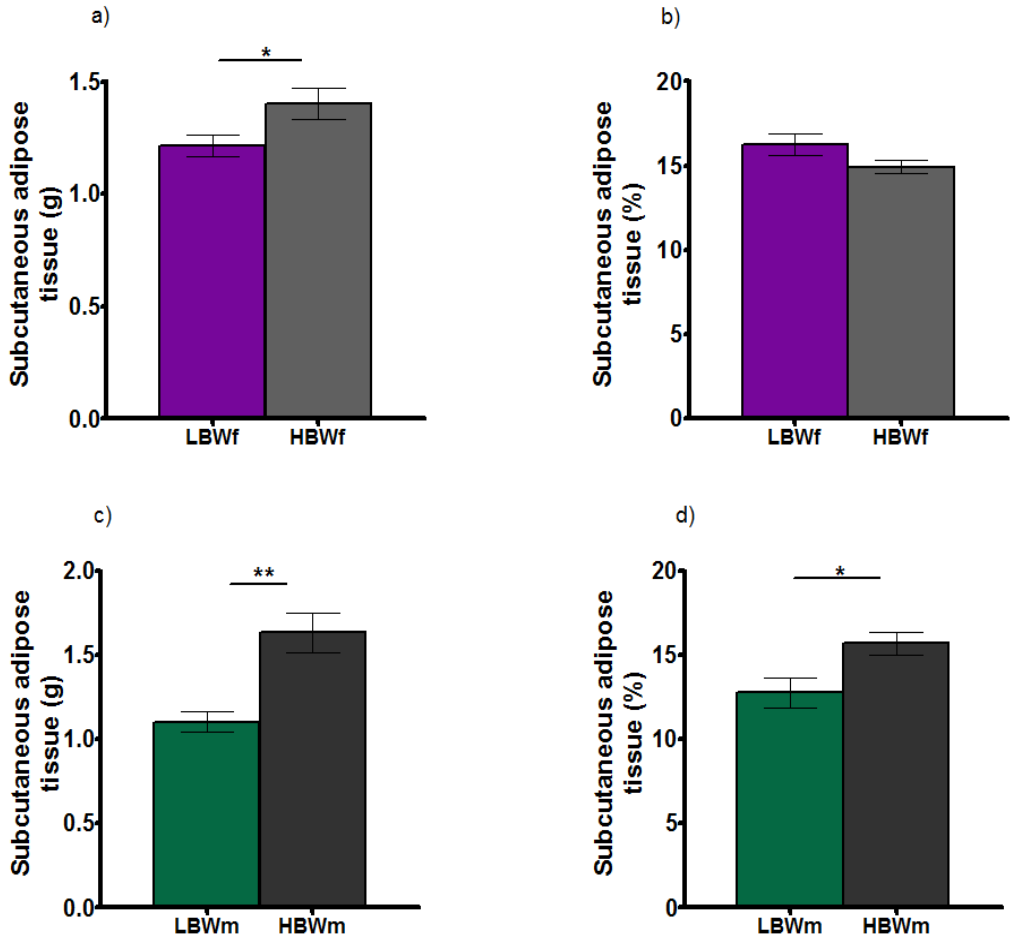

Figure 3.3.2.2 Subcutaneous adipose tissue content from female and male offspring at weaning. Subcutaneous adipose tissue content in grams a) and c) and as a percentage of body weight b) and d). Figures on the top correspond to females and figures below to males. Subcutaneous adipose tissue was quantified from MR images using segmentation analysis. Statistical analysis was performed using a two-tailed *unpaired student t-test.* Data presented as mean ±SEM. **LBWf** n=5; **HBWf** n=6; **LBWm** n=7; **HBWm** n=6. * p≤0.05, **p≤0.01.

Analysis of absolute internal adipose tissue showed no differences between groups (**LBWf**=0.785±0.132g; **HBWf**=0.556±0.07g; p=0.143; figure 3.3.2.3a). However, when normalising internal adipose tissue to body weight, differences were significant with **LBWf** having a higher internal adipose content (**LBWf=**10.43±1.789%; **HBWf**=5.985±0.742%; **p=0.036**; figure 3.3.2.3b).

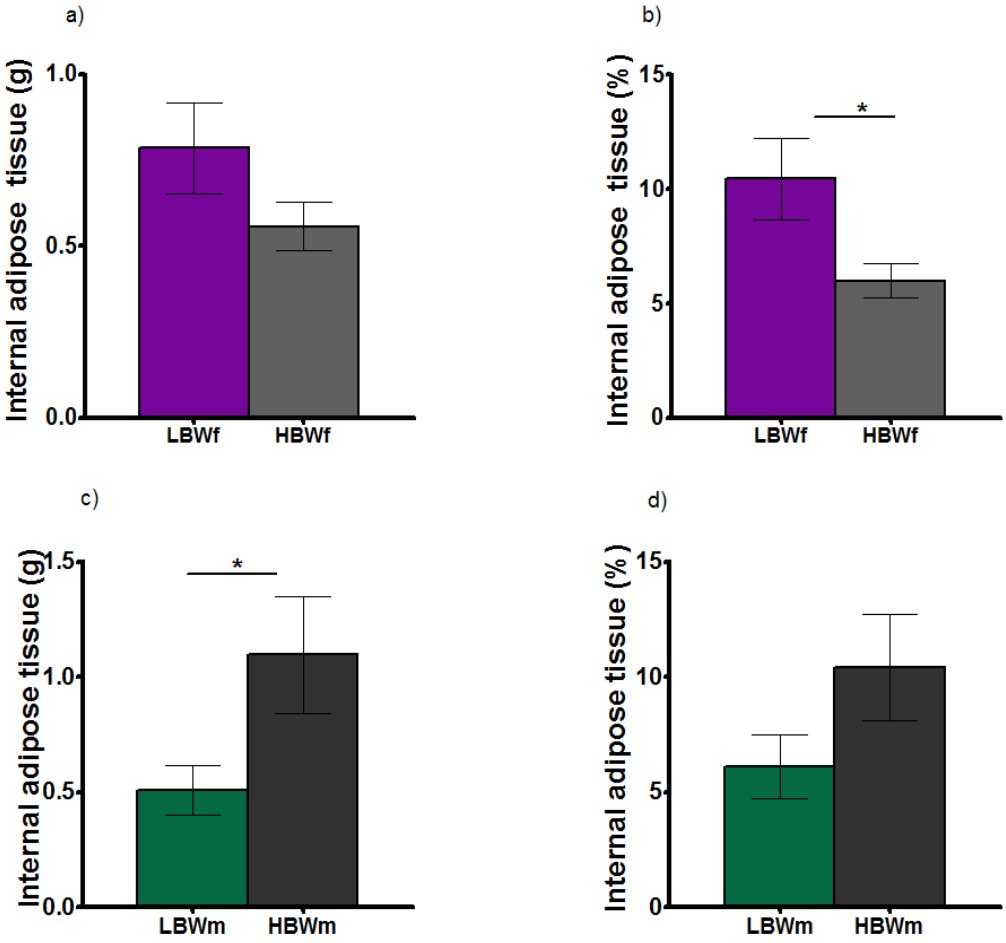

Figure 3.3.2.3 Internal adipose tissue content from female and male offspring at weaning. Internal adipose tissue content in grams a) and c) and as a percentage of body weight b) and d). Figures on the top correspond to females and figures below to males. Internal adipose tissue was quantified from MR images using segmentation analysis Statistical analysis was performed using a two-tailed *unpaired student t-test.* Data presented as mean ±SEM. **LBWf** n=5; **HBWf** n=6; **LBWm** n=7; **HBWm** n=6. * p≤0.05.

Assessment of internal:subcutaneous adipose tissue ratio showed an opposite pattern compared to males. **LBWf** had a significantly higher ratio compared to **HBWf** mice (**LBWf**=0.632±0.09; **HBWf**=0.399±0.044; **p=0.037**; figure 3.3.2.4).

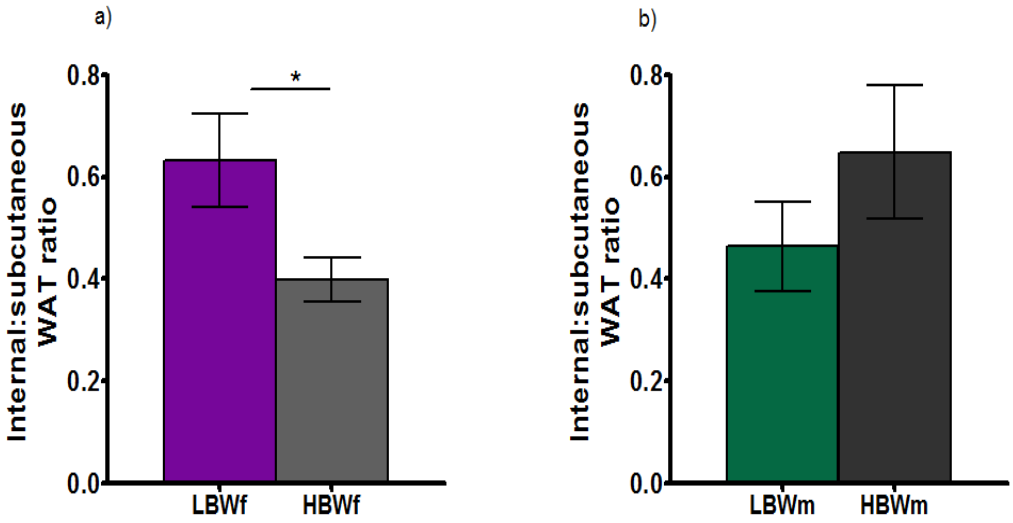

Figure 3.3.2.4 Internal to subcutaneous adipose tissue ratio from female and male offspring at weaning. Statistical analysis was performed using a two-tailed *unpaired student t-test.* Data presented as mean ±SEM. **LBWf** n=5; **HBWf** n=6; **LBWm** n=7; **HBWm** n=6. * p≤0.05.

The table below summarises the distribution of adipose tissue for both male and female mice (table 3.3.1).

	LBWm	HBWm	p	LBWf	HBWf	p	m vs. f difference
Total fat (g)	-	↑	✓	↑	-	x	✓
Total fat (%)	-	↑	x	↑	-	✓	✓
SAT (g)	-	↑	✓	-	↑	✓	x
SAT (%)	-	↑	✓	↑	-	x	✓
IAT (g)	-	↑	✓	↑	-	x	✓
IAT (%)	-	↑	x	↑	-	✓	✓
IAT:SAT ratio	-	↑	x	↑	-	✓	✓

Table 3.3.1 Summary table of the adipose tissue distribution in both male and female mice at weaning. Arrows indicate that the measurement was higher in the respective group compared to its counterpart. ✓indicates that the difference between groups was significantly different in p column (p value); in the last column indicates a different finding between genders. x indicates that the difference between groups was not significantly different in p column; in the last column indicates a similar finding between genders. IAT= internal adipose tissue; SAT= subcutaneous adipose tissue.

3.4 The Effects of Birth Weight and Accelerated Growth on Metabolic Markers at Weaning (3 Weeks)

Plasma samples were used to assess the impact of birth weight and accelerated growth in some metabolic markers.

3.4.1 Metabolic markers in Males

Whole blood glucose levels were significantly higher in **HBWm** compared to **LBWm** mice (**HBWm** =7.614±0.414 mmol/L, **LBWm=**6.375±0.372 mmol/L, **p=0.044**; figure 3.4.1.1).

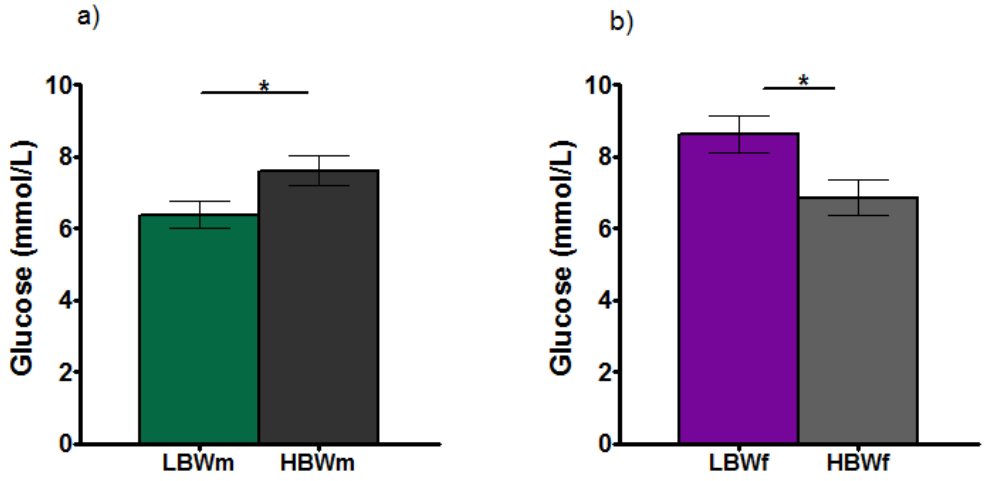

Figure 3.4.1.1 Whole blood glucose levels in male and female offspring at weaning. Glucose concentration units: mmol/L. Figure a) corresponds to males and figure b) to females. Statistical analysis was performed using a two-tailed *unpaired student t-test.* Data presented as mean ±SEM. **LBWm** n=7; **HBWm** n=7; **LBWf** n=8; **HBWf** n=7. * p≤0.05.

C-peptide plasma levels were not significantly different between groups (C-peptide: **LBWm=** 2153.073± 307.977pg/ml, **HBWm**=1959.828± 344.359 pg/ml, p=0.682; figure 3.4.1.2a), as insulin (**LBWm**=1146.124± 232.716pg/ml, **HBWm=**847.333± 199.027 pg/ml, p=0.344; figure 3.4.1.2b). and glucagon levels (**LBWm** =154.31± 19.772 pg/ml, **HBWm=**124.37± 8.315 pg/ml, p=0.195; figure 3.4.1.2c).

Interestingly, the incretin glucose-dependent insulinotropic peptide (GIP) was significantly higher in **LBWm** compared to **HBWm** mice (**LBWm** =338.485± 91.403 pg/ml, **HBWm=**116.036± 11.625 pg/ml, **p=0.045**; figure 3.4.1.2d). This may suggest that GIP greatly stimulated beta cells in the pancreas in order to produce the high amount of insulin that effectively reduced the level of glucose in peripheral circulation in **LBWm** mice.

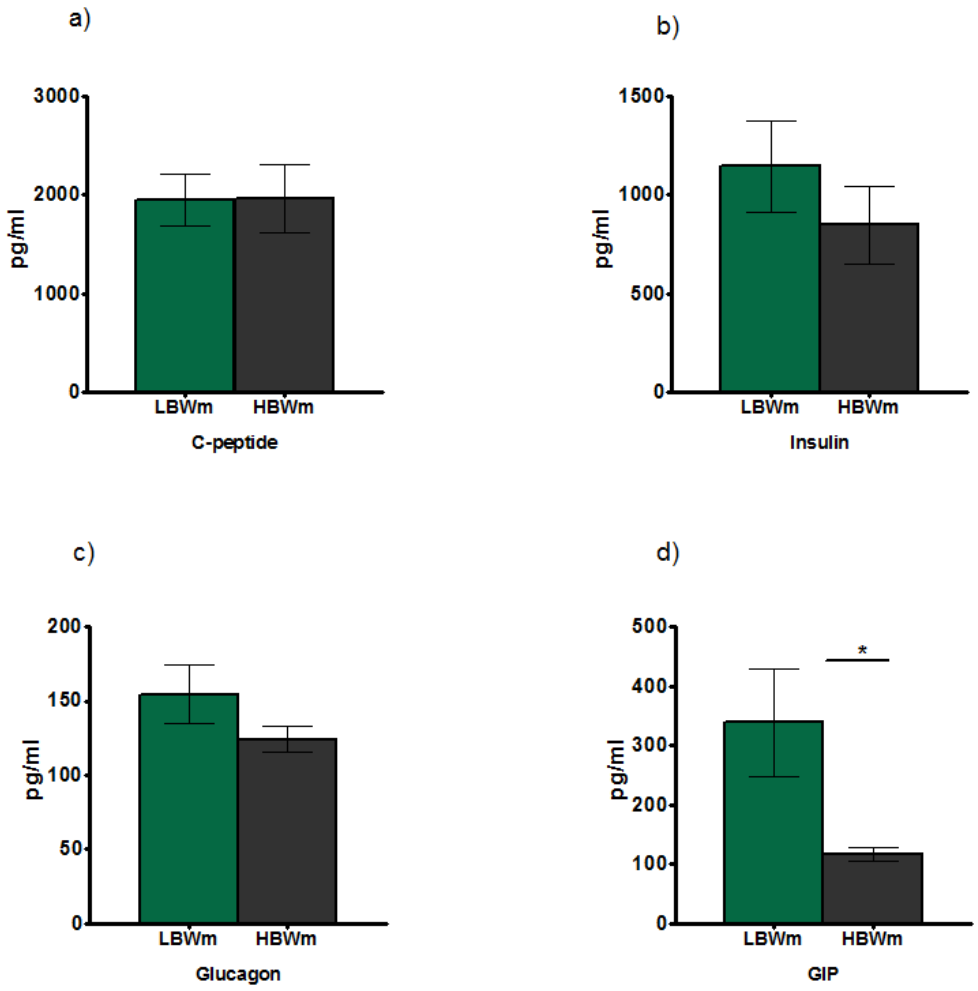

Figure 3.4.1.2 Metabolic markers related to pancreatic stimulation and function measured in male offspring at weaning. Metabolic markers were measured in plasma samples in 3 hour fasted male offspring at weaning. Plasma concentration of c-peptide a), insulin b), glucagon c), give information about the pancreatic secretion/stimulation of b cells (a,b) and delta cells (c) and GIP=glucose-dependent insulinotropic peptide gives information about intestinal stimulation of the pancreas to release insulin d) in **LBWm** and **HBWm** at weaning. Statistical analysis was performed using a two-tailed *unpaired student t-test.* Data are presented as mean ±SEM. **LBWm** n=7; **HBWm** n=7; * p≤0.05.

The appetite related gut hormone ghrelin did not show differences between groups (**LBWm=** 475.4± 96.687 pg/ml, **HBWm=** 553.151± 115.4 pg/ml, p=0.611; figure 3.4.1.3).

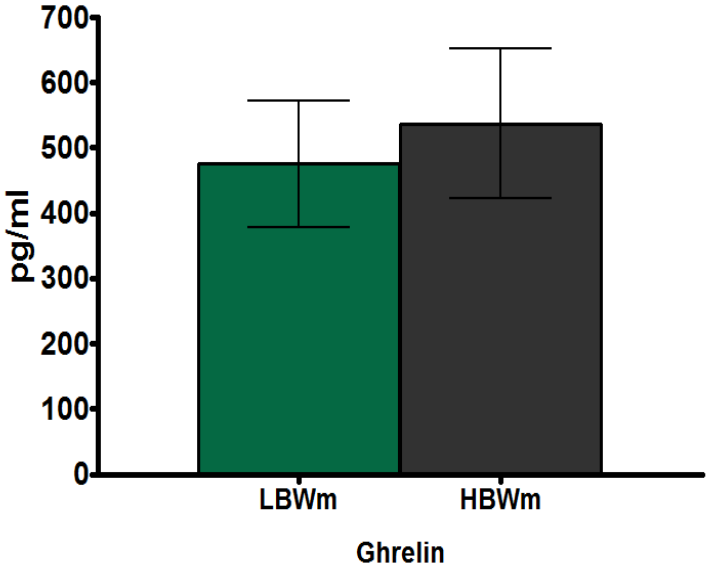

Figure 3.4.1.3 Appetite related gut hormone ghrelin levels in plasma measured in male offspring at weaning. Statistical analysis was performed using a two-tailed *unpaired student t-test*. Data presented as mean ±SEM. **LBWm** n=7; **HBWm** n=7.

Adipokines, including leptin and resistin were not significantly different between groups (**leptin**: **LBWm**=930.399± 269.01pg/ml, **HBWm**=503.232± 126.946 pg/ml, p=0.194; figure 3.4.1.4a; **resistin**: **LBWm**=10597.304± 1653.523 pg/ml, **HBWm**=10945.594± 1662.376 pg/ml, p=0.884; figure 3.4.1.4b). However, the proinflammatory adipokine monocyte chemotactic protein-1 (MCP-1) was significantly higher in **LBWm** mice (**LBWm=** 209.047± 13.786 pg/ml, **HBWm**=162.859± 10.873 pg/ml, **p=0.018**; figure 3.4.1.5a). Tumor Necrosis Factor alpha (TNF-alpha) and interleukin 6 (IL-6) plasma levels were not significantly different between groups (TNF-alpha: **LBWm=** 44.154± 3.399 pg/ml, **HBWm=**47.1019± 2.208 pg/ml, p=0.478; figure 3.4.1.5b; IL-6: **LBWm=** 66.083± 5.131 pg/ml, **HBWm=**75.642± 8.284 pg/ml, p=0.331; figure 3.4.1.5c).

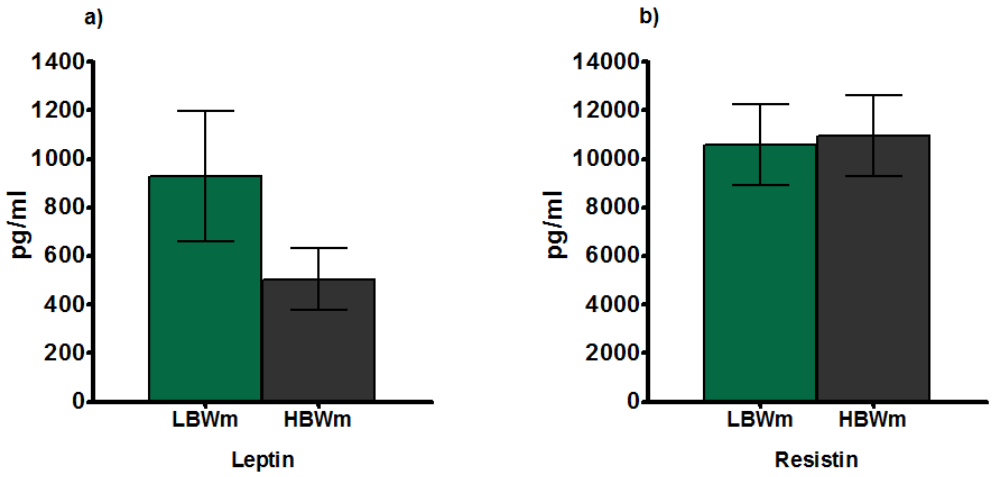

Figure 3.4.1.4 Adipokines leptin and resistin measured in male offspring at weaning. Plasma levels of leptin a) and resistin b) in **LBWm** and **HBWm** at week 3 of age. Statistical analysis was performed using a two-tailed *unpaired student t-test*. Data presented as mean ±SEM. **LBWm** n=7; **HBWm** n=7.

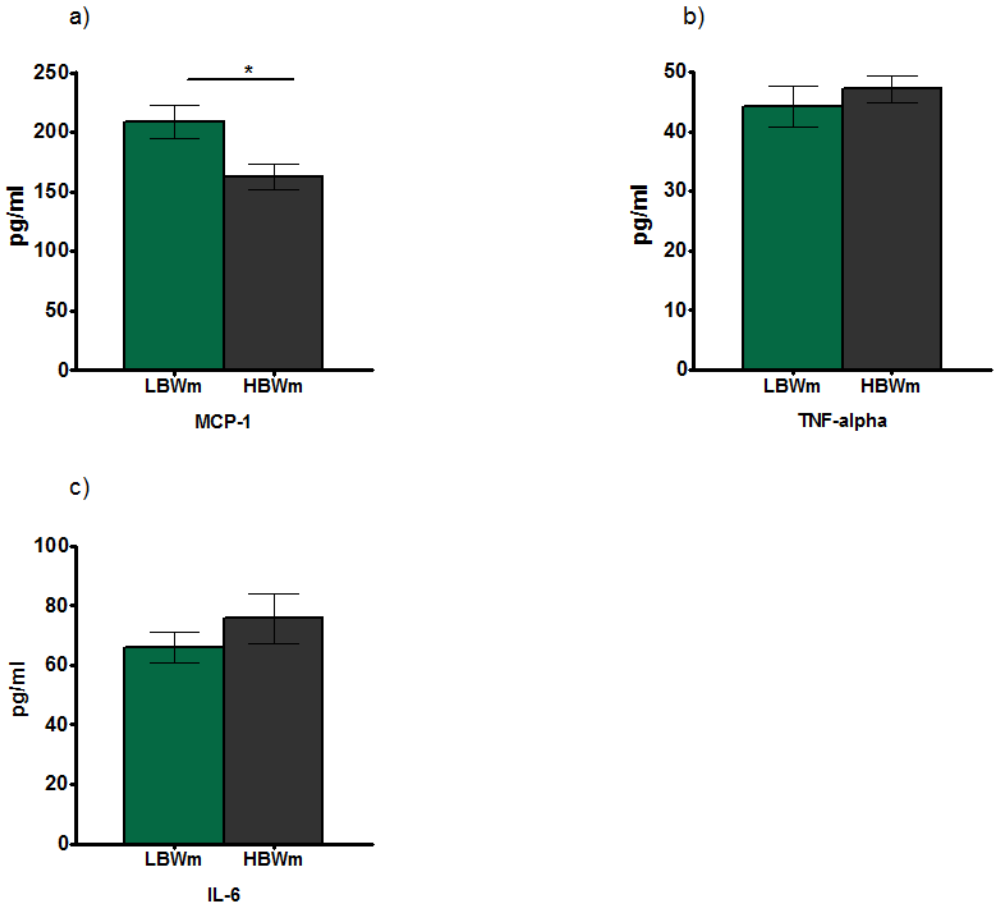

Figure 3.4.1.5 Proinflammatory adipokines measured in male offspring at weaning. Plasmatic levels of MCP-1= monocyte chemotactic protein-1 a), TNF-alpha= tumor necrosis factor alpha b) and IL-6= interleukin 6 c). Statistical analysis was performed using a two-tailed *unpaired student t-test*. Data presented as mean ±SEM. **LBWm** n=7; **HBWm** n=7; * p≤0.05.

3.4.2 Metabolic markers in Females

The metabolic effect of birth weight and accelerated growth in females was different from males in some of the metabolites analysed. Glucose levels in blood were significantly different between female groups, but in the opposite direction to that found in males, the **LBWf** mice had a higher level than **HBWf** mice (**LBWf**=8.629 ±0.532mmol/L, **HBWf** =6.867 ± 0.503mmol/L; **p=0.036;** figure 3.4.2.1).

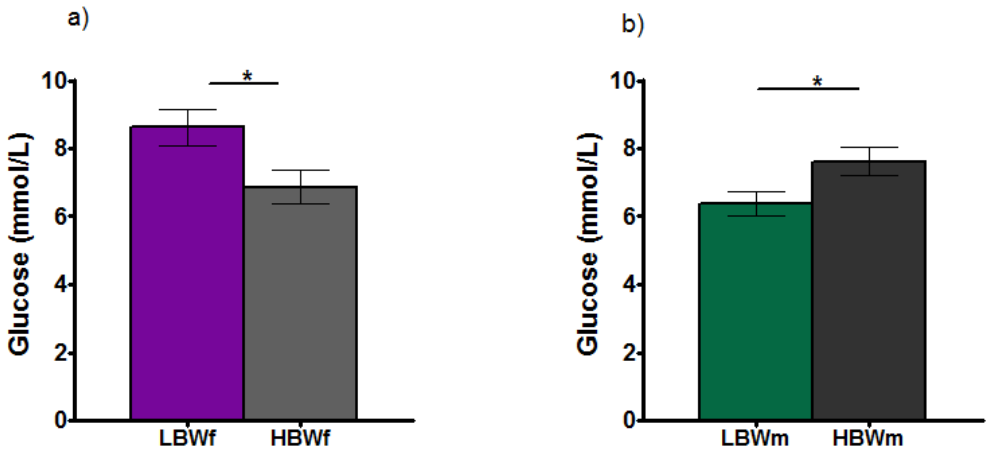

Figure 3.4.2.1 Whole blood glucose levels in female and male offspring at weaning. Glucose concentration units: mmol/L. Statistical analysis was performed using a two-tailed *unpaired student t-test.* Data presented as mean ±SEM. **LBWf** n=8; **HBWf** n=7; **LBWm** n=7; **HBWm** n=7. * p≤0.05.

Although levels of C-peptide were higher in **LBWm** compared to **HBWm** differences did not reach significance difference. On the contrary, in females, levels were substantially higher in **LBWf** compared to **HBWf** (**LBWf=**2949.769 ±431.534 pg/ml, **HBWf** =1467.631 ± 224.253 pg/ml; **p=0.019;** figure 3.4.2.2a). Also insulin reached statistical significance between females with higher values in **LBWf** mice (**LBWf=**1485 (1071,1934) pg/ml, **HBWf** =733.9 (446.8,888.8) pg/ml; **p=0.005;** figure 3.4.2.2b).

There was also a difference between male and female mice in the levels of glucagon. **LBWf** did have a substantial higher level of glucagon than **HBWf** (**LBWf=** 154.163±16.841, **HBWf** =111.167 ±5.699; **p=0.04;** figure 3.4.2.2c). Male mice did not show any significance.

A similar significant pattern in the levels of GIP was seen in males and females respective groups (**LBWf=** 414.553 ±108.553, **HBWf** =138.295 ± 29.731; **p=0.04**; figure 3.4.2.2d).

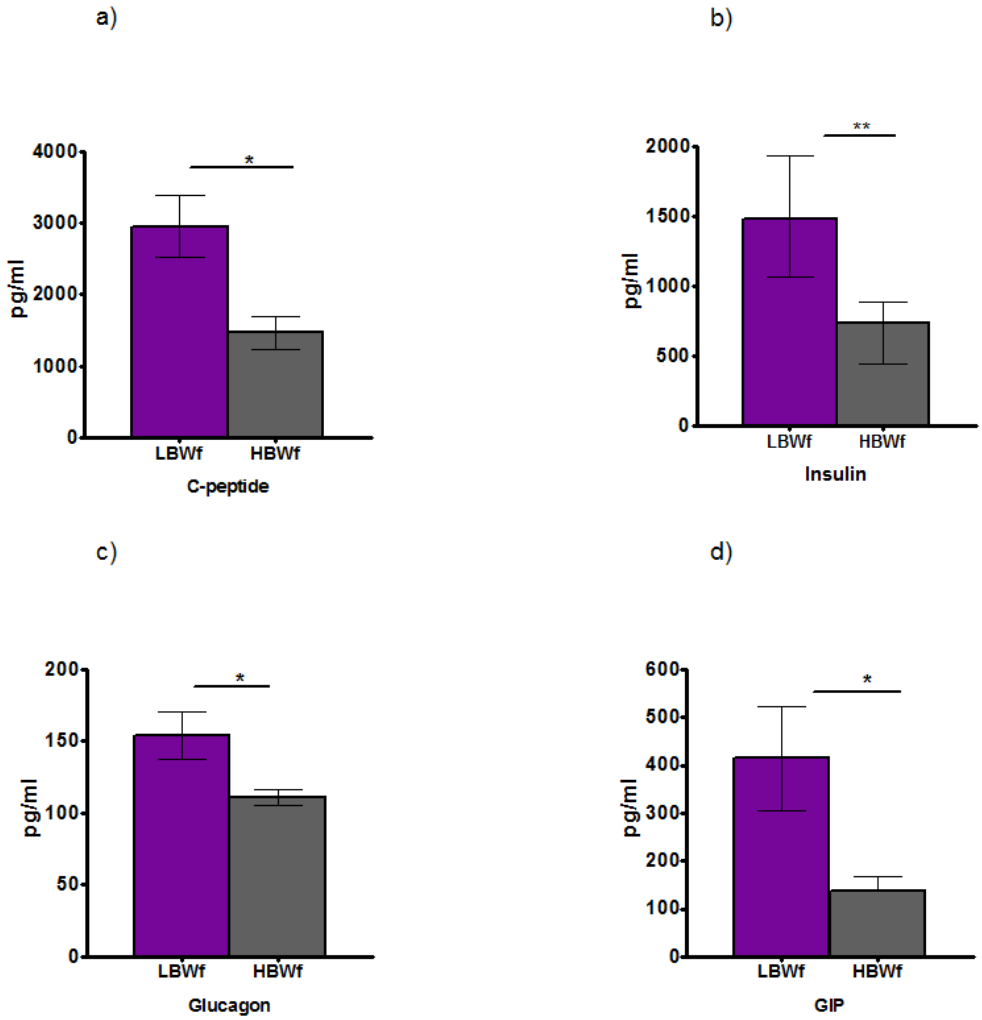

Figure 3.4.2.2 Metabolic markers related to pancreatic function and stimulation measured in female offspring at weaning. Plasma concentration of c-peptide a), insulin b), glucagon c), give information about the pancreatic secretion/stimulation of b cells (a,b) and delta cells (c) and GIP=glucose-dependent insulinotropic peptide gives information about intestinal stimulation of the pancreas to release insulin d) in **LBWf** and **HBWf** at weaning. Statistical analysis for c-peptide, glucagon and GIP was performed using a two-tailed *unpaired student t-test.* Statistical analysis for insulin was performed using a *Mann Whitney test*. Data presented as mean ±SEM for a), c) and d) and as median with interquartile range (25%,75%) for b. **LBWf** n=8; **HBWf** n=7; * p≤0.05, ** p p≤0.001.

The appetite related gut hormone ghrelin was not significantly different between female groups as in males (**LBWf=** 473.1 ±151.921 pg/ml, **HBWf=** 633.787± 165.692 pg/ml, p=0.611; figure 3.4.2.3).

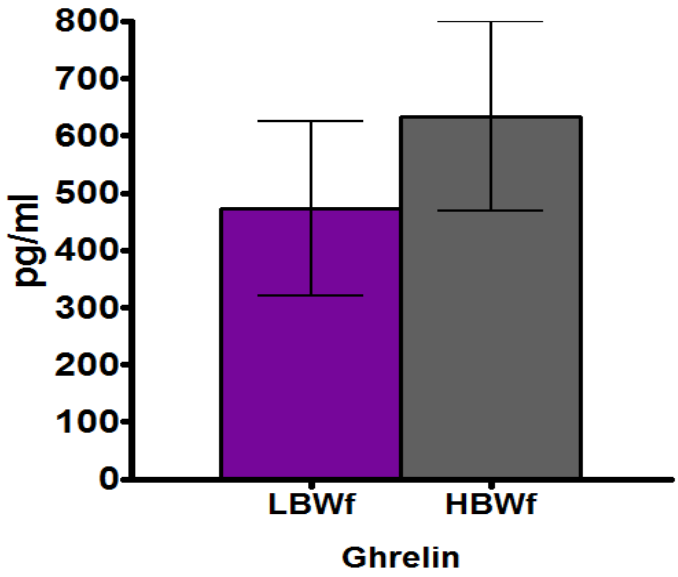

Figure 3.4.2.3 Appetite related gut hormone ghrelin (active) levels in plasma measured in female offspring at weaning. Statistical analysis was performed using a two-tailed *unpaired student t-test*. Data presented as mean ±SEM. **LBWf** n=8; **HBWf** n=7.

Adipokines such as leptin and resistin did not show significant differences between females groups as in male mice (leptin: **LBWf**=939.544 ±238.651 pg/ml, **HBWf**=772.575 ±276.334 pg/ml, p=0.654; figure 3.4.2.4a; resistin: **LBWf**=12232.751 ±2321.519 pg/ml, **HBWf**=13088.417 ±1380.059 pg/ml, p=0.765; figure 3.4.2.4b).

Whilst the levels of the proinflammatory adipokine MCP-1 were significant different between male groups, the level of lL-6 (also proinflammatory adipokine) was significantly different between females as well as MCP-1 (IL-6: **LBWf**= 76.925± 16.448 pg/ml, **HBWf**=33.215 ±9.131 pg/ml, **p=0.039**; figure 3.4.2.5a; MCP-1: **LBWf**= 162.7 ±4.459 pg/ml, **HBWf**=124.2 ±11.94 pg/ml, **p=0.023**; figure 3.4.2.5b). TNF-alpha was not significant different between female groups as between male groups (**LBWf**=42.199 ±3.923 pg/ml, **HBWf**=33.384 ±6.32 pg/ml, p=0.247; figure 3.4.2.5c).

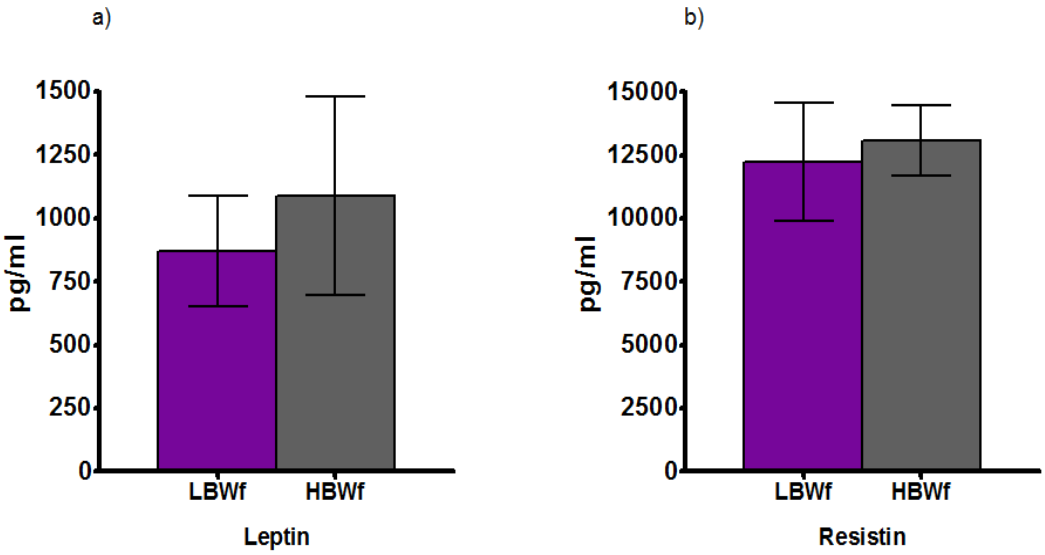

Figure 3.4.2.4 Adipokines leptin and resistin measured in female offspring at weaning. Plasma levels of leptin a) and resistin b) in **LBWf** and **HBWf** at week 3 of age. Statistical analysis was performed using a two-tailed *unpaired student t-test*. Data presented as mean ±SEM. **LBWf** n=8; **HBWf** n=7.

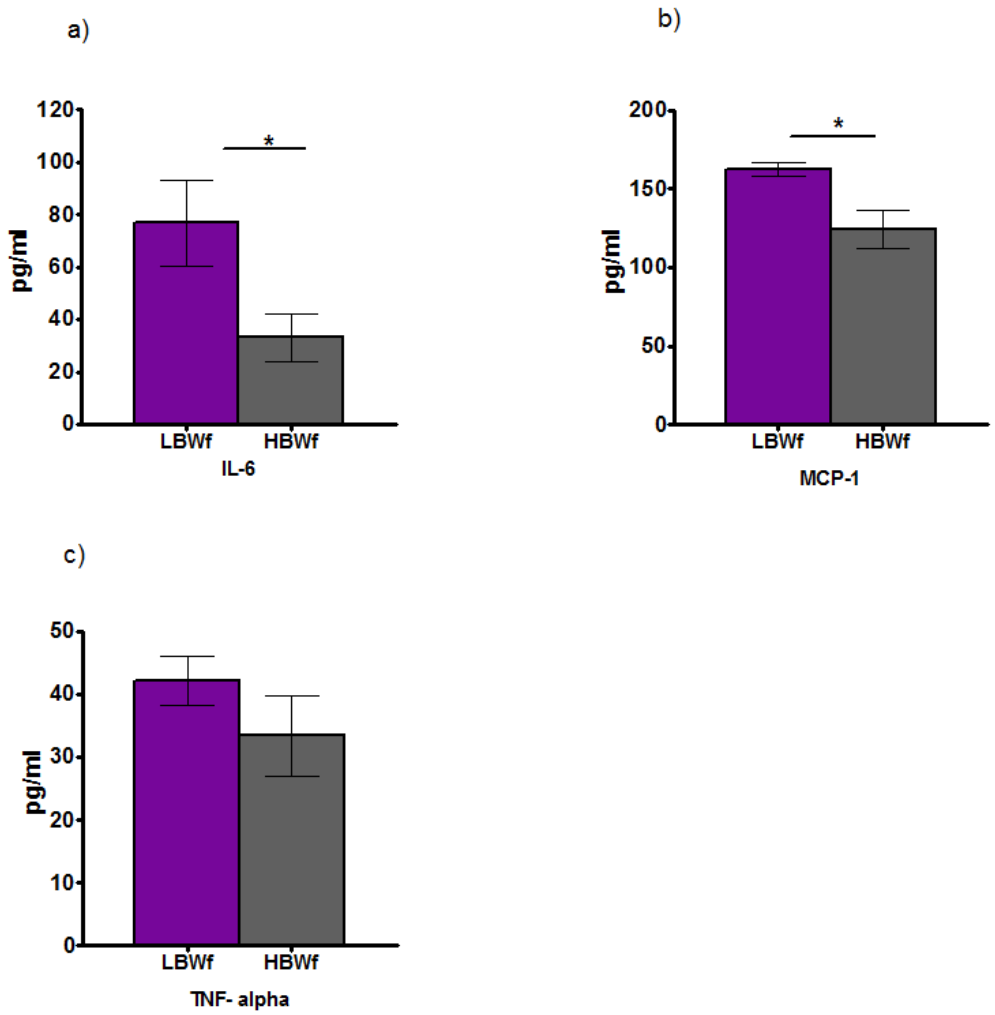

Figure 3.4.2.5 Proinflammatory adipokines measured in female offspring at weaning. Plasma levels of IL-6= interleukin 6 a), MCP-1= monocyte chemotactic protein-1 b) and TNF-alpha= tumor necrosis factor alpha c). Statistical analysis was performed using a two-tailed *unpaired student t-test*. Data presented as mean ±SEM. **LBWf** n=8; **HBWf** n=7; * p≤0.05.

The table below summarises the metabolic profiles for both male and female mice (table 3.4.1).

Metabolite	LBWm	HBWm	p	LBWf	HBWf	p	m vs. f difference
Glucose	-	↑	✓	↑	-	✓	✓
C-peptide	↑	-	x	↑	-	✓	✓
Insulin	↑	-	x	↑	-	✓	x
Glucagon	↑	-	x	↑	-	✓	x
GIP	↑	-	✓	↑	-	✓	x
Ghrelin	-	↑	x	-	↑	x	x
Leptin	↑	-	x	-	↑	x	✓
Resistin	-	↑	x	-	↑	x	x
MCP-1	↑	-	✓	↑	-	✓	x
TNF-a	-	↑	x	↑	-	x	✓
IL-6	-	↑	x	↑	-	✓	✓

Table 3.4.1 Summary of the metabolic profiles of both male and female mice. Arrows indicate that the measurement was higher in the respective group compared to its counterpart. ✓indicates that the difference between groups was significantly different in p column (p value); in the last column indicates a different finding between genders. x indicates that the difference between groups was not significantly different in p column; in the last column indicates a similar finding between genders.

3.5 The Effects of Birth weight and Accelerated Growth on Organs Mass at Weaning (3 Weeks)

At week 3, which was the end of the lactation, offspring was separated from their litters and mothers (weaning). As aforementioned, mice were classified as either Low birth weight male/female mice (**LBWm/f**) or High birth weight male/female (**HBWm/f**) mice. Pups were dissected at this time point as described previously in methods 2.1.4. Organ mass and proportional organ weights to current body weight were recorded and analysed.

3.5.1 Organ mass in Males

At weaning, **LBWm** mice had a lower body weight compared to the **HBWm** mice (**LBWm=** 8.566±0.12, **HBWm=** 9.916±0.12; **p<0.001**). Absolute weight in grams of heart, pancreas, kidneys, liver and muscle were significantly lighter in **LBWm** mice than **HBWm** mice (heart: **p=0.005**; pancreas: **p=0.038**; kidneys: **p=0.028**, liver: **p<0.001**; muscle: **p<0.001**; figure 3.5.1.1 and table 3.5.1.1). Brain, brown adipose tissue and spleen were not significantly different between groups (brain: p=0.275; brown adipose tissue: p=0.163; spleen: p=0.081; figure 3.5.1.1 and table 3.5.1.1).

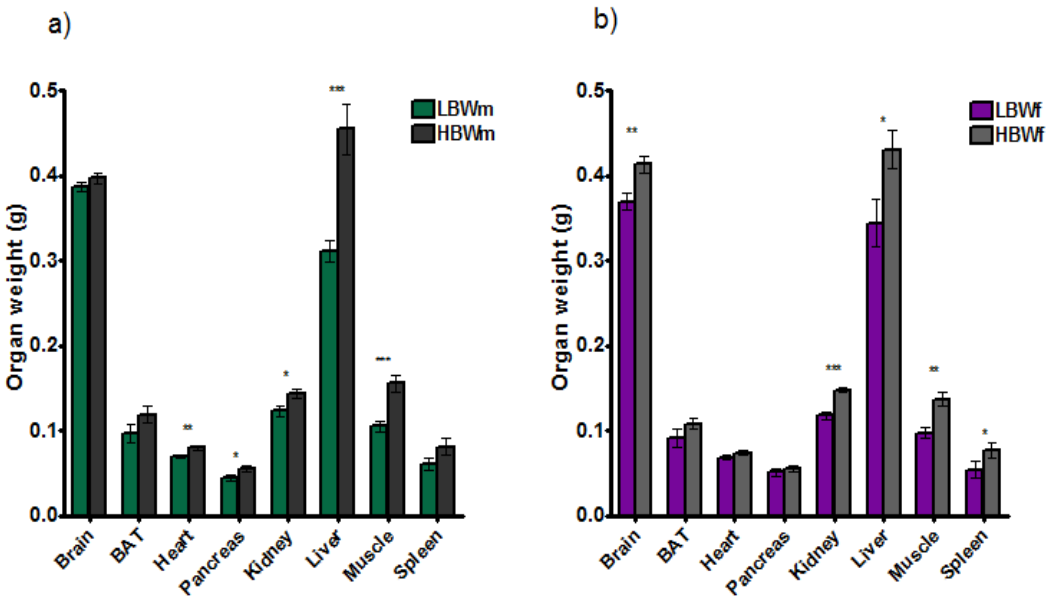

Figure 3.5.1.1 Organ mass of male and female offspring at week 3 (weaning). BAT=brown adipose tissue. Figure a) corresponds to males and figure b) to females. Statistical analysis was performed using a two-tailed *unpaired student t-test* per each organ. Data presented as mean ±SEM. **LBWm** n=10; **HBWm** n=10; **LBWf** n=9; **HBWf** n=9. * p≤0.05, ** p≤0.01, *** p≤0.001.

Upon normalising organ mass to current body weight, relative weight of brain was increased in **LBWm** in respect to **HBWm** mice (**p=0.001**; figure 3.5.1.2 and table 3.5.1.1), contrary to rest of organs weighed. Liver and muscle were still lighter in **LBWm** mice (liver: **p=0.015**; muscle: **p<0.001**; figure 3.5.1.2 and table 3.5.1.1). Furthermore, the relative weight of pancreas, kidneys and heart was not significantly different between groups (pancreas: p=0.732; kidneys: p=0.496; heart: p=0.161; figure 3.5.1.2 and table 3.5.1.1). Brown adipose tissue remained not significantly different between both groups (brown adipose tissue: p=0.995; figure 3.5.1.2 and table 3.5.1.1).

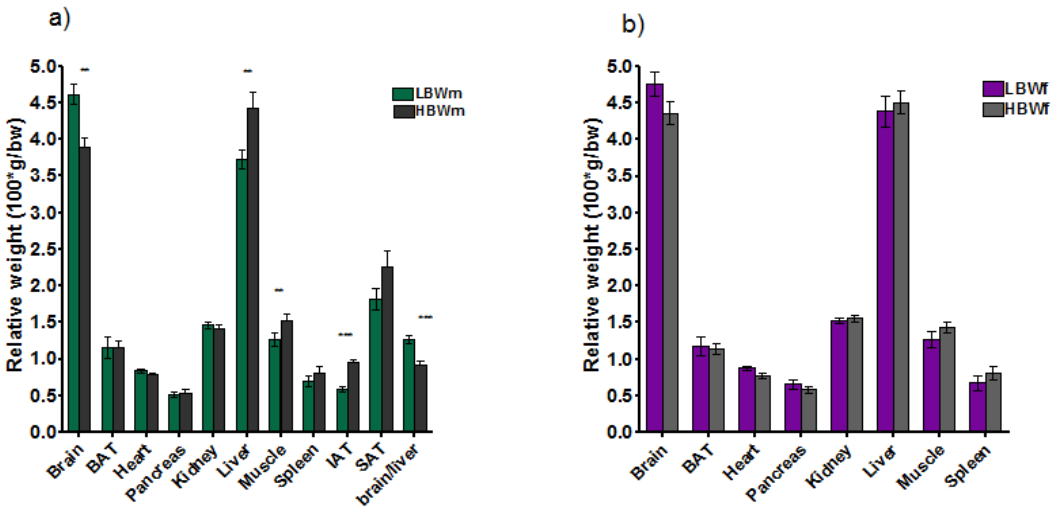

Figure 3.5.1.2 Organ mass as a percentage of current body weight of male and female offspring at week 3 (weaning). BAT=brown adipose tissue. Figure a) corresponds to males and figure b) to females. Statistical analysis was performed using a two-tailed *unpaired student t-test* with *Welch's correction* for unequal variances when necessary. Data presented as mean ±SEM. **LBWm** n=10; **HBWm** n=10; **LBWf** n=9; **HBWf** n=9. * p≤0.05, ** p≤0.01, *** p≤0.001.

	LBWm	HBWm	P value
Brain	**0.387±0.006**	**0.397±0.007**	0.275
Brain (%)	4.618±0.139	3.897±0.125	**0.001**
BAT	**0.097±0.011**	**0.119±0.01**	0.163
BAT (%)	1.16±0.142	1.161±1.371	0.995
Heart	**0.069±0.002**	**0.080±0.003**	**0.005**
Heart (%)	0.837±0.024	0.787±0.024	0.161
Pancreas	**0.044±0.003**	**0.055±0.003**	**0.038**
Pancreas (%)	0.522±0.038	0.542±0.041	0.732
Kidneys	**0.123±0.007**	**0.144±0.005**	**0.028**
Kidneys (%)	1.467±0.049	1.413±0.192	0.496
Liver	**0.311±0.013**	**0.455±0.003**	**<0.001**
Liver (%)	3.728±0.13	4.425±0.217	**0.013**
Muscle	**0.105±0.006**	**0.163±0.008**	**<0.001**
Muscle (%)	1.267±0.085	1.597±0.068	**0.008**
Spleen	**0.06±0.007**	**0.085±0.01**	0.081
Spleen (%)	0.705±0.072	0.826±0.099	0.343

Table 3.5.1.1 Absolute organ mass and as a percentage of current body weight of male offspring at week 3 (weaning). BAT=brown adipose tissue. Statistical analysis was performed using a two-tailed *unpaired student t-test*. Data presented as mean ±SEM. **LBWm** n=10; **HBWm** n=10.

3.5.2 Organ mass in Females

Female absolute weight in grams of kidneys, liver and muscle had a similar phenotype as in the male groups, being lighter in **LBWf** than **HBWf** ((kidneys: **p<0.001**; liver**: p=0.03**; muscle: **p=0.005**; figure and 3.5.2.1 and table 3.5.2.1). However, **LBWf** did have a significantly lighter brain than **HBWf,** whilst differences between males were not significantly different (**LBWf** vs. **HBWf** brain: **p=0.002**; figure and 3.5.2.1 and table 3.5.2.1. **LBWm** vs. **HBWm** brain: p=0.275; figure and 3.5.1.1 and table 3.5.1.1). Moreover, heart and pancreas were not significantly different between females groups, but were between the male groups being both lighter in **LBWm** mice (**LBWf** vs. **HBWf** heart: p=0.092; pancreas: p=0.484; figure and 3.5.2.1 and table 3.5.2.1 **LBWm** vs. **HBWm** heart: **p=0.005**; pancreas: **p=0.038**; figure and 3.5.1.1 and table 3.5.1.1). Spleen mass was nearly significant between males, with a lighter spleen in **LBWm** mice vs. **HBWm** (p=0.081; figure and 3.5.1.1 and table 3.5.1.1). On the contrary, it was significantly different between females, although it had the same pattern as seen in the male groups (**LBWf** spleen was lighter than **HBWf** mice; **p=0.021**). Brown adipose tissue was similarly not significant between both females and males (**LBWf** vs. **HBWf** brown adipose tissue: p=0.195; **LBWm** vs. **HBWm** brown adipose tissue: p=0.163).

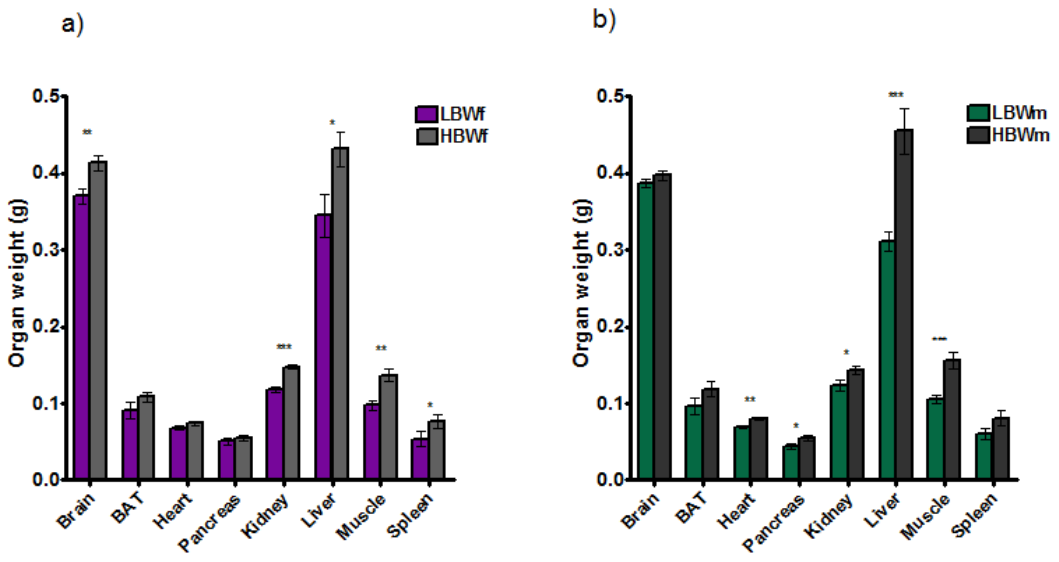

Figure 3.5.2.1 Organ mass of female and male offspring at week 3 (weaning). BAT=brown adipose tissue. Figure a) corresponds to females and figure b) to males. Statistical analysis was performed using a two-tailed *unpaired student t-test or Mann Whitney test* when necessary. Data presented as mean ±SEM. **LBWf** n=9; **HBWf** n=9; **LBWm** n=10; **HBWm** n=10. *p≤0.05, ** p≤0.01, *** p≤0.001.

After normalising organ mass to current body weight, **LBWf** had a heavier brain that **HBWf,** although it did not reach significance (**LBWf** vs. **HBWf** p=0.09 figure 3.5.2.2 and table 3.5.2.1). The rest of the organs did not show any differences between female groups (figure 3.5.2.2 and table 3.5.2.1).

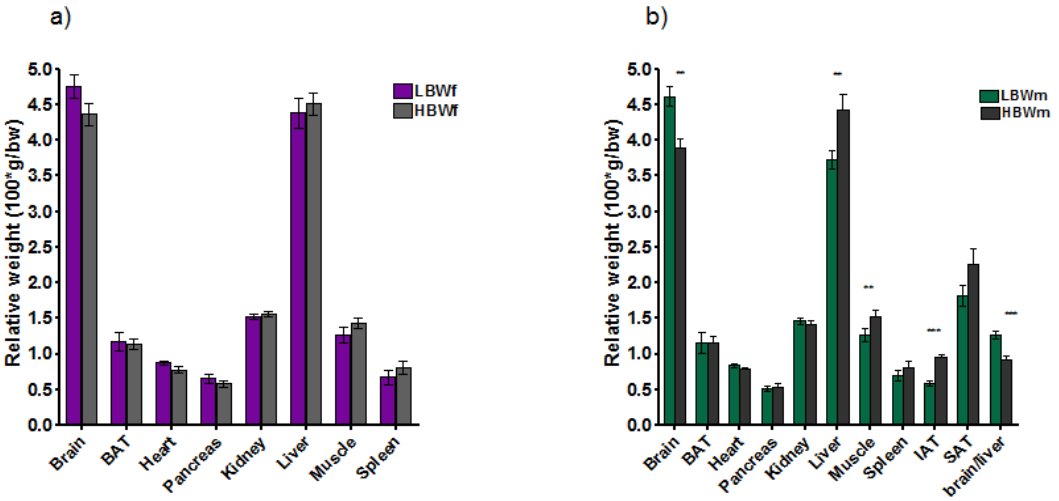

Figure 3.5.2.2 Organ mass as a percentage of current body weight of female and male offspring at week 3 (weaning). BAT=brown adipose tissue. Figure a) corresponds to females and figure b) to males. Statistical analysis was performed using a two-tailed *unpaired student t-test* with *Welch's correction* for unequal variances when necessary. Data presented as mean ±SEM. **LBWf** n=9; **HBWf** n=9; **LBWm** n=10; **HBWm** n=10. *p≤0.05, ** p≤0.01, *** p≤0.001.

	LBWf	HBWf	P value
Brain	**0.369±0.01**	**0.413±0.009**	**<0.001**
Brain (%)	4.759±0.166	4.363±0.147	0.094
BAT	**0.091±0.011**	**0.108±0.006**	0.195
BAT (%)	1.176±0.13	1.141±0.07	0.931
Heart	**0.068±0.003**	**0.075±0.002**	0.092
Heart (%)	0.837±0.024	0.787±0.024	**0.077**
Pancreas	**0.051±0.005**	**0.055±0.003**	0.484
Pancreas (%)	0.522±0.038	0.542±0.041	0.364
Kidneys	**0.118±0.004**	**0.148±0.003**	**<0.001**
Kidneys (%)	1.524±0.033	1.559±0.043	0.528
Liver	**0.344±0.028**	**0.431±00.022**	**0.028**
Liver (%)	4.384±0.207	4.509±0.159	0.638
Muscle	**0.097±0.007**	**0.137±0.008**	**<0.001**
Muscle (%)	**1.275±0.109**	**1.437±0.076**	0.242
Spleen	**0.054±0.009**	**0.082±0.008**	**0.021**
Spleen (%)	0.676±0.103	0.865±0.089	0.191

Table 3.5.2.1 Absolute organ mass and as a percentage of current body weight of female offspring at week 3 (weaning). BAT=brown adipose tissue. Statistical analysis was performed using a two-tailed *unpaired student t-test*. Data presented as mean ±SEM. **LBWf** n=9, **HBWf** n=9.

The table below summarises the organ masses for both male and female mice (table 3.5.2.2).

	LBWm	HBWm	p	LBWf	HBWf	p	m-f diff.
Brain (g)	-	↑	x	-	↑	✓	x
Brain (%)	↑	-	✓	↑	-	x	x
BAT (g)	-	↑	x	-	↑	x	x
BAT(%)	-	-	x	↑	-	x	✓
Heart (g)	-	↑	✓	-	↑	x	✓
Heart (%)	↑	-	x	↑	-	x	x
Pancreas (g)	-	↑	✓	-	↑	x	x
Pancreas (%)	-	↑	x	↑	-	x	✓
Kidneys (g)	↑	-	x	-	↑	✓	✓
Kidneys (%)	↑	-	x	-	↑	x	✓
Liver (g)	-	↑	✓	-	↑	✓	x
Liver (%)	-	↑	✓	-	↑	x	x
Muscle (g)	-	↑	✓	-	↑	✓	x
Muscle (%)	-	↑	✓	-	↑	x	x
Spleen (g)	-	↑	x	-	↑	✓	x
Spleen (%)	-	↑	x	-	↑	x	x

Table 3.5.2.2 Summary of organ masses results by gender. Arrows indicate that the measurement was higher in the respective group compared to its counterpart. ✓indicates that the difference between groups was significantly different in p column (p value); in the last column indicates a different finding between genders. x indicates that the difference between groups was not significantly different in p column; in the last column indicates a similar finding between genders.

3.6 The Effects of Birth weight and Accelerated Growth on White Adipose Tissue Mass at Weaning (3 Weeks)

White adipose tissue was (WAT) was extracted and subdivided into subcutaneous (SAT) and internal adipose tissue (IAT). IAT was further subdivided into gonadal, retroperitoneal and mesenteric fat depots.

3.6.1 White adipose tissue mass in Males

Total WAT was heavier in **HBWm** mice than in **LBWm** (**p=0.003**, figure, 3.6.1.1 and table 3.6.1.1) as well as all the regional white fat depots (SAT: **p=0.014**, gonadal fat: **p<0.001**, retroperitoneal fat: **p=0.043**, mesenteric fat: **p=0.035**; IAT: **p<0.001**; figure 3.6.1.1 and table 3.6.1.1).

After normalisation to current body weight (relative body weight), total WAT, gonadal and IAT remained heavier in **HBWm** mice compared to **LBWm** mice (total WAT: **p=0.023**, gonadal: **p<0.001**, IAT: **p<0.001**; figure 3.6.1.2, and table 3.6.1.1). On the contrary, SAT, retroperitoneal and mesenteric fat were not significantly different between groups (SAT: p=0.119, retroperitoneal fat: p=0.121, mesenteric: p=0.131; figure 3.6.1.2 table 3.6.1.1).

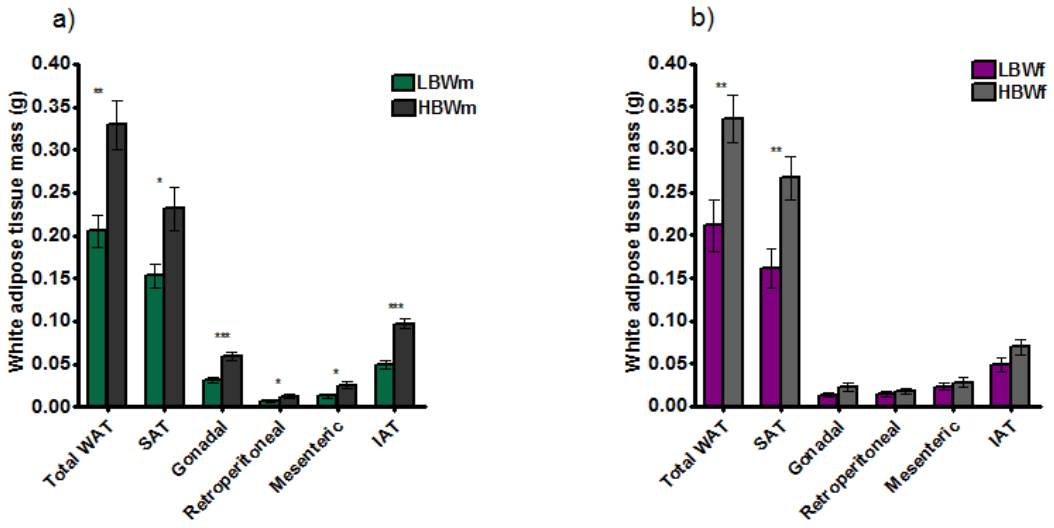

Figure 3.6.1.1 Absolute white adipose tissue mass of male and female offspring at week 3 (weaning). Figure a) corresponds to males and figure b) to females. Statistical analysis was performed using a two-tailed *unpaired student t-test*. Data presented as mean ±SEM. **LBWm** n=10; **HBWm** n=10; **LBWf** n=9; **HBWf** n=9. *p≤0.05, *** p≤0.001. WAT= white adipose tissue, SAT=subcutaneous adipose tissue, IAT=internal adipose tissue (as the sum of gonadal, retroperitoneal and mesenteric fat).

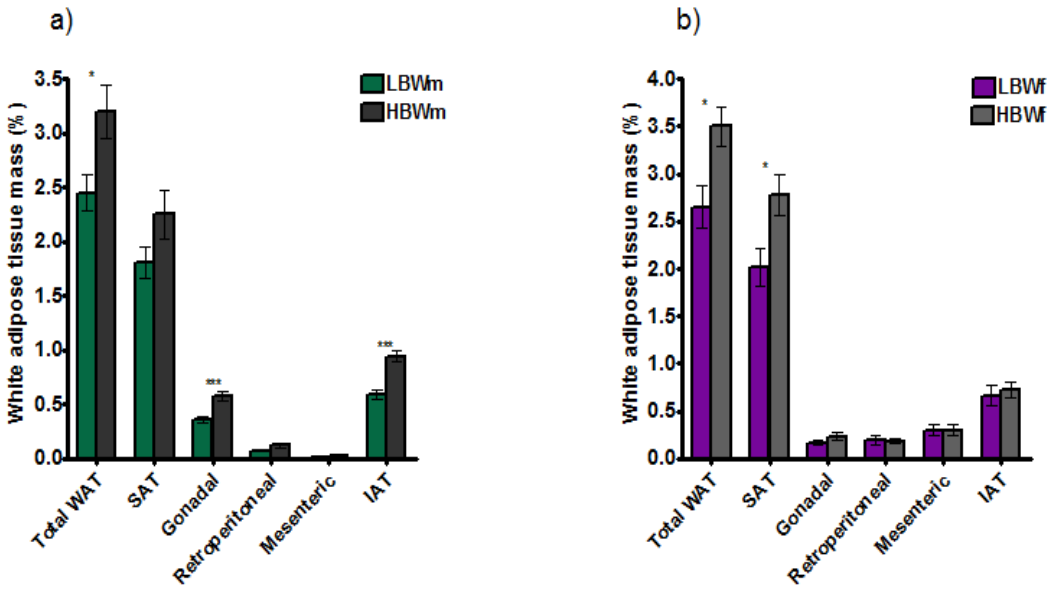

Figure 3.6.1.2 Relative white adipose tissue mass of male and female offspring at week 3 (weaning). Figure a) corresponds to males and figure b) to females. Statistical analysis was performed using a two-tailed *unpaired student t-test*. Data presented as mean ±SEM. **LBWm** n=10; **HBWm** n=10; **LBWf** n=9; **HBWf** n=9. *p≤0.05, *** p≤0.001. WAT= white adipose tissue, SAT=subcutaneous adipose tissue, IAT=internal adipose tissue (as the sum of gonadal, retroperitoneal and mesenteric fat).

	LBWm	HBWm	P value
Total WAT	**0.205±0.019**	**0.329±0.028**	**0.003**
Total WAT %	2.45±0.162	3.199±0.245	**0.023**
SAT	**0.153±0.014**	**0.231±0.025**	**0.014**
SAT%	1.812±0.145	2.252±0.225	0.119
Gonadal	**0.031±0.003**	**0.059±0.004**	**<0.001**
Gonadal%	0.362±0.029	0.577±0.038	**<0.001**
Retroperitoneal	**0.006±0.001**	**0.013±0.003**	**0.043**
Retroperitoneal%	0.078±0.011	0.121±0.024	0.121
Mesenteric	**0.013±0.002**	**0.025±0.004**	**0.035**
Mesenteric%	0.162±0.031	0.249±0.043	0.131
IAT	**0.053±0.006**	**0.097±0.006**	**<0.001**
IAT%	0.591±0.044	0.947±0.045	**<0.001**
IAT/SAT	**0.335±0.035**	**0.453±0.042**	**0.047**

Table 3.6.1.1 White adipose tissue mass and as a percentage of current body weight of male offspring at week 3 (weaning). SAT= subcutaneous adipose tissue, IAT= internal adipose tissue (as the sum of gonadal, retroperitoneal and mesenteric fat depots). Statistical analysis was performed using a two-tailed *unpaired student t-test*. Data presented as mean ±SEM. **LBWm** n=10, **HBWm** n=10.

A comparison of the ratio of IAT to SAT tissue mass between the groups showed that **LBWm** had a lower ratio compared to **HBWm** (**p=0.047**, table 3.6.1.1). This suggests that an enhanced adipose tissue mass was mostly related to a higher internal fat deposition in **HBWm** vs. **LBWm.**

The distribution of different WAT depots as a percentage of the total WAT showed that **HBWm** had a significantly higher gonadal fat content in comparison to **LBWm** (**HBWm**=18.51±1.213%; **LBWm**=14.33±0.874%, **p=0.014**; figure 3.6.1.3). On the contrary, the percentage of subcutaneous fat mass was significantly reduced in **HBWm** mice than **LBWm** mice (**HBWm=** 69.31±1.963%; **LBWm=** 75.3±1.985%; **p=0.047**). The distribution of the retroperitoneal and mesenteric fat depots was not different between groups (figure 3.6.1.3). This showed that although differences in relative SAT were not evident in both groups, the distribution of WAT showed that **LBWm** did have a preference for SAT deposition compared to other compartments and **HBWm** for IAT, especially gonadal fat deposition.

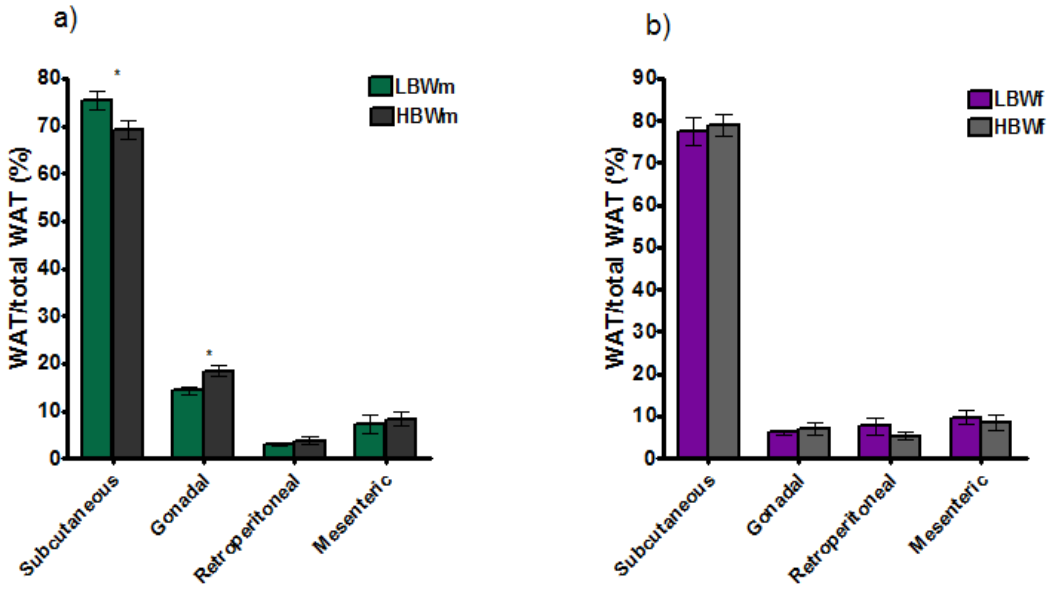

Figure 3.6.1.3 Relative distribution of white adipose tissue mass as a percentage of total WAT of male and female offspring at week 3 (weaning). Figure a) corresponds to males and figure b) to females. Statistical analysis was performed using a two-tailed *unpaired student t-test*. Data presented as mean ±SEM. **LBWm** n=10; **HBWm** n=10; **LBWf** n=9; **HBWf** n=9. *p≤0.05.

3.6.2 White adipose tissue mass in Females

In the female groups, only total WAT and absolute SAT mass were significantly higher in **HBWf** than in **LBWf** (WAT: **p=0.008**; SAT: **p=0.007**; figure 3.6.2.1 and table 3.6.2.1). Moreover, this difference was still significant when normalising to body weight (WAT: **p=0.013**; SAT: **p=0.017**; figure 3.6.2.2 and table 3.6.2.1). In general, females had more total WAT% than their respective male group and subcutaneous adipose tissue than males.

Although absolute mass of gonadal, retroperitoneal and mesenteric tended to be less in **LBWf** as in **LBWm** (figure 3.6.2.1 and table 3.6.2.1), differences were not significantly different between females. This pattern was maintained for gonadal and retroperitoneal fat when normalising to body weight but differences did not reach significance. However, mesenteric fat was similar between groups contrary to the males groups. In general, female mice had less gonadal than males (**LBWf=** 53.315% less gonadal fat than **LBWm** mice and **HBWf=** 59.272 % less than **HBWm** mice) but more retroperitoneal fat than males (**LBWf=** 89.743% more than **LBWm** and **HBWf=** 71.074% more than **HBWm**) as well as mesenteric fat (**LBWf=** 87.037% more than **LBWm** and **HBWf=** 19.277% more than **HBWm**).

IAT in both, absolute values (g) and relative values (%), was not significantly different between groups (table 3.6.2.1), contrary to the respective male groups. Interestingly, IAT% in **LBWf** mice was approximately 12.69% more than in **LBWm** mice but **HBWf** had 23.44% less IAT% than **HBWm.**

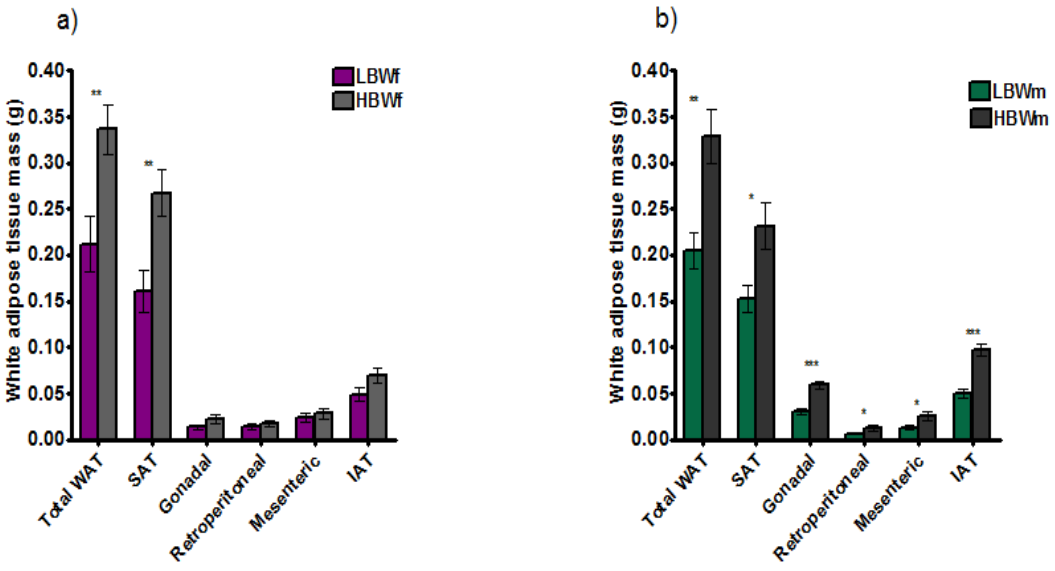

Figure 3.6.2.1 Absolute white adipose tissue mass of female and male mice offspring at week 3 (weaning). Figure a) corresponds to females and figure b) to males. Statistical analysis was performed using a two-tailed *unpaired student t-test*. Data presented as mean ±SEM. **LBWf** n=9; **HBWf** n=9; **LBWm** n=10; **HBWm** n=10. *p≤0.05, **p≤0.01, ***p≤0.001. WAT= white adipose tissue, SAT=subcutaneous adipose tissue, IAT=internal adipose tissue (as the sum of gonadal, retroperitoneal and mesenteric fat).

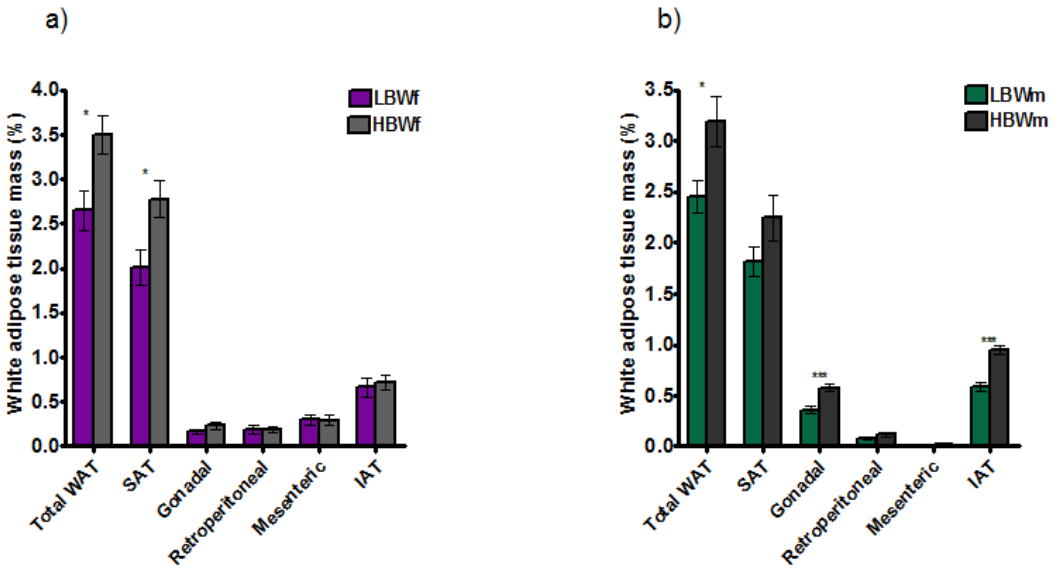

Figure 3.6.2.2 Relative white adipose tissue mass of female and male offspring at week 3 (weaning). Figure a) corresponds to females and figure b) to males. Statistical analysis was performed using a two-tailed *unpaired student t-test*. Data presented as mean ±SEM. **LBWf** n=9; **HBWf** n=9; **LBWm** n=10; **HBWm** n=10. *p≤0.05, ***p≤0.001. WAT= white adipose tissue, SAT=subcutaneous adipose tissue, IAT=internal adipose tissue (as the sum of gonadal, retroperitoneal and mesenteric fat).

	LBWf	HBWf	P value
Total WAT	**0.212±0.03**	**0.336±0.027**	**0.008**
Total WAT%	2.654±0.222	3.501±0.201	**0.013**
SAT	**0.161±0.022**	**0.267±0.025**	**0.007**
SAT%	2.01±0.198	2.781±0.21	**0.017**
Gonadal	**0.014±0.002**	**0.023±0.004**	0.092
Gonadal%	0.169±0.023	0.235±0.044	0.198
Retroperitoneal	**0.015±0.003**	**0.018±0.003**	0.491
Retroperitoneal%	0.194±0.048	0.187±0.03	0.902
Mesenteric	**0.024±0.004**	**0.028±0.005**	0.528
Mesenteric%	0.303±0.06	0.297±0.059	0.948
IAT	**0.052±0.008**	**0.069±0.009**	0.164
IAT%	0.666±0.106	0.725±0.086	0.669
IAT/SAT	**0.358±0.079**	**0.274±0.041**	0.344

Table 3.6.2.1 White adipose tissue mass and as a percentage of current body weight of female offspring at week 3 (weaning). SAT= subcutaneous adipose tissue, IAT= internal adipose tissue (as the sum of gonadal, retroperitoneal and mesenteric fat depots). Statistical analysis was performed using a two-tailed *unpaired student t-test*. Data presented as mean ±SEM. **LBWf** n=9, **HBWf** n=9.

Contrary to what was seen in male groups, a comparison of the ratio IAT/SAT showed no difference between groups (p=0.344; table 3.6.2.1). **LBWf** had a 6.866% higher ratio than **LBWm,** but **HBWf** had a 39.514% lower ratio than **HBWm** mice.

The distribution of different WAT depots as a percentage of the total WAT did not show significant differences between the groups, opposite to what was seen in the male groups (figure 3.6.2.3). SAT was the adipose tissue with the highest percentage from the total WAT in both genders. The difference between **LBWf** and **LBWm** was 0.47%, where females had the highest percentage (**LBWf=** 75.77±3.389%, **LBWm**=75.30±1.985%). A 9.64% difference was seen between **HBWf** and **HBWm** (**HBWf**=78.95±2.441%; **HBWm**=69.31±1.963%), as well as similar trend in deposition as in **LBW** mice. However, gonadal adipose tissue was preferentially accumulated in males than in females with a 133% increment compared to females (**LBWf**=6.142±0.522% vs. **LBWm**=14.33±0.874%), and a 161.8% more deposition in **HBWm** in respect to **HBWf** mice **(HBWf**=7.071±1.381% vs. **HBWm**=18.51±1.213%).

Retroperitoneal (**LBWm=** 3.076±0.343%, **HBWm=** 3.828±0.682%; **LBWf=** 6.856±1.939%, **HBWf**=5.746±0.87%) as well as mesenteric distribution (**LBWm**=7.295±1.827%, **HBWm**=8.349±1.54%; **LBWf**=11.30±2.193%, **HBWf**=8.607±1.789%) was augmented in females in respect to the respective male groups.

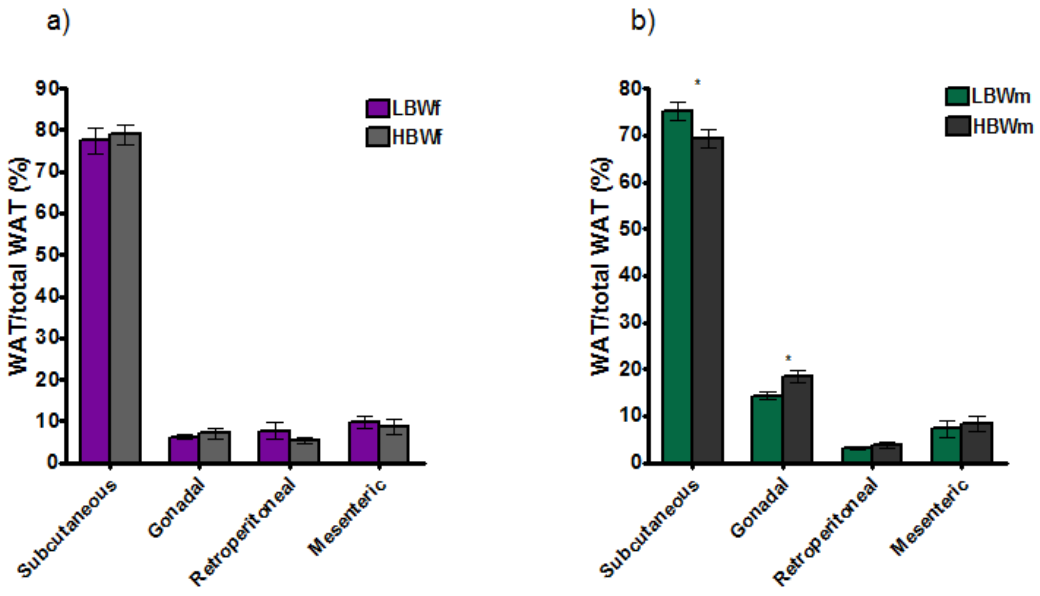

Figure 3.6.2.3 Relative distribution of white adipose tissue mass as a percentage of total WAT of female and male offspring at week 3 (weaning). Figure a) corresponds to females and figure b) to males. Statistical analysis was performed using a two-tailed *unpaired student t-test*. Data presented as mean ±SEM. **LBWf** n=9; **HBWf** n=9; **LBWm** n=10; **HBWm** n=10. *p≤0.05. WAT= white adipose tissue.

The table below summarises the white adipose tissue masses for both male and female mice (table 3.6.3).

	LBWm	HBWm	p	LBWf	HBWf	p	m-f diff.
WAT (g)	-	↑	✓	-	↑	✓	x
WAT (%)	-	↑	✓	-	↑	x	x
SAT (g)	-	↑	✓	-	↑	✓	x
SAT(%)	-	↑	x	-	↑	x	x
Gonadal (g)	-	↑	✓	-	↑	x	x
Gonadal (%)	-	↑	✓	-	↑	x	x
Retrop. (g)	-	↑	✓	-	↑	x	x
Retrop.(%)	-	↑	x	↑	-	x	✓
Mesent. (g)	-	↑	✓	-	↑	x	x
Mesent.(%)	-	↑	x	↑	-	x	✓
IAT (g)	-	↑	✓	-	↑	x	x
IAT (%)	-	↑	✓	-	↑	x	x
IAT/SAT	-	↑	✓	↑	-	x	✓

Table 3.6.3 Summary of white adipose tissue depots findings by gender. Arrows indicate that the measurement was higher in the respective group compared to its counterpart. ✓indicates that the difference between groups was significantly different in p column (p value); in the last column indicates a different finding between genders. x indicates that the difference between groups was not significantly different in p column; in the last column indicates a similar finding between genders.

3.7 The Effects of Birth Weight and Accelerated Growth on Adipose Tissue Gene Expression at Weaning (3 Weeks)

Subcutaneous adipose tissue was harvested and processed as mentioned in section 2.4.8. qPCR was used to assess changes in adipose tissue gene expression. mRNA expression of genes involved in insulin signaling, adipocyte differentiation, lipid metabolism, and non-shivering thermogenesis in white adipose tissue were determined.

In the insulin pathway, insulin receptor substrate 1 (IRS-1), Phosphatidylinositol-3 Kinase catalytic subunit p110b (PIK3/p110b), protein kinase C isoform zeta (PKC-Z), and Glucose Transporter 4 (GLUT4) genes were assessed.

Key transcriptional regulators of adipogenesis and lipogenesis such as Peroxisome Proliferator Activated Receptor Gamma 2(PPARg-2), CCAAT/enhancer-binding protein alpha (CEBPa), and Sterol Regulatory Element Binding Protein 1c (SREBP1c) were analysed. SREBP1c downstream target gene Fatty Acid Synthase (FASN) and Lipoprotein Lipase (LPL) expression were also analysed. To assess mobilization of lipids from adipose tissue to circulation (lipolytic function) mRNA expression of Hormone Sensitive Lipase (HSL) was determined.

To investigate changes in mitochondrial biogenesis and adaptive thermogenesis, Peroxisome Proliferator-activated Receptor Gamma Coactivator 1 alpha (PGC1a) and its downstream target gene Uncoupling Protein 1 (UCP1) expression were evaluated. PGC1a expression and activity are regulated directly by the beta-adrenergic signaling. Adrenergic expression was also assessed measuring mRNA levels of beta-3 adrenergic receptor (adrb3).

3.7.1 Adipose tissue expression of insulin signaling related genes at weaning (3 weeks)

3.7.1.1 Expression of insulin signaling related genes in Males

mRNA expression of IRS-1, (**p<0.001**), PIK3/p110b (**p<0.001**), Akt2 (**p<0.001**), PKC-Z (**p=0.027**) and GLUT4 (**p<0.001**) were significantly higher in **LBWm** mice than in **HBWm** mice (figure 3.6.1). This data suggests that transcriptional insulin signaling was highly activated in SAT in **LBWm**, which could contribute to the increment in SAT mass in this group of mice (figure 3.7.1.1.1).

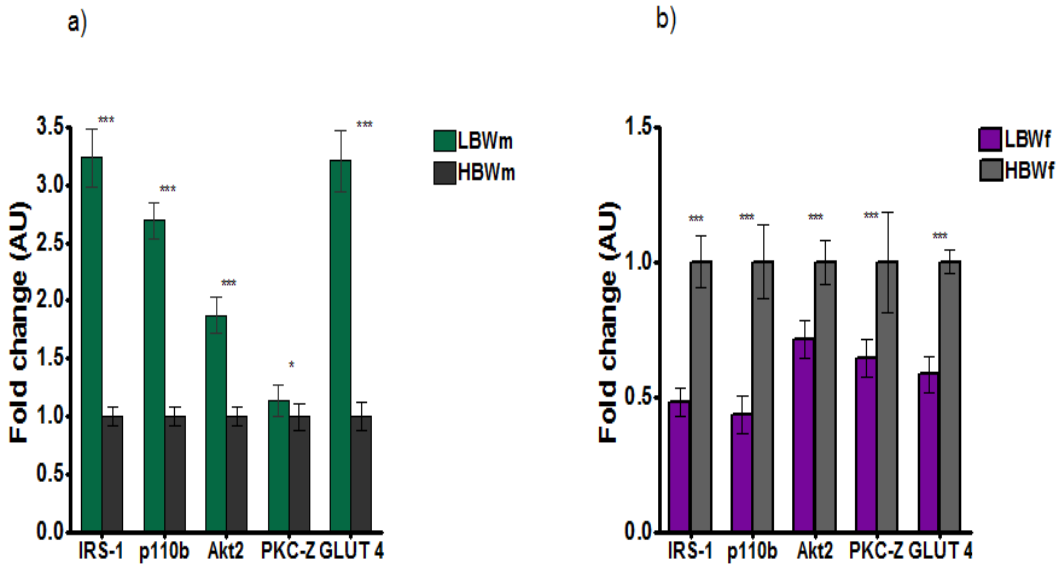

Figure 3.7.1.1.1 mRNA expression of insulin-signaling components in subcutaneous adipose tissue from male and female offspring at weaning. Figure a) corresponds to males and figure b) to females. Data presented as fold change of **LBWm/f** mice in relation to **HBWm/f** mice respectively. mRNA expression was determined by RT-qPCR and normalised to mRNA expression of housekeeping gene actin beta (Actb). Statistical analysis was performed using an *unpaired student t-test*. Data presented as mean± SD. **LBWm** n=8; **HBWm** n=8; **LBWf** n=6; **HBWf** n=5. *p≤0.05, ***p≤0.001.

3.7.1.2 Expression of insulin signaling related genes in Females

Different mRNA expression was seen between female groups. Contrary to **LBWm, LBWf** had a reduction of the expression of IRS-1 (**p<0.001**; figure 3.7.1.2.1), PIK-3/p110b (**p<0.001**; figure 3.4.2), PCK-Z (**p<0.001**) and GLUT4 (**p<0.001**; figure 3.7.1.2.1).

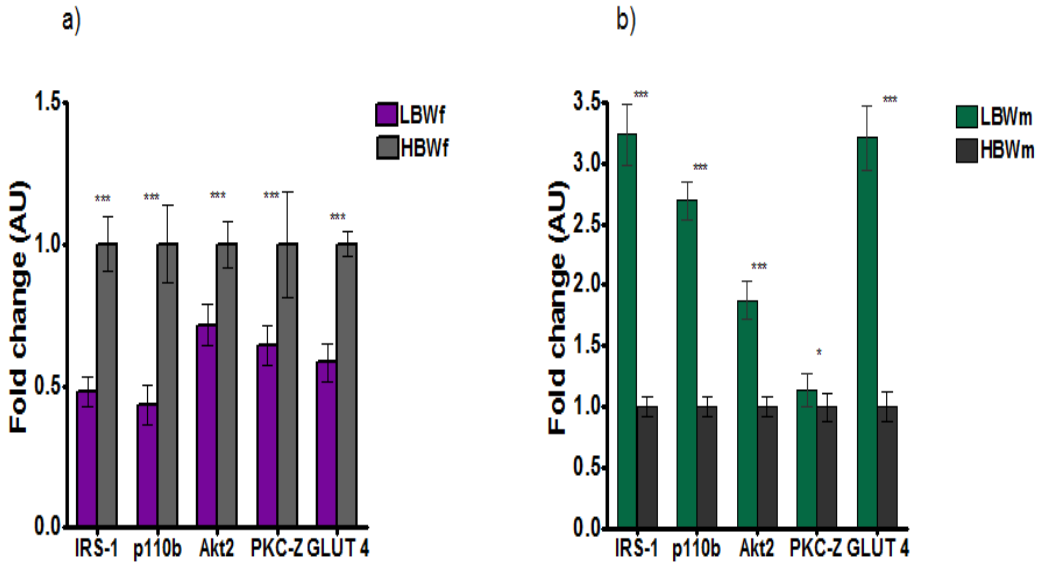

Figure 3.7.1.2.1 mRNA expression of insulin-signaling components in subcutaneous adipose tissue from female and male offspring at weaning. Figure a) corresponds to females and figure b) to males. Data presented as fold change of **LBWf/m** mice in relation to **HBWf/m** mice respectively. mRNA expression was determined by RT-qPCR and normalised to mRNA expression of housekeeping gene actin beta (Actb). Statistical analysis was performed using an *unpaired student t-test*. Data presented as mean± SD. **LBWf** n=6; **HBWf** n=5; **LBWm** n=8; **HBWm** n=8. *p≤0.05, *** p≤0.001.

3.7.2 Adipose tissue expression of adipogenic and lipid related genes at weaning (3 weeks)

3.7.2.1 Expression of adipogenic related genes in Males

Adipogenic key regulators $PPARG_2$ and CEBPa were significantly higher in **LBWm** mice than **HBWm** mice (**p<0.001** both; figure 3.7.2.1.1). This suggests that adipogenesis was more active in SAT of these mice which correlates with the overexpression of genes regulated by insulin as aforementioned. Insulin action is very important in triggering differentiation of adipocytes as the key regulators $PPARG_2$ and CEBPa.

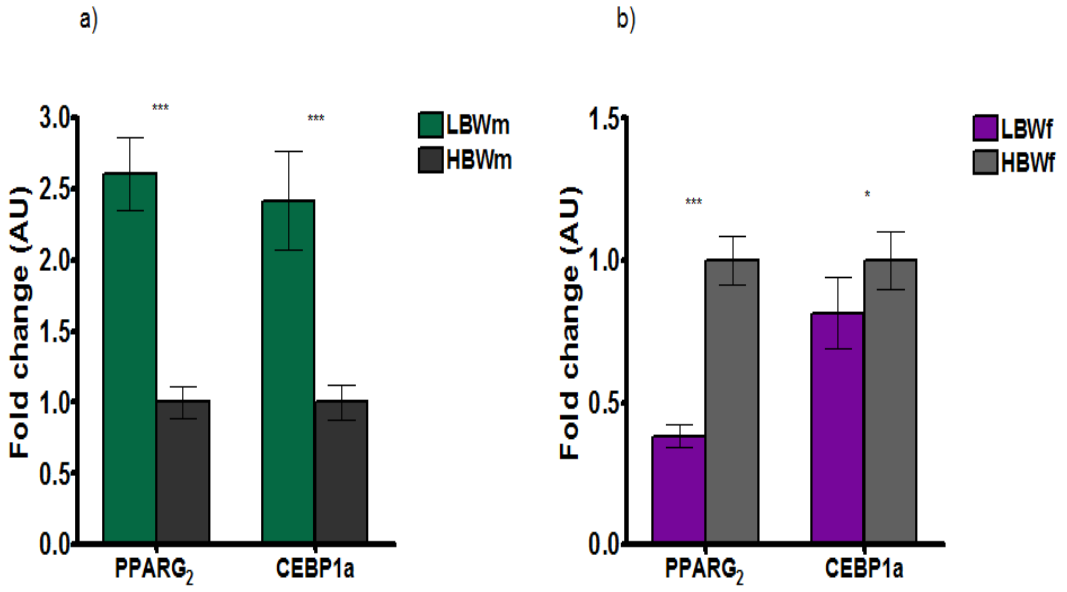

Figure 3.7.2.1.1 mRNA expression of key adipogenic transcriptional regulators in subcutaneous adipose tissue from male and female offspring at weaning. Figure a) corresponds to males and figure b) to females. Peroxisome proliferator activated receptor gamma 2= $PPARG_2$, CCAAT/enhancer-binding protein alpha=CEBPa. Data presented as fold change of **LBWm/f** mice in relation to **HBWm/f** mice respectively. mRNA expression was determined by RT-qPCR and normalised to mRNA expression of housekeeping gene actin beta (Actb). Statistical analysis was performed using an *unpaired student t-test*. Data presented as mean± SD. **LBWm** n=8; **HBWm** n=8; **LBWf** n=6; **HBWf** n=5. *p≤0.05, *** p≤0.001.

3.7.2.2 Expression of adipogenic related genes in Females

Contrary to **LBWm, LBWf** had a reduction in fold change in PPARG-2 and CEBP1a compared to **HBWf** (**p<0.001; p=0.016** respectively; figure 3.7.2.2.1)**.**

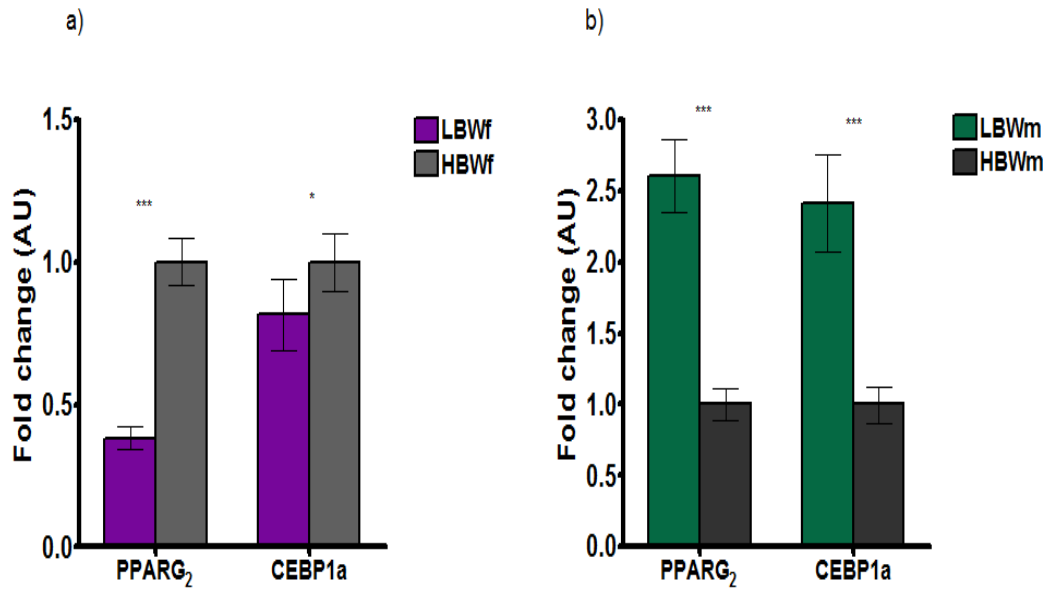

Figure 3.7.2.2.1 mRNA expression of key adipogenic transcriptional regulators in subcutaneous adipose tissue from female and male offspring at weaning. Figure a) corresponds to females and figure b) to males. Peroxisome proliferator activated receptor gamma 2= $PPARG_2$, CCAAT/enhancer-binding protein alpha=CEBPa. Data presented as fold change of **LBWf/m** mice in relation to **HBWf/m** mice respectively. mRNA expression was determined by RT-qPCR and normalised to mRNA expression of housekeeping gene actin beta (Actb). Statistical analysis was performed using an *unpaired student t-test*. Data presented as mean± SD. **LBWf** n=6; **HBWf** n=5; **LBWm** n=8; **HBWm** n=8. *p≤0.05, ***p≤0.001.

3.7.2.3 Expression of lipogenic related genes in Males

Fold change of the lipogenic regulator SREBP1c was substantially increased in **LBWm** in relation to **HBWm** (**p<0.001**; figure 3.7.2.3.1). FASN and LPL fold change was also increased in **LBWm** (**p<0.001** both genes; figure 3.7.2.3.1).

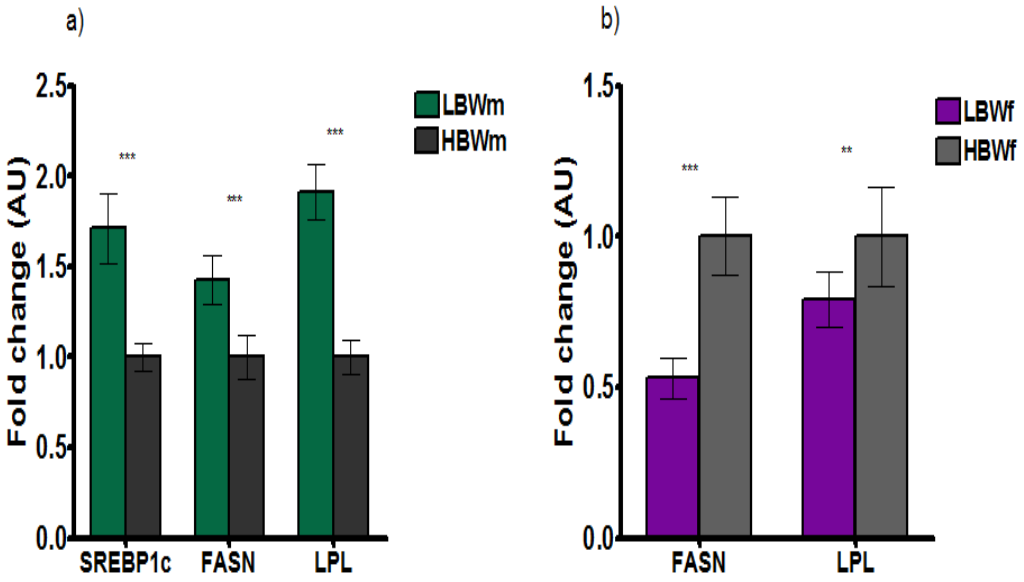

Figure 3.7.2.3.1 mRNA expression of lipogenic genes in subcutaneous adipose tissue from male and female offspring at weaning. Figure a) corresponds to males and figure b) to females. Sterol regulatory element binding protein 1c =SREBP1c, fatty acid synthase =FASN, and lipoprotein lipase =LPL. mRNA expression was determined by RT-qPCR and normalised to mRNA expression of housekeeping gene actin beta (Actb). Statistical analysis was performed using an *unpaired student t-test*. Data presented as mean± SD. **LBWm** n=8; **HBWm** n=8; **LBWf** n=6; **HBWf** n=4. ** p≤0.01, *** p≤0.001

3.7.2.4 Expression of lipogenic related genes in Females

In females, SREBP1c expression was undetectable in the samples used. However, FASN and LPL expression was significantly reduced in **LBWf** compared to **HBWf** (**p<0.001**; **p= 0.003** respectively; figure 3.7.2.4.1). It would be expected to have a lower expression of SREBP1c, as its downstream target gene FASN is down regulated.

These results suggest that **LBWf** accumulated less lipid in the SAT than **HBWf**, contrary to what was observed between male groups were **LBWm** presented a higher accumulation of lipid in SAT according to mRNA levels of lipogenic regulators.

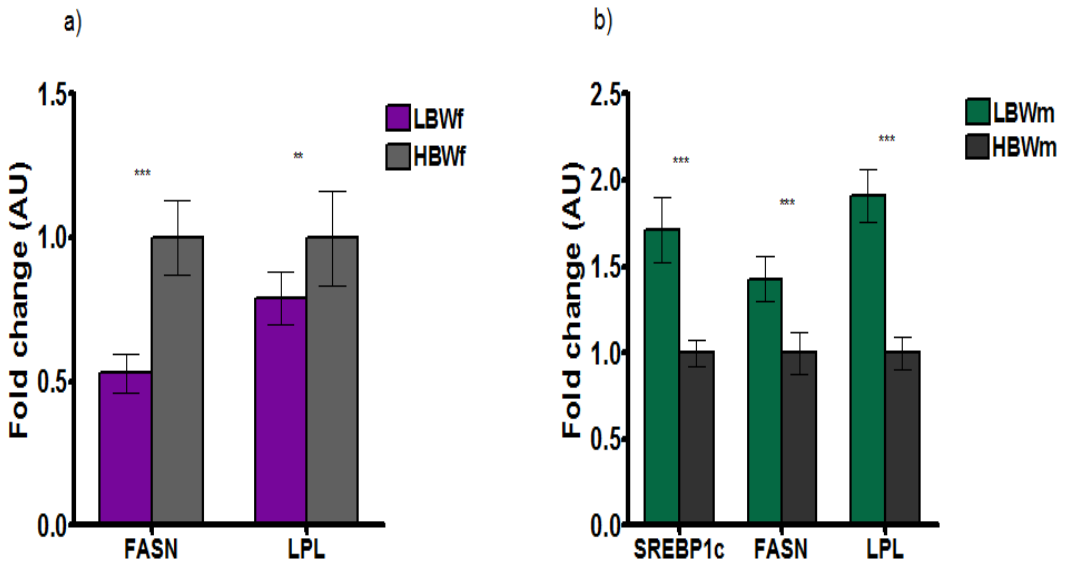

Figure 3.7.2.4.1 mRNA expression of lipogenic genes in subcutaneous adipose tissue from female and male offspring at weaning. Figure a) corresponds to females and figure b) to males. Sterol regulatory element binding protein 1c =SREBP1c, fatty acid synthase =FASN, and lipoprotein lipase =LPL. mRNA expression was determined by RT-qPCR and normalised to mRNA expression of housekeeping gene actin beta (Actb). Statistical analysis was performed using an *unpaired student t-test*. Data presented as mean± SD. **LBWf** n=6; **HBWf** n=4; **LBWm** n=8; **HBWm** n=8. **p≤0.01, *** p≤0.001.

3.7.2.5 Expression of a lipolytic related gene in Males

To assess lipolytic function in SAT, HSL mRNA levels were determined. **LBWm** did have an enhanced fold change in expression of HSL in respect to **HBWm** (**p<0.001**, figure 3.7.2.5.1). *De novo* lipogenesis (as measured by FAS expression) and lipid uptake from circulating lipids (estimating LPL expression) in **LBWm** was increased, as did HSL. This may suggests an increased in lipid turnover (synthesis-uptake-lipolysis) in SAT of **LBWm** mice.

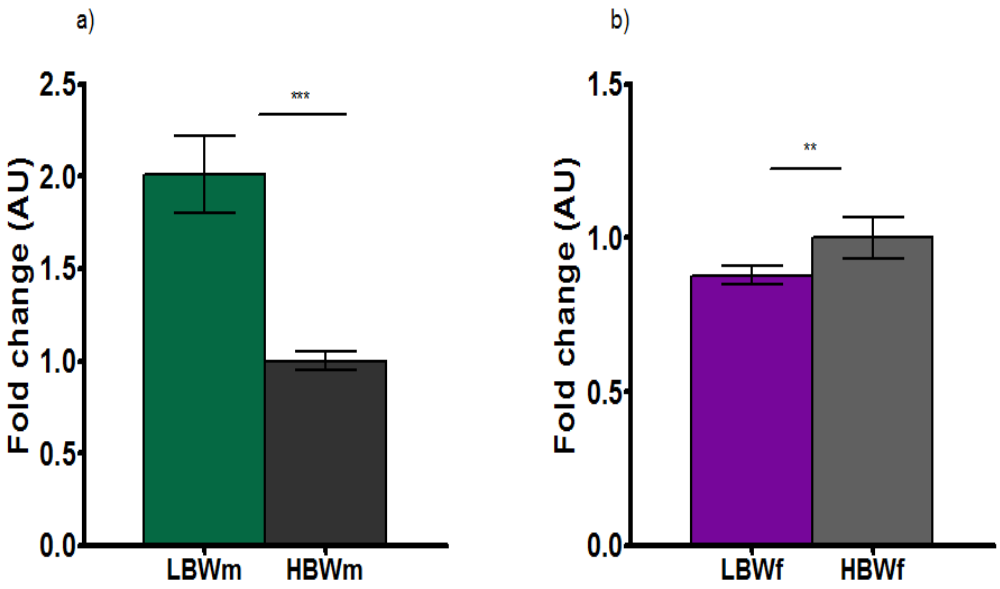

Figure 3.7.2.5.1 mRNA expression of the lipolytic hormone sensitive lipase (HSL) in subcutaneous adipose tissue from male and female offspring at weaning. Figure a) corresponds to males and figure b) to females. Hormone sensitive lipase was assessed as lipolytic regulator. mRNA expression was determined by RT-qPCR and normalised to mRNA expression of housekeeping gene actin beta (Actb). Statistical analysis was performed using an *unpaired student t-test*. Data presented as mean± SD. **LBWm** n=8; **HBWm** n=8; **LBWf** n=6; **HBWf** n=5. ** p≤0.01, *** p≤0.001.

3.7.2.6 Expression of a lipolytic related gene in Females

mRNA levels of HSL in females were contrary to what was seen in males. **LBWf** had a lower fold change in respect to **HBWf** (**p=0.009**, figure 3.7.2.6.1).

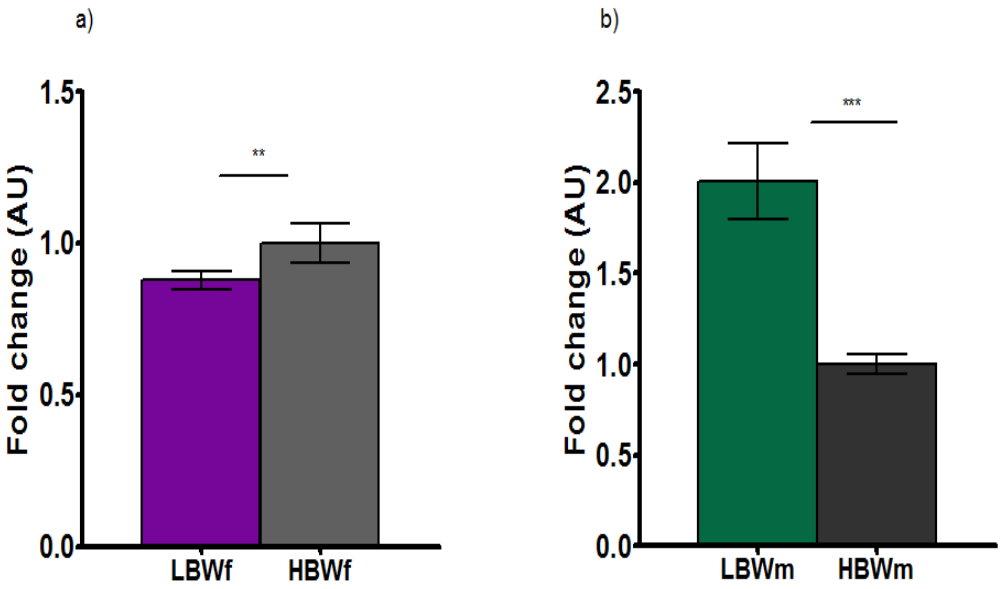

Figure 3.7.2.6.1 mRNA expression of the lipolytic hormone sensitive lipase (HSL) in subcutaneous adipose tissue from female and male offspring at weaning. Figure a) corresponds to females and figure b) to males. Hormone sensitive lipase was assessed as lipolytic regulator. mRNA expression was determined by RT-qPCR and normalised to mRNA expression of housekeeping gene actin beta (Actb). Statistical analysis was performed using an *unpaired student t-test*. Data presented as mean± SD. **LBWf** n=6; **HBWf** n=5; **LBWm** n=8; **HBWm** n=8. ** p≤0.01, *** p≤0.001 .

3.7.3 Adipose tissue expression of thermogenic genes at weaning (3 weeks)

3.7.3.1 Adipose tissue expression of thermogenic genes in Males

PGC1a and UCP-1 mRNA expression in **LBWm** were increased compared to **HBWm** (**p<0.001** in both; figure 3.7.3.1.1). This is accordance to the results obtained for the adrenergic receptor adrb3, whose mRNA expression was also increased in **LBWm** (**p<0.001**; figure 3.7.3.1.2).

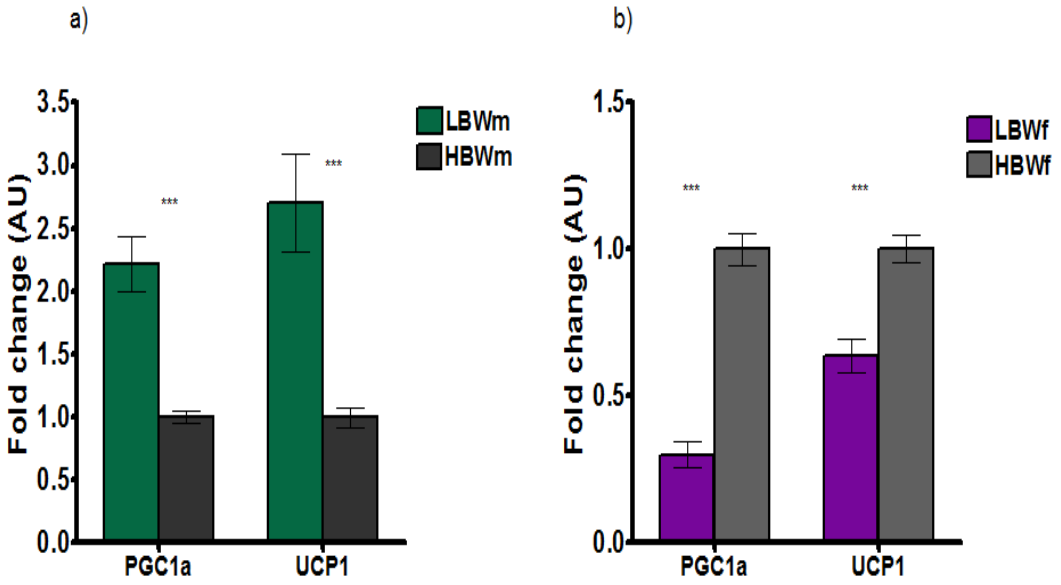

Figure 3.7.3.1.1 mRNA expression of genes related to thermogenic activity in subcutaneous adipose tissue from male and female offspring at weaning. Figure a) corresponds to males and figure b) to females. Peroxisome proliferator-activated receptor gamma coactivator 1 alpha (PGC1a) and its downstream target gene uncoupling protein 1 (UCP1) expression were evaluated. mRNA expression was determined by RT-qPCR and normalised to mRNA expression of housekeeping gene actin beta (Actb). Statistical analysis was performed using an *unpaired student t-test*. Data presented as mean± SD. **LBWm** n=7; **HBWm** n=7; **LBWf** n=6; **HBWf** n=5. *** p≤0.001.

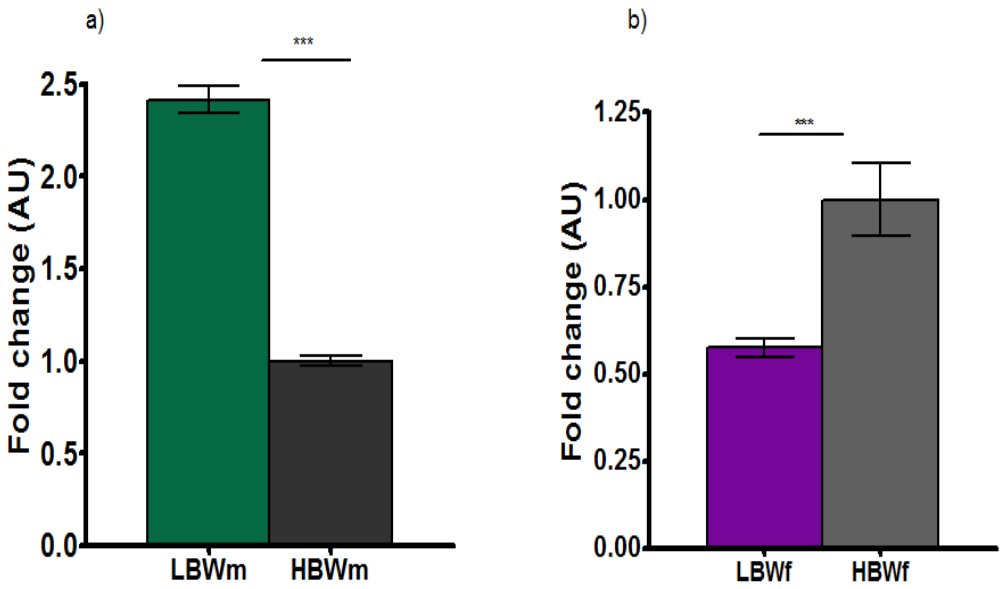

Figure 3.7.3.1.2 mRNA expression of beta 3 adrenergic receptor in subcutaneous adipose tissue from male and female offspring at weaning. Figure a) corresponds to males and figure b) to females. Beta-adrenergic transcriptional regulation of PGC1a was analysed measuring beta 3 adrenergic receptor expression. mRNA expression was determined by RT-qPCR and normalised to mRNA expression of housekeeping gene actin beta (Actb). Statistical analysis was performed using an *unpaired student t-test*. Data presented as mean± SD. **LBWm** n=6; **HBWm** n=6; **LBWf** n=6; **HBWf** n=5. *** p≤0.001.

3.7.3.2 Adipose tissue expression of thermogenic genes in Females

In females, **LBWf** mice had a reduced fold change in the expression of PGC1a and UCP1 **(p<0.001** in both; figure 3.7.3.2.1) as well as beta 3 adrenergic receptor expression (Adrb3) (**p< 0.001**; figure 3.7.3.2.2).

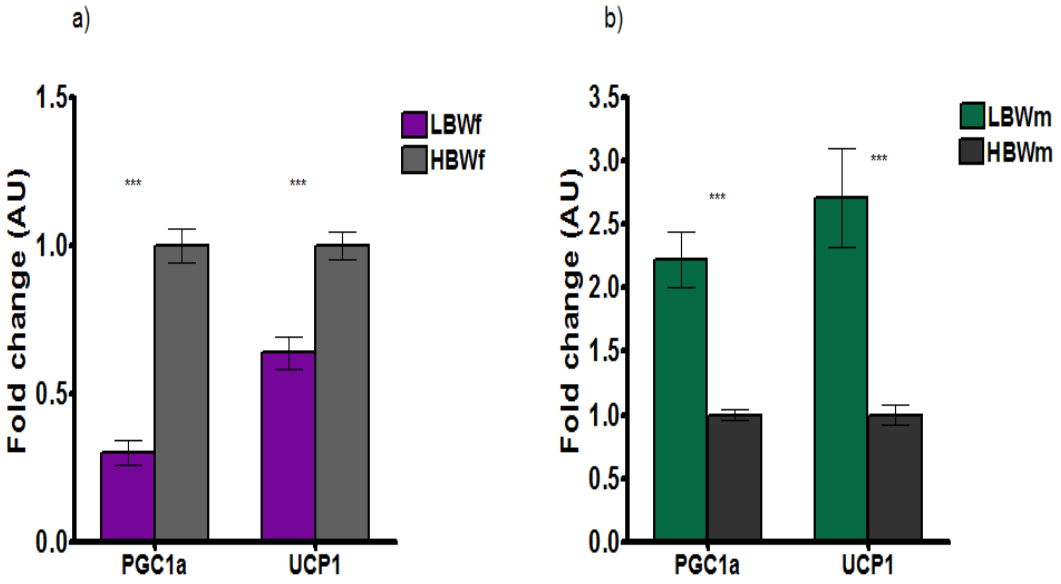

Figure 3.7.3.2.1 mRNA expression of genes related to thermogenic activity in subcutaneous adipose tissue from female and male offspring at weaning. Figure a) corresponds to females and figure b) to males. Peroxisome proliferator-activated receptor gamma coactivator 1 alpha (PGC1a) and its downstream target gene uncoupling protein 1 (UCP1) expression were evaluated. mRNA expression was determined by RT-qPCR and normalised to mRNA expression of housekeeping gene actin beta (Actb). Statistical analysis was performed using an *unpaired student t-test*. Data presented as mean± SD. **LBWf** n=6; **HBWf** n=5; **LBWm** n=7; **HBWm** n=7. *** p≤0.001.

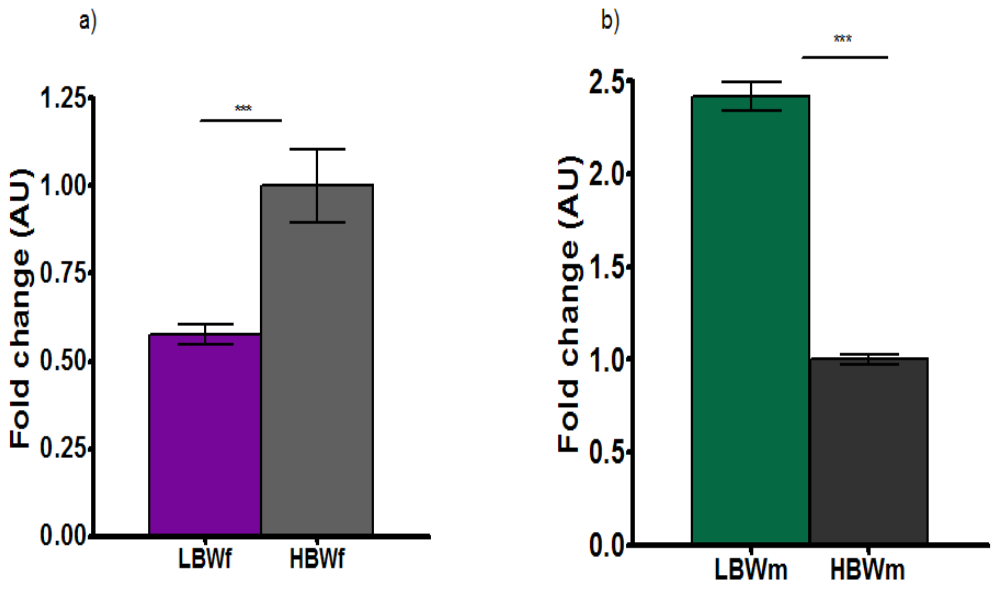

Figure 3.7.3.2.2 mRNA expression of beta 3 adrenergic receptor in subcutaneous adipose tissue from female and male offspring at weaning. Figure a) corresponds to females and figure b) to males. Beta-adrenergic transcriptional regulation of PGC1a was analysed measuring beta 3 adrenergic receptor expression. mRNA expression was determined by quantitative reverse transcriptase PCR RT-qPCR and normalised to mRNA expression of housekeeping gene actin beta (Actb). Statistical analysis was performed using an *unpaired student t-test*. Data presented as mean± SD. **LBWf** n=6; **HBWf** n=5; **LBWm** n=6; **HBWm** n=6. *** p≤0.001.

The table below summarises the adipose tissue gene expression for both male and female mice (table 3.7.1).

	LBWm	HBWm	p	LBWf	HBWf	p	m-f diff.
IRS-1	↑	-	✓	-	↑	✓	✓
p110b	↑	-	✓	-	↑	✓	✓
Akt2	↑	-	✓	-	↑	✓	✓
PKC-Z	↑	-	✓	-	↑	✓	✓
GLUT4	↑	-	✓	-	↑	✓	✓
$PPARG_2$	↑	-	✓	-	↑	✓	✓
CEBP1a	↑	-	✓	-	↑	✓	✓
SREBP1c	↑	-	✓	-	↑	✓	✓
FASN	↑	-	✓	-	↑	✓	✓
LPL	↑	-	✓	-	↑	✓	✓
HSL	↑	-	✓	-	↑	✓	✓
PGC1a	↑	-	✓	-	↑	✓	✓
UCP1	↑	-	✓	-	↑	✓	✓
Adrb3	↑	-	✓	-	↑	✓	✓

Table 3.7.1 Summary of adipose tissue gene expression by gender. Arrows indicate that the measurement was higher in the respective group compared to its counterpart. ✓indicates that the difference between groups was significantly different in p column (p value); in the last column indicates a different finding between genders. x indicates that the difference between groups was not significantly different in p column; in the last column indicates a similar finding between genders. Adrb3= beta 3 adrenergic receptor.

3.8 Summary

LBWm/f mice grew faster than **HBWm/f** mice but did not catch up in weight with **HBWm/f** mice.

There were sexually dimorphic differences at weaning: **LBWm** mice had an asymmetrical growth with an enhanced brain growth (measured as weight). In contrast, liver, muscle, and white adipose tissue growth was rectricted. No differences in growth were found between female groups, although brain and heart weights tended to be higher in **LBWf** mice.

Adipose tissue distribution was sexually dimorphic with **LBWm** mice having a lower SAT% than **HBWm** mice, whereas **LBWf** mice had a higher IAT% compared to **HBWf** mice. Intrahepatocellular lipid content (IHCL) was lower in **LBWm/f** compared to **HBWm/f** mice.

Fasting glucose levels were significantly higher in **LBWm** mice than **HBWm** mice. Levels of insulin were higher in **LBWm** mice than **HBWm** mice but it did not reach statistical significance. GIP levels were higher in **LBWm** than **HBWm** mice. **LBWf** had an impaired fasting glucose compared to **HBWf** mice accompanied by high c-peptide, insulin, GIP and glucagon levels in plasma.

Proinflammatory markers MCP-1 and IL-6 were significantly higher in **LBWf** compared to **HBWf** mice, but only MCP-1 in **LBWm** compared to **HBWm** mice.

SAT translational insulin signaling, adipogenesis and lipid metabolism were upregulated in **LBWm** mice and downregulated in **LBWf** mice compared to their respective counterparts (**HBWm/f**).

4. Study 2. Effects of Birth Weight and Diet on Body Composition and Appetite Regulation in Young Mice (From Week 3 Until Week 15)

At weaning (week 3 of life), pups were separated from their litters and divided by birth weight into two categories taking into account the parameters mentioned in study 1 (section 2.1.3). These two groups were: Low birth weight mice (**LBW**) and High birth weight mice (**HBW**). Offspring was further subdivided by diet (section 2.2.2: control fat diet =9%kcal fat intake) and a moderated high fat diet =27% kcal) and by gender: male (**m**) or female (**f**) mice. In total, four groups were formed per gender as follow: 1). Low birth weight mice fed a Normal Fat diet (**LBWm/f-NF**), 2). High birth weight mice fed a Normal Fat diet (**HBWm/f-NF**), 3). Low birth weight mice fed a High Fat diet (**LBWm/f-HF**) and 4). High birth weight mice fed a High Fat diet (**HBWm/f-HF**).

4.1 The Effects of Birth Weight and Diet on Body Weight in Young Mice (From Week 3 Until Week 15)

Body weight was monitored weekly, starting when the pups were 3 weeks old and ending at age 15 weeks. Detailed information of the protocol used for this study can be found in section 2.2.4.

4.1.1 Body weight in Male mice

Figures 4.1.1.1 and 4.1.1.2 show the growth pattern of the 4 groups following maintenance on both normal fat control diet (9% kcal fat intake) and purified moderated high fat diet (27% kcal fat intake).

Mice fed a **HF** diet increased rapidly their body weight; by week 5 of age **HBWm-HF** had significantly higher body weights compared to **HBWm-NF** mice (**HBWm-HF** =20.613±0.286g vs. **HBWm-NF** =19.49±0.236g, **p=0.025**; figures 4.1.1.1 and 4.1.1.2b) and one week later between **LBWm** mice (**LBWm-HF**=21.061±0.248g vs. **LBWm-NF**=19.769±0.22g, **p=0.002**; figures 4.1.1.1 and 4.1.1.2a). Comparison between **LBWm** mice and **HBWm** mice showed significant differences in weight until the age of 9 weeks on a **NF** diet (figures 4.1.1 and 4.1.2c), and until the age of 11 weeks on a **HF** diet (figures 4.1.1.1 and 4.1.1.2d).

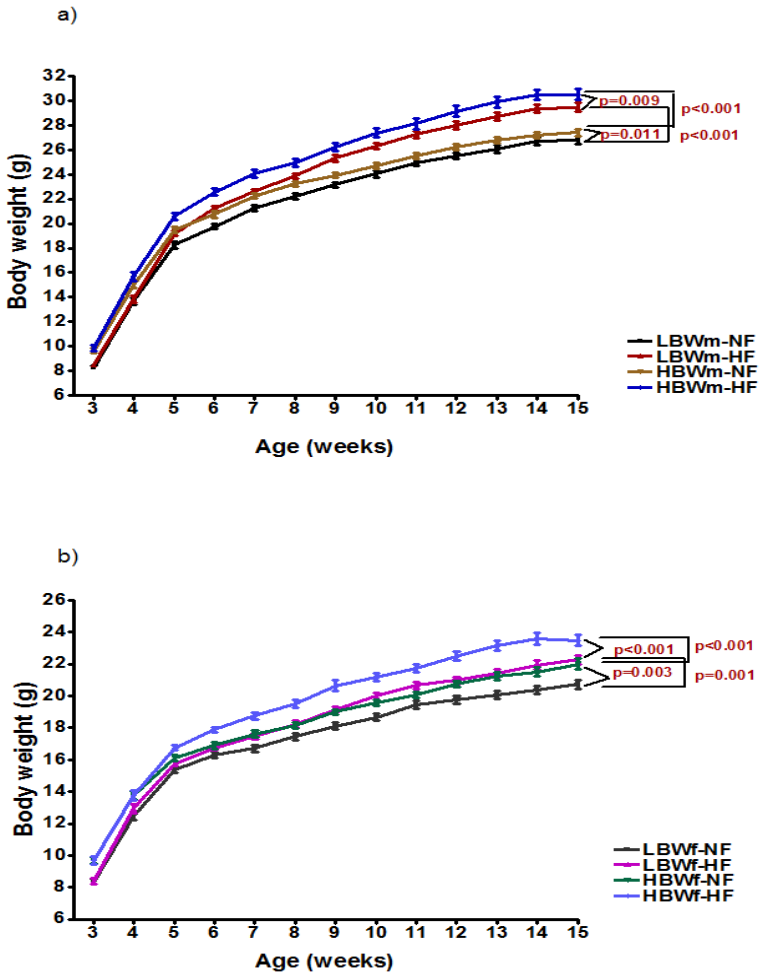

Figure 4.1.1.1 Body weight of male and female mice from weaning (week 3) until early adulthood (week 15). **LBWm/f** and **HBWm/f** were subdivided into 4 further groups according to the diet given from weaning until week 51, either a normal fat diet =**NF** (9% kcal fat) or moderated high fat diet =**HF** (27% fat intake). The groups were: Low birth weight males/females fed a normal fat diet =**LBWm/f-NF**; Low birth weight males/females fed a high fat diet= **LBWm/f-HF**; High birth weight males/females fed a normal fat diet =**HBWm/f-NF;** High birth weight males/females fed a high fat diet**=HBWm/f-HF**. Statistical analysis was performed using a mixed general linear model (GLM) followed by a Games-Howell post hoc analysis for unequal variances. Data presented as mean± SEM. **LBWm-NF** n=40; **LBWm-HF** n=42; **HBWm-NF** n=33; **HBWm-HF** n=38; **LBWf-NF** n=39; **LBWf-HF** n=36; **HBWf-NF** n=24, **HBWf-HF** n=30. Figure a) corresponds to males and figure b) to females.

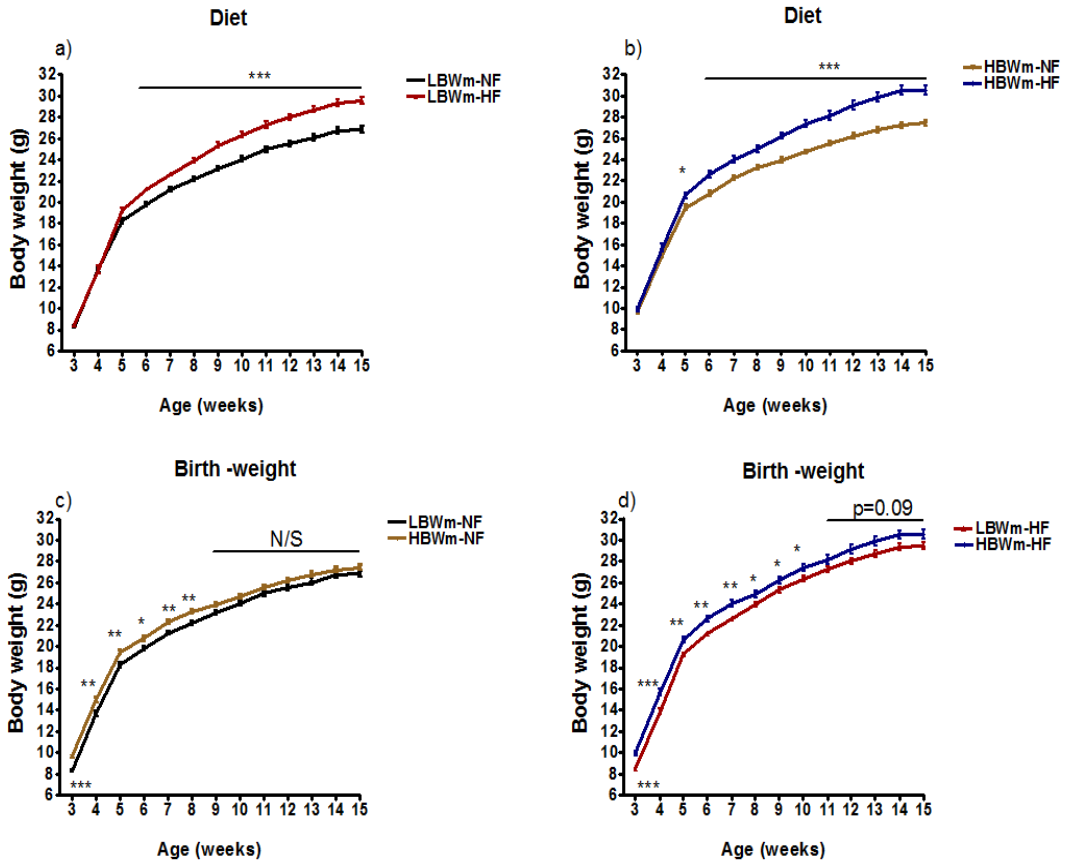

Figure 4.1.1.2 Body weight of male mice from weaning (week 3) until early adulthood (week 15). Figures a) and b) show the body weights throughout the study by diets (**NF-HF** respectively) in mice within the same birth weight category. Figure c) and d) show the body weights throughout the study by (**LBWm-HBWm** respectively) in mice within the same diet category. Statistical analysis was performed using a mixed general linear model (GLM) followed by a Games-Howell post hoc analysis for unequal variances. Data presented as mean± SEM. **LBWm-NF** n=40; **LBWm-HF** n=42; **HBWm-NF** n=33, **HBWm-HF** n=38. * p≤0.05, **p≤0.01, *** p≤0.001.

4.1.2 Body weight in Female mice

As with males, diet affected the body weight of mice, with higher body weights in females fed a **HF** diet. Differences between **HBWf** mice reached significance by week 6, compared to 5 weeks in males (**HBWf-HF** =17.884±0.162g vs. **HBWm-NF** =16.886±0.242g, **p=0.004**; figures 4.1.2.1 and 4.1.2.2b); by week 7 differences between **LBWf** mice reached significance, whilst in small males was one week before (**LBWm-HF**=17.466±0.1742g vs. **LBWm-NF**=16.709±0.16.292g, **p=0.023**; figures 4.1.2.1 and 4.1.2.2a).

Contrary to males, compared to **HBWf** mice **LBWf** mice had a significant lower body weight throughout the study (females: figures 4.1.2.1 and figures 4.1.2.2c-d; males: figures 4.1.1.1 and 4.1.1.2c-d).

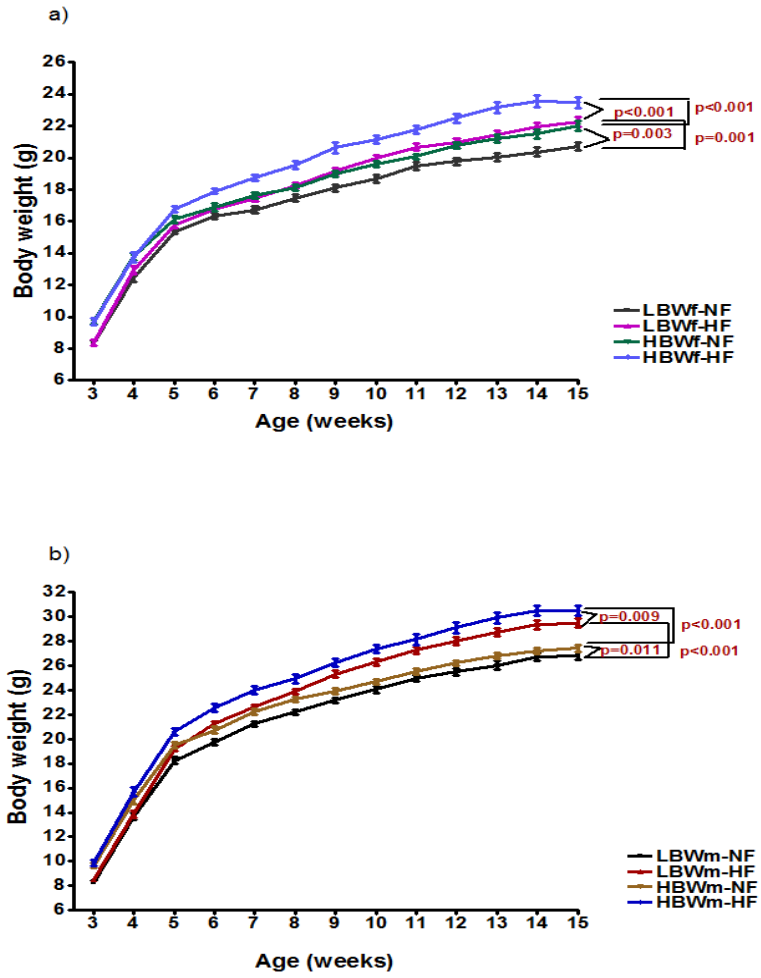

Figure 4.1.2.1 Body weight of female and male mice from weaning (week 3) until early adulthood (week 15). **LBWf/m** and **HBWf/m** were subdivided into 4 further groups according to the diet given from weaning until week 51, either a normal fat diet =**NF** (9% kcal fat) or moderated high fat diet =**HF** (27% fat intake). Statistical analysis was performed using a mixed general linear model (GLM) followed by a Tukey's high significance difference (HSD) post hoc analysis. Data presented as mean± SEM. **LBWf-NF** n=39; **LBWf-HF** n=36; **HBWf-NF** n=24, **HBWf-HF** n=30; **LBWm-NF** n=40; **LBWm-HF** n=42; **HBWm-NF** n=33, **HBWm-HF** n=38. Figure a) corresponds to females and figure b) to males.

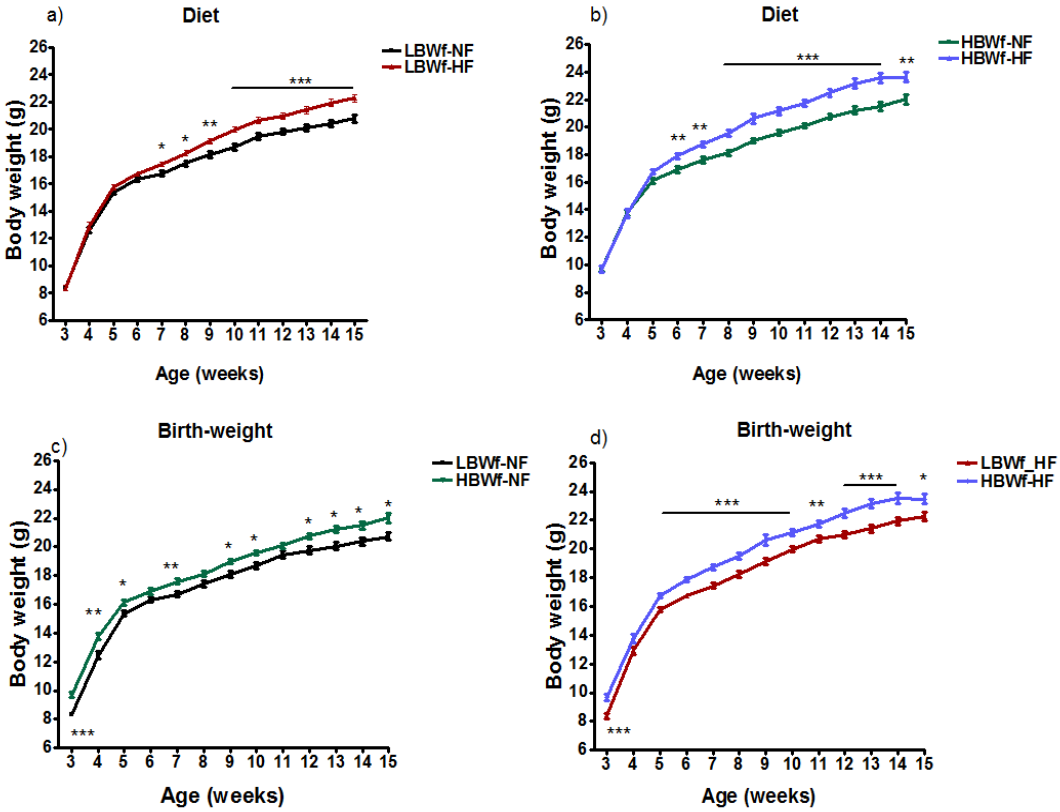

Figure 4.1.2.2 Body weight of female mice from weaning (week 3) until early adulthood (week 15). Figures a) and b) show the body weights throughout the study by diets (**NF-HF** respectively) in mice within the same birth weight category. Figure c) and d) show the body weights throughout the study by (**LBWf-HBWf** respectively) in mice within the same diet category. Statistical analysis was performed using a mixed general linear model (GLM) followed by a Tukey's high significance difference (HSD) post hoc analysis. Data presented as mean± SEM. **LBWf-NF** n=39; **LBWf-HF** n=36; **HBWf-NF** n=24, **HBWf-HF** n=30. * p≤0.05, **p≤0.01, *** p≤0.001.

4.1.3 Body weight gain in Male mice

A 2x2 factorial ANOVA was performed to examine the independent effects of birth weight and diet on body weight gain as well as a possible interaction between these two factors.

Assessment of body weight gain (g) from week 3 to week 15 showed that both factors, birth weight and diet, had an effect on body weight gained during this period (: $F(1,134)=4.338$ **p=0.039**; diet: $F(1,134)=41.53$ **p<0.001**; figure 4.1.3.1a and table 4.1.3.1(left)) and these effects were independent as the interaction between and diet was not significant (interaction birth weight x diet: $F(1,134)=0.026$ $p=0.873$; figure 4.1.3.1a and table 4.1.3.1(left). This suggests that **LBWm** mice gained more weight than **HBWm** irrespective of the diet given, and at the same time, mice fed a **HF** diet gained more weight than mice fed a **NF** diet, independently of the size at birth.

Assessment of body weight gain normalised to initial body weight (relative body weight gain or total growth %) showed a similar pattern as seen in absolute body weight gain (g) where birth weight and diet effects were maintained without an interaction (birth weight: $F(1,134)=30.826$ **p<0.001**; diet: $F(1,134)=10.986$ **p=0.001**; interaction birth weight x diet: $F(1,134)=0.156$ $p=0.693$; figure 4.1.3.1b and table 4.1.3.1 (right).

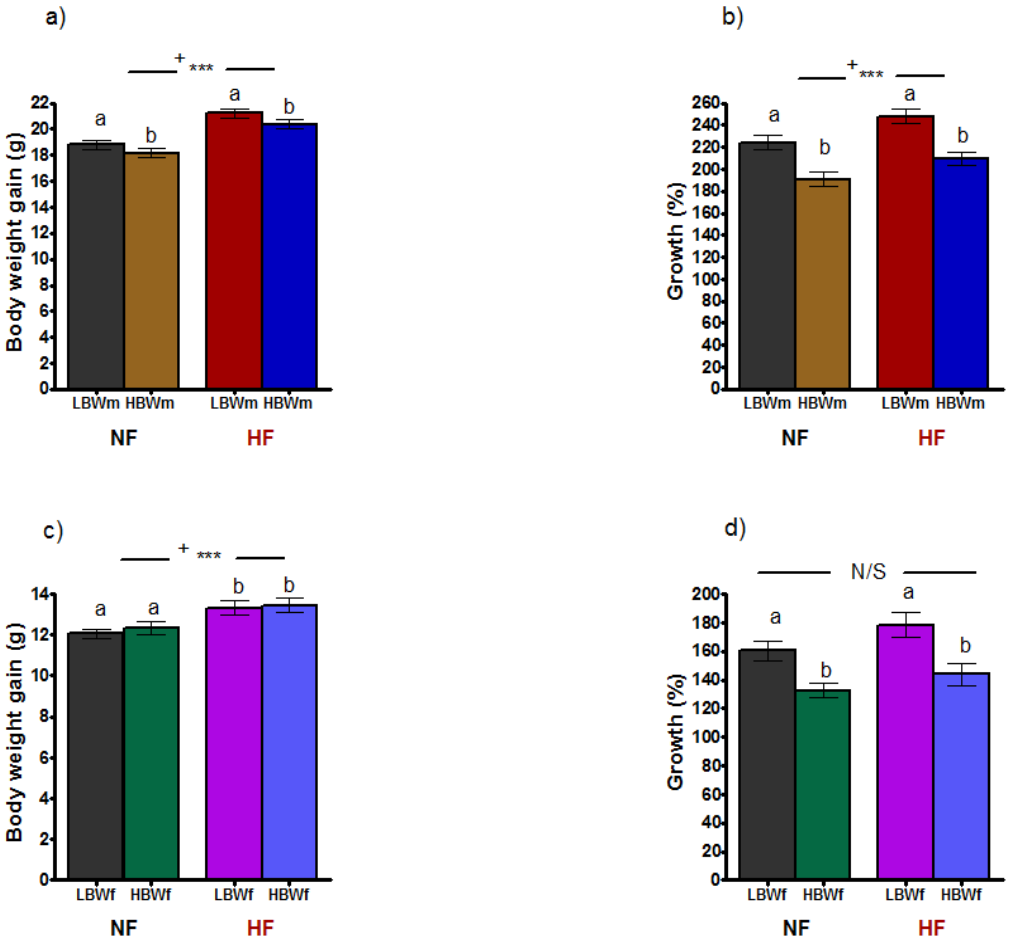

Figure 4.1.3.1 Body weight gain of male and female offspring from week 3 to week 15. Total body weight gains in grams a) and c) and body weight gains normalised to initial body weight (growth%) b) and d). Figures on the top correspond to males and figures below to females. Statistical analysis was performed using a 2x2 factorial ANOVA analysis. Data presented as mean± SEM. Main effect of diet= **+** p≤0.001 in a), b) and c); significant main effect of birth weight represented with different letters p≤0.05 in a) and p≤0.001 in b) and d). **LBWm-NF** n=30; **LBWm-HF** n=40; **HBWm-NF** n=30, **HBWm-HF** n=40; **LBWf-NF** n=30; **LBWf-HF** n=27; **HBWf-NF** n=22, **HBWf-HF** n=25.

Birth weight	Diet	Total body weight gain (g)	Total body weight gain (growth%)
LBWm	**NF**	18.799± 0.387	224.158±7.066
	HF	21.057± 0.329	248.088±5.912
HBWm	**NF**	17.993± 0.387	190.893±6.827
	HF	20.366± 0.329	209.725±5.912
Birth weight effect		**p=0.039**	**p<0.001**
Diet		**p<0.001**	**p=0.001**
Interaction (x diet)		p=0.873	p=0.693

Table 4.1.3.1 Body weight gain of male offspring from week 3 to week 15. Total body weight gains in grams (left) and body weight gains normalised to initial body weight (growth%; left). Statistical analysis was performed using a 2x2 factorial ANOVA analysis. Data presented as mean± SEM. **LBWm-NF** n=30; **LBWm-HF** n=40; **HBWm-NF** n=30, **HBWm-HF** n=40.

4.1.4 Body weight gain in Female mice

Contrary to males, only diet had a significant main effect *per se* on body weight gained in females (diet: F(1,100)=13.858 **p<0.001**; birth weight: F(1,100)=0.248 p=0.619; interaction diet x birth weight: F(1,100)=0.007 p=0.932; figures 4.1.4.1a and table 4.1.4.1(left)). This suggests that females that were fed a **HF** diet had a greater body weight gain compared to females fed a **NF** diet, and this effect was not dependent on birth weight.

However, evaluation of normalised body weight to initial body weight (%) showed a different pattern with a significant main effect of birth weight on body weight and a marginal effect of diet with no interaction between both factors (birth weight: F(1,100)=16.275 **p<0.001**; diet: F(1,100)=3.492 p=0.065; interaction diet x birth weight: F(1,100)=0.348 p=0.557; figures 4.1.4.1b and table 4.1.4.1(right)). This indicated that females accelerated more their weight gain if they had a lower birth weight (**LBWf**) compared to their heavier counterparts (**HBWf**).

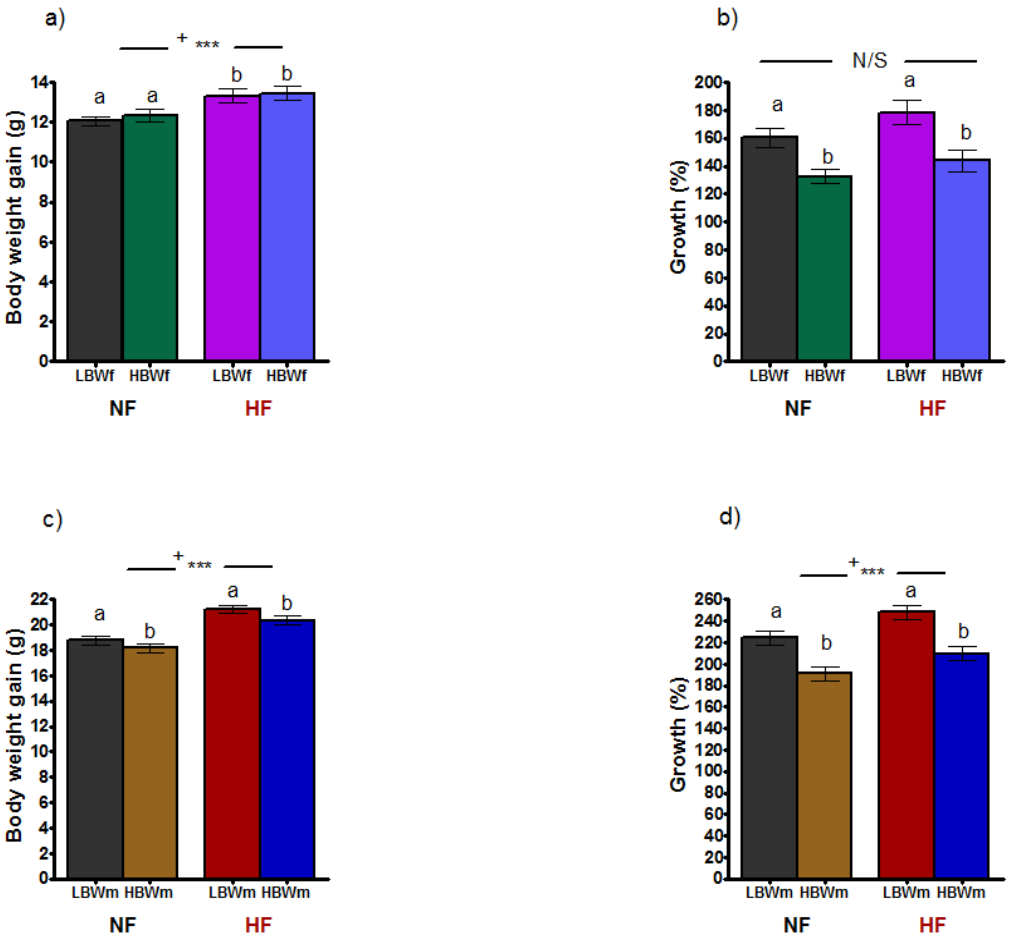

Figure 4.1.4.1 Body weight gain of female and male offspring from week 3 to week 15. Total body weight gains in grams a) and c) and body weight gains normalised to initial body weight (growth%) b) and d). Figures on the top correspond to females and figures below to males. Statistical analysis was performed using a 2x2 factorial ANOVA analysis. Data presented as mean± SEM. Significant main effect of diet= **+** p≤0.001 in a), c) and d) and N/S=no significant (p=0.065) in b). No significant effect of birth weight (p=0.619) represented with equal letters in a) and significant main effect of birth weight represented with different letters, p≤0.05 in c), and p≤0.001 in b) and d). **LBWf-NF** n=30; **LBWf-HF** n=27; **HBWf-NF** n=22, **HBWf-HF** n=25; **LBWm-NF** n=30; **LBWm-HF** n=40; **HBWm-NF** n=30, **HBWm-HF** n=40.

Birth Weight	Diet	Total body weight gain (g)	Total body weight gain (growth%)
LBWf	**NF**	12.098± 0.303	159.937±6.958
	HF	13.322± 0.314	178.168±7.211
HBWf	**NF**	12.286± 0.341	134.397±7.813
	HF	13.455± 0.327	143.878±7.648
Birth weight effect		p=0.619	**p<0.001**
Diet		**p<0.001**	p=0.065
Interaction (birth weight x diet)		p=0.932	p=0.557

Table 4.1.4.1 Body weight gain of female offspring from week 3 to week 15. Total body weight gains in grams (left) and body weight gains normalised to initial body weight (growth%; right). Statistical analysis was performed using a 2x2 factorial ANOVA analysis. Data presented as mean± SEM. **LBWf-NF** n=30; **LBWf-HF** n=27; **HBWf-NF** n=22, **HBWf-HF** n=25.

4.2 The Effects of Birth Weight and Diet on Caloric Intake in Young Mice (From Week 3 Until Week 15)

Total kilocalorie intake was calculated using weekly food intake measurements and the values of the caloric content of the diets described in section 2.2, table 2.2.1, and section 2.3. A 2x2 factorial ANOVA was performed to examine the independent effects of birth weight and diet on total kilocalorie intake and a possible interaction between these two factors.

4.2.1 Total kilocalorie intake in Male mice

Figure 4.2.1.1a and table 4.2.1.1(left) shows the total kilocalorie intake of **LBWm** and **HBWm** mice fed both a control fat diet (9% kcal fat intake) and a purified moderated high fat diet (27% kcal fat intake).

There was a main effect of both, diet and birth weight on the total kilocalorie intake in mice (diet: $F(1,22)=25.363$ **$p<0.001$**; birth weight: $F(1,22)=5.826$ **$p=0.025$**; figure 4.2.1a and table 4.2.1(left)) but the interaction was not significant (interaction diet x birth weight: $F(1,22)=0.497$ $p=0.488$; figure 4.2.1a and table 4.2.1(left). This indicated that mice fed **HF** diet had a higher intake of kilocalories independently of the birth weight of mice. However, birth weight *per se* had an effect on kilocaloric intake as well. This means that both factors presented in the study can affect food intake independently of each other.

Normalisation of kilocalorie intake to body weight$^{0.75}$ showed that differences between groups had a different pattern. The two independent factors (diet and birth weight) did not have a main effect *per se* (diet: F(1,72)=1.895 p=0.173; birth weight: F(1,72)=0.261 p=0.611; figure 4.2.1.1b and table 4.2.1.1(right) but the effect of each factor depended on the other factor (interaction diet x birth weight: F(1,72)=5.643 **p=0.02**; figure 4.2.1.1b and table 4.2.1.1(right). This indicated that the effect of diet depended on the birth weight of mice and vise versa. **LBWm-NF** had a higher kilocaloric intake that **LBWm-HF** but the difference did not reach significance (p=0.472; figure 4.2.1.1b and table 4.2.1.1(right). On the contrary, **HBWm-NF** had a lower intake that **HBWm-HF** (**p=0.011**; figure 4.2.1.1b). Moreover, **LBWm-NF** had a higher intake than **HBWm-NF** but differences did not reach significance (p=0.243; figure 4.2.1.1b). However, **LBWm-HF** did consume less kilocalories than **HBWm-HF** mice (**p=0.021**; figure 4.2.1.1b).

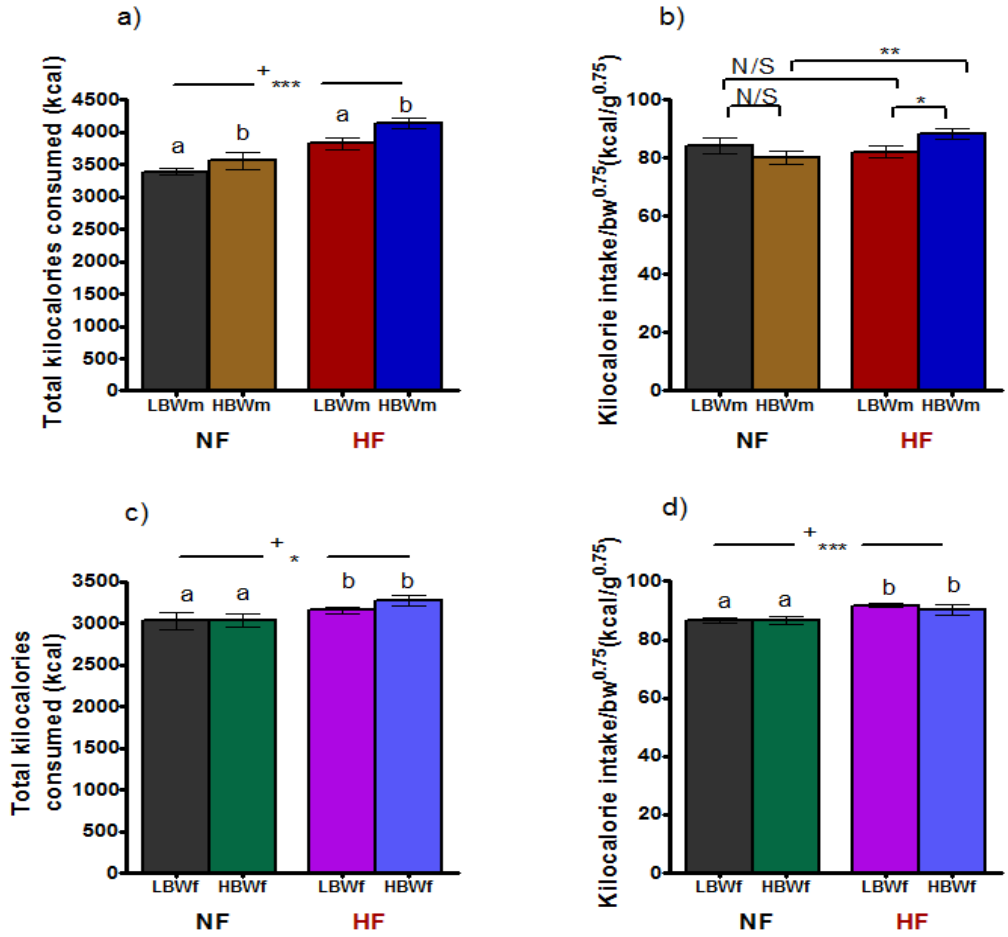

Figure 4.2.1.1 Total kilocalorie intake of male and female mice from week 3 to week 15 of age. Total kilocalories consumed in absolute values a) and c) and normalised to body weight$^{0.75}$ b) and d). Statistical analysis was performed using a 2x2 factorial ANOVA analysis. Significant main effect of diet= **+** *p≤0.05 in c) and *** p≤0.001 in a) and d). Significant main effect of birth weight= different letters in a), **p=0.025**. Simple main effects were assessed in b) as interaction was significant. Data presented as mean± SEM. **LBWm-NF** n=5/14; **LBWm-HF** n=9/27; **HBWm-NF** n=5/14, **HBWm-HF** n=7/21; **LBWf-NF** n=10/27; **LBWf-HF** n=5/15; **HBWf-NF** n=6/18, **HBWf-HF** n=6/16.

Birth weight	Diet	Total kilocalories (kcal)	Total kilocalories / $bw^{0.75}$ ($kcal/g^{0.75}$)
LBWm	**NF**	3386.898± 110.109	84.219±2.495
	HF	3818.115± 82.07	81.996±1.797
HBWm	**NF**	3557.038± 110.109	80.068±2.495
	HF	4128.565± 93.059	88.422±2.037
Birth weight effect		**p=0.025**	p=0.173
Diet		**p≤0.001**	p=0.611
Interaction (Birth weight x diet)		p=0.488	**p=0.02**

Table 4.2.1.1 Total kilocalories consumed from week 3 until week 15 in male offspring. Total kilocalories consumed in absolute values (left) and normalised to body $weight^{0.75}$ (right). Statistical analysis was performed using a 2x2 factorial ANOVA analysis. Data presented as mean± SEM. Data for kilocalories in absolute values was analysed by cage and by mouse/cage for normalised data. **LBWm-NF** n=5/14; **LBWm-HF** n=9/257; **HBWm-NF** n=5/14, **HBWm-HF** n=7/21.

4.2.2 Total kilocalorie intake in Female mice

As in males, females were affected by the diet given during the study but there was not a main effect of birth weight or interaction between both variables (diet: $F(1,23)=4.123$ **p=0.05**; birth weight: $F(1,23)=0.385$ $p=0.541$; interaction diet x birth weight: $F(1,23)=0.352$ $p=0.559$; figure 4.2.2.1a and table 4.2.2.1(left).

This pattern was maintained after normalisation to body weight$^{0.75}$ (diet: $F(1,72)=11.567$ **p=0.001**; birth weight: $F(1,72)=0.416$ $p=0.521$; interaction diet x birth weight: $F(1,72)=0.507$ $p=0.479$; figure 4.2.2.1b and table 4.2.2.1 (right).

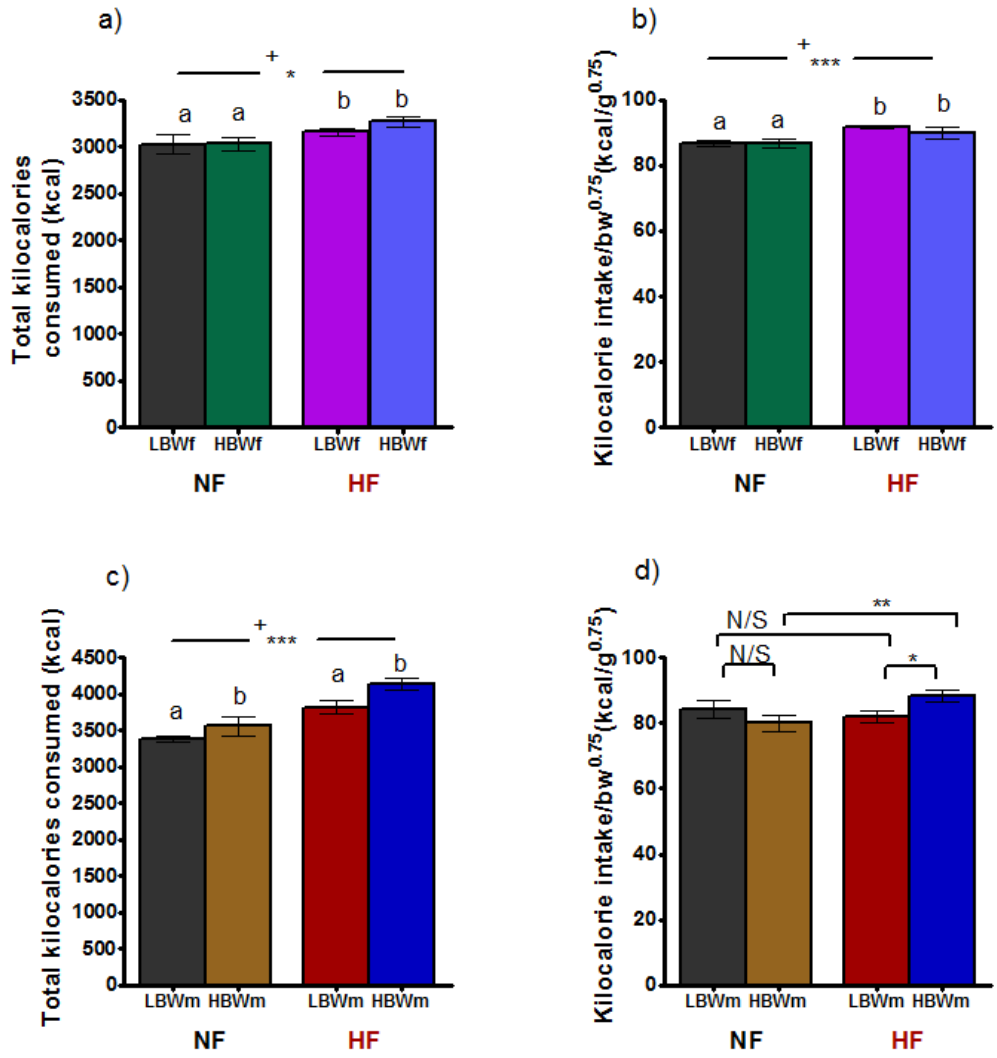

Figure 4.2.2.1 Total kilocalorie intake of female and male mice from week 3 to week 15 of age. Total kilocalories consumed in absolute values a) and c) and normalised to body weight$^{0.75}$ b) and d). Figures on the top correspond to females and figures below to males. Statistical analysis was performed using a 2x2 factorial ANOVA analysis. Data presented as mean± SEM. Main effect of diet= $^{+}$ and main effect of birth weight= lowercase letters (different letters= significant effect; **p=0.025** in c)). **LBWf-NF** n=10/27; **LBWf-HF** n=5/15; **HBWf-NF** n=6/18, **HBWf-HF** n=6/16; **LBWm-NF** n=5/14; **LBWm-HF** n=9/27; **HBWm-NF** n=5/14, **HBWm-HF** n=7/21. *p≤0.05, **p≤0.01, ***p≤0.001.

Birth weight	Diet	Total kilocalories (kcal)	Total kilocalories / $bw^{0.75}$ ($kcal/g^{0.75}$)
LBWf	**NF**	3026.01± 72.099	86.649±1.035
	HF	3156.416± 101.963	91.728±1.319
HBWf	**NF**	3028.505± 93.079	86.732±1.244
	HF	3266.511± 93.079	90.052±1.319
Birth weight effect		p=0.541	p=0.521
Diet		**p=0.05**	**p=0.001**
Interaction (Birth weight x diet)		p=0.559	p=0.479

Table 4.2.2.1 Total kilocalories consumed from week 3 until week 15 in female offspring. Total kilocalories consumed in absolute values (left) and normalised to body weight$^{0.75}$ (right). Statistical analysis was performed using a 2x2 factorial ANOVA analysis. Data presented as mean± SEM. Data for kilocalories in absolute values was analysed by cage and by mouse/cage for normalised data. **LBWf-NF** n=10/27; **LBWf-HF** n=5/15; **HBWf-NF** n=6/18, **HBWf-HF** n=6/16.

4.3 The Effects of Birth Weight and Diet on Feed Efficiency in Young Mice (From Week 3 Until Week 15)

Feed efficiency was calculated as the body weight gain divided by total kilocalories consumed. Total kilocalorie intake was calculated using weekly food intake measurements and the values of the caloric content of the diets mentioned in section 2.2, table 2.2.1. A 2x2 factorial ANOVA was performed to examine the independent effects of birth weight and diet on feed intake and a possible interaction between these two factors.

4.3.1 Feed efficiency in Males

Figure 4.3.1.1 and table 4.3.1.1 show that **LBWm** mice were more efficient in gaining weight per kilocalorie consumed than **HBWm** mice (birth weight: $F(1,72)=26.267$ **$p<0.001$**), and there was not a significant effect of diet (diet: $F(1,72)=3.184$ $p=0.079$), or interaction between birth weight and diet (interaction diet x birth weight: $F(1,72)=0.159$, $p=0.691$).

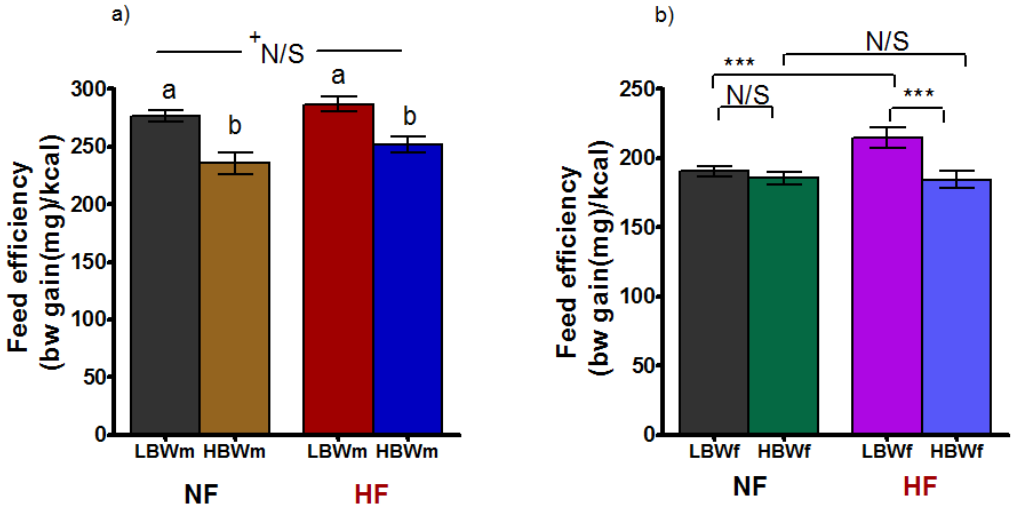

Figure 4.3.1.1 Feed efficiency of male and female mice from week 3 until week 15. Figure a) corresponds to males and figure b) to females. Total kilocalories were obtained from weekly-recorded food intake and the calculated kilocaloric content per gram of each diet (**NF**= 3.6 kcal/g and **HF**=4.1 kcal/g). Statistical analysis was performed using a 2x2 factorial ANOVA analysis. Data presented as mean± SEM. $^{+}$ Main effect of diet: p=0.079 in males a); significant main effect of birth weight represented with different letters: **p≤0.001** in males a). As interaction was significant between groups in b), simple main effects were assessed after the factorial ANOVA. N/S= No significant difference. **LBWm-NF** n=14; **LBWm-HF** n=27; **HBWm-NF** n=14, **HBWm-HF** n=20; **LBWf-NF** n=26; **LBWf-HF** n=14; **HBWf-NF** n=19, **HBWf-HF** n=15.

Birth weight	Diet	Feed efficiency (mg/kcal)
LBWm	**NF**	276.286± 8.274
	HF	286.515± 5.958
HBWm	**NF**	235.5± 8.274
	HF	251.619± 6.756
Birth weight effect		**p<0.001**
Diet		**p=0.079**
Interaction (Birth weight x diet)		p=0.691

Table 4.3.1.1 Feed efficiency of male mice from week 3 until week 15. Statistical analysis was performed using a 2x2 factorial ANOVA analysis. Data presented as mean± SEM. **LBWm-NF** n=14; **LBWm-HF** n=27; **HBWm-NF** n=14, **HBWm-HF** n=20.

4.3.2 Feed efficiency in Females

Contrary to what was seen in males, there was an interaction between both birth weight and diet in female mice (interaction diet x birth weight: $F(1,70)=5.673$ **p=0.02**; figure 4.3.2.1 and table 4.3.2.1). This indicated that the effect of both variables depended on each other. **LBWf-NF** mice had a lower efficiency in gaining weight per kilocalorie consumed than **LBWf-HF** mice (**p=0.001**; figure 4.3.2.1 and table 4.3.2.1). However, there was not a significant difference between **HBWf** mice (p=0.904; figure 4.3.2.1 and table 4.3.2.1). Furthermore, there was a significance difference between mice fed a **HF** diet, with a higher feed efficiency in **LBWf-HF** mice compared to **HBWf-HF** mice (**p<0.001**; figure 4.3.2.1 and table 4.3.2.1) but not difference was seen between females fed a **NF** diet (p=0.455; figure 4.3.2.1 and table 4.3.2.1).

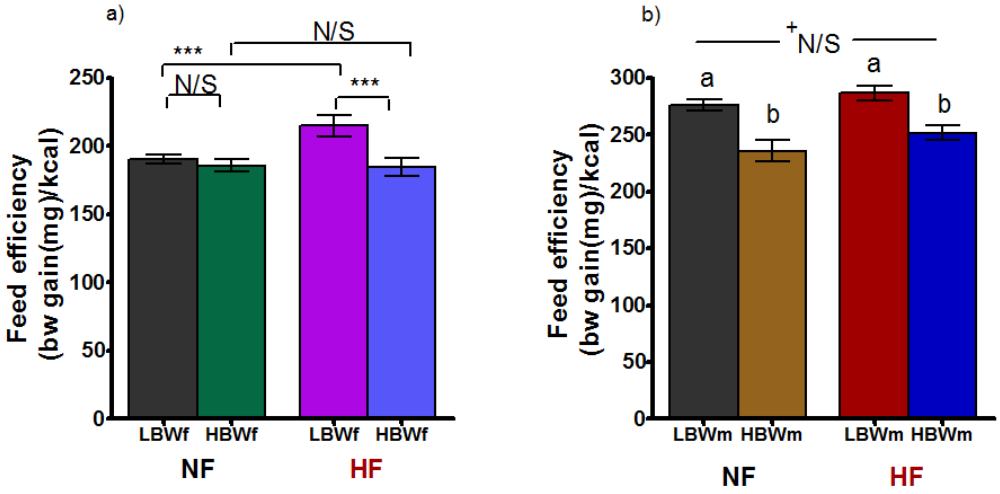

Figure 4.3.2.1 Feed efficiency of female and male mice from week 3 until week 15. Total kilocalories were obtained from weekly-recorded food intake and the calculated kilocaloric content per gram of each diet (**NF**= 3.6 kcal/g and **HF**=4.1 kcal/g). Statistical analysis was performed using a 2x2 factorial ANOVA analysis. Data presented as mean± SEM. As interaction was significant between groups in females a), simple main effects with Bonferroni correction were assessed after the factorial ANOVA. $^{+}$Main effect of diet: p=0.079 in b); significant main effect of birth weight represented with different letters: **p≤0.001** in b). N/S= No significant difference (**LBWf-NF** vs. **HBWf-NF** p=0.455; **HBWm-NF** vs. **HBWf-HF** p=0.904); ***p≤0.001** (**LBWf-NF** vs. **LBWf-HF**; **LBWf-HF** vs. **HBWf-HF**). **LBWf-NF** n=26; **LBWf-HF** n=14; **HBWf-NF** n=19, **HBWf-HF** n=15; **LBWm-NF** n=14; **LBWm-HF** n=27; **HBWm-NF** n=14, **HBWm-HF** n=20.

Birth weight	Diet	Feed efficiency (mg/kcal)
LBWf	**NF**	190.41± 4.355
	HF	214.804± 5.934
HBWf	**NF**	185.377± 5.094
	HF	184.452± 5.733
Interaction (birth weight x diet)		**p=0.02**

Table 4.3.2.1 Feed efficiency of female mice from week 3 until week 15. Statistical analysis was performed using a 2x2 factorial ANOVA analysis. Data presented as mean± SEM. **LBWf-NF** n=26; **LBWf-HF** n=14; **HBWf-NF** n=19, **HBWf-HF** n=15.

4.4 The Effects of Birth Weight and Diet on Total Body Adiposity and Intrahepatocellular Lipid Content in Young Mice (From Week 3 Until Week 15)

15 weeks old mice were fasted overnight before assessing non-invasively the whole body adiposity and intrahepatocellular lipid content (IHCL) using ^{1}H MRS and MRI techniques. Detailed information of the parameters of these methods is described in section 2.4.1. A 2x2 factorial ANOVA was performed to examine the independent effects of birth weight and diet on body adiposity and hepatic lipid content and a possible interaction between these two factors.

4.4.1 Whole body adiposity in Males and intrahepatocelullar lipid content (IHCL)

Whole body adiposity showed an interaction between both diet and birth weight (interaction diet x birth weight: F(1,68)=3.874 **p=0.05**; figure 4.4.1.1). Simple main effects assessment revealed that in general mice fed a **HF** diet had a higher adiposity than mice fed a **NF** diet, but the difference only reached significance between **HBWm** mice (**HBWm-HF**=21.327±1.156% vs. **HBWm-NF**=15.697±1.156%, **p=0.001**; **LBWm-HF**=20.635±1.016% vs. **LBWm-NF**= 19.461±1.191%, p=0.456; figure 4.4.1.1). Furthermore, **LBWm-NF** had a significantly higher adiposity than **HBWm-NF** mice (**p=0.027**; figure 4.4.1.1), but it was comparable between **LBWm-HF** and **HBWm-HF** (p=0.654; figure 4.4.1.1).

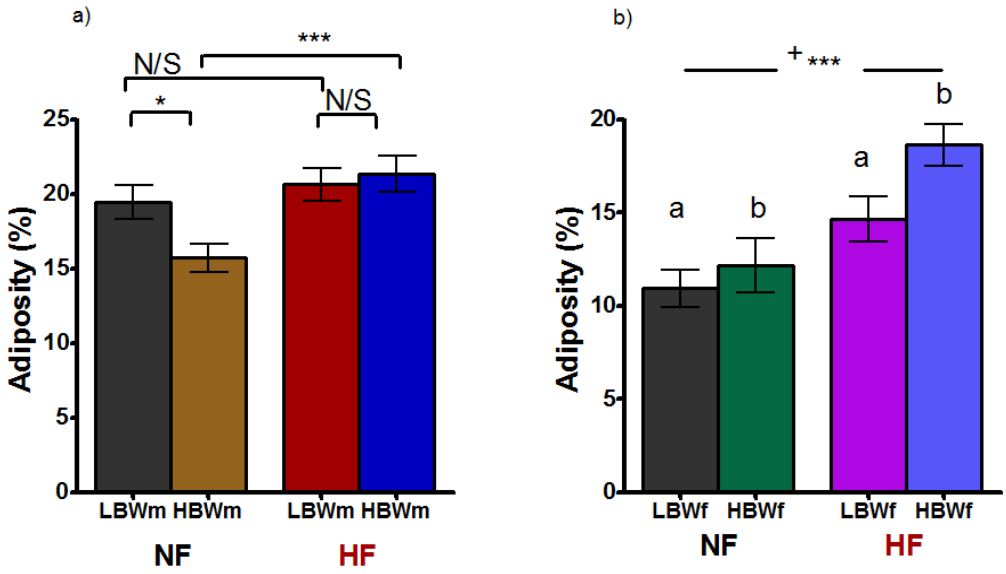

Figure 4.4.1.1 Whole body adiposity (%) of male and female mice at the end of the study (week 15). Whole body adiposity was assessed using ^{1}H MRS. Statistical analysis was performed using a 2x2 factorial ANOVA analysis. Data presented as mean± SEM. As interaction was significant between groups in males a), simple main effects with Bonferroni correction were assessed after the factorial ANOVA. N/S= No significant difference (**LBWm-NF** vs. **LBWm-HF** p=0.456; **LBWm-HF** vs. **HBWm-HF** p=0.654); * **p≤0.05** (**LBWm-NF** vs. **HBWm-NF**); ***p≤0.001** (**HBWm-NF vs. HBWm-HF**). **LBWm-NF** n=16; **LBWm-HF** n=22; **HBWm-NF** n=17, **HBWm-HF** n=17. Main effect of diet $^{+}$=***p≤0.001 in females b). Significant main effect of birth wieght represented with different letters (**p=0.037**) in female mice b). **LBWf-NF** n=12; **LBWf-HF** n=12; **HBWf-NF** n=12, **HBWf-HF** n=15.

Birth weight	Diet	Adiposity (%)
LBWm	**NF**	19.461± 1.191
	HF	20.635± 1.016
HBWm	**NF**	15.697± 1.156
	HF	21.327± 1.156
Interaction (birth weight x diet)		**p=0.05**

Table 4.4.1.1 Whole body adiposity (%) of male mice at the end of the study (week 15). Whole body adiposity was assessed using ^{1}H MRS. Statistical analysis was performed using a 2x2 factorial ANOVA analysis. Data presented as mean± SEM. **LBWm-NF** n=16; **LBWm-HF** n=22; **HBWm-NF** n=17, **HBWm-HF** n=17.

Assessment of the intrahepatocellular lipid content (IHCL) showed a significant main effect of birth weight on the percentage of hepatic lipid content in male mice ($F(1,61)=5.063$ **$p=0.028$**; figure 4.4.2.1 and table 4.4.2.1). This indicated that **LBWm** mice had a higher lipid content compared to **HBWm** mice independently of the diet given throughout the study. There was not a main effect of diet or significant interaction between both variables (diet: $F(1,61)=0.832$ $p=0.365$; interaction birth weight x diet: $F(1,61)=0.124$ $p=0.725$; figure 4.4.1.2 and table 4.4.1.2).

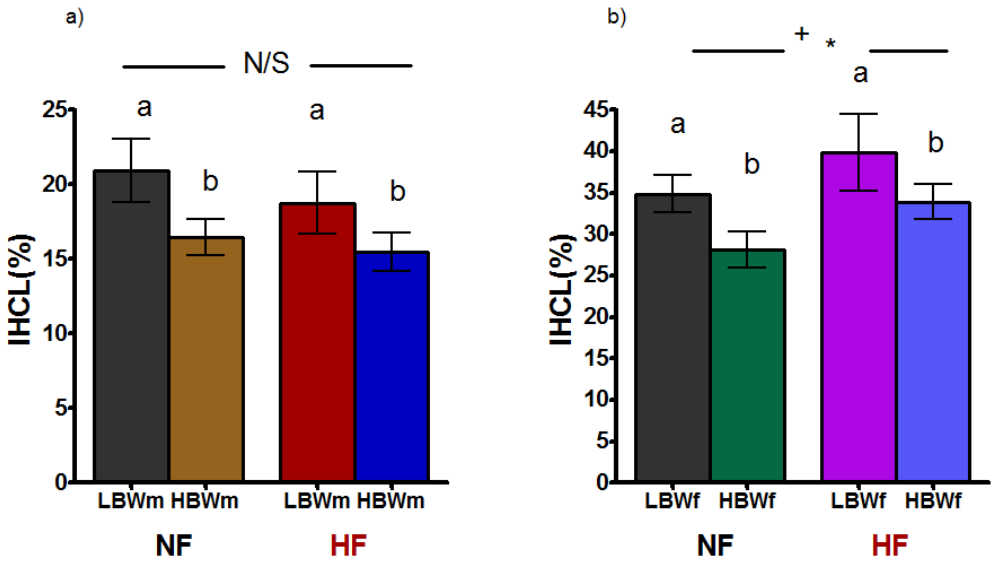

Figure 4.4.1.2 Intrahepatocellular lipid content (IHCL%) of male and female mice at the end of the study (week 15). IHCL was assessed using localised ^{1}H MRS. Statistical analysis was performed using a 2x2 factorial ANOVA analysis. Data presented as mean± SEM. Main effect of diet: N/S= No significant difference (p=0.365) in male mice a) and significantly different in female mice b) $^{+}$= * **p≤0.05**. Main effect of birth weight represented with different letters in a), **p=0.028** and b), **p=0.034**. **LBWm-NF** n=15; **LBWm-HF** n=17; **HBWm-NF** n=16, **HBWm-HF** n=17; **LBWf-NF** n=8; **LBWf-HF** n=8; **HBWf-NF** n=10, **HBWf-HF** n=13.

Birth weight	Diet	IHCL (%)
LBWm	**NF**	20.947± 1.798
	HF	18.759± 1.689
HBWm	**NF**	16.444± 1.741
	HF	15.476± 1.689
Birth -weight effect		**p=0.028**
Diet		p=0.365
Interaction (birth weight x diet)		p=0.725

Table 4.4.1.2 Intrahepatocellular lipid content (IHCL%) of male mice at the end of the study (week 15) using localised ^{1}H MRS. Statistical analysis was performed using a 2x2 factorial ANOVA analysis. Data presented as mean± SEM. **LBWm-NF** n=15; **LBWm-HF** n=17; **HBWm-NF** n=16, **HBWm-HF** n=17.

4.4.2 Whole body adiposity in Females and intrahepatocellular lipid content (IHCL)

Contrary to male mice, females did not have an interaction between both birth weight and diet ($F(1,47)=1.282$ $p=0.263$; figure 4.4.2.1 and table 4.4.2.1). However, there was a independent main effect of both birth weight ($F(1,47)=4.595$ **$p=0.037$**; figure 4.4.2.1 and table 4.4.2.1) and diet ($F(1,47)=17.405$ **$p<0.001$**; figure 4.4.2.1 and table 4.4.2.1). This indicated that **LBWf** mice had a lower adiposity compared to **HBWf** mice and furthermore, females fed a **HF** had a higher lipid content than females fed **NF** diet. Female mice had in general a lower adiposity compared to their respective male group (figures 4.4.1.1 and 4.4.1.2 and tables 4.4.1.1 and 4.4.1.2).

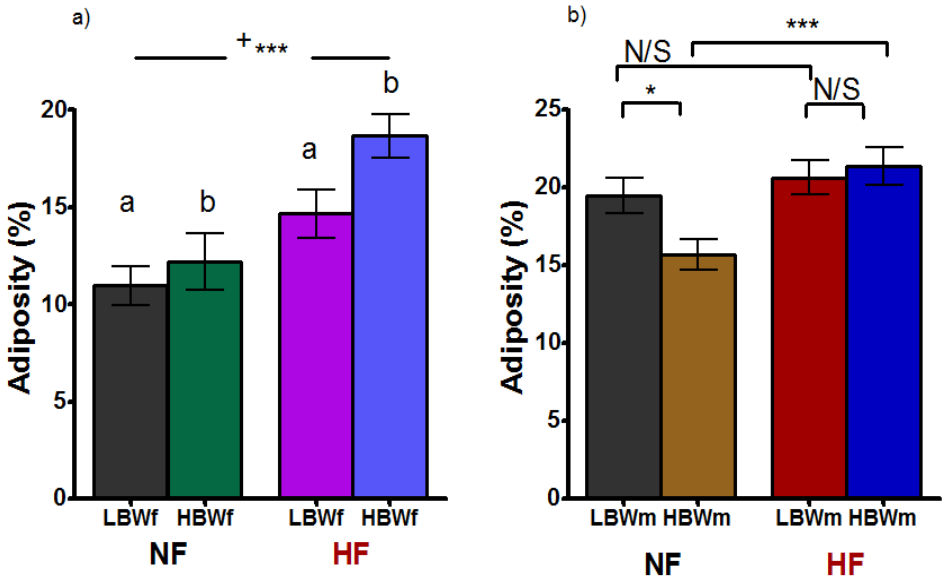

Figure 4.4.2.1 Whole body adiposity (%) of female and male mice at the end of the study (week 15). Whole body adiposity was assessed using ^{1}H MRS. Statistical analysis was performed using a 2x2 factorial ANOVA analysis. Data presented as mean± SEM. Main effect of diet **$^{+}$=***p≤0.001** in female mice a). Significant main effect of birth weight represented with different letters (**p=0.037**) in a). **LBWf-NF** n=12; **LBWf-HF** n=12; **HBWf-NF** n=12, **HBWf-HF** n=15. As interaction was significant between groups in male mice b), simple main effects with Bonferroni correction were assessed after the factorial ANOVA. N/S= No significant difference (**LBWm-NF** vs. **LBWm-HF** p=0.456; **LBWm-HF** vs. **HBWm-HF** p=0.654); *** p≤0.05** (**LBWm-NF** vs. **HBWm-NF**); ***p≤0.001** (**HBWm-NF vs. HBWm-HF**). **LBWm-NF** n=16; **LBWm-HF** n=22; **HBWm-NF** n=17, **HBWm-HF** n=17.

Birth weight	Diet	Adiposity (%)
LBWf	**NF**	10.955± 1.249
	HF	14.654± 1.249
HBWf	**NF**	12.186± 1.249
	HF	18.641± 1.117
Birth weight effect		**p=0.037**
Diet		**p<0.001**
Interaction (x diet)		p=0.263

Table 4.4.2.1 Whole body adiposity (%) of female mice at the end of the study (week 15). Whole body adiposity was assessed using ^{1}H MRS. Statistical analysis was performed using a 2x2 factorial ANOVA analysis. Data presented as mean± SEM. **LBWf-NF** n=12; **LBWf-HF** n=12; **HBWf-NF** n=12, **HBWf-HF** n=15.

Evaluation of the hepatic lipid content in female mice showed, as in males, showed a main effect of birth weight (F(1,35)=4.871 **p=0.034**; figure 4.4.2.2 and table 4.4.2.2). However, female mice were also affected by the diet given throughout the study with a higher IHCL% in females fed a **HF** diet than **NF** fed females (F(1,35)=4.131 **p=0.05**; figure 4.4.2.2 and table 4.4.2.2). There was not an interaction between variables (F(1,35)=0.044 p=0.835; figure 4.4.4 and table 4.4.4). Interestingly, females had higher lipid content in the liver compared to their respective male group (figures 4.4.1.2 and 4.4.2.2 and tables 4.4.1.2 and 4.4.2.2).

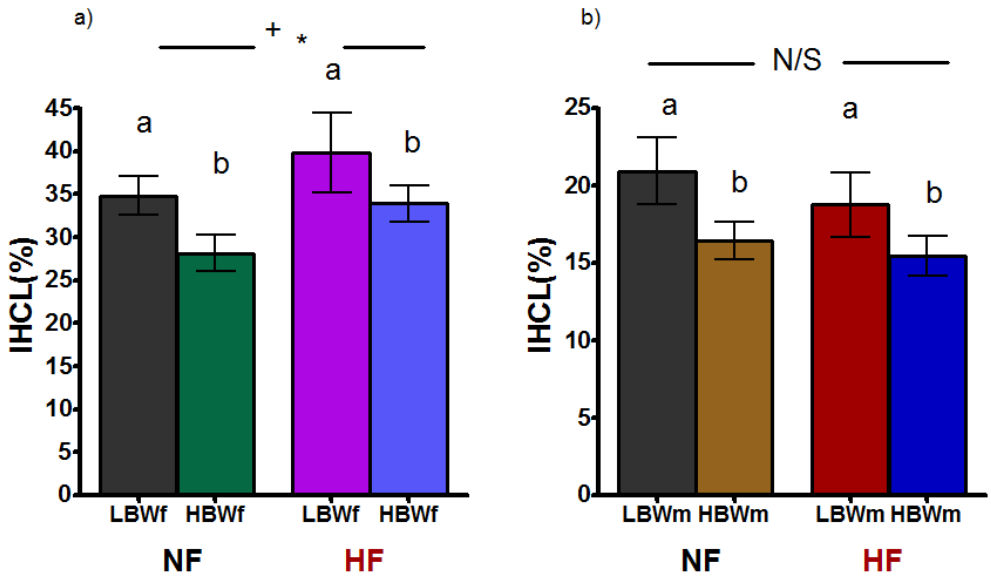

Figure 4.4.2.2 Intrahepatocellular lipid content (IHCL%) of female and male mice at the end of the study (week 15). Statistical analysis was performed using a 2x2 factorial ANOVA analysis. Data presented as mean± SEM. Main effect of diet $^{+}$ =*$\mathbf{p \leq 0.05}$ in female mice a). No significant different=N/S in male mice b), p=0.365. Significant main effect of birth weight represented with different letters in a), $\mathbf{p=0.034}$ and b) $\mathbf{p=0.028}$. **LBWf-NF** n=8; **LBWf-HF** n=8; **HBWf-NF** n=10, **HBWf-HF** n=13; **LBWm-NF** n=15; **LBWm-HF** n=17; **HBWm-NF** n=16, **HBWm-HF** n=17.

Birth weight	Diet	IHCL (%)
LBWf	**NF**	34.838± 2.999
	HF	39.888± 2.999
HBWf	**NF**	28.14± 2.682
	HF	34.354± 2.352
Birth weight effect		**p=0.034**
Diet		**P=0.05**
Interaction (x diet)		p=0.835

Table 4.4.4 Intrahepatocellular lipid content (IHCL%) of female mice at the end of the study (week 15). IHCL was assessed using ^{1}H MRS. Statistical analysis was performed using a 2x2 factorial ANOVA analysis. Data presented as mean± SEM. **LBWf-NF** n=8; **LBWf-HF** n=8; **HBWf-NF** n=10, **HBWf-HF** n=13.

4.5.1 The Effects of birth weight and diet on adipose tissue distribution in young mice (From week 3 until week 15)

15 weeks old offspring was fasted overnight before assessing non-invasively adipose tissue content and distribution by using MRI for localisation followed by subsequent quantification and distribution of adipose tissue by segmentation analysis, as described in section 2.4.1. A 2x2 factorial ANOVA was performed to examine the independent effects of birth weight and diet on adipose tissue distribution and a possible interaction between these two factors.

4.5.1 Adipose tissue distribution in Male offspring

For male offspring, data for total and regional distribution of fat content in grams as well as data normalised to current body weight was naturally log transformed (Ln) in order to correct for unequal variances within groups.

Figure 4.5.1.1a and table 4.5.1.1 show the results of total fat in grams after Ln transformation (Log total fat_g). There was an interaction between both birth weight and diet given to mice throughout the study ($F(1,66)=5.198$ **p=0.026**). This indicated that differences between groups depended on the relationship between variables. Mice fed a **HF** diet had a higher total fat content compared to those mice fed a **NF** diet (**LBWm-HF** vs. **LBWm-NF p=0.042**; **HBWm-HF** vs. **HBWm-NF p<0.001**). Furthermore, there was a significant difference between mice fed a **NF** diet, with a higher total fat content in **LBWm-NF** mice than **HBWm-NF** mice (**p=0.036**) but the

difference did not reach significance between mice fed a **HF** diet (**LBWm-HF** vs. **HBWm-HF** p=0.29).

After normalisation to current body weight, Log total $fat_{\%}$ (Ln) maintained a comparable pattern between groups. Interaction was significant between variables (F(1,66)=5.136 **p=0.027**). Difference between **LBWm-HF** vs. **LBWm-NF** was comparable (p=0.122; figure 4.5.1.1b and table 4.5.1.1).

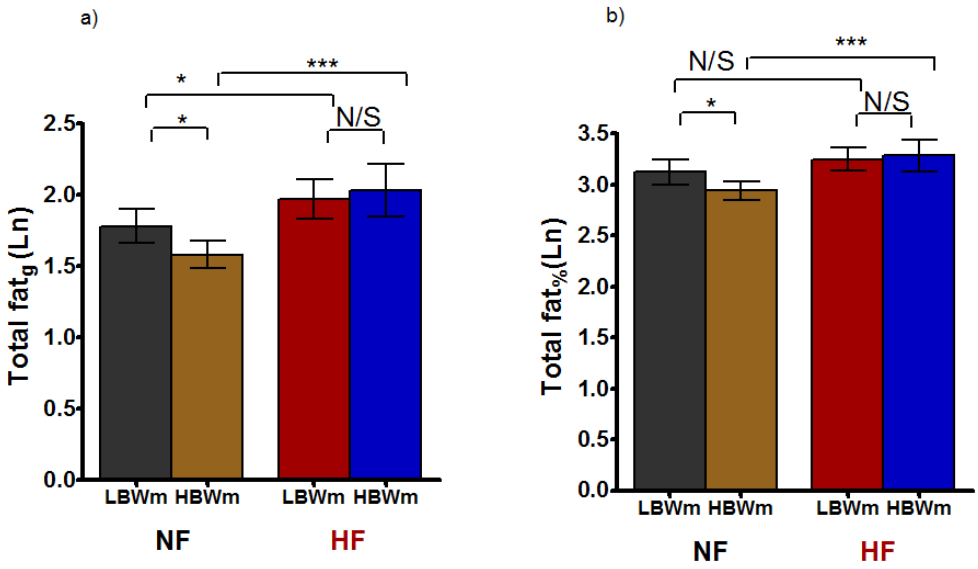

Figure 4.5.1.1 Total fat content of male offspring at 15 weeks of age. Total fat in grams a) and normalised to current body weight (%) b) were natural log transformed (Ln) to correct for unequal variances. *p≤0.05,***p≤0.001. N/S= no significant difference. As interaction was significant between variables, simple main effects with Bonferroni correction were assessed after the factorial ANOVA. N/S= No significant difference (**LBWm- HF** vs. **HBWm-HF** p=0.29 in a); **LBWm-HF** vs. **LBWm-NF** p=0.122 and **LBWm-HF** vs. **HBWm-HF** p=0.371 in b)). *p≤0.05 **(LBWm-NF** vs. **HBWm-NF** a) and b) and **LBWm-HF** vs. **LBWm-NF** in a); *p≤0.001 (**HBWm-NF vs. HBWm-HF** a) and b). Data presented as mean with 95% confidence interval (CI). **LBWm-NF** n=16; **LBWm-HF** n=20; **HBWm-NF** n=18, **HBWm-HF** n=16.

Absolute values (grams) of subcutaneous adipose tissue (SAT) and internal adipose tissue (IAT) had similar trends as seen in total fat content. Interactions were significant for both fat depots (log transformed SAT in grams (Ln SAT_g): (F(1,66)=6.124 **p=0.016**; table 4.5.1. Log transformed IAT in grams (Ln IAT_g): (F(1,66)=4.204 **p=0.044;** table 4.5.1). Mice fed a **HF** diet had a higher SAT (Ln) and IAT (Ln) compared to mice fed a **NF** diet (SAT (Ln): **LBWm-HF** vs. **LBWm-NF p=0.03**; **HBWm-HF** vs. **HBWm-NF p<0.001;** figure 4.5.1.2a and table 4.5.1. IAT (Ln): **LBWm-HF** vs. **LBWm-NF p=0.049**; **HBWm-HF** vs. **HBWm-NF p<0.001**; figure 4.5.1.2c and table 4.5.1.1).

Interactions were maintained after normalisation to current body weight (log transformed SAT normalised to body weight (Ln $SAT_{\%}$): (F(1,66)=6.124 **p=0.016;** table 4.5.1. Log transformed IAT normalised to body weight (Ln $IAT_{\%}$): (F(1,66)=4.204 **p=0.044**; table 4.5.1). However, the significant difference between **LBWm** mice disappeared in both fat depots (SAT (Ln): **LBWm-HF** vs. **LBWm-NF** p=0.19; figure 4.5.1.2b and table 4.5.1.1. IAT (Ln): **LBWm-HF** vs. **LBWm-NF** p=0.258; figure 4.5.1.2d and table 4.5.1.1).

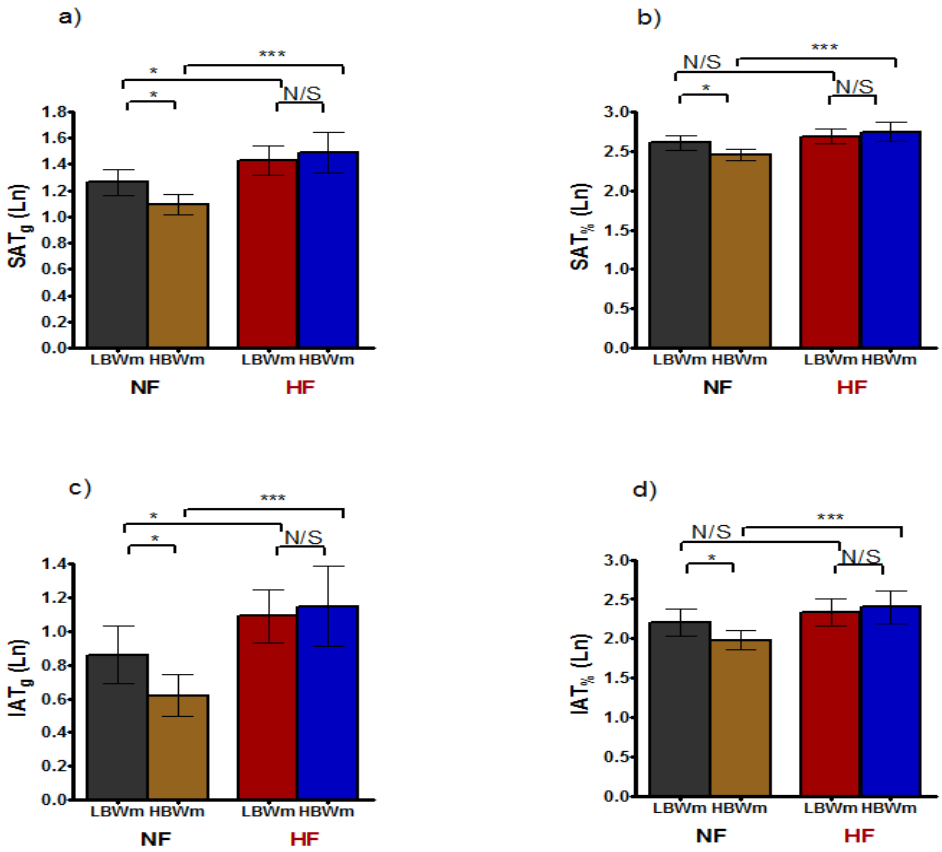

Figure 4.5.1.2 Adipose tissue distribution of male offspring at 15 weeks of age. SAT_g (Ln)= natural log transformed subcutaneous adipose tissue in grams a); $SAT_{\%}$ (Ln)= natural log transformed subcutaneous adipose tissue normalised to body weight b); IAT_g (Ln)= natural log transformed internal adipose tissue in grams c); $IAT_{\%}$(Ln)= natural log transformed internal adipose tissue normalised to body weight d). As interaction was significant between variables, simple main effects with Bonferroni correction were assessed after the factorial ANOVA. N/S= No significant difference (**LBWm- HF** vs. **HBWm-H** a); **LBWm-HF** vs. **LBWm-NF** and **LBWm-HF** vs. **HBWm-HF** p=0.371 b)). *p≤0.05 **(LBWm-NF** vs. **HBWm-NF** a)-d) and **LBWm-HF** vs. **LBWm-NF** in a) and c); ***p≤0.001 (**HBWm-NF vs. HBWm-HF** a)-d). Data presented as mean with 95% confidence interval (CI). **LBWm-NF** n=16; **LBWm-HF** n=20; **HBWm-NF** n=18, **HBWm-HF** n=16.

Assessment of internal to adipose tissue ratio showed a main effect of birth-weight (F(1,65)=4.176 **p=0.045**; figure 4.5.1.3 and table 4.5.1.1) and diet *per se* (diet: F(1,66)=9.997 **p=0.002**; table 4.5.1.1). No interaction between variables was found (F(1,65)=1.079 p=0.303; table 4.5.1.1).This indicated that **LBWm** mice had a higher ratio compared to **HBWm** mice. Moreover, mice fed a **HF** had a higher ratio compared to mice fed a **NF** diet independently of the birth weight.

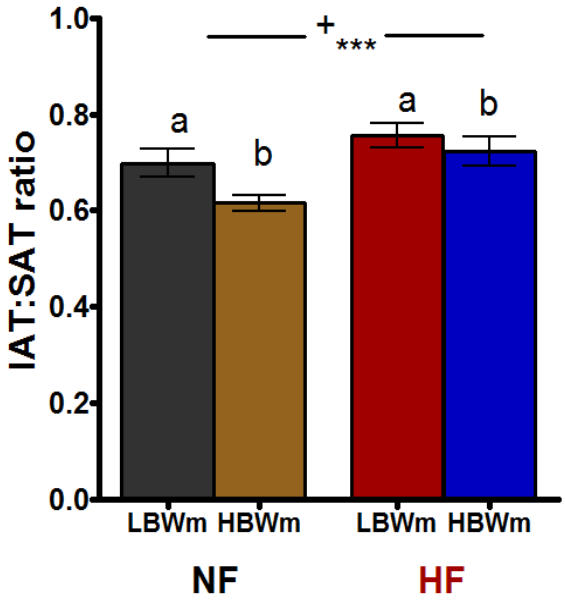

Figure 4.5.1.3 Internal to subcutaneous adipose tissue ratio of male offspring at 15 weeks of age. Statistical analysis was performed using a 2x2 factorial ANOVA analysis. Main effect of diet $^{+}$ =***p≤0.001. Significant main effect of birth weight represented with different letters (p=0.045). Data presented as mean± SEM. **LBWm-NF** n=15; **LBWm-HF** n=20; **HBWm-NF** n=18, **HBWm-HF** n=16.

	LBWm-NF_1	LBWm-HF_2	HBWm-NF_3	HBWm-HF_4	p-value
Total WAT_g (Ln)	1.78 (1.646-1.815)	1.969 (1.848-2.09)	1.581 (1.454-1.708)	2.066 (1.931-2.2)	**1 vs.2=0.042 3vs.4<0.001 1vs.3=0.036** 2vs.4=0.29
Total $WAT_{\%}$ (Ln)	3.125 (3.008-3.242)	3.248 (3.144-3.353)	2.941 (2.83-3.051)	3.319 (3.202-3.436)	**1 vs.2**=0.122 **3vs.4<0.001 1vs.3=0.025** 2vs.4=0.371
SAT_g (Ln)	1.264 (1.154-1.373)	1.427 (1.329-1.525)	1.096 (0.992-1.199)	1.521 (1.329-1.631)	**1 vs.2=0.03 3vs.4<0.001 1vs.3=0.03** 2vs.4=0.209
$SAT_{\%}$ (Ln)	2.608 (2.514-2.703)	2.691 (2.607-2.776)	2.455 (2.366-2.544)	2.775 (2.68-2.869)	**1 vs.2**=0.198 **3vs.4<0.001 1vs.3=0.022** 2vs.4=0.193
IAT_g (Ln)	0.862 (0.691-1.033)	1.092 (0.939-1.245)	0.62 (0.459-0.782)	1.188 (1.017-1.358)	**1 vs.2=0.049 3vs.4<0.001 1vs.3=0.044** 2vs.4=0.41
$IAT_{\%}$ (Ln)	2.207 (2.039-2.376)	2.336 (2.186-2.487)	1.98 (1.821-2.139)	2.441 (2.273-2.61)	**1 vs.2**=0.258 **3vs.4<0.001 1vs.3=0.05** 2vs.4=0.357
IAT:SAT ratio	0.699±0.029	0.756±0.024	0.616±0.027	0.729±0.028	**Main effect birth weight: p=0.045 Main effect diet: p=0.002**

Table 4.5.1 Adipose tissue distribution in male offspring at 15 weeks. Total WAT_g (Ln)= natural log transformed total fat in grams, **Total $WAT_{\%}$ (Ln)**= natural log transformed total fat normalised to body weight as percentage, SAT_g (Ln)= natural log transformed subcutaneous adipose fat in grams, **$SAT_{\%}$ (Ln)**= natural log transformed subcutaneous adipose fat normalised to body weight as percentage, IAT_g (Ln)= natural log transformed internal adipose fat in grams, **$IAT_{\%}$ (Ln)**= natural log transformed internal adipose fat normalised to body weight as percentage. Statistical analysis was performed using a 2x2 factorial ANOVA. When interaction was significant between variables, simple main effects with Bonferroni correction were assessed after the factorial ANOVA. Data presented as mean with 95% confidence intervals (CI) except from IAT:SAT ratio (presented as mean± SEM).

4.5.2 Adipose tissue distribution in Female offspring

After normalisation, assessment of total fat showed that diet had a significantly main effect on total fat (total fat_g (Ln): $F(1,37)=14.708$ **$p<0.001$**). Birth weight did not have an independent effect on total fat (Ln) ($F(1,37)=1.516$ $p=0.226$) and there was not an interaction between birth weight and diet ($F(1,37)=0.18$ $p=0.674$). This indicated that females that were fed a **HF** diet had a higher total adiposity compared to females fed a **NF** diet irrespectively of their birth weight (figure 4.5.2.1a and table 4.5.2.1). These differences were maintained after normalisation of total body fat to current body weight (%) (diet: ($F(1,37)=7.866$ **$p=0.008$;** birth weight: $F(1,37)=0.068$ $p=0.796$; interaction diet x birth weight: $F(1,37)=0.141$ $p=0.71$; figure 4.5.2.1b and table 4.5.2.1). As aforementioned in section 4.1 (figure 4.1.2.1 and 4.1.2.2), **LBWf** mice had a lower body weight throughout the study. Therefore, although these females were lighter in weight they had a comparable total fat_g (Ln) and total fat (%) to the heavier females.

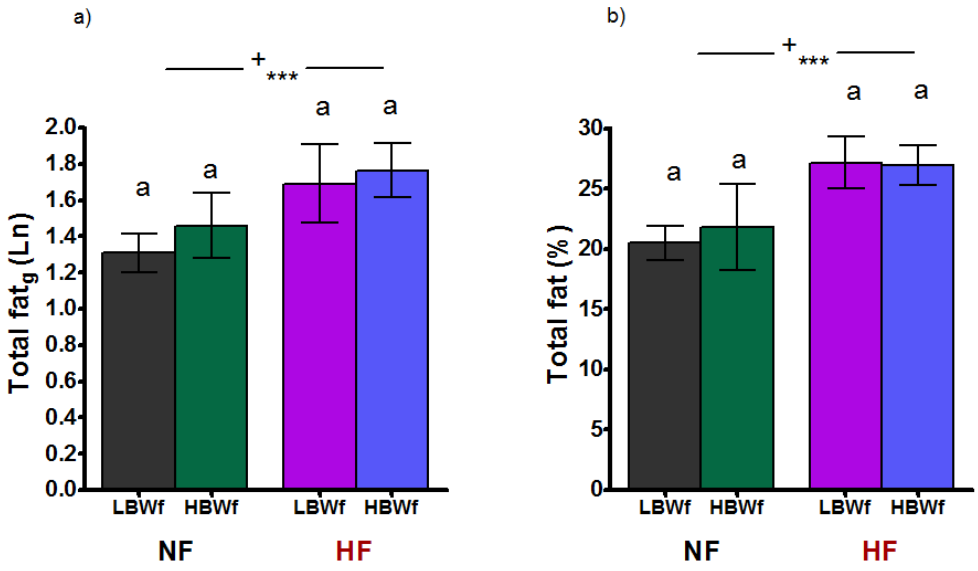

Figure 4.5.2.1 Total fat content of female offspring at 15 weeks of age. Total fat in grams a) was natural log transformed (Ln) to correct for unequal variances. Total fat %= total fat normalised to current body weight expressed as percentage (%). Main effect of diet $^{+}$ =***p≤0.001 a) and b). No significant main effect of birth weight represented with equal letters (p=0.226 in a) p=0.796 in b)). Data presented as mean with 95% confidence interval (CI) for total fat$_g$ (Ln) and as mean± SEM for Total fat (%). **LBWf-NF** n=12; **LBWf-HF** n=9; **HBWf-NF** n=5, **HBWf-HF** n=15.

Subcutaneous adipose tissue (SAT) and internal adipose in grams (IAT) had similar patterns as seen in total fat_g (Ln), with a main effect of diet only (SAT(g): F(1,37)=14.266 **p=0.001**; IAT(g): F(1,37)=14.266 **p=0.002**; figures 4.5.2.2a and 4.5.2.2c respectively; table 4.5.2.1). The main effect of diet was maintained when normalising to body weight for both regional fat depots (SAT%: (F(1,37)=9.316 **p=0.004**; IAT%: (F(1,37)=6.286 **p=0.017**; figures 4.5.2.2b and 4.5.2.2d; table 4.5.2.1).

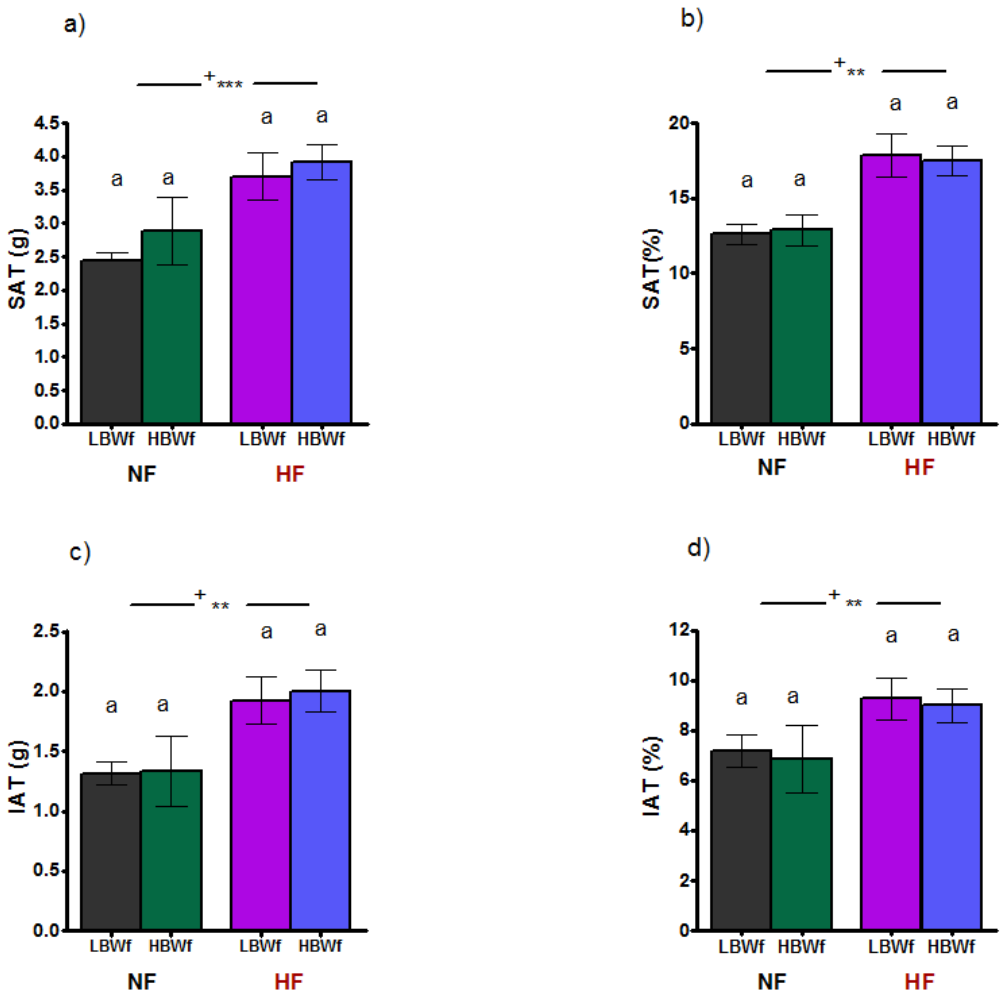

Figure 4.5.2.2 Adipose tissue distribution of female offspring at 15 weeks of age. SAT (g)= subcutaneous adipose tissue in grams a); SAT(%)= subcutaneous adipose tissue expressed as percentage of body weight b); IAT(g)= internal adipose tissue in grams c); IAT(%)=internal adipose tissue expressed as percentage of body weight d). Main effect of diet $^{+}$=***p≤0.001 in a) and **p≤0.01 in c)-d). No significant main effect of birth weight represented with equal letters (p=0.277 in a), p=0.441 in b), p=0.803 in c) and p=0.721 in d)). Data presented as mean± SEM. **LBWf-NF** n=12; **LBWf-HF** n=9; **HBWf-NF** n=5, **HBWf-HF** n=15.

	LBWf-NF_1	LBWf-HF_2	HBWf-NF_3	HBWf-HF_4	Effects and Interaction
Total WAT_g (Ln)	1.31 (1.156-1.465)	1.692 (1.514-1.87)	1.458 (1.219-1.698)	1.764 (1.626-1.902)	**Birth weight:** p=0.226 **Diet: p<0.001** **Interaction:** p=0.674
Total WAT (%)	20.482 ±1.848	27.14 ±2.134	21.811 ±2.614	26.899 ±1.653	**Birth weight:** p=0.796 **Diet: p=0.008** **Interaction:** p=0.71
SAT (g)	2.442 ±0.267	3.701 ±0.309	2.892 ±0.378	3.92 ±0.239	**Birth weight:** p=0.277 **Diet: p=0.001** **Interaction:** p=0.706
SAT (%)	12.609 ±1.169	17.872 ±1.292	14.966 ±1.582	17.51 ±1.01	**Birth weight:** p=0.441 **Diet: p=0.004** **Interaction:** p=0.295
IAT (g)	1.314 ±0.166	1.925 ±0.192	1.333 ±0.235	2.01 ±0154	**Birth weight:** p=0.803 **Diet: p=0.002** **Interaction:** p=0.882
IAT (%)	7.184 ±0.742	9.267 ±0.856	6.845 ±1.049	8.998 ±0.687	**Birth weight:** p=0.721 **Diet: p=0.017** **Interaction:** p=0.968

Table 4.5.2.1 Adipose tissue distribution in female offspring at 15 weeks. Total WAT_g (Ln)=natural log transformed total fat in grams, Total WAT(%)=total fat normalised to body weight (%), SAT(g)=subcutaneous adipose fat in grams, SAT (%)=subcutaneous adipose fat normalised to body weight (%), IAT (g)=internal adipose fat in grams, IAT(%)=internal adipose fat normalised to body weight as percentage. Statistical analysis was performed using a 2x2 factorial ANOVA analysis.Data presented as mean± SEM except from Total WAT_g (Ln) which is presented as mean with 95% confidence intervals (CI). **LBWf-NF** n=12; **LBWf-HF** n=9; **HBWf-NF** n=5, **HBWf-HF** n=15.

Assessment of the internal to subcutaneous adipose tissue ratio showed a marginal effect of diet (F(1,37)=3.153 p=0.084; figure 4.5.2.3 ant table 4.5.2.2). There was not a main effect of birth weight or interaction between variables (: (F(1,37)=1.686 p=0.202; interaction diet x birth- weight: (F(1,37)=1.126 p=0.296).

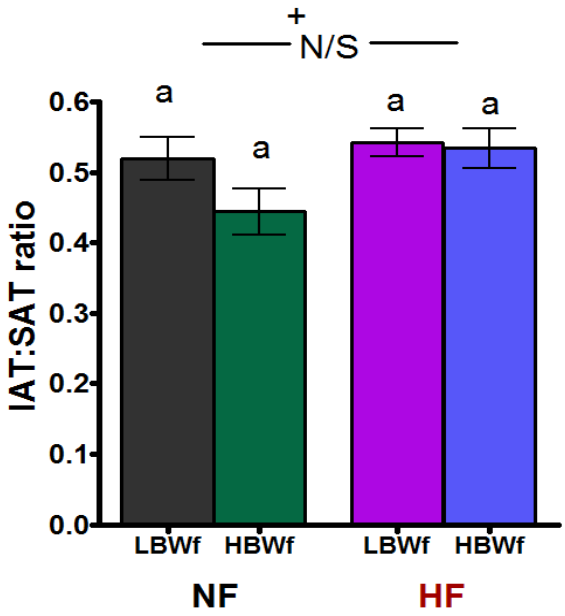

Figure 4.5.2.3 Internal to subcutaneous adipose tissue ratio of female offspring at 15 weeks of age. Statistical analysis was performed using a 2x2 factorial ANOVA analysis. Effect of diet $^{+}$: N/S= no significant (p=0.084). No significant effect of birth weight represented with equal letters. Data presented as mean± SEM. **LBWf-NF** n=12; **LBWf-HF** n=9; **HBWf-NF** n=5, **HBWf-HF** n=15.

	LBWf-NF_1	LBWf-HF_2	HBWf-NF_3	HBWf-HF_4	Effects and Interaction
IAT:SAT ratio	0.519±0.029	0.542±0.033	0.444±0.039	0.534±0.024	**Birth weight:** p=0.296 **Diet:** p=0.084 **Interaction:** p=0.296

Table 4.5.2.2 Internal to subcutaneous adipose tissue ratio in female offspring at 15 weeks. Statistical analysis was performed using a 2x2 factorial ANOVA. Data presented as mean± SEM. **LBWf-NF** n=12; **LBWf-HF** n=9; **HBWf-NF** n=5, **HBWf-HF** n=15.

4.6 The Effects of Birth Weight and Diet on Metabolic Markers and Glucose Tolerance in Young Mice (From Week 3 Until Week 15)

Plasma samples were used to assess metabolic markers in both male and female mice at week 15 of age. Samples were collected in a postprandial state.

To assess changes in glucose tolerance due to the effect of birth weight and diet an intraperitoneal glucose tolerance test (IPGTT) was performed. Mice were fasted overnight for 16-18 hours prior to the test. The protocol for this test is described in detailed in section 2.4.3.

4.6.1 Metabolic markers in Male mice

Whole blood glucose assessment showed a main effect of birth weight on the level of glucose ($F(1,43)=4.698$ **p=0.036**; figure 4.6.1.1). This indicated that **LBWm** mice had a higher glucose level than **HBWm** mice, independently of the diet given throughout the study; no main effect of diet was found ($F(1,43)=1.87$ $p=0.179$; figure 4.6.1.1 and table 4.6.1.1). Furthermore, there was not a significant interaction between variables ($F(1,43)=0.668$ $p=0.418$; figure 4.6.1.1 ant table 4.6.1.1).

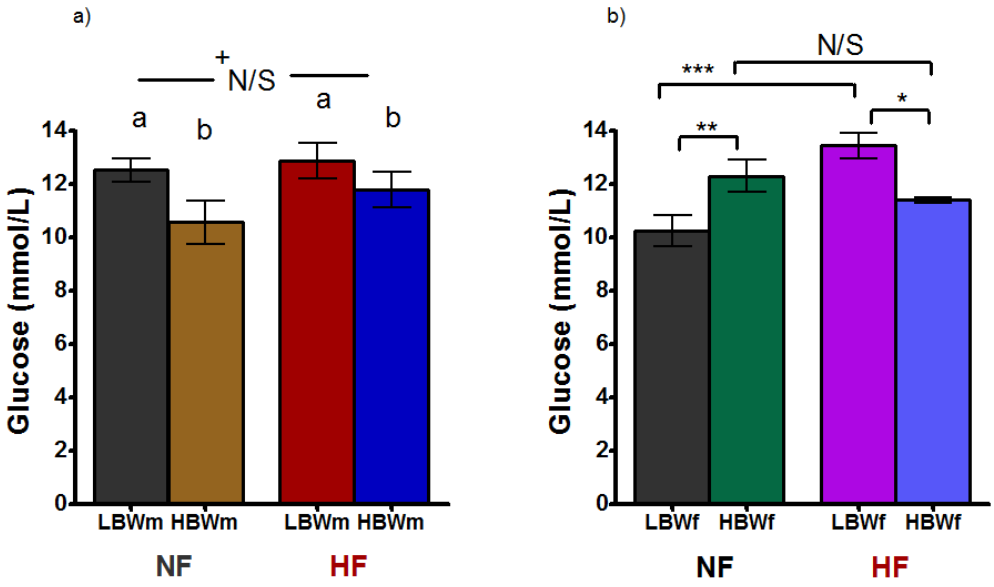

Figure 4.6.1.1 Glucose level in male and female offspring at 15 weeks of age. Glucose was measured in whole blood at the time of tissue collection. Statistical analysis was performed using a 2x2 factorial ANOVA test. Main effect of diet $^{+}$: N/S= no significant (p=0.179). Main effect of birth weight represented with different letters. Data presented as mean± SEM. **LBWm-NF** n=12; **LBWm-HF** n=11; **HBWm-NF** n=10, **HBWm-HF** n=15. 2x2 factorial ANOVA test was followed by simple main effects analysis in female mice b), as the interaction was significant. N/S= no significant difference (p=0.309); *p≤0.05, **p≤0.01, ***p≤0.001. **LBWf-NF** n=10; **LBWf-HF** n=13; **HBWf-NF** n=8, **HBWf-HF** n=6.

Following the evaluation of insulin (Ln), there was a comparable level between groups by birth weight (birth weight: (F(1,42)=1.058 p=0.31) but there was main effect of diet: (F(1,42)=4.867 **p=0.033**) without interaction (F(1,42)=1.439 p=0.237; figure 4.6.1.2a and table 4.6.1.1). Mice fed a **HF** diet had higher insulin than mice fed a **NF** diet.

Insulin related markers such as c-peptide, GIP and glucagon were also assessed. There was not a significant main effect of either birth weight or diet between groups in the level of c-peptide ((birth weight: (F(1,45)=0.042 p=0.838; diet: (F(1,45)=0.205 p=0.653; interaction (F(1,45)=0.096 p=0.758; figure 4.6.1.2b and table 4.6.1.1). Natural log transformed GIP (Ln) showed a significant interaction between both birth weight and diet (F(1,39)=5.02 **p=0.031**; figure 4.6.1.2c and table 4.6.1.1). After simple main effects analysis, no significant difference was found between mice fed a **NF** diet or a **HF** diet (**LBWm-NF** vs. **HBWm-NF** p=0.133; **LBWm-HF** vs. **HBWm-HF** p=0.108). Whilst levels of **LBWm-NF** mice tended to be higher than **HBWm-NF** mice, GIP levels of **LBWm-HF** mice tended to be lower than **HBWm-HF** mice. Furthermore, GIP levels were significantly higher in **HBWm-HF** compared to **HBWm-NF** (**p=0.037**). Differences between **LBWm** mice did not reach significance (p=0.326). Glucagon was only affected by the diet given to mice and not for the birth weight (diet: F(1,40)=6.469 **p=0.015**; F(1,40)=0.168 p=0.684; interaction: F(1,40)=1.295 p=0.262; figure 4.6.1.2d and table 4.6.1.1). Mice fed a **NF** diet had higher levels of glucagon than mice fed a **HF** diet.

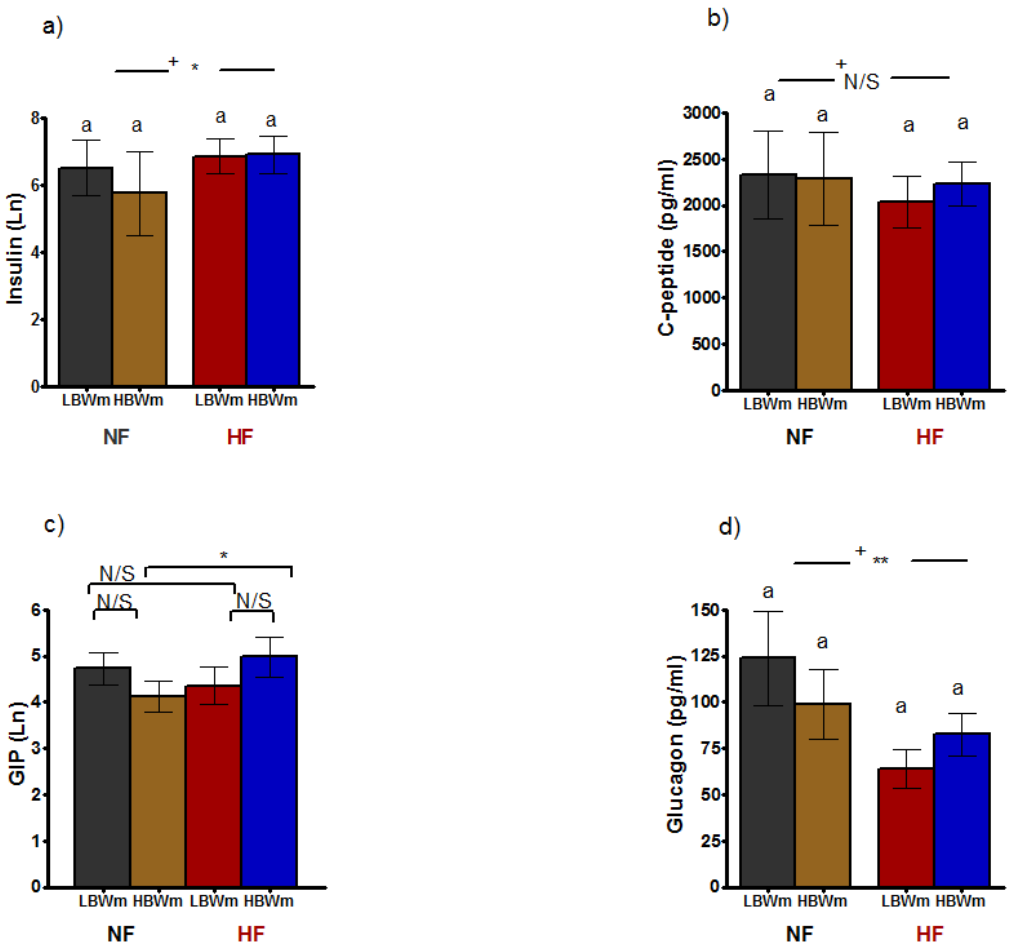

Figure 4.6.1.2 Metabolic markers in plasma of male mice fed both a **NF** diet and **HF** diet at 15 weeks of age. This figure shows insulin levels a) and some metabolic markers related to insulin secretion and stimulation/regulation such as c-peptide b), GIP c) and glucagon d). GIP= glucose dependant- insulinotropic peptide GIP values were natural log transformed before the analysis. Statistical analysis was performed using a 2x2 factorial ANOVA test followed by simple main effects when interaction was significant (only c). Main effect of diet $^{+}$: N/S= no significant for b); *p≤0.05 in a) and ** p≤0.01 in d). Data presented as mean± SEM, except from insulin and GIP, which are presented as mean with 95% confidence interval (CI). **LBWm-NF** n=10-12; **LBWm-HF** n=11-12; **HBWm-NF** n=9-11, **HBWm-HF** n=13-15.

The gut peptide ghrelin was affected by the interaction between both birth weight and diet (F(1,43)=5.251 **p=0.027**; figure 4.6.1.3 and table 4.6.1.1). Ghrelin levels were lower in **LBWm-NF** mice compared to **HBWm-NF** mice (**p=0.003**); difference between mice fed a HF diet was not significant (p=0.955). Furthermore, **HBWm-NF** mice had a significant higher level compared to **HBWm-HF** mice (**p=0.028**). Different pattern was seen between **LBWm** mice with a higher level of ghrelin in **LBWm-HF** compared to **LBWm-NF** but the difference did not reach statistical significance (p=0.321).

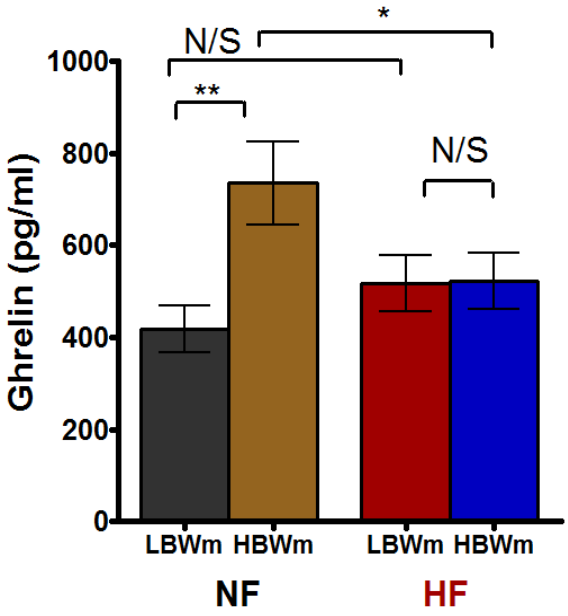

Figure 4.6.1.3 Ghrelin levels in plasma of male offspring at 15 weeks of age. Statistical analysis was performed using a 2x2 factorial ANOVA test followed by simple main effects, as interaction was significant. N/S= no significant difference: (**LBWm-NF** vs. **LBWm-HF** p=0.321; **LBWm-HF** vs. **HBWm-HF** p=0.955). *p≤0.05, **p≤0.01. Data presented as mean± SEM. **LBWm-NF** n=10; **LBWm-HF** n=12; **HBWm-NF** n=11, **HBWm-HF** n=14.

Adipokines such as leptin and resistin were also evaluated. Both birth weight and diet interacted affecting the levels of leptin in males (F(1,41)=7.004 **p=0.011**; figure 4.6.1.4a and table 4.6.1.1). There was significant difference between males fed a **NF** diet with a higher level in **LBWm** mice (**p=0.045**; figure 4.6.1.4a and table 4.6.1.1) but there was not a significant difference between males fed a **HF** diet (p=0.105). Furthermore, there was a significant difference between **HBWm** mice (**p<0.001;** but not between **LBWm** mice (p=0.356. Resistin was also affected by the interaction of diet and birth-weight (F(1,40)=5.803 **p=0.021**; figure 4.6.1.4b and table 4.6.1.1). Mice fed a **HF** had a significant difference with **LBWm-HF** having a lower level than **HBWm-HF** (**p=0.041**) but not significant difference was found between mice fed **NF** diet (p=0.194). Comparable differences were found between **LBWm** mice (p=0.516) but there was a significant difference between **HBWm** mice (**p<0.001**).

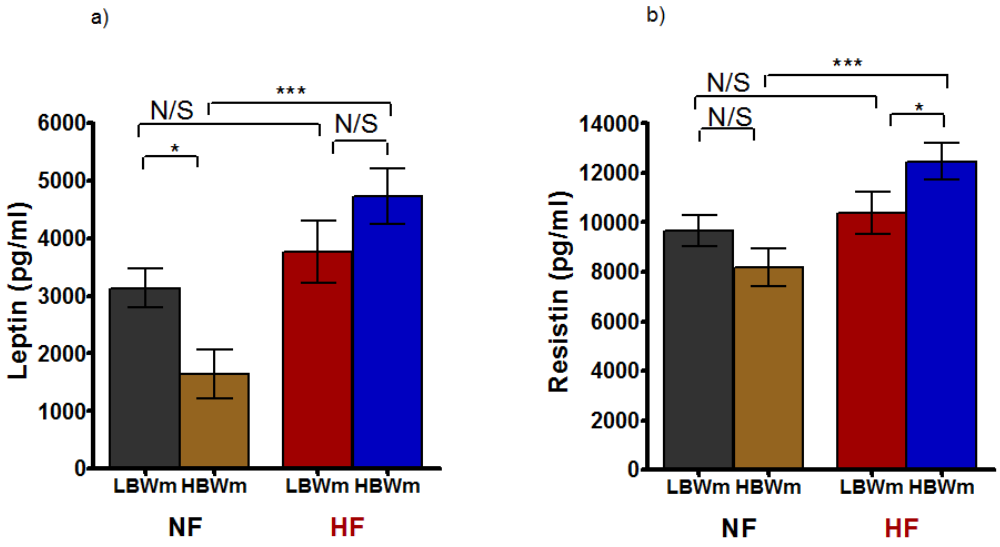

Figure 4.6.1.4 Leptin and resistin levels in plasma of male offspring at 15 weeks of age. Leptin a) and resistin b) levels. Statistical analysis was performed using a 2x2 factorial ANOVA test followed by simple main effects, as interaction was significant. N/S= no significant difference. *p≤0.05, ***p≤0.001. Data presented as mean± SEM. **LBWm-NF** n=11; **LBWm-HF** n=11-12; **HBWm-NF** n=9-10, **HBWm-HF** n=12-13.

Proinflammatory cytokines such as IL-6 and MCP-1 were also assessed.

IL-6 levels were significantly affected by birth weight *per se* but not for diet; there was not a significant interaction between both (birth weight: F(1,21)=6.687 **p=0.017**; diet: F(1,21)=0.205 p=0.656; interaction: F(1,21)=0.869 p=0.362; figure 4.6.1.5a and table 4.6.1.1). **HBWm** mice had a higher level of IL-6 in plasma than **LBWm** mice irrespectively of the diet given to them. However, the MCP-1 levels in plasma were affected by both birth weight and diet, in a independent manner with no interaction between both (birth weight: F(1,40)=4.24 **p=0.046**; diet: F(1,40)=5.826 **p=0.02**;

interaction: F(1,40)=0.002 p=0.967; figure 4.6.1.5b and table 4.6.1.1). **LBWm** mice had a higher MCP-1 level concentration than **HBWm** mice, but at the same time, mice fed a **HF** diet had a higher level of MCP-1 compared to mice fed a **NF** diet, independently of birth weight and vise versa.

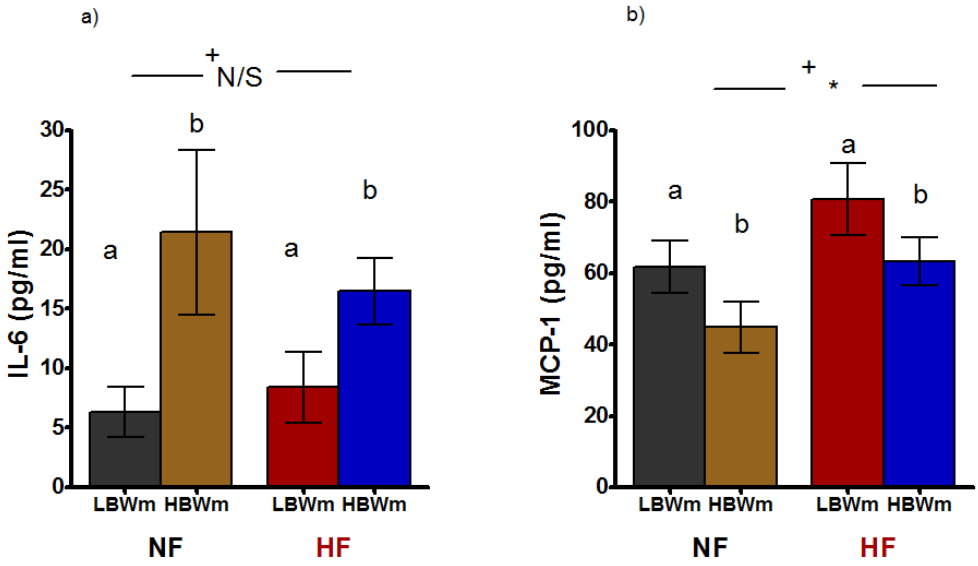

Figure 4.6.1.5 Proinflammatory cytokines of male offspring plasma at 15 weeks of age. IL-6= interleukine 6 a) and MCP-1= monocyte chemotactic peptide 1 b). Main effect of diet $^{+}$ = N/S= no signficant in a) and *p≤0.05 in b). Significant main effect of birth weight represented with different letters. Statistical analysis was performed using a 2x2 factorial ANOVA analysis. Data presented as mean± SEM. **LBWm-NF** n=4/10; **LBWm-HF** n=5/10; **HBWm-NF** n=5/10, **HBWm-HF** n=11/14.

	LBWm-NF_1	LBWm-HF_2	HBWm-NF_3	HBWm-HF_4	P value
C-peptide pg/ml	2328.178 ±381.033	2039.78 ±381.033	2288.813 ±397.976	2234.733 ±352.768	**Birth weight:** p=0.838 **Diet:** p=0.653 **Interaction:** p=0.758
GIP (Ln)	4.722 ±0.274	4.354 ±0.25	4.111 ±0.289	4.935 ±0.25	**1 vs.2**=0.326 **3vs.4=0.037** **1vs.3=**0.133 **2vs.4**=0.108
Glucagon pg/ml	123.694 ±16.8	63.931 ±24.273	98.575 ±17.709	75.76 ±14.199	**Birth weight:** p=0.684 **Diet: p=0.015** **Interaction:** p=0.262
Insulin (Ln)	6.524 (5.8-7.22)	6.863 (6.2-7.527)	5.773 (4.995-6.552)	6.921 (6.352-7.489)	**Birth weight:** p=0.416 **Diet:** p=0.703 **Interaction:** p=0.797
Ghrelin pg/ml	417.373 ±73.197	516.951 ±66.82	734.42 ±69.791	522.149 ±61.863	**1 vs.2**=0.321 **3vs.4=0.028** **1vs.3=0.003** **2vs.4**=0.955
Leptin pg/ml	3133.036 ±482.55	3756.486 ±462.007	1647.123 ±533.48	4819.86 ±443.882	**1 vs.2**=0.356 **3vs.4<0.001** **1vs.3=0.045** **2vs.4**=0.105
Resistin pg/ml	9659.14 ±769.751	10372.459 ±769.751	8186.564 ±807.321	12617.217 ±736.98	**1 vs.2**=0.516 **3vs.4<0.001** **1vs.3**=0.194 **2vs.4=0.041**
Il-6 pg/ml	6.326 ±4.985	8.385 ±4.459	21.422 ±4.459	15.481 ±3.01	**Birth weight: p=0.017** **Diet:** p=0.656 **Interaction:** p=0.362
MCP-1 pg/ml	61.597 ±8.318	80.609 ±8.318	44.749 ±8.318	64.431 ±7.03	**Birth weight: p=0.046** **Diet: p=0.02** **Interaction:** p=0.967

Table 4.6.1.1 Metabolic markers measured in plasma from male mice at week 15 of age. Data presented as mean± SEM except from GIP (Ln) and insulin (Ln), which are presented as mean with 95% confidence interval (CI).

4.6.2 Metabolic markers in Female mice

Contrary to males, there was an interaction between variables in the female group (F(1,33)=13.457 **p=0.001**; figure 4.6.2.1) when assessing blood glucose concentration. **LBWf-NF** mice had a higher blood glucose compared to **LBWf-NF** mice (**p=0.012**). However, **LBWf-HF** had a higher blood glucose level than **HBWf-HF** mice (**p=0.016**). Difference between **LBWf** mice was significantly different (**p<0.001**), whilst the difference between **HBWf** did not reach significance (p=0.309).

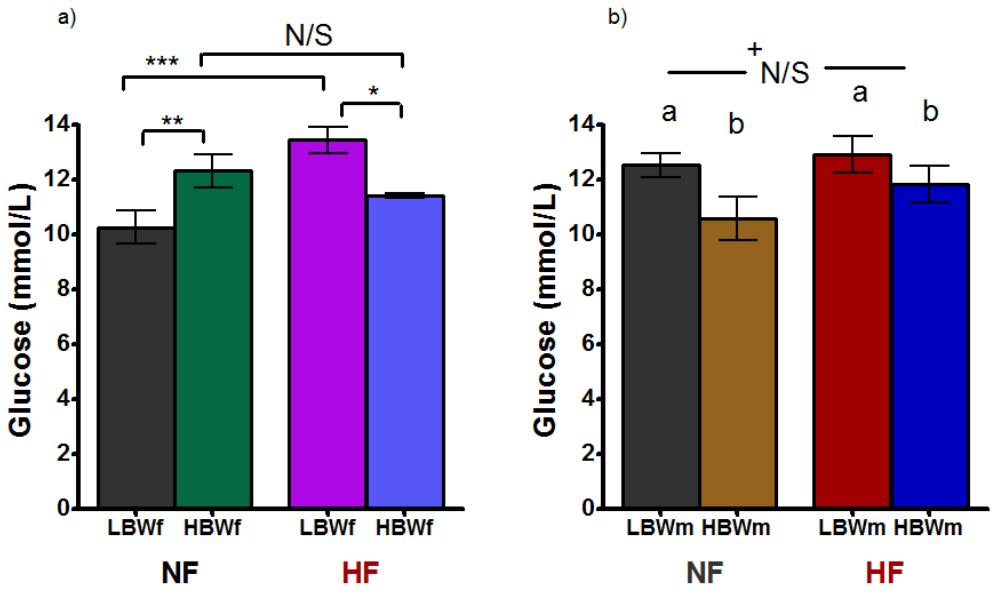

Figure 4.6.2.1 Glucose level in female and male offspring at 15 weeks of age. Glucose was measured in whole blood at the time of tissue collection. Statistical analysis was performed using a 2x2 factorial ANOVA test followed by simple main effects analysis, as the interaction was significant in female mice a). N/S= no significant difference (p=0.309); *p≤0.05, **p≤0.01, ***p≤0.001. Data presented as mean± SEM. **LBWf-NF** n=10; **LBWf-HF** n=13; **HBWf-NF** n=8, **HBWf-HF** n=6. Main effect of diet in male mice b) $^{+}$: N/S= no significant (p=0.179). Main effect of birth weight represented with different letters in male mice b). **LBWm-NF** n=12; **LBWm-HF** n=11; **HBWm-NF** n=10, **HBWm-HF** n=15.

Log transformed insulin (Ln) analysis showed diet had an effect on the level of insulin independently of (F(1,19)=7.192 **p=0.015**; figure 4.6.2.2a and table 4.6.2.1), with **HF** fed females having a higher insulin level compared to **NF** fed females.

Insulin related markers such as c-peptide, GIP and glucagon were also assessed as in males. C-peptide levels between groups were marginally significant for main effect of birth weight (birth weight: (F(1,29)=3.405 p=0.075; figure 4.6.2.2b and table 4.6.2.1), with **LBWf** mice having a lower value than **HBWf** mice. Diet effect was no significant (F(1,29)=0.102 p=0.752) and there was no interaction between variables (F(1,29)=0.057 p=0.812; figure 4.6.2.2b and table 4.6.2.1). GIP levels was not affected by the interaction between variables as in males, but there was an effect of diet (F(1,30)=4.371 **p=0.045**; figure 4.6.2.2c and table 4.6.2.1). **HF** fed mice had a higher level of GIP compared to mice fed a **NF** diet. Glucagon was not affected by either diet or birth weight *per se* (diet: F(1,31)=0.143 p=0.707; birth weight: (F(1,31)=0.49 p=0.489; figure 4.6.2.2d and table 4.6.2.1) and there was not interaction between both variables (F(1.31)=0.481 p=0.493).

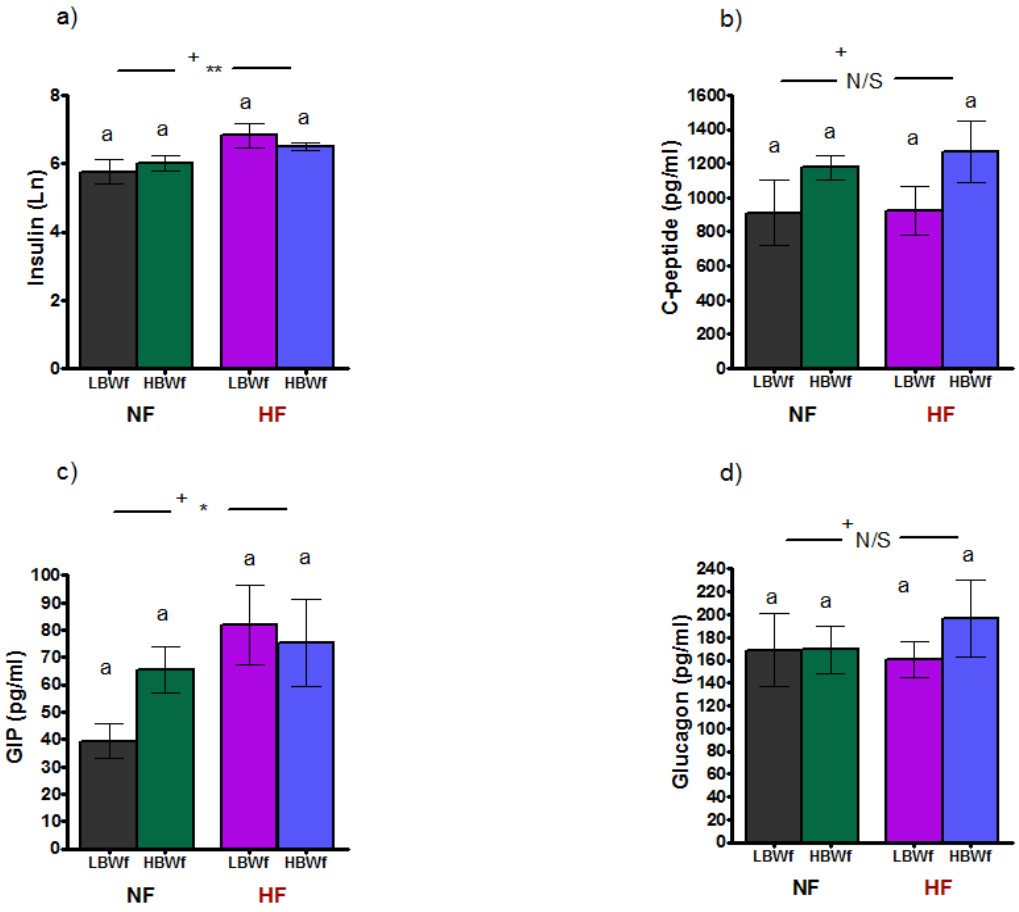

Figure 4.6.2.2 Metabolic markers in plasma from female mice fed both a **NF** diet and **HF** diet at 15 weeks of age. This figure shows insulin levels a) and some metabolic markers related to insulin secretion and stimulation/regulation such as c-peptide b), GIP c) and glucagon d). Insulin values were natural log transformed before the analysis. Statistical analysis was performed using a 2x2 factorial ANOVA test. Main effect of diet $^{+}$: N/S= no significant for b) and d); *p≤0.05 in c) and ** p≤0.01 in a). No significant effect of birth weight represented with equal letters. Data presented as mean± SEM, except from insulin, which is presented as mean with 95% confidence interval (CI). **LBWfNF** n=6-8; **LBWf-HF** n=7-12; **HBWf-NF** n=6-7, **HBWf-HF** n=5-8.

The gut peptide ghrelin was affected by the interaction between both birth weight and diet (F(1,28)=5.706 **p=0.024**; figure 4.6.2.3 and table 4.6.2.1). Ghrelin levels were lower in **HBWf-NF** mice compared to **HBWf-HF** mice (**p=0.014**) but there was a comparable level between mice fed a **NF** diet (p=0.498). Moreover, there was a significant difference between **HBWf** mice (**p=0.009**) but not between **LBWf** mice (p=0.784).

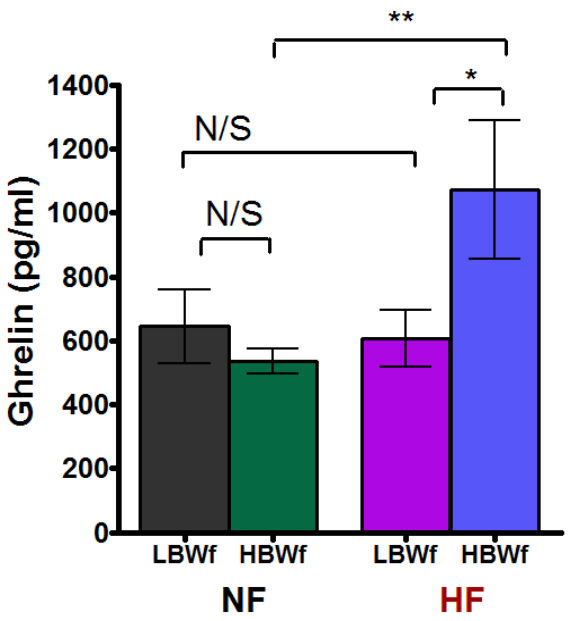

Figure 4.6.2.3 Ghrelin levels in plasma of female offspring at 15 weeks of age. Statistical analysis was performed using a 2x2 factorial ANOVA test followed by simple main effects, as interaction was significant. N/S= no significant difference: (**LBWf-NF** vs. **LBWf-HF** p=0.784; **LBWf-NF** vs. **HBWf-NF** p=0.498). *p≤0.05, **p≤0.01. Data presented as mean± SEM. **LBWf-NF** n=9; **LBWf-HF** n=11; **HBWf-NF** n=7, **HBWf-HF** n=7.

Adipokines such as leptin and resistin were also evaluated. Leptin was affected by both birth weight (F(1,33)=4.008 **p=0.05**; figure 4.6.2.4a and table 4.6.2.1) and diet (F(1,33)=8.135 **p=0.007**; figure 4.6.2.4a and table 4.6.2.1) independently as their interaction was not significant (F(1,33)=0.478 p=0.494). Resistin on the contrary, was not affected by any of the variables (diet: F(1,35)=0.283 p=0.598; birth weight: (F(1,35)=0.757 p=0.39); interaction: F(1,35)=1.426 p=0.24; figure 4.6.2.4b and table 4.6.2.1).

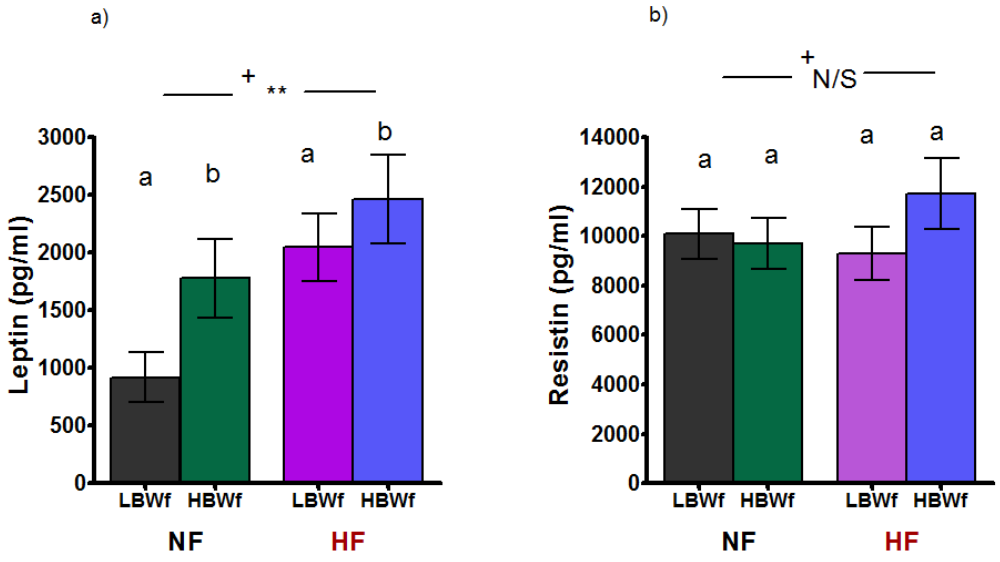

Figure 4.6.2.4 Leptin and resistin levels in plasma of female offspring at 15 weeks of age. Statistical analysis was performed using a 2x2 factorial ANOVA. Main effect of diet $^{+}$: **p≤0.01 in a) and N/S= no significant difference in b). Main effect of birth weight represented with different letters in a) and no significant effect represented with equal letters in b). Data presented as mean± SEM. **LBWf-NF** n=9-10; **LBWf-HF** n=13; **HBWf-NF** n=8, **HBWf-HF** n=7-8.

Proinflammatory cytokines such as IL-6 and MCP-1 were again assessed.

IL-6 levels of **HBWf-NF** were below the detection limit and could not be assessed. However, when comparing the rest of the groups with a one-way ANOVA test, significant differences were found between **LBWf** mice (**p=0.05**) and between mice fed a **HF** diet (**p=0.024**). As the values of **HBWf-NF** were lower than the minimum detectable level, it suggested that **LBWf-NF** had a higher level than this groups as well as **HBWf-HF** (figure 4.6.2.5a and table 4.6.2.1). MCP-1 levels was affected by birth weight ($F(1,26)=4.218$ **p=0.05**; figure 4.6.2.5b) but it was not affected by diet ($F(1,26)=0.001$ $p=0.981$).

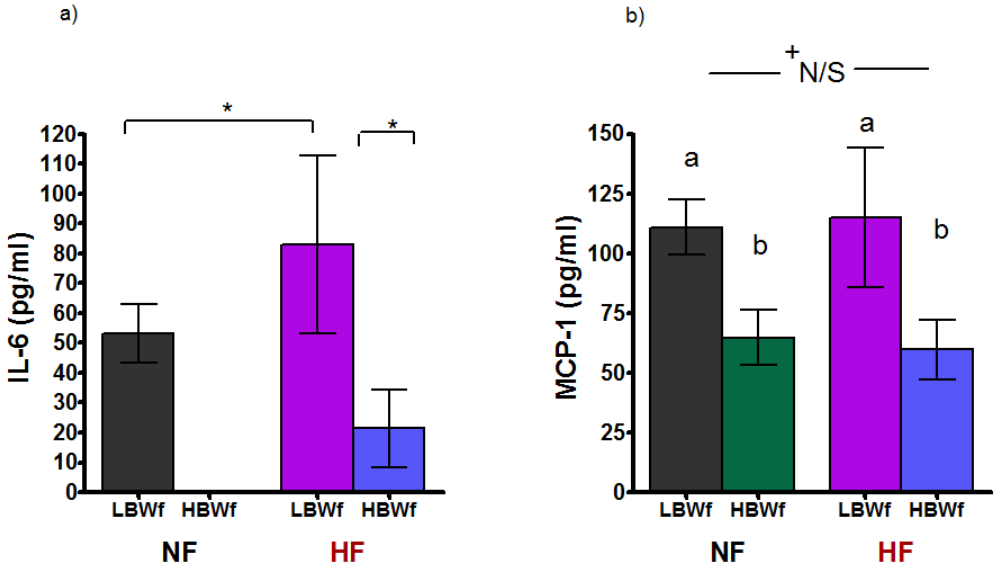

Figure 4.6.2.5 Proinflammatory cytokines of female offspring plasma at 15 weeks of age. IL-6 a) and MCP-1 b). Main effect of diet $^{+}$= N/S= no signficant in b). Significant main effect of birth weight represented with different letters in b). Statistical analysis was performed using a one-way ANOVA for IL-6 and 2x2 factorial ANOVA analysis for MCP-1. Data presented as mean± SEM. **LBWf-NF** n=8; **LBWf-HF** n=11; **HBWf-NF** n=6, **HBWf-HF** n=5. *p≤0.05.

	LBWf-NF_1	LBWf-HF_2	HBWf-NF_3	HBWf-HF_4	P value
C-peptide pg/ml	911.926 ±161.694	924.96 ±132.022	1176.196 ±172.858	1268.026 ±186.708	**Birth weight:** **p=0.075** **Diet:** p=0.752 **Interaction:** p=0.812
GIP pg/ml	39.249 ±19.773	76.121 ±16.144	65.564 ±21.138	110.873 ±21.138	**Birth weight:** **p=0.131** **Diet:** **p=0.045** **Interaction:** p=0.832
Glucagon pg/ml	168.945 ±26.367	160.853 ±21.529	169.111 ±28.188	196.697 ±26.367	**Birth weight:** p=0.489 **Diet:** p=0.707 **Interaction:** p=0.493
Insulin (Ln)	5.768 (5.181-6.356)	6.822 (6.234-7.4)	6.023 (5.435-6.61)	6.512 (5.9-7.16)	**Birth weight:** p=0.925 **Diet:** **p=0.015** **Interaction:** p=0.34
Ghrelin pg/ml	644.582 ±105.106	605.403 ±95.072	535.566 ±119.179	1052.39 ±141.014	**1 vs.2**=0.784 **3vs.4=0.009** **1vs.3**=0.498 **2vs.4=0.014**
Leptin pg/ml	918.382 ±314.492	2047.126 ±261.673	1776.291 ±333.569	2464.528 ±356.601	**Birth weight:** **p=0.05** **Diet:** **p=0.007** **Interaction:** p=0.494
Resistin pg/ml	10081.595 ±1130.645	9307.544 ±991.642	9702.868 ±1264.1	11718.658 ±1264.1	**Birth weight:** p=0.39 **Diet:** p=0.598 **Interaction:** p=0.24
Il-6 pg/ml	45.761 ±10.979	101.397 ±29.96	No detected	21.498 ±12.988	**1 vs.2=0.05** **2vs.4=0.024**
MCP-1 pg/ml	110.906 ±22.847	114.85 ±19.484	64.803 ±26.381	59.652 ±28.899	**Birth weight:** **p=0.05** **Diet:** **p=0.981** **Interaction:** p=0.855

Table 4.6.2.1 Metabolic markers measured in plasma of female mice at week 15 of age. Data presented as mean± SEM except from insulin (Ln), which is presented as mean with 95% confidence interval (CI).

4.6.3 Glucose tolerance in Male mice

Intraperitoneal glucose tolerance test (IPGTT) assessment in males showed significant differences in the fasting state, before the administration of the bolus of glucose in the peritoneum. Mice fed a **HF** diet had a higher basal glucose level than mice fed a **NF** diet (**LBWm-HF** vs. **LBWm-NF p=0.027**; **HBWm-HF** vs. **HBWm-NF p=0.027**; figure 4.6.3.1a). Furthermore, **LBWm-NF** had a higher glucose than **HBWm-NF** (**p=0.049**; figure 4.6.3.1a). A marginal difference was seen between mice fed a **HF** diet (p=0.094; figure 4.6.3.1a). However, there were not significant differences between groups at 15, 30, 60 or 120 minutes after the glucose administration. This may suggest that mice fed a **HF** diet and **LBWm-NF** had an impaired fasting glucose compared to their counterparts.

Further evaluation of the area under the curve (AUC) revealed a significant main effect of both birth weight and diet on the level of the glucose throughout the test duration, which was 120 minutes (birth weight: $F(1,28)=4.333$ **p=0.047**; diet: $F(1,28)=4.63$ **p=0.04**; figure 4.6.3.1b). There was not a significant interaction between factors ($F(1,28)=0.144$ $p=0.707$; figure 4.6.5b). Overall, **LBWm** mice had a higher AUC than **HBWm** mice, but similarly, mice fed a **HF** diet had a significantly higher AUC than mice fed a **NF** diet. These effects were independent one of each other. These may suggest that **LBWm** mice and mice fed a **HF** diet have an impaired glucose metabolism at 15 weeks old.

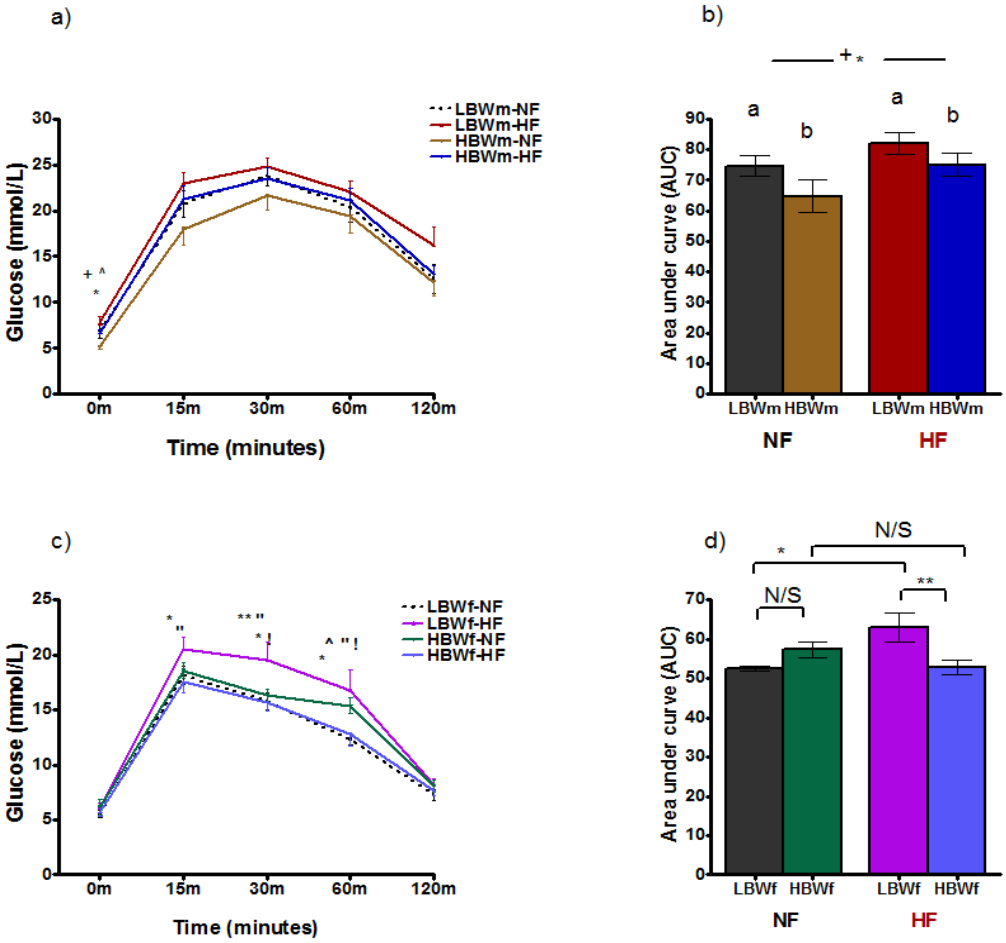

Figure 4.6.3.1 Glucose tolerance results in male and female offspring at 15 weeks old. Intraperitoneal glucose tolerance test (IPGTT) after administration of a glucose bolus a) and area under the curve (AUC) analysis of the IPGTT b). +: significant difference between **LBWm-HF** vs. **LBWm-NF**, and **HBWm-HF** vs. **HBWm-NF** in a) and main effect of diet in b). ^: significant difference between **LBWm-NF** vs. **HBWm-NF**. Significant main effect of birth weight represented with different letters in b). **"**: significant difference between **LBWf-HF** vs. **HBWf-HF**; **!**: significant difference between **LBWf-HF** vs. **LBWf-NF**; ^: significant difference between **LBWf-NF** vs. **HBWf-NF** c). Kruskal Wallis analysis was performed in a) and c) and 2x2 ANOVA analysis in c) and d). *p≤0.05. **p≤0.001.

4.6.4 Glucose tolerance in Female mice

Contrary to the results obtained in males, female mice were not significantly different at the basal time (0 minutes). However, 15 minutes after the glucose administration, there was a significant difference between mice fed a **HF**, with **LBWf-HF** having the highest glucose at this time point compared to their counterparts (**p=0.027**; figure 4.6.4.1a). **LBWf-HF** had the highest level of glucose 30 minutes and 60 minutes after glucose injection. At 30 minutes, **LBWf-HF** had a significantly higher glucose level compared to **HBWf-HF** (**p=0.007**; figure 4.6.4.1a) and compared to **LBWf-NF** mice (**p=0.029**; figure 4.6.4.1a). After 60 minutes of starting the test, significant differences were maintained between the groups mentioned before (**LBWf-HF** vs. **HBWf-HF** **p=0.021**; **LBWf-HF** vs. **LBWf-NF** **p=0.029**), and also, there was a significant difference between mice fed a **NF** diet, with **HBWf-NF** having the highest glucose level (**p=0.024**; figure 4.6.4.1a).

Assessment of the area under the curve (AUC) revealed a significant interaction between both birth weight and diet ($F(1,27)=8.945$ **p=0.006**; figure 4.6.4.1b). Therefore, a simple main effect was performed. **LBWf-HF** had a higher AUC compared to **HBWf-HF** (**p=0.003**) and compared to **LBWf-NF** mice (**p=0.01**). There were not significant differences between mice fed a **NF** diet (p=0.263) or between **HBWf** mice (p=0.186).

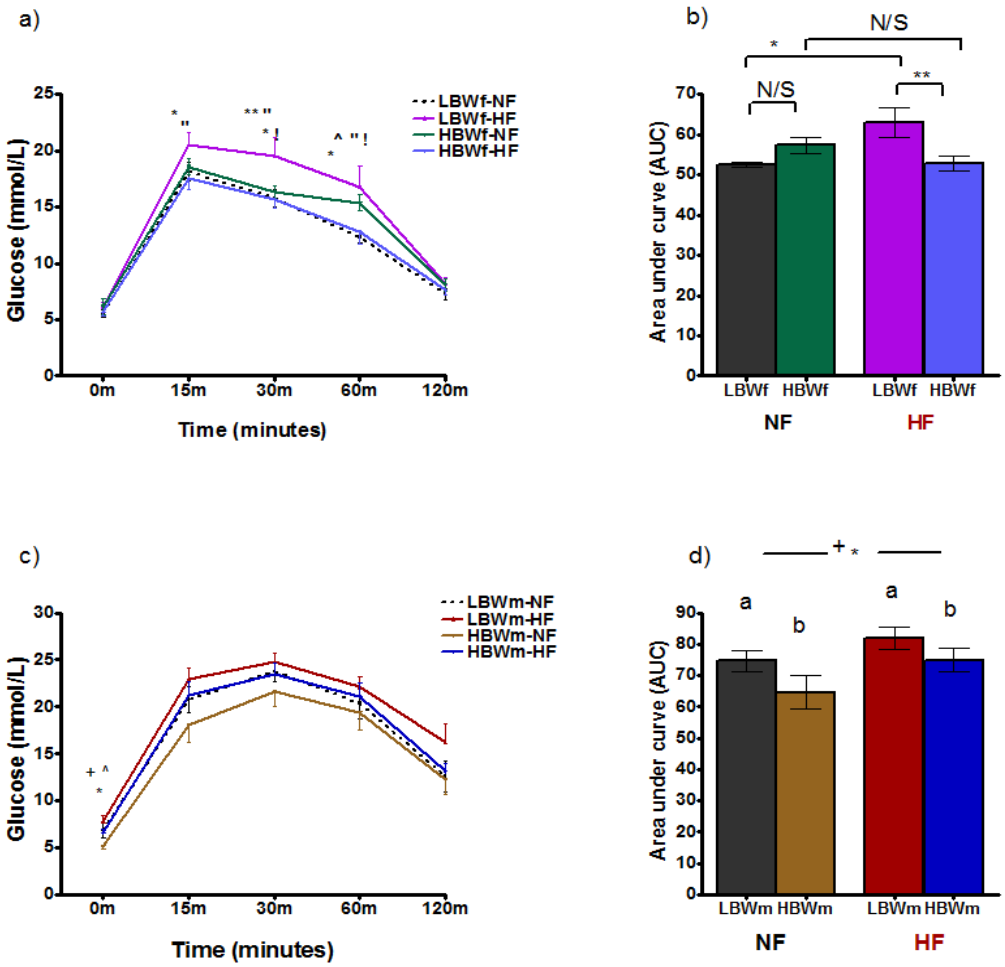

Figure 4.6.4.1 Glucose tolerance results in female and male offspring at 15 weeks old. Intraperitoneal glucose tolerance test (IPGTT) performed at 15, 30, 60 and 120 minutes after administration of a glucose bolus a) and c) and area under the curve (AUC) analysis of the IPGTT b) and d). **"**: significant difference between **LBWf-HF** vs. **HBWf-HF**; **!**: significant difference between **LBWf-HF** vs. **LBWf-NF**; ^: significant difference between **LBWf-NF** vs. **HBWf-NF** . +: significant difference between **LBWm-HF** vs. **LBWm-NF**, and **HBWm-HF** vs. **HBWm-NF** in c) and main effect of diet in d). ^: significant difference between **LBWm-NF** vs. **HBWm-NF**. Significant main effect of birth weight represented with different letters in b). Statistical analysis was performed using a Kruskal Wallis analysis a) and c) or 2x2 ANOVA b) and d). *p≤0.05, **p≤0.01.

4.7 The Effects of Birth Weight and on Organ Mass in Young Mice (From Week 3 Until Week 15)

Offspring was dissected at the end of the study (15 weeks old) as described previously in methods 2.1.4. Organ mass and proportional organ weights to current body weight were recorded and analysed. A one-way ANOVA analysis was used to assess differences between groups.

4.7.1 Organ mass in Males

4.7.1.1 Brain mass in Males

Brain mass in grams was significantly different between **LBWm** mice, with a higher mass in **LBWm-HF** mice (**p=0.023;** figure 4.7.1.1.1a and table 4.7.1.1.1). However, after normalising to current body weight (%), the relative mass of brain was not significantly different between **LBWm** mice any longer (p=0.516; figure 4.7.1.1.1b and table 4.7.1.1.1). Furthermore, differences between **HBWm** mice appeared significant, being higher in **HBWm-NF** mice (**p=0.004**; figure 4.7.1.1.1b and table 4.7.1.1.1) and marginally significant between mice fed a **HF** diet, with a higher mass in **LBWm-HF** mice (p=0.065; figure 4.7.1.1.1b and table 4.7.1.1.1). Comparable differences were maintained between mice fed a **NF** diet (p=0.567; figure 4.7.1.1.1b and table 4.7.1.1.1).

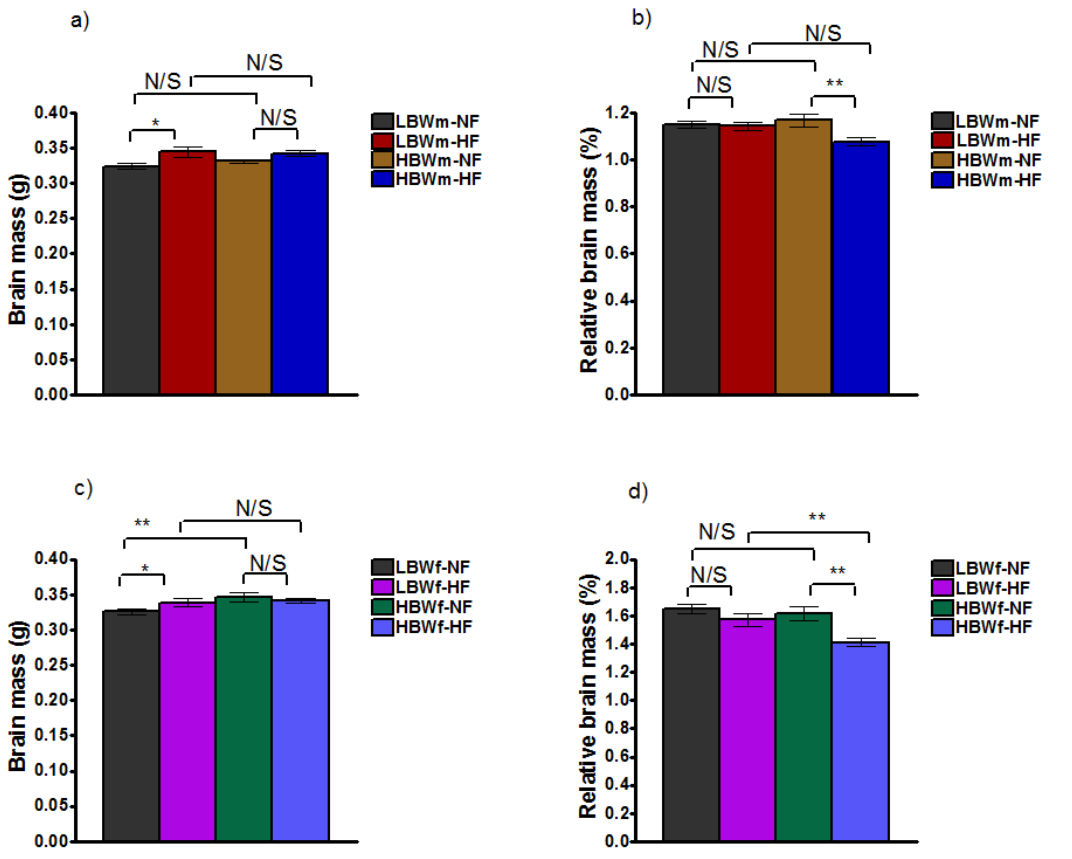

Figure 4.7.1.1.1 Brain mass in male and female offspring at 15 weeks old. Brain mass in grams a) and c) and normalised to current body weight expressed as percentage (relative brain mass %) b) and d). Figures on the top correspond to males and figures below to females. Statistical analysis was performed using a one-way ANOVA followed by a protected Fisher's least significant difference (LSD) post hoc analysis. Data presented as mean± SEM. **LBWm-NF** n=10; **LBWm-HF** n=14; **HBWm-NF** n=11, **HBWm-HF** n=14; **LBWf-NF** n=11; **LBWf-HF** n=14; **HBWf-NF** n=8, **HBWf-HF** n=8. N/S= no significant; *p≤0.05; **p≤0.01.

Organ mass	LBWm-NF_1	LBWm-HF_2	HBWm-NF_3	HBWm-HF_4	P value
Brain (g)	0.322 ±0.004	0.34 ±0.006	0.331 ±0.007	0.342 ±0.002	**1 vs.2=0.023** **3vs.4**=0.111 **1vs.3**=0.319 **2vs.4**=0.745
Brain (%)	1.15 ±0.014	1.13 ±0.021	1.169 ±0.027	1.077 ±0.018	**1 vs.2**=0.516 **3vs.4=0.004** **1vs.3**=0.567 **2vs.4=0.065**

Table 4.7.1.1.1 Brain mass of male offspring at 15 weeks old. Brain (g)= brain mass in grams and Brain (%)= normalised brain mass to current body weight expressed as percentage. Statistical analysis was performed using a one-way ANOVA followed by a protected Fisher's least significant difference (LSD) post hoc analysis. Data presented as mean± SEM.

4.7.1.2 Brown adipose tissue mass (BAT) in Males

Brown adipose tissue (BAT) in grams was significantly different between **HBWm** mice with a higher mass in **HBWm-HF** mice (**p<0.001**) but not between **LBWm** mice (p=0.691; figure 4.7.1.2.1a and table 4.7.1.2.1). A marginal difference was found between mice fed a **NF** diet, with higher mass in **LBWm-NF** mice (p=0.056; figure 4.7.1.2.1a and table 4.7.1.2.1) and not significant difference between mice fed a **HF** diet (p=0.201; figure 4.7.1.2.1a and table 4.7.1.2.1). Upon normalising BAT mass to body weight and expressed as percentage, the significant difference between **HBWm** mice was maintained (**p=0.003**; figure 4.7.1.2.1b and table 4.7.1.2.1) and the marginal difference between mice fed a **NF** diet became significant (**p=0.013**;

figure 4.7.1.2.1b and table 4.7.1.2.1). The comparable differences found in absolute values were maintained after normalisation (**LBWm-NF** vs. **LBWm-HF** p=0.669; **LBWm-HF** vs. **HBWm-HF** p=0.382; figure 4.7.1.2.1b and table 4.7.1.2.1).

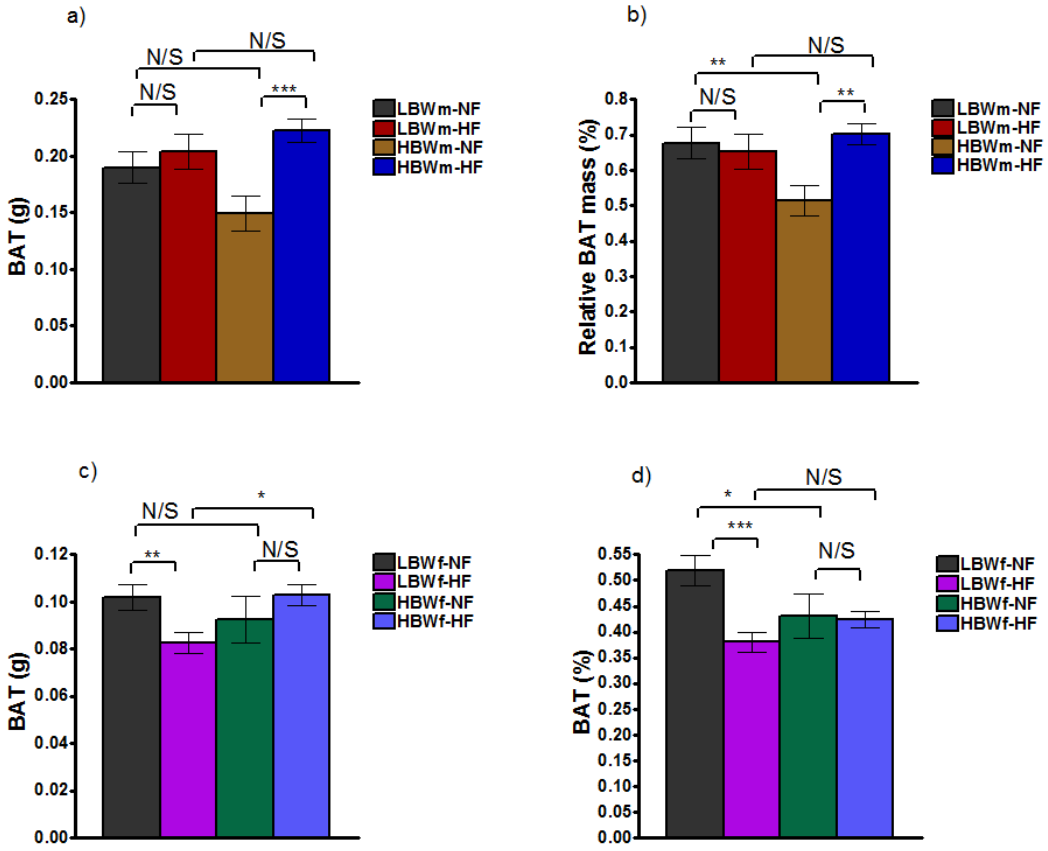

Figure 4.7.1.2.1 Brown adipose tissue (BAT) mass of male and female offspring at 15 weeks old. BAT mass in grams a) and c) and normalised to current body weight expressed as percentage (relative BAT mass %) b) and d). Figures on the top correspond to males and figures below to females. Statistical analysis was performed using a one-way ANOVA followed by a protected Fisher's least significant difference (LSD) post hoc analysis. Data presented as mean± SEM. **LBWm-NF** n=13; **LBWm-HF** n=14; **HBWm-NF** n=11, **HBWm-HF** n=15; **LBWf-NF** n=11; **LBWf-HF** n=14; **HBWf-NF** n=8, **HBWf-HF** n=8. N/S= no significant; *p≤0.05; **p≤0.01; ***p≤0.001.

Organ mass	LBWm-NF_1	LBWm-HF_2	HBWm-NF_3	HBWm-HF_4	P value
BAT (g)	0.189 ± 0.137	0.198 ±0.016	0.149 ±0.015	0.222 ±0.01	**1 vs.2**=0.691 **3vs.4<0.001** **1vs.3**=0.056 **2vs.4**=0.201
BAT (%)	0.677 ±0.045	0.651 ±0.049	0.514 ±0.043	0.702 ±0.296	**1 vs.2**=0.669 **3vs.4=0.003** **1vs.3**=0.013 **2vs.4**=0.382

Table 4.7.1.2.1 Brown adipose tissue (BAT) mass of male offspring at 15 weeks old. BAT (g)= brown adipose tissue mass in grams and BAT (%)= normalised brown adipose tissue mass to current body weight expressed as percentage. Statistical analysis was performed using a one-way ANOVA followed by a protected Fisher's least significant difference (LSD) post hoc analysis. Data presented as mean± SEM.

4.7.1.3 Liver mass in Males

Liver mass as absolute value (grams) was significantly different between mice fed a **HF** diet, being lower in **LBWm-HF** (**p=0.022**; figure 4.7.1.3.1a and table 4.7.1.3.1). Not differences were seen between the rest of the groups. However, after normalisation, differences between **LBWm** mice became significant, with **LBWm-HF** mice having a lower mass compared to **LBWm-NF** (**p=0.011**; figure 4.7.1.3.1a and table 4.7.1.3.1), and the significant difference between mice fed **HF** diet was maintained (**p=0.005**; figure 4.7.1.3.1a and table 4.7.1.3.1).

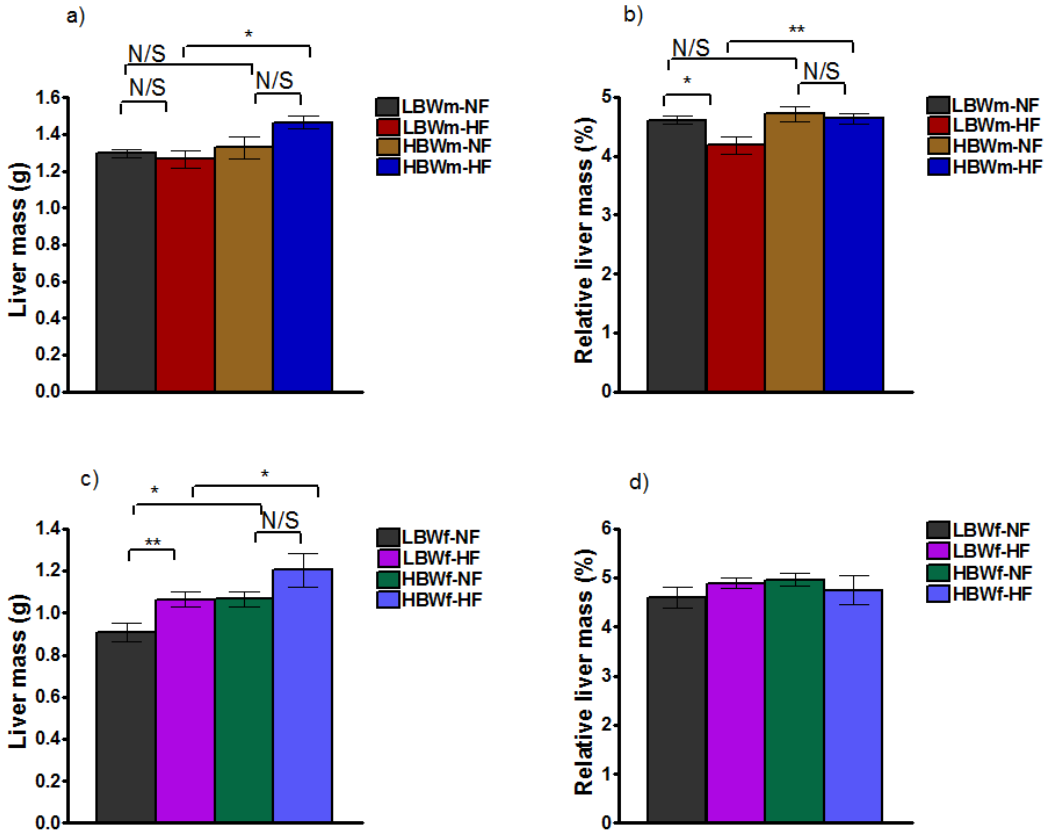

Figure 4.7.1.3.1 Liver mass of male and female offspring at 15 weeks old. Liver mass in grams a) and c) and normalised to current body weight expressed as percentage (relative liver mass %) b) and d). Figures on the top correspond to males and figures below to females. Statistical analysis was performed using a one-way ANOVA followed by a protected Fisher's least significant difference (LSD) post hoc analysis. Data presented as mean± SEM. **LBWm-NF** n=11; **LBWm-HF** n=12; **HBWm-NF** n=11, **HBWm-HF** n=15; **LBWf-NF** n=12; **LBWf-HF** n=14; **HBWf-NF** n=8, **HBWf-HF** n=8. N/S= no significant; *p≤0.05; **p≤0.01.

Organ mass	LBWm-NF_1	LBWm-HF_2	HBWm-NF_3	HBWm-HF_4	P value
Liver (g)	1.296 ±0.023	1.264 ±0.052	1.327 ±0.059	1.465 ±0.024	**1 vs.2**=0.942 **3vs.4**=0.232 **1vs.3**=0.959 **2vs.4=0.022**
Liver (%)	4.613 ±0.074	4.189 ±0.147	4.715 ±0.135	4.534 ±0.061	**1 vs.2=0.011** **3vs.4**=0.598 **1vs.3**=0.546 **2vs.4=0.005**

Table 4.7.1.3.1 Liver mass of male offspring at 15 weeks old. Liver (g)= liver mass in grams and liver (%)= normalised liver mass to current body weight expressed as percentage. Statistical analysis was performed using a one-way ANOVA followed by a protected Fisher's least significant difference (LSD) post hoc analysis. Data presented as mean± SEM.

4.7.1.4 Pancreas, spleen and heart masses in Males

Assessment of pancreas, spleen and heart did not show any significant difference between groups in either absolute (grams) or relative (%) values (pancreas: figure 4.7.1.4.1 and table 4.7.1.4.1; spleen: figure 4.7.1.4.2 and table 4.7.1.4.1; heart 4.7.1.4.3 and table 4.7.1.4.1).

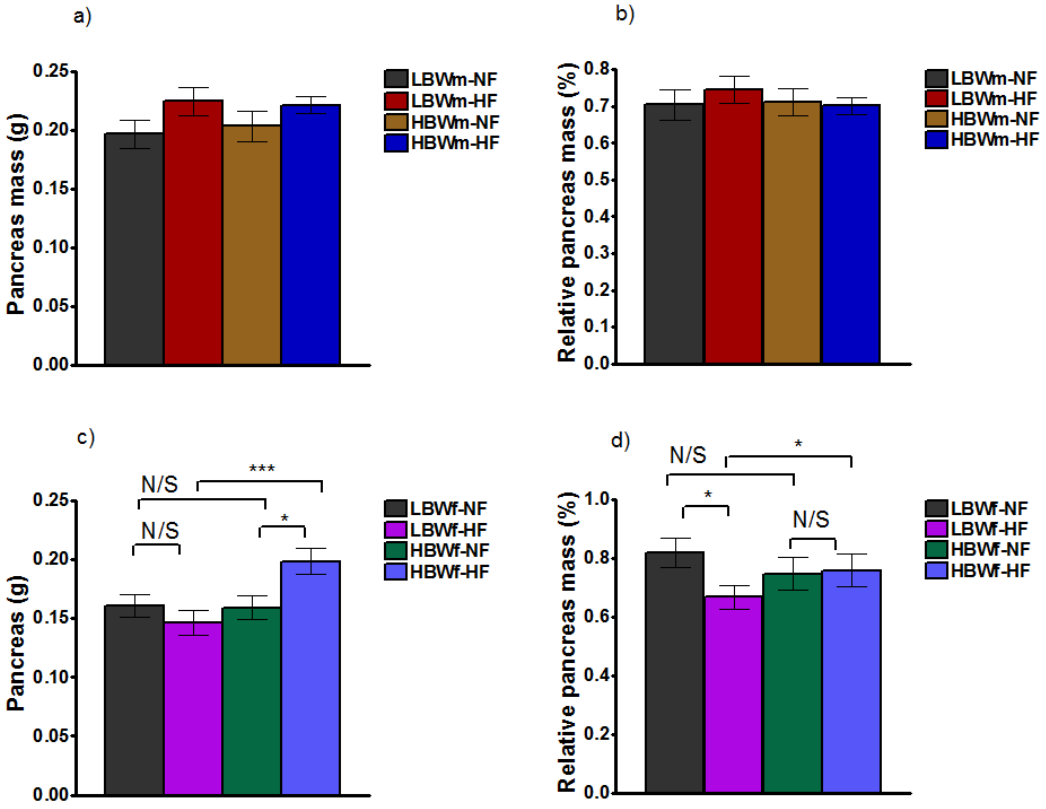

Figure 4.7.1.4.1 Pancreas mass of male and female offspring at 15 weeks old. Pancreas mass in grams a) and c) and normalised to current body weight expressed as percentage (relative pancreas mass%) b) and d). Figures on the top correspond to males and figures below to females. Statistical analysis was performed using a one-way ANOVA followed by a protected Fisher's least significant difference (LSD) post hoc analysis. Data presented as mean± SEM. **LBWm-NF** n=13; **LBWm-HF** n=14; **HBWm-NF** n=11, **HBWm-HF** n=15; **LBWf-NF** n=12; **LBWf-HF** n=14; **HBWf-NF** n=8, **HBWf-HF** n=8. N/S= no significant; *p≤0.05; ***p≤0.001.

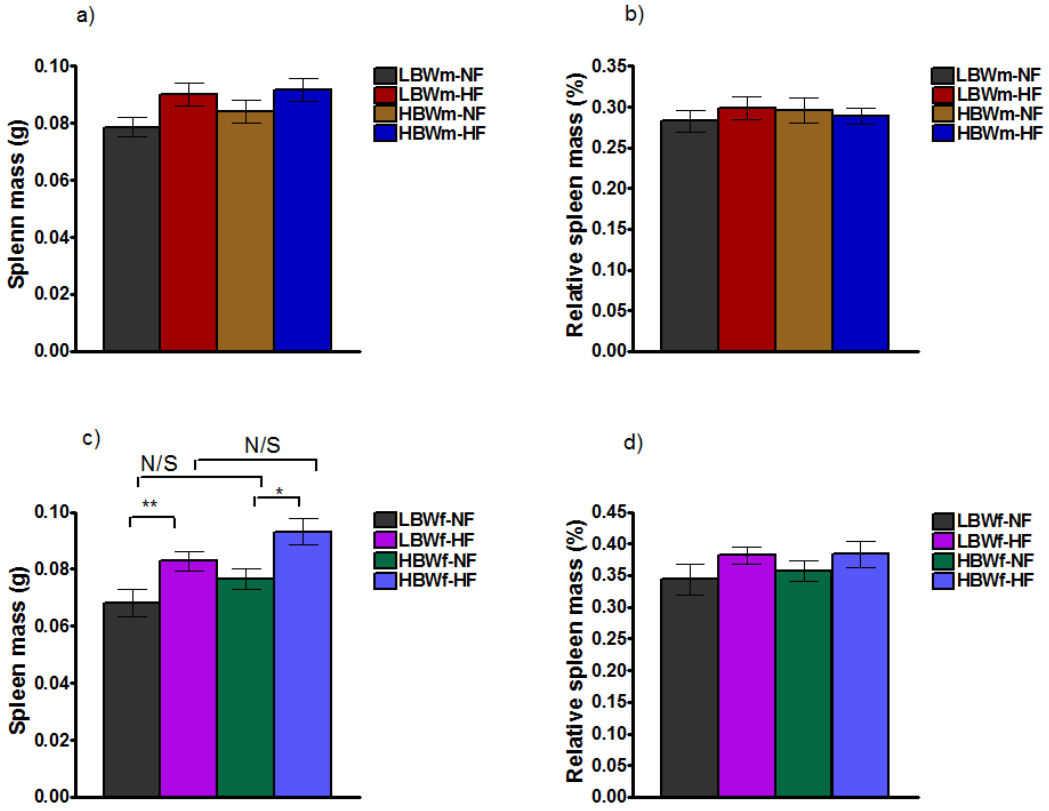

Figure 4.7.1.4.2 Spleen mass of male and female offspring at 15 weeks old. Spleen mass in grams a) and c) and normalised to current body weight expressed as percentage (relative spleen mass%) b) and d). Figures on the top correspond to males and figures below to females. Statistical analysis was performed using a one-way ANOVA followed by a protected Fisher's least significant difference (LSD) post hoc analysis. Data presented as mean± SEM. **LBWm-NF** n=13; **LBWm-HF** n=13; **HBWm-NF** n=11, **HBWm-HF** n=15; **LBWf-NF** n=10; **LBWf-HF** n=14; **HBWf-NF** n=8, **HBWf-HF** n=7. N/S= no significant; *p≤0.05; **p≤0.01.

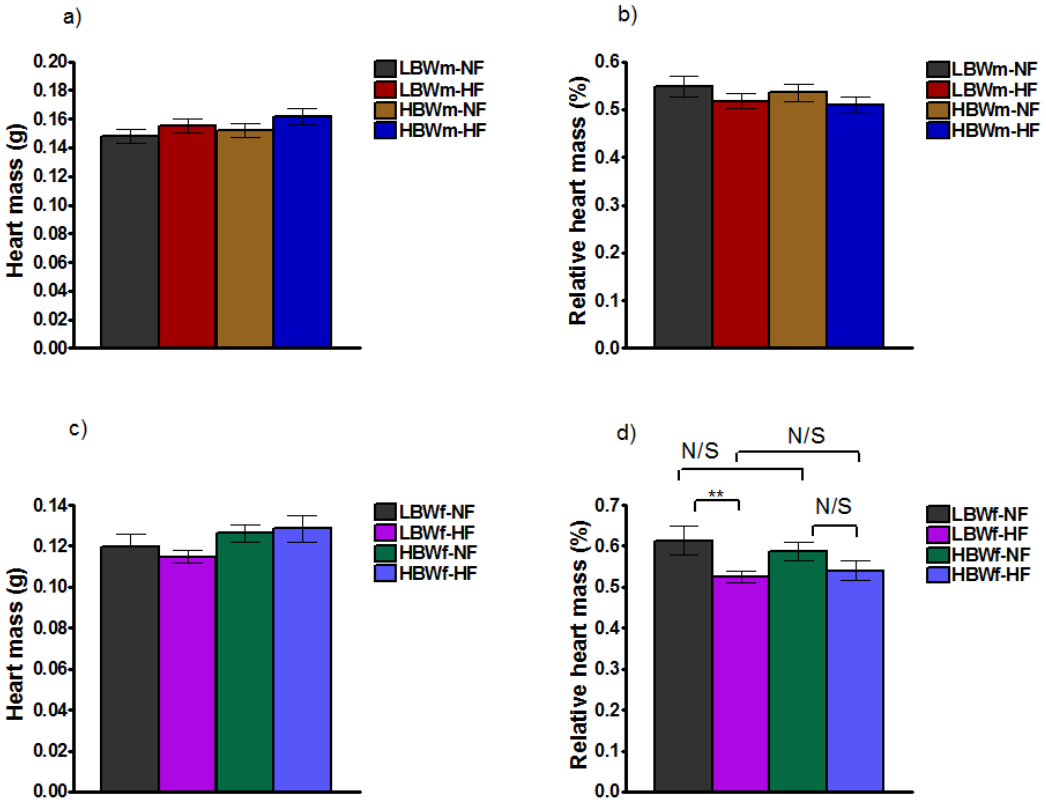

Figure 4.7.1.4.3 Heart mass of male and female offspring at 15 weeks old. Heart mass in grams a) and c) and normalised to current body weight expressed as percentage (relative heart mass%) b) and d). Figures on the top correspond to males and figures below to females. Statistical analysis was performed using a one-way ANOVA followed by a protected Fisher's least significant difference (LSD) post hoc analysis. Data presented as mean± SEM. **LBWm-NF** n=12; **LBWm-HF** n=13; **HBWm-NF** n=11, **HBWm-HF** n=14; **LBWf-NF** n=10; **LBWf-HF** n=14; **HBWf-NF** n=7, **HBWf-HF** n=8. N/S= no significant; **p≤0.01.

Organ mass	LBWm-NF_1	LBWm-HF_2	HBWm-NF_3	HBWm-HF_4	P value
Pancreas (g)	0.197 ±0.012	0.225 ±0.012	0.204 ±0.013	0.221 ±0.007	**1 vs.2**=0.275 **3vs.4**=0.676 **1vs.3**=0.975 **2vs.4**=0.996
Pancreas (%)	0.705 ±0.041	0.745 ±0.038	0.711 ±0.037	0.702 ±0.023	**1 vs.2**=0.847 **3vs.4**=0.998 **1vs.3**=0.999 **2vs.4**=0.799
Spleen (g)	0.079 ±0.003	0.089 ±0.004	0.084 ±0.004	0.091 ±0.004	**1 vs.2**=0.201 **3vs.4**=0.551 **1vs.3**=0.799 **2vs.4**=0.991
Spleen (%)	0.282 ±0.013	0.299 ±0.014	0.296 ±0.015	0.289 ±0.101	**1 vs.2**=0.807 **3vs.4**=0.982 **1vs.3**=0.894 **2vs.4**=0.946
Heart (g)	0.148 ±0.004	0.155 ±0.005	0.152 ±0.005	0.161 ±0.006	**1 vs.2**=0.736 **3vs.4**=0.584 **1vs.3**=0.955 **2vs.4**=0.811
Heart (%)	0.529 ±0.013	0.517 ±0.016	0.535 ±0.019	0.509 ±0.159	**1 vs.2**=0.947 **3vs.4**=0.674 **1vs.3**=0.996 **2vs.4**=0.984

Table 4.7.1.4.1 Pancreas, spleen and heart masses of male offspring at 15 weeks old. Pancreas, spleen and heart (g)= respective masses in grams and pancreas, spleen and heart (%)= normalised masses to current body weight expressed as percentage. Statistical analysis was performed using a one-way ANOVA followed by a protected Fisher's least significant difference (LSD) post hoc analysis. Data presented as mean± SEM.

4.7.1.5 Kidneys mass in Males

Kidneys mass in grams was significantly higher in **LBWm-HF** compared to **LBWm-NF** (**p=0.015**; figure 4.7.1.5.1a and table 4.7.1.5.1) but not between **HBWm** mice (p=0.628; figure 4.7.1.5.1a and table 4.7.1.5.1). Furthermore, there was a significant difference between mice fed a **NF** diet with a higher mass in **HBWm-NF** mice han **LBWm-NF** mice (**p=0.033**; figure 4.7.1.5.1a and table 4.7.1.5.1) but it was comparable between mice fed a **HF** diet (p=0.919; figure 4.7.1.5.1a and table 4.7.1.5.1). After normalisation, relative kidneys mass was not longer significant, but it was marginal, between **LBWm** mice (p=0.062; figure 4.7.1.5.1b and table 4.7.1.5.1). The difference between mice fed a **NF** diet was maintained (**HBWm-NF** vs. **LBWm-NF** mice (**p=0.015**; figure 4.7.1.5.1b and table 4.7.1.5.1) as well as comparable differences between **HBWm** mice (p=0.181) and mice fed a **HF** diet (p=0.506; figure 4.7.1.5.1b and table 4.7.1.5.1).

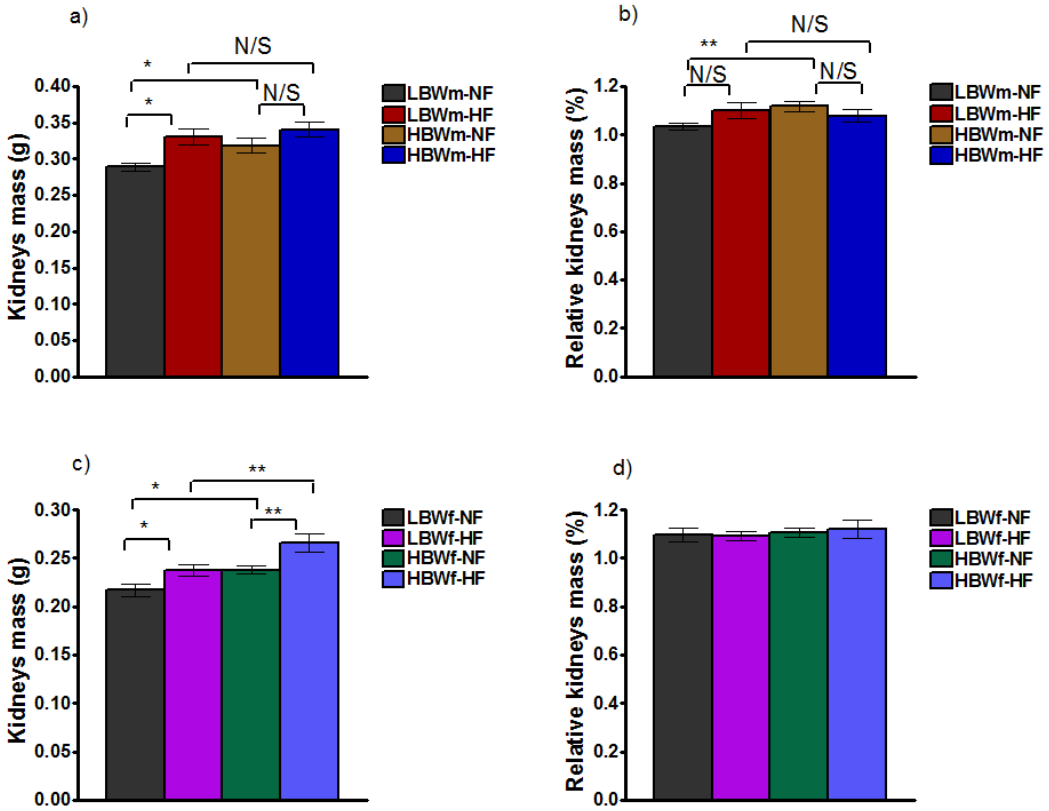

Figure 4.7.1.5.1 Kidneys mass of male and female offspring at 15 weeks old. Kidneys mass in grams a) and c) and normalised to current body weight expressed as percentage (relative brain mass%) b) and d). Figures on the top correspond to males and figures below to females. Statistical analysis was performed using a one-way ANOVA followed by a protected Fisher's least significant difference (LSD) post hoc analysis. Data presented as mean± SEM. **LBWm-NF** n=13; **LBWm-HF** n=12; **HBWm-NF** n=10, **HBWm-HF** n=15; **LBWf-NF** n=10; **LBWf-HF** n=14; **HBWf-NF** n=8, **HBWf-HF** n=8. N/S= no significant; *p≤0.05; **p≤0.01.

Organ mass	LBWm-NF_1	LBWm-HF_2	HBWm-NF_3	HBWm-HF_4	P value

Kidneys (g)	0.289 ±0.005	0.331 ±0.011	0.324 ±0.009	0.341 ±0.009	**1 vs.2=0.015** **3vs.4**=0.628 **1vs.3=0.033** **2vs.4**=0.919
Kidneys (%)	1.035 ±0.014	1.101 ±0.031	1.126 ±0.018	1.079 ±0.026	**1 vs.2=0.062** **3vs.4**=0.181 **1vs.3=0.015** **2vs.4**=0.506

Table 4.7.1.5.1 Kidneys mass of male offspring at 15 weeks old. Kidneys (g)= kidneys mass in grams and kidneys (%)= normalised kidneys mass to current body weight expressed as percentage. Statistical analysis was performed using a one-way ANOVA followed by a protected Fisher's least significant difference (LSD) post hoc analysis. Data presented as mean± SEM.

4.7.1.6 Skeletal muscle mass in Males

Assessment of skeletal muscle mass (from right hind leg) in grams showed a significant difference between mice fed a **HF** diet, with a lower muscle mass in **LBWm-HF** than **HBWm-HF** mice (**p<0.001**; figure 4.7.1.6.1a and table 4.7.1.6.1). There was also a significant difference between **HBWm** mice with a higher muscle mass in **HBWm-HF** than **HBWm-NF** mice (**p=0.003**; figure 4.7.1.6.1a and table 4.7.1.6.1). However after normalisation, the significant difference between mice fed a **HF** diet was maintained (**p=0.004**; figure 4.7.1.6.1a and table 4.7.1.6.1), but not the significant difference between **HBWm** mice (p=0.141; figure 4.7.1.6.1a and table 4.7.1.6.1), although the pattern was similar.

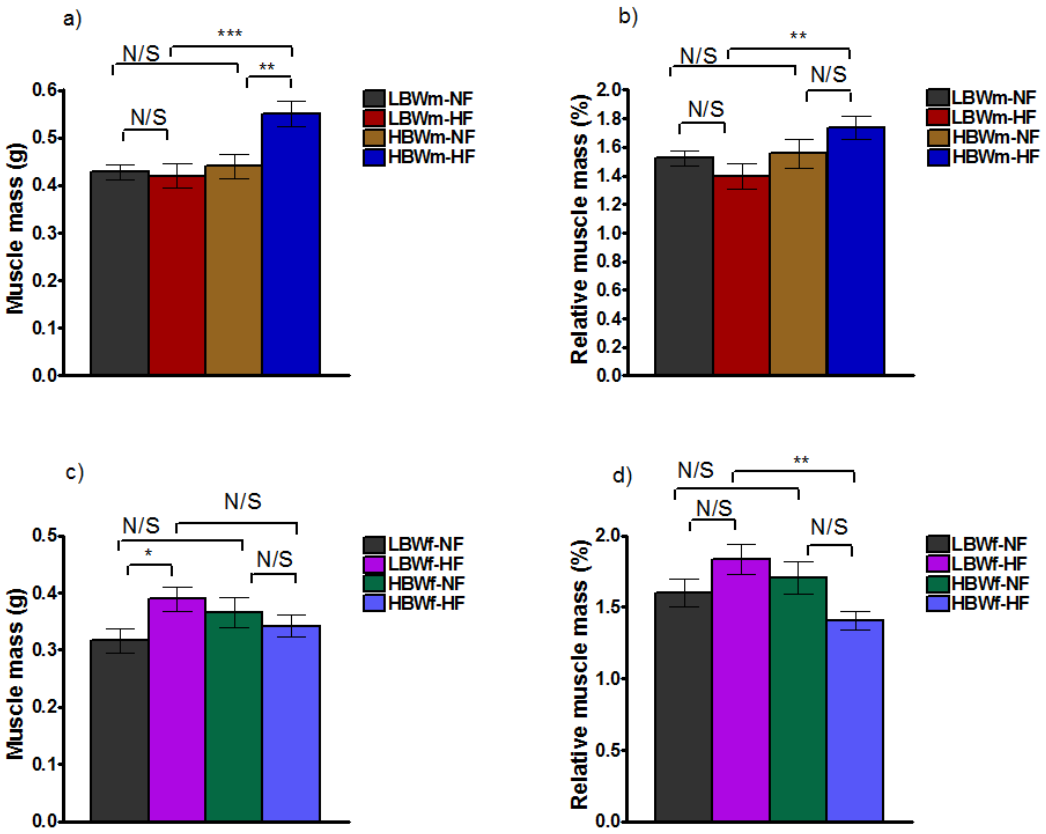

Figure 4.7.1.6.1 Skeletal muscle mass of male and female offspring at 15 weeks old. Muscle mass in grams a) and c) and normalised to current body weight expressed as percentage (relative brain mass%) b) and d). Figures on the top correspond to males and figures below to females. Statistical analysis was performed using a one-way ANOVA followed by a protected Fisher's least significant difference (LSD) post hoc analysis. Data presented as mean± SEM. **LBWm-NF** n=12; **LBWm-HF** n=14; **HBWm-NF** n=11, **HBWm-HF** n=14; **LBWf-NF** n=11; **LBWf-HF** n=14; **HBWf-NF** n=8, **HBWf-HF** n=8. N/S= no significant; *p≤0.05; **p≤0.01***p≤0.001.

Organ mass	LBWm-NF_1	LBWm-HF_2	HBWm-NF_3	HBWm-HF_4	P value
Muscle (g)	0.428 ±0.016	0.419 ±0.025	0.44 ±0.026	0.55 ±0.026	**1vs.2**=0.809 **3vs.4=0.003** **1vs.3**=0.734 **2vs.4<0.001**
Muscle (%)	1.523 ±0.051	1.398 ±0.089	1.556 ±0.102	1.734 ±0.079	**1vs.2**=0.289 **3vs.4**=0.141 **1vs.3**=0.787 **2vs.4=0.004**

Table 4.7.1.6.1 Skeletal muscle mass of male offspring at 15 weeks old. Muscle (g)= muscle mass in grams and muscle (%)= normalised muscle mass to current body weight expressed as percentage. Statistical analysis was performed using a one-way ANOVA followed by a protected Fisher's least significant difference (LSD) post hoc analysis. Data presented as mean± SEM.

4.7.2 Organ mass in Females

4.7.2.1 Brain mass in Females

Brain mass as grams in females showed a significant difference between **LBWf** mice with a higher weight in **LBWf-HF** mice than **LBWf-NF** (**p=0.05**; figure 4.7.2.1.1a and table 4.7.2.1.1), but the difference between **HBWf** mice did not reach significance (p=0.576; figure 4.7.2.1.1a and table 4.7.2.1.1). Furthermore, **LBWf-NF** had a lower brain mass compared to **HBWf-NF** mice (**p=0.009**; figure 4.7.2.1.1a and table 4.7.2.1.1). Comparable masses were found between females fed a **HF** diet (p=0.663; figure 4.7.2.1.1a and table 4.7.2.1.1). Similar brain masses were seen in their respective male groups, except from **HBWm-NF** mice, which had 0.015 ±0.006g less than its respective female group.

Upon normalising brain mass to body weight and expressed as percentage, differences between **LBWf** mice and between females fed a **NF** diet were not maintained (p=0.144; p=0.589 respectively; figure 4.7.2.1.1b and table 4.7.2.1.1). This suggested that the brain mass was proportional to their body weights. However, the difference between **HBWf** mice appeared significant, with a lower mass in **HBWf-HF** mice (**p=0.004**; figure 4.7.2.1.1b and table 4.7.2.1.1), as well as the difference between females fed a **HF** diet with again a lower mass in **HBWf-HF** mice (**p=0.012**; figure 4.7.2.1.1b and table 4.7.2.1.1). Similar pattern was found in males, but relative brain masses tended to be higher in males than their respective female groups (figure 4.7.1.1.1 and table 4.7.1.1.1).

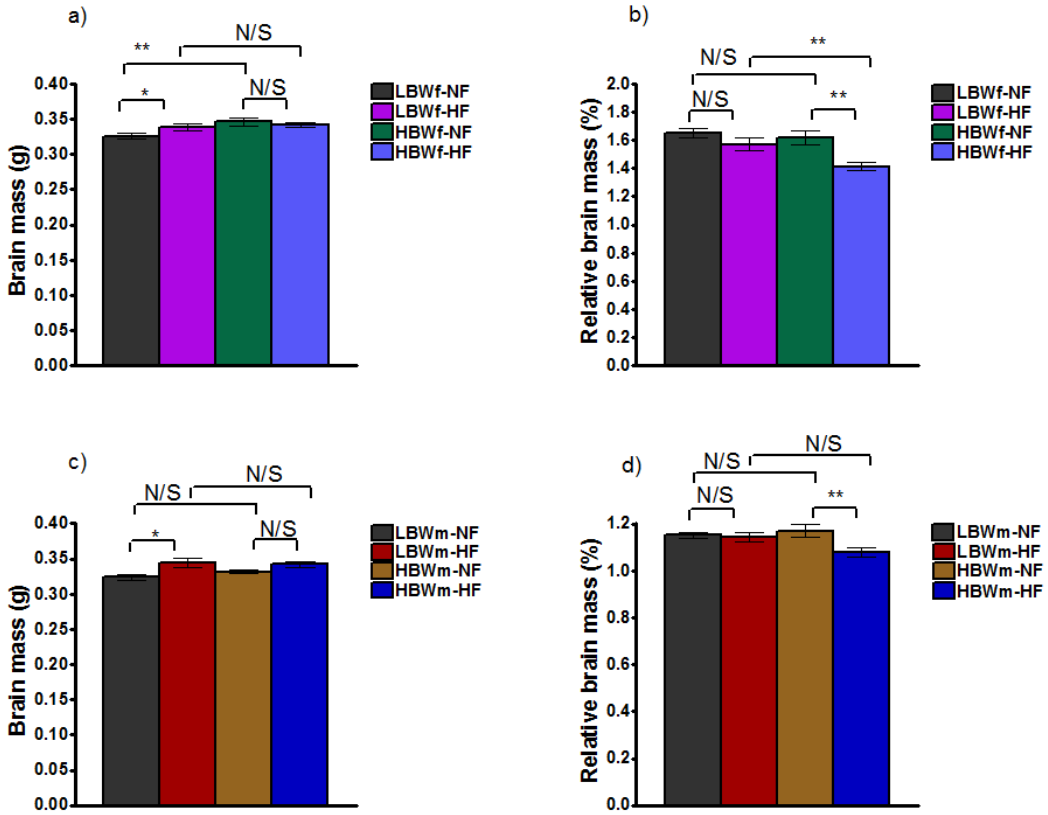

Figure 4.7.2.1.1 Brain mass of female and male offspring at 15 weeks old. Brain mass in grams a) and c) and normalised to current body weight expressed as percentage (relative brain mass %) b) and d). Figures on the top correspond to females and figures below to males. Statistical analysis was performed using a one-way ANOVA followed by a protected Fisher's least significant difference (LSD) post hoc analysis. Data presented as mean± SEM. **LBWf-NF** n=11; **LBWf-HF** n=14; **HBWf-NF** n=8, **HBWf-HF** n=8. **LBWm-NF** n=10; **LBWm-HF** n=14; **HBWm-NF** n=11, **HBWm-HF** n=14. N/S= no significant; *p≤0.05; **p≤0.01.

Organ mass	LBWf-NF_1	LBWf-HF_2	HBWf-NF_3	HBWf-HF_4	P value
Brain (g)	0.326 ±0.004	0.339 ±0.005	0.346 ±0.006	0.342 ±0.003	**1 vs.2=0.05** **3vs.4**=0.576 **1vs.3=0.009** **2vs.4**=0.663
Brain (%)	1.652 ±0.033	1.571 ±0.045	1.618 ±0.05	1.412 ±0.029	**1vs.2**=0.144 **3vs.4=0.004** **1vs.3**=0.589 **2vs.4=0.012**

Table 4.7.2.1.1 Brain mass of female offspring at 15 weeks old. Brain (g)= brain mass in grams and Brain (%)= normalised brain mass to current body weight expressed as percentage. Statistical analysis was performed using a one-way ANOVA followed by a protected Fisher's least significant difference (LSD) post hoc analysis. Data presented as mean± SEM.

4.7.2.2 Brown adipose tissue (BAT) mass in Females

Brown adipose tissue analysis showed differences between **LBWf** mice (**p=0.013**; figure 4.7.2.2.1a and table 4.7.2.2.1) and females fed a **HF** diet (**p=0.017**; figure 4.7.2.2.1a and table 4.7.2.2.1), with **LBWf-HF** mice having a lower BAT mass in both cases. After normalisation to body weight, the significant difference between **LBWf** mice was maintained (**p<0.001**; figure 4.7.2.2.1b and table 4.7.2.2.1), which was not significant between respective male groups (figure 4.7.1.2.1 and table 4.7.1.2.1). However, the significance was not maintained between mice fed a **HF** diet, which it was in males (figure 4.7.1.2.1 and table 4.7.1.2.1). Moreover, difference between females fed a **NF** diet became significant with **LBWf-NF** mice having the highest mass (**p=0.038**; figure 4.7.2.2.1b and table 4.7.2.2.1), but it was not in the respective male groups (figure 4.7.1.2.1 and table 4.7.1.2.1).

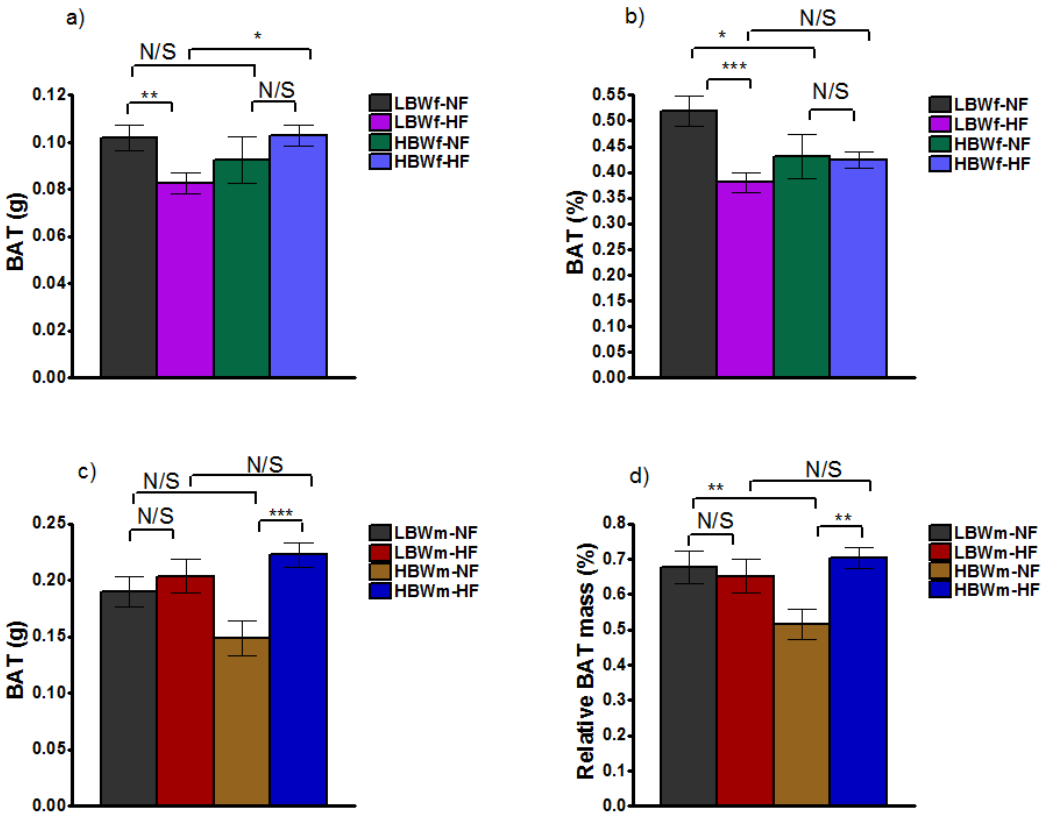

Figure 4.7.2.2.1 Brown adipose tissue (BAT) mass of female and male offspring at 15 weeks old. BAT mass in grams a) and c) and normalised to current body weight expressed as percentage (relative BAT mass %) b) and d). Figures on the top correspond to females and figures below to males. Statistical analysis was performed using a one-way ANOVA followed by a protected Fisher's least significant difference (LSD) post hoc analysis. Data presented as mean± SEM. **LBWf-NF** n=11; **LBWf-HF** n=14; **HBWf-NF** n=8, **HBWf-HF** n=8; **LBWm-NF** n=13; **LBWm-HF** n=14; **HBWm-NF** n=11, **HBWm-HF** n=15. N/S= no significant; *p≤0.05, **p≤0.01, ***p≤0.001.

Organ mass	LBWf-NF_1	LBWf-HF_2	HBWf-NF_3	HBWmfHF_4	P value
BAT (g)	0.102 ± 0.005	0.083 ±0.004	0.092 ±0.009	0.1029 ±0.004	**1 vs.2=0.013** **3vs.4**=0.255 **1vs.3**=0.275 **2vs.4=0.017**
BAT (%)	0.519 ±0.03	0.380 ±0.02	0.431 ±0.043	0.424 ±0.015	**1 vs.2<0.001** **3vs.4**=0.872 **1vs.3=0.038** **2vs.4**=0.261

Table 4.7.2.2.1 Brown adipose tissue (BAT) mass of female offspring at 15 weeks old. BAT (g)= brown adipose tissue mass in grams and BAT (%)= normalised brown adipose tissue mass to current body weight expressed as percentage. Statistical analysis was performed using a one-way ANOVA followed by a protected Fisher's least significant difference (LSD) post hoc analysis. Data presented as mean± SEM.

4.7.2.3 Liver mass in Females

Absolute liver mass (g) was significantly different between **LBWf** mice, with **LBWf-HF** mice having a higher liver mass than **LBWf-NF** mice (**p=0.01**; figure 4.7.2.3.1a and table 4.7.2.3.1). Significance was also found between mice fed a **NF** diet with a higher liver mass in **HBWf-NF** mice than **LBWf-NF** mice (**p=0.023**; figure 4.7.2.3.1a and table 4.7.2.3.1) and between females fed a **HF** diet, with **LBWf-HF** mice having a lower liver mass than their counterpart (**p=0.047**; figure 4.7.2.3.1a and table 4.7.2.3.1). There was a marginal significant difference between **HBWf** mice (**p=0.077**; figure 4.7.2.3.1a and table 4.7.2.3.1). However, after normalisation, differences were comparable between groups (figure 4.7.2.3.1b and table 4.7.2.3.1). The trends seen in males were different, as **LBWm-HF** had the lowest

relative mass compared to the other groups and the differences were significant between groups (figure 4.7.1.3.1 and table 4.7.1.3.1).

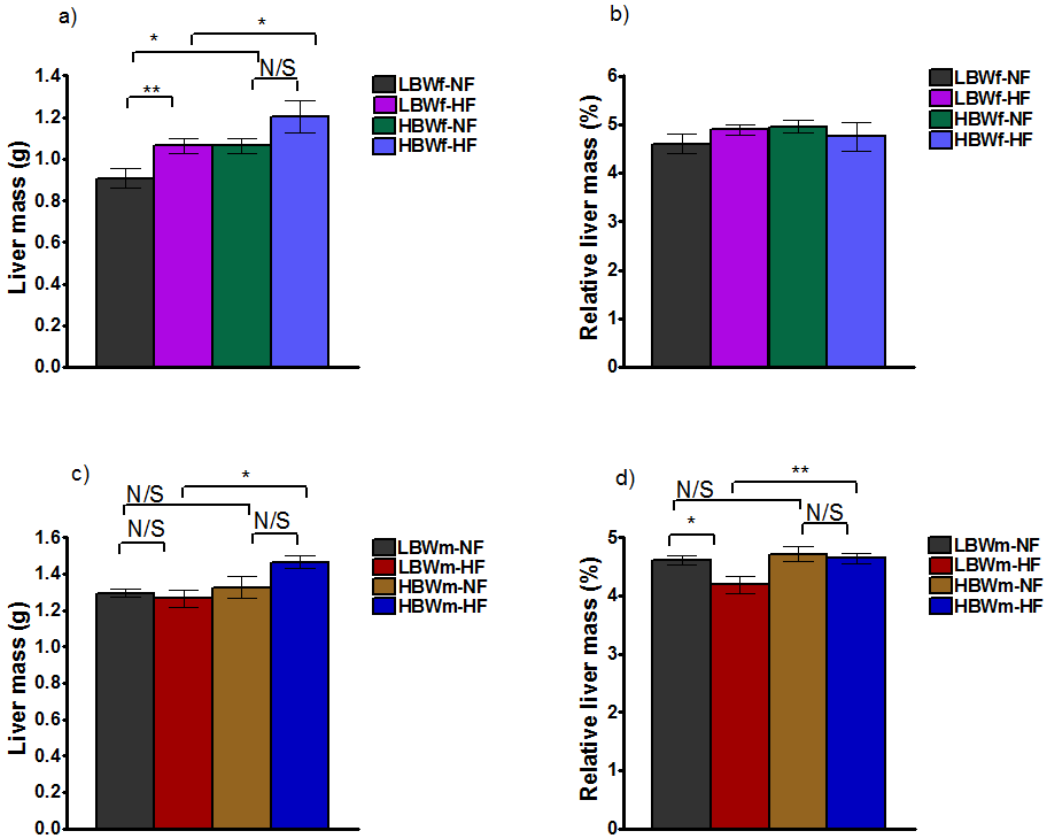

Figure 4.7.2.3.1 Liver mass of female and male offspring at 15 weeks old. Liver mass in grams a) and c) and normalised to current body weight expressed as percentage (relative liver mass %) b) and d). Figures on the top correspond to females and figures below to males. Statistical analysis was performed using a one-way ANOVA followed by a protected Fisher's least significant difference (LSD) post hoc analysis. Data presented as mean± SEM. **LBWf-NF** n=12; **LBWf-HF** n=14; **HBWf-NF** n=8, **HBWf-HF** n=8; **LBWm-NF** n=11; **LBWm-HF** n=12; **HBWm-NF** n=11, **HBWm-HF** n=15. N/S= no significant; *p≤0.05, **p≤0.01.

Organ mass	LBWf-NF$_1$	LBWf-HF$_2$	HBWf-NF$_3$	HBWf-HF$_4$	P value
Liver (g)	0.907 ±0.046	1.064 ±0.036	1.065 ±0.036	1.20 ±0.067	**1 vs.2=0.01** **3vs.4=0.077** **1vs.3=0.023** **2vs.4=0.047**
Liver (%)	4.597 ±0.205	4.893 ±0.109	4.957 ±0.131	5.036 ±0.208	**1 vs.2**=0.165 **3vs.4**=0.768 **1vs.3**=0.143 **2vs.4**=0.553

Table 4.7.2.3.1 Liver mass of female offspring at 15 weeks old. Liver (g)= liver mass in grams and liver (%)= normalised liver mass to current body weight expressed as percentage. Statistical analysis was performed using a one-way ANOVA followed by a protected Fisher's least significant difference (LSD) post hoc analysis. Data presented as mean± SEM.

4.7.2.4 Pancreas, spleen and heart masses in Females

Contrary to the comparable differences between males (figure 4.7.1.4.1 and table 4.7.1.4.1), pancreas (g) was significantly higher in **HBWf-HF** mice than **HBWf-NF** mice (**p=0.026**; figure 4.7.2.4.1a and table 4.7.2.4.1) and it was also higher when compared to **LBWf-HF** mice (**p=0.001**; figure 4.7.2.4.1a and table 4.7.2.4.1). Comparable masses were found between **LBWf** mice (p=0.29; figure 4.7.2.4.1a and table 4.7.2.4.1) and females fed a **NF** diet (p=0.915; figure 4.7.2.4.1a and table 4.7.2.4.1). After normalising to body weight, the difference between **HBWf** mice disappeared (p=0.329; figure 4.7.2.4.1b and table 4.7.2.4.1) but the significant difference between females fed a **HF** diet was maintained (**p=0.029**; figure 4.7.2.4.1b and table 4.7.2.4.1) as well as the comparable masses between those fed a **NF** diet (p=0.312; figure 4.7.2.4.1b and table 4.7.2.4.1). However, differences between **LBWf**

mice were significant, with **LBWf-HF** mice having the lowest mass (**p=0.02**; figure 4.7.2.4.1b and table 4.7.2.4.1).

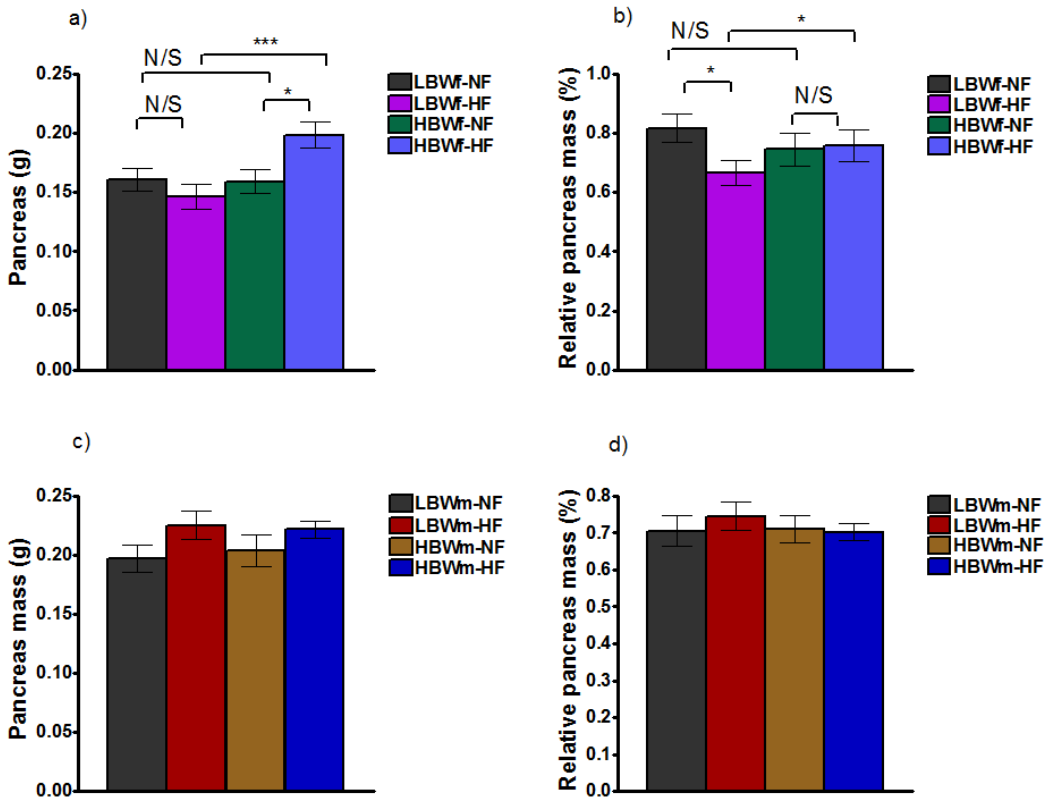

Figure 4.7.2.4.1 Pancreas mass of female and male offspring at 15 weeks old. Pancreas mass in grams a) and c) and normalised to current body weight expressed as percentage (relative pancreas mass%) b) and d). Figures on the top correspond to females and figures below to males. Statistical analysis was performed using a one-way ANOVA followed by a protected Fisher's least significant difference (LSD) post hoc analysis. Data presented as mean± SEM. **LBWf-NF** n=12; **LBWf-HF** n=14; **HBWf-NF** n=8, **HBWf-HF** n=8; **LBWm-NF** n=13; **LBWm-HF** n=14; **HBWm-NF** n=11, **HBWm-HF** n=15. N/S= no significant; *p≤0.05, ***p≤0.001.

Organ mass	LBWf-NF_1	LBWf-HF_2	HBWf-NF_3	HBWf-HF_4	P value
Pancreas (g)	0.161 ±0.009	0.146 ±0.011	0.159 ±0.0103	0.198 ±0.011	**1 vs.2**=0.29 **3vs.4=0.026** **1vs.3**=0.915 **2vs.4=0.001**
Pancreas (%)	0.818 ±0.049	0.667 ±0.041	0.746 ±0.054	0.821 ±0.047	**1 vs.2=0.02** **3vs.4**=0.329 **1vs.3**=0.312 **2vs.4=0.029**

Table 4.7.2.4.1 Pancreas mass of female offspring at 15 weeks old. Pancreas (g)= pancreas mass in grams and pancreas (%)= normalised pancreas mass to current body weight expressed as percentage. Statistical analysis was performed using a one-way ANOVA followed by a protected Fisher's least significant difference (LSD) post hoc analysis. Data presented as mean± SEM.

Contrary to the similar differences seen between male groups (figure 4.7.1.4.2 and table 4.7.1.4.2), assessment of spleen mass in grams showed that mice fed a **HF** diet had a heavier spleen than their counterparts (**LBWf-HF** vs. **LBWf-NF p=0.009**; **HBWf-HF** vs. **HBWf-NF p= 0.02**; figure 4.7.2.4.2a and table 4.7.2.4.2). However after normalisation to body weight, there were not significant differences between groups but the pattern was maintained (figure 4.7.2.4.2b and table 4.7.2.4.2).

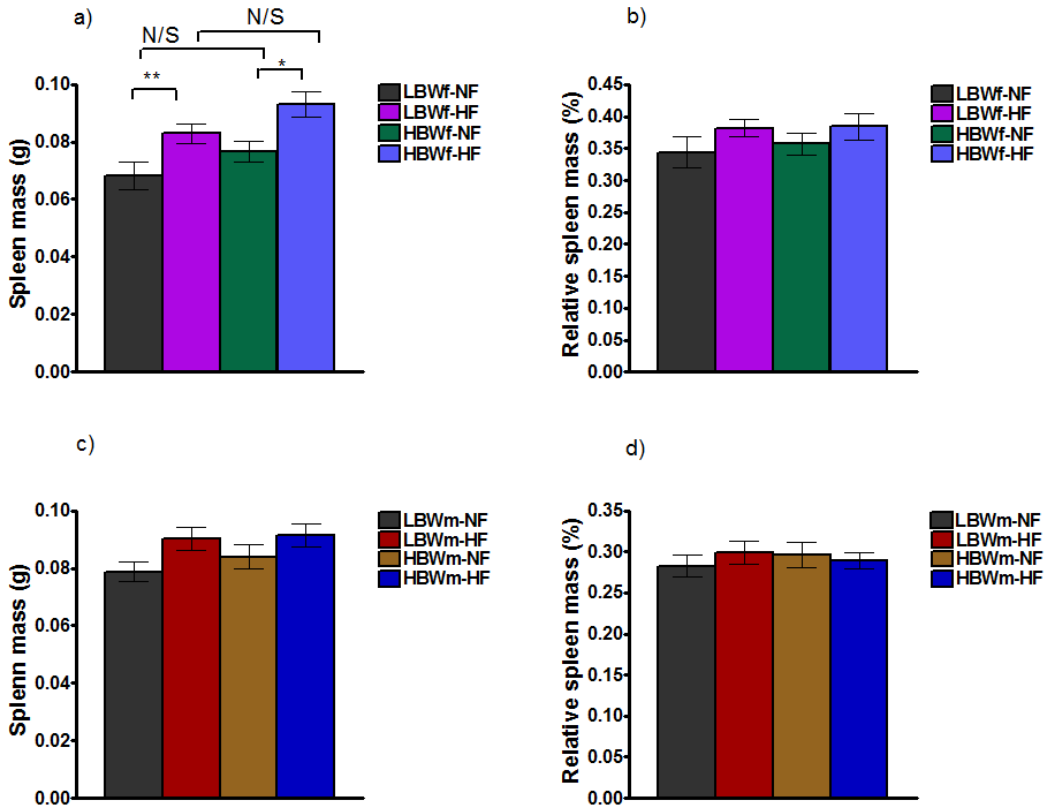

Figure 4.7.2.4.2 Spleen mass of female and male offspring at 15 weeks old. Spleen mass in grams a) and c) and normalised to current body weight expressed as percentage (relative spleen mass%) b) and d). Figures on the top correspond to females and figures below to males. Statistical analysis was performed using a one-way ANOVA followed by a protected Fisher's least significant difference (LSD) post hoc analysis. Data presented as mean± SEM. **LBWf-NF** n=10; **LBWf-HF** n=14; **HBWf-NF** n=8, **HBWf-HF** n=7; **LBWm-NF** n=13; **LBWm-HF** n=13; **HBWm-NF** n=11, **HBWm-HF** n=15. N/S= no significant; *p≤0.05, **p≤0.01.

Organ mass	LBWf-NF_1	LBWf-HF_2	HBWf-NF_3	HBWf-HF_4	P value
Spleen (g)	0.068 ±0.005	0.083 ±0.003	0.077 ±0.004	0.093 ±0.004	**1 vs.2=0.009** **3vs.4=0.02** **1vs.3**=0.174 **2vs.4**=0.10
Spleen (%)	0.344 ±0.024	0.382 ±0.014	0.357 ±0.017	0.384 ±0.021	**1 vs.2**=0.125 **3vs.4**=0.382 **1vs.3**=0.634 **2vs.4**=0.939

Table 4.7.2.4.2 Spleen mass of female offspring at 15 weeks old. Spleen (g)= pancreas mass in grams and spleen (%)= normalised spleen mass to current body weight expressed as percentage. Statistical analysis was performed using a one-way ANOVA followed by a protected Fisher's least significant difference (LSD) post hoc analysis. Data presented as mean± SEM.

Heart mass (g) was similar between groups as it was in male groups (figure 4.7.2.4.3a and table 4.7.2.4.3). However, relative values (%) between **LBWf** mice were significantly different, with a higher mass in **LBWm-NF** mice compared to **LBWf-HF** mice (**p=0.012**; figure 4.7.2.4.3b and table 4.7.2.4.3), but there were similar between males. Comparable differences were maintained between others female groups.

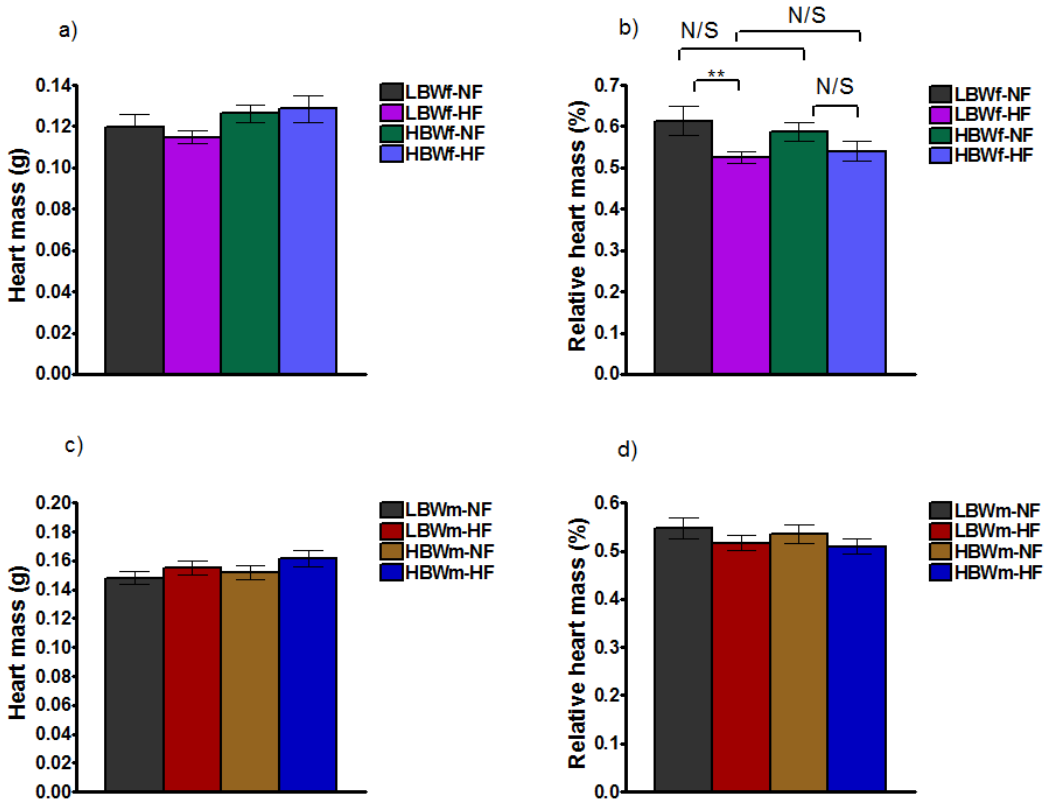

Figure 4.7.2.4.3 Heart mass of female and male offspring at 15 weeks old. Heart mass in grams a) and c) and normalised to current body weight expressed as percentage (relative heart mass%) b) and d). Figures on the top correspond to females and figures below to males. Statistical analysis was performed using a one-way ANOVA followed by a protected Fisher's least significant difference (LSD) post hoc analysis. Data presented as mean± SEM. **LBWf-NF** n=10; **LBWf-HF** n=14; **HBWf-NF** n=7, **HBWf-HF** n=8; **LBWm-NF** n=12; **LBWm-HF** n=13; **HBWm-NF** n=11, **HBWm-HF** n=14. N/S= no significant; **p≤0.01.

Organ mass	LBWf-NF_1	LBWf-HF_2	HBWf-NF_3	HBWf-HF_4	P value
Heart (g)	0.119 ±0.006	0.115 ±0.003	0.126 ±0.004	0.128 ±0.006	**1 vs.2**=0.863 **3vs.4**=0.993 **1vs.3**=0.825 **2vs.4**=0.185
Heart (%)	0.613 ±0.035	0.529 ±0.014	0.587 ±0.023	0.539 ±0.023	**1 vs.2=0.012** **3vs.4**=0.219 **1vs.3**=0.503 **2vs.4**=0.767

Table 4.7.2.4.3 Heart mass of female offspring at 15 weeks old. Heart (g)= heart mass in grams and heart (%)= normalised heart mass to current body weight expressed as percentage. Statistical analysis was performed using a one-way ANOVA followed by a protected Fisher's least significant difference (LSD) post hoc analysis. Data presented as mean± SEM.

4.7.2.5 Kidneys mass in Females

Absolute value of kidneys mass (g) was significantly higher in mice fed a **HF** diet compared to their counterparts (**LBWf-HF** vs. **LBWf-NF p=0.031**; **HBWf-HF** vs. **HBWf-NF p= 0.014**; figure 4.7.2.5.1a and table 4.7.2.5.1). Also, **HBWf-NF** mice had a higher kidneys mass compared to **LBWf-NF** mice (**p=0.05**; figure 4.7.2.5.1a and table 4.7.2.5.1) as well as **HBWf-HF** vs. **LBWf-HF p=0.005**; figure 4.7.2.5.1a and table 4.7.2.5.1). However, relative values (%) were similar between groups (figure 4.7.2.5.1b and table 4.7.2.5.1). Although a significant difference between females fed a **NF** diet was not evident, it was between their respective male groups (figure 4.7.1.5.1 and table 4.7.1.5.1).

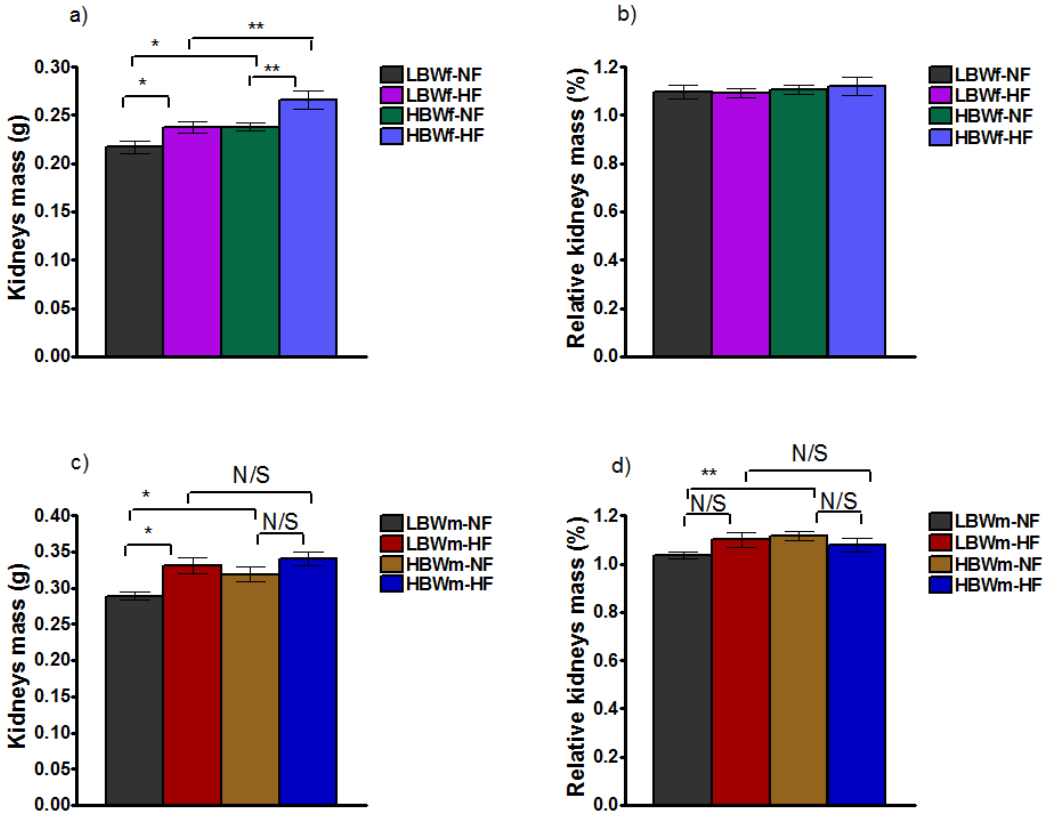

Figure 4.7.2.5.1 Kidneys mass of female and male offspring at 15 weeks old. Kidneys mass in grams a) and c) and normalised to current body weight expressed as percentage (relative brain mass%) b) and d). Figures on the top correspond to females and figures below to males. Statistical analysis was performed using a one-way ANOVA followed by a protected Fisher's least significant difference (LSD) post hoc analysis. Data presented as mean± SEM. **LBWf-NF** n=10; **LBWf-HF** n=14; **HBWf-NF** n=8, **HBWf-HF** n=8; **LBWm-NF** n=13; **LBWm-HF** n=12; **HBWm-NF** n=10; **HBWm-HF** n=15. N/S= no significant; *p≤0.05, **p≤0.01.

Organ mass	LBWf-NF_1	LBWf-HF_2	HBWf-NF_3	HBWf-HF_4	P value
Kidneys (g)	0.217 ±0.007	0.237 ±0.003	0.238 ±0.004	0.265 ±0.009	**1 vs.2=0.031** **3vs.4=0.014** **1vs.3=0.05** **2vs.4=0.005**
Kidneys (%)	1.095 ±0.028	1.093 ±0.018	1.108 ±0.018	1.119 ±0.039	**1 vs.2**=0.94 **3vs.4**=0.781 **1vs.3**=0.746 **2vs.4**=0.466

Table 4.7.2.5.1 Kidneys mass of female offspring at 15 weeks old. Kidneys (g)= kidneys mass in grams and kidneys (%)= normalised kidneys mass to current body weight expressed as percentage. Statistical analysis was performed using a one-way ANOVA followed by a protected Fisher's least significant difference (LSD) post hoc analysis. Data presented as mean± SEM.

4.7.2.6 Skeletal muscle mass in Females

Skeletal muscle assessment showed a different pattern between females and males. **LBWf-HF** mice had a higher muscle mass in grams compared to **LBWf-NF** mice (**p=0.017**; figure 4.7.2.6.1a and table 4.7.2.6.1), which was the contrary in males (figure 4.7.2.6.1 and table 4.7.2.6.1). The difference between **HBWf** mice did not reach significance (p=0.49; figure 4.7.2.6.1a and table 4.7.2.6.1), which it did between males (figure 4.7.1.6.1 and table 4.7.1.6.1). Comparable differences between females fed a **NF** diet (p=0.127; figure 4.7.2.6.1a and table 4.7.2.6.1) and females fed a **HF** diet were found (p=0.147; figure 4.7.2.6.1a and table 4.7.2.6.1).

After normalisation, relative muscle mass was marginally significant between **LBWf** mice, maintaining the same pattern as in mass in absolute values (g) (p=0.092; figure 4.7.2.6.1b and table 4.7.2.6.1) as well as between **HBWf** mice (p=0.067; figure 4.7.2.6.1b and table 4.7.2.6.1). However, differences between females fed a **HF** diet became significantly different, with a higher relative mass in **LBWf-HF** mice, (**p=0.006**; figure 4.7.2.6.1b and table 4.7.2.6.1), what was opposite in males (figure 4.7.1.6.1 and table 4.7.1.6.1). Comparable difference was maintained between females fed a **NF** diet (p=0.492; figure 4.7.2.6.1b and table 4.7.2.6.1).

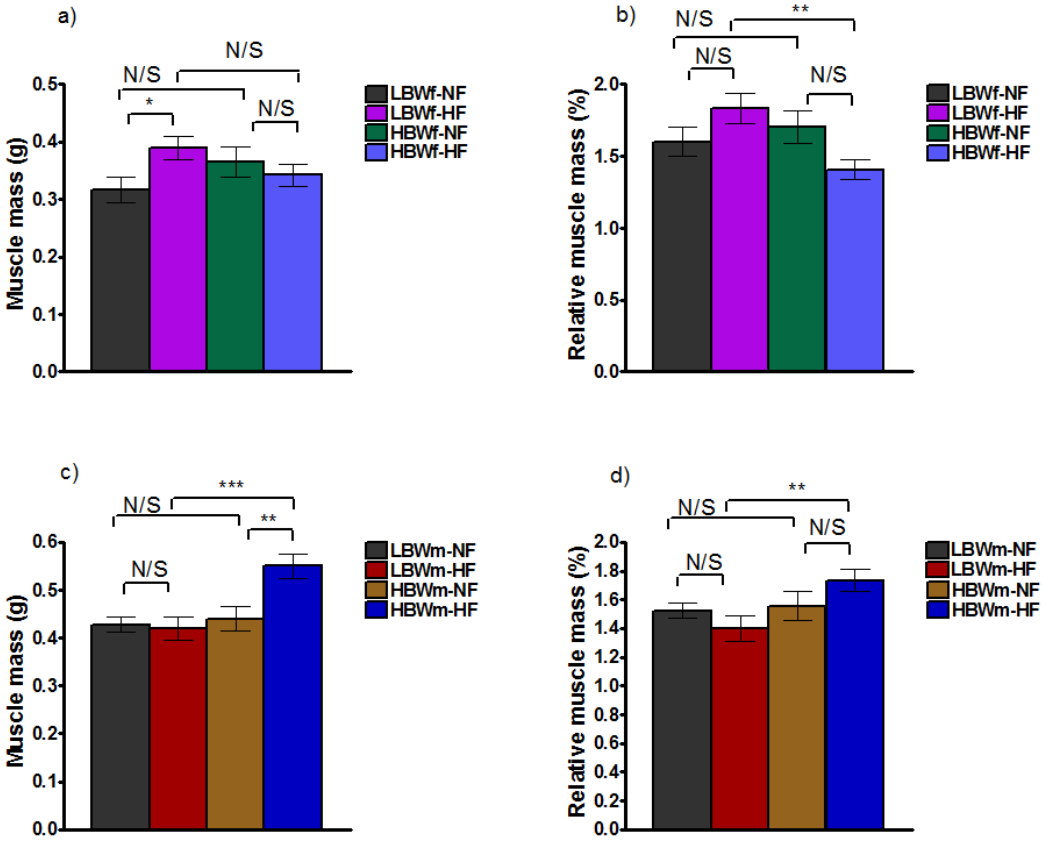

Figure 4.7.2.6.1 Skeletal muscle mass of female and male offspring at 15 weeks old. Muscle mass in grams a) and c) and normalised to current body weight expressed as percentage (relative brain mass%) b) and d). Figures on the top correspond to females and figures below to males. Statistical analysis was performed using a one-way ANOVA followed by a protected Fisher's least significant difference (LSD) post hoc analysis. Data presented as mean± SEM. **LBWf-NF** n=11; **LBWf-HF** n=14; **HBWf-NF** n=8, **HBWf-HF** n=8; **LBWm-NF** n=12; **LBWm-HF** n=14; **HBWm-NF** n=11; **HBWm-HF** n=14. N/S= no significant; *p≤0.05, **p≤0.01, ***p≤0.001.

Organ mass	LBWf-NF_1	LBWf-HF_2	HBWf-NF_3	HBWf-HF_4	P value
Muscle (g)	0.317 ±0.022	0.389 ±0.021	0.366 ±0.026	0.342 ±0.019	**1 vs.2=0.017** **3vs.4**=0.49 **1vs.3**=0.127 **2vs.4**=0.147
Muscle (%)	1.602 ±0.099	1.834 ±0.111	1.704 ±0.114	1.407 ±0.067	**1 vs.2=0.092** **3vs.4=0.067** **1vs.3**=0.492 **2vs.4=0.006**

Table 4.7.2.6.1 Muscle mass of female offspring at 15 weeks old. Muscle (g)= muscle mass in grams and muscle (%)= normalised muscle mass to current body weight expressed as percentage. Statistical analysis was performed using a one-way ANOVA followed by a protected Fisher's least significant difference (LSD) post hoc analysis. Data presented as mean± SEM.

4.8 The Effects of Birth Weight and Diet on White Adipose Tissue Mass in Young Mice (From Week 3 Until Week 15)

White adipose tissue was (WAT) was extracted and subdivided into subcutaneous (SAT) and internal adipose tissue (IAT). IAT was further subdivided into gonadal, retroperitoneal and mesenteric fat depots for regional analysis. Data was analysed based on absolute values (grams) and relative values (expressed as percentage of current body weight). A 2x2 factorial ANOVA was performed to assess the effects of both birth weight and diet on white adipose tissue mass.

4.8.1 White adipose tissue mass in Males

Significant interactions were found between both birth weight and diet in all the independent white fat depots as well as in total white adipose tissue and internal adipose tissue expressed in grams (figure 4.8.1.1 and tables 4.8.1.1 and 4.8.1.2).

Total white adipose tissue in grams (Total WAT), subcutaneous (SAT), mesenteric adipose tissue and internal adipose tissue (IAT), were marginally significant between mice fed a **NF** diet, with **LBWm-NF** mice having higher masses compared to **HBWm-NF** mice (total WAT: p=0.057; SAT: p=0.063; mesenteric: p=0.07; IAT: p=0.056; figure 4.8.1.1 and tables 4.8.1.1 and 4.8.1.2). However, retroperitoneal fat was significantly different between mice groups (**p=0.042**; figure 4.8.1.1 and tables 4.8.1.1 and 4.8.1.2).

However, an opposite pattern was seen in mice fed a **HF** diet, with **HBWm-HF** mice having significant higher masses than **LBWm-HF** mice, except from gonadal and mesenteric fat, which were comparable between groups (gonadal: p=0.191; mesenteric; p=0.106; figure 4.8.1.1 and tables 4.8.1.1 and 4.8.1.2).

Furthermore, **HBWm-HF** mice had higher total WAT, SAT, IAT, and independent regional internal depots (gonadal, retroperitoneal and mesenteric adipose tissues) compared to **HBWm-NF** mice (figure 4.8.1.1 and tables 4.8.1.1 and 4.8.1.2). Significant differences between **LBWm** mice were also found, except from retroperitoneal and mesenteric fat, which were comparable between groups (retroperitoneal: p=0.747; mesenteric: p=0.346; figure 4.8.1.1 and tables 4.8.1.1 and 4.8.1.2).

Significant interactions and therefore differences were maintained after normalising white fat masses to current body weight (%), except from Total WAT and IAT between **LBWm** mice, which became nearly significant (total WAT: p=0.067; IAT: p=0.057; figure 4.8.1.2 and table 4.8.1.1; figure 4.8.1.2 and table 4.8.1.2), as well as IAT differences between **HBWm-HF** and **LBWm-HF** mice (p=0.096; figure 4.8.1.2 and table 4.8.1.2) maintaining all a similar trend as in absolute values. Comparable differences between groups were also maintained (figure 4.8.1.2 and tables 4.8.1.1 and 4.8.1.2). The marginal difference obtained in grams for mesenteric fat was significant in relative values (%) between mice fed a **NF** diet (**p=0.02**; figure 4.8.1.2 and table 4.8.1.2).

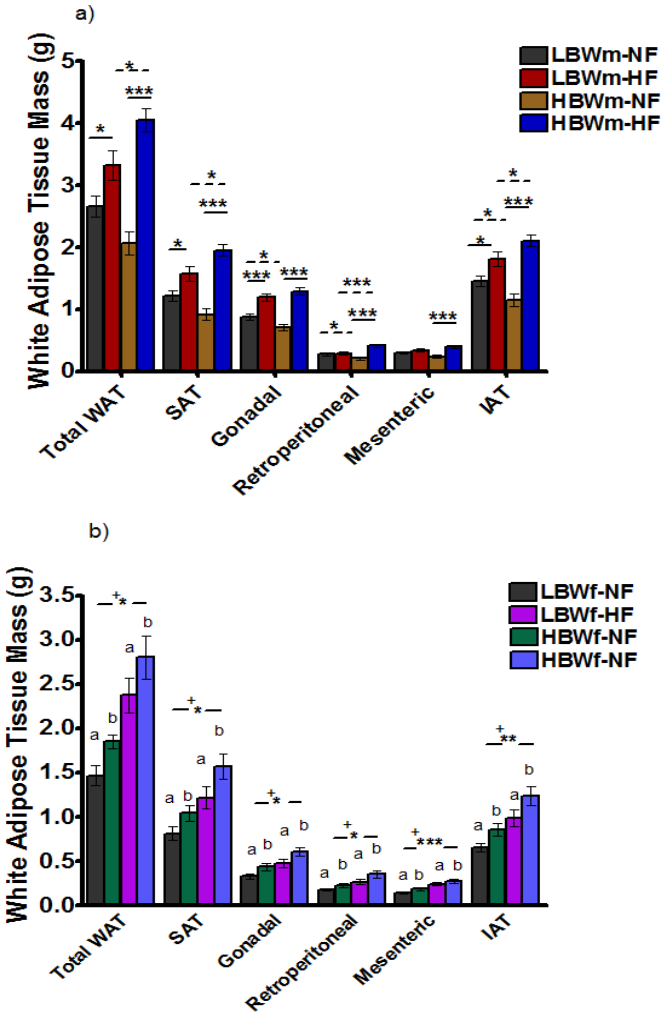

Figure 4.8.1.1 White adipose tissue mass in grams from male and female mice at week 15. Total WAT= total white adipose tissue, SAT=subcutaneous adipose tissue, IAT= internal adipose tissue as the sum of gonadal, retroperitoneal and mesenteric fat depots. Statistical analysis was performed using a 2x2 factorial ANOVA test..Data presented as mean± SEM. Dotted line in a)= for significant differences between mice fed a **NF** diet and mice fed a **HF** diet having the same birth weight. Continuous line in a)= for significant differences between **LBWm** mice and **HBWm** mice having the same diet. **LBWm-NF** n=11; **LBWm-HF** n=14; **HBWm-NF** n=10, **HBWm-HF** n=15. Significant main effect of diet in b) $^{+}$: *p≤0.05,** p≤0.01, ***p≤0.001. Main effect of birth weight represented with different letters in b). **LBWf-NF** n=12; **LBWf-HF** n=13; **HBWf-NF** n=7, **HBWf-HF** n=8.

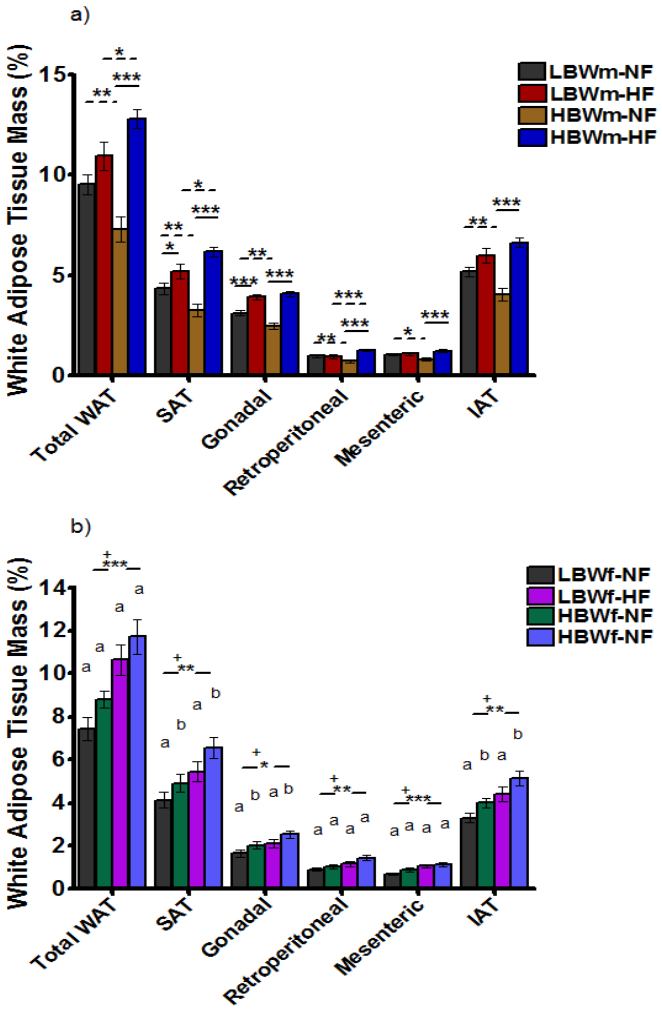

Figure 4.8.1.2 White adipose tissue mass in percentage (%) from male and female mice at week 15. Total WAT= total white adipose tissue, SAT=subcutaneous adipose tissue, IAT= internal adipose tissue as the sum of gonadal, retroperitoneal and mesenteric fat depots. Statistical analysis was performed using a 2x2 factorial ANOVA test. Data presented as mean± SEM. Dotted line in a)= for significant differences between mice fed a **NF** diet and mice fed a **HF** diet having the same birth weight. Continuous line in a)= for significant differences between **LBWm** mice and **HBWm** mice having the same diet. **LBWm-NF** n=11; **LBWm-HF** n=14; **HBWm-NF** n=10, **HBWm-HF** n=15. Significant main effect of diet in b) $^{+}$: *p≤0.05, **p≤0.01, ***p≤0.001. Main effect of birth weight represented with different letters in b). **LBWf-NF** n=12; **LBWf-HF** n=13; **HBWf-NF** n=7, **HBWf-HF** n=8.

	LBWm-NF_1	LBWm-HF_2	HBWm-NF_3	HBWm-HF_4	P value
Total WAT (g)	2.779 ±0.205	3.453 ±0.18	2.064 ±0.205	4.056 ±0.168	**1 vs.2=0.018 3vs.4<0.001 1vs.3=0.018 2vs.4=0.018**
Interaction: F(1,44)=12.014 p=0.001					
Total WAT (%)	9.859 ±0.599	11.351 ±0.525	7.302 ±0.599	12.796 ±0.489	**1 vs.2=0.067 3vs.4<0.001 1vs.3=0.004 2vs.4=0.05**
Interaction: F(1,44)=12.977 p=0.001					
SAT (g)	1.274 ±0.105	1.638 ±0.092	0.918 ±0.105	1.954 ±0.086	**1 vs.2=0.013 3vs.4<0.001 1vs.3=0.021 2vs.4=0.016**
Interaction: F(1,44)=11.848 p=0.001					
SAT (%)	4.521 ±0.321	5.406 ±0.281	3.254 ±0.321	6.169 ±0.262	**1 vs.2=0.044 3vs.4<0.001 1vs.3=0.008 2vs.4=0.05**
Interaction: F(1,44)=11.664 p=0.001					

Table 4.8.1.1 Total white adipose tissue and subcutaneous adipose tissue from males at 15 weeks old. Total WAT (g)= total white adipose tissue; Total WAT (%)= total white adipose tissue as percentage of body weight. SAT (g)= subcutaneous adipose tissue in grams; SAT (%)= subcutaneous adipose tissue as percentage of body weight. Statistical analysis was performed using a 2x2 factorial ANOVA test followed by simple main effects analysis, as interactions were significant. Data presented as mean± SEM.

	LBWm-NF_1	LBWm-HF_2	HBWm-NF_3	HBWm-HF_4	P value
Gonadal (g)	0.878 ±0.058	1.192 ±0.056	0.704 ±0.061	1.291 ±0.05	**1 vs.2<0.001 3vs.4<0.001 1vs.3=0.046 2vs.4**=0.191
Interaction: F(1,44)=5.838 p=0.02					
Gonadal (%)	3.135 ±0.161	3.928 ±0.154	2.494 ±0.169	4.079 ±0.138	**1 vs.2=0.001 3vs.4<0.001 1vs.3=0.009 2vs.4**=0.471
Interaction: F(1,44)=6.43 p=0.015					
Retrop. (g)	0.278 ±0.021	0.302 ±0.021	0.208 ±0.024	0.414 ±0.019	**1 vs.2**=0.437 **3vs.4<0.001 1vs.3=0.034 2vs.4<0.001**
Interaction: F(1,44)=17.845 p<0.001					
Retrop. (%)	0.993 ±0.066	1.009 ±0.059	0.736 ±0.072	1.302 ±0.059	**1 vs.2**=0.86 **3vs.4<0.001 1vs.3=0.012 2vs.4=0.002**
Interaction: F(1,44)=17.311 p<0.001					
Mesent. (g)	0.306 ±0.026	0.354 ±0.025	0.233 ±0.028	0.397 ±0.023	**1 vs.2**=0.188 **3vs.4<0.001 1vs.3=0.062 2vs.4**=0.208
Interaction: F(1,44)=5.196 p=0.027					
Mesent. (%)	1.092 ±0.074	1.164 ±0.071	0.818 ±0.081	1.246 ±0.066	**1 vs.2**=0.486 **3vs.4<0.001 1vs.3=0.016 2vs.4**=0.403
Interaction: F(1,44)=5.891 p=0.019					
IAT (g)	1.451 ±0.107	1.815 ±0.099	1.146 ±0.112	2.102 ±0.092	**1 vs.2=0.016 3vs.4<0.001 1vs.3=0.056 2vs.4=0.039**
Interaction: F(1,44)=8.301 p=0.006					
IAT (%)	5.18 ±0.302	5.982 ±0.278	4.048 ±0.316	6.627 ±0.258	**1 vs.2=0.057 3vs.4<0.001 1vs.3=0.013 2vs.4=0.096**
Interaction: F(1,44)=9.416 p=0.004					

Table 4.8.1.2 Internal adipose tissue from males at 15 weeks old. Gonadal, retroperitoneal and mesenteric adipose tissues in grams (g)= and as percentages of body weight (%). IAT= internal adipose tissue as the sum of the aforementioned white adipose tissues in grams (g) and as percentage of body weight (%). Statistical analysis was performed using a 2x2 factorial ANOVA test followed by simple main effects analysis, as interactions were significant. Data presented as mean± SEM.

Assessment of the internal to subcutaneous adipose tissue ratio showed an interaction between both birth weight and diet. Unexpectedly **HBWm-NF** had a higher ratio than **HBWm-HF** (**p≤0.001**; figure 4.8.1.3 and table 4.8.1.3), whilst differences between others groups did not reach significance. It was noticed that also in **LBWm** mice there was a similar trend as seen in the **HBWm** mice.

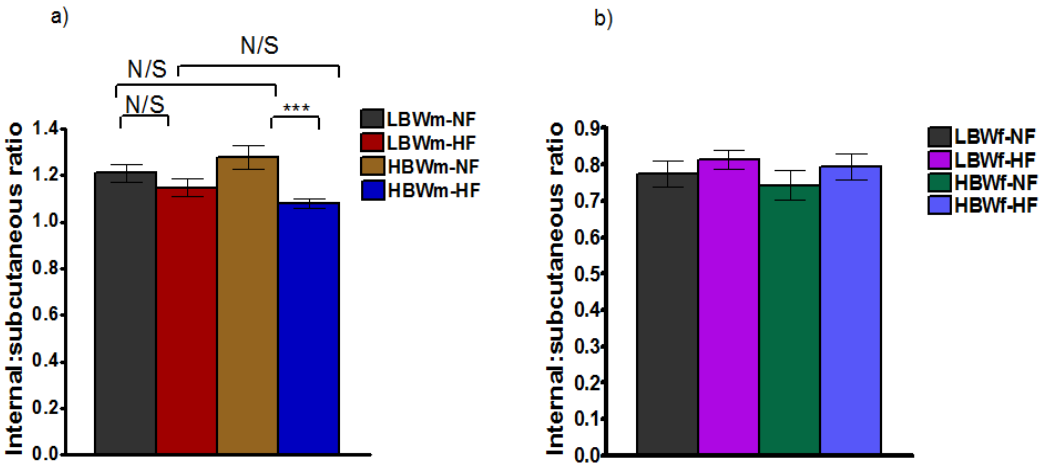

Figure 4.8.1.3 Internal to subcutaneous adipose tissue ratio in male and female offspring at 15 weeks old. Statistical analysis was performed using a 2x2 factorial ANOVA test. Data presented as mean± SEM. **LBWm-NF** n=11; **LBWm-HF** n=14; **HBWm-NF** n=10, **HBWm-HF** n=15; **LBWf-NF** n=12; **LBWf-HF** n=13; **HBWf-NF** n=7, **HBWf-HF** n=8. ***p≤0.001.

	LBWm-NF_1	LBWm-HF_2	HBWm-NF_3	HBWm-HF_4	P value
IAT:SAT	1.21 ±0.037	1.147 ±0.034	1.315 ±0.04	1.081 ±0.031	**1 vs.2**=0.21 **3vs.4<0.001** **1vs.3**=0.063 **2vs.4**=0.158
Interaction: F(1,44)=5.691 p=0.021					

Table 4.8.1.3 Internal to subcutaneous adipose tissue ratio of male offspring at 15 weeks old. Statistical analysis was performed using a 2x2 factorial ANOVA test followed by simple main effects analysis, as interaction was significant. Data presented as mean± SEM.

4.8.2 White adipose tissue mass in Females

Contrary to males, there was a significant effect of both birth weight and diet on total WAT (g), SAT (g), retroperitoneal (g), mesenteric (g), gonadal fat (g), and IAT (g), and the interaction was not significant between variables, which suggested that both variables might affect adipose tissue mass independently one of each other. All the depots mentioned before were significantly higher in females fed a **HF** diet compared to female mice fed a **NF** diet, and at the same time, in those females with a high birth weight (**HBWf**) compared to females with a low birth weight (**LBWf**) (figure 4.8.2.1 and tables 4.8.2.1 and 4.8.2.2).

After normalisation to current body weight (relative body weight as percentage), significant differences were maintained when assessing SAT(%) (figure 4.8.2.2 and table 4.8.2.1), gonadal (%) and IAT (%) (figure 4.8.2.2 and table 4.8.2.2). However, main effect of birth weight was marginally significant after assessing total WAT (%) (p=0.086; figure 4.8.2.2

and tables 4.8.2.1) and retroperitoneal fat (%) (p=0.067; figure 4.8.2.2 and table 4.8.2.2). It was not significant for mesenteric (%) (p=0.152; figure 4.8.2.2 and table 4.8.2.2). Moreover, the diet effect was maintained in these depots (total WAT(%): **p<0.001**; retroperitoneal (%): **p=0.004**; mesenteric (%): **p<0.001**; figure 4.8.2.2 and tables 4.8.2.1 and table 4.8.2.2).

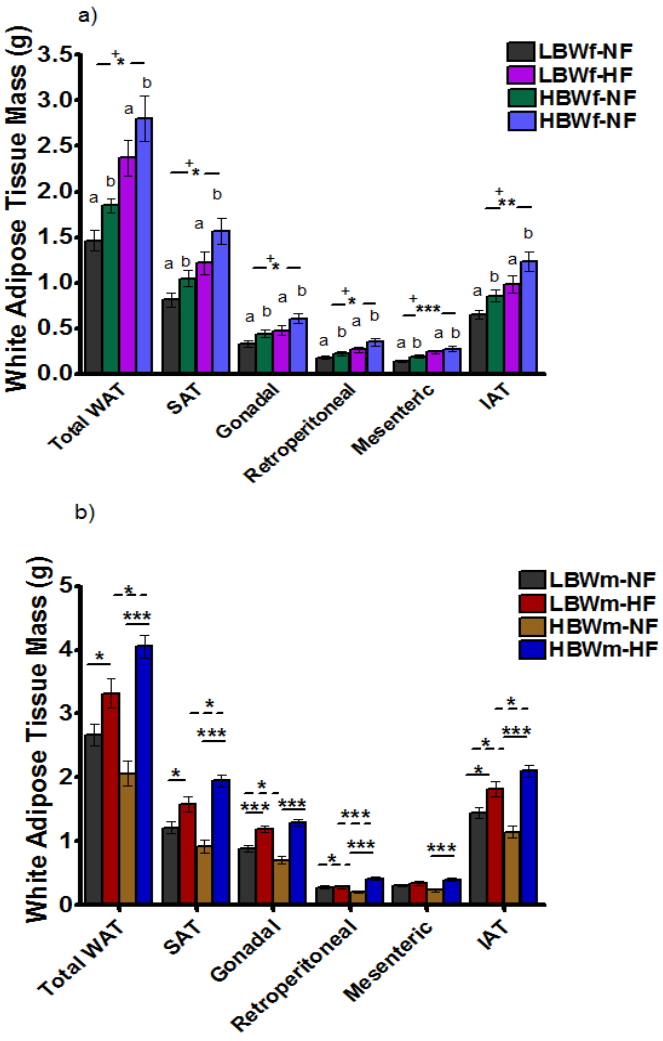

Figure 4.8.2.1 White adipose tissue mass in grams from female and male mice at week 15. Total WAT= total white adipose tissue, SAT=subcutaneous adipose tissue, IAT= internal adipose tissue as the sum of gonadal, retroperitoneal and mesenteric fat depots. Statistical analysis was performed using a 2x2 factorial ANOVA test. Data presented as mean± SEM. Significant main effect of diet in a) $^{+}$: *p≤0.05,** p≤0.01, ***p≤0.001. Main effect of birth weight represented with different letters in a). **LBWf-NF** n=12; **LBWf-HF** n=13; **HBWf-NF** n=7, **HBWf-HF** n=8. Dotted line in b)= for significant differences between mice fed a **NF** diet and mice fed a **HF** diet having the same birth weight. Continuous line in b)= for significant differences between **LBWm** mice and **HBWm** mice having the same diet. **LBWm-NF** n=11; **LBWm-HF** n=14; **HBWm-NF** n=10, **HBWm-HF** n=15.

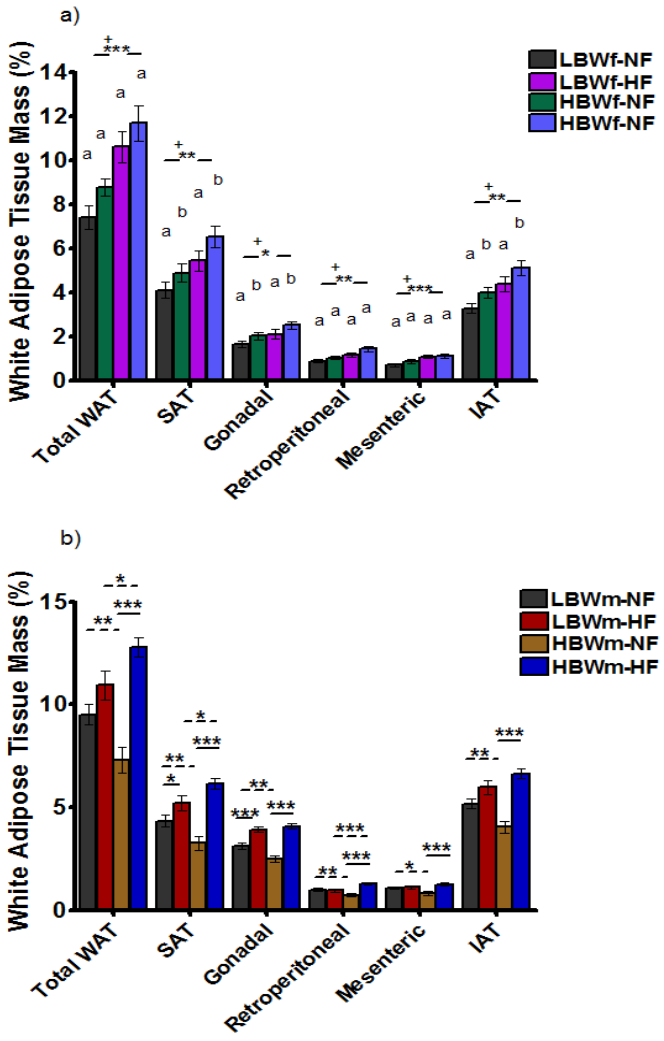

Figure 4.8.2.2 White adipose tissue mass as percentage (%) from female and male mice at week 15. Statistical analysis was performed using a 2x2 factorial ANOVA test. Data presented as mean± SEM. Significant main effect of diet in a) $^{+}$: *p≤0.05,** p≤0.01, ***p≤0.001. Main effect of birth weight represented with different letters in a). **LBWf-NF** n=12; **LBWf-HF** n=13; **HBWf-NF** n=7, **HBWf-HF** n=8. Dotted line in b)= for significant differences between mice fed a **NF** diet and mice fed a **HF** diet having the same birth weight. Continuous line in b)= for significant differences between **LBWm** mice and **HBWm** mice having the same diet. **LBWm-NF** n=11; **LBWm-HF** n=14; **HBWm-NF** n=10, **HBWm-HF** n=15.

	LBWf-NF_1	LBWf-HF_2	HBWf-NF_3	HBWf-HF_4
Total WAT (g)	1.465 ±0.163	2.372 ±0.156	1.851 ±0.213	2.801 ±0.199
Birth weight: F(1,36)=4.865 **p=0.034; diet:** F(1,36)=25.138 **p<0.001; interaction:** F(1,36)=0.014 p=0.907				
Total WAT (%)	7.427 ±0.608	10.646 ±0.584	8.795 ±0.796	11.708 ±0.744
Birth weight: F(1,36)=3.115 **p=0.086; diet:** F(1,36)=19.821 **p<0.001; interaction:** F(1,36)=0.049 p=0.825				
SAT (g)	0.813 ±0.104	1.217 ±0.1	1.046 ±0.136	1.567 ±0.127
Birth weight: F(1,36)=6.153 **p=0.018; diet:** F(1,36)=15.475 **p<0.001; interaction:** F(1,36)=0.246 p=0.623				
SAT (%)	4.124 ±0.415	5.457 ±0.399	4.918 ±0.543	6.556 ±0.508
Birth weight: F(1,36)=4.053 **p=0.05; diet:** F(1,36)=9.98 **p=0.003; interaction**: F(1,36)=0.105 p=0.748				

Table 4.8.2.1 Total white adipose tissue and subcutaneous adipose tissue from females at 15 weeks old. Total WAT (g)= total white adipose tissue; Total WAT (%)= total white adipose tissue as percentage of body weight. SAT (g)= subcutaneous adipose tissue in grams; SAT (%)= subcutaneous adipose tissue as percentage of body weight. Statistical analysis was performed using a 2x2 factorial ANOVA test followed by simple main effects analysis, as interactions were significant. Data presented as mean± SEM.

	LBWf-NF_1	LBWf-HF_2	HBWf-NF_3	HBWf-HF_4
Gonadal (g)	0.328 ±0.043	0.477 ±0.041	0.438 ±0.056	0.609 ±0.052
Birth weight: F(1,36)=6.2 **p=0.018; diet:** F(1,36)=10.857 **p=0.002; interaction**: F(1,36)=0.051 p=0.822				
Gonadal (%)	1.665 ±0.171	2.134 ±0.165	2.047 ±0.224	2.545 ±0.21
Birth weight: F(1,36)=4.167 **p=0.049; diet:** F(1,36)=6.201 **p=0.018; interaction:** F(1,36)=0.006 p=0.94				
Retrop. (g)	0.181 ±0.026	0.266 ±0.025	0.228 ±0.034	0.352 ±0.032
Birth weight: F(1,36)=5.14 p=0.029; diet: F(1,36)=12.647 **p=0.001; interaction:** F(1,36)=0.436 p=0.513				
Retrop. (%)	0.913 ±0.098	1.187 ±0.094	1.06 ±0.128	1.46 ±0.12
Birth weight: F(1,36)=3.572 p=0.067; diet: F(1,36)=9.222 p=0.004; interaction: F(1,36)=0.323 p=0.573				
Mesent. (g)	0.143 ±0.018	0.242 ±0.017	0.192 ±0.023	0.274 ±0.022
Birth weight: F(1,36)=4.174 p=0.048; diet: F(1,36)=20.715 **p<0.001; interaction:** F(1,36)=0.17 p=0.682				
Mesent. (%)	0.725 ±0.069	1.09 ±0.066	0.896 ±0.09	1.147 ±0.084
Birth weight: F(1,36)=2.14 p=0.152**;** diet: F(1,36)=15.515 **p<0.001; interaction**: F(1,36)=0.535 p=0.469				
IAT (g)	0.652 ±0.077	0.985 ±0.074	0.858 ±0.101	1.235 ±0.095
Birth weight: F(1,36)=6.765 p=0.013; diet: F(1,36)=16.397 **p<0.001; interaction:** F(1,36)=0.064 p=0.802				
IAT (%)	5.18 ±0.302	5.982 ±0.278	4.048 ±0.316	6.627 ±0.258
Birth weight: F(1,36)=4.925 p=0.033; diet: F(1,36)=12.077 **p=0.001; interaction:** F(1,36)=0.004 p=0.949				

Table 4.8.2.2 Internal adipose tissue from females at 15 weeks old. Gonadal, retroperitoneal and mesenteric adipose tissues in grams (g)= and as percentages of body weight (%). IAT= internal adipose tissue as the sum of the aforementioned white adipose tissues in grams (g) and as percentage of body weight (%). Analysis was performed using a 2x2 factorial ANOVA. Data presented as mean± SEM.

Internal to subcutaneous adipose tissue ratio was not significantly affected by birth weight or diet, and there was not interaction between both. Contrary to males, the differences tended to be higher in males fed a **HF** diet and in **LBWf** mice (figures 4.8.1.3 and 4.8.2.3 and tables 4.8.1.3 and table 4.8.2.3).

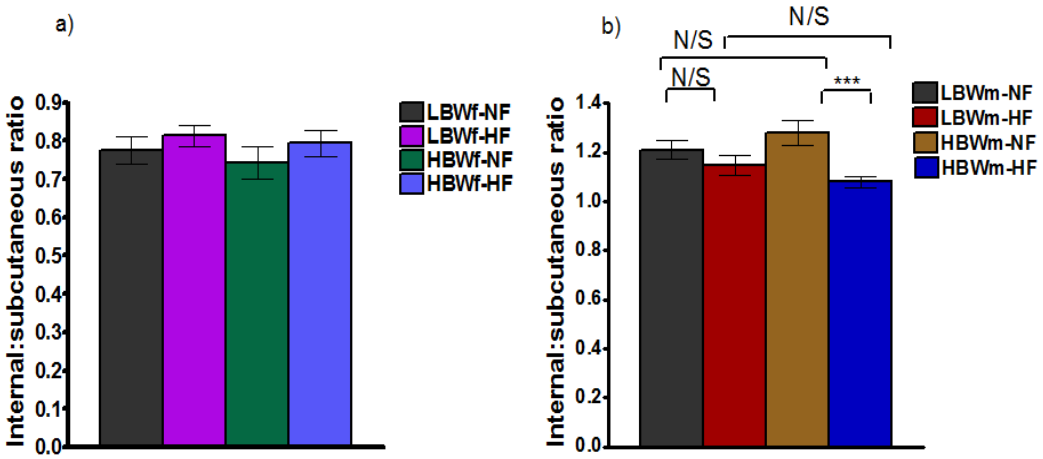

Figure 4.8.2.3 Internal to subcutaneous adipose tissue ratio of female and male offspring at 15 weeks old. Statistical analysis was performed using a 2x2 factorial ANOVA test. Figure a) corresponds to males and figure b) to females. Data presented as mean± SEM. **LBWf-NF** n=12; **LBWf-HF** n=13; **HBWf-NF** n=7, **HBWf-HF** n=8; **LBWm-NF** n=11; **LBWm-HF** n=14; **HBWm-NF** n=10, **HBWm-HF** n=15. ***p≤0.001.

	LBWf-NF_1	LBWf-HF_2	HBWf-NF_3	HBWf-HF_4
IAT:SAT	0.775 ±0.033	0.817 ±0.03	0.757 ±0.045	0.793 ±0.039
Birth weight: F(1,36)=0.324 p=0.573; diet: F(1,36)=1.1 p=0.302; Interaction: F(1,36)=0.006 p=0.941				

Table 4.8.2.3 Internal to subcutaneous adipose tissue ratio of female offspring at 15 weeks old. Statistical analysis was performed using a 2x2 factorial ANOVA test followed by simple main effects analysis, as interaction was significant. Data presented as mean± SEM.

4.9 Adipocyte Size Distribution in White Adipose Tissue

Subcutaneous and gonadal adipose tissue from male mice (only) were collected and processed as described in section 2.4.6. Total adipocyte number was analysed as per gram of tissue extracted and per total fat depot.

Assessment of adipocyte number per gram of tissue showed comparable levels between groups (figure 4.9.1a). However, a significant interaction between both birth weight and diet was found when evaluating adipocyte number per fat depots ($F(1,39)=4.921$ **p=0.032**; figure 4.9.1b). **HBWm-HF** had a higher number of adipocytes when compared to **HBWm-NF** mice (**p=0.008**). Although **LBWm-NF** had a higher number of adipocytes than **HBWm-NF**, the difference did not reach statistical significance (p=0.144). An opposite trend was found between mice fed a **HF** diet, with **LBWm-HF** having a lower cell number than **HBWm-HF** but again, the difference was not significant (p=0.102).

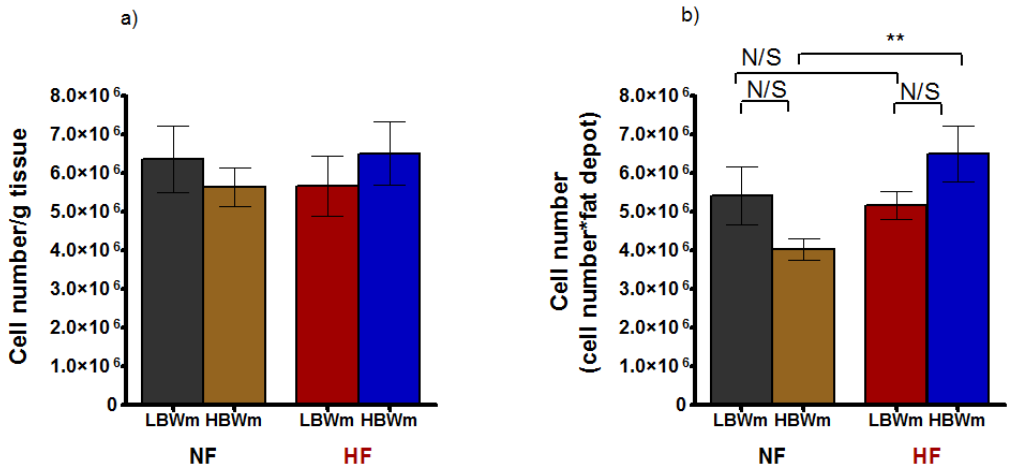

Figure 4.9.1 Adipocyte number in gonadal adipose tissue from male mice at week 15. Cell number expressed as per gram of tissue extracted (adipocyte number/gram tissue) a), and multiply by the amount of total gonadal tissue per mouse per group b). Statistical analysis was performed using a 2x2 factorial ANOVA test followed by a simple main effect analysis, as the interaction was significant between variables. Data presented as mean± SEM. **LBWm-NF** n=10; **LBWm-HF** n=12; **HBWm-NF** n=8, **HBWm-HF** n=13. * p≤0.05, ** p≤0.01.

Evaluation of subcutaneous adipose tissue per gram showed no differences between groups (figure 4.9.2a); but as in gonadal fat tissue, the total number of adipocytes per total fat depots were affected by birth weight and diet ($F(1,42)=5.481$ **p=0.024**; figure 4.9.2b). Differences between **HBWm** mice were significantly different, as in gonadal, with a higher adipocyte number in **HBWm-HF** mice compared to **HBWm-NF** mice (**p<0.001**). Furthermore, **HBWm-HF** mice had a significantly higher cell number than **LBWm-HF** mice (**p=0.036**). Comparable differences were found between mice fed a **NF** diet (p=0.231) or between **LBWm** mice (p=0.252).

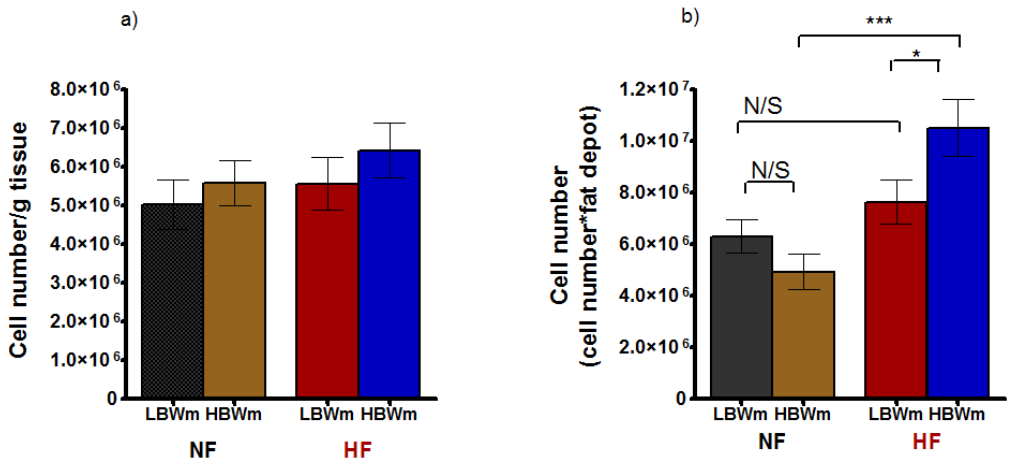

Figure 4.9.2 Adipocyte number in subcutaneous adipose tissue from male mice. Adipocyte number expressed as per gram of tissue extracted (cell number/gram tissue) a), and multiply by the amount of total gonadal tissue per mouse per group b). Statistical analysis was performed using a 2x2 factorial ANOVA test followed by a simple main effect analysis, as the interaction was significant between variables. Data presented as mean± SEM. **LBWm-NF** n=11; **LBWm-HF** n=13; **HBWm-NF** n=9, **HBWm-HF** n=13. * p≤0.05, ** p≤0.01.

After assessing adipocyte number in both gonadal and subcutaneous adipose tissue, an analysis of the relative frequency of adipocyte size distribution (%) was performed in order to see whether there was any difference in size between groups.

There was a general bimodal distribution (two separated populations) of adipocytes in all groups when assessing both adipose tissues (figure 4.7.1.1.3). The nadir, which is the lowest point in frequency, (i.e. where the curve between two populations was flat, the midpoint was designated the nadir) was used as the cut point between two cell populations, small and large adipocytes. The percentages of adipocytes below the nadir were designated as “small adipocytes” and above the nadir as the “large adipocytes”.

There was a significant main effect of birth weight on the amount of small adipocytes in gonadal fat, with **LBWm** mice having a higher number of small adipocytes compared to **HBWm** mice ($F(1,39)=7.312$ **p=0.01**; figure 4.9.3 and table 4.9.1). The main effect of birth weight in large adipocytes was **HBWm** mice having larger adipocytes than **LBWm** mice ($F(1,40)=6.074$ **p=0.018**; figure 4.9.3 and table 4.9.1).

The small to large adipocytes ratio confirmed the results above, as it was significantly affected by birth weight, with the **LBWm** mice having a higher ratio compared to **HBWm** mice ($F(1,39)=11.48$ **p=0.002**; table 4.9.1).

The peak diameter of large adipocytes, defined as the mean diameter at which frequency of the large adipocytes reached a maximum, was shifted to the right in **HBWm-HF** mice compared to **HBWm-NF** mice (**p=0.001**; figure 4.9.3b and table 4.9.1). However, a comparable difference was seen between **LBWm** mice (p=0.479; figure 4.9.3a and table 4.9.1). There were not significant differences between mice fed a **NF** diet (p=0.078) or mice fed a **HF** diet (p=0.169; figure 4.9.3c-d and table 4.9.1).

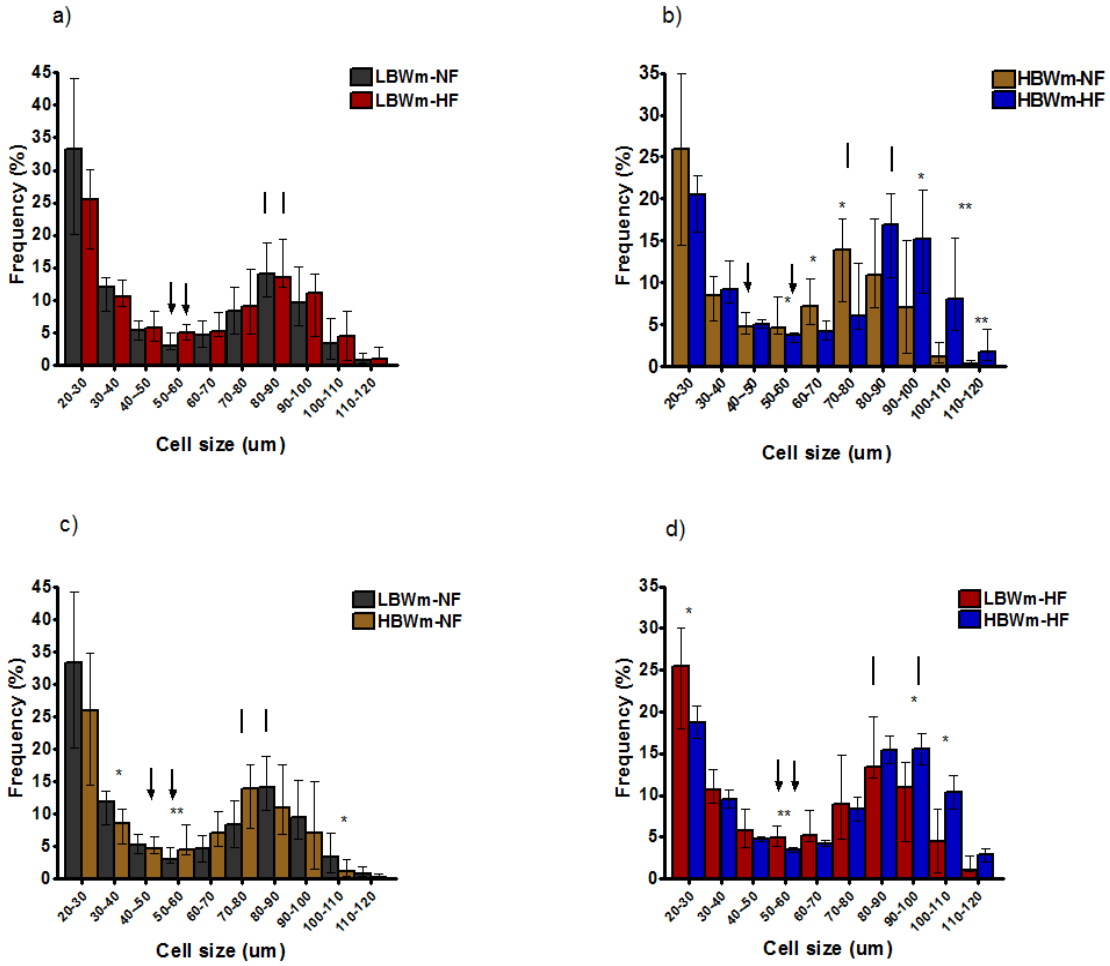

Figure 4.9.3 Frequency distribution (%) of adipocytes extracted from gonadal adipose tissue from male mice at 15 weeks. Arrowheads indicate the nadir of each group, which corresponds to the lowest point between two populations of adipocytes (small-large adipocytes). Headless arrows indicate the peak diameter of large cells in each group. Statistical analysis was performed using a *Kruskal-Wallis* test followed by a Mann-Whitney test for range analysis. Data presented as median with interquartile range (25%-75%). **LBWm-NF** n=9-11; **LBWm-HF** n=13-14; **HBWm-NF** n=8-9, **HBWm-HF** n=13-14. * p≤0.05,**p≤0.01.

	LBWm-NF_1	LBWm-HF_2	HBWm-NF_3	HBWm-HF_4	P value
Nadir (um)	56.818 ±2.482	54.231 ±2.283	50 ±2.911	59.615 ±2.283	
Below nadir (small adipocytes) %	52.728 ±5.329	46.318 ±4.674	38.176 ±5.618	31.23 ±5.329	**Birth weight effect: p=0.01 Diet effect:** p=0.167 **Interaction:** p=0.936
Above nadir (large adipocytes) %	46.955 ±5.187	50.69 ±4.598	57.75 ±5.735	65.807 ±5.441	**Birth weight effect: p=0.018 Diet effect:** p=0.269 **Interaction:** p=0.683
Large peak (um)	85 ±2.246	87.143 ±1.991	78.75 ±2.634	91.154 ±2.066	**1 vs.2**=0.479 **3vs.4=0.001 1vs.3**=0.078 **2vs.4**=0.169
Small:large adipocytes ratio	1.632 ±0.252	1.105 ±0.202	0.603 0.267	0.502 ±0.239	**Birth weight effect: p=0.002 Diet effect:** p=0.201 **Interaction:** p=0.381

Table 4.9.1 Frequency distribution (%) of adipocytes extracted from gonadal adipose tissue from male mice at 15 weeks. Nadir was the lowest point (cut off point) that separated two cell populations (small and large adipocytes). Statistical analysis was performed using a 2x2 factorial ANOVA. Interaction was significant for the analysis of large peak ($F(1,42)=5.208$ **p=0.02**), and therefore a simple main effect analysis was performed. Data presented as mean±SEM. **LBWm-NF** n=9-11; **LBWm-HF** n=13-14; **HBWm-NF** n=8-9, **HBWm-HF** n=13-14. * p≤0.05,**p≤0.01.

There was a general bimodal distribution on subcutaneous adipose cells as in gonadal adipose cells (figure 4.9.4). There was not a significant difference in small or large adipocytes percentages, or in their ratio (table 4.9.2). However, when assessing the distribution of cells by range, there was a significant shift towards the right in the **HBWm-HF** group in respect to **HBWm-NF** group, with a higher frequency of adipocytes between 80-120μm (figure 4.9.4b). The difference between mice fed a **HF** diet was significant between 90-110 μm with a higher frequency of adipocytes in the **HBWm-HF** group in respect to **LBWm-HF** group (figure 4.9.4d). There was a significant higher percentage of adipocytes between 90-100μm in **LBWm-NF** mice compared to **HBWm-NF** mice (figure 4.9.4a); but a comparable difference between **LBWm** mice was seen (4.9.4c).

Differences in the peak diameter of large adipocytes showed the same right shift of the **HBWm-HF** group when compared to **HBWm-NF** (**p<0.001**; figure 4.9.4b and table 4.9.2) and to **LBWm- HF** groups (**p<0.001**; figure 4.9.4d ant table 4.9.2). However, the peak diameter of large adipocytes was not significantly different between mice fed a **NF** diet (p=0.155; figure 4.9.4c and table 4.9.2) or between **LBWm** mice (p=0.787; figure 4.9.4 and table 4.9.2).

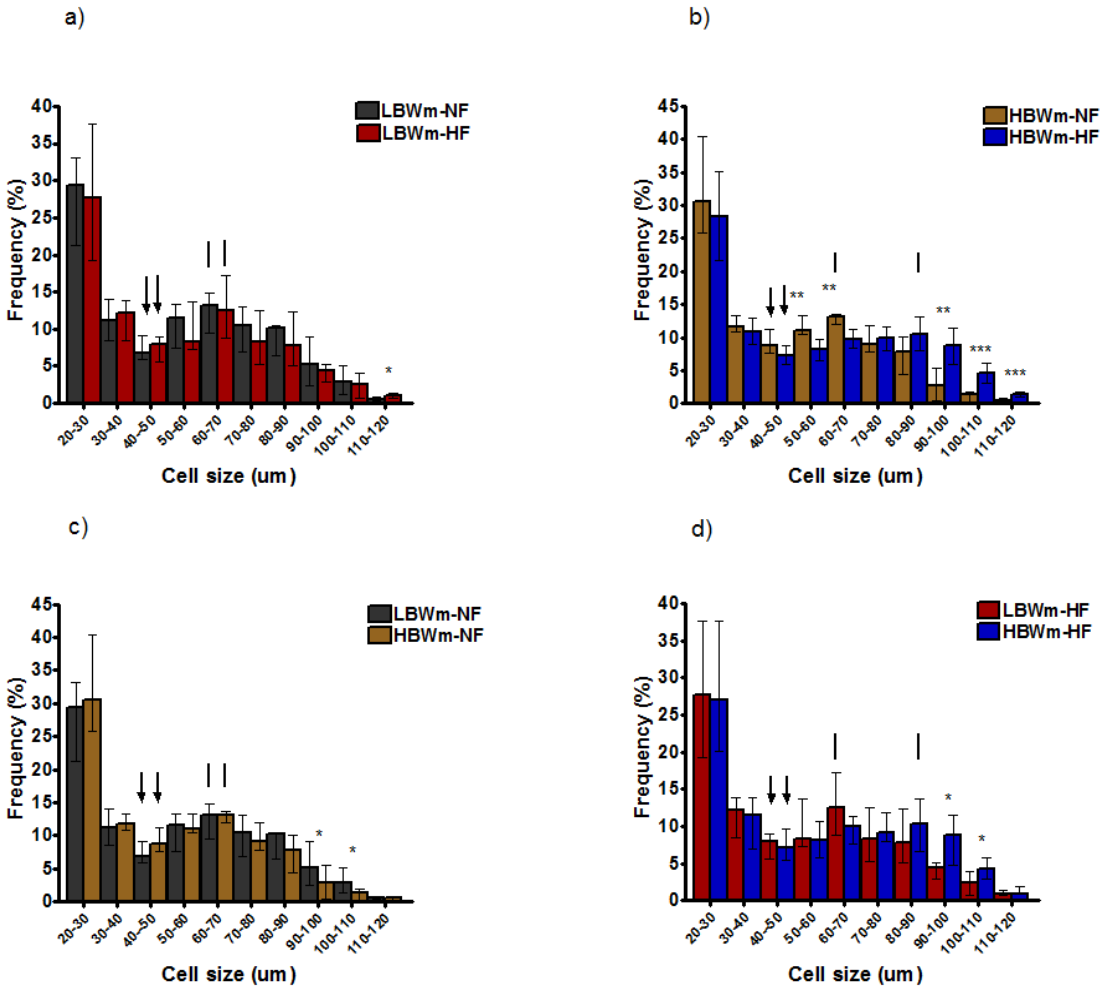

Figure 4.9.4 Frequency distribution (%) of adipocytes extracted from subcutaneous adipose tissue from male mice at 15 weeks. Arrowheads indicate the nadir of each group, which corresponds to the lowest point between two populations of cells (small-large adipocytes). Headless arrows indicate the peak diameter of large adipocytes in each group. Statistical analysis was performed using a *Kruskal-Wallis* test followed by a Mann-Whitney test for range analysis. Data presented as median with interquartile range (25%-75%). **LBWm-NF** n=9-11; **LBWm-HF** n=13-14; **HBWm-NF** n=8-9, **HBWm-HF** n=13-14. * p≤0.05,**p≤0.01.

	LBWm-NF_1	LBWm-HF_2	HBWm-NF_3	HBWm-HF_4	P value
Nadir (um)	45 ±1.85	48.571 ±1.483	44.091 ±1.673	50.714 ±1.483	
Below nadir (small adipocytes) %	41.873 ±4.821	44.498 ±4.273	41.497 ±5.33	44.156 ±4.273	**Birth weight effect:** p=0.939 **Diet effect:** p=0.576 **Interaction:** p=0.997
Above nadir (large adipocytes) %	51.08 ±4.945	51.75 ±4.195	45.698 ±4.56	49.054 ±4.042	**Birth weight effect:** p=0.618 **Diet effect:** p=0.945 **Interaction:** p=0.519
Large peak (um)	68 ±2.412	67.143 ±2.038	63.182 ±2.299	80.833 ±2.202	**1 vs.2**=0.787 **3vs.4<0.001** **1vs.3=**0.155 **2vs.4<0.001**
Small:large adipocytes ratio	0.771 ±0.953	0.985 ±0.18	0.837 ±0.216	1.058 ±0.18	**Birth weight effect:** p=0.722 **Diet effect:** p=0.273 **Interaction:** p=0.986

Table 4.9.2 Frequency distribution (%) of adipocytes extracted from subcutaneous adipose tissue from male mice at 15 weeks. Nadir was the lowest point (cut off point) that separated two adipocyte populations (small and large adipocytes). Statistical analysis was performed using a 2x2 factorial ANOVA. Interaction was significant for the analysis of large peak ($F(1,44)=57.1$ **p=0.011**), and therefore a simple main effect analysis was performed. Data presented as mean± SEM. **LBWm-NF** n=9-11; **LBWm-HF** n=13-14; **HBWm-NF** n=8-9, **HBWm-HF** n=13-14.

* p≤0.05,**p≤0.01.

Comparison of gonadal and subcutaneous adipocytes distribution within groups showed that **LBWm** mice gonadal adipocytes had a shift to the right (larger adipocytes) in respect to subcutaneous adipocytes with a significance difference between peaks of the large adipocytes (**LBWm-NF**: **p=0.001**; **LBWm-HF**: **p<0.001**; figure 4.9.5a-b and tables 4.9.1 and 4.9.2). Although the shift was less evident in **HBWm** mice (as seen in the figure below), it was however significantly different with a higher peak of large adipocytes in gonadal adipocytes than subcutaneous adipose cells (**HBWm-NF**: **p<0.001**; **HBWm-HF**: **p=0.002**; figure 4.9.5c-d and tables 4.9.1 and 4.9.2).

Small adipocytes were significantly higher in subcutaneous adipose tissue compared to gonadal fat of **HBWm-HF** mice (**p=0.037**; figure 4.9.5d and tables 4.9.1 and 4.9.2). However, comparable differences were seen within others groups. Furthermore, the large adipocytes were significantly higher in gonadal than subcutaneous tissue of **HBWm-HF** mice (**p=0.018**; figure 4.9.5d and tables 4.9.1 and 4.9.2).

The small to large adipocytes ratio was significantly higher from gonadal tissue of **LBWm-NF** mice (**p=0.031**; figure 4.9.5a and tables 4.9.1 and 4.9.2). Significant difference was also seen in the ratio of **HBWm-HF** mice, but with an opposite trend: the highest ratio was seen in subcutaneous adipose tissue rather than gonadal. There were not significant differences within others groups.

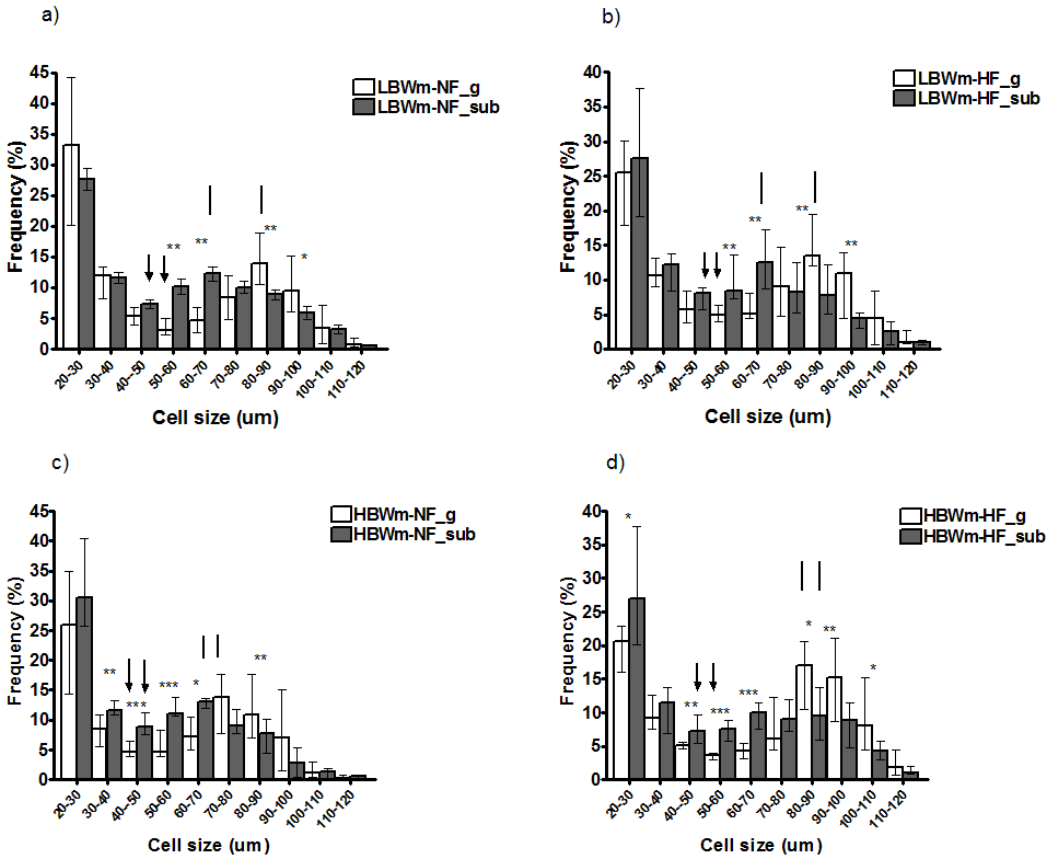

Figure 4.9.5 Frequency distribution (%) of adipocytes extracted from gonadal and subcutaneous adipose tissue from male mice at 15 weeks. Arrowheads indicate the nadir of each group, which corresponds to the lowest point between two populations of adipocytes (small-large adipocytes). Headless arrows indicate the peak diameter of large adipcoytes in each group. g= gonadal fat tissue, sub=subcutaneous adipose tissue. Statistical analysis was performed using a *Kruskal-Wallis* test followed by a Mann-Whitney test for range analysis. Data presented as median with interquartile range (25%-75%). **LBWm-NF** n=9-11; **LBWm-HF** n=13-14; **HBWm-NF** n=8-9, **HBWm-HF** n=13-14. * p≤0.05,**p≤0.01.

4.10 The Effects of Birth Weight and Diet on Hypothalamic Activation in Young Mice at Week 15

Neural activity in specific hypothalamic appetite centres was measured by using Manganese Enhancement (MEMRI), as described in section 2.4.2. Neural activity was analysed by measuring changes in Signal Intensities (SI), which were normalised and presented as normalised percentage enhancement (NPE). NPE were analysed in four hypothalamic centres: arcuate nucleus (ARC), paraventricular nucleus (PVN), ventromedial hypothalamus (VMH) and periventricular nucleus (Pe).

4.10.1 Hypothalamic activity in Males

Figures 4.10.1 and 4.10.2 showed the neural activity (NPE) within the ARC nucleus. Activity did not show a similar pattern between mice within the same birth weight category or fed the same diet. This suggested a possible dependency of activity on both factors. **LBWm-HF** had a significantly lower activity than **LBWm-NF** (**p=0.002**; figures 4.10.1.1 and 4.10.1.2a). However, the pattern was different between **HBWm** mice, with a higher neural activity in **HBWm-HF** mice compared to **HBWm-NF** mice, but the difference was not significantly different (p=0.11; figures 4.10.1.1 and 4.10.1.2b). Furthermore, there was a significant difference between mice fed a **HF** diet, with a higher activity in **HBWm-HF** mice compared to **LBWm-HF** mice (**p<0.001**; figures 4.10.1.1 and 4.10.1.2d). Comparable difference was seen between mice fed a **NF** diet (p=0.44; figures 4.10.1.1 and 4.10.1.2c).

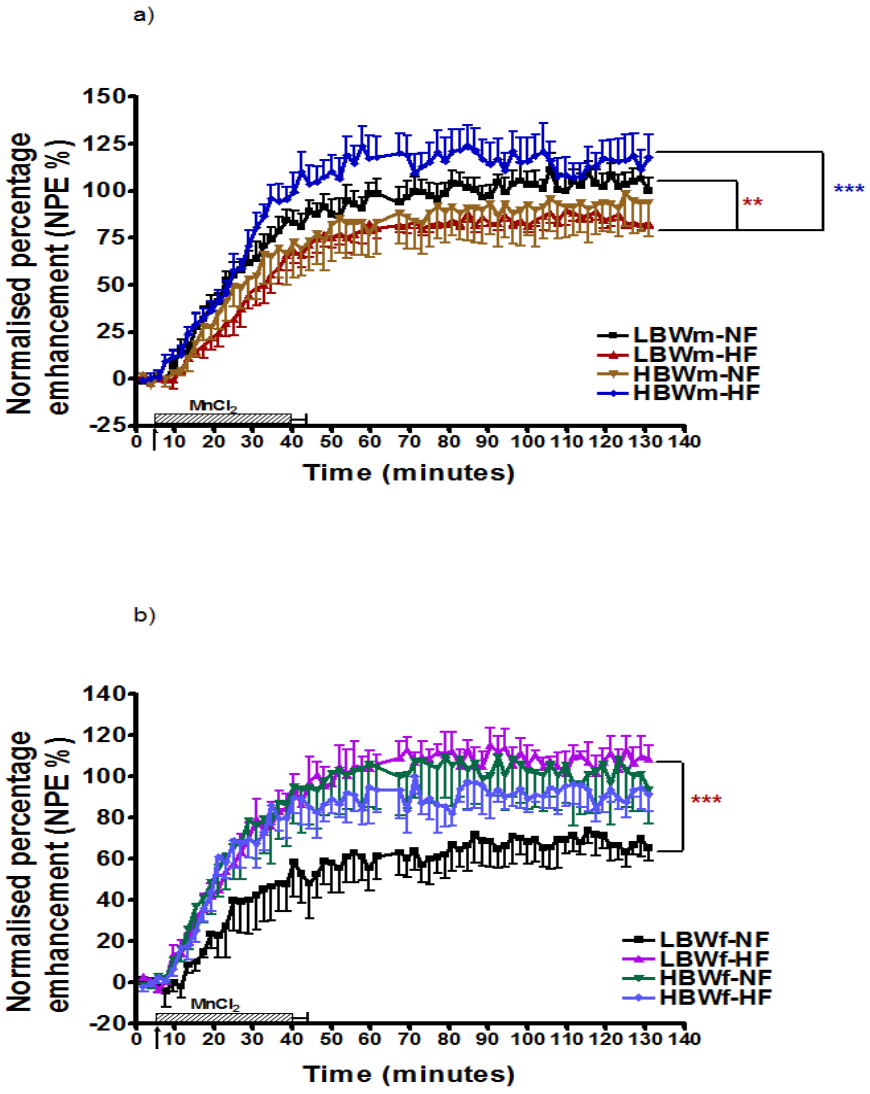

Figure 4.10.1.1 Neural activity measured within the hypothalamic ARC nucleus in male and female offspring at 15 weeks. Neural activity was analysed by measuring time course changes in SIs and presented as normalised percentage enhancement (NPE %) from the ARC nucleus within the hypothalamus. The arrow indicates the start of intravenous (i.v.) $MnCl_2$ infusion and the hatched bars indicate the duration of the i.v. infusion. Figure a) corresponds to males and figure b) to females. Statistical analysis was performed using a general estimated equation (GEE) test. Data presented as mean±SEM. **LBWm-NF** n=5; **LBWm-HF** n=5; **HBWm-NF** n=5, **HBWm-HF** n=5; **LBWf-NF** n=4; **LBWf-HF** n=3; **HBWf-NF** n=4, **HBWf-HF** n=3.

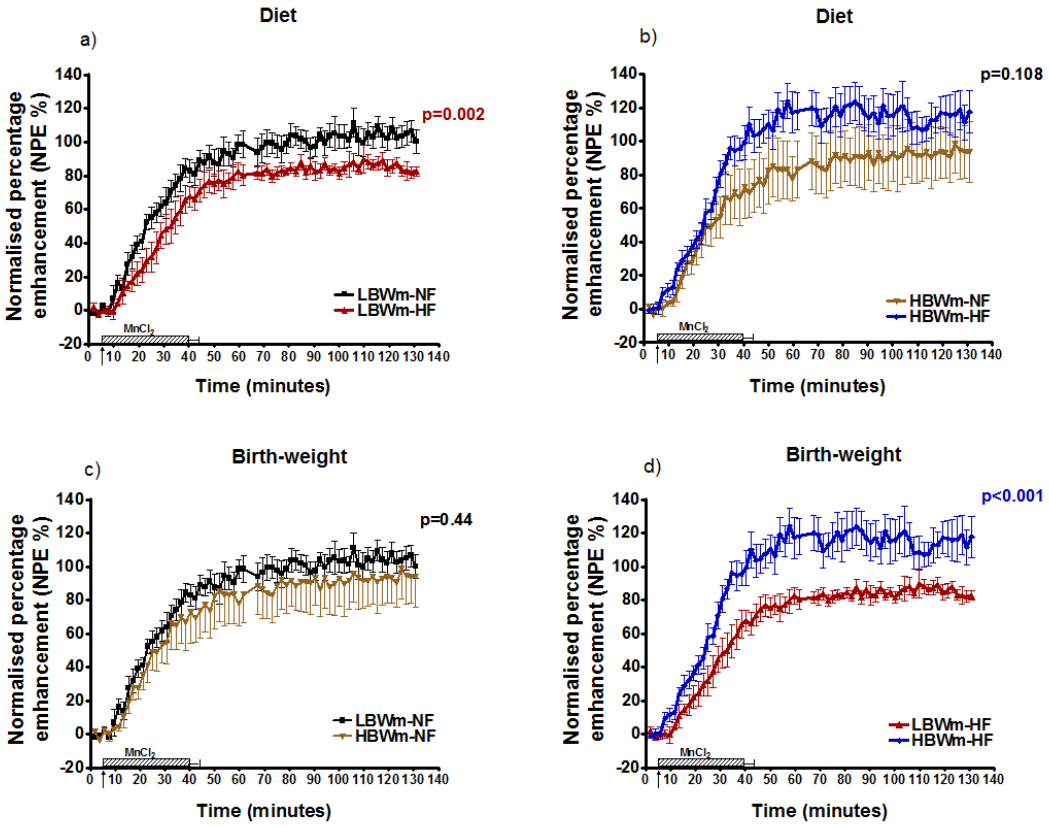

Figure 4.10.1.2 Neural activity measured within the hypothalamic ARC nucleus in male offspring at 15 weeks. Neural activity was analysed by measuring time course changes in SIs and presented as normalised percentage enhancement (NPE %) from the ARC nucleus within the hypothalamus. Figures a) and b) show the time course activity by diets (**NF-HF** respectively) in mice within the same birth weight category. Figure c) and d) show the time course activity by birth weight (**LBWm-HBWm** respectively) in mice within the same diet category. The arrow indicates the start of intravenous (i.v.) $MnCl_2$ infusion and the hatched bars indicate the duration of the i.v. infusion. Statistical analysis was performed using a general estimated equation (GEE) test. Data presented as mean± SEM. **LBWm-NF** n=5; **LBWm-HF** n=5; **HBWm-NF** n=5, **HBWm-HF** n=5.

Neural activity within the PVN, VMH and Pe nuclei showed, as in the ARC nucleus, a possible dependency of activity on the different levels of each factor.

In the PVN nucleus, **LBWm-NF** has a significantly higher activity than both, **LBWm-HF** mice (**p<0.001**; figures 4.10.1.3 and 4.10.1.4a) and **HBWm-NF** mice; figures 4.10.1.3 and 4.10.1.4c). Similarly, **HBWm-HF** had a higher activity than **HBWm-NF** mice (**p=0.03**; figures 4.10.1.3 and 4.10.1.4b), and **LBWm-HF** mice (**p<0.001**; figures 4.10.1.3 and 4.10.1.4d).

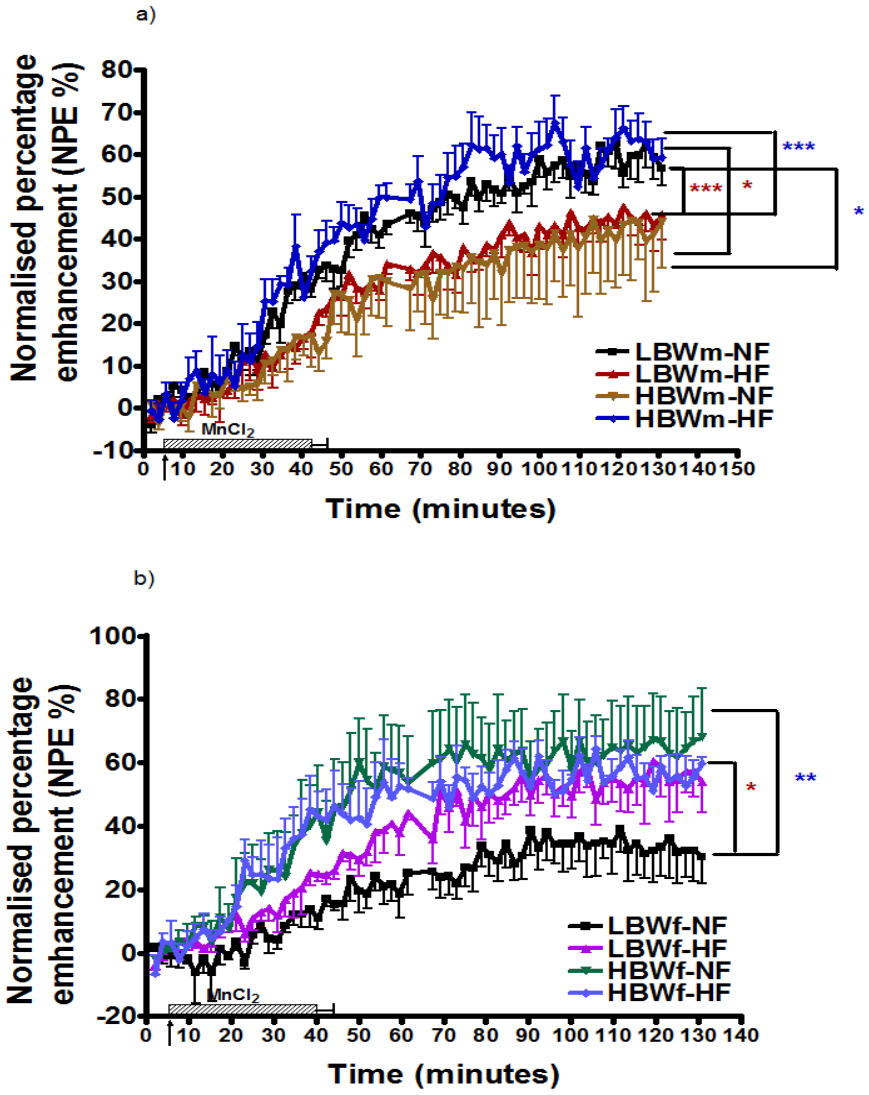

Figure 4.10.1.3 Neural activity measured within the hypothalamic PVN nucleus in male and female offspring at 15 weeks. Neural activity was analysed by measuring time course changes in SIs and presented as normalised percentage enhancement (NPE %) from the PVN nucleus within the hypothalamus. The arrow indicates the start of intravenous (i.v.) $MnCl_2$ infusion and the hatched bars indicate the duration of the i.v. infusion. Figure a) corresponds to males and figure b) to females. Statistical analysis was performed using a general estimated equation (GEE) test. Data presented as mean± SEM. **LBWm-NF** n=5; **LBWm-HF** n=5; **HBWm-NF** n=5, **HBWm-HF** n=5; **LBWf-NF** n=4; **LBWf-HF** n=3; **HBWf-NF** n=4, **HBWf-HF** n=3.

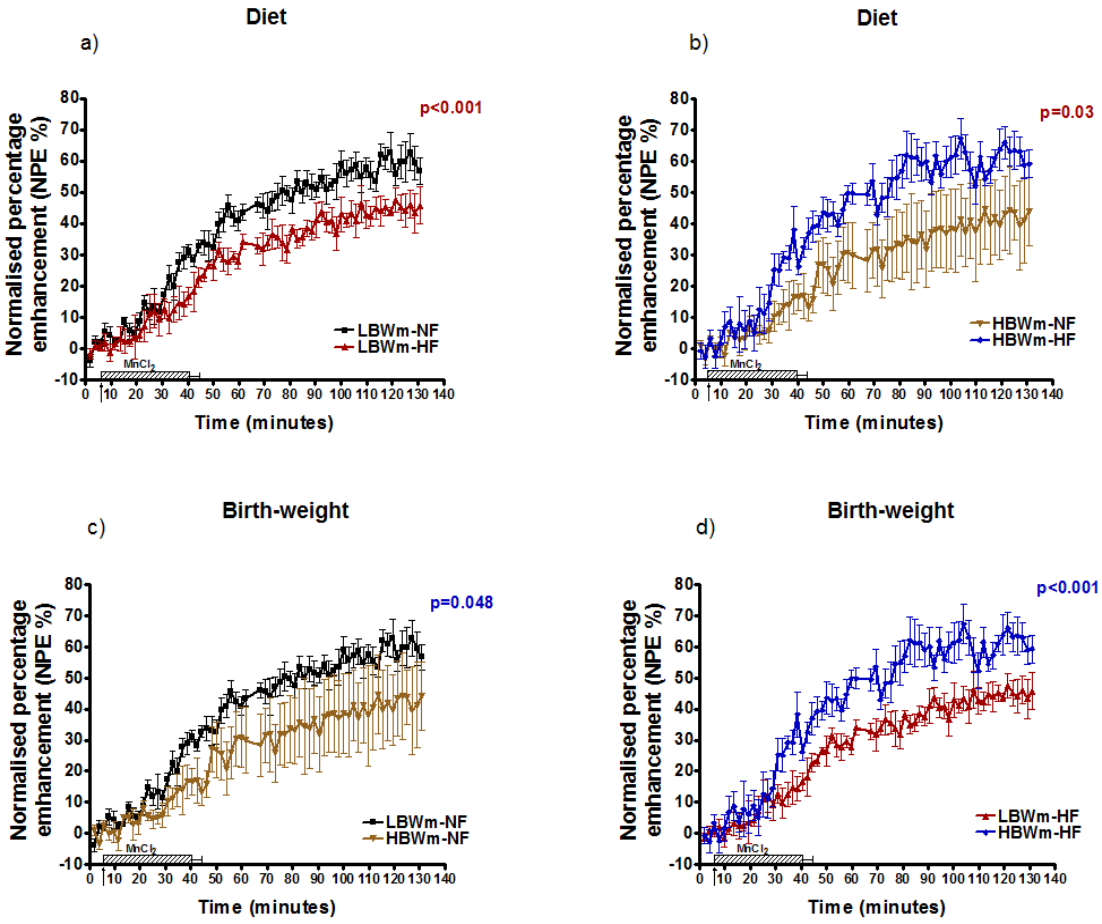

Figure 4.10.1.4 Neural activity measured within the hypothalamic PVN nucleus in male offspring at 15 weeks. Neural activity was analysed by measuring time course changes in SIs and presented as normalised percentage enhancement (NPE %) from the PVN nucleus within the hypothalamus. Figures a) and b) show the time course activity by diets (**NF-HF** respectively) in mice within the same birth weight category. Figure c) and d) show the time course activity by birth weight (**LBWm-HBWm** respectively) in mice within the same diet category. The arrow indicates the start of intravenous (i.v.) $MnCl_2$ infusion and the hatched bars indicate the duration of the i.v. infusion. Statistical analysis was performed using a general estimated equation (GEE) test. Data presented as mean± SEM. **LBWm-NF** n=5; **LBWm-HF** n=5; **HBWm-NF** n=5, **HBWm-HF** n=5.

In the VMH nucleus, **LBWm-NF** and **HBWm-HF** maintained a significantly higher activity and pattern compared to their counterparts as in the PVN (figures 4.10.1.5 and 4.10.1.6). **LBWm-NF** and **HBWm-HF** mice had a significantly higher NPE than **LBWm-HF** mice.

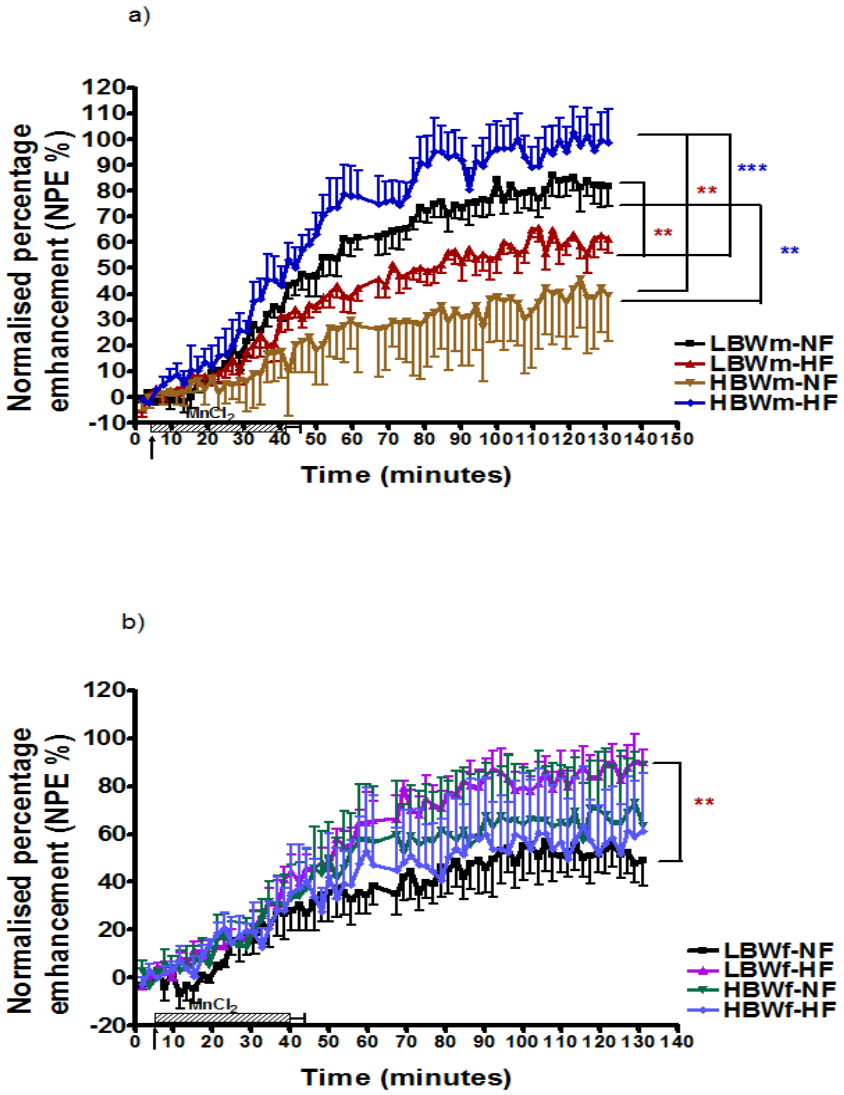

Figure 4.10.1.5 Neural activity measured within the hypothalamic VMH nucleus in male and female offspring at 15 weeks. Neural activity was analysed by measuring time course changes in SIs and presented as normalised percentage enhancement (NPE %) from the VMH nucleus within the hypothalamus. The arrow indicates the start of intravenous (i.v.) $MnCl_2$ infusion and the hatched bars indicate the duration of the i.v. infusion. Figure a) corresponds to males and figure b) to females. Statistical analysis was performed using a general estimated equation (GEE) test. Data presented as mean± SEM. **LBWm-NF** n=5; **LBWm-HF** n=5; **HBWm-NF** n=5, **HBWm-HF** n=5; **LBWf-NF** n=4; **LBWf-HF** n=3; **HBWf-NF** n=4, **HBWf-HF** n=3.

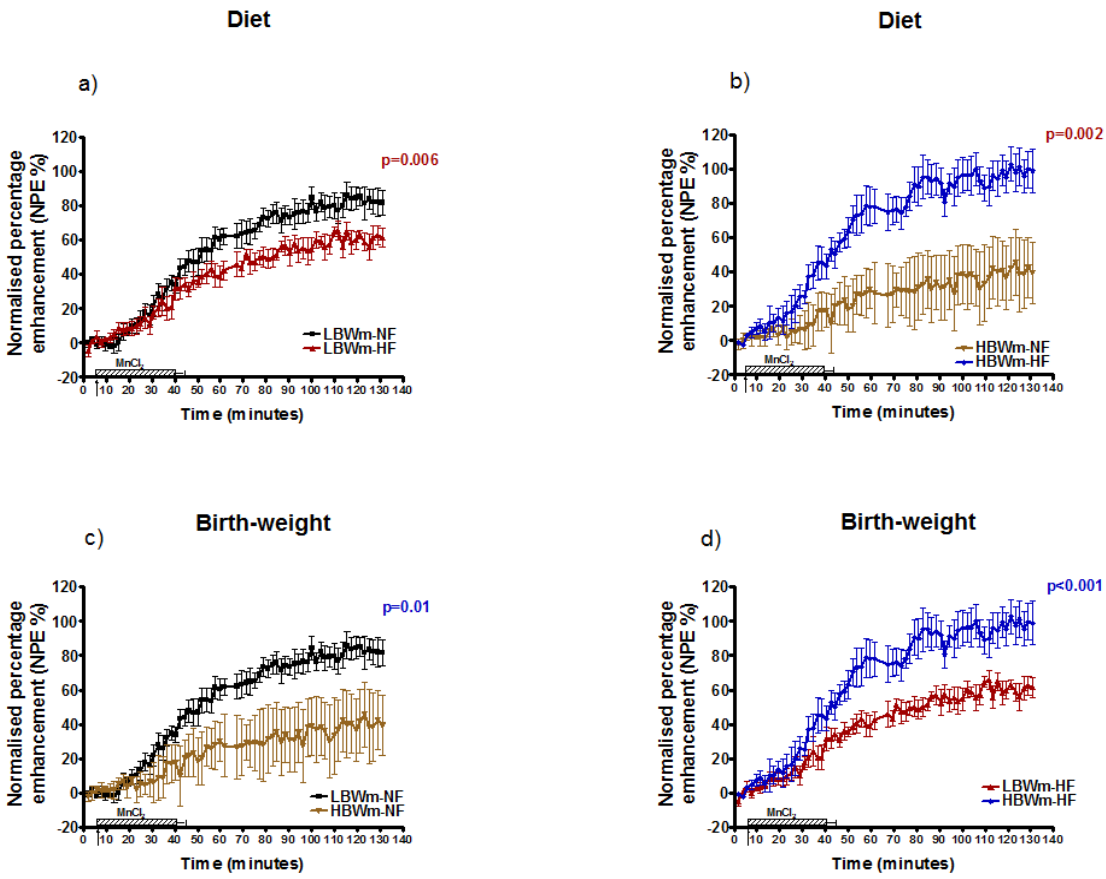

Figure 4.10.1.6 Neural activity measured within the hypothalamic VMH nucleus in male offspring at 15 weeks. Neural activity was analysed by measuring time course changes in SIs and presented as normalised percentage enhancement (NPE %) from the VMH nucleus within the hypothalamus. Figures a) and b) show the time course activity by diets (**NF-HF** respectively) in mice within the same birth weight category. Figure c) and d) show the time course activity by birth weight (**LBWm-HBWm** respectively) in mice within the same diet category. The arrow indicates the start of intravenous (i.v.) $MnCl_2$ infusion and the hatched bars indicate the duration of the i.v. infusion. Statistical analysis was performed using a general estimated equation (GEE) test. Data presented as mean± SEM. **LBWm-NF** n=5; **LBWm-HF** n=5; **HBWm-NF** n=5, **HBWm-HF** n=5.

In the Pe nucleus, male groups showed significant differences between **LBWm** mice with the highest activity in **LBWm-NF** mice (**p<0.001**; figures 4.10.1.7 and 4.10.1.8a) and mice fed a **HF** with **HBWm-HF** having a higher NPE than **LBWm-HF** mice (**p<0.001**; figure 4.10.1.7 and 4.10.1.8b), but no between mice fed a **NF** diet (p=0.14; figures 4.10.1.7 and 4.10.1.8c). The difference between **HBWm** mice was marginally significant (p=0.08; figures 4.10.1.7 and 4.10.1.8b).

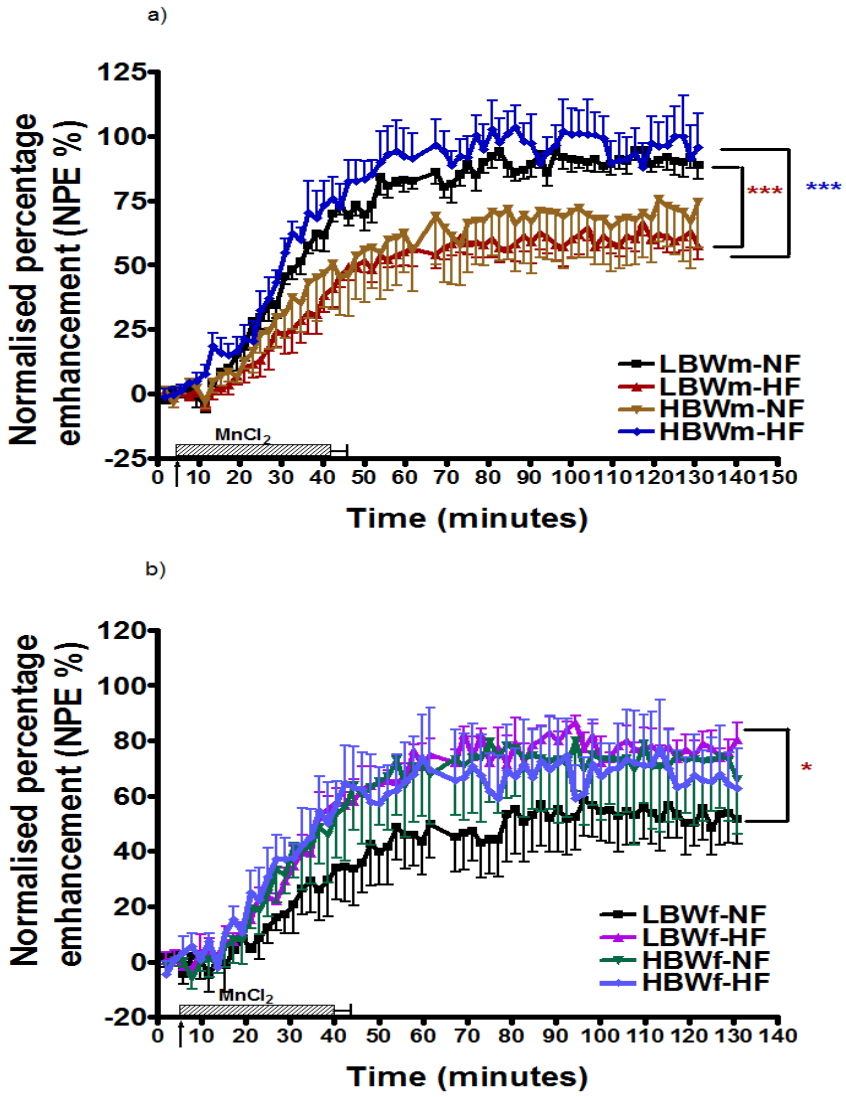

Figure 4.10.1.7 Neural activity measured within the hypothalamic Pe nucleus in male and female offspring at 15 weeks. Neural activity was analysed by measuring time course changes in SIs and presented as normalised percentage enhancement (NPE %) from the Pe nucleus within the hypothalamus. The arrow indicates the start of intravenous (i.v.) $MnCl_2$ infusion and the hatched bars indicate the duration of the i.v. infusion. Figure a) corresponds to males and figure b) to females. Statistical analysis was performed using a general estimated equation (GEE) test. Data presented as mean± SEM. **LBWm-NF** n=5; **LBWm-HF** n=5; **HBWm-NF** n=5, **HBWm-HF** n=5; **LBWf-NF** n=4; **LBWf-HF** n=3; **HBWf-NF** n=4, **HBWf-HF** n=3.

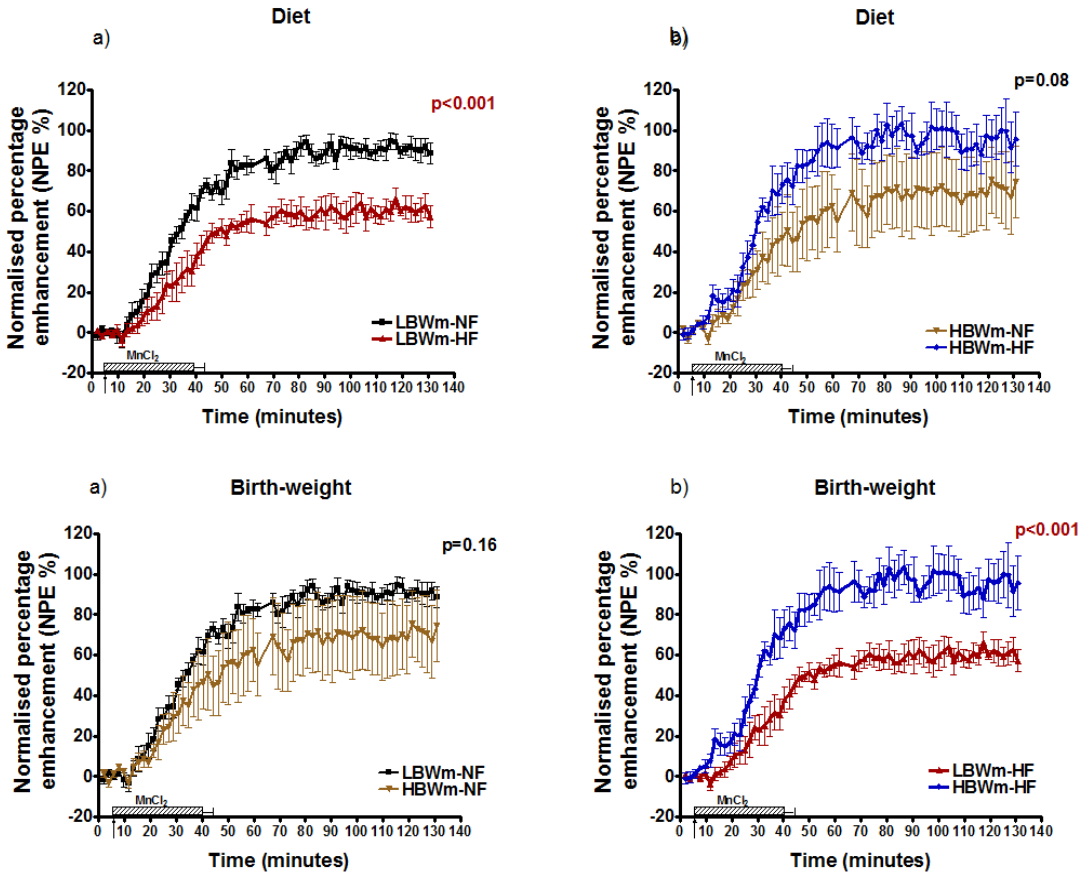

Figure 4.10.1.8 Neural activity measured within the hypothalamic Pe nucleus in male offspring at 15 weeks. Neural activity was analysed by measuring time course changes in SIs and presented as normalised percentage enhancement (NPE %) from the Pe nucleus within the hypothalamus. Figures a) and b) show the time course activity by diets (**NF-HF** respectively) in mice within the same birth weight category. Figure c) and d) show the time course activity by birth weight (**LBWm-HBWm** respectively) in mice within the same diet category. The arrow indicates the start of intravenous (i.v.) $MnCl_2$ infusion and the hatched bars indicate the duration of the i.v. infusion. Statistical analysis was performed using a general estimated equation (GEE) test. Data presented as mean± SEM. **LBWm-NF** n=5; **LBWm-HF** n=5; **HBWm-NF** n=5, **HBWm-HF** n=5.

4.10.2 Hypothalamic activity in Females

As in males, regional hypothalamic activation was different between depending on both birth weight and diet, but it did not seem to have independent factor effects. However, the patterns seen in female groups in all nuclei were contrary to the ones seen in their male counterparts.

In the ARC nucleus, there was a significant difference between **LBWf** mice, with **LBWf-HF** having a higher NPE (activity) than **LBWf-NF** mice (**p<0.001**; figures 4.10.2.1 and 4.10.2.2a), whilst the opposite was observed between their male counterparts (figures 4.10.1.1 and 4.10.1.2a). **HBWf-HF** mice had a lower activity than **HBWm-NF** mice but the difference did not reach significance (p=0.69; figures 4.10.2.1 and 4.10.2.2b). Furthermore, **LBWf-NF** mice had a significantly lower activity when compared to **HBWf-NF** mice (**p=0.03**; figures 410.2.1 and 4.10.2.2c), which was also contrary to the pattern seen in their male counterparts (figures 4.10.1.1 and 4.10.1.2c). **LBWf-HF** had a higher activity than **HBWf-HF** mice but the difference was not significant (p=0.19; figures 4.10.2.1 and 4.10.2.2d), whilst the pattern in males was opposite and significant (figures 4.10.1.1 and 4.10.1.2d).

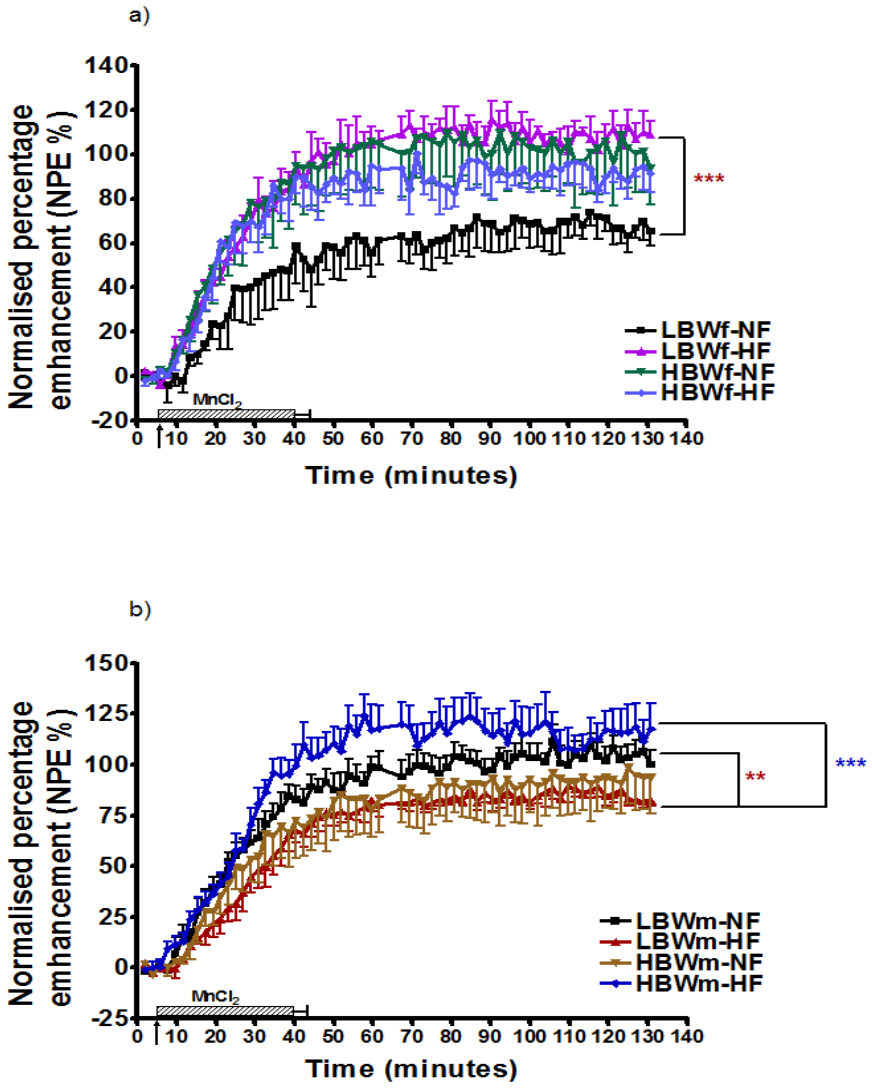

Figure 4.10.2.1 Neural activity measured within the hypothalamic ARC nucleus in female and male offspring at 15 weeks. Neural activity was analysed by measuring time course changes in SIs and presented as normalised percentage enhancement (NPE %) from the ARC nucleus within the hypothalamus. The arrow indicates the start of intravenous (i.v.) $MnCl_2$ infusion and the hatched bars indicate the duration of the i.v. infusion. Figure a) corresponds to females and figure b) to males. Statistical analysis was performed using a general estimated equation (GEE) test. Data presented as mean± SEM. **LBWf-NF** n=4; **LBWf-HF** n=3; **HBWf-NF** n=4, **HBWf-HF** n=3; **LBWm-NF** n=5; **LBWm-HF** n=5; **HBWm-NF** n=5, **HBWm-HF** n=5.

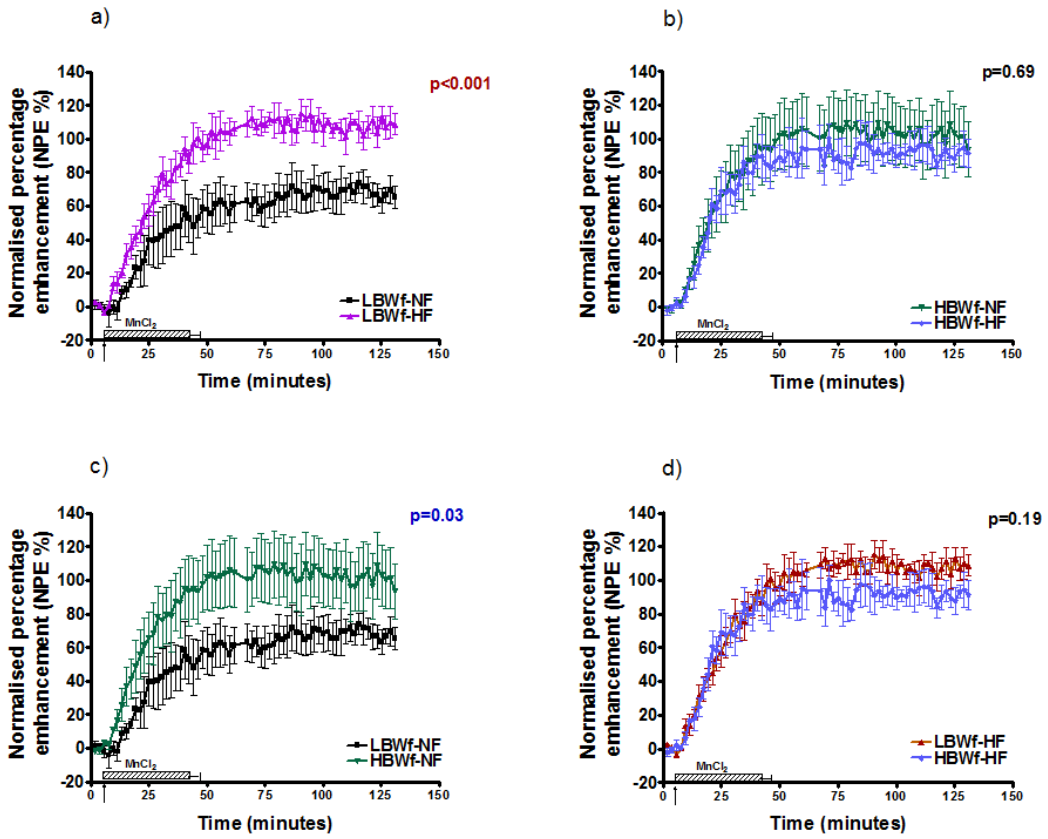

Figure 4.10.2.2 Neural activity measured within the hypothalamic ARC nucleus in female offspring at 15 weeks. Neural activity was analysed by measuring time course changes in SIs and presented as normalised percentage enhancement (NPE %) from the ARC nucleus within the hypothalamus. Figures a) and b) show the time course activity by diets (**NF-HF** respectively) in mice within the same birth weight category. Figure c) and d) show the time course activity by birth weight (**LBWm-HBWm** respectively) in mice within the same diet category. The arrow indicates the start of intravenous (i.v.) $MnCl_2$ infusion and the hatched bars indicate the duration of the i.v. infusion. Statistical analysis was performed using a general estimated equation (GEE) test. Data presented as mean± SEM. **LBWf-NF** n=4; **LBWf-HF** n=3; **HBWf-NF** n=4, **HBWf-HF** n=3.

Similarly, the activity in the PVN was significantly higher in **LBWf-HF** mice compared to **LBWf-NF** (**p=0.02**; figures 4.10.2.3 and 4.10.2.4a), and in **HBWf-NF** mice in respect to **LBWf-NF** mice. However, the difference was not significantly different between **HBWf** mice as in the ARC nucleus (p=0.69; figures 4.10.2.3 and 4.10.2.4b). Male mice had again an opposite activity in respect to female groups (figures 4.10.1.3 and 4.10.1.4).

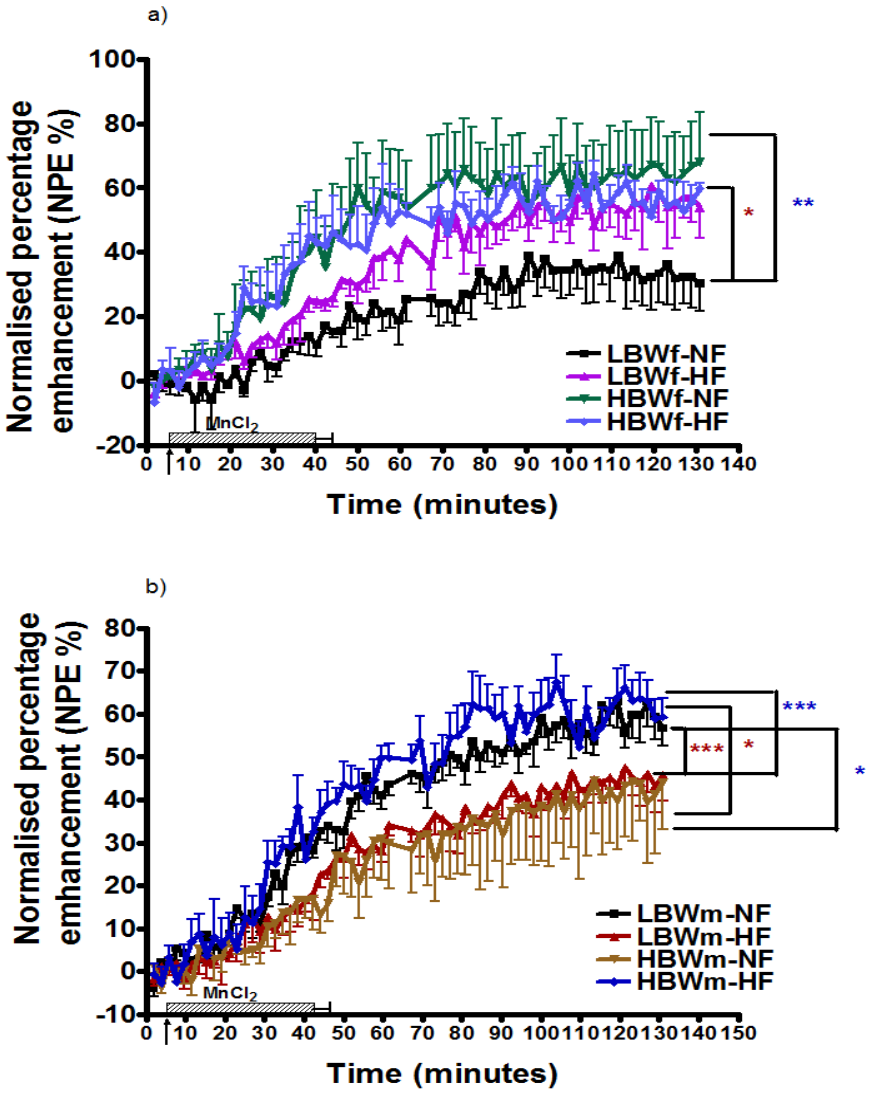

Figure 4.10.2.3 Neural activity measured within the hypothalamic PVN nucleus in female and male offspring at 15 weeks. Neural activity was analysed by measuring time course changes in SIs and presented as normalised percentage enhancement (NPE %) from the PVN nucleus within the hypothalamus. The arrow indicates the start of intravenous (i.v.) $MnCl_2$ infusion and the hatched bars indicate the duration of the i.v. infusion. Figure a) corresponds to females and figure b) to males. Statistical analysis was performed using a general estimated equation (GEE) test. Data presented as mean± SEM. **LBWf-NF** n=4; **LBWf-HF** n=3; **HBWf-NF** n=4, **HBWf-HF** n=3; **LBWm-NF** n=5; **LBWm-HF** n=5; **HBWm-NF** n=5, **HBWm-HF** n=5.

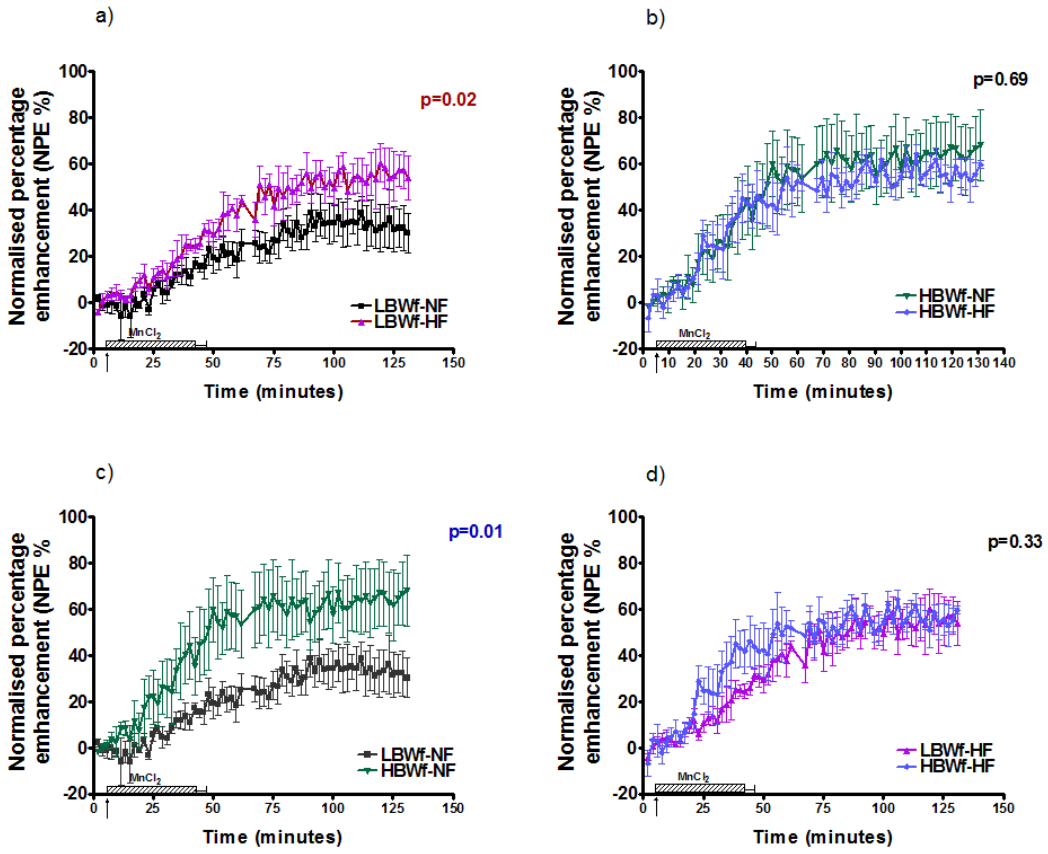

Figure 4.10.2.4 Neural activity measured within the hypothalamic PVN nucleus in female offspring at 15 weeks. Neural activity was analysed by measuring time course changes in SIs and presented as normalised percentage enhancement (NPE %) from the PVN nucleus within the hypothalamus. Figures a) and b) show the time course activity by diets (**NF-HF** respectively) in mice within the same birth weight category. Figure c) and d) show the time course activity by birth weight (**LBWm-HBWm** respectively) in mice within the same diet category. The arrow indicates the start of intravenous (i.v.) $MnCl_2$ infusion and the hatched bars indicate the duration of the i.v. infusion. Statistical analysis was performed using a general estimated equation (GEE) test. Data presented as mean± SEM. **LBWf-NF** n=4; **LBWf-HF** n=3; **HBWf-NF** n=4, **HBWf-HF** n=3.

In the VMH and Pe nuclei, the only significant difference seen was between **LBWf** mice, with the highest activity in **LBWf-HF** mice (**p=0.009** and **p=0.03** respectively; figures 4.10.2.5, 4.10.2.6a, 4.10.2.7 and 4.10.2.8a). However, **HBWf-NF** mice activity tended to be higher than in both **HBWf-HF** and **LBWf-NF** mice (VMH: p=0.77 and p=0.47 respectively; Pe: p=0.91 and 0.26 respectively; figures 4.10.2.5, 4.10.2.6b-c, 4.10.2.7 and 4.10.2.8b-c). Similarly, **LBWf-HF** tended to be higher than **HBWf-HF** mice (p=0.36; figures 4.10.2.5, 4.10.2.6d, 4.10.2.7 and 4.10.2.8d). Again, the patterns seen in male mice were different compared to their female counterparts (figures 4.10.1.5 and 4.10.1.6).

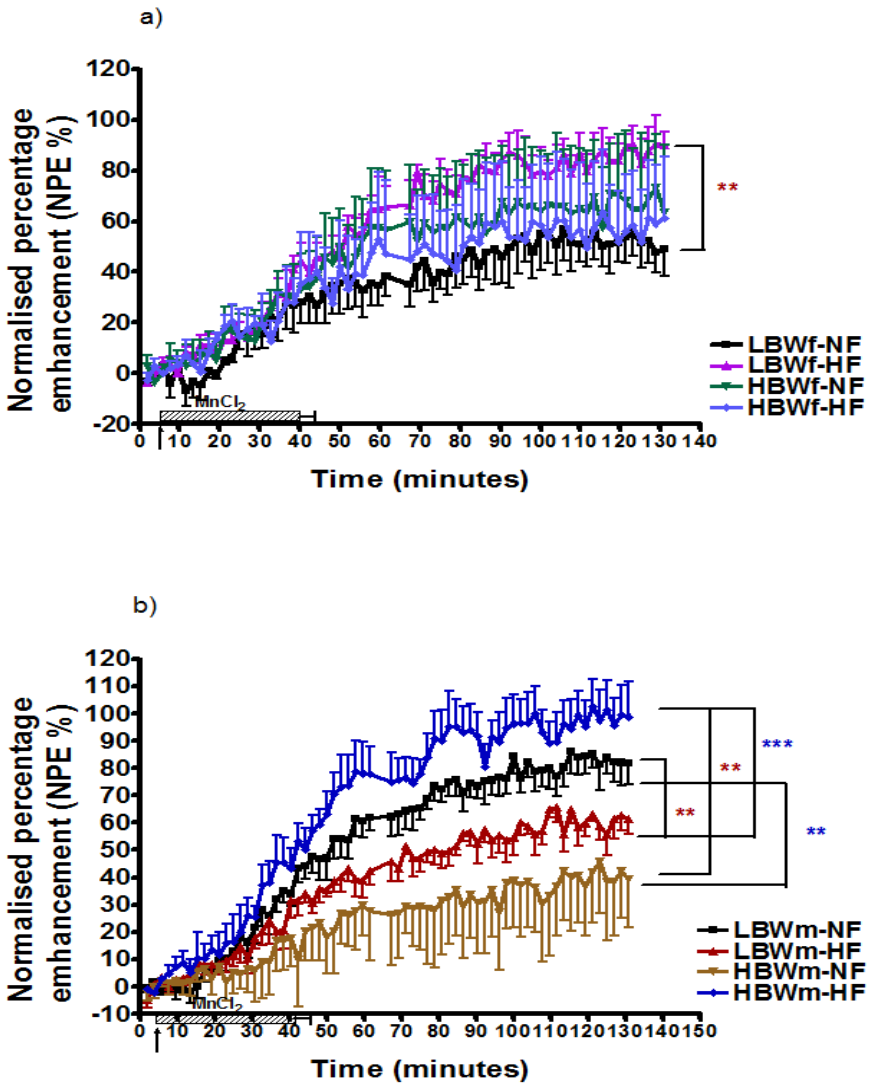

Figure 4.10.2.5 Neural activity measured within the hypothalamic VMH nucleus in female and male offspring at 15 weeks. Neural activity was analysed by measuring time course changes in SIs and presented as normalised percentage enhancement (NPE %) from the VMH nucleus within the hypothalamus. The arrow indicates the start of intravenous (i.v.) $MnCl_2$ infusion and the hatched bars indicate the duration of the i.v. infusion. Figure a) corresponds to females and figure b) to males. Statistical analysis was performed using a general estimated equation (GEE) test. Data presented as mean± SEM. **LBWf-NF** n=4; **LBWf-HF** n=3; **HBWf-NF** n=4, **HBWf-HF** n=3; **LBWm-NF** n=5; **LBWm-HF** n=5; **HBWm-NF** n=5, **HBWm-HF** n=5.

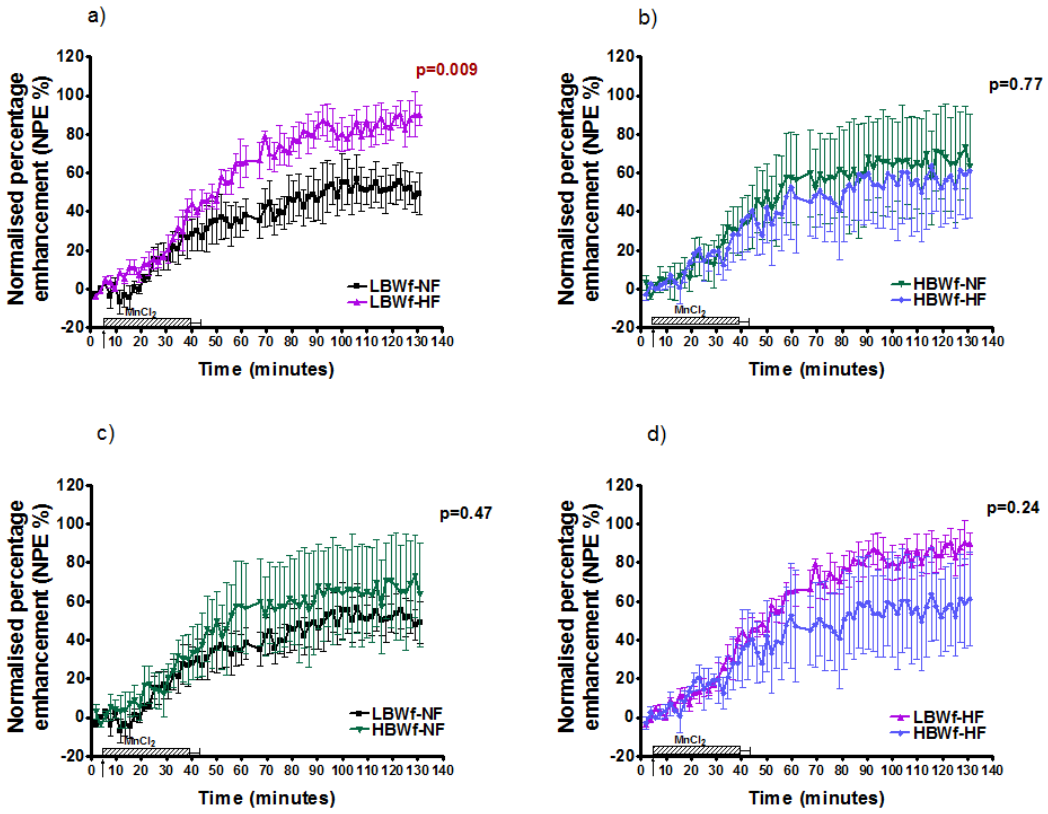

Figure 4.10.2.6 Neural activity measured within the hypothalamic VMH nucleus in female offspring at 15 weeks. Neural activity was analysed by measuring time course changes in SIs and presented as normalised percentage enhancement (NPE %) from the VMH nucleus within the hypothalamus. Figures a) and b) show the time course activity by diets (**NF-HF** respectively) in mice within the same birth weight category. Figure c) and d) show the time course activity by birth weight (**LBWm-HBWm** respectively) in mice within the same diet category. The arrow indicates the start of intravenous (i.v.) $MnCl_2$ infusion and the hatched bars indicate the duration of the i.v. infusion. Statistical analysis was performed using a general estimated equation (GEE) test. Data presented as mean± SEM. **LBWf-NF** n=4; **LBWf-HF** n=3; **HBWf-NF** n=4, **HBWf-HF** n=3.

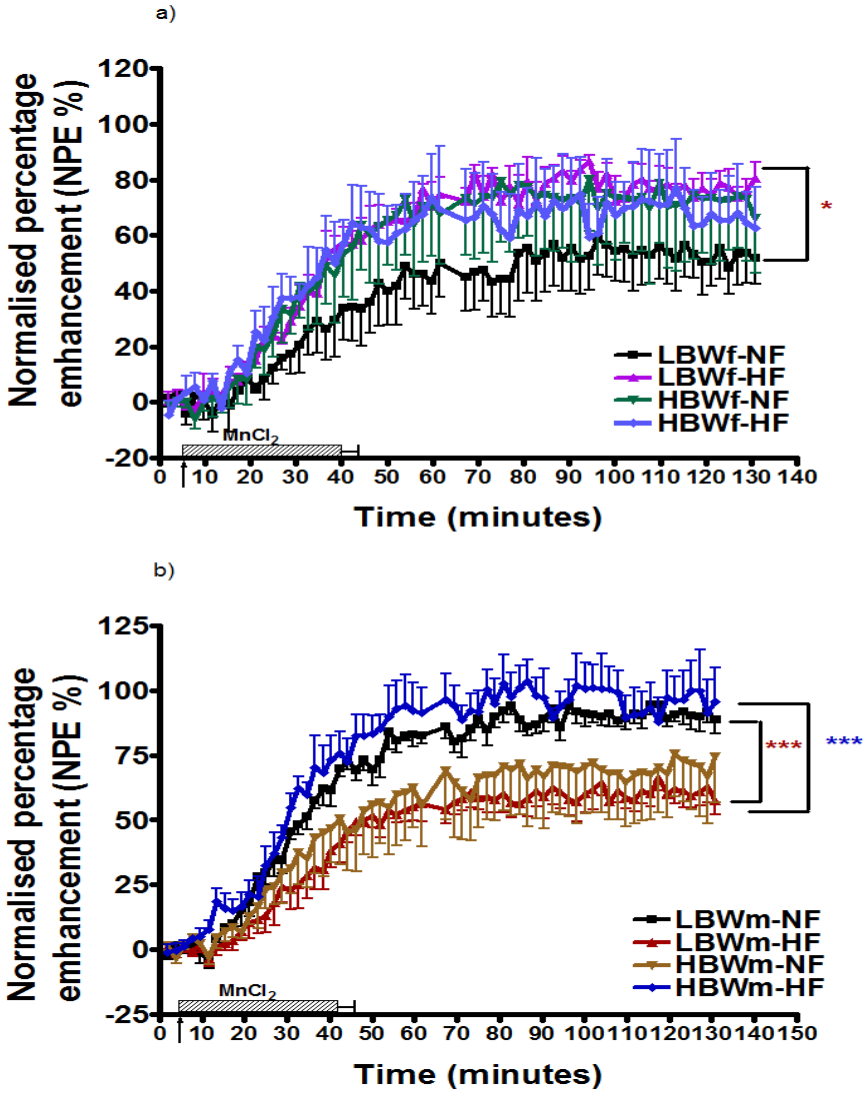

Figure 4.10.2.7 Neural activity measured within the hypothalamic Pe nucleus in female and male offspring at 15 weeks. Neural activity was analysed by measuring time course changes in SIs and presented as normalised percentage enhancement (NPE %) from the Pe nucleus within the hypothalamus. The arrow indicates the start of intravenous (i.v.) $MnCl_2$ infusion and the hatched bars indicate the duration of the i.v. infusion. Figure a) corresponds to females and figure b) to males. Statistical analysis was performed using a general estimated equation (GEE) test. Data presented as mean± SEM. **LBWf-NF** n=4; **LBWf-HF** n=3; **HBWf-NF** n=4, **HBWf-HF** n=3**; LBWm-NF** n=5; **LBWm-HF** n=5; **HBWm-NF** n=5, **HBWm-HF** n=5.

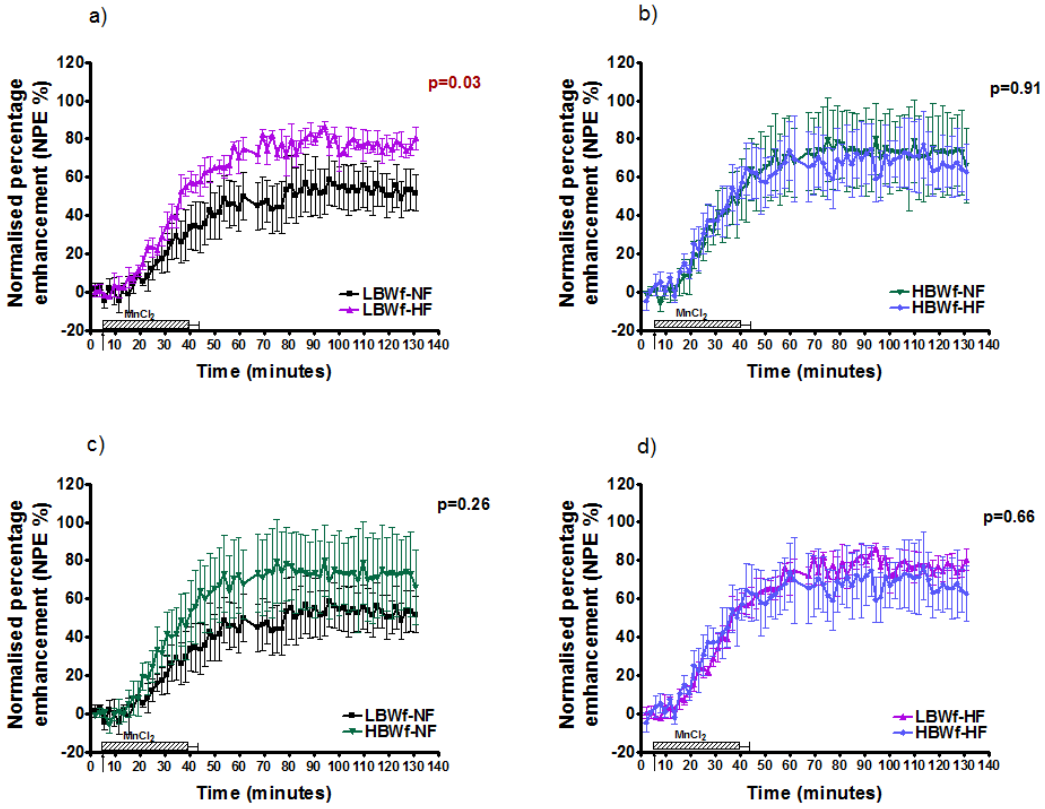

Figure 4.10.2.8 Neural activity measured within the hypothalamic Pe nucleus in female offspring at 15 weeks. Neural activity was analysed by measuring time course changes in SIs and presented as normalised percentage enhancement (NPE %) from the Pe nucleus within the hypothalamus. Figures a) and b) show the time course activity by diets (**NF-HF** respectively) in mice within the same birth weight category. Figure c) and d) show the time course activity by birth weight (**LBWm-HBWm** respectively) in mice within the same diet category. The arrow indicates the start of intravenous (i.v.) $MnCl_2$ infusion and the hatched bars indicate the duration of the i.v. infusion. Statistical analysis was performed using a general estimated equation (GEE) test. Data presented as mean± SEM. **LBWf-NF** n=4; **LBWf-HF** n=3; **HBWf-NF** n=4, **HBWf-HF** n=3.

4.11 Summary

LBWm mice had an increased accelerated growth and caught up in weight with **HBWm** mice at the age 9 weeks when fed a **NF** diet and at 11 weeks when fed a **HF** diet. However, **LBWf** mice remained smaller than **HBWf** mice throughout the study, despite the fact that they had a higher accelerated growth rate.

There was a significant effect of birth weight and diet (interaction) on the total kilocaloric intake in males. **HBWm-HF** mice had a higher intake than **LBWm-HF** and **HBWm-NF** mice. No significant differences were found between mice fed a **NF** diet (**LBWm-NF** vs. **HBWm-NF)** or between **LBW** mice (**LBWm-NF** vs. **HBWm-HF**). In female mice, diet exerted total kilocaric intake independently of birth weight, with a higher intake in females fed a **HF** diet than females fed a **NF** diet. **LBWm** mice were more efficient in gaining weight (FE) than **HBWm** mice irrespectively of the diet ingested. However, an interaction on factors (birth weight and diet) was evident in the female groups. **LBWf** mice had the highest FE when compared to their respective counterparts (**LBWf-NF** and **HBWf-HF**).

Total body adiposity was affected by the interaction between birth weight and diet. **LBWm-NF** had a higher percentage of total adiposity compared to **HBWm-NF** mice, but similar percentage to **LBWm-HF** mice. **HBWm-HF** diet had a higher percentage of total adiposity than **HBWm-NF** mice, but similar percentage to **LBWm-HF** mice. However, birth weight and diet *per se*

influenced adiposity in female mice. **HBWf** mice had a higher adiposity than **LBWf** mice and at the same time, **HF** fed females had a higher adiposity than females fed a **NF** diet.

IHCL in males was affected by birth weight only. **LBWm** mice had a higher IHCL content than **HBWm** mice, irrespectively of the diet consumed. Similarly, **LBWf** mice had a higher IHCL content than **HBWf** mice. Moreover, female mice were also affected by the diet *per se.* Female mice fed a **HF** diet had a significantly higher IHCL content than **NF** fed females.

Adipose tissue distribution varied according to the interaction between diet and birth weigh in males. **LBWm** mice had a signficanlty higher SAT and IAT tissue content than **HBWm-NF** mice but similar relative levels to **LBWm-HF** mice. Female mice were affected only by diet. **LBWf** and **HBWf** that were fed a **HF** diet ahd the highest SAT and IATcontent.

Glucose levels in a fed state were significantly higher in mice with a low birth weight (**LBW**) irrespectively of the diet ingested throughout the study. **LBWf** mice had the highest level of glucose when compared to both **LBWf-NF** and **HBWf-HF** mice. Similar levels of glucose were seen between **HBWf** mice. Insulin was increased in male mice fed a **HF** diet with a concomitant increase in glucagon levels in plasma. Females fed a **HF** diet had increased levels of insulin as males, but there was not a change in glucagon levels.

LBWm mice had an impaired fasting glucose as well as glucose intolerance compared to **HBWm** mice. Moreover, male mice fed a **HF** diet were glucose intolerant independently of the birth weight of mice. Conversely, female mice did not have significant differences in fasting glucose. However, **LBWf-HF** had higher levels of glucose during IPGTT test than both **LBWf-NF** and **HBWf-HF** mice.

The number of adipocytes was significantly higher in **HBWm-HF** mice in subcutaneous adipose tissue only when compared to **LBWm-HF** mice. Larger adipocytes were found in the gonadal and subcutaneous adipose tissue of **HBWm-HF** mice compared to **LBWm-HF** mice. **LBWm** mice had a higher small to large adipocyte ratio than **HBWm** irrespectively of the diet consumed only in the gonadal adipose tissue.

Neural acitivity in the hypothalamus was modulated by birth weight and diet and by gender. Overall, **LBWm-HF** mice presented the lowest activity in the centres of interest compared to **LBWm-NF** and **HBWm-HF** mice. Furthermore, **LBWm-NF** had a higher neural activity than **HBWm-NF** mice as well as **HBWm-HF** mice compared to this latter group.

Conversely, **LBWf-NF** mice had a lower activity than **LBWf-HF** mice and **HBWf-NF** mice. No differences were detected between females fed a **HF** diet or between **HBWf** mice.

5. Study 3. Effects of Birth Weight and Diet on Body Composition in Matured Mice (from 16 weeks to 51 weeks old)

5.1 The Effects of Birth Weight and Diet on Body Weight in Matured Mice (from 16 weeks to 51 weeks old)

Body weights of offspring were monitored weekly for a period of 36 weeks, from early adulthood (week 16) until middle age (51 weeks). **LBWm/f** and **HBWm/f** were maintained on the same dietary regime as in study 2 (section 2.2.3). The protocol of this preliminary study is described in section 2.3.

5.1.1 Body weight in Male mice

Figures 5.1.1.1 and 5.1.1.2 show the growth pattern of the 4 male groups following maintenance on both normal fat control diet (9% kcal fat intake) and purified moderated high fat diet (27% kcal fat intake).

As expected, male mice fed a **HF** diet had a higher weight than those fed a NF diet in both, **LBWm-HF (LBWm-HF vs. LBWm-NF p= 0.002**, figures 5.1.1.1 and 5.1.1.2a) mice and **HBWm-HF** mice **(HBWm-HF vs. HBWm-NF p<0.001**; figures 5.1.1.1 and 5.1.1.2b). This result suggests that birth weight did not affected body weight per se but the effect of diet was strong enough to modulate the body weight of male mice.

LBWm-NF and **HBWm-NF** were not significantly different at any time point as seen in figures 5.1.1.1 and 5.1.1.2c (**LBWm**-**NF** vs. **HBWm**-**NF** p=0.803).

Differences between **LBWm**-**HF** and **HBWm**-**HF** were not significantly different throughout the 36 weeks period (**LBWm-HF** vs. **HBWm-HF** p= 0.181; figures 5.1.1.1 and 5.1.1.2d). Although between groups difference was not significantly different, significant time point differences were seen during the first 9 weeks. After week 24, differences were not longer significant. This explains why the between groups analysis did not reach significance.

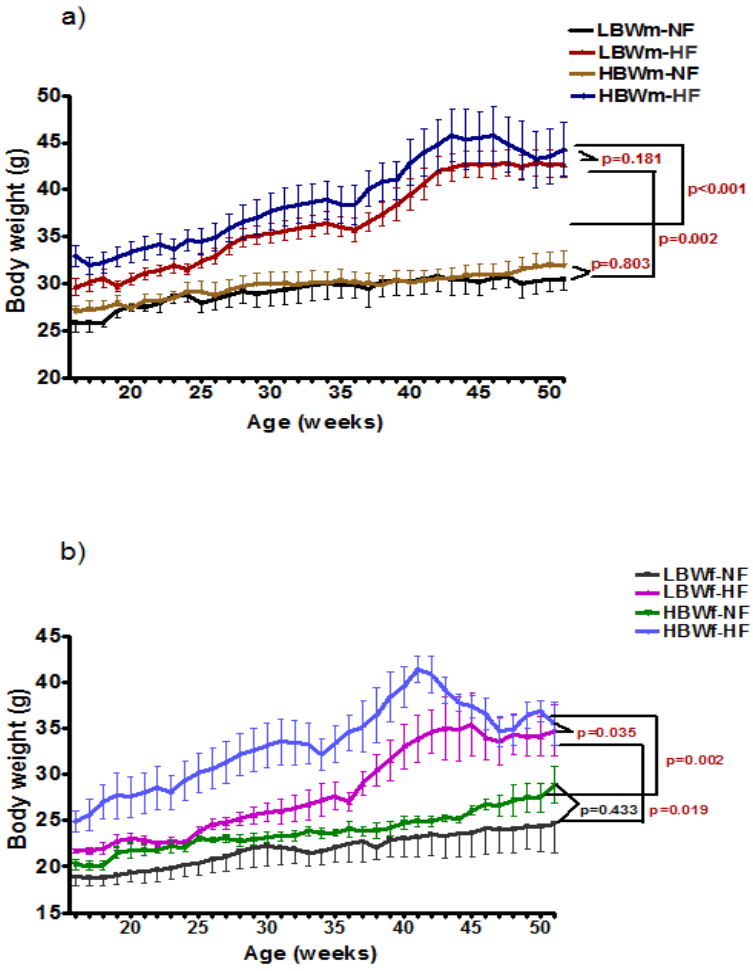

Figure 5.1.1.1 Body weight of male and female mice from early adulthood (week 16) until middle age week (week 51). **LBWm/f** and **HBWm/f** were subdivided into 4 further groups according to the diet given from weaning until week 51, either a normal fat diet =**NF** or moderated high fat diet =**HF**. The groups were: Low birth weight males/females fed a normal fat diet =**LBWm/f-NF**; Low birth weight males/females fed a high fat diet= **LBWm/f-HF**; High birth weight males/females fed a normal fat diet =**HBWm/f-NF;** High birth weight males/females fed a high fat diet= **HBWm/f-HF.** Figure a) corresponds to males and b) to females. Statistical analysis was performed using a mixed general linear model (GLM) followed by a protected Fisher's least significant difference (LSD) post hoc analysis. Data presented as mean± SEM. **LBWm-NF** n=4; **LBWm-HF** n=10; **HBWm-NF** n=5, **HBWm-HF** n=5; **LBWf-NF** n=4; **LBWf-HF** n=4; **HBWf-NF** n=4, **HBWf-HF** n=5.

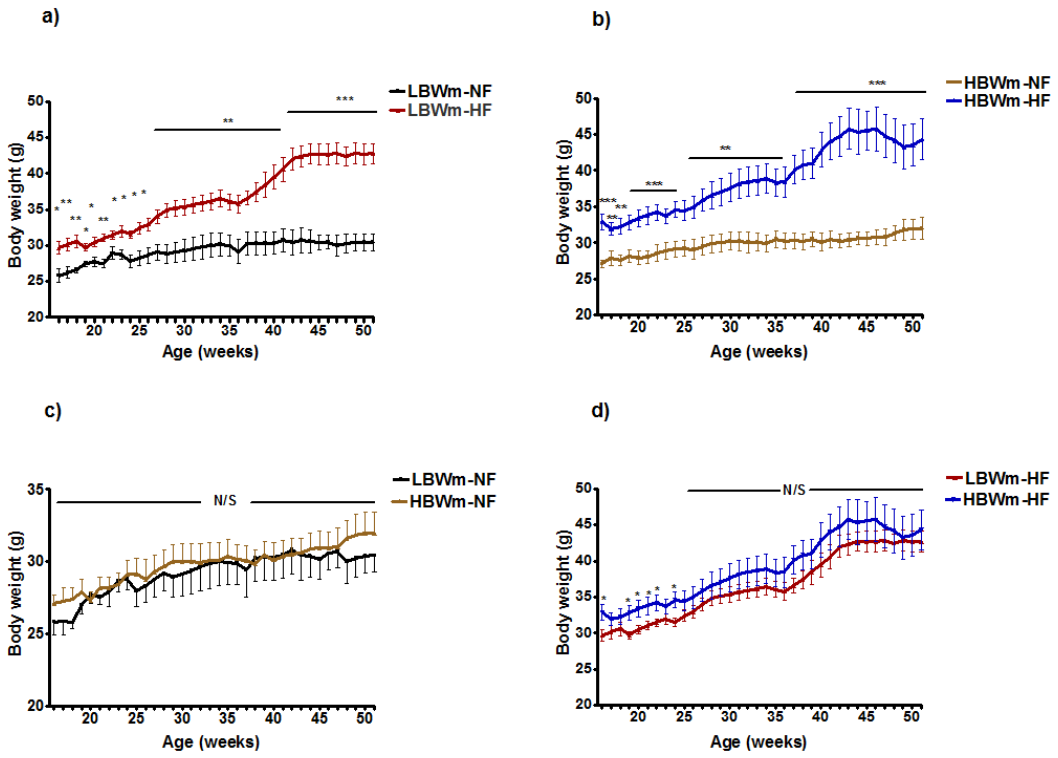

Figure 5.1.1.2 Body weight of male mice from early adulthood (week 16) until middle age week (week 51). a) **LBWm-NF** vs. **LBWm-HF**; b) **HBWm-NF** vs. **HBWm-HF**; c) **LBWm-NF** vs. **HBWm-NF**; d) **LBWm-HF** vs. **HBWm-HF**. Statistical analysis was performed using a mixed general linear model (GLM) followed by a protected Fisher's least significant difference (LSD) post hoc analysis. Data presented as mean± SEM. **LBWm-NF** n=4; **LBWm-HF** n=10; **HBWm-NF** n=5, **HBWm-HF** n=5. N/S= no significant differences, *p≤0.05; ** p≤0.01, ***p≤0.001.

5.1.2 Body weight in Female mice

Figures 5.1.2.1 and 5.1.2.2 show the body weights of female offspring from week 16 until week 51. **HF** diet had a similar effect on female mice as in male offspring, with females fed a **HF** having a higher body weight than those females fed a NF diet (**LBWf-HF** vs. **LBWf-NF p=0.019,** figures 5.2.1 and 5.2.2a; **HBWf-HF** vs. **HBWf-NF p=0.002**; figures 5.1.2.1 and 5.1.2.2b).

Differences between **LBWf-NF** and **HBWf-NF** were not significant as seen in male mice (**LBWf-NF** vs. **HBWf-NF** p=0.433; figures 5.1.2.1 and 5.1.2.2c). However, there was a significant difference between mice fed a **HF** diet with **LBWf-HF** having a lower weight than **HBWf-HF.** Despite the fact that between groups difference was significant, **LBWf-HF** caught up in weight with **HBWf-HF** at week 43 (**LBWf-HF** vs. **HBWf-HF p=0.035**; figure 5.1.2.1 and 5.1.2.2d). This catch up in weight was reached in part due to a decline in body weight of the **HBWf-HF** mice from week 42. Thus, the difference between groups was significant because of the body weight differences during week 16 until week 43. Contrary to males, **LBWf-HF** mice caught up in weight 9 weeks before the end of the study, whilst **LBWm-HF** mice caught up in weight 10 weeks after beginning the study.

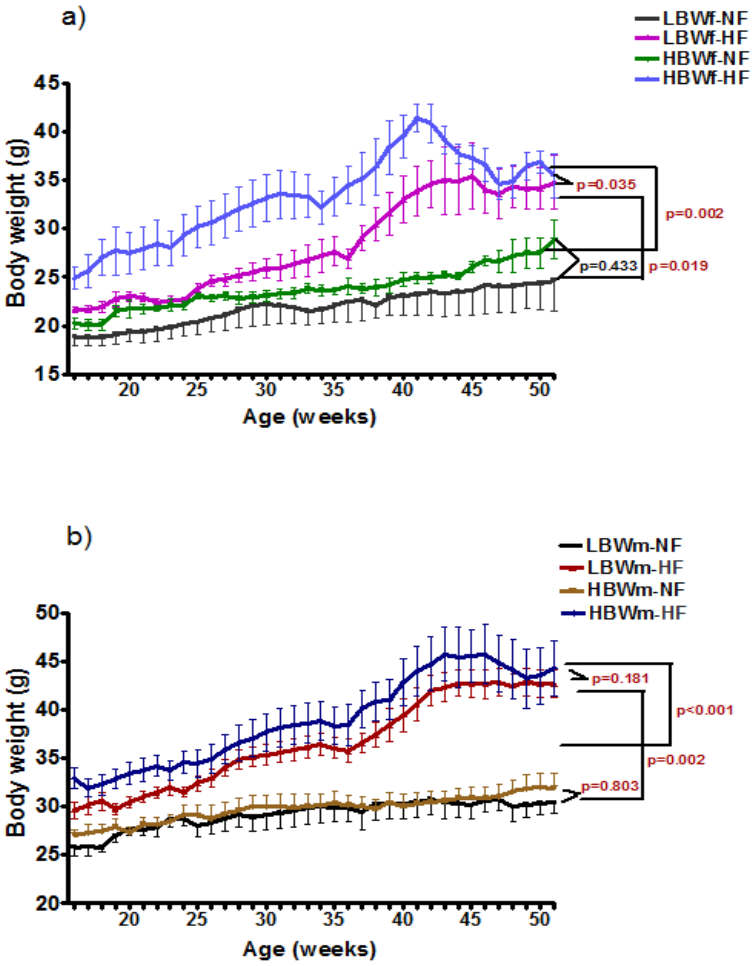

Figure 5.1.2.1 Body weight of female and male mice from early adulthood (week 16) until middle age week (week 51). **LBWf/m** and **HBWf/m** were subdivided into 4 further groups according to the diet given from weaning until week 51 (normal fat diet =**NF** or moderated high fat diet =**HF**. The groups were: Low birth weight females/males fed a normal fat diet =**LBWf/m-NF**; Low birth weight females/males fed a high fat diet= **LBWf/m-HF**; High birth weight females/males fed a normal fat diet =**HBWf/m-NF;** High birth weight females/males fed a high fat diet= **HBWf/m-HF**. Statistical analysis was performed using a mixed general linear model (GLM) followed by a protected Fisher's least significant difference (LSD) post hoc analysis. Data presented as mean± SEM. **LBWf-NF** n=4; **LBWf-HF** n=4; **HBWf-NF** n=4, **HBWf-HF** n=5. **LBWm-NF** n=4; **LBWm-HF** n=10; **HBWm-NF** n=5, **HBWm-HF** n=5.

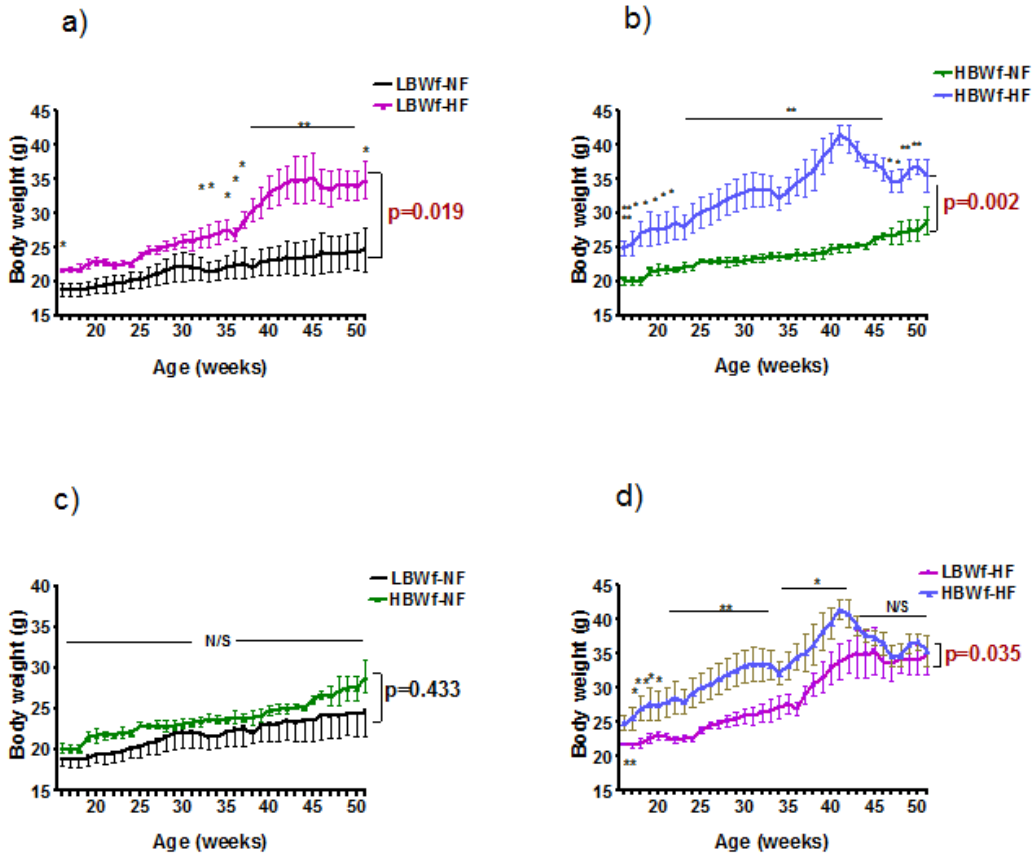

Figure 5.1.2.2 Body weight of <u>female</u> mice from early adulthood (week 16) until middle age week (week 51). a) **LBWf-NF** vs. **LBWf-HF**; b) **HBWf-NF** vs. **HBWf-HF**; c) **LBWf-NF** vs. **HBWf-NF**; d) **LBWf-HF** vs. **HBWf-HF**. Statistical analysis was performed using a Mixed general linear model (GLM) followed by a protected Fisher's least significant difference (LSD) post hoc analysis. Data presented as mean± SEM. **LBWF-NF** n=4; **LBWf-HF** n=4; **HBWf-NF** n=4, **HBWf-HF** n=5. N/S= no significant differences, *p≤0.05; ** p≤0.01, ***p≤0.001.

5.1.3 Body weight gain in Male mice

Assessment of body weight gain from week 19 to week 51 showed an enhanced total body weight gain in male mice fed a **HF** compared to mice fed a **NF** diet (**LBWm-HF**=12.952±1.107g, **LBWm-NF=** 4.615 ±0.436g, **p<0.001**; figure 5.1.3.1; **HBWm-HF=** 12.42±1.815g vs. **HBWm-NF=** 4.84±1.1973g, **p=0.001**; figure 5.1.3.1). Difference between mice fed a NF was not significantly different (**LBWm-NF** vs. **HBW-NF** p=0.918; figure 5.1.3.1). Similar body weight gain was seen between LBWm-**HF** and **HBWm-HF** (p=0.767; figure 5.1.3.1).

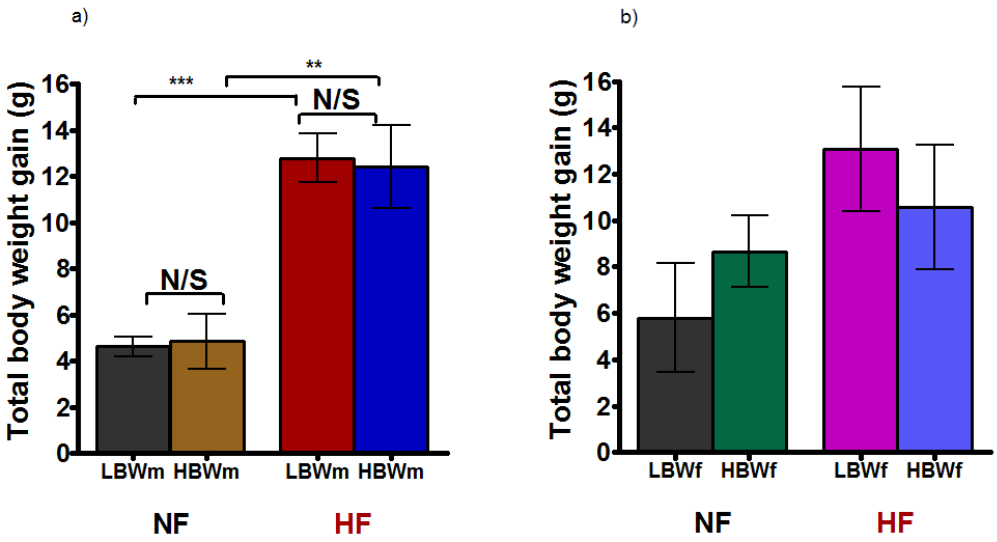

Figure 5.1.3.1 Total body weight gain of male and female offspring from week 16 to week 51. Absolute values are given in grams. Figure a) corresponds to males and figure b) to females. Statistical analysis was performed using a one-way anova test followed by a protected Fisher's least significant difference (LSD) a) or Tukey high significant difference (HSD) b) post hoc analysis. Data presented as mean± SEM. **LBWm-NF** n=4; **LBWm-HF** n=10; **HBWm-NF** n=5, **HBWm-HF** n=5; **LBWf-NF** n=4; **LBWf-HF** n=4; **HBWf-NF** n=4, **HBWf-HF** n=5. N/S or figures without symbols/letters= no significant, **p≤0.01,***p≤0.001.

Similar pattern was seen when evaluating body weight gain normalised to initial body weight expressed as percentage (growth or relative body weight gain%). **HF** fed mice had a significantly higher relative body weight compared to mice fed a **NF** (**LBWm-HF**=45.722±3.896%, **LBWm-NF=** 17.882 ±1.612%, **p<0.001**; figure 5.1.3.2; **HBWm-HF=** 36.691±4.491%, **HBWm-NF=** 17.764±4.251%, **p=0.009**; figure 5.1.3.2). Differences between mice fed a **NF** were not significantly different (**LBWm-NF** vs. **HBW-NF** p=0.987; figure 5.1.3.2). Although **LBWm-HF** had a higher relative body weight gain than **HBWm-HF**, it was not enough to reach statistical significance. (p=0.128; figure 5.1.3.2).

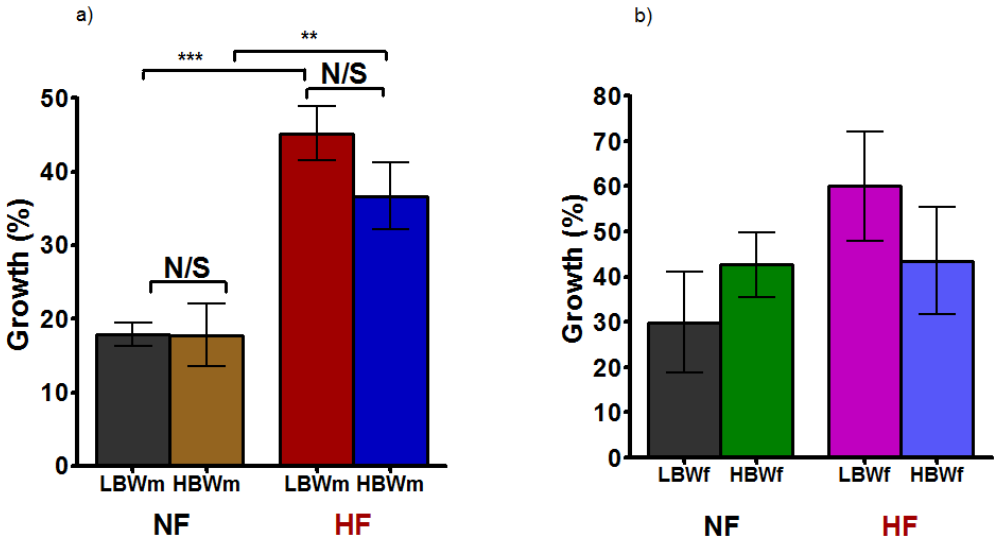

Figure 5.1.3.2 Relative body weight gain of male and female offspring from week 16 to week 51. Relative values or growth change given as a percentage of the initial body weight: 100*(body weight 51 week- body weight 16 week)/ body weight 16 week. Figure a) corresponds to males and figure b) to females. Statistical analysis was performed using a one-way ANOVA test followed by a protected Fisher's least significant difference (LSD) a) or Tukey high significant difference (HSD) post hoc analysis b) post hoc analysis. Data presented as mean± SEM. **LBWm-NF** n=4; **LBWm-HF** n=10; **HBWm-NF** n=5, **HBWm-HF** n=5; **LBWf-NF** n=4; **LBWf-HF** n=4; **HBWf-NF** n=4, **HBWf-HF** n=5. N/S or figure without symbols/letters= no significant, **p≤0.01, ***p≤0.001.

5.1.4 Body weight gain n Female mice

HF feeding in female mice did not have the same significant impact as seen in males. **LBWf-HF** gained more weight than **LBWf-NF** but the difference did not reach statistical significance (**LBWf-HF=** 13.075±2.692g, **LBWf-NF =** 5.8± 2.358g, p=0.244; figure 5.1.4.1). A narrower difference was seen between **HBWF-HF** and **HBWf-NF** (**HBWf-HF=** 10.575±2.7g, **HBWf-NF=** 8.667± 1.551g, p=0.95; figure 5.1.4.1). As in males, no differences were seen between female mice fed a **NF** diet (p=0.877; figure 5.1.4.1) or between female mice fed a **HF** (p=0.875; figure 5.1.4.1).

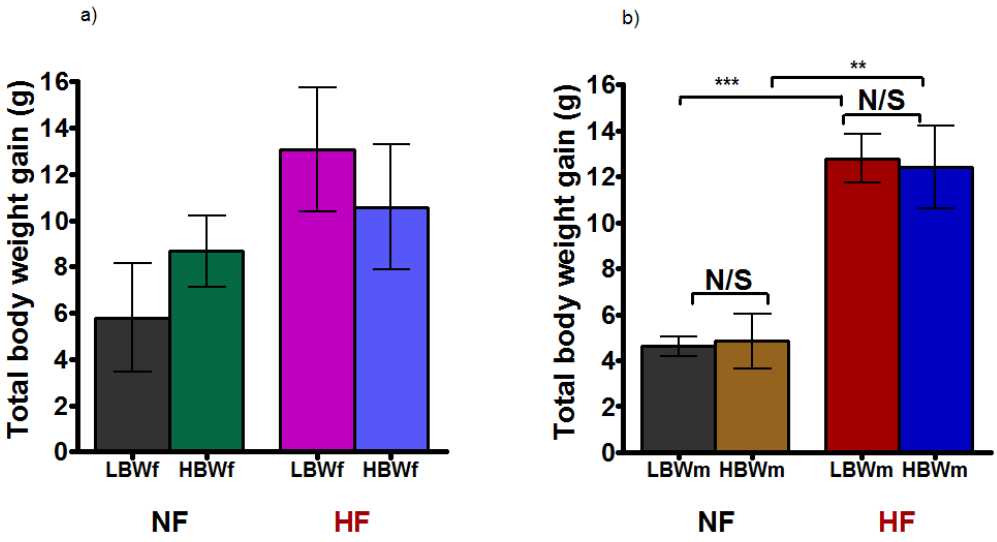

Figure 5.1.4.1 Total body weight gain of female and male offspring from week 16 to week 51. Absolute values are given in grams. Figure a) corresponds to females and figure b) to males. Statistical analysis was performed using a one-way ANOVA test followed by a Tukey high significant difference (HSD) a) or protected Fisher's least significant difference (LSD) b) post hoc analysis. Data presented as mean± SEM. **LBWf-NF** n=4; **LBWf-HF** n=4; **HBWf-NF** n=4, **HBWf-HF** n=5; **LBWm-NF** n=4; **LBWm-HF** n=10; **HBWm-NF** n=5, **HBWm-HF** n=5. N/S or figure without symbols/letters= no significant, **p≤0.01, ***p≤0.001.

Similar pattern was seen when normalising body weight gain to initial body weight (growth or relative body weight gain%). **LBWf-HF** had the highest growth percentage but it was not significantly different from **LBWf-NF** or **HBWf-HF** (**LBWf-HF**= 60.088±12.0783%, **LBWf-NF** = 29.914± 11.234%, p=0.302; **HBWf-HF** =43.515±11.861% p=0.695; figure 5.1.4.2). There was not difference between female mice fed a **NF** diet (**LBWf-NF**= 29.914± 11.234%, **HBWf-NF** = 42.674±7.122, p=0.88; figure 5.1.4.2). **HBWf** had a similar growth irrespective of the diet (p=0.999; figure 5.1.4.2).

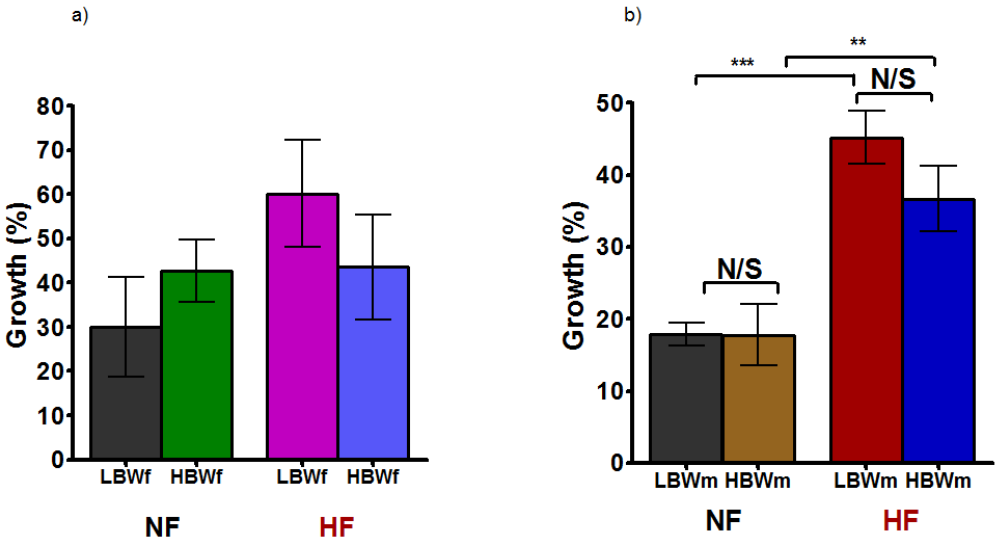

Figure 5.1.4.2 Relative body weight gain of female and male offspring from week 16 to week 51. Relative values or growth change given as a percentage of the initial body weight: 100*(body weight 51 week body weight 16 week)/ body weight 16 week. Statistical analysis was performed using a one-way ANOVA test followed by a Tukey high significant difference (HSD) or protected Fisher's least significant difference (LSD) b) post hoc analysis. Data presented as mean± SEM. **LBWf-NF** n=4; **LBWf-HF** n=4; **HBWf-NF** n=4, **HBWf-HF** n=5; **LBWm-NF** n=4; **LBWm-HF** n=10; **HBWm-NF** n=5, **HBWm-HF** n=5. N/S or figure without symbols/letters= no significant, **p≤0.01, ***p≤0.001

5.2 The Effects of Birth Weight and Diet on Caloric Intake in Matured Mice (from 16 weeks to 51 weeks old)

Total kilocalorie intake was calculated using weekly food intake measurements and the values of the caloric content of the diets mentioned in section 2.2, table 2.2.1, and section 2.3.

5.2.1 Total kilocalorie intake in Male mice

Figure 5.2.1.1 shows the total kilocalorie intake of **LBWm** and **HBWm** mice fed both a control fat diet (9% kcal fat intake) and a purified moderated high fat diet (27% kcal fat intake).

Both groups fed a **HF** diet had a higher kilocalorie intake than those mice fed a **NF**. However, only **HBWm**-**HF** mice had a significantly higher intake than **HBWm**-**NF** mice (**HBWm-HF**=3440.687±136.566 kcalories, **HBWm-NF**=2996.093±94.317 kcalories, **p=0.016**; **LBWm**-**HF**=3129.783±94.129 kcalories, **LBWm**-**NF**=2849.415±47.526 kcalories, p=0.102; figure 5.2.1.1). Interestingly, there was a significant difference between mice fed a **HF** diet with **LBWm-HF** having a lower intake than **HBWm-HF** (**p=0.04**; figure 5.2.1.1). There was not a statistical significance between mice fed a **NF** diet (p=0.445; figure 5.2.1.1).

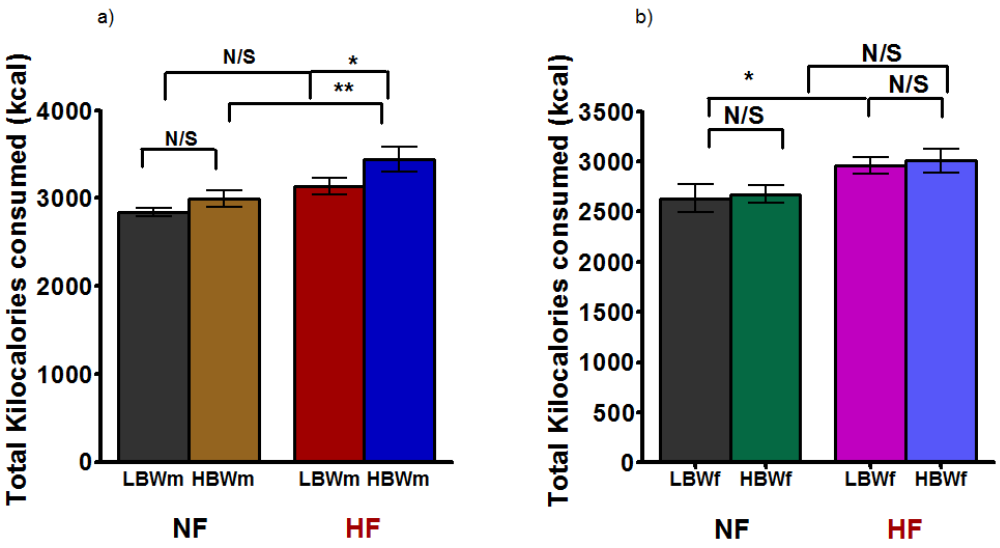

Figure 5.2.1.1 Male and female kilocalorie consumption from week 16 until week 51 (36 weeks). Total kilocalories were obtained from calculated weekly-recorded food intake and the kilocalorie content per gram of each diet (**NF**= 3.6 kcal/g and **HF**=4.1 kcal/g). Figure a) corresponds to males and figure b) to females. Statistical analysis was performed using a one-way ANOVA test followed by a protected Fisher's least significant difference (LSD) post hoc analysis. Data presented as mean± SEM. **LBWm-NF** n=4; **LBWm-HF** n=11; **HBWm-NF** n=5, **HBWm-HF** n=6; **LBWf-NF** n=4; **LBWf-HF** n=4; **HBWf-NF** n=4, **HBWf-HF** n=5. *p≤0.05, ** p≤0.01, N/S= no significant difference.

However, when normalising kilocalorie intake to body weight$^{0.75}$(g), significant differences were not longer present (**HBWm-HF**= 219.196±6.653 kcalories/bodyweight$^{0.75}$, **HBWm-NF**= 225.092 ±6.794 kcalories/body weight$^{0.75}$, p=0.896; **HBWm-HF** vs. **LBWm-HF** p=0.995; figure 5.2.1.2). **LBWm-HF** vs. **LBWm-NF** was not significantly different as seen in the absolute kilocalorie intake as well as mice fed a **NF** (**LBWm-**

HF=217.441±4.099 kcalories/body weight$^{0.75}$, **LBWm-NF**=221.332 ±4.999 kcalories/body weight$^{0.75}$, p=0.964; **LBWm-NF** vs. **HBWm-NF** p=0.977).

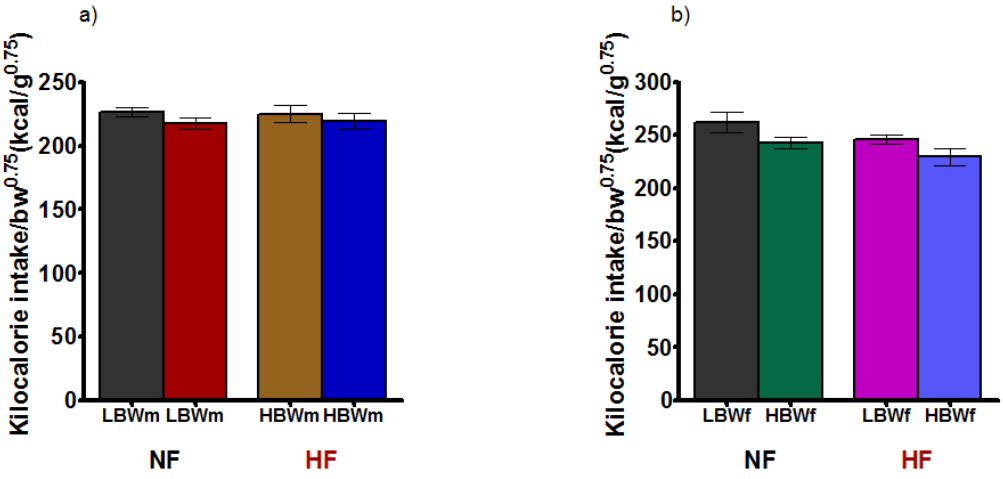

Figure 5.2.1.2 Male and female kilocalorie consumption from week 16 until week 51 normalised to body weight$^{0.75}$ (36 weeks). Total kilocalories were obtained from calculated weekly-recorded food intake and the kilocalorie content per gram of each diet (**NF**= 3.6 kcal/g and **HF**=4.1 kcal/g) and subsequent normalisation to body weight$^{0.75}$. Figure a) corresponds to males and figure b) to females. Statistical analysis was performed using a one-way ANOVA test followed by a Tukey high significant difference (HSD) post hoc analysis. Data presented as mean± SEM. **LBWm-NF** n=4; **LBWm-HF** n=11; **HBWm-NF** n=5, **HBWm-HF** n=6. ; **LBWf-NF** n=4; **LBWf-HF** n=4; **HBWf-NF** n=4, **HBWf-HF** n=5; **LBWm-NF** n=4; **LBWm-HF** n=11; **HBWm-NF** n=5, **HBWm-HF** n=6.

5.2.2 Total caloric intake in Female mice

As in males, female mice fed a **HF** diet had a higher kilocalorie intake compared to those females fed a **NF** diet. However, only **LBWf-HF** had a significantly higher intake than **LBWf-NF** (**LBWf**-**HF**=2962.356±84.08 kcalories, **LBWf-NF**=2568.192±176.764 kcalories, **p=0.019**; **HBWf-HF**=2889.949±43.561kcalories, **HBWf**-**NF**=2674.112±89.932 kcalories, p=0.134; figure 5.2.2.1). No differences were seen between female groups fed a **NF** (**LBWf-NF** vs. **HBWf-NF** p=0.477; figure 5.2.2.1) or between females fed a **HF** diet (**LBWf-HF** vs. **HBWf-HF** p=0.598; figure 5.2.2.1).

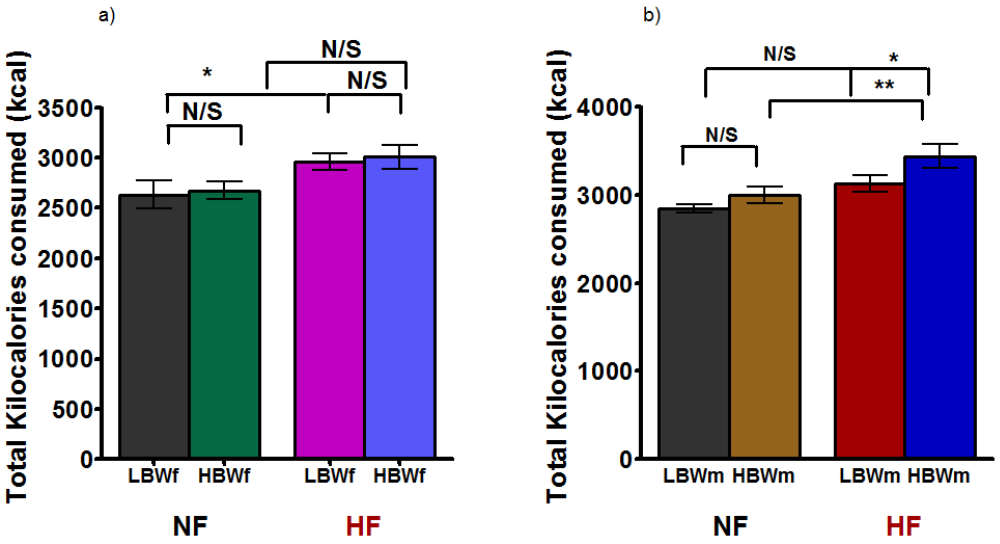

Figure 5.2.2.1 Female and male kilocalorie consumption from week 16 until week 51 (36 weeks). Total kilocalories were obtained from calculated weekly-recorded food intake and the kilocalorie content per gram of each diet (**NF**= 3.6 kcal/g and **HF**=4.1 kcal/g). Figure a) corresponds to females and figure b) to males. Statistical analysis was performed using a one-way ANOVA test followed by a protected Fisher's least significant difference (LSD) post hoc analysis. Data presented as mean± SEM. **LBWf-NF** n=4; **LBWf-HF** n=4; **HBWf-NF** n=4, **HBWf-HF** n=5. **LBWm-NF** n=4; **LBWm-HF** n=11; **HBWm-NF** n=5, **HBWm-HF** n=6. * p≤0.05, ** p≤0.01, N/S= no significant difference.

However, when normalising kilocalorie intake to body weight$^{0.75}$(g), significant differences were not longer present (**LBWf-HF**= 246.352±4.346 kcalories/bodyweight$^{0.75}$,**LBWf-NF**=262.534±13.915kcalories/bodyweight$^{0.75}$ p=0.185; figure 5.2.2.2). **LBWf-NF** vs. **HBWf-NF** was not significantly different as seen in the absolute kilocaloric intake (**LBWf-NF**=262.534±13.915 kcalories/body weight$^{0.75}$, **HBWf-NF**=243.053±5.437; p=0.117; figure 5.2.2.2). **LBWf-HF** had a higher kilocalorie intake than **HBWf-HF** but the difference did not reach statistical significance (**LBWf-HF**=246.352±4.346 kcalories/bodyweight$^{0.75}$, **HBWf-HF**= 225.969±7.02 kcalories/bodyweight$^{0.75}$; p=0.067; figure 5.2.2.2). There was not a significant difference between **HBWf** mice (**HBWf-NF** vs. **HBWf-HF** p=0.117; figure 5.2.2.2).

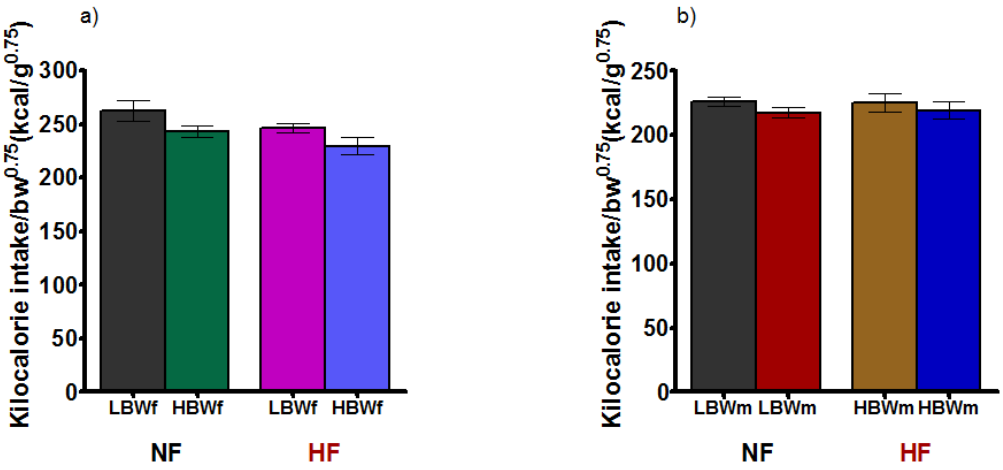

Figure 5.2.2.2 Female and male kilocalorie consumption from week 16 until week 51 normalised to body weight$^{0.75}$ (36 weeks). Total kilocalories were obtained from calculated weekly-recorded food intake and the kilocalorie content per gram of each diet (**NF=** 3.6 kcal/g and **HF**=4.1 kcal/g) and subsequent normalisation to body weight$^{0.75}$. Figure a) corresponds to females and figure b) to males. Statistical analysis was performed using a one-way ANOVA test followed by a Tukey's high significant difference (HSD) post hoc analysis. Data presented as mean± SEM. **LBWf-NF** n=4; **LBWf-HF** n=4; **HBWf-NF** n=4, **HBWf-HF** n=5; **LBWm-NF** n=4; **LBWm-HF** n=11; **HBWm-NF** n=5, **HBWm-HF** n=6.

5.3 The Effects of Birth Weight and Diet on Feed Efficiency in Matured Mice (from 16 weeks to 51 weeks old)

Feed efficiency was calculated as the body weight gain divided by total kilocalories consumed. Total caloric intake was calculated using weekly food intake measurements and the values of the caloric content of the diets mentioned in section 2.2, table 2.2.1, and section 2.3.

5.3.1 Feed efficiency in Male mice

Figure 5.3.1.1 show the feed efficiency of male groups. Male mice fed a **HF** diet gained more weight per kilocalories consumed than mice fed a **NF** diet (**LBWm-HF=** 3.749±0.347 mg/kcalorie, **LBWm-NF**=1.341±0.23 mg/kcalorie **p=0.001**; **HBWm-HF=** 3.416±0.499 mg/kcalorie, **HBWm-NF**=1.759±0.319 mg/kcalorie **p=0.014**; figure 5.3.1.1). No differences were seen between mice fed both **NF** and **HF** (**LBWm-NF** vs. **HBWm-NF** p=0.552; **LBWm-HF** vs. **HBWm-HF** p=0.531; figure 5.3.1.1).

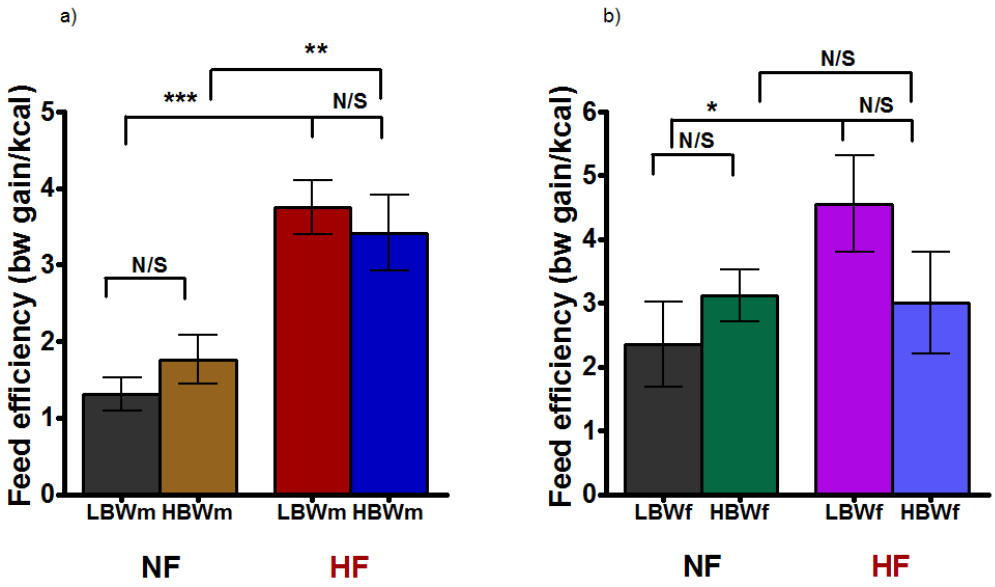

Figure 5.3.1.1 Feed efficiency of male and female mice from week 16 until week 51 (36 weeks). Total kilocalories were obtained from weekly-recorded food intake and the calculated kilocaloric content per gram of each diet (**NF**= 3.6 kcal/g and **HF**=4.1 kcal/g). Figure a) corresponds to males and figure b) to females. Statistical analysis was performed using a one-way ANOVA test followed by a protected Fisher's least significant difference (LSD) post hoc analysis. Data presented as mean± SEM. **LBWm-NF** n=4; **LBWm-HF** n=11; **HBWm-NF** n=5, **HBWm-HF** n=6; **LBWf-NF** n=4; **LBWf-HF** n=4; **HBWf-NF** n=4, **HBWf-HF** n=5. * p≤0.05, *** p≤0.001,N/S= no significant difference.

5.3.2 Feed efficiency in Female mice

Contrary to males, female mice fed a **HF** diverged in their feed efficiency. Whilst **LBWf-HF** had a higher feed efficiency than **LBWf-NF** (**LBWf-HF=** 4.554±0.756 mg/kcalorie, **LBWf-NF**=2.356±0.665 mg/kcalorie; **p=0.05**; figure 5.3.2.1), **HBWf-HF** had a very similar feed efficiency compared to **HBWf-NF** (**HBWf-HF**=3.502±0.8 mg/kcalorie, **HBWf-NF**=3.458±0.444 mg/kcalorie; p=0.964; figure 5.3.2.1). No differences were seen between mice fed **NF** or mice fed a **HF** (**LBWf-NF** vs. **HBWf-NF** p=0.302; **LBWf-HF** vs. **HBWf-HF** p=0.288; figure 5.3.2.1).

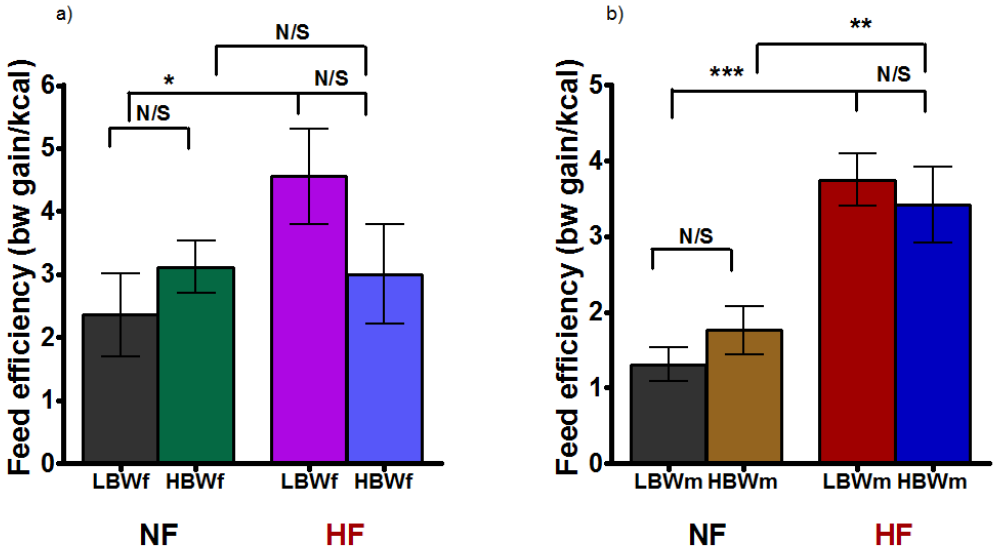

Figure 5.3.2.1 Feed efficiency of female and male mice from week 16 until week 51 (36 weeks). Total kilocalories were obtained from weekly-recorded food intake and the calculated kilocaloric content per gram of each diet (**NF**= 3.6 kcal/g and **HF**=4.1 kcal/g). Figure a) corresponds to females and figure b) to males. Statistical analysis was performed using a one-way ANOVA test followed by a protected Fisher's least significant difference (LSD) post hoc analysis. Data presented as mean± SEM. **LBWf-NF** n=4; **LBWf-HF** n=4; **HBWf-NF** n=4, **HBWf-HF** n=5; **LBWm-NF** n=4; **LBWm-HF** n=11; **HBWm-NF** n=5, **HBWm-HF** n=6; *p≤0.05, *** p≤0.001, N/S= no significant difference.

5.4 The Effects of Birth Weight and Diet on White Adipose Tissue Mass in Matured Mice (51 weeks old)

White adipose tissue was (WAT) was extracted and subdivided into subcutaneous (SAT) and internal adipose tissue (IAT). IAT was further subdivided into gonadal, retroperitoneal and mesenteric fat depots. Male and female analysis is presented separately.

5.4.1 White Adipose Tissue Mass

5.4.1.1 White adipose tissue mass in Male mice

At the time of the collection of tissues (week 51), body weights of mice fed a **HF** diet were heavier than mice fed a **NF** (**LBWm-HF**= 41.33±1.888g vs. **LBWm-NF**= 30.667±1.576g**, p=0.009**; **HBWm-HF**= 44.3±2.826g vs. **HBWm-NF**= 32.02±0.1.533g, **p=0.002**; figure 5.4.1.1.1). No differences were seen between males fed a **NF** diet (**LBWm-NF** vs. **HBWm-NF** p=0.743; figure 5.4.1.1.1) and between males fed a **HF** diet (**LBWm-HF** vs. **HBWm-HF** p=0.315; figure 5.4.1.1.1).

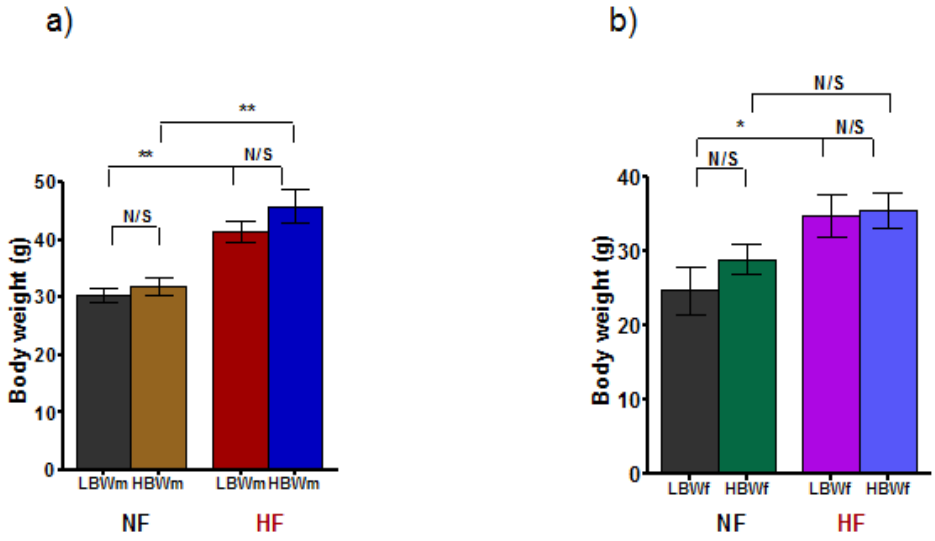

Figure 5.4.1.1.1 Body weight of male and female mice fed a **NF** and **HF** diet at week 51 of age. Figure a) corresponds to males and figure b) to females. Statistical analysis was performed using a one-way ANOVA test followed by a protected Fisher's least significant difference (LSD) post hoc analysis. Data presented as mean± SEM. **LBWm-NF** n=4; **LBWm-HF** n=11; **HBWm-NF** n=5, **HBWm-HF** n=6; **LBWf-NF** n=4; **LBWf-HF** n=4; **HBWf-NF** n=4, **HBWf-HF** n=5. * p≤0.05, ** p≤0.01, N/S= no significant difference.

Total white adipose tissue was significantly higher in mice fed a **HF** than mice fed a **NF** (**LBWm-HF** vs. **LBWm-NF p=0.004**; **HBWm-HF** vs. **HBWm-NF p=0.006**; figure 5.4.1.1.2). No differences were seen in mice fed a **NF** (**LBWm-NF** vs. **HBWm-NF** p=0.946; figure 5.4.1.1.2 and table 5.4.1.1.1) or between mice fed a **HF** (**LBWm-HF** vs. **HBWm-HF** p=0.663; figure 5.4.1.1.2 and table 5.4.1.1.1).

After normalisation of total white adipose tissue to current body weight (as percentage), differences between groups were maintained as seen in total white adipose tissue mass in grams (**LBWm-HF** vs. **LBWm-NF p=0.002**; **HBWm-HF** vs. **HBWm-NF p=0.011**; table 5.4.1.1.1 and figure 5.4.1.1.3). No differences were seen between males fed a **NF diet** (**LBWm-NF** vs**. HBWm-NF** p=0.856; table 5.4.1.1.1 and figure 5.4.1.1.3) or between males fed a **HF** diet (**LBWm-HF** vs. **HBWm-HF** p=0.219; table 5.4.1.1.1 and figure 5.4.1.1.3). This suggests that at this time point of study, the dietary intervention had a major impact in total white adipose tissue independently of birth weight.

	LBWm-NF_1	LBWm-HF_2	HBWm-NF_3	HBWm-HF_4	P value
Total WAT (g)	3.269±0.81	7.869±0.671	3.161±0.725	7.383±1.089	**1 vs.2=0.004** **3vs.4=0.006** **1vs.3=**0.946 **2vs.4=**0.663
Total WAT %	10.452±2.043	18.491±0.981	9.975±1.76	16.204±1.601	**1 vs.2=0.002** **3vs.4=0.011** **1vs.3=**0.856 **2vs.4=**0.219

Table 5.4.1.1.1 Total white adipose tissue mass from male mice fed a **NF** and a **HF** diet. Total WAT (g)= total white adipose tissue in grams, total WAT= total white adipose tissue mass normalised to current body weight and presented as percentage. Statistical analysis was performed using a one-way ANOVA test followed by a protected Fisher's least significant difference (LSD) post hoc analysis. Data presented as mean± SEM. **LBWm-NF** n=4; **LBWm-HF** n=10; **HBWm-NF** n=5, **HBWm-HF** n=6.

Subcutaneous adipose tissue (SAT) had the same pattern as the total white adipose tissue with mice fed a **HF** having a higher SAT content than their counterparts (**LBWm-HF** vs. **LBWm-NF p=0.001**; **HBWm-HF** vs. **HBWm-NF p=0.004**; figure 5.4.1.1.2 and table 5.4.1.1.2). No differences were seen in mice fed a **NF** (**LBWm-NF** vs. **HBWm-NF** p=0.909; table 5.4.1.1.2 and figure 5.4.1.1.2) and between mice fed a **HF** (**LBWm-HF** vs. **HBWm-HF** p=0.206; table 5.4.1.1.2 and figure 5.4.1.1.2).

Assessment of normalised SAT showed a similar trend as seen in absolute values (in grams) with a higher SAT depot in mice fed a **HF** (**LBWm-HF** vs. **LBWm-NF p<0.001**; **HBWm-HF** vs. **HBWm-NF p=0.01**; table 5.4.1.1.2 and figure 5.4.1.1.3). However, contrary to the SAT in grams, there was a significantly higher amount of SAT (%) in **LBWm-HF** compared to **HBWm-HF** (**LBWm-HF** vs. **HBWm-HF p=0.03**; table 5.4.1.1.2 and figure 5.4.1.1.3).

	LBWm-NF$_1$	**LBWm-HF$_2$**	**HBWm-NF$_3$**	**HBWm-HF$_4$**	**P value**
SAT (g)	1.6±0.407	3.992±0.251	1.524±0.355	3.385±0.461	**1 vs.2<0.001** **3vs.4=0.004** **1vs.3=**0.909 **2vs.4=**0.206
SAT %	5.115±1.028	9.297±0.2061	4.811±0.867	7.478±0.709	**1 vs.2=0.003** **3vs.4=0.01** **1vs.3=**0.783 **2vs.4=0.03**

Table 5.4.1.1.2 Subcutaneous white adipose tissue (SAT) mass from male mice fed a **NF** and a **HF** diet. SAT (g)= subcutaneous adipose tissue in grams, SAT (%)= subcutaneous adipose tissue mass normalised to current body weight and presented as percentage. Statistical analysis was performed using a one-way ANOVA test followed by a protected Fisher's least significant difference (LSD) post hoc analysis. Data presented as mean± SEM. **LBWm-NF** n=4; **LBWm-HF** n=10; **HBWm-NF** n=5, **HBWm-HF** n=6.

Gonadal, retroperitoneal and mesenteric fat depots were also significantly higher in mice fed a **HF** compared to those mice fed a **NF** (Gonadal: **LBWm-HF** vs. **LBWm-NF p=0.002**; **HBWm-HF** vs. **HBWm-NF p=0.006**; retroperitoneal: **LBWm-HF** vs. **LBWm-NF p=0.047**; **HBWm-HF** vs. **HBWm-NF p=0.021**; mesenteric: **LBWm-HF** vs. **LBWm-NF p=0.01**; **HBWm-HF** vs. **HBWm-NF p=0.003**; table 5.4.1.1.3 and figure 5.4.1.1.2).

Differences between **NF** fed mice were not significantly different (Gonadal: **LBWm-NF** vs. **HBWm-NF** p=0.937; retroperitoneal: **LBWm-NF** vs. **HBWm-NF** p=0.986; mesenteric: **LBWm-NF** vs. **HBWm-NF** p=0.947; figure 5.4.1.1.2 and table 5.4.1.1.3) as in between **HF** fed mice (Gonadal: **LBWm-HF** vs. **HBWm-HF** p=0.403; retroperitoneal: **LBWm-HF** vs. **HBWm-HF** p=0.715; mesenteric: **LBWm-HF** vs. **HBWm-HF** p=0.487; table 5.4.1.1.3 and figure 5.4.1.1.2).

After normalisation of these regional fat compartments, significant differences were maintained (table 5.4.1.1.3 and figure 5.4.1.1.3).

	LBWm-NF_1	LBWm-HF_2	HBWm-NF_3	HBWm-HF_4	P value
Gonadal (g)	1.029±0.248	2.452±0.203	0.992±0.198	2.182±0.296	**1 vs.2=0.002** **3vs.4=0.006** **1vs.3**=0.937 **2vs.4**=0.403
Gonadal %	3.291±0.627	5.632±0.316	3.141±0.463	4.981±0.469	**1 vs.2=0.001** **3vs.4=0.012** **1vs.3**=0.844 **2vs.4**=0.162
Retrop. (g)	0.327±0.097	0.916±0.119	0.321±0.085	1.042±0.273	**1 vs.2=0.047** **3vs.4=0.021** **1vs.3**=0.986 **2vs.4**=0.715
Retrop. %	1.041±0.257	2.204±0.228	1.009±0.219	2.212±0.464	**1 vs.2=0.04** **3vs.4=0.03** **1vs.3**=0.959 **2vs.4**=0.985
Mesent. (g)	0.313±0.063	0.698±0.056	0.323±0.09	0.774±0.113	**1 vs.2=0.01** **3vs.4=0.003** **1vs.3**=0.947 **2vs.4**=0.487
Mesent. (%)	1.005±0.151	1.646±0.076	1.012±0.232	1.703±0.167	**1 vs.2=0.011** **3vs.4=0.005** **1vs.3**=0.978 **2vs.4**=0.752
IAT (g)	1.669±0.408	4.107±0.377	1.637±0.371	3.998±0.659	**1 vs.2=0.007** **3vs.4=0.007** **1vs.3**=0.972 **2vs.4**=0.865
IAT%	5.337±1.034	9.63±0.578	5.163±0.903	8.726±0.985	**1 vs.2=0.004** **3vs.4=0.012** **1vs.3**=0.909 **2vs.4**=0.394

Table 5.4.1.1.3 Regional internal fat depots mass from male mice fed a **NF** and a **HF** diet. Gonadal, retroperitoneal and mesenteric fat depots mass in grams (g), and normalised to current body weight and presented as percentage (%). IAT= internal adipose tissue mass as the sum of gonadal, retroperitoneal and mesenteric fat depots. Statistical analysis was performed using a one-way ANOVA test followed by a protected Fisher's least significant difference (LSD) post hoc analysis. Data presented as mean± SEM. **LBWm-NF** n=4; **LBWm-HF** n=10; **HBWm-NF** n=5, **HBWm-HF** n=6.

Evaluation of the total internal adipose tissue as the sum of the gonadal, retroperitoneal and mesenteric fat depots, showed a similar pattern as the total adipose tissue and regional fat depots. **HF** mice had the highest IAT (**LBWm-HF** vs. **LBWm-NF p=0.007**; **HBWm-HF** vs. **HBWm-NF p=0.007**) with no significant differences between both groups fed either a **HF** diet or a **NF** diet (**LBWm-NF** vs. **HBWm-NF** p=0.972; **LBWm-HF** vs. **HBWm-HF** p=0.865; table 5.4.1.1.3 and figure 5.4.1.1.2). Differences were maintained after normalisation to current body weight as percentage (table 5.4.1.1.3 and figure 5.4.1.1.3).

A comparison of the ratio of IAT to SAT tissue mass, showed not significant difference between groups (table 5.4.1.1.4).

	LBWm-NF$_1$	**LBWm-HF$_2$**	**HBWm-NF$_3$**	**HBWm-HF$_4$**	**P value**
IAT:SAT	1.047±0.666	1.094±0.049	1.078±0.048	1.165±0.078	**1 vs.2**=0.649 **3vs.4**=0.385 **1vs.3**=0.794 **2vs.4**=0.385

Table 5.4.1.1.4 Ratio of internal adipose tissue and subcutaneous adipose tissue from male mice fed a **NF** and a **HF** diet. IAT= Internal adipose tissue (as the sum of gonadal, retroperitoneal and mesenteric fat depots mass). Statistical analysis was performed using a one-way ANOVA test followed by a Tukey High significance difference (HSD) post hoc analysis. Data presented as mean± SEM. **LBWm-NF** n=4; **LBWm-HF** n=10; **HBWm-NF** n=5, **HBWm-HF** n=6.

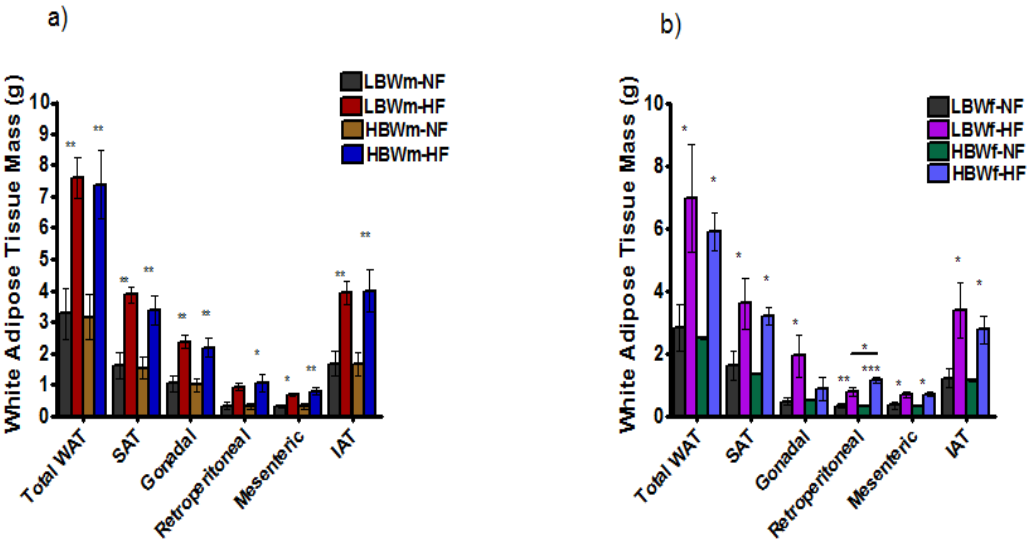

Figure 5.4.1.1.2 White adipose tissue mass from male and female mice fed a **NF** and a **HF** diet at week 51. Total WAT= total white adipose tissue, SAT=subcutaneous adipose tissue, IAT= internal adipose tissue as the sum of gonadal, retroperitoneal and mesenteric fat depots. Significant differences in the figure correspond to mice fed a **HF** diet against mice fed a **NF** diet (**LBWm/f-HF** vs. **LBWm/f-NF** and **HBWm/f-HF** vs. **HBWm/f-NF**). Differences between male mice fed a **NF** as between mice fed a **HF** diet were not significantly different a). In the female group, there was a significant difference in the retroperitoneal fat depots, which were significantly different between mice fed a **HF** diet (**LBWf-HF** vs. **HBWf-HF p=0.02**) b). Statistical analysis was performed using a one-way ANOVA test followed by a protected Fisher's least significant difference (LSD) post hoc analysis. Data presented as mean± SEM. **LBWm-NF** n=4; **LBWm-HF** n=10; **HBWm-NF** n=5, **HBWm-HF** n=6. * p≤0.05, ** p≤0.01; **LBWf-NF** n=4; **LBWf-HF** n=4; **HBWf-NF** n=4, **HBWf-HF** n=5.

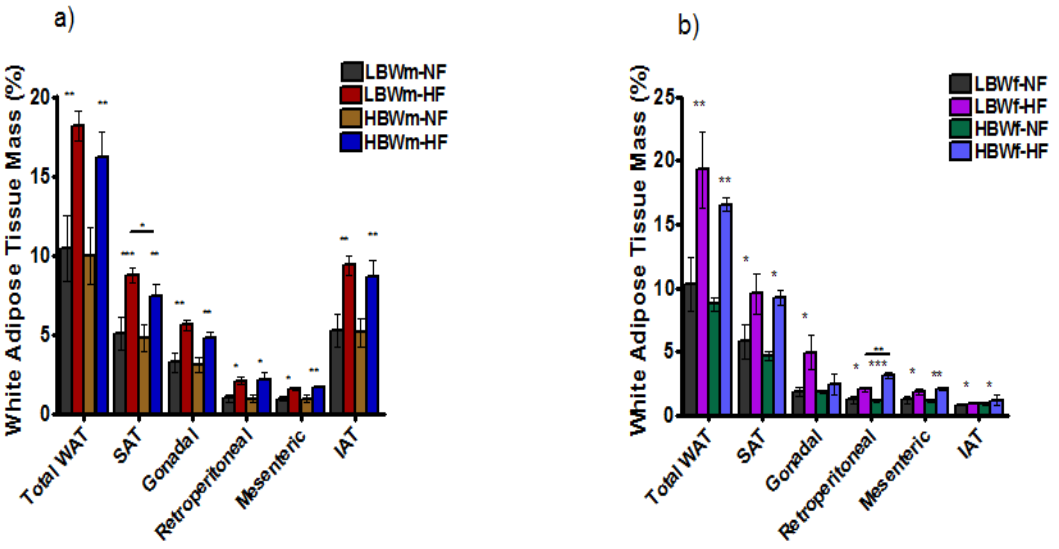

Figure 5.4.1.1.3 White adipose tissue mass normalised to current body weight (%) from male mice fed a **NF** and a **HF** diet at week 51. Total WAT= total white adipose tissue, SAT=subcutaneous adipose tissue, IAT= internal adipose tissue as the sum of gonadal, retroperitoneal and mesenteric fat depots. Significant differences in the figure correspond to mice fed a **HF** diet against mice fed a **NF** diet (**LBWm/f-HF** vs. **LBWm/f-NF** and **HBWm/f-HF** vs. **HBWm/f-NF**), except from gonadal fat between **HBWf-HF** vs. **HBWf-NF** b). Differences between male mice fed a **NF** as between mice fed a **HF** diet were not significantly different, except from SAT between **LBWm-HF** vs. **HBWm-HF** **p=0.035** a), as well as retroperitoneal fat depots in the female group b) which were significantly different between females fed a **HF** diet (**p=0.004**). Statistical analysis was performed using a one-way ANOVA test followed by a protected Fisher's least significant difference (LSD) post hoc analysis. Data presented as mean± SEM. **LBWm-NF** n=4; **LBWm-HF** n=11; **HBWm-NF** n=5, **HBWm-HF** n=6. * p≤0.05, ** p≤0.01, *** p≤0.001; **LBWf-NF** n=4; **LBWf-HF** n=4; **HBWf-NF** n=4, **HBWf-HF** n=5.

5.4.1.2 White adipose tissue mass in Female mice

Female mice assessment showed some differences in respect to male mice in body weights as well as for some of the fat depot masses at 51 weeks old. As in males, females fed a **HF** diet had a higher body weight but differences were only significant between **LBWf** mice (**LBWf-HF**=34.775±2.814g vs. **LBWf-NF**= 24.667±3.135g, **p=0.023**; **HBWf-HF**=35.475±2.322g vs. **HBWf-NF**=28.867±1.988g, p=0.109; figure 5.4.1.2.1). It was noticed that **HBWf-HF** started losing weight from week 42 in comparison to the other groups as mentioned in section 5.1 (figures 5.1.2.1 and 5.1.2.2). This weight loss seemed to reduce the significant difference between **HBWf**.

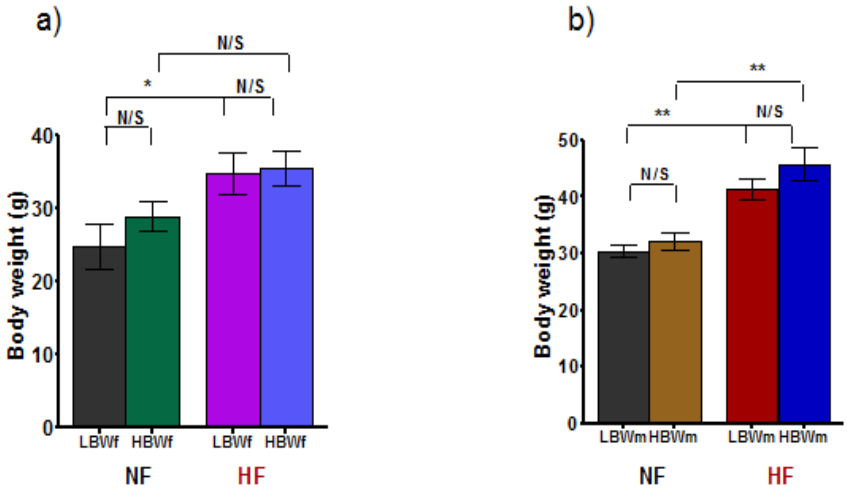

Figure 5.4.1.2.1 Body weight of female and male mice fed a **NF** and **HF** diet at week 51 of age. Statistical analysis was performed using a one-way ANOVA test followed by a protected Fisher's least significant difference (LSD) post hoc analysis. Data presented as mean± SEM. **LBWf-NF** n=4; **LBWf-HF** n=4; **HBWf-NF** n=4, **HBWf-HF** n=5; **LBWm-NF** n=4; **LBWm-HF** n=11; **HBWm-NF** n=5, **HBWm-HF** n=6. *p≤0.05, ** p≤0.01, N/S= no significant difference.

Total white adipose tissue mass in grams was significantly higher in **LBWf-HF** compared to **LBWf-NF** (**p=0.013**; table 5.4.1.2.1 an figure 5.4.1.2.2) and **HBWf-HF** compared to **LBWf-NF** (**p=0.05**; table 5.4.1.2.1 an figure 5.4.1.2.2). Differences between mice fed both **NF** and **HF** diets were not significantly different (**LBWf-NF** vs. **HBWf-NF** p=0.835; **LBWf- HF** vs. **HBWf-HF** p=0.319; table 5.4.1.2.1 and figure 5.4.1.2.2).

After normalisation to current body weight, total WAT remained significantly higher in **LBWf-HF** compared to **LBWf-NF** (**p=0.005**; table 5.4.1.2.1 and figure 5.4.1.2.3) and **HBWf-HF** vs. **HBWf-NF** (**p=0.014**; table 5.4.1.2.1 and figure 5.4.1.2.3). Mice fed a **NF** and **HF** did remain not significantly different (p=0.602 and 0.29 respectively).

	LBWf-NF_1	LBWf-HF_2	HBWf-NF_3	HBWf-HF_4	P value
Total WAT (g)	2.823±0.755	6.964±1.709	2.498±0.052	5.565±0.687	**1 vs.2=0.013** **3vs.4=0.05** **1vs.3=**0.835 **2vs.4=**0.319
Total WAT %	10.252±2.092	19.311±3	8.723±0.528	16.537±0.527	**1 vs.2=0.005** **3vs.4=0.014** **1vs.3=**0.602 **2vs.4=**0.29

Table 5.4.1.2.1 Total white adipose tissue mass from female mice fed a **NF** and a **HF** diet. Total WAT (g)= total white adipose tissue in grams, total WAT= total white adipose tissue mass normalised to current body weight and presented as percentage. Statistical analysis was performed using a one-way ANOVA test followed by a protected Fisher's least significant difference (LSD) post hoc analysis. Data presented as mean± SEM. **LBWf-NF** n=4; **LBWf-HF** n=4; **HBWf-NF** n=4, **HBWf-HF** n=5.

Subcutaneous adipose tissue in grams was, as in males, higher in mice fed a **HF** compared to mice fed a **NF** diet (**LBWf-HF** vs. **LBWf-NF p=0.021**; **HBWf-HF** vs. **HBWf-NF p=0.041**; table 5.4.1.2.2 and figure 5.4.1.2.2). **NF** fed female mice did not differed significantly (**LBWf-NF** vs. **HBWf-NF** p=0.744; table 5.4.1.2.2 and figure 5.4.1.2.2) as well as **HF** fed mice (**LBWf-HF** vs. **HBWf-HF** p=0.587; table 5.4.1.2.2 and figure 5.4.1.2.2).

After normalisation to current body weight, SAT % was again significantly different in mice fed a **HF** (**LBWf-HF** vs. **LBWf-NF p=0.039**; **HBWf-HF** vs. **HBWf-NF p=0.022**; table 5.4.1.2.2 and figure 5.4.1.2.3). **NF** fed female mice did not differed significantly (**LBWf-NF** vs. **HBWf-NF** p=0.529; table 5.4.1.2.2 and figure 5.4.1.2.3) as well as **HF** fed female mice (**LBWf-HF** vs. **HBWf-HF** p=0.868; table 5.4.1.2.2 and figure 5.4.1.2.3).

	LBWf-NF$_1$	LBWf-HF$_2$	HBWf-NF$_3$	HBWf-HF$_4$	P value
SAT (g)	1.6±0.474	3.597±0.475	1.338±0.024	3.183±0.288	**1 vs.2=0.021** **3vs.4=0.041** **1vs.3=**0.744 **2vs.4=**0.587
SAT %	5.802±1.354	9.542±1.551	4.683±0.348	9.269±0.601	**1 vs.2=0.039** **3vs.4=0.022** **1vs.3=**0.529 **2vs.4=**0.868

Table 5.4.1.2.2 Subcutaneous white adipose tissue (SAT) mass from female mice fed a **NF** and a **HF** diet. SAT (g)= subcutaneous adipose tissue in grams, SAT (%)= subcutaneous adipose tissue mass normalised to current body weight and presented as percentage. Statistical analysis was performed using a one-way ANOVA test followed by a protected Fisher's least significant difference (LSD) post hoc analysis. Data presented as mean± SEM. **LBWf-NF** n=4; **LBWf-HF** n=4; **HBWf-NF** n=4, **HBWf-HF** n=5.

Gonadal adipose tissue mass in female mice was lower compared to male mice in all the groups (tables 5.4.1.1.3 and 5.4.1.2.3 and figures 5.4.1.1.2 and 5.4.1.2.2). This fat depot mass was only significantly different between **LBWf-HF** vs. **LBWf-NF** (**p=0.046**). Moreover, the significance was maintained when normalising to current body weight (gonadal %; **p=0.045**). Although the difference between female mice fed was marginally significant, **LBWf-HF** had a two fold increase compared to **HBWf-HF** (**p=0.076**; table 5.4.1.2.3 and figure 5.4.1.2.3).

Retroperitoneal fat (g) was significantly higher in females fed a **HF** (**LBWf-HF** vs. **LBWf-NF p=0.009**; **HBWf-HF** vs. **HBWf-NF p<0.001**; table 5.4.1.2.3 and figure 5.4.1.2.2). Furthermore, there was a significant difference between those mice fed a **HF** diet with **LBWf-HF** having a lower fat depot compared to **HBWf-HF** (**p=0.02**; table 5.4.1.2.3 and figure 5.4.1.2.2). Mice fed a **NF** were not significantly different (**LBWf-NF** vs. **HBWf-NF** p=0.938). Similar differences were maintained after normalisation to current body weight (table 5.4.1.2.3 and figure 5.4.1.2.3).

Mesenteric adipose tissue was significantly different between diets in both grams and relative values (%), with a higher mass in those females fed a **HF** diet (in grams: **LBWf-HF** vs. **LBWf-NF p=0.017**; **HBWf-HF** vs. **HBWf-NF p=0.011**; table 5.4.1.2.3 and figure 5.4.1.2.2; as percentage: (**LBWf-HF** vs. **LBWf-NF p=0.032**; **HBWf-HF** vs. **HBWf-NF p=0.004**; table 5.4.1.2.3 and figure 5.4.1.2.3).

	LBWf-NF$_1$	LBWf-HF$_2$	HBWf-NF$_3$	HBWf-HF$_4$	P value
Gonadal (g)	0.473±0.134	1.92±0.663	0.516±0.028	0.876±0.296	**1 vs.2=0.046** **3vs.4**=0.584 **1vs.3**=0.951 **2vs.4**=0.107
Gonadal %	1.841±0.332	4.92±1.351	1.791±0.026	2.45±0.551	**1 vs.2=0.045** **3vs.4=0.635** **1vs.3**=0.973 **2vs.4=0.076**
Retrop. (g)	0.335±0.089	0.765±0.135	0.323±0.005	1.137±0.091	**1 vs.2=0.009** **3vs.4<0.001** **1vs.3**=0.938 **2vs.4=0.02**
Retrop. %	1.228±0.275	2.029±0.19	1.129±0.071	3.119±0.237	**1 vs.2=0.031** **3vs.4<0.001** **1vs.3**=0.786 **2vs.4=0.004**
Mesent. (g)	0.341±0.096	0.681±0.099	0.32±0.017	0.697±0.08	**1 vs.2=0.017** **3vs.4=0.011** **1vs.3**=0.879 **2vs.4**=0.89
Mesent. (%)	1.225±0.272	1.852±0.207	1.119±0.097	2.061±0.132	**1 vs.2=0.032** **3vs.4=0.004** **1vs.3**=0.715 **2vs.4**=0.413
IAT (g)	1.218±0.291	3.367±0.885	1.159±0.036	3.022±0.443	**1 vs.2=0.017** **3vs.4=0.045** **1vs.3**=0.944 **2vs.4**=0.659
IAT%	4.45±0.783	8.8±1.656	4.039±0.18	8.245±1.077	**1 vs.2=0.02** **3vs.4=0.028** **1vs.3**=0.82 **2vs.4**=0.724

Table 5.4.1.2.3 Regional internal fat depots mass from female mice fed a **NF** and a **HF** diet. Gonadal, retroperitoneal and mesenteric fat depots mass in grams (g), and normalised to current body weight and presented as percentage (%). IAT= internal adipose tissue mass as the sum of gonadal, retroperitoneal and mesenteric fat depots. Statistical analysis was performed using a one-way ANOVA test followed by a protected Fisher's least significant difference (LSD) post hoc analysis. Data presented as mean± SEM. **LBWf-NF** n=4; **LBWf-HF** n=4; **HBWf-NF** n=4, **HBWf-HF** n=5.

Evaluation of the total internal adipose tissue as the sum of the gonadal, retroperitoneal and mesenteric fat depots showed the diet had a major impact in the distribution of internal adipose. Female mice had the highest amount of IAT in both grams and as percentage of the current body weight (in grams: **LBWf-HF** vs. **LBWf-NF p=0.017**; **HBWf-HF** vs. **HBWf-NF p=0.045**; table 5.4.1.2.3 and figure 5.4.1.2.2; as percentage: (**LBWf-HF** vs. **LBWf-NF p=0.02**; **HBWf-HF** vs. **HBWf-NF p=0.028**; table 5.4.1.2.3 and figure 5.4.1.2.3).

A comparison of the ratio of IAT to SAT tissue mass between the female groups showed not significant difference (table 5.4.1.2.4).

	LBWf-NF$_1$	**LBWf-HF$_2$**	**HBWf-NF$_3$**	**HBWf-HF$_4$**	**P value**
IAT:SAT	0.802±0.062	0.918±0.055	0.866±0.024	0.84±0.177	**1 vs.2**=0.853 **3vs.4**=0.998 **1vs.3**=0.975 **2vs.4**=0.949

Table 5.4.1.2.4 Ratio of internal adipose tissue and subcutaneous adipose tissue from female mice fed a **NF** and a **HF** diet. IAT= Internal adipose tissue (as the sum of gonadal, retroperitoneal and mesenteric fat depots mass). Statistical analysis was performed using a one-way ANOVA test followed by a Tukey High significance difference (HSD) post hoc analysis. Data presented as mean± SEM. **LBWf-NF** n=4; **LBWf-HF** n=4; **HBWf-NF** n=4, **HBWf-HF** n=5.

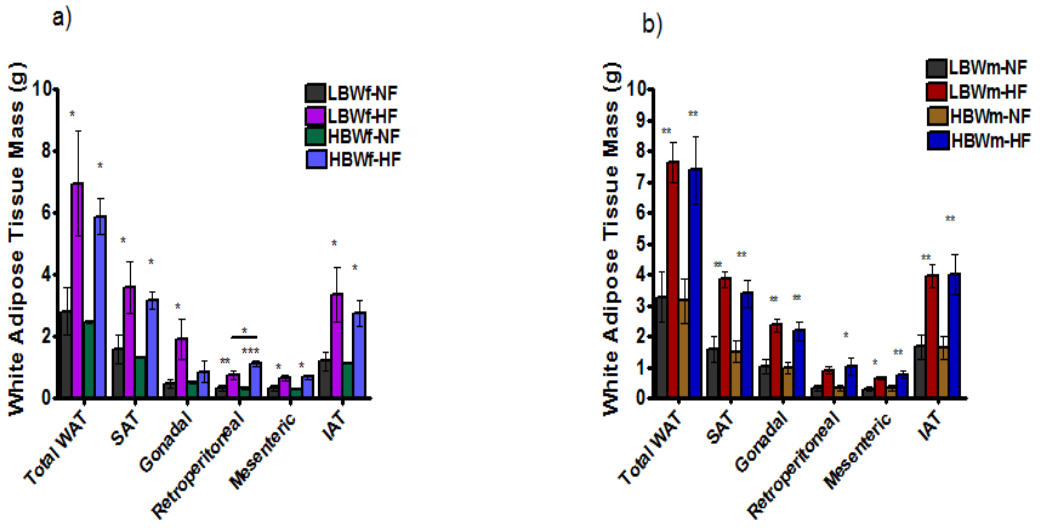

Figure 5.4.1.2.2 White adipose tissue mass from female and male mice fed a **NF** and a **HF** diet at week 51. Total WAT= total white adipose tissue, SAT=subcutaneous adipose tissue, IAT= internal adipose tissue as the sum of gonadal, retroperitoneal and mesenteric fat depots. Significant differences in the figure correspond to mice fed a **HF** diet against mice fed a **NF** diet (**LBWf/m-HF** vs. **LBWf/m-NF** and **HBWf/m-HF** vs. **HBWf/m-NF**), except from gonadal fat between **HBWf-HF** vs. **HBWf-NF** a). The differences between mice fed a **NF** as between mice fed a **HF** diet were not significantly different in female and male mice, except from retroperitoneal fat depots in the female group, which were significantly different between mice fed a **HF** diet (**p=0.02**). Statistical analysis was performed using a one-way ANOVA test followed by a protected Fisher's least significant difference (LSD) post hoc analysis. Data presented as mean± SEM. **LBWf-NF** n=4; **LBWf-HF** n=4; **HBWf-NF** n=4, **HBWf-HF** n=5; **LBWm-NF** n=4; **LBWm-HF** n=10; **HBWm-NF** n=5, **HBWm-HF** n=6. * p≤0.05, ** p≤0.01, *** p≤0.001.

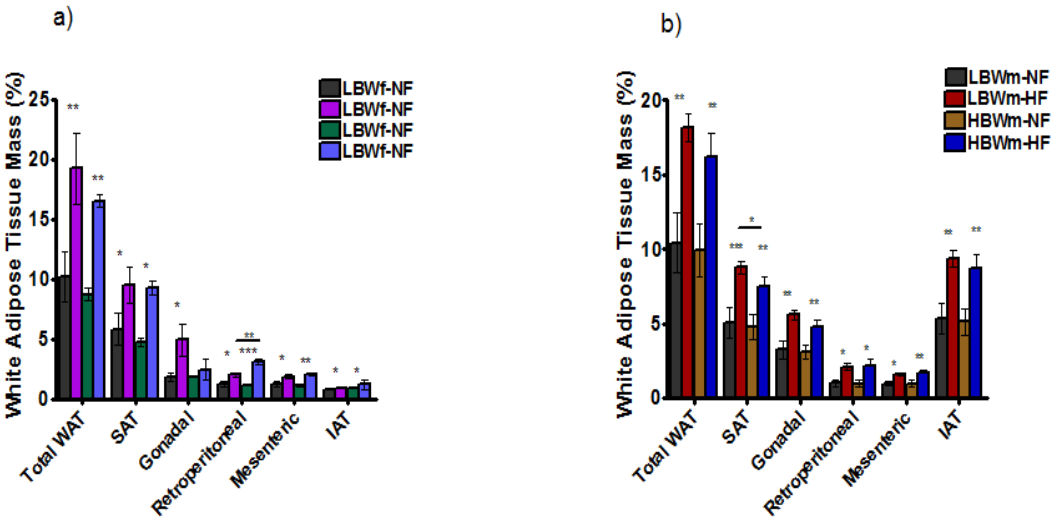

Figure 5.4.1.2.3 White adipose tissue mass normalised to current body weight (%) from female and male mice fed a **NF** and a **HF** diet at week 51. Total WAT= total white adipose tissue, SAT=subcutaneous adipose tissue, IAT= internal adipose tissue as the sum of gonadal, retroperitoneal and mesenteric fat depots. Significant differences in the figure correspond to mice fed a **HF** diet against mice fed a **NF** diet (**LBWf/m-HF** vs. **LBWf/m-NF** and **HBWf/m-HF** vs. **HBWf/m-NF**), except from gonadal fat between **HBWf-HF** vs. **HBWf-NF** a). The differences between mice fed a **NF** as between mice fed a **HF** diet were not significantly different, except from retroperitoneal fat depots, which were significantly different between female mice fed a **HF** diet (**p=0.004**) a) as well as SAT between **LBWm-HF** vs. **HBWm-HF p=0.035 b)**. Statistical analysis was performed using a one-way ANOVA test followed by a protected Fisher's least significant difference (LSD) post hoc analysis. Data presented as mean± SEM. **LBWf-NF** n=4; **LBWf-HF** n=4; **HBWf-NF** n=4, **HBWf-HF** n=5**; LBWm-NF** n=4; **LBWm-HF** n=11; **HBWm-NF** n=5, **HBWm-HF** n=6. * p≤0.05, ** p≤0.01, *** p≤0.001.

5.5 The Effects of Birth Weight and Diet on Adipocyte Size Distribution in Matured Mice (51 weeks old)

Subcutaneous and gonadal adipose tissues from male mice were subdivided at the time of collection: approximately 50-60mg of tissue were used for adipocyte extraction and the remained tissue was stored at -80°C for further analysis. Detailed information of the protocol can be found in section 2.4.6. Adipocyte distribution assessment was performed in males only.

Assessment of adipocyte number per gram of gonadal adipose tissue showed that mice fed a **HF** diet had a lower number of adipocytes per gram of tissue and no differences were seen between mice fed a **NF** diet (**LBWm-NF** vs. **LBWm-HF p=0.016**; **HBWm-NF** vs. **HBWm-HF p= 0.007**; **LBWm-NF** vs. **HBWm-NF** p=0.35; figure 5.5.1.1a). No differences were found between mice fed a **HF** diet (**LBWm-HF** vs. **HBWm-HF** p=0.384; figure 5.5.1a). This result may suggest that **HF** fed mice had bigger adipocytes per gram of tissue compared to the mice fed a **NF** diet and therefore, appears as having a lower number of cells per gram. However, when analysing cell number per fat depot, the significant difference disappeared as well as the pattern. Mice fed a **HF** diet had a higher adipocytes number compared to **NF** fed mice but there was not a statistical significance between groups (**LBWm-HF** vs. **LBWm-NF** p=0.265; **HBWm-HF** vs. **HBWm-NF** p=0.619; figure 5.5.1b).

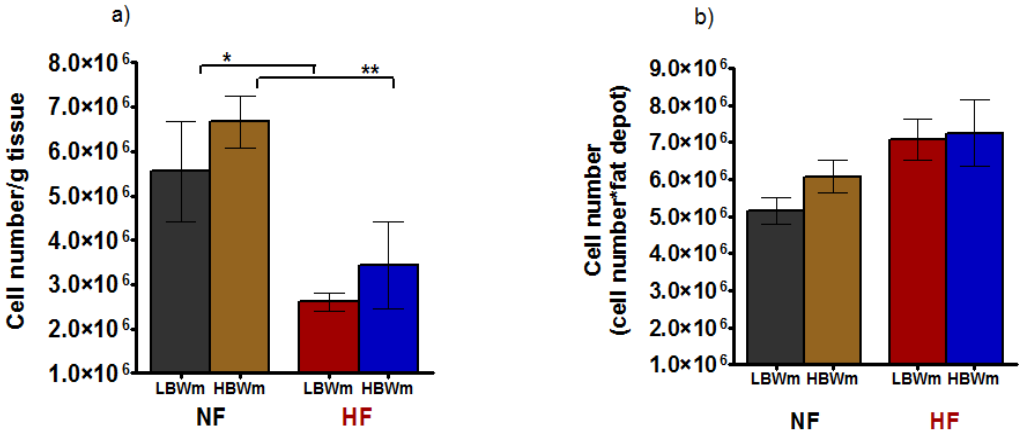

Figure 5.5.1 Adipocyte number in gonadal adipose tissue from male mice. Adipocyte number expressed as per gram of tissue extracted (adipocyte number/gram tissue) a), and multiply by the amount of total gonadal tissue per mouse per group b). Statistical analysis was performed using a one-way ANOVA test followed by a protected Fisher's least significant difference (LSD) post hoc analysis. Data presented as mean± SEM. **LBWm-NF** n=3; **LBWm-HF** n=6; **HBWm-NF** n=5, **HBWm-HF** n=6. * p≤0.05, ** p≤0.01.

Assessment of subcutaneous adipose tissue showed a different pattern. There was a significant difference between **HBWm** mice with **HBWm-NF** having a higher number of adipocytes than **HBWm-HF** (**HBWm-NF** vs. **HBWm-HF p=0.006**; figure 5.5.2a). No difference was seen between **LBWm** mice (**LBWm-NF** vs. **LBWm-HF** p=0.679; figure 5.5.2a) or between mice fed a **HF** diet (**LBWm-HF** vs. **HBWm-HF** p=0.143; figure 5.5.2a). **LBWm** mice had a higher number of adipocytes compared to **HBWm-NF** but the difference was marginally significant (**LBWm-NF** vs. **HBWm-NF** p=0.07; figure 5.5.2a).

Evaluation of subcutaneous adipose tissue per total amount of fat depot showed a similar pattern as seen in gonadal adipose tissue. Mice fed a **HF** diet had a higher adipocytes number compared to **NF** fed mice and the difference between **LBWm** mice was significant, whilst the difference between **HBWm** mice was marginally significant (**LBWm-HF** vs. **LBWm-NF** **p<0.001**; **HBWm-HF** vs. **HBWm-NF** p=0.061; figure 5.5.2b).

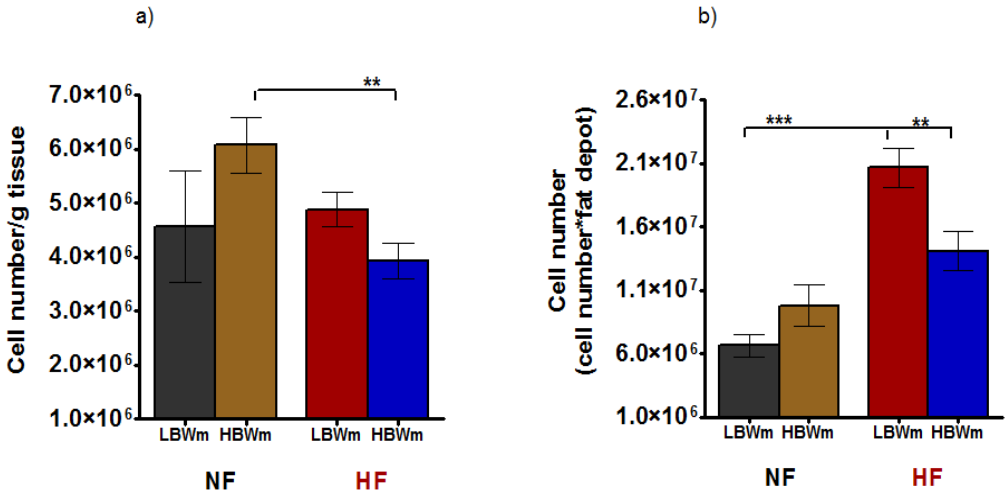

Figure 5.5.2 Adipocyte number in subcutaneous adipose tissue from male mice. Adipocyte number expressed as per gram of tissue extracted (adipocyte number/gram tissue) a), and multiply by the amount of total gonadal tissue per mouse per group b). Statistical analysis was performed using a one-way ANOVA test followed by a protected Fisher's least significant difference (LSD) post hoc analysis. Data presented as mean± SEM. **LBWm-NF** n=3; **LBWm-HF** n=6; **HBWm-NF** n=5, **HBWm-HF** n=6. ** p≤0.01,*** p≤0.001.

After assessing adipocyte number in both gonadal and subcutaneous adipose tissue, an analysis of the relative frequency of cell size distribution (%) was performed in order to see whether there was any difference in size between groups in both adipose tissues.

There was a general bimodal distribution (two separated populations) of cells in all groups when assessing gonadal adipose tissue. Assessment of the nadir showed that the nadir of **LBWm-NF** group was 48.667± 3.167μm whilst the nadir of **LBWm-HF** group was 71±2.449μm (**p=0.001;** figure 5.5.3a). **HBWm-NF** mice had a significantly lower nadir than **HBWm-HF** (**HBWm-NF** =46.25±3.146μm vs. **HBWm-HF**= 60±5μm, **p=0.018;** figure 5.5.3b) but it was similar nadir as **LBWm-NF** mice (p=0.662; figure 5.5.3c). **HBWm-HF** nadir was significantly lower than **LBWm-HF** mice (**p=0.039**; figure 5.5.3d).

The percentages of cells below the nadir were designated as small adipocytes and above the nadir as the large adipocytes. **LBWm-HF** mice had the highest percentage of adipocytes below the nadir (44.718±3.801%) and it was significantly different when compared to **LBWm-NF** (14.172±2.831%; **p<0.001**; figure 5.5.3a) and against **HBWm-HF** mice (24.713±3.225%, **p<0.001**; figure 5.5.3d). Moreover, **HBWm-HF** had a higher percentage of adipocytes below the nadir than **HBWm-NF** (9.999±0.484%; **p=0.008**; figure 5.5.3b). No differences were found between mice fed a **NF** diet (p=0.45; figure 5.5.3c).

The small to large adipocytes ratio was higher in mice fed a **HF** diet than mice fed a **NF** diet (**LBWm-HF**=0.965±0.161 vs. **LBWm-NF**=0.16±0.029, **p=0.014**; **HBWm-HF**= 0.256±0.077 vs. **HBWm-NF**=0.115±0.005, **p=0.046**). At the same time, **LBWm-HF** had a significantly higher ratio than **HBWm-HF** (**p=0.023**).

It was noticed that the peak diameter of large adipocytes in mice fed a **HF** diet was shifted to the right when compared to the mice fed a **NF** diet (**LBWm-HF**=105μm vs. **LBWm-NF**=88.333±3.333μm, **p<0.001**; figure 5.5.3a; **HBWm-HF**= 105μm vs. **HBWm-NF**=87.5±2.5μm, **p<0.001**; figure 5.5.3b). This means that a **HF** diet increased the diameter of adipocytes in mice at the same time that had a higher number of small adipocytes. No differences were seen between mice fed a **NF** diet or a **HF** (**LBWm-NF** vs. **HBWm-NF** p=0.746; figure 5.5.3c; **LBWm-HF** vs. **HBWm-HF** p=1.0; figure 5.5.3d).

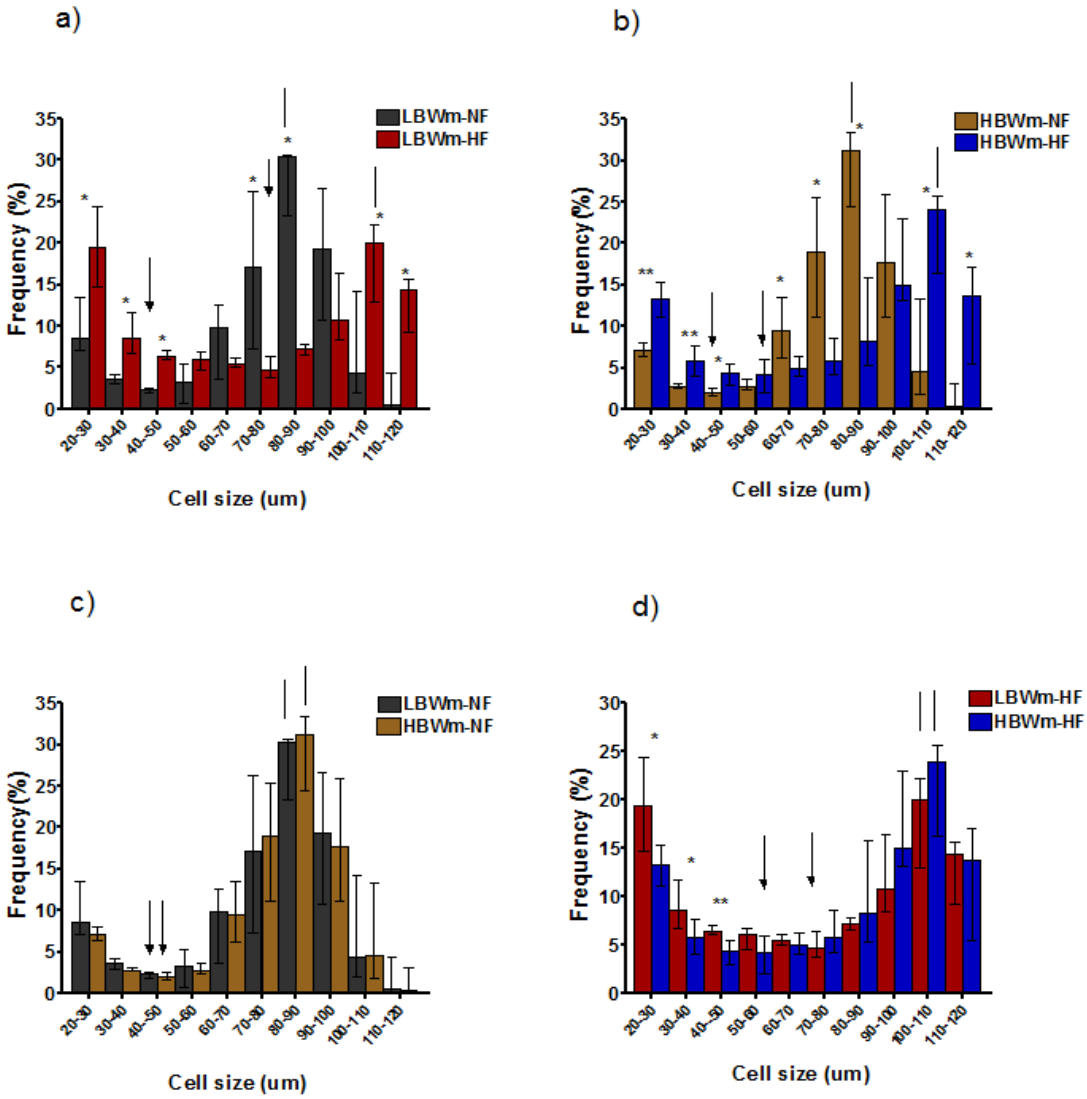

Figure 5.5.3 Frequency distribution (%) of adipocytes extracted from gonadal adipose tissue from male mice fed both a **NF** and **HF** diet. Arrowheads indicate the nadir of each group, which corresponds to the lowest point between two populations of adipocytes (small-large adipocytes). Headless arrows indicate the peak diameter of large adipcoytes in each group. Statistical analysis was performed using a *Kruskal-Wallis* test followed by a Mann-Whitney test for range analysis. Data presented as median with interquartile range (25%-75%). **LBWm-NF** n=3; **LBWm-HF** n=6; **HBWm-NF** n=5, **HBWm-HF** n=6. * p≤0.05,**p≤0.01.

Analysis of the relative frequency of cell size distribution (%) of subcutaneous adipose showed a general bimodal distribution (two separated populations) of adipocytes in all groups as it was seen in gonadal adipose tissue. Assessment of the nadir showed no differences between different diets (**LBWm-NF**=38.333± 3.333µm vs. **LBWm-HF**= 45±3.087µm (p=0.412; figure 5.5.4a; **HBWm-NF**=43±2µm vs. **HBWm-HF**=43.333±1.666µm, p=0.999; figure 5.5.4b) or between different birth weights (**LBWm-NF** vs. **HBWm-NF** p=0.723; figure 5.5.4c; **LBWm-HF** vs. **HBWm-HF** p=0.96; figure 5.5.4d).

The percentages of cells below the nadir (small adipocytes) was no different between diets (**LBWm-NF**=18.044± 3.39% vs. **LBWm-HF**= 21.676±3.15% (p=0.872; figure 5.5.4a; **HBWm-NF**=12.747±1.339% vs. **HBWm-HF**=16.122±1.605%, p=0.874; figure 5.5.1.4b) or between different birth weights (**LBWm-NF** vs. **HBWm-NF** p=0.753; figure 5.5.4c; **LBWm-HF** vs. **HBWm-HF** p=0.496; figure 5.5.4d).

The small to large adipocytes ratio was no different between groups (**LBWm-NF**=0.228± 0.051 vs. **LBWm-HF**= 0.309±0.593, p=0.789; **HBWm-NF**=0.202±0.052 vs. **HBWm-HF**=0.2104±0.109, p=0.999; **LBWm-NF** vs. **HBWm-NF** p=0.993; **LBWm-HF** vs. **HBWm-HF** p=0.517).

Assessment of the peak diameter of large adipocytes showed a similar pattern as seen in the gonadal fat. The peak diameter of large adipocytes in mice fed a **HF** diet was shifted to the right when compared to the mice fed a

NF diet (**LBWm-HF**=87.857±5.654μm vs. **LBWm-NF**=58.333±4.409μm, **p<0.001**; figure 5.5.4a; **HBWm-HF**= 90±2.236μm vs. **HBWm-NF**=65μm, **p=0.001**; figure 5.5.4b). This means that a **HF** diet increased the diameter of adipocytes in mice but contrary to gonadal adipose tissue, it was not accompanied by a higher number of small adipocytes. No differences were seen between mice fed a **NF** diet or a **HF** (**LBWm-NF** vs. **HBWm-NF** p=0.361; figure 5.5.4c; **LBWm-HF** vs. **HBWm-HF** p=0.697; figure 5.5.4d).

A further investigation on the differences between subcutaneous and gonadal fat adipocytes distribution within the same groups showed that subcutaneous adipose tissue nadir was higher in most of the groups in respect to gonadal adipose tissue (figures 5.5.5). Only **HBWm-NF** had a similar nadir in both fat depots (figures 5.5.5c).

Comparisons of percentages between gonadal and subcutaneous fat showed a significantly lower percentage of small cells in the subcutaneous fat of **LBWm-HF** mice compared to gonadal fat (21.676±3.15% vs. 44.718±3.801% **p=0.001;** figure 5.5.5b). The difference between **HBWm-HF** subcutaneous and gonadal fat depots was marginally significant (16.122±1.605% vs. 24.713±3.225% respectively, p=0.082; figure 5.5.5d). No differences were found between **LBWm-NF** subcutaneous and gonadal fat depots (18.044± 3.39% vs. 14.172±2.831% respectively, p=0.43; figure 5.5.5a) or between **HBWm-NF** fat depots (12.747±1.339% vs. 9.999±0.484%, p=0.15; figure 5.5.5c).

LBWm-HF subcutaneous adipocytes ratio (small to large adipocytes ratio) was significantly lower compared to the gonadal ratio (0.309±0.059 vs. 0.965±0.161 respectively). This means that there were a higher number of small adipocytes in the gonadal fat of this group compared to their subcutaneous fat. No differences were seen between both fat depots within the others groups (**LBWm-NF** subcutaneous cell ratio: 0.228±0.051 vs. gonadal cell ratio: 0.16±0.029**,** p=0.311; **HBWm-NF** subcutaneous adipocytes ratio: 0.202 ±0.052 vs. gonadal cell ratio: 0.115±0.005, p=0.186; **HBWm-HF** subcutaneous adipocytes ratio: 0.2104±0.045 vs. gonadal adipocytes ratio: 0.256±0.077, p=0.451).

Interestingly, the peak diameter of large adipocytes in subcutaneous adipose tissue was significantly lower compared to the peak of large adipocytes in gonadal adipose tissue within the groups (**LBWm-NF** subcutaneous large adipocytes peak: 58.333±4.409µm vs. gonadal large adipocytes peak: 88.333±3.333µm**, p=0.006;** figure 5.5.1.5a; **HBWm-NF** subcutaneous large adipocytes peak: 65µm vs. gonadal large adipocytes peak: 87.5±2.5µm, **p=0.003;** figure 5.5.5c; **LBWm-HF** subcutaneous large adipocytes peak: 93.333±1.666µm vs. gonadal large adipocytes peak: 105µm, **p=0.001;** figure 5.5.5b; **HBWm-HF** subcutaneous large adipocytes peak: 90±2.236µm vs. gonadal large adipocytes peak: 105µm, **p=0.001;** figure 5.5.5d).

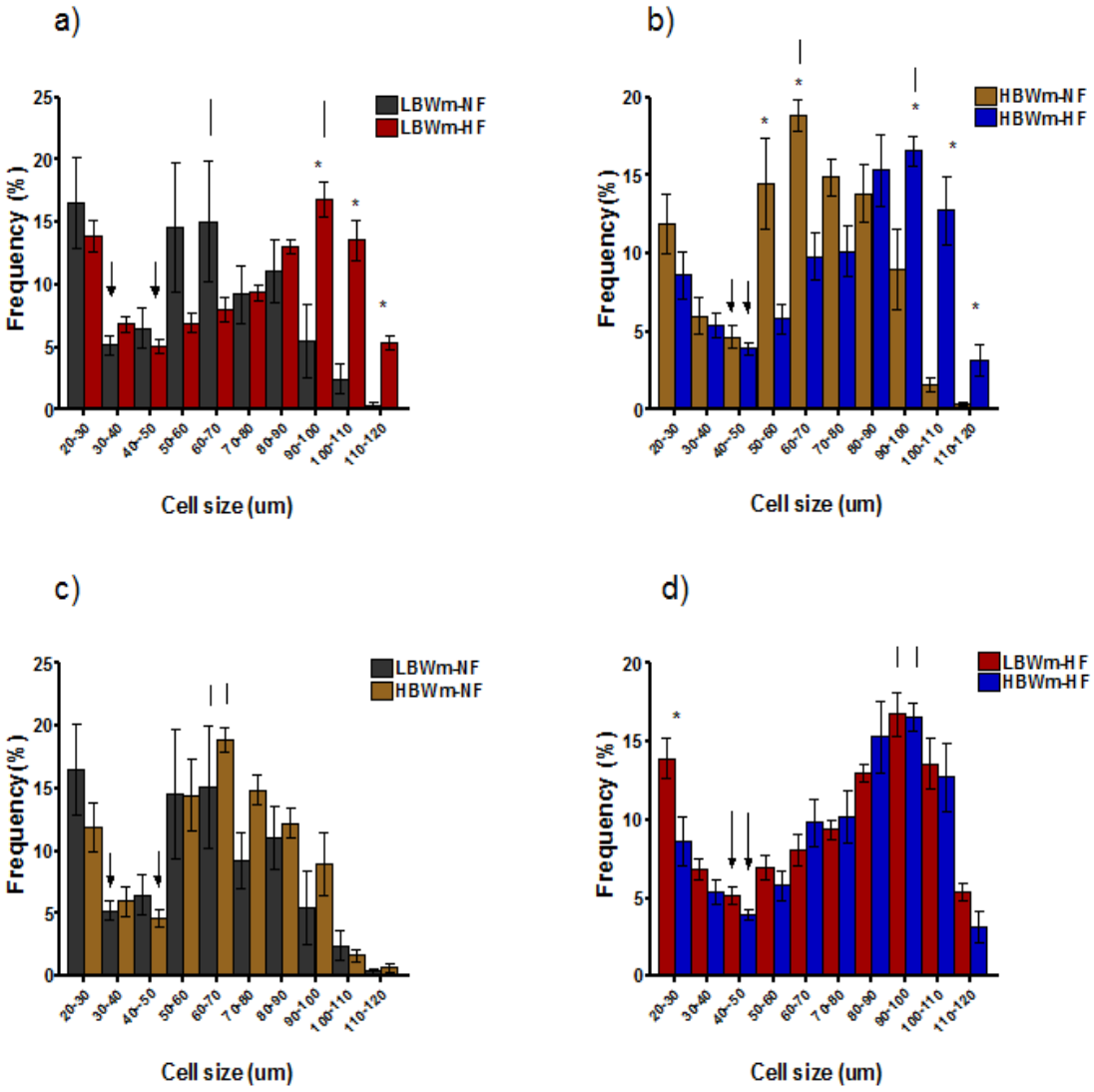

Figure 5.5.4 Frequency distribution (%) of adipocytes extracted from subcutaneous adipose tissue from male mice fed both a **NF** and **HF** diet. Arrowheads indicate the nadir of each group, which corresponds to the lowest point between two populations of cells (small-large adipocytes). Headless arrows indicate the peak diameter of large adipocytes in each group. Statistical analysis was performed using a *Kruskal-Wallis* test followed by a Mann-Whitney test for range analysis. Data presented as median with interquartiles range (25%-75%). **LBWm-NF** n=3; **LBWm-HF** n=6; **HBWm-NF** n=5, **HBWm-HF** n=6. * p≤0.05,**p≤0.01.

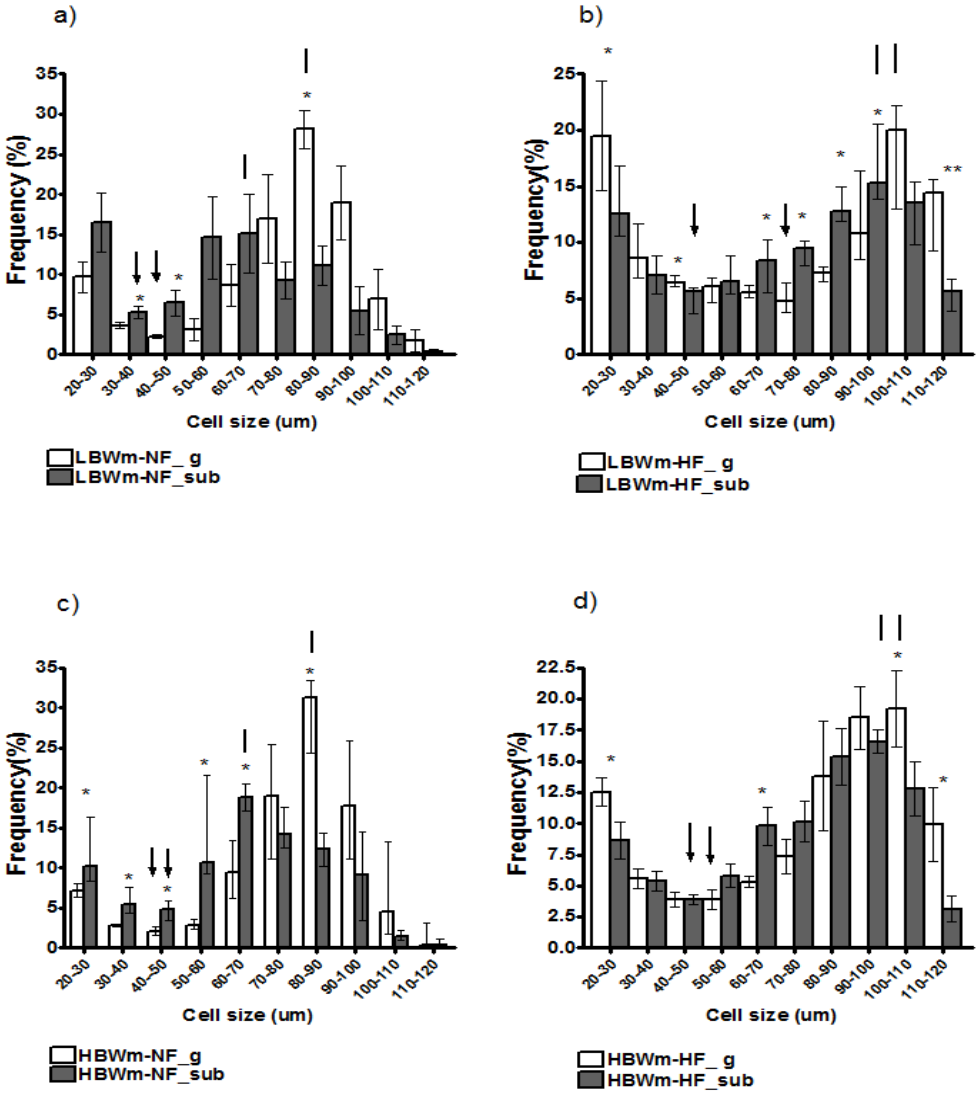

Figure 5.5.5 Frequency distribution (%) of adipocytes extracted from gonadal and subcutaneous adipose tissue of male mice fed both a **NF** and **HF** diet. Arrowheads indicate the nadir of each group, which corresponds to the lowest point between two populations of cells (small-large adipocytes). Headless arrows indicate the peak diameter of large adipcytes in each group. g= gonadal fat tissue, sub=subcutaneous adipose tissue. Statistical analysis was performed using a *Kruskal-Wallis* test followed by a Mann-Whitney test for range analysis. Data presented as median with interquartiles range (25%-75%). **LBWm-NF** n=3; **LBWm-HF** n=6; **HBWm-NF** n=5, **HBWm-HF** n=6. * p≤0.05, **p≤0.01.

5.6 The Effects of Birth Weight and Diet on Metabolic Markers in Matured Mice (51 weeks old)

Plasma samples were used to assess metabolic markers in both male and female mice at week 51 after 36 weeks of dietary intervention. Samples were collected in a postprandial state.

5.6.1 Metabolic markers in Male mice

Whole blood glucose levels were similar between all the groups, although a marginal difference was seen between **HBWm** mice: **HBWm-HF=** 11.42 ±0.591mmol/L, **HBWm-NF**=9.933 ±0.569mmol/L p=0.067; **LBWm-HF**=11.237 ±0.244mmol/L vs. **LBWm-NF**=10.167 ±0.775mmol/L p=0.586; **LBWm-NF** vs. **HBWm-NF** p=0.785; **LBWm-HF** vs. **HBWm-HF** p=0.76.

Markers related to insulin secretion and insulin stimulation/regulation such as C-peptide, GIP and glucagon were not significantly different between groups (figure 5.6.1.1 and table 5.6.1.1). However, natural log values of insulin concentration in plasma were significantly different between **HBWm** mice only**: HBWm-NF** vs. **HBWm-HF p=0.035** (figure 5.6.1.1 and table 5.6.1.1).

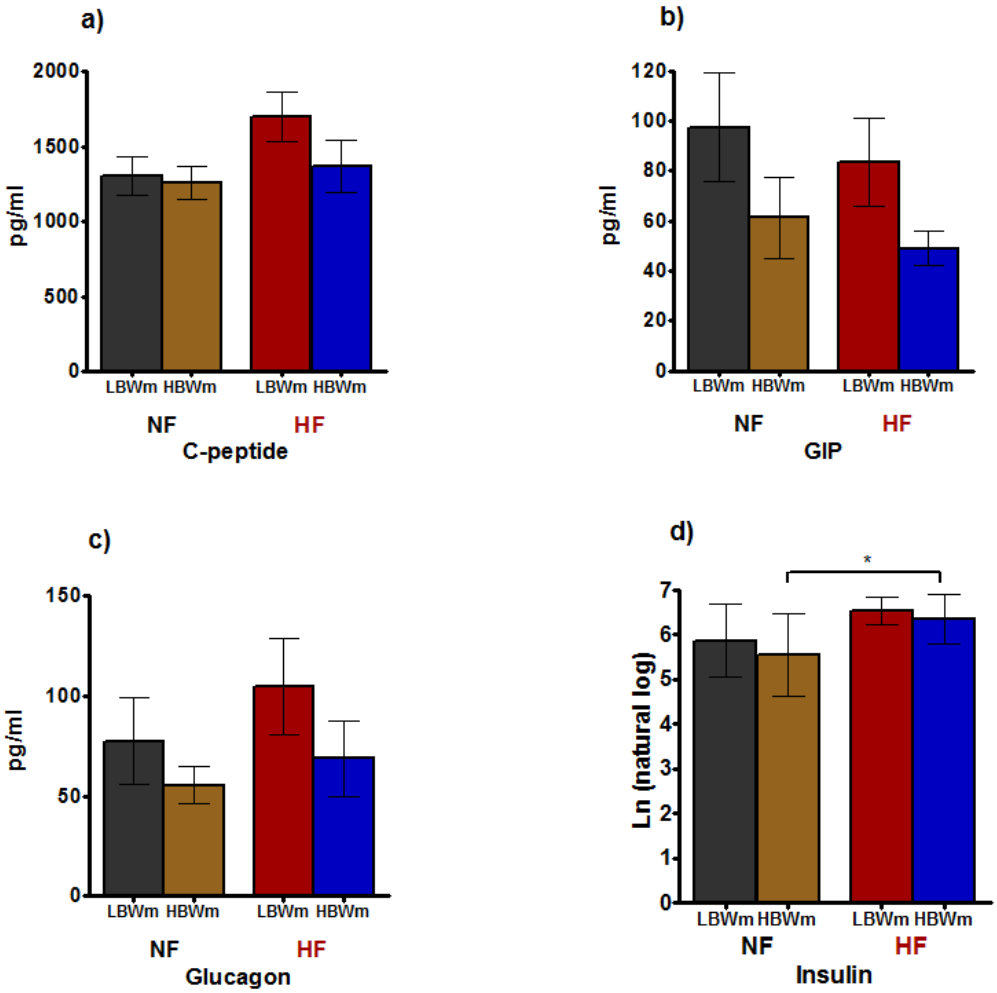

Figure 5.6.1.1 Metabolic markers in plasma from male mice fed both a **NF** and **HF** diet. This figure shows some metabolic markers related to insulin secretion and stimulation/regulation such as c-peptide a), GIP b) and glucagon c), as well as levels of insulin in plasma. Insulin values were positively skewed for some of the groups and therefore, the data was natural log transformed before the analysis. Results for Ln (natural log) insulin are presented as mean with 95% confidence interval (CI). Statistical analysis was performed using a one-way ANOVA test followed by a protected Fisher's least significant difference (LSD) post hoc analysis for c-peptide, GIP and glucagon. Data presented as mean± SEM. **LBWm-NF** n=4; **LBWm-HF** n=9; **HBWm-NF** n=4, **HBWm-HF** n=6. *p≤0.05.

The gut peptide ghrelin was affected by the different diet given to the mice; male mice fed **NF** had a higher ghrelin concentration in plasma compared to the male mice fed a **HF** diet. **LBWm-NF** vs. **LBWm-HF** **p=0.016**; **HBWm-NF** vs. **HBWm-HF** **p=0.013**. Differences were similar between groups of different that were fed the same diet **LBWm-NF** vs. **HBWm-NF** p=0.491; **LBWm-HF** vs. **HBWm-HF** p=0.286 (figure 5.6.1.2 and table 5.6.1.1).

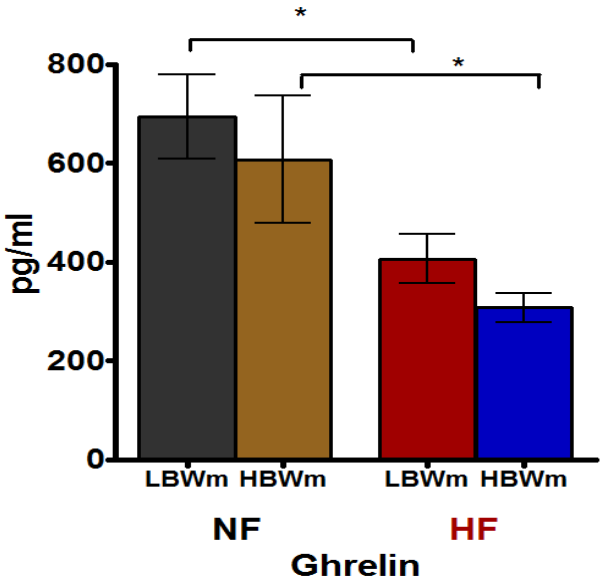

Figure 5.6.1.2 Ghrelin levels in plasma from male mice fed both a **NF** and **HF** diet. Statistical analysis was performed using a one-way ANOVA test followed by a protected Fisher's least significant difference (LSD) post hoc analysis. Data presented as mean± SEM. **LBWm-NF** n=4; **LBWm-HF** n=9; **HBWm-NF** n=4, **HBWm-HF** n=6. *p≤0.05.

Adipokines such as leptin and resistin were generally higher in mice fed **HF** but only reached significance between **LBWm** mice: (leptin: **LBWm-HF** vs. **LBWm-NF p=0.022**; **HBWm-HF** vs. **HBWm-NF** p=0.072; resistin: **LBWm-HF** vs. **LBWm-NF p=0.033**; **HBWm-HF** vs. **HBWm-NF** p=0.837; figure 5.6.1.3 and table 5.6.1.1). Resistin was marginally significant between mice fed a **HF** diet, with **LBWm-HF** having a higher level compared to **HBWm-HF** (p=0.064 figure 5.6.1.3 and table 5.6.1.1).

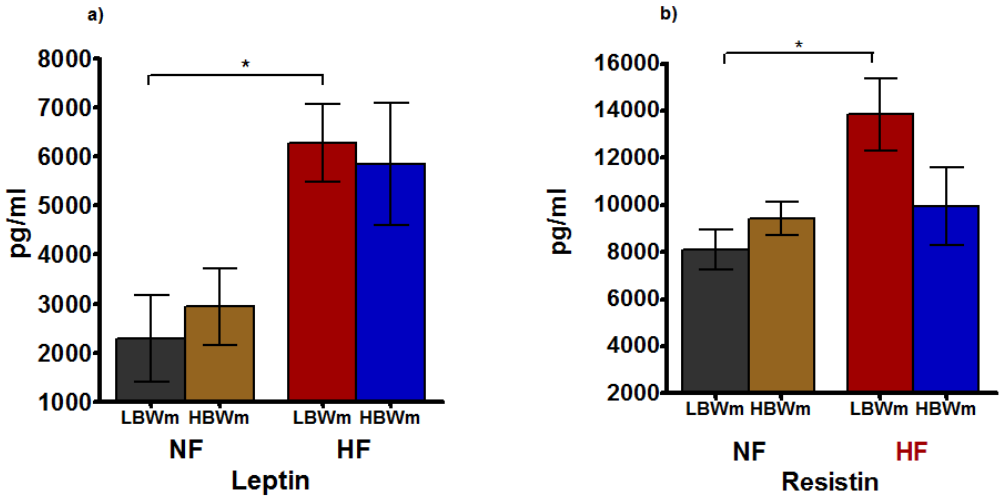

Figure 5.6.1.3 Leptin and resistin levels in plasma from male mice fed both a **NF** and **HF** diet. Statistical analysis was performed using a one-way ANOVA test followed by a protected Fisher's least significant difference (LSD) post hoc analysis. Data presented as mean± SEM. **LBWm-NF** n=4; **LBWm-HF** n=9; **HBWm-NF** n=4, **HBWm-HF** n=6. *p≤0.05.

Proinflammatory cytokines markers such as IL-6 and MCP-1 were also assessed. IL-6 was higher in mice fed a HF but the differences only reached significance between **HBWm** mice. Moreover, **HBWm-HF** mice had a higher level of IL-6 compared to **LBWm-HF** mice (**HBWm-HF** vs. **HBWm-NF** **p<0.001**; **LBWm-HF** vs. **LBWm-NF** p=0.445; **HBWm-HF** vs. **LBWm-HF** **p=0.017** figure 5.6.1.4 and table 5.6.1.1). MCP-1 did not differed significantly between groups (figure 5.6.1.4 and table 5.6.1.1).

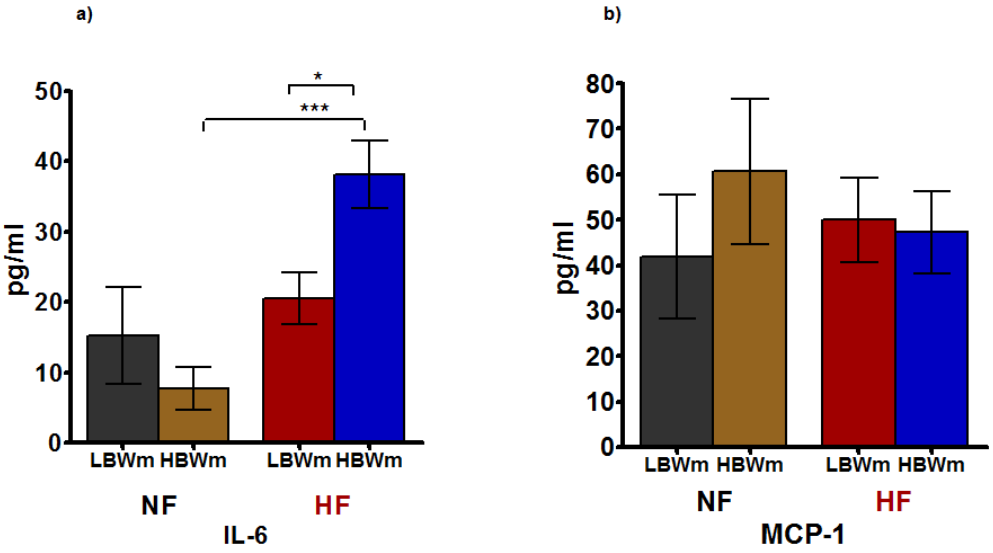

Figure 5.6.1.4 Proinflammatory markers in plasma from male mice fed both a **NF** and **HF** diet. Statistical analysis was performed using a one-way ANOVA test followed by a protected Fisher's least significant difference (LSD) post hoc analysis. Data presented as mean± SEM. **LBWm-NF** n=4; **LBWm-HF** n=9; **HBWm-NF** n=4, **HBWm-HF** n=6. *p≤0.05,***p≤0.001.

	LBWm-NF$_1$	LBWm-HF$_2$	HBWm-NF$_3$	HBWm-HF$_4$	P value
C-peptide pg/ml	1303.034 ±131.658	1696.258 ±164.892	1260.298 ±110.689	1368.484 ±173.369	**1 vs.2**=0.504 **3vs.4**=0.977 **1vs.3**=0.331 **2vs.4**=0.46
GIP pg/ml	97.46 ±21.852	83.784 ±17.606	61.433 ±16.247	49.065 ±7.034	**1 vs.2**=0.959 **3vs.4**=0.97 **1vs.3=**0.673 **2vs.4**=0.46
Glucagon pg/ml	77.456 ±21.81	104.905 ±24.273	55.439 ±9.258	69.947 ±18.817	**1 vs.2**=0.882 **3vs.4**=0.984 **1vs.3=**0.955 **2vs.4**=0.665
Insulin (Ln)	5.863 (5.042-6.685)	6.528 (6.22-6.84)	5.257 (3.108-7.406)	6.367 (5.817-6.448)	**1 vs.2**=0.098 **3vs.4=0.035** **1vs.3**=0.466 **2vs.4**=0.605
Ghrelin pg/ml	693.819 ±85.577	406.148 ±49.611	607.407 ±129.488	307.234 ±29.452	**1 vs.2=0.016** **3vs.4=0.013** **1vs.3**=0.491 **2vs.4**=0.286
Leptin pg/ml	2284.774 ±873	6271.472 ±794.119	2935.85 ±777.344	5840.955 ±851.068	**1 vs.2=0.022** **3vs.4**=0.072 **1vs.3**=0.721 **2vs.4**=0.738
Resistin pg/ml	8092.363 ±862.868	13831.979 ±1545.701	9432.845 ±703.675	9924.049 ±1657.524	**1 vs.2=0.033** **3vs.4**=0.837 **1vs.3**=0.637 **2vs.4=0.064**
Il-6 pg/ml	15.266 ±6.285	21.773 ±4.209	7.702 ±3.059	38.149 ±4.865	**1 vs.2**=0.445 **3vs.4<0.001** **1vs.3**=0.393 **2vs.4=0.017**
MCP-1 pg/ml	41.948 ±13.658	49.997 ±9.339	47.696 ±18.757	47.26 ±9.089	**1 vs.2**=0.971 **3vs.4**=0.999 **1vs.3**=0.992 **2vs.4**=0.998

Table 5.6.1.1 Metabolic markers measured in plasma from male mice fed both a **NF** and a **HF** diet at week 51 of age. GIP= glucose dependant- insulinotropic peptide, IL6= interleukine 6, MCP-1= monocyte chemotactic peptide 1. Insulin values were positively skewed for some of the groups and therefore, the data was natural log transformed before the analysis. Results for Ln (natural log) insulin are presented as mean with 95% confidence interval (CI). Statistical analysis was performed using a one-way ANOVA test followed by a protected Fisher's least significant difference (LSD) post hoc analysis. Data presented as mean± SEM. **LBWm-NF** n=4; **LBWm-HF** n=9; **HBWm-NF** n=4, **HBWm-HF** n=6.

5.6.2 Metabolic markers in Female mice

Female mice had significant differences between groups. **LBWf** mice had significantly higher levels of glucose than **HBWf** mice fed a **NF** diet (**LBWf-NF=** 9.65±0.328mmol/L vs. **HBWf-NF=** 6.767±1.197mmol/L **p=0.04**) but differences did not reach significance between females fed a **HF** diet (**LBWf-HF**=10.733±0.338mmol/L vs. **HBWf-HF**=9.35±0.3778mmol/L, p=0.203). Also, although diet affected **HBWf** mice (**HBWf-HF** vs. **HBWf-NF**, **p=0.028**), it did not affect **LBWf** mice (**LBWf-HF**=10.733±0.338mmol/L vs. **LBWf-NF**=9.65±0.328mmol/L p=0.11).

C-peptide levels and GIP were not significantly different between groups (figure 5.6.2.1a-b and table 5.6.2.1). However, the plasmatic levels of glucagon were significantly higher in **LBWf-NF** mice compared to **HBWf-NF** mice (**p=0.009**; figure 5.6.2.1c and table 5.6.2.1) and in the **HBWf-HF** mice compared to **HBWf-NF** mice (**p=0.012**; figure 5.6.2.1c and table 5.6.2.1). These significances were not seen between male groups (figure 5.6.1.1 and table 5.6.1.1). Insulin was not significantly different between groups (figure 5.6.2.1d and table 5.6.2.1). In the male group there was a significant difference between **HBWm** mice (figure 5.6.1.1d and table 5.6.1.1), whilst **HBWf** mice tended to have a very similar level of insulin.

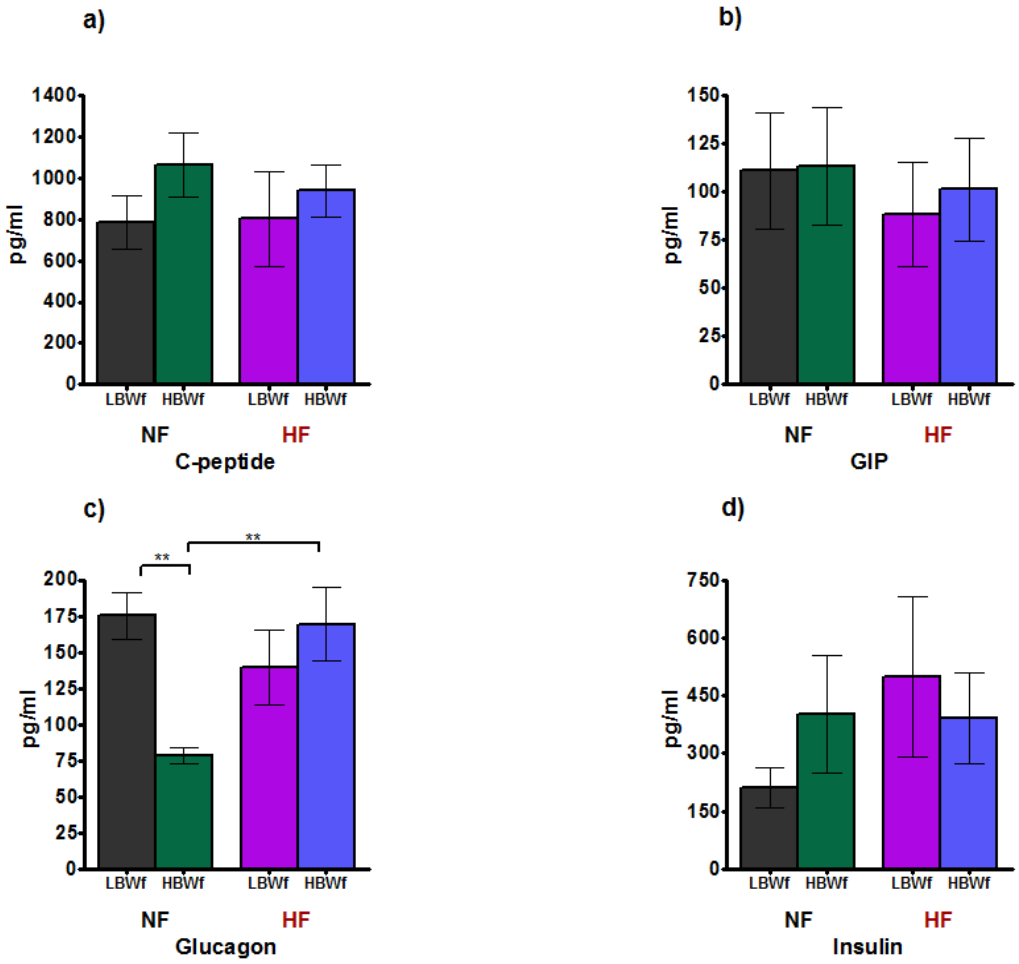

Figure 5.6.2.1 Metabolic markers in plasma from female mice fed both a **NF** and **HF** diet. This figure shows some metabolic markers related to insulin secretion and stimulation/regulation such as c-peptide a), GIP b) and glucagon c), as well as levels of insulin in plasma. Statistical analysis was performed using a one-way ANOVA test followed by a protected Fisher's least significant difference (LSD) post hoc analysis. Data presented as mean± SEM. **LBWf-NF** n=4; **LBWf-HF** n=3; **HBWf-NF** n=4, **HBWf-HF** n=5. **p≤0.01.

The gut peptide ghrelin was not significantly different between groups. However, levels between **HBWf-NF** vs. **HBWf-HF** were marginally significant (p=0.068; figure 5.6.2.2 and table 5.6.2.1). The pattern seen between the female groups was similar to that seen between the male groups, but differences were more marked between males (figure 5.6.1.2 and table 5.6.1.1).

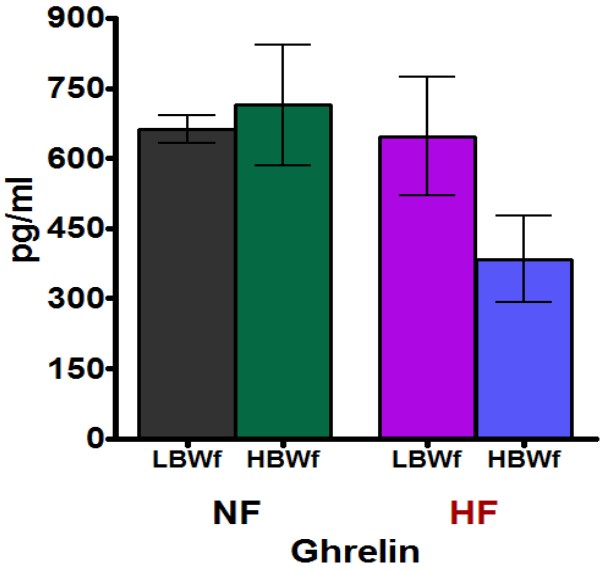

Figure 5.6.2.2 Ghrelin levels in plasma from female mice fed both a **NF** and **HF** diet. Statistical analysis was performed using a one-way ANOVA test followed by a protected Fisher's least significant difference (LSD) post hoc analysis. Data presented as mean± SEM. **LBWf-NF** n=4; **LBWf-HF** n=3; **HBWf-NF** n=4, **HBWf-HF** n=5.

Leptin was significantly different between female mice fed a **NF** diet with a higher level in **LBWf-NF** mice compared to **HBWf-NF** mice (**p=0.044;** figure

5.6.2.3a and table 5.6.2.1). Differences were also significantly different between **HBWf** mice (**HBWf-NF** vs. **HBWf-HF** **p=0.013** figure 5.6.2.3a and table 5.6.2.1). Resistin was not statistically significant between groups (figure 5.6.2.3b and table 5.6.2.1).

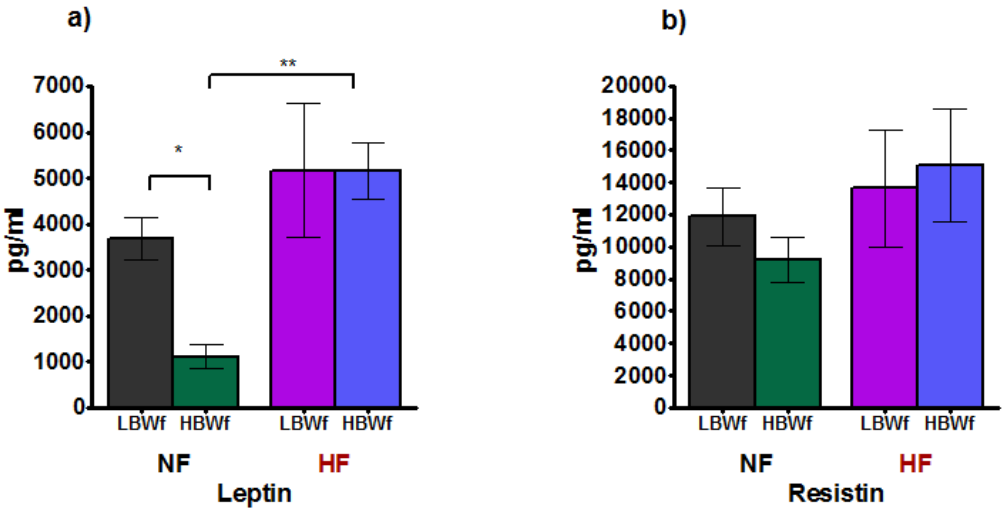

Figure 5.6.2.3 Leptin and resistin levels in plasma from female mice fed both a **NF** and **HF** diet. Statistical analysis was performed using a one-way ANOVA test followed by a protected Fisher's least significant difference (LSD) post hoc analysis. Data presented as mean± SEM. **LBWf-NF** n=4; **LBWf-HF** n=3; **HBWf-NF** n=4, **HBWf-HF** n=5. *p≤0.05, ** p≤0.01.

Proniflammatory cytokine IL-6 was higher in **HBWf-HF** compared to **HBWf-NF** (**p=0.019** figure 5.6.2.4a and table 5.6.2.1) as when compared to **LBWf-**

HF (**p=0.048** figure 5.6.2.4a and table 5.6.2.1). MCP-1 was not different between groups (figure 5.6.2.4b and table 5.6.2.1) Although **HBWf-HF** had a higher level of MCP-1 in respect to the others groups, differences were not significantly different (figure 5.6.2.4b and table 5.6.2.1).

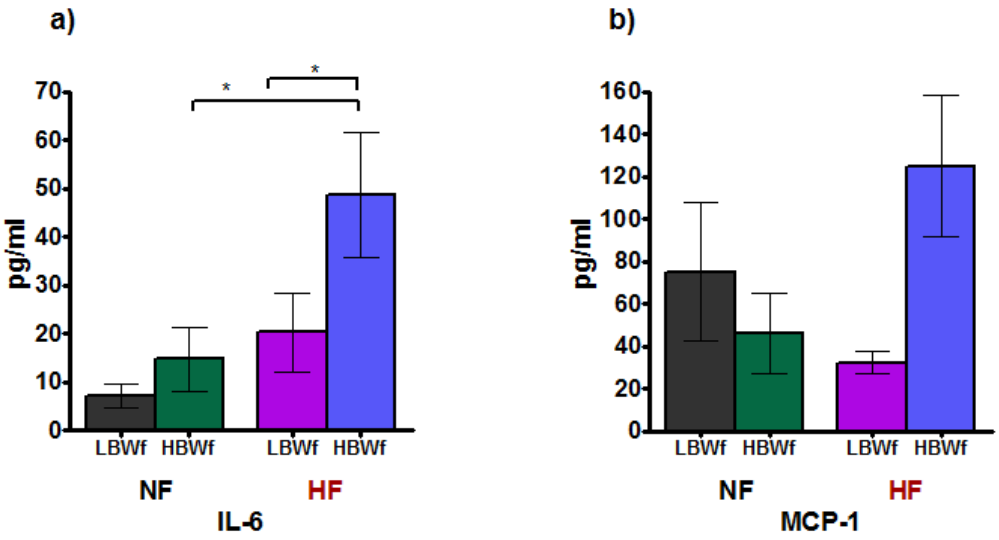

Figure 5.6.2.4 Proinflammatory markers in plasma from female mice fed both a **NF** and **HF** diet. Statistical analysis was performed using a one-way ANOVA test followed by a protected Fisher's least significant difference (LSD) post hoc analysis. Data presented as mean± SEM. **LBWf-NF** n=4; **LBWf-HF** n=3; **HBWf-NF** n=4, **HBWf-HF** n=5. *p≤0.05.

	LBWf-NF_1	LBWf-HF_2	HBWf-NF_3	HBWf-HF_4	P value
C-peptide pg/ml	784.769 ±128.722	803.279 ±228.928	1061.313 ±156.047	939.224 ±127.168	**1 vs.2**=0.936 **3vs.4**=0.596 **1vs.3**=0.244 **2vs.4**=0.556
GIP pg/ml	110.906 ±30.262	88.345 ±27.319	113.359 ±30.824	101.178 ±26.963	**1 vs.2**=0.953 **3vs.4**=0.991 **1vs.3**=0.999 **2vs.4**=0.989
Glucagon pg/ml	175.292 ±16.1	139.537 ±26.31	78.668 ±5.619	169.457 ±25.276	**1 vs.2**=0.256 **3vs.4=0.012** **1vs.3=0.009** **2vs.4**=0.337
Insulin pg/ml	211.531 ±51.818	498.542 ±208.695	401.296 ±152.919	391.105 ±117.986	**1 vs.2**=0.541 **3vs.4**=0.999 **1vs.3**=0.799 **2vs.4**=0.944
Ghrelin pg/ml	671.743 ±23.332	647.17 ±126.585	714.567 ±128.934	447.495 ±87.049	**1 vs.2**=0.855 **3vs.4=0.068** **1vs.3**=0.75 **2vs.4**=0.158
Leptin pg/ml	3.677.637 ±459.097	5170.113 ±1448.257	1114.674 ±260.278	5146.828 ±608.8	**1 vs.2**=0.773 **3vs.4=0.013** **1vs.3=0.044** **2vs.4**=0.999
Resistin pg/ml	11875.329 ±1771.242	13645.245 ±3652.078	9191.403 ±1379.455	15064.9926 ±3521.526	**1 vs.2**=0.978 **3vs.4**=0.539 **1vs.3**=0.93 **2vs.4**=0.539
Il-6 pg/ml	7.28 ±2.475	20.333 ±8.161	8.518 ±3.713	48.706 ±12.948	**1 vs.2**=0.306 **3vs.4=0.019** **1vs.3**=0.928 **2vs.4=0.019**
MCP-1 pg/ml	75.24 ±32.814	32.567 ±4.929	46.439 ±18.802	125.089 ±33.467	**1 vs.2**=0.67 **3vs.4**=0.242 **1vs.3**=0.888 **2vs.4**=0.107

Table 5.6.2.1 Metabolic markers measured in plasma from female mice fed both a **NF** and a **HF** diets at week 51 of age. GIP= glucose dependant- insulinotropic peptide, IL6= interleukine 6, MCP-1= monocyte chemotactic peptide 1. Statistical analysis was performed using a one-way ANOVA test followed by a protected Fisher's least significant difference (LSD) post hoc analysis. Data presented as mean± SEM. **LBWf-NF** n=4; **LBWf-HF** n=3; **HBWf-NF** n=4, **HBWf-HF** n=5.

5.7 Summary

Mice fed a **HF** diet were heavier than mice fed a **NF** diet throughout the study. **LBWm** mice had similar body weights to **HBWm** mice. Similarly, females fed a **HF** diet were the heaviest and **LBWf-NF** mice weight was similar to **HBWf-NF** mice throughout the study. However, **LBWf-HF** mice did not catch up in weight until week 43 of age.

Body weight gains and percentage of growth in male mice was mainly modulated by the diet, with **HF** fed mice gaining more weight and faster. Conversely, differences between female groups were not statistically significant.

Total kilocaloric intake was not significantly different between male mice as well as between female mice. FE was influenced by the diet. Male mice fed a **HF** diet were more efficient in gaining weight than males fed a **NF** diet. This pattern was seen also in **LBWf-HF** but not for **HBWf-HF** mice when compared to their respective counterparts.

Adipsoe tissue distribution was modulated by the diet only irrespective of birth weights. Total WAT, SAT and IAT were higher in male amd female mice fed a **HF** diet than mice fed a **NF** diet. Moreover, **LBWm-HF** mice had a higher level of SAT than **HBWm-HF** mice and **LBWf-HF** mice had a lower retroperitoneal content than **HBWf-HF** mice.

Adipocytes number per fat depot was not different in the gonadal fat of male mice but in the subcutaneous adipose tissue was significantly higher in mice

fed a **HF** diet. This group of mice had larger adipocytes than **NF** fed mice in both fat depots (gonadal and subcutaneous). **LBWf-HF** mice tended to have more small adipocytes than **HBWm-HF** mice.

Glucose levels in a fed state were not statistically significant between male groups. However, **LBWf-NF** had higher glucose levels than **HBWf-NF** mice as well as **HBWf-HF** mice compared to **HBWm-NF** mice. Insulin was higher in **HBWm-HF** diet compared to **HBWm-NF** mice and no differences were found between other groups. In females, insulin levels were similar between groups. **HBWm/f** fed a **HF** diet had the highest level of IL-6 in plasma. MCP-1 levels in plasma were not diferent between groups in both genders. However, it tended to be higher in **HBWf-HF** mice than **HBWf-NF** and **LBWf-HF** mice.

6. Discussions and Conclusion

Epidemiological, clinical and experimental data have shown that low birth weight, as an indicator of prenatal development conditions, may influence the risk of developing health complications later in life, such as insulin resistance, overweight/obesity, and further metabolic syndrome and non-insulin dependent diabetes (type 2 diabetes) (Hales, Barker et al. 1991, Ozanne and Hales 2002, Poore and Fowden 2004, Poore and Fowden 2004, Gluckman, Hanson et al. 2008). Moreover, some studies argue that the influence of birth weight on the onset of the aforementioned health risks seemed to be conditioned to a postnatal nutritional mismatch (Gluckman and Hanson 2004, Gluckman and Hanson 2004).

Different studies have indicated that a positive deviation from the normal growth trajectory for specific species is more relevant than birth weight *per se* or that the additive effect of both factors is more deleterious in later life (Baird J *et al,* 2005; Isgainitis E, Jimenez-Chillaron, 2009; Ibanez L, et al, 2006).

In the current study, a murine model based on extremes (low and high) birth weights combined with a postnatal diet intervention, was used in order to identify the changes in different phenotypes and hypothalamic neural activity that can be connected to possible physiological alterations. To be able to determine whether the changes were linked to different life stages (in chronological age), the study was subdivided in 3 different studies that covered: **lactation-prepubertal period (study1)**, **puberty-early adulthood**

(study2) and **middle age (study3)**.

6.1 Body Weight, Weight Gain, Feed Efficiency and Kilocaloric Intake

Body weights were lower in **LBWm/f** mice compared to **HBWm/f** mice during lactation and at the time of weaning **(study 1)** and a similar trend was seen after the introduction of either a **NF** or a **HF** diet from week 3 until week 15 of age **(study 2)**. However, differences between males were reduced between weeks 9 (**LBWm-NF**) to 11 of age (**LBWm-HF**). In **study 3** (from week 16 to week 51 of age), **LBWm/f-NF** mice had similar body weight to **HBWm/f-NF** mice. However, **LBWm-HF** mice remained smaller until week 23 than **HBWm-HF** mice and **LBWf-HF** mice until week 42. Similar body weight differences have been seen in both genders in pigs at 3 months of age (Poore and Fowden 2004), as well as in children and young adults (Binkin, Yip et al. 1988, Matthes, Lewis et al. 1996, Hediger, Overpeck et al. 1998, Bouhours-Nouet, Dufresne et al. 2008); although these studies did not use nutritional interventions as here. Additionally, studies in monozygotic twins have reported that twins with that were heavier at birth were also taller and heavier as adults (Loos, Beunen et al. 2002). As expected, **HF** diet increased the body weight in mice irrespective of birth weight.

Body weight gain, measured as weight gain in grams or as acceleration in growth, have been indicated as a common subsequent consequence of growth restriction *in utero*, reflected in low weight at birth (Bhargava, Sachdev et al. 2004, Isganaitis, Jimenez-Chillaron et al. 2009). In this study, this observation was corroborated in **LBWm** mice, which had a higher weight

gain (accelerated growth%) than **HBWm** mice during lactation **(study 1)** and (as grams and accelerated growth%) at young age **(study2)**. In **study 2**, the increment in weight gain could be partially due to the higher feed efficiency (FE) seen in these mice in respect to **HBWm** mice. Furthermore, there was an independent main effect of diet, with a higher weight gain in males fed a **HF** diet. This enhanced weight gain could also be attributed to a higher FE in these mice.

Other studies, have demonstrated a higher increase in FE after introducing a **HF** diet to mice (Corbett, Stern et al. 1986, Barbosa-da-Silva, Fraulob-Aquino et al. 2012); although a decrease FE has also been described in a short term overfeeding model (Rothwell and Stock 1979, Young, Saville et al. 1982). Moreover, **HBWm-HF** mice had a higher total kilocaloric intake than **HBWm-NF** mice before and after nomalisation, which indicated that hyperphagia and FE were, at least in part, responsible for the higher weight gain of these mice. However, when **HBWm-HF** mice were compared to **LBWm-HF** mice, the latter had a lower feed intake, indicating that **LBWm-HF** mice gained weight by having a higher FE in the presence of hypophagia.

In contrast, **LBWm-HF** mice compared to **LBWm-NF** mice had a higher intake before normalisation but tending to have a lower feed intake after normalisation to metabolic body mas ($bw^{0.75}$) (Tschop, Speakman et al. 2012). Dulloo's studies and others have shown that acceleration in growth after early growth restriction or during weight recovery in adults could occur by different control systems such as overcompensatory hyperphagia, shift in

fuel partitioning or increased efficiency of the metabolic machinery (Crescenzo, Samec et al. 2003, Dulloo 2006, Dulloo, Jacquet et al. 2006), and that the response could be amplified when introducing a **HF** diet. According to this, it could be suggested that **LBWm-NF** mice accelerated their growth due in part to a higher feed efficiency (FE) in the absence of hyperphagia, and when fed a HF diet, it was due to a higher FE in the presence of hypophagia, perhaps as a compensatory effect to reduce further weight gain.

Although **LBWf** mice were smaller than **HBWf** mice, absolute weight gain (in grams) was similar between them; however, females fed a **HF** diet had a higher weight gain irrespectively of birth weight, as seen in males. This is in accordance with the kilocaloric intake, where females fed a **HF** diet had the highest intake. Accelerated growth (%) was confirmed in **LBWf** mice, which had the highest percentage of growth, but there was not a significant effect of diet, contrary to males. Again, the high feed efficiency seen in **LBWf-HF** mice may contribute to an enhanced weight gain in respect to **LBWf-NF** and **HBWf-HF**.

In **study 3** (from week 16 to week 51 of age), body weight gain was modulated mainly by the diet, being enhanced in male mice fed a **HF** diet. Although energy intake was higher in males fed a **HF** diet before normalisation, there was not a significant difference between groups after normalisation to metabolic body mass, indicating that the intake was proportional to their metabolic needs. However, FE was higher in these mice

and also tended to be higher in **LBWm-HF** in respect to **HBWm-HF** mice, which could also be related to a pattern of higher weight gain in this group. These results suggested that **HF** diet did not further amplify ingestion of food but affected the efficiency of gaining weight per kilocalorie consumed (FE).

In the female groups, there was not a significant difference in weight gain between groups, although **LBWf-HF** mice tended to have the highest weight gain. The higher weight gain presented in **LBWf-HF** mice could be mainly related to their higher FE as no changes in energy intake were seen (as in males).

FE involves many complex processes and therefore, a gross change in FE does not assume net changes in all the processes. Energy intake, digestibility of nutrients, metabolism (anabolism and catabolism), body composition and energy expenditure (physical activity, basal metabolic rate and thermoregulation as production of heat), are some of the mechanisms associated with FE (Herd and Arthur 2009, Harris, Patience et al. 2012). To be able to understand what exactly caused an increase in FE, it would be necessary to assess each of these mechanisms. In the present study, it was not possible to evaluate each of these components. However, it has been suggested in other studies that accelerated growth after early growth arrest is a phenomenon that can occur in the absence of hyperphagia and therefore arises the possibility that sustained reduction in energy expenditure *per se* (decrease of thermogenesis in certain organs/tissues) as a compensatory metabolic process for the purpose of sparing energy for catch

up in growth (Cettour-Rose, Samec et al. 2005). Furthermore, it has been argued that because the rate of carbohydrate and protein oxidation is determined by intake of these nutrients, whereas the rate of fat oxidation is determined mainly by the gap between total energy expenditure and energy intake, excessive weight gain (mainly fat accretion) is the natural result of a diet rich in fat (Flatt 1987, Barbosa-da-Silva, Fraulob-Aquino et al. 2012).

Another potential mechanism suggested to be involved in gaining weight is a decreased physical activity (Marques, Motta et al. 2010, Barbosa-da-Silva, Fraulob-Aquino et al. 2012).

6.2 Body Composition by MRS and MRI

Total body adiposity measured by MRS showed that at weaning (**study 1**), **LBWm/f** mice had a lower adiposity than **HBWm/f** mice. Murine studies with nutritional interventions during perinatal life have demonstrated that low birth weight mice under caloric restriction or low protein diets during gestation and lactation tended to have lower body weights and lower fat deposition than control mice (Shepherd, Crowther et al. 1997), corroborating the results in the present study. However, studies on low birth weigh infants showed that those born small for gestational age and that underwent increased weight gain, and caught up in weight with controls at the postnatal stage have higher fat deposition (Ounsted and Sleigh 1975, Ozanne and Hales 2004, Ozanne, Lewis et al. 2004, Desai, Gayle et al. 2005). In the present study, **LBWm** accelerated their growth but they did not catch up in weight, which could partially explain the low increment in fat deposition.

Total fat as measured by MRI, showed a different pattern in males and females. Whereas total fat, as measured by MRS, IAT, SAT and internal to subcutaneous ratio were lower on **LBWm** mice, they were higher in **LBWf** mice, especially total fat, IAT and internal to subcutaneous ratio. This suggested that female mice had a different fat patterning than males, and it seems to have a higher deposition of fat in adipose tissues than in other areas of the body. These differences in fat deposition exclude the hormonal changes related to puberty as the time of evaluation was before the onset of puberty. Previous reports have indicated that females haver higher body adiposity than males at birth, and tend to have higher skin fold thicknesses (Rodriguez, Samper et al. 2005). Both sexes also seemed to show relative decreases in body fat between 1 to 6 years; however, whereas girls then begin to increase in fatness again, increases in boys are mainly attributed to lean mass (Fomon, Haschke et al. 1982, Akinyinka, Sanni et al. 1999, Wells 2000).

There was also a lower IHCL content in both LBW males and females. This low level of hepatic content could also due to the fact that less fat is available to be stored or an alteration in the production long chain fatty acids (Goodridge, Klautky et al. 1996).

In **study 2** (from week 3 to week 15 of age), total body adiposity was affected by the interaction between birth weight and diet. The measurement of adiposity was performed at the end of the study, when mice were 15

weeks old. By this time, **LBWm** mice caught up in weight with their respective counterparts. There is evidence that mammalian catch up growth is characterised by a disproportionately higher rate of body fat than lean tissue gain (Graham, Cordano et al. 1969, Castilla-Serna, Perez-Ortiz et al. 1996, Dulloo, Jacquet et al. 2002). This is partially in accordance with the present study. As mentioned before, there was an interaction between factors, which means that the effects of birth weight depended on the diets given to mice and vice versa. Although there was a higher adiposity level (MRS) and fat content (MRI) in **LBWm-NF** mice compared to **HBWm-NF** mice, it was not the case for **LBWm-HF** mice compared to **HBWm-HF** mice, which had similar fat content. Moreover, the levels of adiposity and total body fat in **LBWm-HF** mice compared to **LBWm-NF** mice were higher but the proportions to body weight (%) were comparable. This result can suggest that a **HF** diet did not further amplify the proportion of fat accretion in **LBWm** mice at this age, which could be in part due to the adaptive effect of a reduction of the kilocalorie intake of **LBWm-HF** mice to comparable levels of **LBWm-NF** mice as a compensatory response to a relatively higher feed efficiency, and therefore, maintained their proportional fat accretion.

In this study, **HF** diet led to an increase accretion in both, subcutaneous and internal adipose tissue; however, after normalisation to body weight the proportion of these regional fat depots were significantly higher only in **HBWm-HF** compared to **HBWm-NF** mice. Birth weight led also to the progression of compartmental fat deposition, but only when fed a **NF** diet. However, when assessing the internal to subcutaneous ratio, diet and birth

weight effect were visible. This means that **LBWm** mice had a higher internal adipose tissue in respect to subcutaneous tissue when compared to **HBWm** mice. Despite the fact that **LBWm-HF** mice had comparable levels of total fat content to **HBWm-HF** mice, IAT and SAT were disproportionately distributed, having more IAT than SAT.

Previous studies have evaluated the relationship between birth weight and body composition at different stages of life using surrogates of body composition such as waist to hip ratio (WHR), skinfold thickness and BMI (in kg/m^2). Some of these studies indicated no association between birth weight and BMI (Rasmussen and Johansson 1998, Kahn, Narayan et al. 2000, Weyer, Pratley et al. 2000, Rogers and Group 2003, Singhal, Wells et al. 2003, Te Velde, Twisk et al. 2003); others indicated a positive association between the two (Gale, Martyn et al. 2001, Oken and Gillman 2003, Sayer, Syddall et al. 2004) and others a negative or J-U shaped association (Valdez, Athens et al. 1994, Fall, Osmond et al. 1995, Curhan, Willett et al. 1996, Yarbrough, Barrett-Connor et al. 1998, Parsons, Power et al. 2001).

Overall, the evidence suggests that although birth weight may be related positively with BMI, it is not necessarily linked to increase adiposity, as BMI cannot differentiate between fat-free mass and adipose tissue. Therefore, misleading results can result from its interpretation. A high birth weight, although usually related to higher BMI later in life, has been also linked to less body fatness assessed by skinfold thickness and DXA (Okosun, Liao et al. 2000, Singhal, Wells et al. 2003), which suggested that the high BMI is

related to a higher lean mass rather than fat mass. However, no association between fat mass and birth weight (Singhal, Wells et al. 2003) or a higher risk of obesity with a higher birth weight has been reported (Yu, Han et al. 2011, Schellong, Schulz et al. 2012).

Overall, there is not a consistent finding in the literature about the effects of birth weight on adiposity and fat distribution, and this is in part due to the different indirect measures used as surrogates of fat content. In this study, more precise techniques were used for the measurement of fat content such as MRI and MRI. Here, I demonstrated that birth weight had an inverse effect on the IAT:SAT ratio, and this effect was independent of the diet given during the study. However, there was an independent effect of diet, with **HF** fed mice having a higher IAT:SAT ratio.

This suggested that either a low birth weight or a high fat diet could independently be a risk of a disproportional fat accretion in young mice, and this could be partially related to higher energy intakes and/or higher feed efficiencies. Moreover, it was demonstrated that intrahepatocellular lipid content (IHCL) was modulated by birth weight and diet *per se*, with a higher hepatic content in **LBWm** mice as well as in **HF** fed males.

Interestingly, in the female group there were independent effects of both birth weight and diet in the percentage of adiposity measured by MRS. **HBWf** mice had the highest adiposity when compared to **LBWf** mice. At the same time, **HF** fed females had the highest adiposity when compared to **NF** fed

females. This is in accordance with the higher energy intake observed in these mice, and the higher efficiency in **LBWf-HF** mice only. However, when looking at adipose tissue distribution, there was an effect of diet only, as it was in the percentage of fat measured by MRS. This result suggests that **LBWf** mice had similar total fat and adipose tissue distribution as the **HBWf** mice, despite the fact of having a lower weight at 15 weeks of age, which could explain the lack of differences in energy intake and feed efficiency by birth weight. As MRS takes into account the whole body adiposity rather that total fat as the sum of IAT and SAT, the results suggested that **HBWf** mice might have higher lipid content in other areas (ectopic deposition), apart from these fat depots. However, the IHCL was higher in **LBWf** mice and females fed a **HF** diet. Therefore, the ectopic deposition should take place in other organs, but this assumption was unfortunately not assessed in this study. The IAT to SAT ratio was not different between groups, which indicated a comparable proportion of these compartmental adipose tissues between groups. As in males, there is much controversy as to the association between birth weight and fat deposition in females (Fall, Osmond et al. 1995, Martyn, Hales et al. 1998, Yarbrough, Barrett-Connor et al. 1998, Parsons, Power et al. 2001, Ros, Lichtenstein et al. 2001, Kuh, Bassey et al. 2002, Kuh, Hardy et al. 2002, Loos, Beunen et al. 2002). Studies in middle aged or elderly subjects have also demonstrated a contradictory role for birth weight on fat deposition. The majority of the studies have shown a negative relationship between birth weight and different surrogates of fat measured in both genders, others found no association (Martyn, Hales et al. 1998, Yarbrough, Barrett-Connor et al. 1998), a positive relationship (Vestbo,

Damsgaard et al. 1996), or a J-U association (Schellong, Schulz et al. 2012).

In **study 3**, (from week 16 to week 51 of age), it was not possible to measure adiposity by MRS or MRI for technical reasons. However, an evaluation of an adipose tissue index was performed, using dissected fat depots. Matured mice (week 51 of age) were mainly affected by the diet rather than for differences, in birth weight in both male and females. As mentioned in section 6.2.1, male mice fed a **HF** diet gain more weight and this weight gain was mainly related to a higher FE rather than hyperphagia. It could be speculated that the body weight gained at this age was related to their higher fat deposition, which at the same time was associated with a higher efficiency of weight gain per kilocalorie consumed. Furthermore, these mice had a higher SAT and IAT (as the sum of retroperitoneal, mesenteric and gonadal fat tissue). Although mice fed a **HF** diet did not have significant differences in total fat, it was observed that **LBWm-HF** mice tended to have a higher total fat content. Furthermore, they had a significantly higher SAT than **HBWm-HF** mice and tended to have higher levels of gonadal fat. This indicated that fat distribution was differently modulated between mice fed a **HF** diet.

In females, there was also a different pattern of distribution in the IAT tissue; there was no difference between **HBWf** mice in the gonadal fat pads, but there was in **LBWf** mice. Furthermore, **LBWf-HF** mice had a higher gonadal fat than **HBWf-HF** mice. However, the latter had a higher retroperitoneal fat than the former.

6.3 Glucose Tolerance and Metabolic Hormones

Previous studies have shown that low birth weight animals that underwent undernutrition in the perinatal period, presented a higher glucose tolerance than those that catch up in weight with control animals or than control animals, and those that catch up after and appropriate postnatal nutrition had similar levels of glucose and insulin as control animals (Shepherd, Crowther et al. 1997, Chen, Martin-Gronert et al. 2009). Other studies conducted in infants have shown similar glucose levels between infants with a low birth weight and high birth weight but higher whole body, muscle and hepatic insulin sensitivities in the latter group (Bouhours-Nouet, Dufresne et al. 2008).

In this study, **LBWm** mice had a lower glucose than **HBWm** mice and higher in **LBWf** than their counterparts. The levels of insulin were slightly higher than **HBWm** mice but not significantly whereas in **LBWf** mice it was significantly higher. **LBWm** mice seemed to have higher levels of insulin for the amount of glucose in periphery, and this could be a sign of early hyperinsulinemia. **LBWf** mice had higher levels of insulin and higher levels of glucose than **HBWf** mice, which could be an indication of lack of insulin sensitivity. As c-peptide levels were not different between males groups, it could be excluded the possibility of a higher secretion in small males. However, c-peptide was much higher in **LBWf** mice, indicating a hypersecretion of insulin in respect to **HBWf** mice. The presence of higher levels of insulin might be linked to other processes such as insulin resistance in certain organs and redistribution of glucose to others (Summermatter,

Marcelino et al. 2009). As previously demonstrated, liver growth was impaired in **LBWm** mice, and therefore this could be a sign of a lower insulin-growth dependent signaling, and thus, be partially involved in the small increase of insulin in periphery. Moreover, muscle growth was also blunted. However, brain growth was spared, which indicated that the glucose might be redirected to this organ mainly. In the case of the **LBWf** mice, there was not an asymmetrical growth of organs relative to their weights, although they tended to have a spared brain growth.

Evidence is available that suggests that the state of hyperinsulinemia or higher insulin to glucose ratio during catch up growth is an early event that has been attributed to a reduction in thermogenesis *per* se rather than hyperphagia, excess fat mass or elevated free fatty acids in circulation (Crescenzo, Samec et al. 2003). This is in accordance with the results of fat content from **LBWm** mice, which did not exceed that in **HBWm** mice. However in the females groups, **LBWf** did exceed the fat content of the **HBWf** mice. Other insulin related hormones were also investigated. While glucose is the most potent stimulus of insulin release, other factors stimulate insulin secretion, such as GIP and GLP-1 (Holst 1994, Drucker 2001). These hormones are released from the gut following a meal. In this study, GIP was measured and its levels were higher in **LBWm/f** mice than **HBWm/f** mice, which implies a higher stimulation of insulin release. Higher GIP levels then could indicate that beta cells had to be highly stimulated in order to secrete similar levels of insulin in the circulation in **LBWm** and higher levels in **LBWf**. In previous studies it has been shown that higher levels of insulin during

catch up seems to reside in a beta cell hyperresponsiveness, and this has not been explained by intra cellular alterations in secretion *per se* nor in the exocytosis mechanisms (Casimir, de Andrade et al. 2011). Instead, this has been attributed to a contribution of neural hormonal effectors such as GLP-1 and GIP (Casimir, de Andrade et al. 2011) as could be linked in the present study.

Previous investigations have reported an increase in glucose intolerance with overweight/obesity, introduction of a **HF** diet (Winzell and Ahren 2004), and high internal or hepatic fat (Gabriely, Ma et al. 2002, Fabbrini, Magkos et al. 2009). Different responses to a **HF** diet have been observed within same strains such as a lean but diabetic phenotype or normal/higher glucose sensitivity when combined with a low protein diet during lactation (Burcelin, Crivelli et al. 2002, Ozanne, Lewis et al. 2004).

In **study 2** (from week 3 until week 15 of age), as aforementioned, **LBWm** mice had a higher level of IAT:SAT ratio as well as IHCL content, independently of the diet. This seemed to be in accordance with the impaired glucose they manifested (in a fed state). Moreover, it was also observed that a **HF** feeding induced a higher IAT:SAT independently of birth weight, which might be associated with the fact that these mice presented an impaired fasting glucose. Interestingly, **LBWm-NF** mice had also impaired fasting glucose when compared to **HBWm-NF** mice but it was not the case between mice fed a **HF** diet. Additionally, the same groups that had impaired fasting glucose presented a higher total adiposity, SAT and IAT when compared to

their respective counterparts. The AUC added also evidence of a relationship between glucose tolerance and internal adiposity.

However, as mice matured (**study 3**), levels of glucose seemed to stabilise decreased and were comparable between groups. It has been shown that glucose levels in non-obese C57BL/6 mice decreased between the 3-12 months of age and then rises again after 24-month of age with an increase in islet size and pancreatic insulin content at the age of 21-24 months (Leiter, Premdas et al. 1988). However, in this study, levels of glucose were generally lower in all mice obese and non-obese. Despite this, **HF** fed mice did tend to have higher levels of glucose, with **HBWm-HF** having a marginal significance against **HBWm-NF** mice.

Previous studies have indicated a higher susceptibility to develop impaired glucose metabolism and diabetes in mammals with a low birth weight that catch up growth (Hales, Barker et al. 1991, Hales and Barker 2001, Dulloo, Jacquet et al. 2006). Dulloo's studies also showed that mice presenting weight recovery after weight loss or early growth restriction, showed hyperinsulinemia with skeletal muscle insulin resistance accompanied by adipose tissue insulin sensitivity. The biological significance of this thrifty metabolism seems to be an adaptive response in order to achieve both blood glucose homeostasis and replenishment of fat stores. A maladaptive response in the presence of an energy dense diet, will lead to a pronounced state of hyperinsulinemia, hyperglycemia and excess fat deposition (Dulloo and Girardier 1990, Dulloo 2006, Summermatter, Marcelino et al. 2009).

In young mice (**study 2**), mice fed a **HF** diet were hyperinsulinemic, deposited higher fat mass (grams) and tended to have higher levels of glucose (fed state) when compared to mice fed a **NF** diet. Higher levels of insulin were needed in **HF** fed mice in order to decrease glucose levels in circulation; however, the **LBWm-HF** mice seemed to have less sensitivity to the effect of insulin as the levels of glucose were higher than in **HBWm-HF** mice. There was no difference between plasma insulin concentrations in mice fed a **NF** diet, despite the fact that **LBWm-NF** mice had higher levels of glucose; this may indicate that the levels of insulin secreted were not enough to decrease glucose levels, which could be attributed to paracrine mechanisms such as glucagon secretion (Cryer 1981, Dinneen, Alzaid et al. 1995). In fact in this study, the levels of glucagon were higher in this group than in other groups, and therefore impairment in the glucagon response might increase the levels of hepatic glucose production and subsequently help to increase the levels of glucose in periphery and decrease the levels of insulin (Cryer 1981, Baron, Schaeffer et al. 1987).

However in older mice (**study 3**), levels of insulin were generally increased in **HF** fed mice but it was only significantly higher in **HBWm-HF** mice in respect to their respective counterparts. Moreover, it was noticed that despite the fact that mice fed a **HF** diet had similar levels of total fat, IAT and internal to subcutaneous ratio, the levels of SAT were reduced in **HBWm-HF** mice, which could caused the reduction of the effect of birth weight at this age.

As the difference in total fat, IAT and SAT between **LBWm** mice was more accentuated than in a young age, it would be expected to have an exacerbated impairment of insulin response in these mice. However, a similar response was seen as in young mice in glucose and insulin concentration. Also, it should not be excluded the possibility of a pronounced impairment of glucose tolerance or impaired fasting glucose in these mice, which could not be assessed in this study. It should be also notice that the sample size was smaller at this time and thus differences are more difficult to be identified. In general, these results suggest that glucose metabolism was not affected by fat mass.

Young females (**study 2**) did have a different metabolic profile than males in general. Fasting glucose was not different between groups. However, **LBWf-HF** mice had impaired glucose tolerance as demonstrated by the IPGTT and AUC, when compared to their counterparts. Moreover, as in males, fed **HF** females had higher levels of insulin than females fed a **NF** diet. IHCL levels seemed to be related to the glucose impairment seen in this group of mice.

Matured females (**study 3**), as in males, did have lower levels of glucose and insulin than younger females. However, by this age, differences in glucose were evident. In general, **LBWf-NF** mice had higher levels of glucose than **HBWf-NF** mice and also in **HBWf-HF** mice when compared to those fed a **NF** diet. However, there were not differences in the levels of insulin, although tended to be lower in **LBWf-NF** mice than in other groups. As insulin levels failed to increase as a compensatory response to decrease the glucose

concentration in plasma, it raises the possibility of an altered response in the secretory/inhibitory mechanisms. Unexpectedly, glucagon levels were significantly higher in **LBWf-NF** mice when compared to **HBWf-NF** mice, which could explain the lower levels of insulin and the higher levels of glucose as the result of an impaired response of glucagon in this group (Cryer 1981, Baron, Schaeffer et al. 1987, Dinneen, Alzaid et al. 1995). Moreover, **HBWf-HF** also had a higher glucagon levels than **HBWf-NF** mice in the presence of higher glucose levels in the former group with no changes in insulin secretion (c-peptide) or insulin level.

Overall, the results in young mice suggested that an increase in total adiposity, internal or IHCL might be linked with an altered glucose metabolism in a fed-fasting dependent manner, whilst the relationship between these factors and glucose metabolism are modulated by an interaction between diet, birth weight and other factors than by changes in fat mass *per se*.

It is known that the central effects of leptin include reduction of food intake and body weight gain and increased energy expenditure (Seeley, van Dijk et al. 1996, Mistry, Swick et al. 1997); but also it has been described a trophic factor in early life (Bouret, Draper et al. 2004, Bouret and Simerly 2004). Leptin levels decrease upon negative balance in both humans and adult mice (Maffei, Halaas et al. 1995). Neonatal mice need to maximise food intake and maintain a high thermoregulatory response to optimise survival, and therefore levels of leptin are high in neonates. This suggests that leptin

may function differently in neonates and adults. Here, it was shown that the levels of leptin tended to be higher in **LBWm** mice but it was similar between females and did not correspond to the levels of fat deposition in these mice as shown in previous studies.

Although the relationship between leptin and obesity is well established, controversy over the alterations in resistin concentration in response to obesity still exists; in humans for example, it has been associated to inflammation rather than obesity (Burcelin 2008, Gharibeh, Al Tawallbeh et al. 2010, Schwartz and Lazar 2011). In the present study, the levels of leptin were more robust and in accordance with previous studies. Leptin and resistin changed according to total fat in young males and leptin changed according to whole body adiposity in young females. In older male mice, levels of leptin changed in accordance to fat mass but resistin was not when comparing **HBWm** mice. Leptin levels in matured females were related to fat mass when comparing mice fed a **NF** vs. **HF** diet; unexpectedly, leptin levels in **LBWf-NF** were higher despite having similar levels of fat mass with **HBWf-NF** mice. This might indicate that higher levels are needed in order to maintained the body weight, lower feed efficiency and/or similar energy intake in the former group.

Proinflammatory adipokines in circulation are usually connected to a low-grade chronic inflammation when developing obesity and/or insulin resistance (Yu and Ginsberg 2005). According to this, at weaning (**study 1**) levels of the proinflammatory cytokines IL-6, MCP-1 and TNF-alpha seemed

to be linked to the insulin resistance state of **LBWf** mice. However, **LBWm** had only a higher MCP-1 levels, suggesting a different role of MCP-1. MCP-1 plays vital roles in immune response, angiogenesis and pregnancy outcome. Increased MCP-1 concentration in intrauterine growth restricted neonates during postnatal life may be attributed to gradual initiation of angiogenesis supporting the initiation of accelerated growth (Briana, Boutsikou et al. 2007).

IL-6 seems to correlate positively with fat mass and insulin resistance and increase adipocyte lipolysis (Yu and Ginsberg 2005). In young adults (**study 2**) and older mice (**study3**), IL-6 and MCP-1 did not correlate with fat mass or insulin resistance in both males and females.

Ghrelin, a peptide hormone is known to affect growth hormone secretion, appetite and energy balance. Its level in the circulation has been considered of prognostic value for catch up growth and it has been found to be elevated in growth restricted infants that accelerated their growth when compared to Appropriate for Gestational Age (AGA) and Large for Gestational Age (LGA) (Fidanci, Meral et al. 2010). Ghrelin concentration was not different between **LBWm/f** and **HBWm/f** mice at weaning (**study 1**), and therefore did not correlate with levels of adiposity at this early age as it has been observed in adults (Tschop, Weyer et al. 2001, Shiiya, Nakazato et al. 2002) or with differences in weight gain. Perhaps, similar levels were enough for **LBWm/f** to accelerate their growth without catching up in weight.

Consistently, fat masses were associated with a reduced concentration of ghrelin in plasma in male mice. The results in males in **study 2** and **study 3** agreed with previous studies showing obesity reduces circulating ghrelin in periphery (Tschop, Weyer et al. 2001, Shiiya, Nakazato et al. 2002). Unexpectedly, ghrelin leves in matured **LBWf-HF** mice was similar to that of **LBWf-NF** despite the fact of having higher fat accumulation.

6.4 Adipocyte Size Distribution in Subcutaneous Adipose Tissue

Models of accelerated growth that mimic fat mass accretion, after weight loss or growth restriction, have shown that the compensatory enhanced capacity of glucose uptake in WAT is associated with adipose tissue hyperplasia and controlled hypertrophic growth, with a maintained small adipose size in respect to the control animals (Cettour-Rose, Samec et al. 2005, Summermatter, Marcelino et al. 2009). Others, have found an increased in adipose size without hyperplasia as early as 3 weeks of age in murine models of growth restriction followed by accelerated growth as well as in diet induced obesity in humans (Desai, Guang et al. 2008).

In young mice (**study 2**), subcutaneous and gonadal adipocyte number was not different between groups when compared per gram of fat mass; however, when comparing cell number per fat depot, significant differences appeared only between **HBWm** mice in both fat depots and between mice fed a **HF** diet in SAT. As mice aged (**study 3**), differences in adipocyte number were seen. Mice that were fed a **HF** diet had a lower number of adipocytes per

gram of gonadal fat, but there were not differences when assessing cell number per fat depot, although there was a trend towards a high number in the same **HF** fed mice in gonadal tissue. In SAT a similar pattern was seen between **LBWm** mice in the adipocyte number per gram of tissue, but it was significantly higher in **LBWm-HF** mice when compared to **LBWm-NF** and **HBWm-HF** mice when assessing adipocytes per fat depot.

Further assessment of adipocyte size distribution indicated that there were not significant differences between young **LBWm** mice in both fat depots, although mice fed a **HF** tended to have a higher number of small adipocytes in SAT but larger adipocytes in gonadal fat tissue. These results indicated that fat mass accretion in **LBWm-HF** mice had a similar adipocyte size distribution, as **LBWm-NF** and therefore it was not greatly affected by the introduction of a **HF** diet at this young age. It would be expected to have an amplified response in these early growth restricted mice after the introduction of an energy dense diet. It could be speculated that the time of exposure was not sufficiently long to show significant changes in adipocyte size distribution or that the concomitant hyperplasia and moderate hypertrophy channeled part of the lipid pool in newly formed adipocytes and matured adipocytes in a proportionate manner (Summermatter, Marcelino et al. 2009). In contrast, **HBWm-HF** mice had a different adipocyte distribution than those fed a **NF** diet. The peak diameter of the large adipocytes in the former group was shifted to the right, which indicated that the mean diameter of large adipocytes was higher in this group compared to mice fed a **NF** diet, with no differences in small adipocytes. Matured mice fed a **HF** had a similar

response; in gonadal adipose tissue **LBWm-HF** and **HBWm-HF** had a higher ratio of small to large adipocytes compared to their counterparts, and also the peak diameter of large adipocytes was shifted to the right indicating there was a concomitant increase in both small and the mean size of large cells. However in SAT there was a shift to the right in the diameter of large adipocytes but it was not accompanied by an increase in small adipocytes.

Despite the fact that young **LBWm** mice had similar adipocyte size distribution and similar adipocyte number in both SAT and gonadal fat tissue, **LBWm-HF** mice presented hyperinsulinemia, impaired fasting glucose and were glucose intolerant compared to **LBWm-NF** mice, as **HBWm-HF** compared to **HBWm-NF** mice. However, it was noticed that the levels of leptin and resistin were higher in **HBWm-HF** than **HBWm-NF** but it was similar between **LBWm** mice. This could indicate that the degree of leptin resistance is related to an increase in the peak diameter of large adipocytes independently of insulin resistance and glucose intolerance status. By week 51 of age (**study 3**), levels of leptin were similarly higher in mice fed a **HF** diet in respect to their counterparts indicating that **LBWm** mice became leptin resistant at a much later stage than **HBWm** mice.

Birth weight seemed to have an effect on SAT and gonadal adipocyte size distribution; young **LBWm-NF** mice had a slight deviation to the right in the SAT, which could be an indication of the initiation of lipid flow going towards mature adipocytes. Moreover, **HBWm-HF** mice were shifted to the right compared to **LBWm-HF** mice. By 51 weeks of age, there were not apparent

differences between mice fed a **NF** diet or **HF** fed mice.

In gonadal fat tissue, young **LBWm** mice (**study 2**) had a higher number of small cells and this pattern was maintained in matured **LBWm-HF** mice only. At the same time, the peak diameter of the large adipocytes was shifted slightly to the right in young **LBWm-NF**, as in the SAT tissue but differences were not apparent at matured age. Young **HBWm-HF** mice were again shifted to the right instead of **LBWm-HF** mice. These results suggested than young **LBWm-HF** mice did not have hypertrophic adipocytes in either SAT or gonadal fat tissue in respect to young **HBWm-HF** mice, which could indicate that there was still an ongoing dynamic process of catch up fat involving a sustained hypersinsulinemia, increased lipogenesis, hyperplastic growth with delay hypertrophy (Summermatter, Marcelino et al. 2009). If a reduced increment of size with no changes in adipogenesis but maintained lipogenesis is present, this could indicate an inability to store excess energy by increasing the size of matured adipocytes and/or by increasing the production of fully differentiated and functionally capable adipocytes (McLaughlin, Sherman et al. 2007). In the case of an increase in storage demand, the inability of the fat depot to mature a new group of adipocytes due to an impaired differentiation, would lead to the storage of lipids in non-adipose tissue (ectopic deposition) (Savage, Petersen et al. 2005). In this study it was shown that **LBWm** mice had a higher IAT:SAT ratio than **HBWm** mice independently of the diet given. This inability if accompanied with a possible reduction in the expression of genes related to adipogenesis could confirm that the excess of small cells is not due to proliferation but rather to

dysfunctional differentiated adipocytes (McLaughlin, Sherman et al. 2007). However, adipogenic gene expression could not be assessed in **study 2** and **study 3**. By week 51 of age (**study 3**), mice fed a **HF** diet had similar mean size of large cells, but **LBWm-HF** mice had again a higher number of small cells in gonadal fat but not in SAT.

6.5 Gene Expression in Subcutaneous Adipose Tissue

Expression of genes involved in insulin signaling, adipogenesis, lipid metabolism (lipogenesis-lipolysis) and thermoregulation were increased in **LBWm** mice in respect to **HBWm** mice at weaning (**study 1).** However, there was a reduction in expression of genes involved in the same pathways in **LBWf** when compared to **HBWf** mice suggesting a gender dependent modulation of these mechanisms.

Previous studies have shown that growth restricted offspring undergoing accelerated growth, exhibited an upregulation in the expression of adipogenic and lipogenic related genes (Summermatter, Marcelino et al. 2009) with an apparent adipose cell hyperplasia without alteration in the IRS-1/PIK3/Akt activation. However, Isganaitis's studies (Isganaitis, Jimenez-Chillaron et al. 2009) have shown that genes controlling the flux of glucose towards lipogenesis were upregulated (i.e., FAS, LPL, SREBP1c), whereas the expression of genes related to adipocyte differentiation /proliferation ($PPARg_2$, CEBP1a) and thermogenesis were unaltered. Isganaitis results were consistent with the marked hypertrophy without hyperplasia seen at the end of catch up which is more likely to predispose to reduce insulin

sensitivity in adipose tissue (Dulloo 2009). These findings are in line with a thrifty hypertrophic catch up fat with impaired adipogenic response (Dulloo 2009). The paradoxical results in these studies could be associated with different murine models used (rat-mice).

The present study seems to be consistent with the onset of a hyperplastic catch up fat. Summermattter and colleagues measured insulin signaling activity but he did not assessed mRNA expression, and therefore it can not be excluded the possibility of an upregulation in the expression of these insulin related genes (Summermatter, Marcelino et al. 2009). The only gene expression he assessed was for the gene GLUT4 and this was upregulated as in the present study.

Expression of genes related to thermogenesis and lipolysis (PGC1a, UCP1, HSL, beta 3 adrenergic receptor) were also upregulated in **LBWm** mice. This suggested that the lipid turnover (lipogenesis-lipolysis) on these mice was increased as well as energy dissipation in the form of heat contributing to the recycling of fatty acids into SAT and/or production of heat for thermoregulation and therefore reducing the accumulation of fatty acids in circulation and redirection to other tissues. These changes seemed to be independent of fat mass.

The reduced SAT insulin signaling in **LBWf** mice might be a reflection of an early impairment of insulin action in adipose tissue increasing the risk of lipid storage in other fat depots as seen in **study 1**(section 3.6.2), and perhaps in

other organs not studied. Models of maternal low protein diet in murine models have associated low birth weigh in females with hyperinsulinemia, in the absence of glucose intolerance, and reduced expression of insulin signaling proteins at 21 months but not at early ages in epidydimal fat and muscle (Hales, Desai et al. 1996, Sugden and Holness 2002). It should be noted that the models in these studies differed from the present study; the maternal nutrition was not altered at any time point, and the differences in body weight at birth and early postnatal age were the result of a natural perinatal growth in an isogenic mice. In this study **LBWf** mice were hyperinsulemic and hyperglycemic suggesting a degree of insulin resistance at young age independently of fat mass as in males.

As young **LBWf** mice (**study 2**) continued being smaller than **HBWf** mice but had similar levels of SAT, the results obtained at young age could indicate that there was a delay in catch-up fat at weaning, but it was not a permanent response. As thermogenesis and lipid turnover were also downregulated, it seemed that these mice have a reduced metabolism suggesting that energy demands at this age were higher than energy supply.

6.6 Hypothalamic Activity in Young Mice (study 2)

The hypothalamus is well recognised for its pivotal role in regulation of food intake and energy homeostasis (Remmers and Delemarre-van de Waal 2011). Appetite regulation involves different signals coming from the periphery and from the central nervous system (Elmquist, Coppari et al. 2005, Chaudhri, Field et al. 2008). Food intake and energy expenditure are

the components of energy balance and both of them are in perfect equilibrium in such a way that body weight is maintained within a specific set point (Sternson, Shepherd et al. 2005). The hypothalamus contains different nuclei that are interconnected among them and therefore they can act under the influence of some of them and/or by themselves, which makes more complex the relationship between hypothalamic activity and energy regulation.

In the current study, functional MEMRI was used to assess neural activity in specific appetite related nuclei within the hypothalamus. Previous studies from our group have demonstrated the use of this technique in evaluating the hypothalamic response to fed/fasted states, as well as the effect of gut peptides injected peripherally on hypothalamic activity (Kuo, Herlihy et al. 2005, Kuo, Herlihy et al. 2006, Parkinson, Chaudhri et al. 2009, Parkinson, Chaudhri et al. 2009).

There was not a clear pattern of an effect of birth weight per se but it seemed that both diet and birth weight interacted in a way that different responses were seen in mice fed a **HF** and **NF** diet depending on the birth weight.

There was an upregulation in **HBWm** mice fed a **HF** diet (**HBWm-HF**) when compared to **HBWm** fed a **NF** diet in the PVN and VMH nuclei but not in the ARC or Pe nuclei, although a similar trend was observed. Moreover, when the former group was compared to its counterpart that was fed the same diet (**LBWm-HF**), it exhibited a constant upregulation in all the nuclei.

In contrast, a different response to **HF** diet was seen in **LBWm-HF** when compared to **LBWm-NF** mice. There was a reduced activity in the former in all nuclei. Furthermore, **LBWm-NF** mice had a higher activity than **HBWm-NF** mice in the PVN and VMH nuclei.

As aforementioned, previous studies have correlated a fasted state with an enhanced SI (activity) in the ARC, PVN and VMH nuclei (Kuo, Herlihy et al. 2006). If fasting, in the context of a reduced satiation state, increases neural activity, then an increase in cumulative caloric intake could imply a similar pattern as a fasted state. In study 2, where neural activity was evaluated, **HBWm-HF** had a higher total kilocaloric intake than both **HBWm-NF** and **LBWm-HF** mice suggesting that these mice had a lower level of satiation. If the levels of satiation are reduced in this group of mice, the high activation in the hypothalamus could indicate an activation of orexigenic rather than anorexigenic neuropeptides (Lin and Huang 1999).

LBWm-NF had a higher kilocaloric intake than both **HBWm-NF** and **LBWm-HF** but differences did not reach significance. However, the pattern seemed to be partially in accordance with the neural activity within the hypothalamus. PVN and VMH were the only nuclei with a significant difference between the former group and **HBWm-NF** mice. However, the pattern of ARC and Pe activity was similar. As ARC nucleus has an incomplete blood brain barrier (BBB), it allows the entrance of signals from periphery (Peruzzo, Pastor et al. 2000). Therefore, the lack of differences between groups could suggest that the changes seen in others nuclei are the result of a feedback between

signaling coming from brain stem, nuclei cross talk or central signaling and not from the ARC nucleus. It should not be excluded that different signals coming to the ARC with different effect could polarise the gross change in activity (Parkinson, Chaudhri et al. 2009).

Ablation of the VMH has been linked to reduce sympathetic activity, which increases weight gain and fat accumulation in the absence of hyperphagia, and therefore increases the chances of developing obesity (Ruffin and Nicolaidis 1999). **LBWm-HF** tended to have a lower intake of energy than **LBWm-NF** but had an increase feed efficiency which means that they gained more weight per kilocalorie consumed with a proportional increase in total fat mass. Consequently, this group of mice had a lower activity in the VMH nucleus than **LBWm-NF** mice suggesting an association with a higher feed efficiency not only with this group but also against **HBWm-HF** mice. This increase in efficiency might be related to, at least in part, the vagus nerve and/or reduce activity of the sympathetic nervous system (Ruffin and Nicolaidis 1999).

It should be noted that whilst MEMRI generates quantitative measure of a stimulus, it cannot discriminate between different neural populations within the same nuclei and therefore, alterations in SI indicate gross changes of stimulatory and inhibitory signals. To be able to distinguish the specific neuropeptides/receptors activated or inhibited, it would be necessary to use in vitro techniques such as co-labeling with c-fos. However, expression of c-fos might be induced by diverse stimuli other than neural activation, such as

growth factors, neural differentiation and apoptosis. Also, as in MEMRI, the absence of c-fos activity does not imply the absence of changes in activation, which makes more complex the interpretation (Yamamori 1991, Yu, Chen et al. 1994, Roca, Shin et al. 2004, Parkinson, Chaudhri et al. 2009).

Neural activity in females was more complex and different to males. Overall **LBWf-HF** mice had a higher neural activity in all the nuclei when compared to **LBWf-NF** mice. However differences between females fed a **HF** diet were not apparent (**LBWf-HF** and **HBWf-HF**) as between **HBWf** mice (**HBWf-NF/HF**). However, **HBWf-NF** had a higher activity in the ARC and PVN nuclei than **LBWf-NF** mice only. In this case, there were not differences in kilocaloric intake. Therefore, different activation could indicate other changes rather than appetite regulation *per se* and further investigation should be carry out in order to clarify what other regulatory responses could be associated with the activity seen in both females and males.

6.7 Conclusion

In this study, I investigated the impact of birth weight and nutritional challenge on different phenotypic traits as well as hypothalamic neural activity in a murine model at different ages.

The results suggest that extreme birth weights within a normal range in an isogenic mouse model, as well as postnatal nutrition, influenced growth, glucose and lipid metabolism, body fat patterning and appetite regulation in an age-gender dependent manner.

6.8 Limitations of the Study

The present study has several limitations. The study only included extreme birth weights, low and high birth weights, from a normal birth weight range excluding mice with an intermediate birth weight. It is assumed that intermediate values would be expected for all the measurements but this fact is only speculative and it should be carried out across all birth weights categories in further studies.

Segmentation analysis following MRI was performed for the quantification of adipose tissue mass but lean mass was not measured; therefore, this only gives partial information of the body composition. However, images were stored and this quantification could be carried out in the future from the same images. Furthermore, although lean and fat mass can be quantified with MRI techniques, bone mineral density cannot be. Therefore, it would still give limited information of the body composition *in vivo*.

Separate groups of animals were used for MEMRI, biochemical analysis and IPGTT, in order to reduce the levels of stress. It is possible that neural changes observed in some animals may not be always reflected in the biochemical phenotypes or with glucose tolerance directly. However, it can be expected that there exist similarities within the groups at least in part, similarities within the groups as an inbred strain was used throughout this study. Thus, the reduced genetic variation might help to overcome potential individual variations to a certain extent.

As MEMRI is a functional technique that gives an overall picture of the possible alterations in hypothalamic neural activation, it does not give information of the particular subset of neural populations activated. Thus, other techniques with better spatial/temporal resolution may be needed to identify the underlying cellular components responsible for the *in vivo* MEMRI images. However, the temporal effects seen with MEMRI cannot be duplicated by *in vitro* techniques, which in turn could complicate the interpretation of the results.

Gene expression in SAT was carried out to evaluate transcriptional changes. However, the changes seen at this level do not imply changes at the posttranscriptional level or in activity. Therefore, protein expression in conjunction with activity assessment should be evaluated in further studies.

In study 3, the number of animals per group was low and therefore, the lack of changes can be related to the sample size introducing false negatives in the interpretation. Furthermore for technical reasons adipose tissue distribution could not be assessed using MRI and could not be associated with changes at younger age. However, fat pad mass collected at the end of the study can give an adipose index relatively similar to that using MRI, although differences can be present as not all the regions quantified by MRI were taken into account in the calculation of adipose index. Changes in hepatic lipid at matured age could not be assessed for the same technical reason and thus, could not be correlated with other changes at this age and earlier stages.

6.9 Future Work

Having observed changes in fat mass and hepatic lipid content at early ages, the next step would be to investigate what molecular changes took place. However, similar changes between groups do not necessary imply the absence of changes at the molecular level and therefore would be interesting to assess if there were underlying changes at the molecular levels even in the absence of phenotypic changes.

I would also like to investigate gene and protein expression as well as activity of certain enzymes in different tissues such as SAT, IAT, and liver. I evaluated gene expression in SAT at weaning, but I would like to extent the assessment to gonadal and retroperitoneal fat and not only for gene expression but to the aforementioned investigation. I would like to carry on evaluating adipogenesis, lipid metabolism and thermoregulation mechanisms.

IPGTT was carried out at 15 weeks of age, but unfortunately changes in insulin levels during the IPGTT could not be measured. It would be interesting to see whether changes insulin could occur as an effect of birth weight and diet at this same age as well as at weaning and 51 weeks of age. It would also bring more information about the state of insulin sensitivity between the groups in the absence or presence of hyperglycemia.

As mentioned previously, changes in neuropeptides and receptors involved in appetite regulation and energy balance should be carried out to identify the possible pathway that was implicated in the changes of neural activity within the hypothalamic nuclei. For example, co-labelling of neuropeptides such as NPY/AgRP and POMC/CART and receptors such as MC3R/MC4R with c-fos could help to discriminate whether an orexigenic or anorexigenic response (respectively) is associated with changes in neural activity (c-fos).

Recent studies have shown that epigenetic modifications might have an important role in altering gene expression. Changes in methylation and histone modification in response to early life programming and HF feeding have been identified (Park, Stoffers et al. 2008, Sandovici, Smith et al. 2011, Sandovici, Hammerle et al. 2013). It would be interesting to evaluate the role of epigenetics in the early programming of glucose/lipid metabolism and fat patterning and to what extent the effect persists after introducing energy dense diet postnatally.

As energy balance is due to an equilibrium between energy intake and energy expenditure, it would be important to assess production of heat, locomotor activity, and resting metabolic rate (energy expenditure) at 15 weeks and 51 weeks of age. I would not expect to evaluate this in mice at 21 days as it would involved too much stress for the young pups.

7. References

Abate, N. and A. Garg (1995). "Heterogeneity in adipose tissue metabolism: causes, implications and management of regional adiposity." Prog Lipid Res **34**(1): 53-70.

Akinyinka, O. O., K. A. Sanni, A. G. Falade, M. O. Akindele and A. Sowumi (1999). "Arm area measurements as indices of nutritional reserves and body water in African newborns." Afr J Med Med Sci **28**(1-2): 5-8.

Anastasovska, J., T. Arora, G. J. Sanchez Canon, J. R. Parkinson, K. Touhy, G. R. Gibson, N. A. Nadkarni, P. W. So, A. P. Goldstone, E. L. Thomas, M. K. Hankir, J. Van Loo, N. Modi, J. D. Bell and G. Frost (2012). "Fermentable carbohydrate alters hypothalamic neuronal activity and protects against the obesogenic environment." Obesity (Silver Spring) **20**(5): 1016-1023.

Armitage, J. A., I. Y. Khan, P. D. Taylor, P. W. Nathanielsz and L. Poston (2004). "Developmental programming of the metabolic syndrome by maternal nutritional imbalance: how strong is the evidence from experimental models in mammals?" J Physiol **561**(Pt 2): 355-377.

Banerjee, R. R., S. M. Rangwala, J. S. Shapiro, A. S. Rich, B. Rhoades, Y. Qi, J. Wang, M. W. Rajala, A. Pocai, P. E. Scherer, C. M. Steppan, R. S. Ahima, S. Obici, L. Rossetti and M. A. Lazar (2004). "Regulation of fasted blood glucose by resistin." Science **303**(5661): 1195-1198.

Barbosa-da-Silva, S., J. C. Fraulob-Aquino, J. R. Lopes, C. A. Mandarim-de-Lacerda and M. B. Aguila (2012). "Weight cycling enhances adipose tissue inflammatory responses in male mice." PLoS One **7**(7): e39837.

Barker, D. J. (1998). "In utero programming of chronic disease." Clin Sci (Lond) **95**(2): 115-128.

Baron, A. D., L. Schaeffer, P. Shragg and O. G. Kolterman (1987). "Role of hyperglucagonemia in maintenance of increased rates of hepatic glucose output in type II diabetics." Diabetes **36**(3): 274-283.

Bartelt, A. and J. Heeren (2014). "Adipose tissue browning and metabolic health." Nat Rev Endocrinol **10**(1): 24-36.

Benoit, S. C., D. J. Clegg, R. J. Seeley and S. C. Woods (2004). "Insulin and leptin as adiposity signals." Recent Prog Horm Res **59**: 267-285.

Berg, A. H. and P. E. Scherer (2005). "Adipose tissue, inflammation, and cardiovascular disease." Circ Res **96**(9): 939-949.

Bhargava, S. K., H. S. Sachdev, C. H. Fall, C. Osmond, R. Lakshmy, D. J. Barker, S. K. Biswas, S. Ramji, D. Prabhakaran and K. S. Reddy (2004). "Relation of serial changes in childhood body-mass index to impaired glucose tolerance in young adulthood." N Engl J Med **350**(9): 865-875.

Bieswal, F., M. T. Ahn, B. Reusens, P. Holvoet, M. Raes, W. D. Rees and C. Remacle (2006). "The importance of catch-up growth after early malnutrition for the programming of obesity in male rat." Obesity (Silver Spring) **14**(8): 1330-1343.

Binkin, N. J., R. Yip, L. Fleshood and F. L. Trowbridge (1988). "Birth weight and childhood growth." Pediatrics **82**(6): 828-834.

Boden, G. (1997). "Role of fatty acids in the pathogenesis of insulin resistance and NIDDM." Diabetes **46**(1): 3-10.

Bouhours-Nouet, N., S. Dufresne, F. B. de Casson, E. Mathieu, O. Douay, F. Gatelais, S. Rouleau and R. Coutant (2008). "High birth weight and early postnatal weight gain protect obese children and adolescents from truncal adiposity and insulin resistance: metabolically healthy but obese subjects?" Diabetes Care **31**(5): 1031-1036.

Bouret, S. G., S. J. Draper and R. B. Simerly (2004). "Trophic action of leptin on hypothalamic neurons that regulate feeding." Science **304**(5667): 108-110.

Bouret, S. G. and R. B. Simerly (2004). "Minireview: Leptin and development of hypothalamic feeding circuits." Endocrinology **145**(6): 2621-2626.

Brasaemle, D. L., B. Rubin, I. A. Harten, J. Gruia-Gray, A. R. Kimmel and C. Londos (2000). "Perilipin A increases triacylglycerol storage by decreasing the rate of triacylglycerol hydrolysis." J Biol Chem **275**(49): 38486-38493.

Briana, D. D., M. Boutsikou, S. Baka, G. Papadopoulos, D. Gourgiotis, K. P. Puchner, D. Hassiakos and A. Malamitsi-Puchner (2007). "Perinatal plasma monocyte chemotactic protein-1 concentrations in intrauterine growth restriction." Mediators Inflamm **2007**: 65032.

Burcelin, R. (2008). "Leptin and resistin: master enemy adipokines unified in brain to control glucose homeostasis." Endocrinology **149**(2): 443-444.

Burcelin, R., V. Crivelli, A. Dacosta, A. Roy-Tirelli and B. Thorens (2002). "Heterogeneous metabolic adaptation of C57BL/6J mice to high-fat diet." Am J Physiol Endocrinol Metab **282**(4): E834-842.

Butte, N. F., W. W. Wong, M. S. Treuth, K. J. Ellis and E. O'Brian Smith (2004). "Energy requirements during pregnancy based on total energy expenditure and energy deposition." Am J Clin Nutr **79**(6): 1078-1087.

Campfield, L. A., F. J. Smith, Y. Guisez, R. Devos and P. Burn (1995). "Recombinant mouse OB protein: evidence for a peripheral signal linking adiposity and central neural networks." Science **269**(5223): 546-549.

Casimir, M., P. B. de Andrade, A. Gjinovci, J. P. Montani, P. Maechler and A. G. Dulloo (2011). "A role for pancreatic beta-cell secretory hyperresponsiveness in catch-up growth hyperinsulinemia: Relevance to thrifty catch-up fat phenotype and risks for type 2 diabetes." Nutr Metab (Lond) **8**(1): 2.

Castilla-Serna, L., B. Perez-Ortiz and J. Cravioto (1996). "Patterns of muscle and fat mass repair during recovery from advanced infantile protein-energy malnutrition." Eur J Clin Nutr **50**(6): 392-397.

Cawston, E. E. and L. J. Miller (2010). "Therapeutic potential for novel drugs targeting the type 1 cholecystokinin receptor." Br J Pharmacol **159**(5): 1009-1021.

Cettour-Rose, P., S. Samec, A. P. Russell, S. Summermatter, D. Mainieri, C. Carrillo-Theander, J. P. Montani, J. Seydoux, F. Rohner-Jeanrenaud and A. G. Dulloo (2005). "Redistribution of glucose from skeletal muscle to adipose tissue during catch-up fat: a link between catch-up growth and later metabolic syndrome." Diabetes **54**(3): 751-756.

Chaudhri, O. B., B. C. Field and S. R. Bloom (2008). "Gastrointestinal satiety signals." Int J Obes (Lond) **32 Suppl 7**: S28-31.

Chaudhri, O. B., J. R. Parkinson, Y. T. Kuo, M. R. Druce, A. H. Herlihy, J. D. Bell, W. S. Dhillo, S. A. Stanley, M. A. Ghatei and S. R. Bloom (2006). "Differential hypothalamic neuronal activation following peripheral injection of GLP-1 and oxyntomodulin in mice detected by manganese-enhanced magnetic resonance imaging." Biochem Biophys Res Commun **350**(2): 298-306.

Chen, J. H., M. S. Martin-Gronert, J. Tarry-Adkins and S. E. Ozanne (2009). "Maternal protein restriction affects postnatal growth and the expression of key proteins involved in lifespan regulation in mice." PLoS One **4**(3): e4950.

Cheung, C. C., D. K. Clifton and R. A. Steiner (1997). "Proopiomelanocortin neurons are direct targets for leptin in the hypothalamus." Endocrinology **138**(10): 4489-4492.

Cinti, S. (2005). "The adipose organ." Prostaglandins Leukot Essent Fatty Acids **73**(1): 9-15.

Cinti, S. (2012). "The adipose organ at a glance." Dis Model Mech **5**(5): 588-594.

Ciofi, P. (2011). "The arcuate nucleus as a circumventricular organ in the mouse." Neurosci Lett **487**(2): 187-190.

Cone, R. D., M. A. Cowley, A. A. Butler, W. Fan, D. L. Marks and M. J. Low (2001). "The arcuate nucleus as a conduit for diverse signals relevant to energy homeostasis." Int J Obes Relat Metab Disord **25 Suppl 5**: S63-67.

Consultation, W. H. O. E. (2004). "Appropriate body-mass index for Asian populations and its implications for policy and intervention strategies." Lancet **363**(9403): 157-163.

Corbett, S. W., J. S. Stern and R. E. Keesey (1986). "Energy expenditure in rats with diet-induced obesity." Am J Clin Nutr **44**(2): 173-180.

Coulter, A. A., C. M. Bearden, X. Liu, R. A. Koza and L. P. Kozak (2003). "Dietary fat interacts with QTLs controlling induction of Pgc-1 alpha and Ucp1 during conversion of white to brown fat." Physiol Genomics **14**(2): 139-147.

Cousin, B., S. Cinti, M. Morroni, S. Raimbault, D. Ricquier, L. Penicaud and L. Casteilla (1992). "Occurrence of brown adipocytes in rat white adipose tissue: molecular and morphological characterization." J Cell Sci **103 (Pt 4)**: 931-942.

Covas, D. T., R. A. Panepucci, A. M. Fontes, W. A. Silva, Jr., M. D. Orellana, M. C. Freitas, L. Neder, A. R. Santos, L. C. Peres, M. C. Jamur and M. A. Zago (2008). "Multipotent mesenchymal stromal cells obtained from diverse human tissues share functional properties and gene-expression profile with CD146+ perivascular cells and fibroblasts." Exp Hematol **36**(5): 642-654.

Cowley, M. A., R. G. Smith, S. Diano, M. Tschop, N. Pronchuk, K. L. Grove, C. J. Strasburger, M. Bidlingmaier, M. Esterman, M. L. Heiman, L. M. Garcia-Segura, E. A. Nillni, P. Mendez, M. J. Low, P. Sotonyi, J. M. Friedman, H. Liu, S. Pinto, W. F. Colmers, R. D. Cone and T. L. Horvath (2003). "The distribution and mechanism of action of ghrelin in the CNS demonstrates a novel hypothalamic circuit regulating energy homeostasis." Neuron **37**(4): 649-661.

Crescenzo, R., S. Samec, V. Antic, F. Rohner-Jeanrenaud, J. Seydoux, J. P. Montani and A. G. Dulloo (2003). "A role for suppressed thermogenesis favoring catch-up fat in the pathophysiology of catch-up growth." Diabetes **52**(5): 1090-1097.

Cripps, R. L., M. S. Martin-Gronert and S. E. Ozanne (2005). "Fetal and perinatal programming of appetite." Clin Sci (Lond) **109**(1): 1-11.

Cryer, P. E. (1981). "Glucose counterregulation in man." Diabetes **30**(3): 261-264.

Curhan, G. C., W. C. Willett, E. B. Rimm, D. Spiegelman, A. L. Ascherio and M. J. Stampfer (1996). "Birth weight and adult hypertension, diabetes mellitus, and obesity in US men." Circulation **94**(12): 3246-3250.

Cypess, A. M., S. Lehman, G. Williams, I. Tal, D. Rodman, A. B. Goldfine, F. C. Kuo, E. L. Palmer, Y. H. Tseng, A. Doria, G. M. Kolodny and C. R. Kahn (2009). "Identification and importance of brown adipose tissue in adult humans." N Engl J Med **360**(15): 1509-1517.

Danielsson, A. (2007). "Insulin signalling in human adipocytes: mechanisms of insulin resistance in type 2 diabetes."

DeFalco, J., M. Tomishima, H. Liu, C. Zhao, X. Cai, J. D. Marth, L. Enquist and J. M. Friedman (2001). "Virus-assisted mapping of neural inputs to a feeding center in the hypothalamus." Science **291**(5513): 2608-2613.

Desai, M., M. Beall and M. G. Ross (2013). "Developmental origins of obesity: programmed adipogenesis." Curr Diab Rep **13**(1): 27-33.

Desai, M., D. Gayle, J. Babu and M. G. Ross (2005). "Programmed obesity in intrauterine growth-restricted newborns: modulation by newborn nutrition." Am J Physiol Regul Integr Comp Physiol **288**(1): R91-96.

Desai, M., H. Guang, M. Ferelli, N. Kallichanda and R. H. Lane (2008). "Programmed upregulation of adipogenic transcription factors in intrauterine growth-restricted offspring." Reprod Sci **15**(8): 785-796.

Dietz, W. H. (1994). "Critical periods in childhood for the development of obesity." Am J Clin Nutr **59**(5): 955-959.

Dinneen, S., A. Alzaid, D. Turk and R. Rizza (1995). "Failure of glucagon suppression contributes to postprandial hyperglycaemia in IDDM." Diabetologia **38**(3): 337-343.

Dinneen, S., J. Gerich and R. Rizza (1992). "Carbohydrate metabolism in non-insulin-dependent diabetes mellitus." N Engl J Med **327**(10): 707-713.

Drucker, D. J. (2001). "Minireview: the glucagon-like peptides." Endocrinology **142**(2): 521-527.

Dulloo, A. G. (2006). "Regulation of fat storage via suppressed thermogenesis: a thrifty phenotype that predisposes individuals with catch-up growth to insulin resistance and obesity." Horm Res **65 Suppl 3**: 90-97.

Dulloo, A. G. (2009). "Adipose tissue plasticity in catch-up-growth trajectories to metabolic syndrome: hyperplastic versus hypertrophic catch-up fat." Diabetes **58**(5): 1037-1039.

Dulloo, A. G. and L. Girardier (1990). "Adaptive changes in energy expenditure during refeeding following low-calorie intake: evidence for a specific metabolic component favoring fat storage." Am J Clin Nutr **52**(3): 415-420.

Dulloo, A. G., J. Jacquet and J. P. Montani (2002). "Pathways from weight fluctuations to metabolic diseases: focus on maladaptive thermogenesis during catch-up fat." Int J Obes Relat Metab Disord **26 Suppl 2**: S46-57.

Dulloo, A. G., J. Jacquet, J. Seydoux and J. P. Montani (2006). "The thrifty 'catch-up fat' phenotype: its impact on insulin sensitivity during growth trajectories to obesity and metabolic syndrome." Int J Obes (Lond) **30 Suppl 4**: S23-35.

Egan, J. J., A. S. Greenberg, M. K. Chang, S. A. Wek, M. C. Moos, Jr. and C. Londos (1992). "Mechanism of hormone-stimulated lipolysis in adipocytes: translocation of hormone-sensitive lipase to the lipid storage droplet." Proc Natl Acad Sci U S A **89**(18): 8537-8541.

Egger, G. and B. Swinburn (1997). "An "ecological" approach to the obesity pandemic." BMJ **315**(7106): 477-480.

Elmquist, J. K., R. Coppari, N. Balthasar, M. Ichinose and B. B. Lowell (2005). "Identifying hypothalamic pathways controlling food intake, body weight, and glucose homeostasis." J Comp Neurol **493**(1): 63-71.

Enerback, S., A. Jacobsson, E. M. Simpson, C. Guerra, H. Yamashita, M. E. Harper and L. P. Kozak (1997). "Mice lacking mitochondrial uncoupling protein are cold-sensitive but not obese." Nature **387**(6628): 90-94.

Eriksson, J. G., T. J. Forsen, E. Kajantie, C. Osmond and D. J. Barker (2007). "Childhood growth and hypertension in later life." Hypertension **49**(6): 1415-1421.

Fabbrini, E., F. Magkos, B. S. Mohammed, T. Pietka, N. A. Abumrad, B. W. Patterson, A. Okunade and S. Klein (2009). "Intrahepatic fat, not visceral fat, is linked with metabolic complications of obesity." Proc Natl Acad Sci U S A **106**(36): 15430-15435.

Fall, C. H., C. Osmond, D. J. Barker, P. M. Clark, C. N. Hales, Y. Stirling and T. W. Meade (1995). "Fetal and infant growth and cardiovascular risk factors in women." BMJ **310**(6977): 428-432.

Fall, C. H., C. E. Stein, K. Kumaran, V. Cox, C. Osmond, D. J. Barker and C. N. Hales (1998). "Size at birth, maternal weight, and type 2 diabetes in South India." Diabet Med **15**(3): 220-227.

Farese, R. V. (2001). "Insulin-sensitive phospholipid signaling systems and glucose transport. Update II." Exp Biol Med (Maywood) **226**(4): 283-295.

Fernandez-Twinn, D. S., A. Wayman, S. Ekizoglou, M. S. Martin, C. N. Hales and S. E. Ozanne (2005). "Maternal protein restriction leads to hyperinsulinemia and reduced insulin-signaling protein expression in 21-mo-old female rat offspring." Am J Physiol Regul Integr Comp Physiol **288**(2): R368-373.

Fidanci, K., C. Meral, S. Suleymanoglu, O. Pirgon, F. Karademir, S. Aydinoz, H. Ozkaya, M. Gultepe and I. Gocmen (2010). "Ghrelin levels and postnatal growth in healthy infants 0-3 months of age." J Clin Res Pediatr Endocrinol **2**(1): 34-38.

Flatt, J. P. (1987). "Dietary fat, carbohydrate balance, and weight maintenance: effects of exercise." Am J Clin Nutr **45**(1 Suppl): 296-306.

Flegal, K. M., J. A. Shepherd, A. C. Looker, B. I. Graubard, L. G. Borrud, C. L. Ogden, T. B. Harris, J. E. Everhart and N. Schenker (2009). "Comparisons of percentage body fat, body mass index, waist circumference, and waist-stature ratio in adults." Am J Clin Nutr **89**(2): 500-508.

Fomon, S. J., F. Haschke, E. E. Ziegler and S. E. Nelson (1982). "Body composition of reference children from birth to age 10 years." Am J Clin Nutr **35**(5 Suppl): 1169-1175.

Fredrikson, G., H. Tornqvist and P. Belfrage (1986). "Hormone-sensitive lipase and monoacylglycerol lipase are both required for complete degradation of adipocyte triacylglycerol." Biochim Biophys Acta **876**(2): 288-293.

Frontini, A. and S. Cinti (2010). "Distribution and development of brown adipocytes in the murine and human adipose organ." Cell Metab **11**(4): 253-256.

Fruhbeck, G., M. Aguado and J. A. Martinez (1997). "In vitro lipolytic effect of leptin on mouse adipocytes: evidence for a possible autocrine/paracrine role of leptin." Biochem Biophys Res Commun **240**(3): 590-594.

Gabriely, I., X. H. Ma, X. M. Yang, G. Atzmon, M. W. Rajala, A. H. Berg, P. Scherer, L. Rossetti and N. Barzilai (2002). "Removal of visceral fat prevents insulin resistance and glucose intolerance of aging: an adipokine-mediated process?" Diabetes **51**(10): 2951-2958.

Gafni, R. I. and J. Baron (2000). "Catch-up growth: possible mechanisms." Pediatr Nephrol **14**(7): 616-619.

Gale, C. R., C. N. Martyn, S. Kellingray, R. Eastell and C. Cooper (2001). "Intrauterine programming of adult body composition." J Clin Endocrinol Metab **86**(1): 267-272.

Gerich, J. E., V. Schneider, S. E. Dippe, M. Langlois, C. Noacco, J. H. Karam and P. H. Forsham (1974). "Characterization of the glucagon response to hypoglycemia in man." J Clin Endocrinol Metab **38**(1): 77-82.

Gesta, S., Y. H. Tseng and C. R. Kahn (2007). "Developmental origin of fat: tracking obesity to its source." Cell **131**(2): 242-256.

Gharibeh, M. Y., G. M. Al Tawallbeh, M. M. Abboud, A. Radaideh, A. A. Alhader and O. F. Khabour (2010). "Correlation of plasma resistin with obesity and insulin resistance in type 2 diabetic patients." Diabetes Metab **36**(6 Pt 1): 443-449.

Giorgino, F., L. Laviola and J. W. Eriksson (2005). "Regional differences of insulin action in adipose tissue: insights from in vivo and in vitro studies." Acta Physiol Scand **183**(1): 13-30.

Glaum, S. R., M. Hara, V. P. Bindokas, C. C. Lee, K. S. Polonsky, G. I. Bell and R. J. Miller (1996). "Leptin, the obese gene product, rapidly modulates synaptic transmission in the hypothalamus." Mol Pharmacol **50**(2): 230-235.

Gluckman, P. D. and M. A. Hanson (2004). "Developmental origins of disease paradigm: a mechanistic and evolutionary perspective." Pediatr Res **56**(3): 311-317.

Gluckman, P. D. and M. A. Hanson (2004). "The developmental origins of the metabolic syndrome." Trends Endocrinol Metab **15**(4): 183-187.

Gluckman, P. D., M. A. Hanson, C. Cooper and K. L. Thornburg (2008). "Effect of in utero and early-life conditions on adult health and disease." N Engl J Med **359**(1): 61-73.

Gluckman, P. D., M. A. Hanson and H. G. Spencer (2005). "Predictive adaptive responses and human evolution." Trends Ecol Evol **20**(10): 527-533.

Goodridge, A. G., S. A. Klautky, D. A. Fantozzi, R. A. Baillie, D. W. Hodnett, W. Chen, D. C. Thurmond, G. Xu and C. Roncero (1996). "Nutritional and hormonal regulation of expression of the gene for malic enzyme." Prog Nucleic Acid Res Mol Biol **52**: 89-122.

Gosmain, Y., N. Dif, V. Berbe, E. Loizon, J. Rieusset, H. Vidal and E. Lefai (2005). "Regulation of SREBP-1 expression and transcriptional action on HKII and FAS genes during fasting and refeeding in rat tissues." J Lipid Res **46**(4): 697-705.

Graham, G. G., A. Cordano, R. M. Blizzard and D. B. Cheek (1969). "Infantile malnutrition. Changes in body composition during rehabilitation." Pediatr Res **3**(6): 579-589.

Grunfeld, C. and K. R. Feingold (1992). "Tumor necrosis factor, interleukin, and interferon induced changes in lipid metabolism as part of host defense." Proc Soc Exp Biol Med **200**(2): 224-227.

Gunnarsdottir, I., B. E. Birgisdottir, R. Benediktsson, V. Gudnason and I. Thorsdottir (2004). "Association between size at birth, truncal fat and obesity in adult life and its contribution to blood pressure and coronary heart disease; study in a high birth weight population." Eur J Clin Nutr **58**(5): 812-818.

Gustavsson, J., S. Parpal, M. Karlsson, C. Ramsing, H. Thorn, M. Borg, M. Lindroth, K. H. Peterson, K. E. Magnusson and P. Stralfors (1999). "Localization of the insulin receptor in caveolae of adipocyte plasma membrane." FASEB J **13**(14): 1961-1971.

Hales, C. N. and D. J. Barker (1992). "Type 2 (non-insulin-dependent) diabetes mellitus: the thrifty phenotype hypothesis." Diabetologia **35**(7): 595-601.

Hales, C. N. and D. J. Barker (2001). "The thrifty phenotype hypothesis." Br Med Bull **60**: 5-20.

Hales, C. N., D. J. Barker, P. M. Clark, L. J. Cox, C. Fall, C. Osmond and P. D. Winter (1991). "Fetal and infant growth and impaired glucose tolerance at age 64." BMJ **303**(6809): 1019-1022.

Hales, C. N., M. Desai, S. E. Ozanne and N. J. Crowther (1996). "Fishing in the stream of diabetes: from measuring insulin to the control of fetal organogenesis." Biochem Soc Trans **24**(2): 341-350.

Hales, C. N. and S. E. Ozanne (2003). "The dangerous road of catch-up growth." J Physiol **547**(Pt 1): 5-10.

Harris, A. J., J. F. Patience, S. M. Lonergan, J. M. D. C and N. K. Gabler (2012). "Improved nutrient digestibility and retention partially explains feed efficiency gains in pigs selected for low residual feed intake." J Anim Sci **90 Suppl 4**: 164-166.

He, Q., M. Horlick, J. Thornton, J. Wang, R. N. Pierson, Jr., S. Heshka and D. Gallagher (2002). "Sex and race differences in fat distribution among Asian, African-American, and Caucasian prepubertal children." J Clin Endocrinol Metab **87**(5): 2164-2170.

Hediger, M. L., M. D. Overpeck, R. J. Kuczmarski, A. McGlynn, K. R. Maurer and W. W. Davis (1998). "Muscularity and fatness of infants and young children born small- or large-for-gestational-age." Pediatrics **102**(5): E60.

Henry, R. R., B. Gumbiner, T. Ditzler, P. Wallace, R. Lyon and H. S. Glauber (1993). "Intensive conventional insulin therapy for type II diabetes. Metabolic effects during a 6-mo outpatient trial." Diabetes Care **16**(1): 21-31.

Herd, R. M. and P. F. Arthur (2009). "Physiological basis for residual feed intake." J Anim Sci **87**(14 Suppl): E64-71.

Hermann, G. M., R. L. Miller, G. E. Erkonen, L. M. Dallas, E. Hsu, V. Zhu and R. D. Roghair (2009). "Neonatal catch up growth increases diabetes susceptibility but improves behavioral and cardiovascular outcomes of low birth weight male mice." Pediatr Res **66**(1): 53-58.

Hietakangas, V. and S. M. Cohen (2009). "Regulation of tissue growth through nutrient sensing." Annu Rev Genet **43**: 389-410.

Hoggard, N., J. G. Mercer, D. V. Rayner, K. Moar, P. Trayhurn and L. M. Williams (1997). "Localization of leptin receptor mRNA splice variants in murine peripheral tissues by RT-PCR and in situ hybridization." Biochem Biophys Res Commun **232**(2): 383-387.

Holm, C. (2003). "Molecular mechanisms regulating hormone-sensitive lipase and lipolysis." Biochem Soc Trans **31**(Pt 6): 1120-1124.

Holst, J. J. (1994). "Glucagonlike peptide 1: a newly discovered gastrointestinal hormone." Gastroenterology **107**(6): 1848-1855.

Huang, H. and D. J. Tindall (2007). "Dynamic FoxO transcription factors." J Cell Sci **120**(Pt 15): 2479-2487.

Iozzo, P. (2009). "Viewpoints on the way to the consensus session: where does insulin resistance start? The adipose tissue." Diabetes Care **32 Suppl 2**: S168-173.

Isganaitis, E., J. Jimenez-Chillaron, M. Woo, A. Chow, J. DeCoste, M. Vokes, M. Liu, S. Kasif, A. M. Zavacki, R. L. Leshan, M. G. Myers and M. E. Patti (2009). "Accelerated postnatal growth increases lipogenic gene expression and adipocyte size in low-birth weight mice." Diabetes **58**(5): 1192-1200.

Kahn, H. S., K. M. Narayan, D. F. Williamson and R. Valdez (2000). "Relation of birth weight to lean and fat thigh tissue in young men." Int J Obes Relat Metab Disord **24**(6): 667-672.

Kahn, S. E., R. L. Hull and K. M. Utzschneider (2006). "Mechanisms linking obesity to insulin resistance and type 2 diabetes." Nature **444**(7121): 840-846.

Karlsson, M., H. Thorn, A. Danielsson, K. G. Stenkula, A. Ost, J. Gustavsson, F. H. Nystrom and P. Stralfors (2004). "Colocalization of insulin receptor and insulin receptor substrate-1 to caveolae in primary human adipocytes. Cholesterol depletion blocks insulin signalling for metabolic and mitogenic control." Eur J Biochem **271**(12): 2471-2479.

Kershaw, E. E. and J. S. Flier (2004). "Adipose tissue as an endocrine organ." J Clin Endocrinol Metab **89**(6): 2548-2556.

Klaus, S. (1997). "Functional differentiation of white and brown adipocytes." Bioessays **19**(3): 215-223.

Kozak, L. P. (2000). "Genetic studies of brown adipocyte induction." J Nutr **130**(12): 3132S-3133S.

Kuh, D., J. Bassey, R. Hardy, A. Aihie Sayer, M. Wadsworth and C. Cooper (2002). "Birth weight, childhood size, and muscle strength in adult life: evidence from a birth cohort study." Am J Epidemiol **156**(7): 627-633.

Kuh, D., R. Hardy, N. Chaturvedi and M. E. Wadsworth (2002). "Birth weight, childhood growth and abdominal obesity in adult life." Int J Obes Relat Metab Disord **26**(1): 40-47.

Kuo, Y. T., A. H. Herlihy, P. W. So and J. D. Bell (2006). "Manganese-enhanced magnetic resonance imaging (MEMRI) without compromise of the blood-brain barrier detects hypothalamic neuronal activity in vivo." NMR Biomed **19**(8): 1028-1034.

Kuo, Y. T., A. H. Herlihy, P. W. So, K. K. Bhakoo and J. D. Bell (2005). "In vivo measurements of T1 relaxation times in mouse brain associated with different modes of systemic administration of manganese chloride." J Magn Reson Imaging **21**(4): 334-339.

Lee, P., M. M. Swarbrick and K. K. Ho (2013). "Brown adipose tissue in adult humans: a metabolic renaissance." Endocr Rev **34**(3): 413-438.

Leiter, E. H., F. Premdas, D. E. Harrison and L. G. Lipson (1988). "Aging and glucose homeostasis in C57BL/6J male mice." FASEB J **2**(12): 2807-2811.

Leone, T. C., J. J. Lehman, B. N. Finck, P. J. Schaeffer, A. R. Wende, S. Boudina, M. Courtois, D. F. Wozniak, N. Sambandam, C. Bernal-Mizrachi, Z. Chen, J. O. Holloszy, D. M. Medeiros, R. E. Schmidt, J. E. Saffitz, E. D. Abel, C. F. Semenkovich and D. P. Kelly (2005). "PGC-1alpha deficiency causes multi-system energy metabolic derangements: muscle dysfunction, abnormal weight control and hepatic steatosis." PLoS Biol **3**(4): e101.

Lin, J., P. H. Wu, P. T. Tarr, K. S. Lindenberg, J. St-Pierre, C. Y. Zhang, V. K. Mootha, S. Jager, C. R. Vianna, R. M. Reznick, L. Cui, M. Manieri, M. X. Donovan, Z. Wu, M. P. Cooper, M. C. Fan, L. M. Rohas, A. M. Zavacki, S. Cinti, G. I. Shulman, B. B. Lowell, D. Krainc and B. M. Spiegelman (2004). "Defects in adaptive energy metabolism with CNS-linked hyperactivity in PGC-1alpha null mice." Cell **119**(1): 121-135.

Lin, S. and X. F. Huang (1999). "Altered hypothalamic c-Fos-like immunoreactivity in diet-induced obese mice." Brain Res Bull **49**(3): 215-219.

Lin, Y. J. and A. P. Koretsky (1997). "Manganese ion enhances T1-weighted MRI during brain activation: an approach to direct imaging of brain function." Magn Reson Med **38**(3): 378-388.

Lollmann, B., S. Gruninger, A. Stricker-Krongrad and M. Chiesi (1997). "Detection and quantification of the leptin receptor splice variants Ob-Ra, b, and, e in different mouse tissues." Biochem Biophys Res Commun **238**(2): 648-652.

Loos, R. J., G. Beunen, R. Fagard, C. Derom and R. Vlietinck (2002). "Birth weight and body composition in young women: a prospective twin study." Am J Clin Nutr **75**(4): 676-682.

Lundgren, M., J. Buren, T. Ruge, T. Myrnas and J. W. Eriksson (2004). "Glucocorticoids down-regulate glucose uptake capacity and insulin-signaling proteins in omental but not subcutaneous human adipocytes." J Clin Endocrinol Metab **89**(6): 2989-2997.

Maffei, M., J. Halaas, E. Ravussin, R. E. Pratley, G. H. Lee, Y. Zhang, H. Fei, S. Kim, R. Lallone, S. Ranganathan and et al. (1995). "Leptin levels in human and rodent: measurement of plasma leptin and ob RNA in obese and weight-reduced subjects." Nat Med **1**(11): 1155-1161.

Makowski, M. R., A. J. Wiethoff, C. H. Jansen and R. M. Botnar (2009). "Molecular imaging with targeted contrast agents." Top Magn Reson Imaging **20**(4): 247-259.

Marques, C. M., V. F. Motta, T. S. Torres, M. B. Aguila and C. A. Mandarim-de-Lacerda (2010). "Beneficial effects of exercise training (treadmill) on insulin resistance and nonalcoholic fatty liver disease in high-fat fed C57BL/6 mice." Braz J Med Biol Res **43**(5): 467-475.

Martin-Gronert, M. S. and S. E. Ozanne (2005). "Programming of appetite and type 2 diabetes." Early Hum Dev **81**(12): 981-988.

Martyn, C. N., C. N. Hales, D. J. Barker and S. Jespersen (1998). "Fetal growth and hyperinsulinaemia in adult life." Diabet Med **15**(8): 688-694.

Matthes, J. W., P. A. Lewis, D. P. Davies and J. A. Bethel (1996). "Body size and subcutaneous fat patterning in adolescence." Arch Dis Child **75**(6): 521-523.

McCance, D. R., D. J. Pettitt, R. L. Hanson, L. T. Jacobsson, W. C. Knowler and P. H. Bennett (1994). "Birth weight and non-insulin dependent diabetes: thrifty genotype, thrifty phenotype, or surviving small baby genotype?" BMJ **308**(6934): 942-945.

McLaughlin, T., A. Sherman, P. Tsao, O. Gonzalez, G. Yee, C. Lamendola, G. M. Reaven and S. W. Cushman (2007). "Enhanced proportion of small adipose cells in insulin-resistant vs insulin-sensitive obese individuals implicates impaired adipogenesis." Diabetologia **50**(8): 1707-1715.

Mistry, A. M., A. G. Swick and D. R. Romsos (1997). "Leptin rapidly lowers food intake and elevates metabolic rates in lean and ob/ob mice." J Nutr **127**(10): 2065-2072.

Mook-Kanamori, D. O., B. Durmus, U. Sovio, A. Hofman, H. Raat, E. A. Steegers, M. R. Jarvelin and V. W. Jaddoe (2011). "Fetal and infant growth and the risk of obesity during early childhood: the Generation R Study." Eur J Endocrinol **165**(4): 623-630.

Must, A., G. E. Dallal and W. H. Dietz (1991). "Reference data for obesity: 85th and 95th percentiles of body mass index (wt/ht2) and triceps skinfold thickness." Am J Clin Nutr **53**(4): 839-846.

Mystkowski, P., E. Shankland, S. A. Schreyer, R. C. LeBoeuf, R. S. Schwartz, D. E. Cummings, M. Kushmerick and M. W. Schwartz (2000). "Validation of whole-body magnetic resonance spectroscopy as a tool to assess murine body composition." Int J Obes Relat Metab Disord **24**(6): 719-724.

Nakaki, T., T. Nakadate and R. Kato (1980). "Alpha 2-adrenoceptors modulating insulin release from isolated pancreatic islets." Naunyn Schmiedebergs Arch Pharmacol **313**(2): 151-153.

Neel, J. V. (1962). "Diabetes mellitus: a "thrifty" genotype rendered detrimental by "progress"?" Am J Hum Genet **14**: 353-362.

Oken, E. and M. W. Gillman (2003). "Fetal origins of obesity." Obes Res **11**(4): 496-506.

Okosun, I. S., Y. Liao, C. N. Rotimi, G. E. Dever and R. S. Cooper (2000). "Impact of birth weight on ethnic variations in subcutaneous and central adiposity in American children aged 5-11 years. A study from the Third National Health and Nutrition Examination Survey." Int J Obes Relat Metab Disord **24**(4): 479-484.

Ong, K. K. (2006). "Size at birth, postnatal growth and risk of obesity." Horm Res **65 Suppl 3**: 65-69.

Ouchi, N., J. L. Parker, J. J. Lugus and K. Walsh (2011). "Adipokines in inflammation and metabolic disease." Nat Rev Immunol **11**(2): 85-97.

Ounsted, M. and G. Sleigh (1975). "The infant's self-regulation of food intake and weight gain. Difference in metabolic balance after growth constraint or acceleration in utero." Lancet **1**(7922): 1393-1397.

Ozanne, S. E. and C. N. Hales (2002). "Early programming of glucose-insulin metabolism." Trends Endocrinol Metab **13**(9): 368-373.

Ozanne, S. E. and C. N. Hales (2004). "Lifespan: catch-up growth and obesity in male mice." Nature **427**(6973): 411-412.

Ozanne, S. E., R. Lewis, B. J. Jennings and C. N. Hales (2004). "Early programming of weight gain in mice prevents the induction of obesity by a highly palatable diet." Clin Sci (Lond) **106**(2): 141-145.

Ozanne, S. E., C. L. Wang, C. J. Petry, J. M. Smith and C. N. Hales (1998). "Ketosis resistance in the male offspring of protein-malnourished rat dams." Metabolism **47**(12): 1450-1454.

Panee, J. (2012). "Monocyte Chemoattractant Protein 1 (MCP-1) in obesity and diabetes." Cytokine **60**(1): 1-12.

Park, J. H., D. A. Stoffers, R. D. Nicholls and R. A. Simmons (2008). "Development of type 2 diabetes following intrauterine growth retardation in rats is associated with progressive epigenetic silencing of Pdx1." J Clin Invest **118**(6): 2316-2324.

Parkinson, J. R., O. B. Chaudhri and J. D. Bell (2009). "Imaging appetite-regulating pathways in the central nervous system using manganese-enhanced magnetic resonance imaging." Neuroendocrinology **89**(2): 121-130.

Parkinson, J. R., O. B. Chaudhri, Y. T. Kuo, B. C. Field, A. H. Herlihy, W. S. Dhillo, M. A. Ghatei, S. R. Bloom and J. D. Bell (2009). "Differential patterns of neuronal activation in the brainstem and hypothalamus following peripheral injection of GLP-1, oxyntomodulin and lithium chloride in mice detected by manganese-enhanced magnetic resonance imaging (MEMRI)." Neuroimage **44**(3): 1022-1031.

Parsons, T. J., C. Power, S. Logan and C. D. Summerbell (1999). "Childhood predictors of adult obesity: a systematic review." Int J Obes Relat Metab Disord **23 Suppl 8**: S1-107.

Parsons, T. J., C. Power and O. Manor (2001). "Fetal and early life growth and body mass index from birth to early adulthood in 1958 British cohort: longitudinal study." BMJ **323**(7325): 1331-1335.

Pautler, R. G. (2004). "In vivo, trans-synaptic tract-tracing utilizing manganese-enhanced magnetic resonance imaging (MEMRI)." NMR Biomed **17**(8): 595-601.

Peruzzo, B., F. E. Pastor, J. L. Blazquez, K. Schobitz, B. Pelaez, P. Amat and E. M. Rodriguez (2000). "A second look at the barriers of the medial basal hypothalamus." Exp Brain Res **132**(1): 10-26.

Petrovic, N., T. B. Walden, I. G. Shabalina, J. A. Timmons, B. Cannon and J. Nedergaard (2010). "Chronic peroxisome proliferator-activated receptor gamma (PPARgamma) activation of epididymally derived white adipocyte cultures reveals a population of thermogenically competent, UCP1-containing adipocytes molecularly distinct from classic brown adipocytes." J Biol Chem **285**(10): 7153-7164.

Poore, K. R. and A. L. Fowden (2004). "The effects of birth weight and postnatal growth patterns on fat depth and plasma leptin concentrations in juvenile and adult pigs." J Physiol **558**(Pt 1): 295-304.

Poore, K. R. and A. L. Fowden (2004). "Insulin sensitivity in juvenile and adult Large White pigs of low and high birthweight." Diabetologia **47**(2): 340-348.

Poston, L. (2010). "Developmental programming and diabetes - The human experience and insight from animal models." Best Pract Res Clin Endocrinol Metab **24**(4): 541-552.

Prentice, A. M., B. J. Hennig and A. J. Fulford (2008). "Evolutionary origins of the obesity epidemic: natural selection of thrifty genes or genetic drift following predation release?" Int J Obes (Lond) **32**(11): 1607-1610.

Proulx, K., D. Richard and C. D. Walker (2002). "Leptin regulates appetite-related neuropeptides in the hypothalamus of developing rats without affecting food intake." Endocrinology **143**(12): 4683-4692.

Puigserver, P., Z. Wu, C. W. Park, R. Graves, M. Wright and B. M. Spiegelman (1998). "A cold-inducible coactivator of nuclear receptors linked to adaptive thermogenesis." Cell **92**(6): 829-839.

Rajala, M. W., S. Obici, P. E. Scherer and L. Rossetti (2003). "Adipose-derived resistin and gut-derived resistin-like molecule-beta selectively impair insulin action on glucose production." J Clin Invest **111**(2): 225-230.

Rangwala, S. M., A. S. Rich, B. Rhoades, J. S. Shapiro, S. Obici, L. Rossetti and M. A. Lazar (2004). "Abnormal glucose homeostasis due to chronic hyperresistinemia." Diabetes **53**(8): 1937-1941.

Rasmussen, F. and M. Johansson (1998). "The relation of weight, length and ponderal index at birth to body mass index and overweight among 18-year-old males in Sweden." Eur J Epidemiol **14**(4): 373-380.

Remmers, F. and H. A. Delemarre-van de Waal (2011). "Developmental programming of energy balance and its hypothalamic regulation." Endocr Rev **32**(2): 272-311.

Ritter, R. C. (2004). "Gastrointestinal mechanisms of satiation for food." Physiol Behav **81**(2): 249-273.

Roca, A., K. J. Shin, X. Liu, M. I. Simon and J. Chen (2004). "Comparative analysis of transcriptional profiles between two apoptotic pathways of light-induced retinal degeneration." Neuroscience **129**(3): 779-790.

Rodriguez, G., M. P. Samper, J. L. Olivares, P. Ventura, L. A. Moreno and J. M. Perez-Gonzalez (2005). "Skinfold measurements at birth: sex and anthropometric influence." Arch Dis Child Fetal Neonatal Ed **90**(3): F273-275.

Rogers, I. and E.-B. S. Group (2003). "The influence of birthweight and intrauterine environment on adiposity and fat distribution in later life." Int J Obes Relat Metab Disord **27**(7): 755-777.

Ros, H. S., P. Lichtenstein, A. Ekbom and S. Cnattingius (2001). "Tall or short? Twenty years after preeclampsia exposure in utero: comparisons of final height, body mass index, waist-to-hip ratio, and age at menarche among women, exposed and unexposed to preeclampsia during fetal life." Pediatr Res **49**(6): 763-769.

Rosen, E. D., C. H. Hsu, X. Wang, S. Sakai, M. W. Freeman, F. J. Gonzalez and B. M. Spiegelman (2002). "C/EBPalpha induces adipogenesis through PPARgamma: a unified pathway." Genes Dev **16**(1): 22-26.

Ross, R., L. Leger, R. Guardo, J. De Guise and B. G. Pike (1991). "Adipose tissue volume measured by magnetic resonance imaging and computerized tomography in rats." J Appl Physiol (1985) **70**(5): 2164-2172.

Rothwell, N. J. and M. J. Stock (1979). "Regulation of energy balance in two models of reversible obesity in the rat." J Comp Physiol Psychol **93**(6): 1024-1034.

Ruan, H., N. Hacohen, T. R. Golub, L. Van Parijs and H. F. Lodish (2002). "Tumor necrosis factor-alpha suppresses adipocyte-specific genes and activates expression of preadipocyte genes in 3T3-L1 adipocytes: nuclear factor-kappaB activation by TNF-alpha is obligatory." Diabetes **51**(5): 1319-1336.

Ruffin, M. and S. Nicolaidis (1999). "Electrical stimulation of the ventromedial hypothalamus enhances both fat utilization and metabolic rate that precede and parallel the inhibition of feeding behavior." Brain Res **846**(1): 23-29.

Saito, M., Y. Okamatsu-Ogura, M. Matsushita, K. Watanabe, T. Yoneshiro, J. Nio-Kobayashi, T. Iwanaga, M. Miyagawa, T. Kameya, K. Nakada, Y. Kawai and M. Tsujisaki (2009). "High incidence of metabolically active brown adipose tissue in healthy adult humans: effects of cold exposure and adiposity." Diabetes **58**(7): 1526-1531.

Saltiel, A. R. and C. R. Kahn (2001). "Insulin signalling and the regulation of glucose and lipid metabolism." Nature **414**(6865): 799-806.

Samuelsson, A. M., P. A. Matthews, M. Argenton, M. R. Christie, J. M. McConnell, E. H. Jansen, A. H. Piersma, S. E. Ozanne, D. F. Twinn, C. Remacle, A. Rowlerson, L. Poston and P. D. Taylor (2008). "Diet-induced obesity in female mice leads to offspring hyperphagia, adiposity, hypertension, and insulin resistance: a novel murine model of developmental programming." Hypertension **51**(2): 383-392.

Sanchez-Gurmaches, J. and D. A. Guertin (2014). "Adipocyte lineages: tracing back the origins of fat." Biochim Biophys Acta **1842**(3): 340-351.

Sandovici, I., C. M. Hammerle, S. E. Ozanne and M. Constancia (2013). "Developmental and environmental epigenetic programming of the endocrine pancreas: consequences for type 2 diabetes." Cell Mol Life Sci **70**(9): 1575-1595.

Sandovici, I., N. H. Smith, M. D. Nitert, M. Ackers-Johnson, S. Uribe-Lewis, Y. Ito, R. H. Jones, V. E. Marquez, W. Cairns, M. Tadayyon, L. P. O'Neill, A. Murrell, C. Ling, M. Constancia and S. E. Ozanne (2011). "Maternal diet and aging alter the epigenetic control of a promoter-enhancer interaction at the Hnf4a gene in rat pancreatic islets." Proc Natl Acad Sci U S A **108**(13): 5449-5454.

Saper, C. B., T. C. Chou and J. K. Elmquist (2002). "The need to feed: homeostatic and hedonic control of eating." Neuron **36**(2): 199-211.

Sato, N., K. Kobayashi, T. Inoguchi, N. Sonoda, M. Imamura, N. Sekiguchi, N. Nakashima and H. Nawata (2005). "Adenovirus-mediated high expression of resistin causes dyslipidemia in mice." Endocrinology **146**(1): 273-279.

Sauma, L., N. Franck, J. F. Paulsson, G. T. Westermark, P. Kjolhede, P. Stralfors, M. Soderstrom and F. H. Nystrom (2007). "Peroxisome proliferator activated receptor gamma activity is low in mature primary human visceral adipocytes." Diabetologia **50**(1): 195-201.

Savage, D. B., K. F. Petersen and G. I. Shulman (2005). "Mechanisms of insulin resistance in humans and possible links with inflammation." Hypertension **45**(5): 828-833.

Sayer, A. A., H. E. Syddall, E. M. Dennison, H. J. Gilbody, S. L. Duggleby, C. Cooper, D. J. Barker and D. I. Phillips (2004). "Birth weight, weight at 1 y of age, and body composition in older men: findings from the Hertfordshire Cohort Study." Am J Clin Nutr **80**(1): 199-203.

Schellong, K., S. Schulz, T. Harder and A. Plagemann (2012). "Birth weight and long-term overweight risk: systematic review and a meta-analysis including 643,902 persons from 66 studies and 26 countries globally." PLoS One **7**(10): e47776.

Schwartz, D. R. and M. A. Lazar (2011). "Human resistin: found in translation from mouse to man." Trends Endocrinol Metab **22**(7): 259-265.

Scott, L. J., K. L. Mohlke, L. L. Bonnycastle, C. J. Willer, Y. Li, W. L. Duren, M. R. Erdos, H. M. Stringham, P. S. Chines, A. U. Jackson, L. Prokunina-Olsson, C. J. Ding, A. J. Swift, N. Narisu, T. Hu, R. Pruim, R. Xiao, X. Y. Li,

K. N. Conneely, N. L. Riebow, A. G. Sprau, M. Tong, P. P. White, K. N. Hetrick, M. W. Barnhart, C. W. Bark, J. L. Goldstein, L. Watkins, F. Xiang, J. Saramies, T. A. Buchanan, R. M. Watanabe, T. T. Valle, L. Kinnunen, G. R. Abecasis, E. W. Pugh, K. F. Doheny, R. N. Bergman, J. Tuomilehto, F. S. Collins and M. Boehnke (2007). "A genome-wide association study of type 2 diabetes in Finns detects multiple susceptibility variants." Science **316**(5829): 1341-1345.

Seale, P., H. M. Conroe, J. Estall, S. Kajimura, A. Frontini, J. Ishibashi, P. Cohen, S. Cinti and B. M. Spiegelman (2011). "Prdm16 determines the thermogenic program of subcutaneous white adipose tissue in mice." J Clin Invest **121**(1): 96-105.

Seeley, R. J., G. van Dijk, L. A. Campfield, F. J. Smith, P. Burn, J. A. Nelligan, S. M. Bell, D. G. Baskin, S. C. Woods and M. W. Schwartz (1996). "Intraventricular leptin reduces food intake and body weight of lean rats but not obese Zucker rats." Horm Metab Res **28**(12): 664-668.

Seidman, D. S., A. Laor, R. Gale, D. K. Stevenson and Y. L. Danon (1991). "A longitudinal study of birth weight and being overweight in late adolescence." Am J Dis Child **145**(7): 782-785.

Sekiya, M., N. Yahagi, T. Matsuzaka, Y. Takeuchi, Y. Nakagawa, H. Takahashi, H. Okazaki, Y. Iizuka, K. Ohashi, T. Gotoda, S. Ishibashi, R. Nagai, T. Yamazaki, T. Kadowaki, N. Yamada, J. Osuga and H. Shimano (2007). "SREBP-1-independent regulation of lipogenic gene expression in adipocytes." J Lipid Res **48**(7): 1581-1591.

Sewter, C., D. Berger, R. V. Considine, G. Medina, J. Rochford, T. Ciaraldi, R. Henry, L. Dohm, J. S. Flier, S. O'Rahilly and A. J. Vidal-Puig (2002). "Human obesity and type 2 diabetes are associated with alterations in SREBP1 isoform expression that are reproduced ex vivo by tumor necrosis factor-alpha." Diabetes **51**(4): 1035-1041.

Shepherd, P. R., N. J. Crowther, M. Desai, C. N. Hales and S. E. Ozanne (1997). "Altered adipocyte properties in the offspring of protein malnourished rats." Br J Nutr **78**(1): 121-129.

Shiiya, T., M. Nakazato, M. Mizuta, Y. Date, M. S. Mondal, M. Tanaka, S. Nozoe, H. Hosoda, K. Kangawa and S. Matsukura (2002). "Plasma ghrelin levels in lean and obese humans and the effect of glucose on ghrelin secretion." J Clin Endocrinol Metab **87**(1): 240-244.

Shimomura, I., R. E. Hammer, J. A. Richardson, S. Ikemoto, Y. Bashmakov, J. L. Goldstein and M. S. Brown (1998). "Insulin resistance and diabetes mellitus in transgenic mice expressing nuclear SREBP-1c in adipose tissue: model for congenital generalized lipodystrophy." Genes Dev **12**(20): 3182-3194.

Siiteri, P. K. (1987). "Adipose tissue as a source of hormones." Am J Clin Nutr **45**(1 Suppl): 277-282.

Singhal, A., J. Wells, T. J. Cole, M. Fewtrell and A. Lucas (2003). "Programming of lean body mass: a link between birth weight, obesity, and cardiovascular disease?" Am J Clin Nutr **77**(3): 726-730.

Sladek, R., G. Rocheleau, J. Rung, C. Dina, L. Shen, D. Serre, P. Boutin, D. Vincent, A. Belisle, S. Hadjadj, B. Balkau, B. Heude, G. Charpentier, T. J. Hudson, A. Montpetit, A. V. Pshezhetsky, M. Prentki, B. I. Posner, D. J. Balding, D. Meyre, C. Polychronakos and P. Froguel (2007). "A genome-wide association study identifies novel risk loci for type 2 diabetes." Nature **445**(7130): 881-885.

Spiegelman, B. M., P. Puigserver and Z. Wu (2000). "Regulation of adipogenesis and energy balance by PPARgamma and PGC-1." Int J Obes Relat Metab Disord **24 Suppl 4**: S8-10.

Spielman, R. S., S. S. Fajans, J. V. Neel, S. Pek, J. C. Floyd and W. J. Oliver (1982). "Glucose tolerance in two unacculturated Indian tribes of Brazil." Diabetologia **23**(2): 90-93.

Stanner, S. A. and J. S. Yudkin (2001). "Fetal programming and the Leningrad Siege study." Twin Res **4**(5): 287-292.

Stenlof, K., I. Wernstedt, T. Fjallman, V. Wallenius, K. Wallenius and J. O. Jansson (2003). "Interleukin-6 levels in the central nervous system are negatively correlated with fat mass in overweight/obese subjects." J Clin Endocrinol Metab **88**(9): 4379-4383.

Steppan, C. M., S. T. Bailey, S. Bhat, E. J. Brown, R. R. Banerjee, C. M. Wright, H. R. Patel, R. S. Ahima and M. A. Lazar (2001). "The hormone resistin links obesity to diabetes." Nature **409**(6818): 307-312.

Sternson, S. M., G. M. Shepherd and J. M. Friedman (2005). "Topographic mapping of VMH --> arcuate nucleus microcircuits and their reorganization by fasting." Nat Neurosci **8**(10): 1356-1363.

Sugden, M. C. and M. J. Holness (2002). "Gender-specific programming of insulin secretion and action." J Endocrinol **175**(3): 757-767.

Summermatter, S., H. Marcelino, D. Arsenijevic, A. Buchala, O. Aprikian, F. Assimacopoulos-Jeannet, J. Seydoux, J. P. Montani, G. Solinas and A. G. Dulloo (2009). "Adipose tissue plasticity during catch-up fat driven by thrifty metabolism: relevance for muscle-adipose glucose redistribution during catch-up growth." Diabetes **58**(10): 2228-2237.

Swinburn, B. and G. Egger (2001). "Prevention of type 2 diabetes. Prevention needs to reduce obesogenic environments." BMJ **323**(7319): 997.

Swinburn, B., G. Egger and F. Raza (1999). "Dissecting obesogenic environments: the development and application of a framework for identifying and prioritizing environmental interventions for obesity." Prev Med **29**(6 Pt 1): 563-570.

Tanti, J. F., S. Grillo, T. Gremeaux, P. J. Coffer, E. Van Obberghen and Y. Le Marchand-Brustel (1997). "Potential role of protein kinase B in glucose transporter 4 translocation in adipocytes." Endocrinology **138**(5): 2005-2010.

Te Velde, S. J., J. W. Twisk, W. Van Mechelen and H. C. Kemper (2003). "Birth weight, adult body composition, and subcutaneous fat distribution." Obes Res **11**(2): 202-208.

Thomas, E. L., J. R. Parkinson, G. S. Frost, A. P. Goldstone, C. J. Dore, J. P. McCarthy, A. L. Collins, J. A. Fitzpatrick, G. Durighel, S. D. Taylor-Robinson and J. D. Bell (2012). "The missing risk: MRI and MRS phenotyping of abdominal adiposity and ectopic fat." Obesity (Silver Spring) **20**(1): 76-87.

Tong, Y., H. F. Zhao, F. Labrie and G. Pelletier (1990). "Regulation of proopiomelanocortin messenger ribonucleic acid content by sex steroids in the arcuate nucleus of the female rat brain." Neurosci Lett **112**(1): 104-108.

Torres-Leal, F. L., M. H. Fonseca-Alaniz, M. M. Rogero and J. Tirapegui (2010). "The role of inflamed adipose tissue in the insulin resistance." Cell Biochem Funct **28**(8): 623-631.

Trayhurn, P., M. E. Thomas, J. S. Duncan and D. V. Rayner (1995). "Effects of fasting and refeeding on ob gene expression in white adipose tissue of lean and obese (oblob) mice." FEBS Lett **368**(3): 488-490.

Trujillo, M. E. and P. E. Scherer (2005). "Adiponectin--journey from an adipocyte secretory protein to biomarker of the metabolic syndrome." J Intern Med **257**(2): 167-175.

Trujillo, M. E. and P. E. Scherer (2006). "Adipose tissue-derived factors: impact on health and disease." Endocr Rev **27**(7): 762-778.

Trujillo, M. E., S. Sullivan, I. Harten, S. H. Schneider, A. S. Greenberg and S. K. Fried (2004). "Interleukin-6 regulates human adipose tissue lipid metabolism and leptin production in vitro." J Clin Endocrinol Metab **89**(11): 5577-5582.

Tschop, M., C. Weyer, P. A. Tataranni, V. Devanarayan, E. Ravussin and M. L. Heiman (2001). "Circulating ghrelin levels are decreased in human obesity." Diabetes **50**(4): 707-709.

Tschop, M. H., J. R. Speakman, J. R. Arch, J. Auwerx, J. C. Bruning, L. Chan, R. H. Eckel, R. V. Farese, Jr., J. E. Galgani, C. Hambly, M. A. Herman, T. L. Horvath, B. B. Kahn, S. C. Kozma, E. Maratos-Flier, T. D. Muller, H. Munzberg, P. T. Pfluger, L. Plum, M. L. Reitman, K. Rahmouni, G. I. Shulman, G. Thomas, C. R. Kahn and E. Ravussin (2012). "A guide to analysis of mouse energy metabolism." Nat Methods **9**(1): 57-63.

Unger, R. H., G. O. Clark, P. E. Scherer and L. Orci (2010). "Lipid homeostasis, lipotoxicity and the metabolic syndrome." Biochim Biophys Acta **1801**(3): 209-214.

Unger, R. H. and L. Orci (2002). "Lipoapoptosis: its mechanism and its diseases." Biochim Biophys Acta **1585**(2-3): 202-212.

Valdez, R., M. A. Athens, G. H. Thompson, B. S. Bradshaw and M. P. Stern (1994). "Birthweight and adult health outcomes in a biethnic population in the USA." Diabetologia **37**(6): 624-631.

Van Coillie, E., J. Van Damme and G. Opdenakker (1999). "The MCP/eotaxin subfamily of CC chemokines." Cytokine Growth Factor Rev **10**(1): 61-86.

van den Top, M., K. Lee, A. D. Whyment, A. M. Blanks and D. Spanswick (2004). "Orexigen-sensitive NPY/AgRP pacemaker neurons in the hypothalamic arcuate nucleus." Nat Neurosci **7**(5): 493-494.

Van Harmelen, V., S. Reynisdottir, P. Eriksson, A. Thorne, J. Hoffstedt, F. Lonnqvist and P. Arner (1998). "Leptin secretion from subcutaneous and visceral adipose tissue in women." Diabetes **47**(6): 913-917.

Vazquez-Vela, M. E., N. Torres and A. R. Tovar (2008). "White adipose tissue as endocrine organ and its role in obesity." Arch Med Res **39**(8): 715-728.

Vestbo, E., E. M. Damsgaard, A. Froland and C. E. Mogensen (1996). "Birth weight and cardiovascular risk factors in an epidemiological study." Diabetologia **39**(12): 1598-1602.

Villena, J. A., S. Roy, E. Sarkadi-Nagy, K. H. Kim and H. S. Sul (2004). "Desnutrin, an adipocyte gene encoding a novel patatin domain-containing protein, is induced by fasting and glucocorticoids: ectopic expression of desnutrin increases triglyceride hydrolysis." J Biol Chem **279**(45): 47066-47075.

von Eynatten, M., J. G. Schneider, P. M. Humpert, G. Rudofsky, N. Schmidt, P. Barosch, A. Hamann, M. Morcos, J. Kreuzer, A. Bierhaus, P. P. Nawroth and K. A. Dugi (2004). "Decreased plasma lipoprotein lipase in hypoadiponectinemia: an association independent of systemic inflammation and insulin resistance." Diabetes Care **27**(12): 2925-2929.

Walden, T. B., I. R. Hansen, J. A. Timmons, B. Cannon and J. Nedergaard (2012). "Recruited vs. nonrecruited molecular signatures of brown, "brite," and white adipose tissues." Am J Physiol Endocrinol Metab **302**(1): E19-31.

Wallenius, V., K. Wallenius, B. Ahren, M. Rudling, H. Carlsten, S. L. Dickson, C. Ohlsson and J. O. Jansson (2002). "Interleukin-6-deficient mice develop mature-onset obesity." Nat Med **8**(1): 75-79.

Walley, A. J., A. I. Blakemore and P. Froguel (2006). "Genetics of obesity and the prediction of risk for health." Hum Mol Genet **15 Spec No 2**: R124-130.

Wang, G. L., X. Shi, E. Salisbury, Y. Sun, J. H. Albrecht, R. G. Smith and N. A. Timchenko (2006). "Cyclin D3 maintains growth-inhibitory activity of C/EBPalpha by stabilizing C/EBPalpha-cdk2 and C/EBPalpha-Brm complexes." Mol Cell Biol **26**(7): 2570-2582.

Wang, H. and R. H. Eckel (2009). "Lipoprotein lipase: from gene to obesity." Am J Physiol Endocrinol Metab **297**(2): E271-288.

Wang, Y. C., K. McPherson, T. Marsh, S. L. Gortmaker and M. Brown (2011). "Health and economic burden of the projected obesity trends in the USA and the UK." Lancet **378**(9793): 815-825.

Wei, J. N., F. C. Sung, C. Y. Li, C. H. Chang, R. S. Lin, C. C. Lin, C. C. Chiang and L. M. Chuang (2003). "Low birth weight and high birth weight infants are both at an increased risk to have type 2 diabetes among schoolchildren in taiwan." Diabetes Care **26**(2): 343-348.

Wells, J. C. (2000). "A Hattori chart analysis of body mass index in infants and children." Int J Obes Relat Metab Disord **24**(3): 325-329.

Welt, C. K., J. L. Chan, J. Bullen, R. Murphy, P. Smith, A. M. DePaoli, A. Karalis and C. S. Mantzoros (2004). "Recombinant human leptin in women with hypothalamic amenorrhea." N Engl J Med **351**(10): 987-997.

Weyer, C., C. Bogardus and R. E. Pratley (1999). "Metabolic characteristics of individuals with impaired fasting glucose and/or impaired glucose tolerance." Diabetes **48**(11): 2197-2203.

Weyer, C., R. E. Pratley, R. S. Lindsay and P. A. Tataranni (2000). "Relationship between birth weight and body composition, energy metabolism, and sympathetic nervous system activity later in life." Obes Res **8**(8): 559-565.

White, M. F. (1998). "The IRS-signaling system: a network of docking proteins that mediate insulin and cytokine action." Recent Prog Horm Res **53**: 119-138.

Williams, J. P. (1981). "Catch-up growth." J Embryol Exp Morphol **65 Suppl**: 89-101.

Winzell, M. S. and B. Ahren (2004). "The high-fat diet-fed mouse: a model for studying mechanisms and treatment of impaired glucose tolerance and type 2 diabetes." Diabetes **53 Suppl 3**: S215-219.

World Health Organisation, W. (2013). "Obesity and overweight Fact sheet N°311."

Wu, J., P. Bostrom, L. M. Sparks, L. Ye, J. H. Choi, A. H. Giang, M. Khandekar, K. A. Virtanen, P. Nuutila, G. Schaart, K. Huang, H. Tu, W. D. van Marken Lichtenbelt, J. Hoeks, S. Enerback, P. Schrauwen and B. M. Spiegelman (2012). "Beige adipocytes are a distinct type of thermogenic fat cell in mouse and human." Cell **150**(2): 366-376.

Yajnik, C. S., C. H. Fall, K. J. Coyaji, S. S. Hirve, S. Rao, D. J. Barker, C. Joglekar and S. Kellingray (2003). "Neonatal anthropometry: the thin-fat Indian baby. The Pune Maternal Nutrition Study." Int J Obes Relat Metab Disord **27**(2): 173-180.

Yamamori, T. (1991). "CDF/LIF selectively increases c-fos and jun-B transcripts in sympathetic neurons." Neuroreport **2**(4): 173-176.

Yarbrough, D. E., E. Barrett-Connor, D. Kritz-Silverstein and D. L. Wingard (1998). "Birth weight, adult weight, and girth as predictors of the metabolic syndrome in postmenopausal women: the Rancho Bernardo Study." Diabetes Care **21**(10): 1652-1658.

Young, J. B., E. Saville, N. J. Rothwell, M. J. Stock and L. Landsberg (1982). "Effect of diet and cold exposure on norepinephrine turnover in brown adipose tissue of the rat." J Clin Invest **69**(5): 1061-1071.

Yu, K., Q. Chen, H. Liu, Y. Zhan and J. L. Stevens (1994). "Signalling the molecular stress response to nephrotoxic and mutagenic cysteine conjugates: differential roles for protein synthesis and calcium in the induction of c-fos and c-myc mRNA in LLC-PK1 cells." J Cell Physiol **161**(2): 303-311.

Yu, Y. H. and H. N. Ginsberg (2005). "Adipocyte signaling and lipid homeostasis: sequelae of insulin-resistant adipose tissue." Circ Res **96**(10): 1042-1052.

Yu, Z. B., S. P. Han, G. Z. Zhu, C. Zhu, X. J. Wang, X. G. Cao and X. R. Guo (2011). "Birth weight and subsequent risk of obesity: a systematic review and meta-analysis." Obes Rev **12**(7): 525-542.

Zhang, Y., R. Proenca, M. Maffei, M. Barone, L. Leopold and J. M. Friedman (1994). "Positional cloning of the mouse obese gene and its human homologue." Nature **372**(6505): 425-432.